Weihong Tan · Xiaohong Fang *Editors*

Aptamers Selected by Cell-SELEX for Theranostics

Springer

Aptamers Selected by Cell-SELEX for Theranostics

Weihong Tan · Xiaohong Fang
Editors

Aptamers Selected by Cell-SELEX for Theranostics

Springer

Editors
Weihong Tan
Molecular Science and Biomedicine
Laboratory, State Key Laboratory for
Chemo/Bio-Sensing and Chemometrics
College of Chemistry and Chemical
Engineering
Hunan University
Changsha
China

and

Department of Chemistry
University of Florida
Gainesville, FL
USA

Xiaohong Fang
Institute of Chemistry
Chinese Academy of Sciences
Beijing
China

ISBN 978-3-662-46225-6 ISBN 978-3-662-46226-3 (eBook)
DOI 10.1007/978-3-662-46226-3

Library of Congress Control Number: 2015931245

Springer Heidelberg New York Dordrecht London

Printed on acid-free paper

Springer-Verlag GmbH Berlin Heidelberg is part of Springer Science+Business Media (www.springer.com)

Foreword

One of the great disappointments in chemistry over the past half-century has been the failure of theory to allow chemists to design molecules that bind specifically in aqueous solution to other molecules. This is, of course, the "medicinal chemistry problem"; a classical pharmaceutical is simply a molecule that binds to a protein target with a therapeutically interesting affinity, say a dissociation constant of less than one nanomolar. While heuristic processes are available to sort through hundreds of lead molecules to get dozens of hits that might generate single drug candidates ready for clinical trials, these rely on only broad theoretical concepts and, more frequently, chemical intuition, rarely on constructively detailed design. Even the three-dimensional molecular models for protein target that are now often routine thanks to modern crystallography have not delivered a definitive solution to this problem. The complexities of molecular interactions as well as the challenges of modeling the solvent in which they must occur continue to defeat the largest computers and the best theory.

The inability of theory to support explicit molecular design stands in stark contrast to the ability of natural biology to deliver molecules that bind other molecules, often with exquisite specificity and enormous affinity. Natural biology does not, of course, exploit explicit design. Rather, the binding molecules that nature delivers come from random variation followed by natural selection, where specifically tight binding enhances the fitness of the host organism. The binding molecules are often proteins and, in the case of antibodies, a protein scaffold that has evolved to support random variation in a binding pocket. Here, natural selection for tightly binding antibodies occurs within a single organism. However, a primary antibody library of perhaps 100 million species is sufficient, following mutation, to generate binders with sub-nanomolar affinities, more than enough to support fitness.

It was against this backdrop of theoretical disappointment that in the late 1980s, synthetic biologists decided to try to do laboratory in vitro evolution (LIVE). Here, nucleic acids, not proteins, were to provide the framework from which selective binding molecules were to be delivered "on demand".

As Jack Szostak, one of the developers of this technology was later to write, it was "an idea whose time had come". Not long before, Thomas Cech, Sidney

Altman, and others had found specific examples where natural biology used RNA molecules to catalyze reactions under physiological conditions. A number of these were involved in the processing of RNA molecules that were used by the ribosome to biosynthesize proteins. The ribosome itself was suspected to be, and later shown to be, a catalytic RNA molecule. Further, an analysis of the commonalities of organisms all cross Earth suggested that we had all descended from an "RNA world", a biosphere where the only genetically encoded biological catalysts were themselves RNA molecules. Indeed, some had suggested that the RNA world had a sufficient number of RNA catalysts to support a complex metabolism.

If libraries of RNA could lead to catalytic RNA molecules on demand, surely (it was thought) that they could solve a simpler problem: creating binding RNA molecules on demand. Accordingly, Larry Gold, Andrew Ellington, and Jack Szostak himself undertook to develop the technology that would create binding molecules starting with RNA libraries. Gerald Joyce and others then followed with efforts to do the same thing where DNA was the matrix.

In either case, perhaps 100 trillion different DNA or RNA (collectively xNA) species were synthesized in a library. The library was then presented to a target receptor, in an experimental architecture that allowed the receptor to extract from these libraries specific binding xNA species. Then, the special ability of nucleic acids to direct their own replication would allow amplification to follow. A few binding molecules would have descendants by the polymerase chain reaction. Perhaps with some mutation, laboratory selection and evolution would produce higher affinity binding molecules by a process analogous to the maturation of antibody affinity. Perhaps xNA "aptamers" (as they came to be called) could have an affinity that would rival the affinity of antibodies.

Of course, this was easier said than done, and a rich literature emerged in the following quarter century attempting to achieve this goal. Much of this literature is represented by the chapters in this book. However, these chapters take the next steps in many dimensions. For example, rather than aptamers that bind to simple protein or small molecule targets, the practitioners who contribute to this volume have included cells as the major targets for binding molecules on demand. The field of "Cell SELEX" is today exploding.

This book is focused on cell-targeted selection, and is edited by the people who first made it work convincingly. In this respect, it has the character of a monograph, with the editors being the co-authors of many chapters, and with still other chapters being written by those who were trained in the editor's laboratories.

Some of the unique features of this book include its description of the cell-SELEX process itself, with potential applications in molecular medicine being linked in a logical and coherent way. This reflects the design of the book chapters by the editors to allow individual authors to make contributions that blend coherently with the other contributions. Thus, the product contrasts with many edited books where each set of authors has written a self-standing chapter that need not blend with the other chapters.

In the chapters on medical applications, the visionary question is addressed: How should we *use* cell-targeted aptamers? Binding is often insufficient to meet a

particular biomedical goal. One often also wants to capture, signal, or create downstream action. This book has numerous chapters that meet this challenge, including labeling, immobilization, and signaling that actually use the binding molecules created "on demand". The book contains individual chapters on each.

My own contributions to this field have been minimal. In December 1985, just before I moved my laboratory to Switzerland to pursue these goals, I had dinner with Jack Szostak, who told me of his plans to do directed evolution of functional RNA libraries. My comment to Jack was based on a chemist's perception. I pointed out to Jack that unlike proteins, which have a rich collection of functional groups, nucleic acids have very few of the moieties that are needed to do catalysis or binding. Further, with only four nucleotides, xNA as delivered to us by prebiotic chemistry and subsequent evolution, has too few folding motifs, too much conformational ambiguity, and too little structural diversity to have any hope of rivaling antibodies as a matrix to support binding molecules on demand.

However, I explained that evening to Jack, there was a solution to this problem, recorded in a witnessed notebook on November 14. All one needed to do was rearrange the hydrogen bonding moieties on the nucleobases to give different hydrogen bonding patterns. If one did so, one could create 12 different nucleotides that should be able to form six independently replicable nucleobase pairs. Some of these could carry functional groups similar to those found on proteins. In short, this was the invention of a single biopolymer that had the replicability of nucleic acids and the functional group diversity of proteins.

Jack's response was prescient. "Steve," I remember him saying, "it will take you 10 years to make these molecules and another 10 years to get polymerases to even accept them" in a PCR reaction. He was approximately correct. Only last year were we finally able to do LIVE with an AEGIS alphabet.

Nevertheless, I am delighted to see a chapter by Liqin Zhang in this volume, showing the first examples where an artificially expanded genetic system has been used to create binding molecules on demand. Catalysts are now following, and the deficiencies of the Darwinian system presented to us by nature might now be solved by molecular design, not explicitly for every specific target-receptor interaction, but rather by the design of a system that is more evolvable and thus better able to create functional species.

Steven A. Benner
Foundation for Applied Molecular Evolution and
The Westheimer Institute for Science and Technology
Gainesville, FL

Contents

Contributors

Naznin Ara Department of Chemistry, Lehman College-City University of New York, Bronx, NY, USA

Tao Bing Beijing National Laboratory for Molecular Sciences, Key Laboratory of Analytical Chemistry for Living Biosystems, Institute of Chemistry, Chinese Academy of Sciences, Beijing, People's Republic of China

Tao Chen Genentech Inc., South San Francisco, CA, USA

Xiaohong Fang Beijing National Laboratory for Molecular Sciences, Key Laboratory of Molecular Nanostructure and Nanotechnology, Institute of Chemistry, Chinese Academy of Sciences, Beijing, China

Da Han Intel Corporation, Hillsboro, OR, USA; Departments of Chemistry Physiology and Functional Genomics, Center for Research at the Bio/Nano Interface, Shands Cancer Center, UF Genetics Institute and McKnight Brain Institute, University of Florida, Gainesville, FL, USA

Yue He Department of Biomedical Engineering and Environmental Sciences, National Tsing Hua University, Hsinchu, Taiwan, ROC

Yu-Fen Huang Department of Biomedical Engineering and Environmental Sciences, National Tsing Hua University, Hsinchu, Taiwan, ROC

Chunmei Li Key Laboratory of Luminescent and Real-Time Analytical Chemistry, Ministry of Education, College of Pharmaceutical Sciences, Southwest University, Chongqing, China; Beijing National Laboratory for Molecular Sciences, Institute of Chemistry, Chinese Academy of Sciences, Beijing, China

Juan Li The Key Lab of Analysis and Detection Technology for Food Safety of the MOE, College of Chemistry, Fuzhou University, Fuzhou, China

Haipeng Liu Department of Chemical Engineering and Materials Science, Wayne State University, Detroit, MI, USA

Chun-Hua Lu The Key Lab of Analysis and Detection Technology for Food Safety of the MOE, College of Chemistry, Fuzhou University, Fuzhou, China

Prabodhika Mallikaratchy Department of Chemistry, Lehman College-City University of New York, Bronx, NY, USA

Lei Mei Departments of Chemistry, Physiology and Functional Genomics, Center for Research at the Bio/Nano Interface, Shands Cancer Center, UF Genetics Institute and McKnight Brain Institute, University of Florida, Gainesville, FL, USA

Hongmin Meng Departments of Chemistry, Physiology and Functional Genomics, Center for Research at the Bio/Nano Interface, Shands Cancer Center, UF Genetics Institute and McKnight Brain Institute, University of Florida, Gainesville, FL, USA

Joseph Phillips Roche Molecular Systems, Marlborough, MA, USA

Xiu-Juan Qi The Key Lab of Analysis and Detection Technology for Food Safety of the MOE, College of Chemistry, Fuzhou University, Fuzhou, China

Liping Qiu Molecular Sciences and Biomedicine Laboratory, State Key Laboratory for Chemo/Biosensing and Chemometrics, College of Biology and College of Chemistry and Chemical Engineering, Collaborative Innovation Center for Chemistry and Molecular Medicine, Hunan University, Changsha, China; Departments of Chemistry, Physiology and Functional Genomics, Center for Research at the Bio/Nano Interface, Shands Cancer Center, UF Genetics Institute and McKnight Brain Institute, University of Florida, Gainesville, FL, USA

Kwame Sefah Roche Molecular Systems, Marlborough, MA, USA

Dihua Shangguan Beijing National Laboratory for Molecular Sciences, Key Laboratory of Analytical Chemistry for Living Biosystems, Institute of Chemistry, Chinese Academy of Sciences, Beijing, People's Republic of China

Yanling Song Department of Chemical Biology, College of Chemistry and Chemical Engineering, Xiamen University, Xiamen, People's Republic of China

Weihong Tan Molecular Science and Biomedicine Laboratory, State Key Laboratory for Chemo/Bio-Sensing and Chemometrics, College of Chemistry and Chemical Engineering, Hunan University, Changsha, People's Republic of China; Department of Chemistry, University of Florida, Gainesville, FL, USA

Andrea del Valle Department of Biomedical Engineering and Environmental Sciences, National Tsing Hua University, Hsinchu, Taiwan, ROC

Cuichen Wu Department of Chemistry and Department of Physiology and Functional Genomics, Center for Research at Bio/Nano Interface, Shands Cancer Center, UF Genetics Institute and McKnight Brain Institute, University of Florida, Gainesville, FL, USA

Chaoyong Yang Department of Chemical Biology, College of Chemistry and Chemical Engineering, Xiamen University, Xiamen, People's Republic of China

Huang-Hao Yang The Key Lab of Analysis and Detection Technology for Food Safety of the MOE, College of Chemistry, Fuzhou University, Fuzhou, China

Ronghua Yang State Key Laboratory of Chemo/Biosensing and Chemometrics, College of Chemistry and Chemical Engineering, College of Biology, and Collaborative Innovation Center for Chemistry and Molecular Medicine, Hunan University, Changsha, China

Huimin Zhang Department of Chemical Biology, College of Chemistry and Chemical Engineering, Xiamen University, Xiamen, People's Republic of China

Nan Zhang Beijing National Laboratory for Molecular Sciences, Key Laboratory of Analytical Chemistry for Living Biosystems, Institute of Chemistry, Chinese Academy of Sciences, Beijing, People's Republic of China

Liqin Zhang Departments of Chemistry, UF Health Cancer Center, University of Florida, Gainesville, FL, USA

Libo Zhao Key Laboratory of Molecular Nanostructure and Nanotechnology, Institute of Chemistry, Chinese Academy of Sciences, Beijing, China

Jing Zheng State Key Laboratory of Chemo/Biosensing and Chemometrics, College of Chemistry and Chemical Engineering, College of Biology, and Collaborative Innovation Center for Chemistry and Molecular Medicine, Hunan University, Changsha, China

Guizhi Zhu Laboratory of Molecular Imaging and Nanomedicine, National Institute of Biomedical Imaging and Bioengineering, National Institutes of Health, Bethesda, MD, USA

Zhi Zhu Department of Chemical Biology, College of Chemistry and Chemical Engineering, Xiamen University, Xiamen, China

Hasan Zumrut Department of Chemistry, Lehman College-City University of New York, Bronx, NY, USA

Chapter 1
Introduction to Aptamer and Cell-SELEX

Libo Zhao, Weihong Tan and Xiaohong Fang

Abstract Aptamers are functional oligonucleic acids that bind to specific targets with high affinity. They have demonstrated their unique advantages as chemical antibodies in molecular recognition for many applications in biomedicine and biotechnology such as biosensing, bioimaging, and drug. In particular, a recently developed method of live cell-based in vitro selection, termed cell-SELEX, has successfully isolated aptamers without prior knowledge of a cell's molecular signature, making such aptamers promising for applications in molecular medicine. This chapter reviews the evolution of cell-SELEX technology and introduces the content of this book, which surveys the advancements in cell-SELEX DNA aptamer selection, characterization, modification, and application for theranostics.

Keywords Aptamer · DNA/RNA oligonucleotide · Antibody · Cell-SELEX · Theranostics

L. Zhao · X. Fang (✉)
Key Laboratory of Molecular Nanostructure and Nanotechnology,
Institute of Chemistry, Chinese Academy of Sciences, Beijing, China
e-mail: xfang@iccas.ac.cn

W. Tan
College of Biology, College of Chemistry and Chemical Engineering,
Collaborative Innovation Center for Chemistry and Molecular Medicine,
Hunan University, Changsha 410082, China

W. Tan
Departments of Chemistry, University of Florida, Gainesville, FL 32611-7200, USA

W. Tan and X. Fang (eds.), *Aptamers Selected by Cell-SELEX for Theranostics*,
DOI 10.1007/978-3-662-46226-3_1

1.1 Aptamer: Chemical Antibody

Together with proteins, nucleic acids are essential biological macromolecules that encode, store, and transmit genetic information. Recent years have seen the rapid development of many new functions of nucleic acids by their ability to bind specifically to target molecules, as notably demonstrated with the in vitro selection of aptamer molecules in 1990 [1, 2]. Aptamers are single-stranded DNA or RNA molecules generated for the recognition of specific targets. The term is derived from the Latin word *aptus*, meaning "to fit," and the Greek *meros*, meaning "region." The molecular basis for their target recognition is not the well-known Watson–Crick base pairing, but rather, it stems from their unique tertiary folding architecture. Structural characterization by nuclear magnetic resonance (NMR) has revealed that aptamers possess various folding topographies composed of different elements, such as loops, hairpins, stems, and quadruplexes [3, 4]. Each nucleotide in an aptamer sequence either has direct contact with the target molecule as a binding site or with another nucleotide within the sequence to sustain the overall aptameric structure. Thus, through the diversity of their tertiary structures, aptamers are able to bind with a wide range of targets.

In many ways, in vitro-selected aptamers mimic antibodies in terms of their capacity for molecular recognition; hence, the term "chemical antibody" has been applied to this unique DNA/RNA oligonucleotide [5]. In fact, with their high binding affinity and specificity toward target molecules, aptamers basically function like antibodies, but since aptamers are chemicals, they have many advantages over antibodies. First, aptamers are chemically synthesized molecules. Compared to the reproduction of antibodies in animals or cultured cells, the synthesis of aptamers is economical and highly reproducible. Second, while site-specific modification of antibodies is difficult to achieve, the nature of nucleic acid chemistry facilitates the easy and controllable chemical modification of aptamers at different sites with different functional groups to fulfill different diagnostic and therapeutic purposes in molecular medicine. Third, whereas antibodies have to be carefully handled to avoid irreversible denaturation, the conformational changes of aptamers are often reversible, making them possible to restore the original structures after denaturation. Such capacity allows aptamers to tolerate a broad range of conditions, including temperature, pH, or ion concentration, providing, in turn, flexibility for their modification, processing, and storage. Other advantages include small size, lack of immunogenicity, and fast tissue penetration. These chemical properties make aptamers ideal molecular probes for theranostics.

Besides their chemical properties, the test tube in vitro selection of aptamers, known as Systematic Evolution of Ligands by EXponential enrichment (SELEX), also has advantages over the generation of antibodies from cells or animals in its applicability to cytotoxic or less immunogenic molecules [6]. The aptamer selection process can be performed against a wide range of targets, including ions, small molecules, peptides, purified proteins, and even whole live cells. For the past few

decades, the use of live cells as targets for aptamer selection, termed cell-SELEX, has gained popularity. Even though this technology is still in its infancy, progress has been very promising, as detailed below.

1.2 Cell-SELEX: Selection from Specific Target Molecules to Intact Complex Systems

The basic principle of SELEX, as well as cell-SELEX, is in vitro Darwinian selection, which can be traced back to 1967 when Spiegelman et al. noticed the function of RNA replicase in the synthesis of RNA molecules and realized the possibility of mimicking a precellular event outside living cells. They conducted an experiment by mixing an RNA from bacteriophage Qβ genome, Qβ's RNA replicase, and free nucleotides in the buffer solution to start RNA replication [7, 8]. The sequence involved in the interaction with the replicase is the only indispensable section for this in vitro RNA replication. Under the selective pressure introduced by reducing the incubation time for each replication, the progression to shorter RNA sequence was observed. This result confirmed the deletion of sequences that did not bind to replicase during the selection, indicating Darwin's theory of natural section is achievable in the test tube. However, in the absence of associated techniques, such as chemical synthesis of DNA or RNA chains consisting of randomized sequences, the idea of isolating functional oligonucleotide molecules, such as aptamers, through in vitro selection remained in the conceptual stage.

The first SELEX experiments for aptamer selection were demonstrated in two independent reports published in 1990 [1, 2]. In one report, Tuerk and Gold constructed a ssRNA pool containing about 65,000 different sequences by randomly mutating the eight-base region of an RNA that can interact with T4 DNA polymerase [1, 2]. This RNA pool flanked by predefined 5′ and 3′ ends as primers was then subjected to an in vitro evolution process in the presence of T4 DNA polymerase. Sequences that bound to T4 DNA polymerase were further isolated for PCR amplification. Resultant sequences were then used as the RNA pool for next run of selection. After multiple runs of selection, those ssRNA sequences with high affinity against the target protein became dominant. Eventually, they were able to produce two RNA sequences, wild-type T4, and another mutant sequence with four mutant nucleotides, which exhibited equivalent binding affinity to T4 DNA polymerase.

Meanwhile, to investigate the possibility that a given random sequence might fold into a desired three-dimensional structure able to meet ligand-specific or catalysis-specific requirements, Ellington and Szostak started with the chemical synthesis of a large RNA pool containing 10^{13} different sequences [2]. The library was then employed for in vitro selection against organic dyes using an approach similar to that in the Gold's report [1]. After multiple cycles of selection, a subpopulation of RNA molecules able to bind specific organic dyes was isolated from

the pool. According to their estimation, roughly one out of 10^{10} random RNA sequences could fold into the desired structure and thus meet the specifications of a target-specific ligand. Two years later, they also realized DNA aptamer selection by SELEX with a DNA library [9].

Since then, aptamers have been generated for a number of targets, including metal ions, small molecules, and purified proteins. Among all these targets, purified proteins have attracted the most attention because protein targets may also be aptamer-mediated therapeutic targets. For example, aptamer NX1838, also known as Macugen, is an antagonist of vascular endothelial growth factor (VEGF), and it was approved for the treatment of neovascular (wet) age-related macular degeneration (AMD) by the US FDA in 2004 [10]. Even with no therapeutic effect by themselves, aptamers can still be used for targeted therapy by coupling them with cytotoxic reagents or drugs [11].

However, while the binding of aptamers to purified proteins may work well in vitro, the same results may not be achieved in vivo. For example, to develop aptamers targeting brain tumors, Liu et al. performed RNA SELEX against histidine-tagged epidermal growth factor receptor variant III (EGFRvIII) ectodomain, which was expressed and purified using an *Escherichia coli* system [12]. The resultant sequence, E21, had high affinity with a K_d of 33 nM, but further experimentation showed that this aptamer could not bind with EGFRvIII expressed in eukaryotic cells. In the absence of post-translational modifications, it is likely that the generated aptamer failed to interact with the full-length EGFRvIII in its natural state. Moreover, even using protein expressed in a eukaryotic system for SELEX, conformational changes during purification, especially for membrane proteins, is a potential problem.

The emergence of cell-SELEX technology solved such problems by directly performing aptamer selection against live cells. In this way, the cellular proteins retain their native conformations. More importantly, cell-SELEX enables the isolation of cell-targeting aptamers without prior knowledge of a cell's molecular signature, e.g., the number and type of proteins on the cell membrane surface. As a demonstration of this phenomenon in 2006, the Tan group [13] used the CCRF-CEM cell line as the target and a B cell line, Ramos (human Burkitt's lymphoma), as negative control, to generate aptamers specific for T-cell acute lymphoblastic leukemia (T-ALL) using cell-SELEX. After about 20 rounds of selection, a panel of 10 aptamers with calculated equilibrium dissociation constants in the nM-to-pM range was obtained. Even though the target molecules of those aptamers were unknown at that time, results showed that the aptamers displayed high binding affinities to CCRF-CEM, but not Ramos, even in clinical samples.

1.3 Aptamers Generated by Cell-SELEX

Table 1.1 summarizes a list of cell-SELEX experiments thus far reported for the selection of aptamers against mammalian cells. Both suspension (e.g., leukemia) and adherent (e.g., epithelial) cells can be found in this table. Further inspection

Table 1.1 Cell-SELEX against mammal cells for aptamer selection

Source	Target cell		Binding protein	Best K_d (nm) of aptamer	References
Leukemia	T-ALL	CEM	PTK7	0.8 ± 0.09	[23, 13]
	B-ALL	Ramos		0.76 ± 0.13	[24]
		Toledo			[41]
	AML	NB4	Siglec-5	~2.77	[42]
		HL-60		5.4 ± 1.6	[25]
Brain		U251	Tenascin-C	104	[14, 43]
	Glioblastoma cell	U118-MG		19 ± 8	[26]
	Glioblastoma multiforme	A-172		61.82 ± 6.37	[27]
	Primary glioblastoma	EGFR vIII over expressed U87	EGFR vIII	0.62 ± 0.04	[15]
Lung	NSCLC	A549		28.2 ± 5.5	[28]
	NSCLC	Vaccinia virus-infected A549		2.7 ± 6.2	[21]
	Lung adenocarcinoma	H23		45 ± 5	[29]
	SCLC	NCI-H69		~38	[30]
		SBC3			[31]
Colon	Colorectal cancer	DLD-1		32.1 ± 3.4	[32]
		HCT 116		3.9 ± 0.4	[32]
	Mouse colon carcinoma	CT26 (HCV E2 positive)	HCV envelope glycoprotein E2	1.05 ± 0.4	[16]
Ovary	Ovarian clear cell adenocarcinoma	TOV-21G		0.25 ± 0.08	[33]
	Ovarian serous adenocarcinoma	CAOV-3		39 ± 20	[33]
Cervix	Cervix adenocarcinoma	HPV-transformed Hela		1.6 ± 0.4	[22]
Breast	Breast cancer	MCF-10AT1			[34]
	Metastatic breast cancer	MDA-MB-231		2.6 ± 1.2	[35]
	Breast cancer	N202.1A	HER2	45.8	[17]
Liver	Hepatocellular carcinoma	BNL 1ME A.7R.1		4.51 ± 0.39	[18]
	Metastatic hepatocellular carcinoma	HCCLM9		167.3 ± 30.2	[19]
Pancreas	Pancreatic carcinoma	Panc-1 and Capan-1	(ALPPL-2)	22.5	[36]
Prostate	Cancer stem cell	DU145 (E-cad positive)		2.2 ± 0.8	[37]
	Prostate cancer	PC3		73.59 ± 11.01	[38]
Adipose tissue	Mature adipocytes	3T3-L1		17.8 ± 5.1	[44]
Adrenal gland	Rat pheochromocytoma	PC12/MEN 2A	RET RTK	35 ± 3	[20]
Mouse embryo	Mouse embryonic Stem cell	CCE			[45]
Lymphoblastoma	Human Burkitt's lymphoma	BJAB	c-kit	12.21	[46]

reveals that the target cells are derived from a variety of organs or tissues, including, for example, brain, lung, colon, and ovary, indicating the universality of the cell-SELEX approach, irrespective of species, tissue origins, or culture conditions.

When complex targets like living cells are used directly for SELEX, simultaneous selections toward multiple individual molecular components are likely to take place. As we know, the live cell membrane is composed of many components shared among different cell types. Therefore, performing exponential enrichment through SELEX could lead to the selection of targets against undesired proteins. To prevent this, cell-SELEX uses an additional counterselection with control cells, allowing the selection of aptamers based on the cellular differences between target and control cells through a comparative strategy. Thus, as shown in Table 1.1, aptamers generated from cell-SELEX can be classified into three types:

1. Aptamers selected for a predefined target
   When the target protein is already known, a strategy termed predefined cell-SELEX is usually applied [14–20]. To construct known cellular differences, the protein of interest can be expressed on positive (target) cells. Their parental cells, which do not express the same protein, will act as mock control and will be employed for counterselection. In this way, the target protein can be differentially expressed and maintained in its native states during selection. Using this approach, Cerchia et al. successfully developed nuclease-resistant aptamers capable of recognizing human receptor tyrosine kinase RET [20]. Following a similar approach, Chen et al. produced aptamer ZE2 that can selectively bind to HCV envelope surface glycoprotein E2 [16].
2. Aptamers selected for induced targets
   Molecular changes occur in cells responding to external stimuli, such as toxic chemicals, bacteria, and viruses [21, 22]. Taking advantage of the ability of cell-SELEX aptamer to differentiate minor cellular differences, it is possible to select aptamers for the molecular-level study of cellular response to the applied stimulus. For example, Tang et al. proposed a method of selecting aptamers capable of binding virus-infected cells [21]. In this study, vaccinia virus (VACV)-infected A549 cells were used as positive target, while normal A549 cells were used for counterselection. This step resulted in a panel of aptamers able to specifically recognize VACV-infected cell lines whose target is most likely a viral protein found on the cell surface.
3. Aptamers selected for unknown target molecules
   Intrinsic cellular differences exist between any two given types of cells. Through the comparative strategy proposed by Tan group, cell-SELEX can be performed and eventually generate aptamers in the absence of prior knowledge of the intrinsic difference between the two cell types [13, 23–38]. Cell-SELEX is so powerful that it can even generate aptamers able to differentiate subpopulations of the same cell line [37]. This is particularly useful for the development of molecular probes to identify and subcategorize pathological cells with unknown biomarkers.

Modern molecular medicine strives to understand the molecular basis of diseases and translate this information into theranostic strategies. Up to now, our ability to understand many complex diseases at the molecular level, such as cancer, has been limited by the lack of tools able to identify and characterize distinct molecular features of the disease state. For example, effective clinical cancer biomarkers are very limited. However, with the technological advancement brought by cell-SELEX, it is now possible to identify the molecular differences between normal and tumor cells, or discriminate among different types of cancer cells at different stages and even among different patients. This offers a new approach for biomarker discovery, as the binding proteins of specific cell-targeting aptamers can be extracted and identified by mass spectroscopy for further validation.

In addition to biomarker discovery, aptamers generated via cell-SELEX hold promise for diverse biomedical applications, such as the detection, imaging, profiling, and targeting of diseased cells [5, 39, 40]. Research efforts in this field have resulted in important progress in the selection and application of cell-SELEX aptamers for theranostics.

1.4 Chapter Summary: From Aptamer Selection to Application

This book focuses on the use of cell-SELEX-selected DNA aptamers for applications in molecular medicine generally, and theranostics specifically. Chapters will be devoted to aptamer selection and characterization, aptamer modification for enhanced functionality, and aptamer–nanomaterials bioconjugates for biomedical applications, in particular cancer theranostics.

The first step in aptamer research involves screening and validating aptamers with high affinity and specificity. Accordingly, Chaps. 2–4 will focus on aptamer selection and characterization. In Chap. 2, Shangguan et al. introduce the process of cell-SELEX. Besides a detailed introduction to the selection protocol, including new methods to improve selection efficiency, key considerations and challenges in cell-SELEX are discussed as a practical reference for those new to this technology.

SELEX has successfully produced many different aptamer ligands from the starting pool of DNA/RNA library. However, natural nucleic acids are built on four different nucleotides that carry only a few key functional groups commonly found in proteins. One feasible strategy to further improve SELEX is incorporating unnatural nucleotides to obtain a DNA/RNA library with higher information density and more functional groups for SELEX. In Chap. 3, Zhang discusses the emergence of unnatural bases with different chemical modifications and their application in SELEX, particularly the example of selecting the cancer cell-targeting aptamers using a new expanded genetic system with six different kinds of nucleotides.

After SELEX screening, thorough characterization of the enriched aptamers is important for subsequent application in either diagnostics or therapeutics. Chap. 4 presents different analytical methods applied to the cell-specific aptamers to measure their binding affinity, binding density, binding sites, and binding strength.

Once the affinity and specificity of the selected aptamers have been validated, the next consideration is functionalization through chemical modification to improve their performance in complex physiological environments. Accordingly, Chaps. 5–8 are focused on molecular engineering to accomplish this goal, including chemical modification of aptamers themselves and the integration of aptamers with other materials.

Chapters 5 and 6 describe several new strategies of molecular engineering inspired by DNA nanotechnology, as well as recent developments in nanomaterials and nanodevices. These strategies lead to the construction of aptamer-based nanoassemblies to increase nuclease resistance and biostability and multivalent aptamers to enhance affinity and selectivity. The Tan group has also developed switchable aptamers and logical aptamer systems for intelligent sensing and therapy, aptamer-incorporated DNA dendrimers as efficient nanocarriers for intracellular sensing, and aptamer-tethered nanotrains for targeted delivery of reagents for cancer theranostics.

Chapters 7 and 8, respectively, discuss two new types of materials to improve aptamer function, nucleic acid-based amphiphiles, and hydrogels. In Chap. 7, Liu focuses on nucleic acid-based amphiphiles, which consist of nucleic acids covalently linked to lipophilic lipid molecules. Combining the functions and properties of both hydrophilic nucleic acids and hydrophobic lipid tails, these functional amphiphiles have been developed to transport therapeutic drugs, penetrate cell membranes, and interact with endogenous proteins. Their synthesis, self-assembly properties, and biomedical applications are described. In Chap. 8, Lu et al. discuss hydrogels, which are water-retainable materials that have been widely used in bioanalysis and biomedicine owing to their physical and chemical properties that change upon external stimulations. The latest developments in target-responsive hydrogel engineering, along with many examples of their application in biomedicine and theranostics, are provided.

Having considered aptamer selection and functionalization, Chaps. 9–13 turn to a survey of advancements in aptamer-mediated biomedical applications, especially those involving cancer diagnosis and therapy.

Since aptamers can discriminate cellular differences and differentiate among cell subpopulations, as explained above, they are able to selectively capture diseased cells. Thus, in Chap. 9, the use of aptamers in cell sorting and disease profiling is demonstrated. First, aptamer-based microfluidic devices have been successfully developed for the detection of rare circulating tumor cells. Next, since cell-SELEX can produce multiple aptamers targeting different disease-related proteins, aptamer technology can also be employed for disease profiling. Therefore, it is advantageous to use a panel of aptamers to fully define the molecular signature of a specific disease, even though the target proteins of aptamers are unknown.

Chapter 10 discusses the detection of cancer cells using the conjugation of cell-specific aptamers with various nanomaterials, including metallic, silica, and magnetic nanoparticles, nanocrystals, and DNA nanostructures. Such aptamer–nanomaterial conjugates combine the high affinity and specificity of aptamers with the ability of nanomaterials to facilitate the sensing process and amplify the signal of recognition events. This provides a powerful tool for highly sensitive cancer cell detection for early cancer diagnosis.

Chapter 11 aims to illustrate the advantages of aptamers as new probes for molecular imaging, which refers to in vivo characterization and measurement of biological processes at the molecular level. By their small size, aptamers can quickly penetrate tissue, be uptaken by target cells, and be rapidly eliminated from nontarget organs, thus showing high potential for cancer cell-specific in vivo imaging.

The discovery of biomarkers is an important by-product of cell-SELEX technology. Accordingly, the significant progress of aptamer-assisted biomarker discovery is emphasized in Chap. 12 with six examples describing the methods of identifying aptamers against cell-surface biomarkers.

Finally, in Chap. 13, Huang and coworkers discuss the conjugation of cell-specific aptamers with drug molecules and gold or magnetic nanoparticles for cancer treatment to improve efficacy and reduce the side effects commonly seen in traditional chemotherapeutic methods. Conjugation strategies through a variety of chemical reactions or physical interactions are described, and current advances in aptamer-mediated targeted delivery for chemotherapy, photodynamic therapy, photothermal therapy, and combinational therapy are highlighted.

As a closing remark, Chap. 14 discusses the potential and challenges in the clinical and biotechnological utilization of aptamers and the requirements for achieving this significant goal.

In summary, the structure of this book is designed to provide a comprehensive understanding of the emerging field of cell-SELEX aptamers, which should appeal to a broad range of researchers in chemistry, cell and molecular biology, biomedical engineering and medicine, as well as theranostics.

References

1. Tuerk C, Gold L (1990) Systematic evolution of ligands by exponential enrichment: RNA ligands to bacteriophage T4 DNA polymerase. Science 249:505–510
2. Ellington AD, Szostak JW (1990) In vitro selection of RNA molecules that bind specific ligands. Nature 346:818–822
3. Feigon J, Dieckmann T, Smith FW (1996) Aptamer structures from A to zeta. Chem Biol 3:611–617
4. Patel DJ, Suri AK, Jiang F, Jiang L, Fan P, Kumar RA, Nonin S (1997) Structure, recognition and adaptive binding in RNA aptamer complexes. J Mol Biol 272:645–664
5. Fang XH, Tan WH (2010) Aptamers generated from cell-SELEX for molecular medicine: a chemical biology approach. Acc Chem Res 43:48–57

6. Jayasena SD (1999) Aptamers: an emerging class of molecules that rival antibodies in diagnostics. Clin Chem 45:1628–1650
7. Spiegelman S (1971) An approach to the experimental analysis of precellular evolution. Q Rev Biophys 4:213–253
8. Mills DR, Peterson RL, Spiegelman S (1967) An extracellular Darwinian experiment with a self-duplicating nucleic acid molecule. Proc Natl Acad Sci U S A 58:217–224
9. Ellington AD, Szostak JW (1992) Selection in vitro of single-stranded DNA molecules that fold into specific ligand-binding structures. Nature 355:850–852
10. Ng EWM, Shima DT, Calias P, Cunningham ET, Guyer DR, Adamis AP (2006) Pegaptanib, a targeted anti-VEGF aptamer for ocular vascular disease. Nat Rev Drug Discov 5:123–132
11. Dhar S, Gu FX, Langer R, Farokhzad OC, Lippard SJ (2008) Targeted delivery of cisplatin to prostate cancer cells by aptamer functionalized Pt(IV) prodrug-PLGA-PEG nanoparticles. Proc Natl Acad Sci U S A 105:17356–17361
12. Liu YM, Kuan CT, Mi J, Zhang XW, Clary BM, Bigner DD, Sullenger BA (2009) Aptamers selected against the unglycosylated EGFRvIII ectodomain and delivered intracellularly reduce membrane-bound EGFRvIII and induce apoptosis, Biol Chem 390:137–144
13. Shangguan D, Li Y, Tang ZW, Cao ZHC, Chen HW, Mallikaratchy P, Sefah K, Yang CYJ, Tan WH (2006) Aptamers evolved from live cells as effective molecular probes for cancer study. Proc Natl Acad Sci U S A 103:11838–11843
14. Hicke BJ, Marion C, Chang YF, Gould T, Lynott CK, Parma D, Schmidt PG, Warren S (2001) Tenascin-C aptamers are generated using tumor cells and purified protein. J Biol Chem 276:48644–48654
15. Tan Y, Shi YS, Wu XD, Liang HY, Gao YB, Li SJ, Zhang XM, Wang F, Gao TM (2013) DNA aptamers that target human glioblastoma multiforme cells overexpressing epidermal growth factor receptor variant III in vitro. Acta Pharmacol Sin 34:1491–1498
16. Chen F, Hu YL, Li DQ, Chen HD, Zhang XL (2009) CS-SELEX generates high-affinity ssDNA aptamers as molecular probes for hepatitis C virus envelope glycoprotein E2. Plos One 4:e8142. doi:10.1371/journal.pone.0008142
17. Thiel KW, Hernandez LI, Dassie JP, Thiel WH, Liu XY, Stockdale KR, Rothman AM, Hernandez FJ, McNamara JO, Giangrande PH (2012) Delivery of chemo-sensitizing siRNAs to HER2(+)-breast cancer cells using RNA aptamers. Nucleic Acids Res 40:6319–6337
18. Shangguan DH, Meng L, Cao ZHC, Xiao ZY, Fang XH, Li Y, Cardona D, Witek RP, Liu C, Tan WH (2008) Identification of liver cancer-specific aptamers using whole live cells. Anal Chem 80:721–728
19. Wang FB, Rong Y, Fang M, Yuan JP, Peng CW, Liu SP, Li Y (2013) Recognition and capture of metastatic hepatocellular carcinoma cells using aptamer-conjugated quantum dots and magnetic particles. Biomaterials 34:3816–3827
20. Cerchia L, Duconge F, Pestourie C, Boulay J, Aissouni Y, Gombert K, Tavitian B, de Franciscis V, Libri D (2005) Neutralizing aptamers from whole-cell SELEX inhibit the RET receptor tyrosine kinase. PLoS Biol 3:697–704
21. Tang ZW, Parekh P, Turner P, Moyer RW, Tan WH (2009) Generating aptamers for recognition of virus-infected cells. Clin Chem 55:813–822
22. Graham JC, Zarbl H (2012) Use of cell-SELEX to generate DNA aptamers as molecular probes of HPV-associated cervical cancer cells. Plos One **7**:e36103. doi:10.1371/journal.pone.0036103
23. Shangguan D, Cao ZH, Meng L, Mallikaratchy P, Sefah K, Wang H, Li Y, Tan WH (2008) Cell-specific aptamer probes for membrane protein elucidation in cancer cells. J Proteome Res 7:2133–2139
24. Tang ZW, Shangguan D, Wang KM, Shi H, Sefah K, Mallikratchy P, Chen HW, Li Y, Tan WH (2007) Selection of aptamers for molecular recognition and characterization of cancer cells. Anal Chem 79:4900–4907
25. Sefah K, Tang ZW, Shangguan DH, Chen H, Lopez-Colon D, Li Y, Parekh P, Martin J, Meng L, Phillips JA, Kim YM, Tan WH (2009) Molecular recognition of acute myeloid leukemia using aptamers. Leukemia 23:235–244

26. Kang DZ, Wang JJ, Zhang WY, Song YL, Li XL, Zou Y, Zhu MT, Zhu Z, Chen FY, Yang CJ (2012) Selection of DNA aptamers against glioblastoma cells with high affinity and specificity. Plos One **7**:e42731. doi:10.1371/journal.pone.0042731
27. Bayrac AT, Sefah K, Parekh P, Bayrac C, Gulbakan B, Oktem HA, Tan WH (2011) In vitro selection of DNA aptamers to glioblastoma multiforme. ACS Chem Neurosci 2:175–181
28. Zhao ZL, Xu L, Shi XL, Tan WH, Fang XH, Shangguan DH (2009) Recognition of subtype non-small cell lung cancer by DNA aptamers selected from living cells. Analyst 134:1808–1814
29. Jimenez E, Sefah K, Lopez-Colon D, Van Simaeys D, Chen HW, Tockman MS, Tan WH (2012) Generation of lung adenocarcinoma DNA aptamers for cancer studies. Plos One **7**: e46222. doi:10.1371/journal.pone.0046222
30. Chen HW, Medley CD, Sefah K, Shangguan D, Tang ZW, Meng L, Smith JE, Tan WH (2008) Molecular recognition of small-cell lung cancer cells using aptamers. ChemMedChem 3:991–1001
31. Kunii T, Ogura S, Mie M, Kobatake E (2011) Selection of DNA aptamers recognizing small cell lung cancer using living cell-SELEX. Analyst 136:1310–1312
32. Sefah K, Meng L, Lopez-Colon D, Jimenez E, Liu C, Tan WH (2010) DNA aptamers as molecular probes for colorectal cancer study. Plos One 5:e14269. doi:10.1371/journal.pone.0014269
33. Van Simaeys D, Lopez-Colon D, Sefah K, Sutphen R, Jimenez E, Tan WH (2010) Study of the molecular recognition of aptamers selected through ovarian cancer cell-SELEX. Plos One 5:e13770. doi:10.1371/journal.pone.0013770
34. Zhang KJ, Sefah K, Tang LL, Zhao ZL, Zhu GZ, Ye M, Sun WJ, Goodison S, Tan WH (2012) A novel aptamer developed for breast cancer cell internalization. ChemMedChem 7:79–84
35. Li XL, Zhang WY, Liu L, Zhu Z, Ouyang GL, An Y, Zhao CY, Yang CJ (2014) In vitro selection of DNA aptamers for metastatic breast cancer cell recognition and tissue imaging. Anal Chem 86:6596–6603
36. Dua P, Kang HS, Hong SM, Tsao MS, Kim S, Lee DK (2013) Alkaline phosphatase ALPPL-2 is a novel pancreatic carcinoma-associated protein. Cancer Res 73:1934–1945
37. Sefah K, Bae KM, Phillips JA, Siemann DW, Su Z, McClellan S, Vieweg J, Tan WH (2013) Cell-based selection provides novel molecular probes for cancer stem cells. Int J Cancer 132:2578–2588
38. Wang YY, Luo Y, Bing T, Chen Z, Lu MH, Zhang N, Shangguan DH, Gao X (2014) DNA aptamer evolved by cell-SELEX for recognition of prostate cancer. Plos One 9:e100243. doi:10.1371/journal.pone.0100243
39. Tan WH, Donovan MJ, Jiang JH (2013) Aptamers from cell-based selection for bioanalytical applications. Chem Rev 113:2842–2862
40. Shen Q, Xu L, Zhao L, Wu D, Fan Y, Zhou Y, OuYang W-H, Xu X, Zhang Z, Song M, Lee T, Garcia MA, Xiong B, Hou S, Tseng H-R, Fang X (2013) Specific capture and release of circulating tumor cells using aptamer-modified nanosubstrates. Adv Mater 25:2368–2373
41. Shangguan DH, Cao ZHC, Li Y, Tan WH (2007) Aptamers evolved from cultured cancer cells reveal molecular differences of cancer cells in patient samples. Clin Chem 53:1153–1155
42. Yang ML, Jiang GH, Li WJ, Qiu K, Zhang M, Carter CM, Al-Quran SZ, Li Y (2014) Developing aptamer probes for acute myelogenous leukemia detection and surface protein biomarker discovery. J Hematol Oncol 7:5. doi:10.1186/1756-8722-7-5
43. Daniels DA, Chen H, Hicke BJ, Swiderek KM, Gold L (2003) A tenascin-C aptamer identified by tumor cell SELEX: systematic evolution of ligands by exponential enrichment. Proc Natl Acad Sci U S A 100:15416–15421
44. Liu J, Liu HX, Sefah K, Liu B, Pu Y, Van Simaeys D, Tan WH (2012) Selection of aptamers specific for adipose tissue. Plos One **7**:e37789. doi:10.1371/journal.pone.0037789
45. Iwagawa T, Ohuchi SP, Watanabe S, Nakamura Y (2012) Selection of RNA aptamers against mouse embryonic stem cells. Biochimie 94:250–257
46. Meyer S, Maufort JP, Nie J, Stewart R, McIntosh BE, Conti LR, Ahmad KM, Soh HT, Thomson JA (2013) Development of an efficient targeted cell-SELEX procedure for DNA aptamer reagents. Plos One 8:e71798. doi:10.1371/journal.pone.0071798

Chapter 2
Cell-SELEX: Aptamer Selection Against Whole Cells

Dihua Shangguan, Tao Bing and Nan Zhang

Abstract Changes at the molecular level always occur at different stages in diseased cells. The detection of these changes is critical for understanding the molecular mechanisms underlying pathogenesis, as well as accurately diagnosing disease states and monitoring therapeutic modalities. Cell-SELEX is a foundational tool used to select probes able to recognize molecular signatures on the surface of diseased cells. This technology has been increasingly used in biomarker discovery, as well as cancer diagnosis and therapy. In this chapter, the whole cell-SELEX process is described, including aptamer selection, identification, and validation. In addition, we will explore the challenges and prospects for cell-SELEX now and in the coming years. It is anticipated that this chapter will guide readers toward a better understanding of the working principles underlying the cell-SELEX technology and serve as a practical reference for bench scientists engaged in cell and molecular biology.

Keywords Aptamers · Cell-SELEX · Molecular probes · Biomarkers · Molecular recognition

2.1 Introduction

Revealing the molecular mechanisms that trigger changes in biological cells is the concern of scientists across a broad spectrum of disciplines. However, the detection of such changes and, hence, their understanding is primarily thwarted by the lack of tools able to recognize features of cellular architecture at the molecular level.

D. Shangguan (✉) · T. Bing · N. Zhang
Beijing National Laboratory for Molecular Sciences, Key Laboratory of Analytical Chemistry for Living Biosystems, Institute of Chemistry, Chinese Academy of Sciences, 100190 Beijing, People's Republic of China
e-mail: sgdh@iccas.ac.cn

W. Tan and X. Fang (eds.), *Aptamers Selected by Cell-SELEX for Theranostics*,
DOI 10.1007/978-3-662-46226-3_2

For cancer diagnosis, pathologists commonly use morphological evidence as a basis for diagnosis, such anatomical features identified through the use of microscopy, for example, cannot reveal changes, including mass-density fluctuations, at the molecular level, even though such data could be critical to the diagnosis of early stage cancer. Indeed, cancer diagnosis based on data collected through the use of proteomic technologies provide the link between genes, proteins, and disease. Current technologies do not provide for the detection of a cancer cell's particular molecular signatures, as most methodologies rely on known biomarkers for the development of corresponding probes. However, the number of biomarkers that have thus far been identified and validated is too small to clearly identify even one particular cancer. Besides cancers, the lack of effective probes and biomarkers is also the challenge of the molecular diagnosis of many other diseases. For example, the infectious diseases are extremely widespread all over the world. Because few biomarkers are currently known and available for effective detection of viruses, bacteria, and fungi, as well as infected cells; the diagnosis of infectious agents is cumbersome. Therefore, new technologies that can be applied to the discovery of unknown molecular features of diseased cells and pathogens are in demand.

Aptamers are single-stranded DNA (ss-DNA) or RNA oligonucleotides, which have the ability to bind to other molecules with high affinity and specificity. Compared with antibodies, aptamers have a unique repertoire of merits, including, for example, ease of chemical synthesis, high chemical stability, low molecular weight, lack of immunogenicity, and ease of modification and manipulation [1]. These characteristics make aptamers good candidates as effective probes for the recognition of molecular signatures and as target cell-specific ligands for therapeutic purposes. Aptamers are evolved from a random oligonucleotide library by repetitive binding of the oligonucleotides to target molecules by a process known as Systematic Evolution of Ligands by EXponential enrichment (SELEX) [2, 3]. In the early stage of aptamer development, aptamers were generated against simple targets, such as small molecules and purified proteins [4]. From 2001 to 2003, aptamer selection against complex targets, such as red blood cell membranes [5] and whole cells [6–8], was demonstrated. However, at that time, the application of aptamers toward cancer detection was limited by the absence of aptamers able to bind target cancer cells, or, more specifically, target proteins on the cell surface.

By 2003, only a few cancer biomarkers had been identified, and there were either known biomarkers, were very expensive, or were not commercially available. Therefore, Tan group at University of Florida conceived of the idea of generating specific aptamers by using whole cancer cells as targets. Differences at the molecular level between any two given cell types, such as normal versus cancer cells, or different types of cancer cells, represent the molecular signatures of a specific type of cancer cells. Therefore, the ability to obtain aptamers able to distinguish one type of cancer cell from another by the identification of particular

molecular signatures would constitute aptamers also able to be used as molecular probes for cancer identification. This approach, now known as cell-based SELEX or cell-SELEX, conveniently circumvents the limitations previously noted, and a cell-SELEX protocol was developed using the human acute lymphoblastic leukemia cell line, CCRF-CEM (T cell line), as target cells, as well as human diffuse large cell lymphoma cell line, Ramos (B-cell line), as control cells. This resulted in a panel of aptamers that could specifically bind target cancer cells [9], including one able to bind to a membrane protein on the surface of CCRF-CEM cells, protein tyrosine kinase 7, which has been identified as a biomarker for leukemia [10, 11]. Since then, many aptamers have been generated by cell-SELEX [12–22], their targets are ranged from cancer cells, virus-infected cells to bacteria. These aptamers have shown their utility in cell capture, detection and imaging, even in vivo cancer imaging [1].

Thus, cell-SELEX offers the following advantages:

1. Prior knowledge about the molecular features of target cells is unnecessary since the cell-SELEX specifically generates aptamers that can recognize and differentiate the molecular signatures found on a range of abnormal cell types.
2. Countless molecules, especially proteins, are found on the cell surface, and the molecular differences between two cells typically relate to a series of molecules. In cell-SELEX, each of these molecules is a potential target. A successful selection will therefore generate a panel of aptamers for many different targets, and, as a result, such panel of aptamer probes will provide more data for accurate disease diagnosis and, hence, new opportunities for personalized medicine.
3. Aptamers bind to the native state of target molecules, making it possible for aptamer probes, through ligand binding, to directly recognize their cognate target, creating, in turn, a true molecular profile of diseased cells. In addition, the target molecules are naturally anchored on cell surface, so that the bound aptamers can be easily partitioned from the unbound oligonucleotides by centrifuge or wash (for adherent cells) during the SELEX process; it is unnecessary to purify the target molecules and fix them on solid supports.
4. Providing the opportunity to discover new biomarker. Pathological or physiological changes are complex processes that involve many molecular-level changes on cells. Many of these changes are unknown. Cell-SELEX provides the opportunity to generate aptamers that bind to unknown biomarkers. Then, the obtained aptamers can be used, through affinity separation, to purify and identify their targets. These targets have the potential to be new biomarkers.

Based on these advantages, nowadays cell-SELEX technology has been widely used all over the world and a large number of aptamers specific to a variety of cells have been reported. Nonetheless, the whole cell-SELEX procedure involves

multiple complex steps; and the beginners often fail to obtain desired aptamers. In this chapter, we present an overview for the development of DNA aptamers against different types of mammalian cells (cancer cells as example) using cell-SELEX technology. The discussions mainly focus on the key considerations in each step of cell-SELEX procedure. The challenges and prospects of cell-SELEX are also discussed.

2.2 Overview of Cell-SELEX Procedure

The SELEX strategy was described primarily in 1990 by Gold and Szostak [2, 3], and then it has been modified over the years in different ways [23]. Briefly, the general process of SELEX involves the incubation of the target of interest with an oligonucleotide library (DNA or RNA), separation of the oligonucleotides-target complexes from the unbound sequences, and amplification of the bound sequences by PCR or RT-PCR to obtain an enriched pool for next round of selection. This process is repeated until the pool is highly enriched for sequences that specifically recognize the target. The enriched pool is then cloned into bacteria and sequenced to obtain the individual sequences. Representatives of these sequences are chemically synthesized, labeled with reporters and tested against the target to determine potential aptamer candidates. In this whole procedure, the most critical step is the partition of the target-bound sequences from unbound sequences, especially for the SELEX using purified target molecules; thus, many modified SELEX strategies have been proposed to simplify this step or to enhance the efficiency of partition [23]. Compared with the SELEX for purified target molecules, the partition step of cell-SELEX is relatively simple, because the unbound sequences can be easily removed by centrifuge or wash (for adherent cells). But after obtaining aptamers using cell-SELEX, a target identification step is necessary.

The typical cell-SELEX procedure is shown in Fig. 2.1. The starting point of a cell-SELEX process is the preparation of a synthesized random oligonucleotide library and the growth of cells of interest, which is discussed in details in Sect. 2.3.

The iterative cycles of cell-SELEX process includes the following steps: incubation of target cells with randomized DNA library or the enriched DNA pool; collection of cells bound with oligonucleotides; elution of bound oligonucleotides on target cells; amplification of eluted oligonucleotides and preparation of enriched oligonucleotide pool; and counter selection (also named subtractive selection) using control cells. The counter selection step is strongly recommended to reduce the nonspecifically binding oligonucleotides and the oligonucleotides that bind common surface molecules present on both types of cells, which can increase the specificity of enriched pool to the target cells. After each or several rounds of selection, a binding assay of the enriched pool to target cells and control cells is performed to monitor the progress of aptamer enrichment. In this iterative process, each round of selection is not a simple repeat of the previous round. In order to obtain aptamers with high affinity and specificity, the pressure of selection is

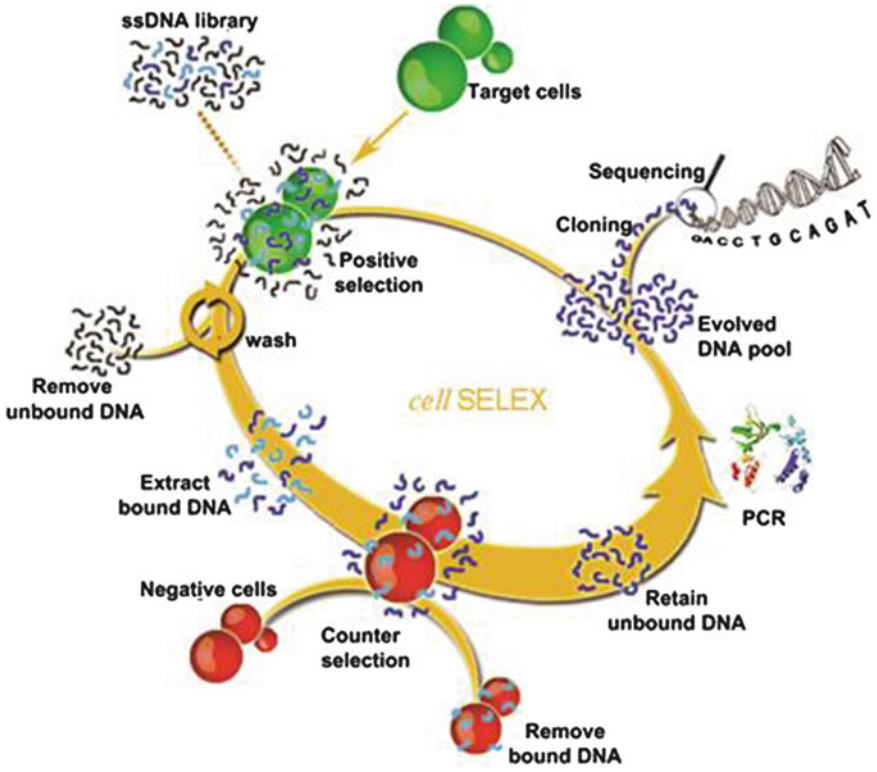

Fig. 2.1 Schematic representation of the cell-SELEX (Reprint with permission from [9], Copyright 2006, National Academy of Sciences, USA)

progressively increased in the course of a SELEX process by modulating the cell number and the binding/washing conditions in later SELEX rounds. For more details concerning the iterative selection process, see Sect. 2.4.

The number of rounds necessary depends on the progress of enrichment (in general 10–20 rounds). If the binding assay shows that the enriched pool has enough affinity and specificity, the PCR products of the last selected pool are cloned and sequenced to obtain the individual sequences. Representative sequences are chosen, synthesized, and applied to binding assays. Finally, the aptamers with high affinity and specificity to target cells can be further optimized and modified for different applications. The details concerning the aptamer identification are shown in Sect. 2.5.

The efficiency of a cell-SELEX depends on many factors, such as the library, the nature and growth state of cells, the selection conditions, the desired target molecules on cell surface, and operation skills. There is no standardized cell-SELEX protocol for any type of cells and purpose. Therefore in the following sections, we do not describe a detailed cell-SELEX protocol (please see our previous paper for

detailed protocol [24]), but give the general principles of each selection step, including library design, cell preparation, choice of selection conditions, enrichment monitoring, and aptamer identification. The key considerations for each step are discussed.

2.3 Preparation of Oligonucleotide Library and Cells

2.3.1 Oligonucleotide Library and Primers

The design and chemical synthesis of a random oligonucleotide library is the start point of any SELEX. This library consists of huge numbers of different ss-DNA sequences that have a central random region (20–80 nt) flanked on either side by constant sequences for primer binding during PCR amplification. For DNA aptamer selection, this library can be directly used for Cell-SELEX. For RNA aptamer selection, the random DNA library has to be converted into a double-stranded DNA (ds-DNA) library by PCR with a sense primer containing the T7 promoter sequence and an antisense primer, and then transformed into a RNA library by T7 RNA polymerase. Since DNA is more stable than RNA, most of cell-SELEX has been performed with DNA oligonucleotide library. In this chapter, we mainly discuss the DNA aptamer selection by cell-SELEX.

Since PCR amplification is an essential step in each selection cycle, a set of DNA sequences including library and primers needs to be prepared before cell-SELEX. An example of primer-library set for cell-SELEX is shown below [9]:

Sense primer: 5′-(dye)-ATACCAGCTTATTCAATT-3′
Antisense primer: 5′-(biotin)-AGATTGCACTTACTATCT-3′
Library: 5′-ATACCAGCTTATTCAATT-N_{52}-AGATAGTAAGTGCAATCT-3′

As shown in above example, the primer sequences and the length of the randomized region are needed to be designed before the library synthesis. The general rules for conventional primer design also apply to primers for cell-SELEX. A good primer pair should result in high PCR amplification efficiency and low nonspecific amplification. For monitoring the progress of selection, the sense primer is labeled at the 5′-end with a fluorescence dye (such as FAM, TMRA, and Cy5). In order to obtain the ss-DNA pool after PCR amplification, the antisense primer is usually labeled with a biotin at the 5′-end, so that the duplex PCR products can adsorbed on the streptavidin-coated matrix, and then the dye-labeled sense strand (aptamer strand) can be separated from the antisense strand by alkaline denaturation. It is worth to remind that the contamination of primers by trace amount of library would severely disrupt the aptamer selection. Thus, synthesis and purification of primers and library should be performed separately.

The length of the randomized region determines the diversity of the library. For cell-SELEX, the length of randomized region is commonly in the range of

20–80 nt. The short libraries are better manageable, cost-effective in chemical synthesis. However, longer randomized regions give the libraries a greater structural complexity, which is important for cell-SELEX because the molecular targets are numerous and unknown. Therefore, a longer random sequence pool may provide better opportunities for the identification of aptamers [23], but too longer random sequence is not necessary.

The amount of synthesized library used for one cell-SELEX is in the range of 20 pmol–20 nmol, which is equivalent to 10^{13}–10^{16} random sequences.

2.3.2 Choice and Maintenance of Cancer Cells

Aptamers have been reported to be generated against various target cells, such as cells highly expressing specific protein of interest [25], a certain type of cancer cells [9], cancer stem cells [17], adipocyte cells [26] virus-infected cells [19, 21], and bacteria [27, 28]. Most of these aptamers are selected by using live cells, except in one case using fixed cells [8], which may due to that the target molecules on live cells are present in their native state. For cancer cell-SELEX, cultured cancer cell lines are usually used. That is because the periods of cell-SELEX are at least 2–3 months; it is hard to obtain enough live cells with stable performance in this long period by primary cell culture.

Although cell-SELEX without counter selection has been reported able to generate aptamers that broadly recognize common cancer biomarkers [12, 29], more specific aptamers for desired cell lines need to be selected by combining a counter selection step. In order to generate aptamers that only recognize the molecular signatures of the target cells, at least one control cell type is used for counter selection to eliminate the sequences that bind to the common molecules present in both types of cells. The choice of target cells and control cells mainly depends on the purpose of the selection and the future applications of aptamers. In general, two closely related cell types are chosen, such as tumor cells and homologous normal cells, differentiated cells and parental cells, drug resistant cancer cells and drug sensitive cancer cells, virus-infected cells and uninfected parental cells, and antibiotic resistant bacterial-strains and antibiotic sensitive bacterial-strains. In the case of aptamer selection for cancer stem cells, the target and control cells were E-cad$^+$ and E-cad$^-$ DU145 cells, respectively, which were isolated by FACS sorting by gating for the top 10 % of E-cad$^+$ cells and the bottom 10 % E-cad$^-$ cells [17].

Cell culture maintenance is very important in cell-SELEX, because improper cell culturing maintenance may influence the aptamer enrichment, and even lead to failure of aptamer selection. For example, overgrowth of cell culture results in higher rates of cell death, which potentially lead to alteration in cell morphology and protein expression, as well as cause collection of a lot of nonspecific oligonucleotide sequences because of the increased membrane permeability of dead cells. The reduction or elimination of dead cells can significantly enhance the

enrichment of selected pool. Also, the change of cell culture condition and cell growth status may result in the changes in expression levels of some target molecules. The viability of adherent monolayer cells may be not a big problem in selection because most dead cells normally float in the medium, and once the medium is removed, relatively healthy cells are obtained. That notwithstanding, cells must not be allowed to overgrow. But for adherent monolayer cells, the density of cells used for each round of selection should keep consistent because the cell-to-cell connections and expression levels of target molecules would be quite different at different cell density.

There are two ways by which adherent monolayer cells can be used for selection: either directly in cultured dish/flask or as dissociated cells. The direct option may offer a better representation of the cells' natural environment. Dissociated cells either by treatment with short-term trypsin treatment or non-enzymatic dissociation buffer or by scraping may result in the change of the surface expression, cell death, and cell rupture.

2.4 Aptamer Selection Against Live Cells

The key principle for a successful SELEX is to keep the specific binding sequences and reduces the nonspecific binding sequences as much as possible during the whole SELEX process. The appropriate selection conditions and selection process are essential to achieve this principle.

2.4.1 Binding Conditions

The selection conditions play an important role in the success of cell-SELEX. These conditions include binding buffer, washing buffer, elution buffer, and binding temperature.

For cell-SELEX, the most essential requirement for buffer condition is to keep the cells intact during the binding and washing steps. Thus, the osmolarity, ion concentrations, and pH value of binding buffer and washing buffer must match those of cells. The commonly used buffers are cell culture media, phosphate buffered saline (PBS), and other buffered salt solution (such as Hank's buffer and Tris-HCl buffer), pH 7.4. In our cases, the washing buffer is PBS plus 4.5 g/L glucose and 5 mM $MgCl_2$. As sequences in initial DNA library or enriched pools may nonspecifically bind to some molecules on cell surface (e.g., electrostatic adsorption), excess other nucleic acid sequences, such as t-RNA, salmon/herring sperm DNA or synthesized oligonucleotides are added to the binding buffer to compete the nonspecifically binding of sequences in library or selected pools. Since the added sequences do not contain the primer binding sites and cannot be amplified by PCR, there is no need to worry about the interference on the selection by these

sequences. In order to reduce the nonspecific sequences that binding to proteins on cell surface and to enhance the utility of aptamers in biological samples or in vivo, albumin (e.g., BSA) or serum is usually added to the binding buffer. Therefore, in our cases, the binding buffer is prepared by adding other nucleic acid sequences (0.1 mg/mL) and bovine serum albumin (BSA, 1 mg/mL) or fetal bovine serum (FBS, 1–10 %) into washing buffer.

The function of elution buffer is to dissociate the potential aptamer sequences from cells. For cell-SELEX, the most commonly used method to recover the sequences binding to target cells is by heating the cell-DNA complex at 95 °C in water or buffer. Compared with other used methods, such as phenol/chloroform extraction, TRIzol extraction and denaturation by 7 M urea, the heating method is simple and efficient. That is because: (i) Elevated temperature will cause denaturing of the cell surface proteins and the folded structure of the DNA, and this will lead to the disruption of the interaction between DNA and protein and the release of DNA from the target protein. (ii) At 95 °C, any DNase that is released after cell disruption at the elevated temperature is inactivated and therefore cannot cause DNA digestion. (iii) After heating, the supernatant containing potential aptamers can be directly used as template for PCR amplification.

The binding temperature depends on the purpose of selection and application of aptamers. In general, 4 °C, room temperature and 37 °C are used in cell-SELEX. However, the higher temperatures such as 37 °C can cause internalization of oligonucleotides into live cells, which may result in the collection of nonspecific sequences because that not all internalizations are caused by the specific binding, such as pinocytosis. In addition, incubation with live cells at 37 °C may increase the probability of DNA digestion by nuclease. Most of our cell-SELEX cases have been performed at 4 °C or on ice. Although the binding affinity of some aptamers selected at 4 °C may decrease at 37 °C, most of the aptamers bind very well at 37 °C [15, 16], especially those with very high affinity. Some of the aptamers generated at 4 °C have been used in various applications at 37 °C [9, 18].

2.4.2 Selection and Counter Selection

As shown in Fig. 2.1, the main body of the cell-SELEX process is the iterative cycles that take most of the time for whole SELEX. Each cycle generally includes steps of target-cell binding, washing, elution, PCR amplification, and enriched pool preparation, as well as a counter selection.

Theoretically, there is only one copy of each sequence in the initial library. Therefore, it is highly possible to lose some of the specific sequences in the first round of selection. When any sequence is lost, it can never be recovered. In order to collect as many specific sequences as possible in the first round of selection, the amount of used target cells should be higher than the subsequent rounds; the incubation time of target cells and initial library should be long enough to let specific sequences have more chance to bind to the target molecules on cells.

In order to avoid loss of specific sequences, the washing strength should be moderate, and the counter selection usually is not performed in the first round. The typical protocol for the first round of selection is as follows: incubate target cells ($1–20 \times 10^6$) with synthesized ss-DNA library (20 pmol–20 nmol, $10^{13}–10^{16}$ random sequences) in 1–5 mL of binding buffer on ice for 0.5–1 h. After incubation, cells are washed with 0.5–1 mL of washing buffer for 1–3 times. Then, the bound sequences are eluted by heating at 95 °C for 5 min in 300 μL of DNase-free water, and all the eluted sequences are directly applied for PCR amplification. Finally, the PCR products are converted to enriched pool for the second round of selection.

From the second round of selection, a counter selection step is usually added into the selection cycle. The counter selection can be carried out before the target-cell binding step [16] or after elution step [9]. In the former case, the selection cycles start with incubation of control cells (10 million or monolayer in a 60 cm^2 dish/T75 flask) with the DNA pool (200 pmol) in binding buffer for 30 min; the supernatant containing unbound sequences is then incubated with target cells, and the other steps from washing to preparation of enriched pool are similar with those described in the first round. In the latter case, the steps before elution are same with those described in the first round. After that, the bound sequences on target cells need to be eluted by heating at 95 °C for 5 min in 300–500 μL of binding buffer, and then incubated with control cells on ice for 1 h. After centrifuge, the supernatant need to be desalted with NAP 5 column (GE Healthcare) and then applied for PCR amplification; and finally, the PCR products are converted to enriched pool for the second round of selection. In order to effectively eliminate the nonspecific sequences, the control cells used for counter selection should be much more than the target cells.

Because after PCR amplification in the first round of selection, the specific sequences in the enriched pool have many copies, the key consideration from the second round is to effectively eliminate the nonspecific binding sequences and weak binding sequences. In order to obtain aptamers with high affinity and specificity, the selection pressure from second round is gradually enhanced by decreasing the amount of the ss-DNA pool (from 200 to 30 pmol), the incubation time for the target-cell binding (from 60 to 10 min), and the target-cell number (from 10 to 0.5 million); and by increasing the number of washes (from 2 to 5), the volume of wash buffer (from 0.5 to 5 mL).

Since cells are grown in suspension or adhesion on a surface, there are some differences in handling the suspension cells and adherent cells during the SELEX process. For suspension cells, the cells bound with DNA sequences are collected by centrifuge in the binding and washing steps. For adherent cells, cells bound with DNA sequences are collected by removing the supernatant with pipette. But after the washing step, the adherent cells need to be scraped off from the bottom of flask or dish, and then cells are collected by centrifuge and applied for elution. Scraping is used to detach cells because it would not affect the binding of aptamers on cell membrane surfaces. The conventional detaching method by trypsin could not be

used because it was demonstrated that trypsin could cleave the target proteins on the cell surface [9, 16].

During the binding and washing steps, strong vortexing/shaking and high-speed centrifuge should be avoided since that can cause cell breakage and may eventually affect selection. When collecting cells bound with DNA sequences in the binding and washing steps, the residue liquid should be removed as much as possible because a small amount of liquid contains a large amount of unbound sequences. Before each round of election, the DNA library or pool needs to be denatured by heating at 95 °C and cooled on ice to obtain folded ss-DNA.

2.4.3 Preparation of Enriched Pool

Compared with other combinatorial chemistry strategy, the most attractive advantage of aptamer selection from nucleic acid library is that nucleic acids can be easily amplified by PCR or in vitro transcription. Unlike the common PCR amplification for a specific template sequence, the DNA library and enriched pool are highly complex. In order to obtain highly efficiency of PCR amplification, an optimization of PCR conditions for library is necessary before SELEX. After PCR amplification of each SELEX cycle, a gel electrophoresis assay is needed to assess the PCR. The PCR contamination should be avoided in the whole SELEX process. The detailed protocol for PCR can be obtained from our previous publication [24].

As the PCR products are ds-DNA, they have to be transformed into a new ss-DNA pool by separating the sense strands from the antisense strands. Several methods have been described in literature for this purpose. Based on our experience, the streptavidin/biotin approach is a very effective way to obtain the sense strand from PCR mixture. The general procedure of streptavidin/biotin approach is as follows: The bound sequences on target cells are amplified by PCR with dye-labeled sense primer and biotin-labeled antisense primers; the PCR products are captured by streptavidin-coated support (such as Sepharose beads and magnetic beads), and then the sense ss-DNA strands are eluted off the beads with 0.1–0.2 M NaOH solution (0.5–1 mL). The eluate is desalted with NAP 5 column (GE Healthcare) and quantified the amount of DNA sequences by absorption at 260 nm. Finally, the desalted solution is dried to obtain the enriched pool for the second round of selection.

2.4.4 Enrichment Monitoring and Selection Procedure Adjustment

The selection cycle is a complex process. It is hard to ensure that the aptamer sequences are enriched in every selection cycle. Therefore, the progress of the

selection is needed to be monitored by binding assay at the end of every cycle or every several cycles. Based on the results of binding assay, the selection procedure can be adjusted. The binding assay of the enriched pool in cell-SELEX usually performed using confocal imaging and flow cytometry.

Flow cytometry assay is the best way to monitor the enrichment progress of cell-SELEX, because this method has high sensitivity, good reproducibility, high degree of statistical precision due to the large number of cells measured, quantitative nature of the analysis, and high speed. For the suspension cells, the binding assay can be carried out by incubation of cells with dye-labeled DNA pool in binding buffer. After washing, cells are applied to flow cytometry assay. For adherent cells, before incubation with selected pool, cells need to be detached and suspended in binding buffer. The cell detachment is performed with non-enzyme cell dissociation solution (including EDTA). Then, the detached cells are gently dispersed with pipette, resuspended in binding buffer and passed through a 40 μm strainer to remove the cell clusters which would block the tube of flow cytometer. Finally, the cells are incubated with selected pool, washed, and applied to flow cytometry assay. The concentration of selected pool for cell binding is set in the range of 0.1–1 μM.

Confocal imaging (or fluorescence microscopy imaging) can provide intuitive information of the DNA binding on cells. After incubation with selected pool and washing, adherent cells can be directly observed when they are attaching on the bottom of the dishes; suspension cells can be detected after dropped on a thin glass slide and covered with a coverslip. Although confocal imaging can show the binding regions of DNA sequences on cells, it is difficult to provide the quantitative information with statistical significance for comparing the binding ability of selected pool from different rounds, thus the results of confocal imaging can be used as a supplement to confirm the binding of selected pool on cells. Usually, the selected pools of the first few rounds have low binding affinity, so that the fluorescence intensity on cells is weak, thus the enrichment of the first few round is hard to be judged by confocal imaging.

In order to estimate the enrichment and specificity of the selected pool, controlled experiments with control sequence (unselected library or non-binding sequence) labeled with the same dye and with control cells must be done. The typical progress of a successful cell-SELEX is shown in Fig. 2.2 [15]. The fluorescence intensity of target cells stained by the selected pools gradually enhances with the increase of selection rounds; and the fluorescence intensity of the control cells does not significantly change with the selection going on. These results indicate the steady progress of the selection and the good specificity of the selected pools to target cells. But in practice, the steady progress and good specificity are not often obtained; if so, the SELEX procedure needs to be adjusted.

Cell-SELEX is a highly complex process; many factors can affect the enrichment of aptamer sequences, such as low sequence diversity of DNA library, contamination of PCR reagent, contamination of eluted sequence from target cells (PCR template) by DNA pool or PCR products from previous round of selection, sequence discrimination in PCR, strong nonspecific binding, low abundance of target molecules on cells, and change of cell states.

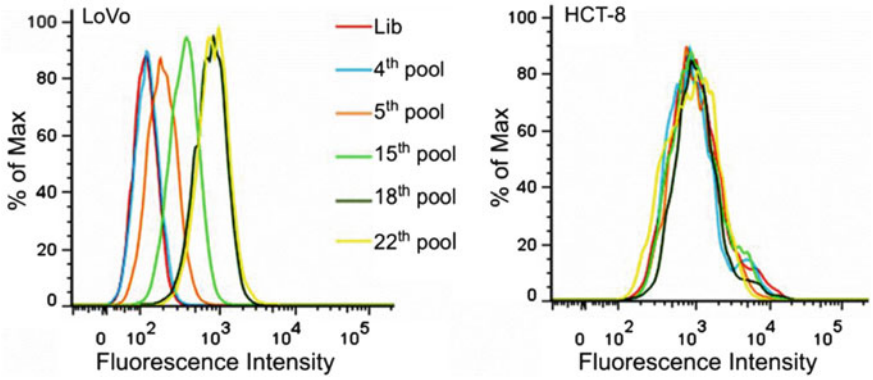

Fig. 2.2 Monitoring of the cell-SELEX progress. Flow cytometry binding assays of the selected pools from the 4th, 5th, 15th, 18th, and 22nd rounds. *Left* LoVo cells (target); *right* HCT-8 cells (control); FITC-labeled ssDNA library as control DNA. Reprinted from Ref. [15], Copyright 2014, with permission from Elsevier

It often happens that no notable progress is observed after many rounds (5–10) of selection. If so, it is necessary to check for any inappropriate operation during the SELEX. If all the selection steps are run correctly, it may be due to too many nonspecific sequences or too few specific sequences in the selected pool. If that is the case, what can we do is to further enhance the selection pressure as describe in the previous section. In one of our previous case [9], we extra added 20 % FBS and 50- to 300-fold molar excess other synthesized DNA in the incubation solution to suppress the nonspecific binding sequences. If all these efforts do not help much, it may be due to the loss of specific sequences in the first round. If so, the SELEX has to be restarted from the first round or even from redesign of the DNA library.

It also often happens that the selected pools bind to both target and control cell lines. It is due to that many of the sequences bound to the common molecules on both cell lines are enriched, and the counter selection is not enough to eliminate these sequences. If that is the case, the counter selection should be strengthened by increasing the number of control cells, reducing the amount of DNA pool, and decreasing the number of target cells. If the enriched sequences bind to highly abundant targets molecules that are present on cell surface of both cell lines, they could not be eliminated only by strengthening the counter selection. In many cases, the counter selection could not completely eliminate the enriched sequences that bind to both cell types. But, if the selected pool bound to target cells stronger than to control cells (Fig. 2.3), aptamers that only bind to target cells may be found in this enriched pool [16].

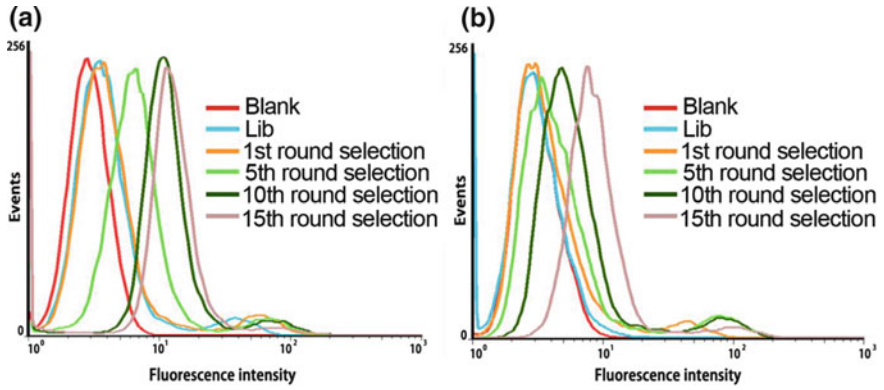

Fig. 2.3 Flow cytometry assay of selected pools binding to target-cell line PC-3 (**a**) and negative control cell line SMMC-7721(**b**), Blank is the background fluorescence of untreated cells. Lib is FITC-labeled DNA library as negative control. Reprinted from Ref. [16]

2.5 Aptamer Identification

2.5.1 Cloning and Sequencing

By iterative cycles of selection and evolution, the complexity of the initial random DNA library is reduced, and aptamer candidates with high affinity and specificity are enriched. The completion of selection is judged by the results of binding assay. The selection circle is finished when the binding assay shows that the selected pool exhibits significant binding ability to target cells, the affinity of the pool cannot be further increased in two or three successive rounds of selection, and the binding of the pool to target cells is higher than that to control cells. Then the final selected pool is PCR-amplified using unmodified primers and cloned into Escherichia coli using the TA cloning kit, and the positive clones (50–100) are sequenced to identify individual aptamer candidates. Since many commercial companies provide cloning and sequencing service and we only need to provide PCR products of the selected pool, the detailed protocol of cloning and sequencing is not described here.

The sequencing result of each clone contains a sense strand or an antisense strand of a potential aptamer. By searching with both primers, the sense and antisense strands of all clones are sought out, and the antisense strands are converted to their complementary strands (sense strands). After removing the primer sequences at both ends, the core sequences (random sequence region) of the potential aptamers are analyzed by sequence alignment using programs, such as Clustal X, clustal omega, and CLUSTAL W. Usually, the sequence alignment groups the potential aptamer sequences in several families (Fig. 2.4). In each family, the sequences are identical or different in only few nucleotide positions. In some cases, special sequence patterns or highly conserved regions are identified among different aptamer groups.

Fig. 2.4 Sample data of sequence alignment. Sequences are grouped in three families. The numbers at the end of sequences indicate the repeat times of this sequence among all the tested clones

New sequencing technology (454 pyrosequencing) together with bioinformatics (MAFFT 6.0, Perl, Jalview 2.4 and ATV 4.0.5 programs) have also been used to analyze the sequences in enriched pools of different rounds of selection in a large scale [29, 30]. The usage of new sequencing technologies with the help of bioinformatics can provide early and detailed information for progress of SELEX by displaying the intensity of selected sequences in the earlier rounds, as well as provide more information for the choice of candidate aptamers.

2.5.2 Aptamer Candidate Screening and Aptamer Validation

The final aptamer pool may be more complex than we thought, not all the sequences are aptamers. We even have met the situation that most of the obtained sequences did not bind to target cells. After known the sequences of the selected pool, it is necessary to seek out the real aptamers in these sequences. There is no need to synthesize all the obtained sequences because the sequences in a family are

almost identical aptamer. Usually, a representative sequence from each family is chosen for validation. Before chemical synthesis, the flanked primer sequences should be added back to the core region, because the primer sequences may directly participate in the target binding or take part in the formation or maintenance of the binding structure. The full-length sequences are synthesized and labeled with fluorescence dye or other reporters. The binding assay of the synthesized sequences is performed by flow cytometry or confocal imaging. Usually, some of the synthesized sequences show high binding ability and specificity to target cells; some of them show binding ability to both target and control cell types; and some of them do not show binding affinity to both cell types. The sequences with high affinity and specificity are identified as aptamers for further characterization.

2.5.3 Characterization of Aptamers

Full-length aptamers generated by SELEX contain 60–120 nucleotides, which include two flanked primer sequences on each end for PCR amplification. Generally, not all the nucleotides are necessary for direct binding to target or for formation and maintenance of binding structure [31, 32]. Longer sequence would result in lower yield and higher cost in chemical synthesis of aptamers. The unnecessary nucleotides would also lead to higher chances of forming various secondary structures, thus destabilizing the target-binding conformation of aptamers. Thus, in practical usage, many selected aptamers are truncated down to a minimal functional sequence after the SELEX process. In general, the truncated sequences possess the same or better binding affinity than the original full-length aptamer. However, the problem here is how to truncate the full-length aptamer sequences or how to determine which nucleotides is unnecessary. RNase footprinting or partial hydrolysis has been used to determine the boundary and binding site of RNA aptamers [33–35]. Partially, fragmenting a full-length aptamer and then selecting the high affinity fragments have been used to determine the minimal sequence of DNA aptamers [36]. In these methods, radioactive labeling has been used to detect the aptamer fragments, and then the predicted potential minimal sequences had to be synthesized to confirm binding capacity.

In our cases, we utilize a relatively easy method to predict the secondary structure of aptamers, as well as the critical sequences for target binding [31, 32]. Secondary structure prediction of the aptamer sequences can provide information about relevant structures for binding [31, 32]. Such prediction is usually carried out by the program mfold [37] (http://www.idtdna.com/unafold/Home/Index), which calculates the possible secondary structures of single-stranded nucleic acids by energy minimizing method. The secondary structure prediction of a sequence often provides many potential structures; a few nucleotides or even single nucleotide change in a sequences can always leads to provide many different predicted structures. The sequences in same family should bind to same target with same secondary structures but different affinity. Therefore, comparing the predicted

structures of sequences in the same family, and even different families, can help to determine the secondary structure for aptamer binding and the binding motif of aptamers [31, 32]. Then, the aptamer sequences can be truncated based on their predicted binding secondary structure and binding motifs. The truncated sequences are synthesized and their binding ability is measured and compared with the original full-length aptamers. The sequence truncation of aptamer may be carried out many times to find out the minimized sequence. Based on the secondary structure and binding motifs, the minimized aptamer sequences can be further optimized to obtain better binding affinity by removing, adding, and/or displacing one or several nucleotides [31, 32, 38–41].

When an optimized aptamer is obtained, its properties need to be further characterized. The properties include dissociation constant (K_d), specificity to many other cell lines, binding sites, tertiary binding structure, molecular target on cells, and interactions with cells (such as cellular internalization [42]), as well as biological activities against cells. The K_d values of an aptamer are usually measured by flow cytometry [9]. It is important to test the *K*d values of aptamers at different temperatures (such as 4, 25, and 37 °C), which would help the subsequent applications of aptamers. The details of cell-specific aptamer characterization and aptamer target identification are discussed in Chaps. 4 and 12.

2.6 Challenges and Perspectives

As discussed above, through cell-SELEX, aptamers that are able to recognize molecular differences on cell membranes can be generated without prior knowledge of their target molecules. These aptamers can be exploited for cell detection, capture, imaging, drug delivery, and biomarker discovery [43–46]. Since its development, cell-SELEX has become an emerging and promising platform for generating large numbers of aptamers against a wide range of cell lines, especially various types of cancer cells. However, although considerable progress has been made, cell-SELEX is still facing many challenges.

First, there is a big gap between theory and practice of cell-SELEX. The whole SELEX process is very complex and like a “black box”; and no one knows exactly at which step the problem occurred when no significant enrichment is observed after many rounds of selection. The sequence discrimination in PCR amplification of the random pools of DNA may greatly hinder the enrichment of aptamer sequences. Additionally, some phenomena are unable to be explained currently; for example, sometimes the high abundant sequences found in the final selected pool do not bind to both target and control cell types. Actually, the success rate of cell-SELEX is not high enough.

Second, the complexity and diversity of the cell surface ligands lead to the difficulties in successful cell-SELEX attempts. Although in theory the selection of aptamers is possible for any target on cell surface, there are preferences for some types of target molecules to successfully select aptamers with high affinity and

specificity. Target molecules with positive charges, hydrogen bond donors/acceptors, and/or aromatic groups facilitate aptamer selection. The high-abundance target molecules facilitate the aptamer selection. However, if these molecules on cell surface are not the desired targets (e.g., they are common molecules on many types of cells), they would disturb the enrichment of desired aptamers. Target molecules with negative charges or highly hydrophobic target molecules do not favor the aptamer selection. The low-abundance target molecules do not favor the aptamer selection. The abundance of some membrane molecules may change with the cell growth status and cell passages, which would interfere in the aptamer selection. Therefore, the good cell culture maintenance is important for cell-SELEX.

Third, in contrast to the traditional SELEX against purified targets, a target identification step is necessary for cell-SELEX after obtained desired aptamers. However, until now, only a limited number of aptamer targets have been identified [11, 47–49], which greatly hindered the further application of aptamers selected against cells. The separation and purification of aptamer targets, especially the membrane protein targets are still a serious limitation for the target identification.

Fourth, the long selection period, complex and tedious process, high experience requirement, and high cost of SELEX still restrict the widely utilization of cell-SELEX.

As a result, some modified cell-SELEX strategies have been reported to exhibit improved selection efficiency. FACS-SELEX integrating flow cytometry and cell sorting into cell-SELEX allows simultaneously removing selection-hampering dead cells and selecting aptamers that are able to differentiate cell subpopulations [50, 51]. An on-chip Cell-SELEX process for automatic selection of aptamers has shorten the selection process to five rounds [52]. In the future for a long period of time, continued efforts on cell-SELEX need focus on the following aspects: (1) Reveal the principle of aptamer enrichment in cell-SELEX; reveal the binding mechanisms of aptamers and the targets on cell surface. (2) Develop new methods to enhance the selection efficiency, shorten the selection period and lower the cost, such as higher automated selection platform. (3) Develop efficient and universal strategies for the target identification of aptamer. (4) Develop data library of aptamers that generated by cell-SELEX, which include the information of target and control cell lines, initial library, selection condition, aptamer sequences, binding affinity, and specificity. This library will provide comprehensive information for further understanding of cell-SELEX and cellular biology.

Although the cell-SELEX methods need to be further improved, current researches have demonstrated that cell-SELEX can do a lot of interesting things, which is encouraging more researchers to develop additional aptamers for different targets. Despite compared with the complex molecular changes on cancer cell surface, the aptamers obtained by cell-SELEX are too less, we believe that further development of cell-SELEX and accumulation of aptamers will lead to an improved understanding of the biochemical and molecular basis of cancer, in turn, spur exciting new technologies for detection, diagnosis, and treatment of cancer. The cell-SELEX strategy can also be applied to the investigation of other diseases, thus expanding our knowledge of disease biology and improving the medical care and

life expectancy of individual patients. We are sure that along with the development of cell-SELEX, it will play a more important role in many fields such as clinical detection, personalized therapy, and cellular biological research.

References

1. Tan W, Donovan MJ, Jiang J (2013) Aptamers from cell-based selection for bioanalytical applications. Chem Rev 113(4):2842–2862. doi:10.1021/cr300468w
2. Ellington AD, Szostak JW (1990) In vitro selection of RNA molecules that bind specific ligands. Nature 346(6287):818–822. doi:10.1038/346818a0
3. Tuerk C, Gold L (1990) Systematic evolution of ligands by exponential enrichment: RNA ligands to bacteriophage T4 DNA polymerase. Science 249(4968):505–510
4. Lee JF, Stovall GM, Ellington AD (2006) Aptamer therapeutics advance. Curr Opin Chem Biol 10(3):282–289. doi:10.1016/j.cbpa.2006.03.015
5. Morris KN, Jensen KB, Julin CM, Weil M, Gold L (1998) High affinity ligands from in vitro selection: complex targets. Proc Natl Acad Sci USA 95(6):2902–2907. doi:10.1073/pnas.95.6.2902
6. Blank M, Weinschenk T, Priemer M, Schluesener H (2001) Systematic evolution of a DNA aptamer binding to rat brain tumor microvessels. selective targeting of endothelial regulatory protein pigpen. J Biol Chem 276(19):16464–16468. doi:10.1074/jbc.M100347200
7. Daniels DA, Chen H, Hicke BJ, Swiderek KM, Gold L (2003) A tenascin-C aptamer identified by tumor cell SELEX: systematic evolution of ligands by exponential enrichment. Proc Natl Acad Sci USA 100(26):15416–15421. doi:10.1073/pnas.2136683100
8. Wang C, Zhang M, Yang G, Zhang D, Ding H, Wang H, Fan M, Shen B, Shao N (2003) Single-stranded DNA aptamers that bind differentiated but not parental cells: subtractive systematic evolution of ligands by exponential enrichment. J Biotechnol 102(1):15–22
9. Shangguan D, Li Y, Tang Z, Cao ZC, Chen HW, Mallikaratchy P, Sefah K, Yang CJ, Tan W (2006) Aptamers evolved from live cells as effective molecular probes for cancer study. Proc Natl Acad Sci USA 103(32):11838–11843. doi:10.1073/pnas.0602615103
10. Jiang GH, Zhang M, Yue BH, Yang ML, Carter C, Al-Quran SZ, Li B, Li Y (2012) PTK7: a new biomarker for immunophenotypic characterization of maturing T cells and T cell acute lymphoblastic leukemia. Leuk Res 36(11):1347–1353. doi:10.1016/j.leukres.2012.07.004
11. Shangguan D, Cao ZH, Meng L, Mallikaratchy P, Sefah K, Wang H, Li Y, Tan WH (2008) Cell-specific aptamer probes for membrane protein elucidation in cancer cells. J Proteome Res 7(5):2133–2139. doi:10.1021/pr700894d
12. Tang Z, Shangguan D, Wang K, Shi H, Sefah K, Mallikratchy P, Chen HW, Li Y, Tan W (2007) Selection of aptamers for molecular recognition and characterization of cancer cells. Anal Chem 79(13):4900–4907. doi:10.1021/ac070189y
13. Chen HW, Medley CD, Sefah K, Shangguan D, Tang Z, Meng L, Smith JE, Tan W (2008) Molecular recognition of small-cell lung cancer cells using aptamers. ChemMedChem 3 (6):991–1001. doi:10.1002/cmdc.200800030
14. Shangguan D, Meng L, Cao ZC, Xiao Z, Fang X, Li Y, Cardona D, Witek RP, Liu C, Tan W (2008) Identification of liver cancer-specific aptamers using whole live cells. Anal Chem 80 (3):721–728. doi:10.1021/ac701962v
15. Li WM, Bing T, Wei JY, Chen ZZ, Shangguan DH, Fang J (2014) Cell-SELEX-based selection of aptamers that recognize distinct targets on metastatic colorectal cancer cells. Biomaterials 35(25):6998–7007. doi:10.1016/j.biomaterials.2014.04.112
16. Wang Y, Luo Y, Bing T, Chen Z, Lu M, Zhang N, Shangguan D, Gao X (2014) DNA aptamer evolved by cell-SELEX for recognition of prostate cancer. PLoS ONE 9(6):e100243. doi:10.1371/journal.pone.0100243

17. Sefah K, Bae KM, Phillips JA, Siemann DW, Su Z, McClellan S, Vieweg J, Tan W (2013) Cell-based selection provides novel molecular probes for cancer stem cells. Int J Cancer 132 (11):2578–2588. doi:10.1002/ijc.27936
18. Sefah K, Tang ZW, Shangguan DH, Chen H, Lopez-Colon D, Li Y, Parekh P, Martin J, Meng L, Phillips JA, Kim YM, Tan WH (2009) Molecular recognition of acute myeloid leukemia using aptamers. Leukemia 23(2):235–244. doi:10.1038/leu.2008.335
19. Tang Z, Parekh P, Turner P, Moyer RW, Tan W (2009) Generating aptamers for recognition of virus-infected cells. Clin Chem 55(4):813–822. doi:10.1373/clinchem.2008.113514
20. Zhao Z, Xu L, Shi X, Tan W, Fang X, Shangguan D (2009) Recognition of subtype non-small cell lung cancer by DNA aptamers selected from living cells. Analyst 134(9):1808–1814. doi:10.1039/b904476k
21. Parekh P, Tang Z, Turner PC, Moyer RW, Tan W (2010) Aptamers recognizing glycosylated hemagglutinin expressed on the surface of vaccinia virus-infected cells. Anal Chem 82 (20):8642–8649. doi:10.1021/ac101801j
22. Sefah K, Meng L, Lopez-Colon D, Jimenez E, Liu C, Tan W (2010) DNA aptamers as molecular probes for colorectal cancer study. PLoS ONE 5(12):e14269. doi:10.1371/journal.pone.0014269
23. Stoltenburg R, Reinemann C, Strehlitz B (2007) SELEX-A (r)evolutionary method to generate high-affinity nucleic acid ligands. Biomol Eng 24(4):381–403. doi:10.1016/j.bioeng.2007.06.001
24. Sefah K, Shangguan D, Xiong X, O'Donoghue MB, Tan W (2010) Development of DNA aptamers using cell-SELEX. Nat Protoc 5(6):1169–1185. doi:10.1038/nprot.2010.66
25. Hicke BJ, Marion C, Chang YF, Gould T, Lynott CK, Parma D, Schmidt PG, Warren S (2001) Tenascin-C aptamers are generated using tumor cells and purified protein. J Biol Chem 276 (52):48644–48654. doi:10.1074/jbc.M104651200
26. Liu J, Liu H, Sefah K, Liu B, Pu Y, Van Simaeys D, Tan W (2012) Selection of aptamers specific for adipose tissue. PLoS ONE 7(5):e37789. doi:10.1371/journal.pone.0037789
27. Cao XX, Li SH, Chen LC, Ding HM, Xu H, Huang YP, Li J, Liu NL, Cao WH, Zhu YJ, Shen BF, Shao NS (2009) Combining use of a panel of ssDNA aptamers in the detection of Staphylococcus aureus. Nucleic Acids Res 37:4621–4628. doi:10.1093/nar/gkp489
28. Turek D, Van Simaeys D, Johnson J, Ocsoy I, Tan W (2013) Molecular recognition of live methicillin-resistant staphylococcus aureus cells using DNA aptamers. World J Transl Med 2 (3):67–74. doi:10.5528/wjtm.v2.i3.67
29. Bayrac AT, Sefah K, Parekh P, Bayrac C, Gulbakan B, Oktem HA, Tan W (2011) In vitro selection of DNA aptamers to glioblastoma multiforme. ACS Chem Neurosci 2(3):175–181. doi:10.1021/cn100114k
30. Jimenez E, Sefah K, Lopez-Colon D, Van Simaeys D, Chen HW, Tockman MS, Tan W (2012) Generation of lung adenocarcinoma DNA aptamers for cancer studies. PLoS ONE 7 (10):e46222. doi:10.1371/journal.pone.0046222
31. Bing T, Yang XJ, Mei HC, Cao ZH, Shangguan DH (2010) Conservative secondary structure motif of streptavidin-binding aptamers generated by different laboratories. Bioorg Med Chem 18(5):1798–1805. doi:10.1016/j.bmc.2010.01.054
32. Shangguan D, Tang ZW, Mallikaratchy P, Xiao ZY, Tan WH (2007) Optimization and modifications of aptamers selected from live cancer cell lines. ChemBioChem 8(6):603–606. doi:10.1002/cbic.200600532
33. Legiewicz M, Yarus M (2005) A more complex isoleucine aptamer with a cognate triplet. J Biol Chem 280(20):19815–19822. doi:10.1074/jbc.M502329200
34. Manimala JC, Wiskur SL, Ellington AD, Anslyn EV (2004) Tuning the specificity of a synthetic receptor using a selected nucleic acid receptor. J Am Chem Soc 126(50):16515–16519. doi:10.1021/ja0478476
35. Sayer NM, Cubin M, Rhie A, Bullock M, Tahiri-Alaoui A, James W (2004) Structural determinants of conformationally selective, prion-binding aptamers. J Biol Chem 279 (13):13102–13109. doi:10.1074/jbc.M310928200

36. Green LS, Jellinek D, Jenison R, Ostman A, Heldin CH, Janjic N (1996) Inhibitory DNA ligands to platelet-derived growth factor B-chain. Biochemistry 35(45):14413–14424. doi:10.1021/bi961544+
37. Zuker M (2003) Mfold web server for nucleic acid folding and hybridization prediction. Nucleic Acids Res 31(13):3406–3415
38. Mei HC, Bing T, Yang XJ, Qi C, Chang TJ, Liu XJ, Cao ZH, Shangguan DH (2012) Functional-group specific aptamers indirectly recognizing compounds with alkyl amino group. Anal Chem 84(17):7323–7329. doi:10.1021/ac300281u
39. Qi C, Bing T, Mei HC, Yang XJ, Liu XJ, Shangguan DH (2013) G-quadruplex DNA aptamers for zeatin recognizing. Biosens Bioelectron 41:157–162. doi:10.1016/j.bios.2012.08.004
40. Yang XJ, Bing T, Mei HC, Fang CL, Cao ZH, Shangguan DH (2011) Characterization and application of a DNA aptamer binding to L-tryptophan. Analyst 136(3):577–585. doi:10.1039/c0an00550a
41. Bing T, Chang TJ, Yang XJ, Mei HC, Liu XJ, Shangguan DH (2011) G-quadruplex DNA aptamers generated for systemin. Bioorg Med Chem 19(14):4211–4219. doi:10.1016/j.bmc.2011.05.061
42. Xiao Z, Shangguan D, Cao Z, Fang X, Tan W (2008) Cell-specific internalization study of an aptamer from whole cell selection. Chem (Easton) 14(6):1769–1775. doi:10.1002/chem.200701330
43. Fang X, Tan W (2010) Aptamers generated from cell-SELEX for molecular medicine: a chemical biology approach. Acc Chem Res 43(1):48–57. doi:10.1021/ar900101s
44. Pu Y, Zhu Z, Liu H, Zhang J, Liu J, Tan W (2010) Using aptamers to visualize and capture cancer cells. Anal Bioanal Chem 397(8):3225–3233. doi:10.1007/s00216-010-3715-7
45. Ye M, Hu J, Peng M, Liu J, Liu J, Liu H, Zhao X, Tan W (2012) Generating aptamers by cell-SELEX for applications in molecular medicine. Int J Mol Sci 13(3):3341–3353. doi:10.3390/ijms13033341
46. Meyer C, Hahn U, Rentmeister A (2011) Cell-specific aptamers as emerging therapeutics. J Nucleic Acids 2011:904750. doi:10.4061/2011/904750
47. Van Simaeys D, Turek D, Champanhac C, Vaizer J, Sefah K, Zhen J, Sutphen R, Tan WH (2014) Identification of cell membrane protein stress-induced phosphoprotein 1 as a potential ovarian cancer biomarker using aptamers selected by cell systematic evolution of ligands by exponential enrichment. Anal Chem 86(9):4521–4527. doi:10.1021/ac500466x
48. Mallikaratchy P, Tang ZW, Kwame S, Meng L, Shangguan DH, Tan WH (2007) Aptamer directly evolved from live cells recognizes membrane bound immunoglobin heavy mu chain in Burkitt's lymphoma cells. Mol Cell Proteomics 6(12):2230–2238. doi:10.1074/mcp.M700026-MCP200
49. Yang ML, Jiang GH, Li WJ, Qiu K, Zhang M, Carter CM, Al-Quran SZ, Li Y (2014) Developing aptamer probes for acute myelogenous leukemia detection and surface protein biomarker discovery. J Hematol Oncol 7:14. doi:10.1186/1756-8722-7-5
50. Raddatz MS, Dolf A, Endl E, Knolle P, Famulok M, Mayer G (2008) Enrichment of cell-targeting and population-specific aptamers by fluorescence-activated cell sorting. Angew Chem Int Ed Engl 47(28):5190–5193. doi:10.1002/anie.200800216
51. Mayer G, Ahmed MS, Dolf A, Endl E, Knolle PA, Famulok M (2010) Fluorescence-activated cell sorting for aptamer SELEX with cell mixtures. Nat Protoc 5(12):1993–2004. doi:10.1038/nprot.2010.163
52. Hung LY, Wang CH, Hsu KF, Chou CY, Lee GB (2014) An on-chip Cell-SELEX process for automatic selection of high-affinity aptamers specific to different histologically classified ovarian cancer cells. Lab Chip. doi:10.1039/c4lc00587b

Chapter 3
Unnatural Nucleic Acids for Aptamer Selection

Liqin Zhang

Abstract Aptamer and SELEX technology have been proposed over 20 years. Despite the huge success in developing aptamers against all kinds of targets, the effort to cover the natural shortages of nucleic acids, including lack of binding functional diversity and low information densities, has never been stopped. Strategies proposed to improve the aptamer properties include post-selective modifications and introducing unnatural nucleic acids in SELEX process. As a perfect binding ligand can hardly be designed and modified on purpose due to the poor understanding of the intricate biological system, the best way to generate improved aptamers would be through modified SELEX experiment, in which unnatural nucleotides are incorporated into library and perform the in vitro evolution. Those unnatural nucleotides include the modifications on almost every components of nucleic acids, (deoxy) ribose, phosphate linkage, and nucleobases. To increase the chemical diversity and the information density of nucleic acids, researchers developed methods to append functional groups as well as to create replicable expanded genetic systems. Some of these unnatural nucleic acids have now been utilized in SELEX, and a panel of improved aptamers has been delivered. In this book chapter, we mainly discuss the emerged unnatural bases which have been used in SELEX or at least have the potential to be used in SELEX, and how these unnatural nucleic acid help generate improved aptamers.

Keywords Unnatural nucleic acids · Modified SELEX · Artificial expanded genetic information system (AEGIS) · Chemical diversity · Information density · Synthetic biology

L. Zhang (✉)
Departments of Chemistry, UF Health Cancer Center, University of Florida, Gainesville, FL 32611-7200, USA
e-mail: liqinzhang@chem.ufl.edu

W. Tan and X. Fang (eds.), *Aptamers Selected by Cell-SELEX for Theranostics*,
DOI 10.1007/978-3-662-46226-3_3

3.1 General

It has been a quarter century since scientists proposed that binding ligands could be generated toward any targets of interest in the forms of nucleic acids [1–3]. The method proposed, termed systematic evolution of ligands by exponential enrichment (SELEX) [1] has been inspiring innumerable efforts committing to deliver aptamers against all kinds of target. Theoretically, with a simple recipe, the DNA or RNA aptamers could be delivered quickly, reliably, and inexpensively, toward any target researchers have in hand. It mimics the natural Darwinism (survival the fittest) that the best fitted nucleic acids will survive and be enriched during the evolution process in the exposure of the environment of targets.

Naturally, the emergence of this method aroused the comparison between nucleic acid aptamers and antibodies, one of the nature's solutions for the generation of biomolecule binders and by far the most useful binding tools in biomedicine. Generally speaking, nucleic acid aptamers share some advantages of antibodies, including high specificity and binding affinity, generated by evolution process, enzymatic pathways available for amplification and degradation, as well as highly biocompatibility. Beyond that, nucleic acid aptamers possess some unique merits. For instance, it could be reproduced simply by chemical synthesis method, equipped with desired chemical modification, with little batch-to-batch variance. They are more likely a product that combining the power of 'chemistry' and power of 'biology' [4]. Indeed, considering the disadvantages of antibodies, including tedious generation process and intrinsic property of instability and immunogenicity, the nucleic acid aptamers and SELEX method were believed to be very competitive.

Despite the high enthusiasm at very beginning, the hope of aptamer rivaling antibodies [5] has never been fully realized. Aptamers have been generated toward a variety of targets ranging from small molecules [6], biomacromolecules [7, 8], to various cancer cells [9–12]. However, very few of these aptamers are now entering the clinical trial phases to be considered as drug leads, nor to be used as detection methods for in vivo application [13]. This fact has always been cited by the sceptics to question the practicability of aptamers.

Honestly, those queries are understandable. The capacity in combinatorial assembly has determined how far natural nucleic acids can go as a therapeutic or diagnostic component. Nucleic acids, after all, are built from merely four different nucleotide building blocks, which render it have therefore, compared to antibodies, much weaker power in terms of binding diversity [14–16]. To be specific, those ligand-receptor co-structure studies revealed that nucleic acid aptamers mainly employ hydrogen bonds, π–π stacking, and electrostatic interactions in the binding process, however, carries little of other key functional groups commonly found in protein, including hydrophobic groups (Leu and Ile), positively charged groups (Lys and Arg), negatively charged groups (Asp and Glu), polarizable binding groups (indole in Trp and thioether in Met), catalytic groups (His), and metal coordinating groups (Cys and His). From this point of view, nucleic acids were indeed far inferior to proteins as matrices for functional performance. Besides, the

pharmacokinetic profile of aptamers is not satisfactory either. Particularly, it is embodied in short plasma half-life due to the nature of small molecule and enzyme vulnerability due to the self-maintaining mechanism of our bodies. Undoubtedly, all above chemical characteristics determined that application of nucleic acid aptamers would be largely limited.

Nevertheless, it would not be wise to throw away the apple because of the core. On the contrary, our scientists are smart enough to overcome those drawbacks by exploiting the chemical knowledge we have. The efforts of dealing with imperfection of aptamers started shortly after the discovery of aptamer, when people realizing the necessity and urgency to do so.

The first strategy is straightforward and feasible, which is usually referred to as 'post-selective' modification. This strategy focuses mainly on improving properties of the existing nucleic acid aptamer. For example, modifications on the ribose–phosphate backbone by introducing phosphorothioates [17] or locked nucleic acids (LNA) [18, 19], both of which are not accepted as substrates by the majority of nucleases, will help maintain stability when applied in vivo. Some other functional groups, those could help aptamers to carry 'cargoes' [20], to cross-linking with its target [21], or to gain improved pharmacokinetic properties [22], have been introduced into post-selective modification method in order to make 'perfect' aptamers. Nowadays, most of these modified phosphoramidites carrying amine, thiol, or carboxyl groups are commercially available, along with a variety of appendents which could be directly labeled on nucleic acid molecules.

The most famous example of successfully utilizing post-selective modification strategies to improve aptamer properties is Pegaptanib (Macugen®, Fig. 3.1) [23]. It is the first and so far the only aptamer therapeutic approved by FDA for the treatment of wet form of age-related macular degeneration (AMD). It was delivered through SELEX against vascular endothelial growth factor (VEGF)-165 in the year of 1994 [24] and it was found that this aptamer can block the actions of its target VEGF. However, it took another 4 years to modify this aptamer to make it resistant to enzyme degradation and renal clearance [25]. Resulting from these modifications, the in vivo

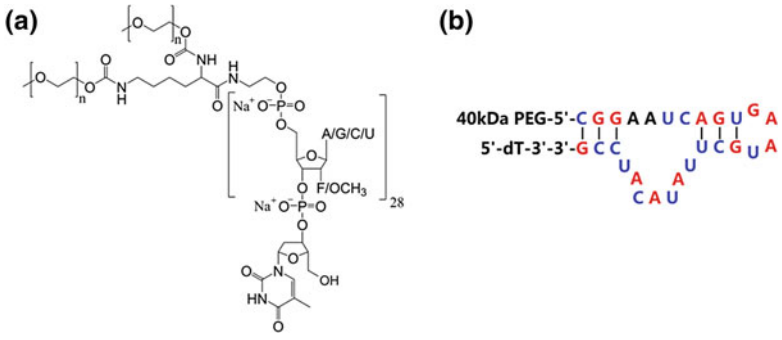

Fig. 3.1 Chemical structure and predicted secondary structure of Pegaptanib. **a** Chemical structure of Pegaptanib. **b** Predicted secondary structure of Pegaptanib. High degree of modification including 2′-fluoro-pyrimidines (in *blue*) and 2′-methoxy-purines (in *red*) replaced nucleotides, capped 3′ end, additional two 20 kDa PEG groups via 5′-end coupling

stability of nucleic acid aptamer has been largely improved, despite a certain degree of reduction in binding affinity for VEGF. The success of Pegaptanib sheds light on the whole aptamer research area and highlighted again the urgency and necessity of chemical modification on natural nucleic acids in aptamer research.

However, those post-selective strategies could not cope with the essential drawback that the building blocks of nucleic acids cannot provide enough chemical diversity, therefore cannot guarantee to generate aptamers with desired affinity when confronting any target. The factors attributed by experimental work as well as theory to low performance of SELEX include the low level of functional groups in nucleic acid molecules and the low information density due to merely four building blocks [26]. Those issues have to be dealt with in the evolution process but not after. Accordingly, another strategy to modify the nucleic acid library in the SELEX experiment has been proposed to cover the shortages, which could be further divided into two methods.

On one hand, various functional groups were introduced onto four standard nucleotides in an attempt to obtain those functional nucleic acid molecules [27–31]. On the other hand, people attempted to increase the number of independently replicating nucleotides in the nucleic acid library, with the purpose of increasing information density carried by nucleic acid and the resultant folding possibility [32–34].

All these efforts of introducing new functionality or novel nucleotides into SELEX process followed similar principles, that is, the biotechnologies developed for SELEX. Three key technologies are involved which include the following: (1) chemical synthesis of phosphoramidites for solid-phase synthesis of nucleic acid and triphosphates for enzymatic amplification, (2) engineering and identifying polymerases to efficiently amplify nucleic acids library using standard four nucleotides plus unnatural nucleotide triphosphates, and (3) sequencing techniques to identify the survivor sequences containing unnatural nucleotides. It is well known that these technologies were originally developed only to natural nucleic acids. To apply those unnatural nucleic acids in SELEX procedure, these technologies need to be adjusted or even compromised to accept unnatural nucleic acids, with satisfactory efficiency and feasibility. From this angle, whether ideally designed unnatural nucleotides can be utilized in SELEX or not largely depends on whether corresponding key technologies could be well developed or not.

Synthesis of phosphoramidites and triphosphates is the first yet fundamental step. It is different from post-selective strategy where only modified phosphoramidites (most of them are commercially available) are needed. To implement those modified nucleic acid building blocks into SELEX process, not only unnatural nucleic acid phosphoramidites, but also the triphosphates, as a key component of recipe for enzymatic amplification, need to be prepared by organic synthetic method.

Maybe sounds a piece of cake for those masters in synthetic chemistry; however, the enzymes for amplification that has been evolved for billion years to accept only natural NTP are never easy to be satisfied. For those who is willing to add functional groups onto natural DNA, the inevasible enzymatic polymerization reactions for amplification involved in SELEX imposes the restriction that the modified NTP has to be perfectly compatible with the usually over 200 rounds of amplification

during SELEX process. By mentioning compatible here, it means these functional groups added should not interfere with the recognition and binding sites of polymerase and should also match with the complementary nucleotides.

To prevent the classical base-pairing interface from disturbing, the modification are usually restricted on those sites which will not be involved in the base paring and polymerase binding process [4, 35] (Fig. 3.2). On nucleobases, the non-Watson-Crick sites, more specifically C5 of pyrimidines are usually the positions where modification proceeded on, which is in the major groove in duplex and will not interfere with approaching by polymerase [35, 36]. Besides, some modifications on ribose–phosphate backbone are also feasible, as long as it will not distort the whole DNA/RNA structure to a large degree. For example, ribose 2′-replacement with

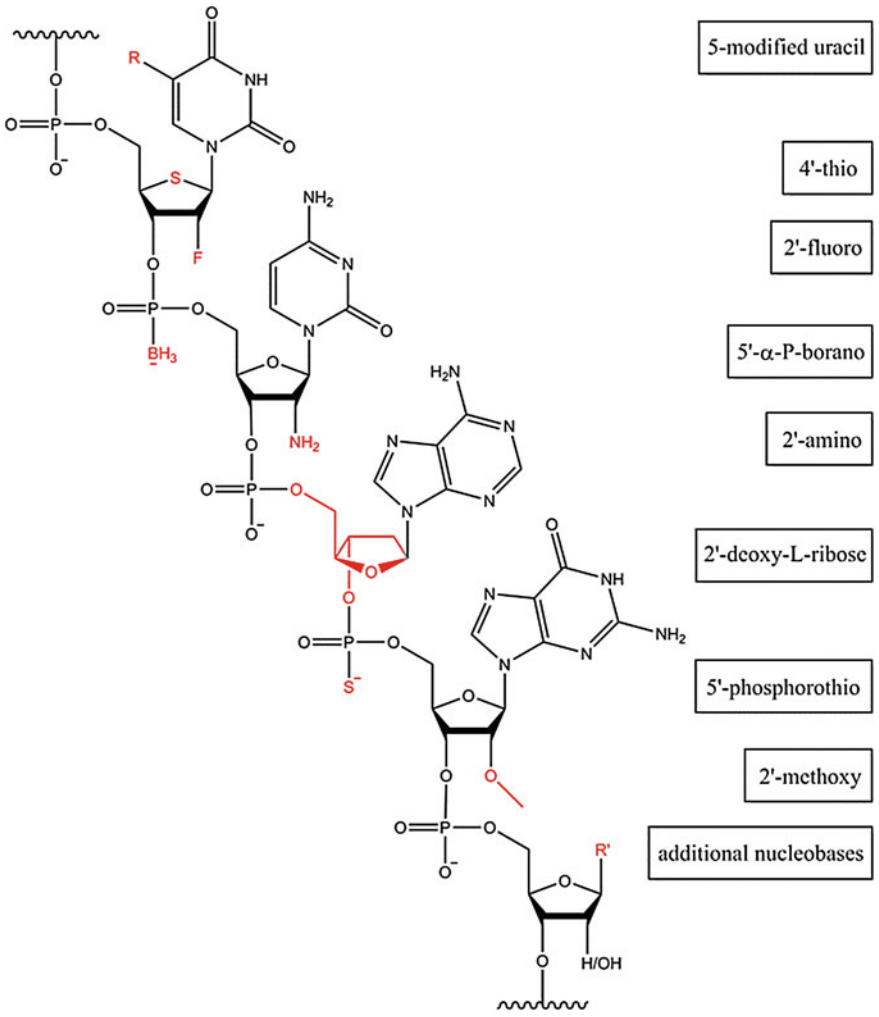

Fig. 3.2 Chemical structure of modified nucleotides reported for SELEX

fluoro, amino, or methoxy group are commonly used generate enzyme resistent nucleic acid library, similarly in the example of Pegaptanib. Another famous example is displacing natural D-ribose with artificial L-ribose to generate the enantiomer of natural DNA (termed Spiegelmer) and thus prevent its degradation by nucleases. These examples will be detailed discussed in the later sections of this chapter.

For those who are dedicating to expand the armory of nucleotides, this concern is even bigger. Artificial designed nucleobases need to be both stable in duplex nucleic acid and replicable by natural existent polymerases. After the idea proposed by Benner in the late 1980s [37, 38], many efforts have been devoted into this area in light of the great potential of encoding additional information by expanded genetic alphabets in both in vitro and in vivo applications, and considerable achievements have been made since then. By adding additional base pair, the drawbacks of nucleic acids mentioned above, that is, lack of functionality and low information density, could be potentially solved at the same time. By far, two main types of approaches to develop such type of unnatural bases have been reported. The first, developed by Benner and coworkers [39], exploited unnatural hydrogen bond patterns between two complementary nucleobases, while maintaining the Watson–Crick geometry. Another one, proposed by Kool and colleagues [40, 41], that interbase hydrogen bonding is not imperative for nucleotide replication has broaden the way of thinking that focused more on van der Waals and hydrophobic interactions. The followers include Hirao [32, 33] and Romesberg [42, 43] and their coworkers have contributed tremendously in this field. The detailed story will also be discussed in later sections.

Since this is a book focusing on cell-SELEX-related technologies, in this chapter, we will mainly pay attention to introduce those unnatural nucleic acids involved strategies which have been used or at least have the potential to be used for SELEX. We will start with strategies that conducting modifications on ribose–phosphate backbone and their application in SELEX will be discussed, including the 2′-modified nucleotides [44], oxygen replacement on phosphate and Spiegelmers developed by Klussmann group [45]. Next, the strategies of adding functional groups to natural nucleobases, including hydrophobic groups, positive charged groups, and amino acid side chain mimicking groups, will be introduced. Following that we will discuss currently emerged replicable artificial nucleobase pairs and one application in SELEX done by Hirao and coworkers [33]. At the end, we will introduce so far the only full SELEX utilizing artificially expanded genetic information system (AEGIS) done by Benner, Tan, and their colleagues.

3.2 Evolution of Aptamers with Artificial Nucleic Acids

One key component of the recipe for success of SELEX technique is that this process highly mimics the natural evolution process. Those binders enriched in the selection process are exactly those survivors who can adjust oneself and adapt to the target environment. Similar to the reason why human being must maintain species

diversity on earth, addition of chemical diversities into nucleic acid library will make this process even more lifelike.

Thanks to the solid fundamental established by organic chemists. Nowadays, human being is processing a huge toolbox with which we design and synthesize almost any chemical structure in need. Of course the ligands are not among these accessible chemical structures, not because of the lack of chemistry knowledge, but simply because the interaction of ligands with their receptors are too complicated for human being to interpret. However, the matured organic chemistry knowledge provides us with all kinds of strategies to modify natural biological molecules. With all this chemical modifications, we can now fulfill our goal of obtaining binders on demand, or even to the bigger picture we could ever imagined.

3.2.1 Modification on Nucleic Acid Backbone to Deliver Improved Aptamers

When people realized that aptamers made of natural nucleic acids have all sorts of drawbacks that severely hindered its wide application, the first solution emerged in mind would be appending functional groups on nucleic acid molecules. These ideas directly root in traditional chemical thought pattern that the function of chemicals could be improved by further chemical modification. If one has a glimpse history of drug discovery, you will find these patterns were applied to almost every type of chemical drugs people ever developed.

It indeed works. To cope with a specific problem emerged, there is always a genius method developed accordingly. That is exactly where the charm of chemistry lies on.

3.2.1.1 Modification on 2′ Site of Ribose

The earliest efforts to apply modified nuclei acids into SELEX were focusing on 2′ site on ribose. The purpose was to increase the nuclease resistance property of aptamers. The functional groups added onto 2′ site of ribose include amino [46], fluoro [47], and methoxyl group [44, 48] (Fig. 3.2). Those techniques were originally proved in post-selective modification, such as in the example of Pegaptanib. However, in order to acquire aptamers more rapidly and conveniently, meanwhile to avoid the potential affinity decreasing resulting from post-selective modification, researchers started to apply those modifications in the selection process. Y639F mutant T7 RNA polymerase was usually used for these modified RNA transcription [47]. 2′-amino pyrimidines, both cytidine (C) and uridine (U), have been used in RNA libraries for SELEX. A variety of targets have now been selected toward using these 2′-modified nucleic acid. These examples include basic fibroblast

growth factor (bFGF) [49], L-selectin [50], human keratinocyte growth factor (hKGF) [51], human neutrophil elastase (HNE) [46], human thyroid stimulating hormone (hTSH) [52], immunoglobulin E (IgE) [53], and interferon-γ (IFN-γ) [54]. Usually the stability could be enhanced that lifetime could be prolonged by 1,000–80,000 times [49, 51].

2′-fluoro replacement method generated a couple of aptamers which has been entered clinical trial. Besides Pegaptanib, there are also anti-Factor IXa aptamer RB006 that binds to members of the coagulation cascade and act as anticoagulants [55] and anti-C5 aptamer which inhibits the complement cascade [56]. Again, 2′-fluoro U and 2′-fluoro C were exploited in library to select aptamers against KGF [51], IFN-γ [54], human thrombin [57], and cluster of differentiation 4 (CD4) [58]. However, someone may concern about its side effect as it was suggested that the administration and degradation of 2′-F-pyrimidine could lead to incorporation into cellular DNA [59, 60].

2′-methoxyl group might be a good alternative. The advantage of this method is that the synthesis is less expensive, and more importantly, the methoxyl group is naturally occurred in as a common moiety in posttranscriptional modification. Methylation of the 2′-hydroxyl groups is a selective protection system used by nature and thus introduced here to reduce the safety concerns. SELEXs using library containing this modification were conducted recently on VEGF-165 [44] and Interleukin 23 (IL-23) [48]. The affinities were high, with a Kd value within nanomolar range.

3.2.1.2 Replacing Oxygen on Phosphate

Another site which could be replaced to functionalize the nucleic acid library is on 5′-α-P-site on phosphate. The functional groups used to replace phosphate linkage this site include boranophosphate [61] and phosphorothioate [62] (Fig. 3.2). For boranophosphate, wild-type T7 RNA polymerase is good enough for the transcription. The initial purpose was to deliver aptamers for boron neutron capture therapy (BNCT), where boron-10 was used as a non-radioactive isotope that has a high propensity to capture slow neutrons to emit high-energy charge particles and result in the cell death. And aptamer would be a perfect probe to deliver this boron-10 to the cancer target. This concept was preliminarily demonstrated by performing a SELEX against ATP [61], with 5′-α-P-borano G or U in the library.

Phosphorothioate internucleotide linkage was utilized to generate nuclease resistance preferred to DNAse. Although the chiral property of phosphorothioate linkage is usually neglected and both diastereomers are used in the phosphoramidite chemistry synthesis, stereoregular phosphorothioate are usually prepared using α-thio-dNTPs in Taq polymerase amplification or T7 RNA polymerase transcription [35]. Examples include cytokine TGF-β1-targeted RNA aptamers [62] and Venezuelan equine encephalitis virus capsid protein [63].

3.2.1.3 Artificial Ribose

An alternative method is to use artificial ribose, to prevent aptamer from nuclease degradation. One way is to replace 4′-oxygen by sulfur on ribose (Fig. 3.2). 4′-thio UTP and CTP were used in library for SELEX to generate aptamers for thrombin [64]. It was claimed that by adding the 4′-thio, besides enhancement of the nuclease resistance by about 50 times, the base pair strength was found to be increased too.

Another heroic work was the generation of Spiegelmers done by Furste and his coworkers [45, 65, 66] (Fig. 3.2). The basic design of the work was based on the fact that all natural enzymes, no matter a polymerase or a nuclease, are all in L-amino acids and born to fit D-nucleosides. In this case, theoretically, an L-oligonucleotide should escape from enzymatic recognition and subsequent degradation. However, because of the same reason those L-oligonucleotides will not be accepted by polymerase so that it cannot be copied in the in vitro selection process. A compromised method was carried out by these smart scientists (Fig. 3.3). Instead of select against natural target, they used the mirror-image target and the natural oligonucleotides in the SELEX process. As long as the natural oligonucleotides targeting, mirror-image target was successfully obtained at the end of SELEX, an L-oligonucleotide would certainly binds to the natural target. And an unnatural enantiomer of aptamer, named Spiegelmer (from German word 'Spiegel,' means mirror), will thus be generated. Based on this technology, a number of spiegelmers have been selected [65–68].

3.2.2 Appending Functionality on Aptamers

On above, we discussed about modifications on (deoxy) ribose-sugar backbone and their applications in SELEX. However, the motivations were more on to enhance the in vivo stability, while contribute little on increasing diversity. The essential shortage

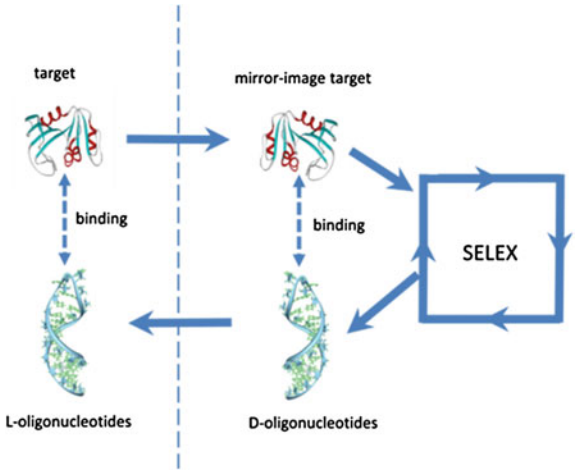

Fig. 3.3 Schematic of spiegelmer technology: mirror-image in vitro selection. Adapted from Eulberg and Klussmann [45]

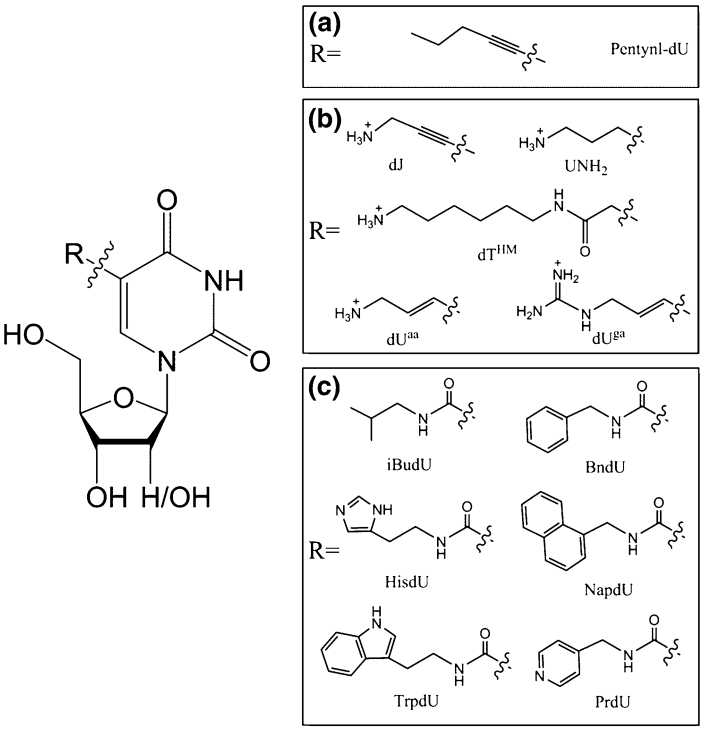

Fig. 3.4 C5-modified deoxyuridines. **a** Hydrophobic group-modified uracil. **b** Cationic group-modified uracil. **c** Protein-like side chain uracil

of nucleic acid as a binding probe lies on its lack of diversified functional groups and thus relatively weak binding capability after combinatorial assembly of them. While the biding sites of aptamers are usually believed to be the unpaired nucleobases (compared with side chains of peptides). Introducing functional groups direct on nucleobases are, therefore, crucial to enlarge the diversity of library. However, as mentioned before, adding functional groups onto nucleic acid has to follow the principle, that is, this addition cannot interfere with the approach and functionalization of polymerase. This limitation largely reduces the possibility of introducing more functional groups. So far, the most permissive sites for modifications are 5-position on U/T, and a variety of functional groups have been successfully appended (Fig. 3.4).

3.2.2.1 Hydrophobic Groups

The earliest attempt using this strategy was done by Latham and his colleagues [69] (Fig. 3.4a). In their design, a 5-pentynyl-modified dU was used to displace dT in the randomized region of DNA library and this library was used to successfully generate aptamers against thrombin. Vent DNA polymerase was used in their

experiment. The survivors at the end of the selection were cloned and sequenced using Sequenase to obtain the specific sequences of candidate aptamers. Because functional group added on C5 cite of pyrimidine, which does not interfere the function of polymerase, the PCR and sequencing were not influenced too much by the modification. Despite that this example was the first attempt to prove the feasibility of introducing a new group onto C5 site of pyrimidine, the affinity of their selected aptamers is not superior of their previous selected aptamers using natural DNA library [70].

3.2.2.2 Positively Charged Groups

Sooner after the success of introducing hydrophobic, another type of functional groups which is lack in natural nucleic acid, cationic group, was also being introduced into SELEX process [71]. In this work, Benner and his coworkers added an aminopropynyl group onto 5 sites of deoxyuridine (**dJ**, Fig. 3.4b), and as an example, the modified nucleotide were incorporated into library and performed a SELEX against ATP molecules. Vent DNA polymerase was used for PCR in this experiment. It was revealed that the selection yielded aptamer having sequences differing from the one generated from standard selection using natural nucleotides. However, convergence including both binding to two ATP molecules and very similar affinity were discovered. This work confirmed the capability to introduce functionality onto natural nucleic acid and use it for in vitro selection.

Another practice was carried out by Szostak and McLaughlin groups several years later [72]. In this work, a 5-(3-aminopropyl)uridine analogue was incorporated into a degenerate RNA library by enzymatic polymerization (**UNH_2**, Fig. 3.4b). Again, this in vitro selection generated an aptamer binding to ATP molecules. And it was observed that the modified RNA can interact with the triphosphate group of ATP, which was not found in the case of natural RNA aptamer. This could further prove the strength of positive charged group.

This line of research continues to develop, and new positive charged nucleobase analogous kept emerging. Sawai and his colleagues successfully incorporated a 1,6-diaminohecyl-N-5-carbamoyl methyl deoxyuridine (**dT^{HM}**, Fig. 3.4b) into DNA library to perform SELEX to generated aptamers against viral infection related cell surface component sialyllactose [73] as well as (*R*)-thalidomide [74]. Recently, Perrin group has expanded introduction of cationic groups onto other standard nucleobases, and those modified nucleotides are being applied in in vitro selection of DNAzyme [27, 75] (**$dU^{aa}TP$**, **$dU^{ga}TP$**, Fig. 3.4b).

3.2.2.3 Mimic of Amino Acid Side Chains

The idea of adding functional groups was initially motivated by presented diversity of amino acids. Recently, this strategy has been propelled one step further by endowing nucleic acids with protein-like properties via functional groups mimicking amino

acid side chains [29]. Eaton and coworkers introduced an amide linkage at the 5 position so that six different side chains could be armed on deoxyuridine, including 5-isobutylaminocarbonyl-dU (**iBudU**), 5-benzylaminocarbonyl-dU (**BndU**), 5-histaminocarbonyl-dU (**HisdU**), 5-naphthylmethylaminocarbonyl-dU (**NapdU**), 5-tryptaminocarbonyl-dU (**TrpdU**), and 5-pyridylmethylaminocarbonyl-dU (**PrdU**) (Fig. 3.4c). Besides mimicking amino acids, other advantages of introducing amide linkage are to restrict rotation of the linkage bond and to provide with extra hydrogen bond acceptors and donors. After screening, all these modified deoxyuridines contained DNA were found to be fully replicated by D.Vent and KOD XL polymerase, which set the foundation for their usage in in vitro selection. Several of these modified deoxyuridines were incorporated into DNA library to perform in vitro selection against tumor necrosis factor receptor superfamily member 9 (TNFRSF9), which used to be considered as a challenging target. BndU and TrpdU incorporated selection generated aptamers having affinity much higher than natural DNA library where deoxythymidine replacing modified deoxyuridines [29].

This approach is now being commercially utilized in SomaLogic, Inc. to generate slow off-rate modified aptamers (SOMAmers), which could significantly increase the number of addressable targets of human proteins as well as the binding affinity [30]. Since the incorporation of four modified nucleotides, **BndU**, **NapdU**, **TrpdU**, and **iBudU**, into SELEX experiments, out of over 1,000 different proteins, the overall success rate rose from below 30 % to around 84 %, with aptamers having satisfactory affinities (Kd < 30 nM) and specificity. Exploiting those SOMAmers, an aptamer-based multiplexed proteomic technology for biomarker discovery, as well as for diagnostic and clinical applications, has been established in their company [28, 31].

3.2.3 Expanded Genetic Alphabets in Aptamer Selection

The effort of adding functional groups has been proved to be successful and productive. All those functional groups added into in vitro selection process indeed help generate aptamers with improved properties and fulfilled the goal in each initial design. However, there is another desire of human for nucleic acid which cannot be covered simply by introducing functional groups, that is, to increase the information density. It would be easier to understand if we transfer this description to chemical terminology. The desired larger chemical diversity could be achieved by introducing functional groups. However, the structural diversity, especially reflected in folding patterns, will not be increased by grafting stuff on one of the four basic building blocks. It is also highly possible that these nucleotides armed with functional groups will be folded into duplex structure and thus losing function, as stem region is usually believed not involved in the binding site. While adding additional nucleotides, also called expanded genetic alphabets, beyond A/G/C/T(U) will give much higher folding diversity and immediately minimize nonfunctioning folds that compete with the folds that have the desired function. Besides, those

expanded genetic systems were usually designed to possess modifiable sites, which allow them to potentially carry functional groups if needed. Therefore, the two strategies could be perfectly combined helped by chemical synthesis method.

However, to create those expanded genetic alphabets is not as easy as to picture it. A successful design of additional nucleotide has to incorporate considerations from broad areas. At first, the additional nucleotide must be stable. Considering the nature of conjugated structures and multiple protonizable and oxidizable sites in aromatic rings, to design a nucleotide stable under different circumstances is definitely not an easy thing to do. Actually most of the expanded genetic systems developed so far have gone through repeating process of modify–test–modify to optimize the most stable structures [76]. Secondly, the designed nucleotides have to be able to be compatible with the enzyme system. Unlike simply adding functional group to replicable uredines, the new designed nucleotides have to be capable of being replicated by polymerase or being transcribed by transcriptase in the evolution process, which of course require not a single, but a pair of complementary nucleotides to be added at the same time. No doubt it took even more effort of scientists, again, to repeat the process of modify–test–modify to cater those enzymes which have been evolved for billions of years to accept only natural nucleotides [77, 78].

It is indeed the essence of synthetic biology, a discipline in which people use tool of synthetic chemistry to modify biological molecules to manipulate the biological systems, more importantly, in which process to understand deeper about biological systems [39].

3.2.3.1 Developed Artificial Genetic Systems

As mentioned above, it is extremely hard to build an artificial genetic system. It has been almost a quarter century since this idea been proposed; however, only several groups in the world have successfully developed artificial genetic systems [34, 77, 78]. Among them, only two examples of in vitro evolution have ever been reported [33, 79].

In 1989, Benner's lab designed a pair of isomers of guanine and cytidine, named **isoG** and **isoC** (Fig. 3.5a), with nonstandard hydrogen-bonding patterns but similar geometry with Watson–Crick pairs [80]. And very soon, another pair (**X** and **K**, Fig. 3.5b) was reported too [37]. Although some shortcomings were found on these pairs, for example, lack of electron pairs in minor groove which were believed to be the polymerase recognition site and keto–enol tautomerization which could induce mismatching **isoG** with T(U), these pioneering studies inspired the subsequent studies to a great extent. And after 25 years of effort to keep improving, Benner's group have now developed a whole system containing up to 12 different nucleotide 'letters' pair via six distinguishable hydrogen-bonding patterns [39, 76]. We will further introduce more details about this system in next section.

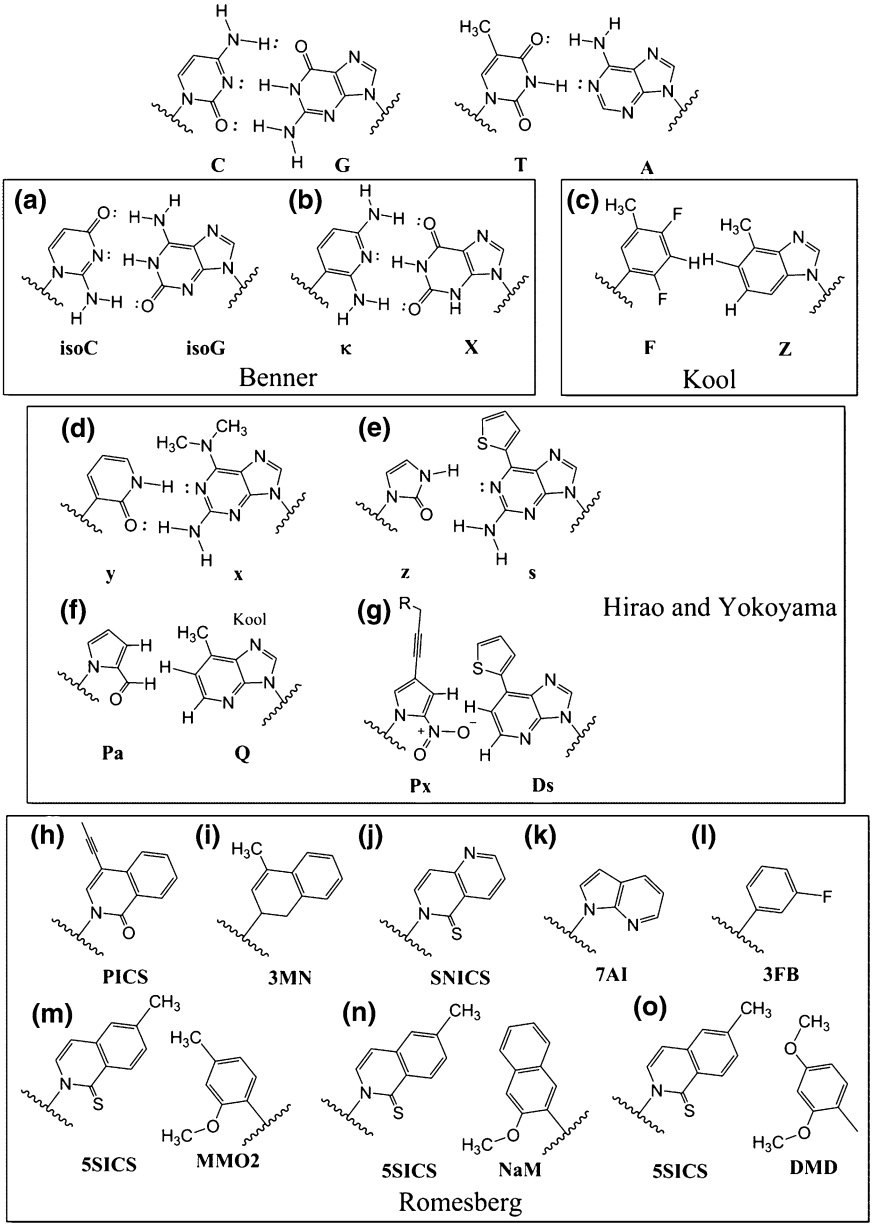

Fig. 3.5 Developed expanded genetic alphabets systems. Images named followed the laboratory who invented it

In 1998, Kool's group proposed their classic non-hydrogen-bonded base pairs. Instead of hydrogen-bonding, they exploited shape analogues of the natural bases, **Z**(**Q**) and **F** (Fig. 3.5c, f), to be incorporated into the replicable nucleic acids [81, 82]. It was the first time researchers realized that the hydrogen bonding between nucleobases is not an absolutely requirement for replication. The role of shape complementarity and hydrophobicity in nucleic acid stability and replication has been illustrated in these works. The absence of hydrogen bonding will inevitably reduce the stability between DNA duplex; however, the pairing between artificial bases is still more stable than mispairing with natural bases; thus, thermal selectivity could be achieved. Similarly, this work inspired a lot of subsequent researches. After all, the strategy of rearrangement of hydrogen bonds between nucleobases could easily reach its limit, that is, maximum 12 bases could be conceived following this rule, and not all of them could be replicated efficiently by enzymes [39].

Hirao, Yokoyama, and their coworkers started from the nonstandard hydrogen-bonding strategy at first, developing **x** and **y** (Fig. 3.5d) as a complementary and replicable pair [83]. A serial of modifications and accommodations were conducted in order to increase the duplex stability and incorporation efficiency, generating base pair of **s** and **z** (Fig. 3.5e), however end up without satisfactory results [84, 85]. Then, they shifted attention to the strategy of exploiting hydrophobicity and stacking interaction, by designing new base (**Pa**, Fig. 3.5f) to be paired with **Q** base developed by Kool's group [86]. And coincidently, they found **Pa** could be paired with **s** also, which pair has higher efficiency compared to the precedent **s**-**z** pair [87, 88]. After another several years of unremitting efforts, the structures were optimized to generate the pair of **Ds** and **Px** (Fig. 3.5g), which was reported that they could be incorporated by Deep Vent DNA polymerase (exo^+) with selectivity of over 99.9 % [89].

Romesburg and colleagues also developed their expanded genetic systems. In 1999, they reported the hydrophobic self-paired **PICS** base (Fig. 3.5h), which was believed to be as stable as G:C pair in duplex DNA [90, 91]. Similarly, due to their hydrophobic stacking ability, this self-paired base could be replicated by KF exo^- polymerase with reasonable efficiency. Another four self-paired bases (**3MN** [91, 92], **SNICS** [93], **7AI** [94], and **3FB** [95], Fig. 3.5i–l) were also developed with incorporation efficiency to a certain extent.

Then, they shifted the way of thinking, and a combinatorial chemistry method was utilized to screen nucleobase pairs for efficient replication [96]. Consequently, following the rule of hydrophobicity, more than 60 base analogues were synthesized and screened for KF exo^- extension. A pair of nucleobases, **SICS** and **MMO2** (Fig. 3.5m), who exhibited the best efficiency and selectivity, was successfully obtained. On basis of structure of **MMO2**, the **5SICS**-**NaM** and **5SICS**-**DMD** (Fig. 3.5n, o) pairs were finally developed [97, 98]. In a newly published work, they applied the **5SICS**-**NaM** pair into the E.coli, proving that the replication could be efficiently achieved in biological system [42].

3.2.3.2 First Example of In Vitro Selection Using Expanded Genetic Alphabets

It was not until 2013 did researches first report utilizing expanded genetic systems for in vitro selection [33]. Hirao and his colleagues have incorporated his **dDs** deoxynucleoside into the DNA library and performed the SELEX experiment to generated aptamers targeting VEGF-165 and IFN-γ with better affinity than what people developed using natural RNA.

Due to the lack of deep sequencing technology for their artificial nucleobase, there were some modifications on most of these SELEX protocol (Fig. 3.6). At first, for each randomized region, only 1-3 **Ds** could be introduced, and it has to be on some predetermined position, and a short tag sequence will be appended. Secondly, the **Ds** has to be allocated several nucleotides away instead of consecutively or closely in consideration of polymerization efficiency. Thirdly, in the PCR amplification, besides natural dNTPs and **dDsTP**, triphosphate of **Px** pairing with **Ds** also needs to be added into the reaction to amplify the **Ds** contained template. And finally, after enrichment of those **Ds** contained DNA, a replacement PCR needed to

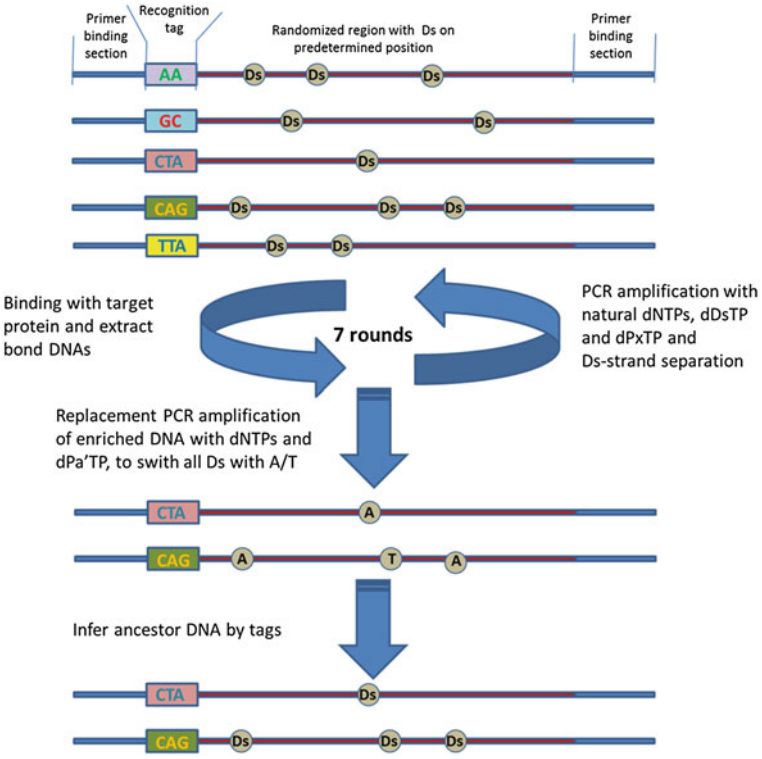

Fig. 3.6 Schematic of in vitro selection using **D**s as the fifth nucleotide. Adapted from Kimoto et al. [33]

be run to switch all **Ds** into either A or T, and after deep sequencing the **Ds** contained sequences will be inferred based on the tag information.

In spite of its success as the first ever use expanded genetic alphabets to do in vitro selection, this method still have lots of room to be improved. As mentioned before, to successfully exploit an unnatural DNA into SELEX experiment, a delicate deep sequencing method should have been established beforehand. To put the artificial base on predetermined position will undoubtedly reduce the randomization effect of the library and thus make the mimicking evolution process less powerful. Besides, only adding one nucleobase into the library cannot help much about the increase of the information density, it is more like an extension of those adding functional group strategies.

However, this example still shows us a lot of potential and sheds light on the future of applying expanded genetic alphabets. After all, the survivors after over 100 round of PCR can still maintain the expanded genetic alphabets. And the high affinity brought by introducing the well-designed fifth 'letter' largely demonstrated what expanded genetic systems can do and how to do it. This work proved the power of synthetic biology and also contributed hugely on the development of SELEX technique.

3.3 AEGIS System and Application in Cell-SELEX

Hirao and his colleagues' work is exciting and it is definitely a milestone in the development of expanded genetic systems. However, they can hardly be called as a complete SELEX. The deep sequencing technology needs to be well developed; the **Ds** and/or **Px** have to be proved to be sustained in closer distance in the evolution process; and only if both complementary bases are added into library could it truly improve SELEX, in terms of increasing information density and chemical diversity.

To date, there is only one pair of expanded nucleotides toward which a deep sequencing method has been reported, along with the solid synthesis technology and PCR amplification technology. This pair is two members of AEGIS developed by Benner and his coworkers [39, 76]. And our collaborative team has been utilizing this system in our cell-SELEX practice and generated a panel of DNA aptamers binding to several kinds of cancer cells. In this section, we will specifically introduce AEGIS system and its application in cell-SELEX. One of our recent work will be presented as an example.

3.3.1 Artificial Expanded Genetic Information Systems

The development of AEGIS was inspired by recognizing that two natural nucleobase pairs (G:C and A:T or U) have not fully exploited all possible hydrogen-bonding patterns (Fig. 3.7). To rearrange hydrogen bond donors and acceptors

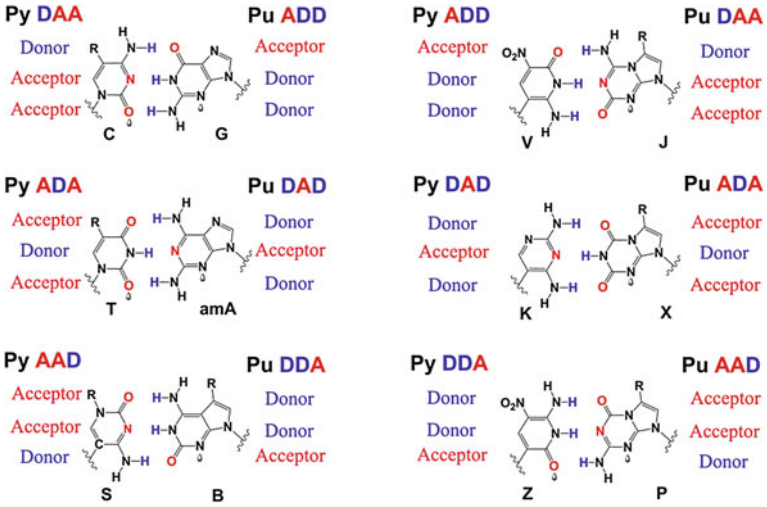

Fig. 3.7 AEGIS system (py stands for pyrimidine, pu stands for purine, A stands for hydrogen bond acceptors, and D stands for hydrogen bond donors)

between nucleotide bases with the help of synthetic chemistry can increase the number of independently replicable nucleosides, from 4 to at most 12 [76]. The hydrogen-bonding pattern assigned to each nucleobase pair is unique and distinguishable that allow the 12 bases to form a system to support the basic DNA properties, that is, to be complemented, to be copied, and, more importantly, to be evolved. At the same time by introducing those much of unnatural nucleotides, the information density will be increased dramatically [39]. We mentioned in last section that the **isoG** and **isoC** pair, as well as **X** and **K** pair developed by Benner group are the prototypes of the current members of AEGIS system. And no doubtfully this system will be kept improving to meet the potential different requirements. As it developed, now the second generation of AEGIS system has overcome these potential tautomerization problems and can carry additional functional groups on those unnatural nucleotides (R group shown in Fig. 3.7). This is to combine the strengths of strategy of adding functionality and the strategy of introducing new nucleotides. AEGIS are now being applied as orthogonal binding elements for human disease diagnosis, including FDA-approved assays for HIV, hepatitis B, and hepatitis C viruses [99].

Among the AEGIS system members, a pair of nucleotides, (2-amino-8-(1′-β-D-2-deoxyribofuranosyl)-imidazo[1,2-a]-1,3,5-triazin-4(8H)one, trivially known as **P**, and 6-amino-5-nitro-3-(1′-β-D-2′-deoxyribofuranosyl)-2(1H)-pyridone, trivially known as **Z**) [100, 101] (Fig. 3.7), were found to be highly suitable for being incorporated into cell-SELEX experiment.

3.3.2 AEGIS Cell-SELEX

The confidence of incorporating **Z** and **P** into cell-SELEX experiment attributes to the successful development of a series of molecular biology technologies: (1) synthesis of DNA libraries containing **Z** and **P** nucleotides together with four natural nucleotides [100], (2) highly efficient PCR amplification of DNA sequences containing **Z** and **P** [102], and (3) deep sequencing of DNA molecule survivors after the evolution process [103]. As mentioned in previous sections, these three key technologies determine whether a designed expanded genetic system can be used for in vitro evolution or not. Based on those fundamental technologies, we have tried multiple AEGIS cell-SELEX on different target cells. In this book, we will cite one of these examples to illustrate the SELEX process [79].

3.3.2.1 Design and Synthesis of AEGIS DNA Primers and Library

The purpose of cell-AEGIS-SELEX is to screen six-letter DNA sequences capable of recognizing and binding to the target cells in the natural state. To achieve this goal, two 16-mer primers were designed with the following principles: unlikely to form intramolecular hairpin structure, similar melting temperature (Tm) between two primers, and unlikely to form neither self-dimer nor hetero-dimer. No artificial bases were included in the primer part. The forward primer was labeled with Fluorescein isothiocyanate (FITC) at the 5′ end, and the reverse primer was labeled with biotin at the 5′ end.

A GACTZP DNA library having a 20-nucleotide random region flanked by two primer binding segments (each 16 nt) was prepared by solid-phase phosphoramidite DNA synthesis. Each of the 20 randomized sites was synthesized to have all six (GACTZP) phosphoramidites in equal amounts (Table 3.1). The presence of **Z** and **P** in the random region was confirmed by digestion of the GACTZP library, with the nucleotide fragments being quantitated by HPLC.

We could do some simple calculations to show the diversity increased by adding new nucleotides. If only four natural nucleotides were involved in 20-nt-long randomized region, the number of all possible sequence would be 4^{20} (1.099×10^{12}). If two more nucleotides added, this number will increases to 6^{20}

Table 3.1 GACTZP DNA library, 6-nucleotide PCR primers, and barcoded primers for deep sequencing

Name	Sequence
Initial GACTZP DNA library	5′-TCCCGAGTGACGCAGC-(N)20-GGACACGGTGGCTGAC-3′ N = A, G, C, T, Z, and P nucleotides mixture
Forward primer	5′-FITC-TCCCGAGTGACGCAGC-3′
Reverse primer	3′-CCTGTGCCACCGACTG- biotin-5′

(3.656×10^{15}), which is 3,000 times more possibilities. When we use longer randomized region, this ratio could be even larger.

3.3.2.2 AEGIS Cell-SELEX Generates GACTZP Aptamers

The procedure for AEGIS cell-SELEX is shown schematically in Fig. 3.8. As a proof of concept, we did not add the counter-selection in this experiment. The aptamers were expected to be generated faster but with less specificity. A breast cancer cell line MDA-MB-231 (from ATCC) was used as the target cell for the positive selection.

In the in vitro selection experiment, an aliquot of the six-letter ssDNA library (20 nmol) was first denatured by heating at 85 °C (different from standard SELEX using 95 °C, to prevent unnatural nucleotides from damage). It was then 'snap cooled' to force the DNA sequences to form their kinetically most accessible secondary structures, incubated with target cells and those binding sequences will be extracted and amplified. These steps followed the protocol of standard cell-SELEX [104].

The enriched GACTZP were amplified by six-nucleotide PCR using Taq polymerase [102, 103] (Table 3.2). Note that we used much larger amount of Taq polymerase and much longer elongation time compared to what were used

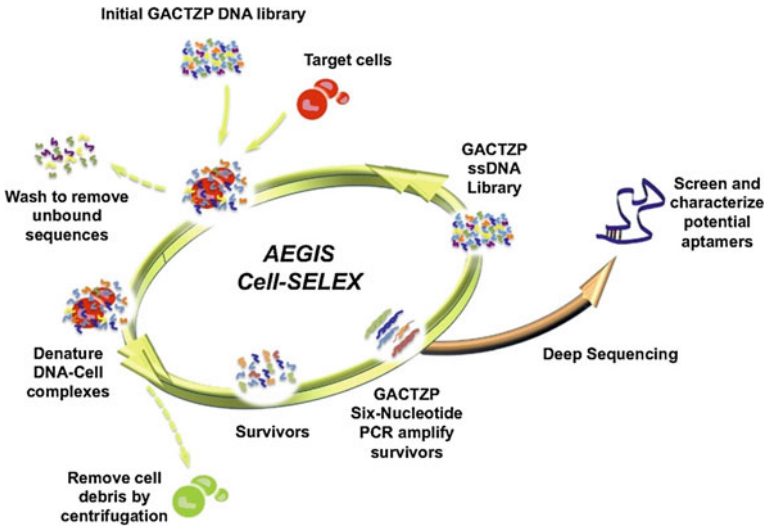

Fig. 3.8 Schematic of AEGIS cell-SELEX process. Reprinted from Ref. [79] by permission of PNAS

Table 3.2 Typical six-nucleotide PCR amplification of GACTZP DNA library

Reagents	Volume (μL)	Final concentration
ddH_2O	30.5	
Forward and reverse primers mixture (each 10 μM)	2.5	0.5 μM
Six-Nucleotide Mix of 10x	5.0	0.1 mM of each
dA,T,G/TPs (1 mM of each)		0.2 mM
dCTP (2 mM)		0.1 mM
dZTP (1 mM)		0.6 mM
dPTP (6 mM)		
10x TaKaRa PCR buffer (pH = 8.3)	5.0	1x
GACTZP DNA library (survivors)	5.0	(10 % of reaction volume)
Takara Taq HS DNA polymerase (5 U/μL)	2	0.10 (U/μL)
Total volume (uL)	50.0	

Note 1x ThermoPol Reaction Buffer (20 mM Tris-HCl, 10 mM $(NH4)2SO_4$, 10 mM KCl, 2 mM $MgSO_4$, 0.1 % Tritonx-100, pH 8.0 at 25 °C); PCR cycling conditions: one cycle of 94 °C for 1 min; 8 cycles–25 cycles of (94 °C for 20 s, 55 °C for 30 s, 72 °C for 5 min); 72 °C for 10 min; 4 °C for extended times
Reprinted with the permission from Ref. [79]. Copyright 2014 National Academy of Sciences, USA

in standard PCR protocol. The polymerase will amplify those standard DNA nucleotides much faster than unnatural ones, larger concentration of polymerase, and longer elongation time will allow polymerase to sufficiently amplify unnatural DNA.

The rest of the selection process is similar to what we used in the standard protocol. A total of 12 rounds of selection were performed. The stringency of the selection was increased in later rounds by decreasing the number cells and the incubation times. Starting from the 9th round, the progress of the selection was monitored by monitoring the ability of the FITC labeled library to fluorescently label individual cells (Fig. 3.9).

It is interesting to find out that the fluorescence intensity keep increasing from rounds 9 to 11 rounds, however back shift in round 12. We assume the reason is

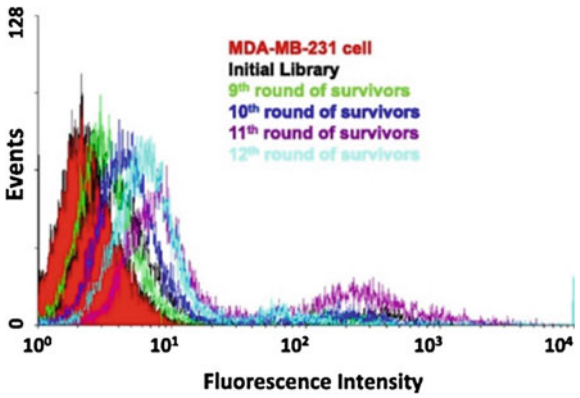

Fig. 3.9 Monitoring the progress of GACTZP AEGIS cell–SELEX using flow cytometer. Reprinted from Ref. [79] by permission of PNAS

dZ-and **dP-**contained DNA were kept losing in the PCR process, although they were supposed to be enriched in the selection process. The selection was then stopped at round 12, and the library from round 11 was prepared for deep sequencing.

3.3.2.3 Deep Sequencing of GACTZP Survivors Using NextGen Sequencing Technology

One of the most advantages that AEGIS has over other artificial genetic system is the well-developed deep sequencing technology. The emerging next-generation sequencing technology provided the chance to identify every single sequence in the enriched pool, avoiding miss any potential aptamer candidate and also avoiding the complicated cloning operation. It is indeed a huge improvement to develop corresponding deep sequencing technology for **Z** and **P** pair, which distinguishes it from others to be used in the in vitro selection process.

We will introduce here briefly about this method. It wisely exploits the strategy that the **Z** and **P** could be directionally controlled to be converted into corresponding natural bases [103]. After conversion, the common deep sequencing methods could be used for the sequencing. Then, the ancestral sequences will be inferred based on the conversion information used. To assure the accuracy of the sequencing, two of the conversion protocols were established and they are usually conducted in parallel (Fig. 3.9). Specifically, in the first protocol, sites holding **Z** and **P** nucleotides in the GACTZP survivors were converted predominantly into sites holding C and G nucleotides, respectively; less than 15 % were other nucleotides. Under the second conversion protocol, sites holding **Z** were converted to sites holding a mixture of C and T, with their ratio lying between 60:40 and 40:60, depending on the sequence surrounding that site. Sites holding **P** is converted to a mixture of G and A with roughly the same range of ratios, again depending on the sequence context surrounding that site.

In this specific SELEX, survivors enriched after 12 rounds of AEGIS-SELEX were divided into two equal portions. These were separately converted by barcoded copying into standard DNA using two conversion protocols. Following conversion, two barcoded samples were combined and submitted for Ion Torrent 'next generation' sequencing. A software was coded to cluster sequenced DNA and infer the ancestral sequences contained **Z** and/or **P** based on the information of conversion strategy. The clustered sequences obtained under the first conversion conditions (Z–C and P–G) serve as reference for the clustered sequences obtained under the second conversion conditions. Sites where C and T were found in approximately equal amounts after conversion under the second conditions were assigned as **Z** in their 'parent.' Sites where G and A were found in approximately equal amounts after conversion under the second conditions were assigned as **P** in their 'parent.' The inferred ancestral sequences were aligned to identify candidate aptamers.

Honestly, this is not a straightforward method as it took complicated steps to do these conversions and even need the help of computer software to run the inference.

However, using this deep sequencing method does help to truly apply expanded genetic systems in the selection process. Compared to Hirao's work mentioned in previous section, now the artificial bases do not have to be put in predetermined positions. This allowed the maximum chemical diversity to be achieved, as well as the pairing of nucleotides to form more complex secondary structures.

3.3.2.4 Characterization of Selected Aptamer

In this specific work, according to the alignment result, the most enriched sequence has around 30 % of populations in the whole pool (ZAP-2012: 5′-TCC CGA GTG ACG CAG CCC CCG G**Z**G GGA TT**P** ATC GGT GGA CAC GGT GGC TGA C-3′). And this very sequence has very strong binding signal on flow cytometry as well as satisfactory affinity according to the low disassociation constant. As expected, it does not have very good specificity as only positive selection was conducted.

In this aptamer we selected, only one **Z** and one **P** are contained. Given the six nucleotides were synthesized equally in amount in the randomized region, it might arouse the skepticism that **Z** and **P** play less important role in the binding process. However, if think about over 200 rounds of PCR performed in the selection process, using the polymerase which has been evolved for billions of years to accept natural nucleobases, this results should be quite gratifying. Those DNA containing only GCAT will be enriched much faster than DNA containing full six letters. And **Z** and **P** tend to keep being lost in the amplification process, resulting in the rare **Z** and **P** present in the winning aptamers.

To show that the AEGIS nucleotides were essential for binding in aptamers, we tried to synthesize those analogs where Z and P are replaced by natural nucleotides. It turned out that in all cases, the binding abilities were largely diminished (Fig. 3.10). We still do not fully understand the role that **Z** and **P** are playing in the aptamer binding process; however, at least we have the clue that they are indispensable (Fig. 3.11).

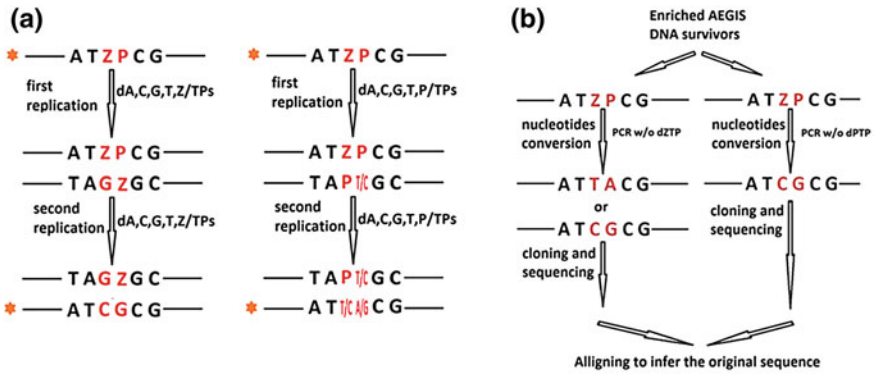

Fig. 3.10 Schematics to show the strategy of sequencing six-letter DNA sequence

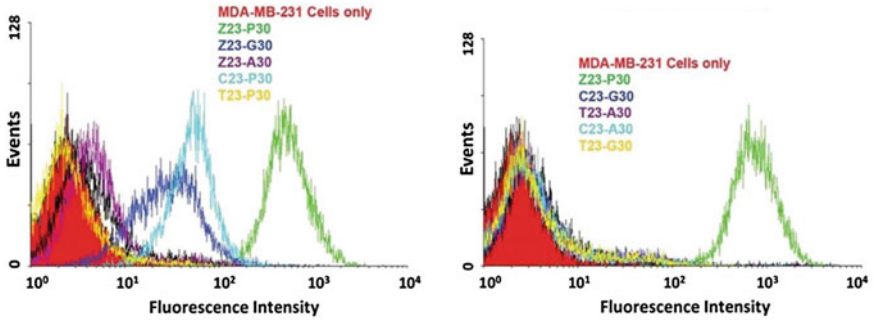

Fig. 3.11 Binding of analogs of aptamer ZAP-2012 with **Z** and **P** replaced by standard nucleotides. Reprinted from Ref. [79] by permission of PNAS

3.3.2.5 Other SELEXs Using AEGIS Nucleotides

This work is the first example of AEGIS cell-SELEX. It is actually first experiment ever to perform a complete in vitro selection using artificial bases exactly following the principle of SELEX. Even though the aptamer we obtained from this work might not have broad application due to its lack of specificity, it proved the concept. We have used this strategy to successfully overcome some very challenging targets. For example, we generated aptamers binding to liver cancer cells, lung cancer cells, and several proteins (data not published). Unlike in this work, only one aptamer carrying only one **Z** and one **P** is recovered; in other cases, we have obtained those aptamers containing 1–4 **Z** and/or **P**, with some of them very close or even adjacent to each other. This method is now becoming a routine method in aptamer generation and could be applied for a wider range of targets.

3.4 Perspective

Modified library and corresponding SELEX have been utilized effectively to generate aptamers with high affinity and specificity for almost two decades. The natural shortages of natural DNA have been largely covered by chemical method. And aptamers with endowed stability, functionality, and diversity are kept being generated using those modified libraries. With all these successful examples of modification achieved by our brilliant scientists, it seems researchers have sufficient reasons to be proud of what we have done. However, our understanding of aptamers and their interactions with their targets are far away from maturation.

Conversely, the studies of unnatural DNA and its application are still on the stage of infant. One can imagine the final goal of researchers is to find a way to generate the aptamers 'on demand.' That means, whenever people need an aptamers binding to whatever target, there is always a method to generate such aptamers in a quick and efficient, maybe also economic way. Those targets could include tumor

sample of individual patient, a mutant Ebola virus, or a new emerged water pollutant. Of course, those aptamers on demand cannot be designed, at least not before human fully understanding every single detail of biological systems. The in vitro selection might be still the only method to generate those aptamers in a long period in future.

The direction and requirements for the development of SELEX are clear. Whether those requirements can be fully fulfilled by effort of chemists is still worth exploring. On one hand, we keep trying to improve our unnatural DNA to accommodate the practical requirement. On the other hand, which is perhaps more important, in the process of improving and testing our modification, the understanding of biology is accumulating. This is the true genius of synthetic biology, which is a subject that requires understanding of biology to synthetically improve or even mimic it and at the same time using synthetic method to understand more about biology [39, 105].

Particularly in the synthetic of unnatural DNA, what we need is larger diversity, more efficient enzyme incorporation, and detail understanding of mechanism of how these unnatural DNAs interact with targets. Obviously, these future goals have to be achieved by involvement of not only organic chemist, but also collaboration of molecular biologists, physical chemists, microbiologist, and a lot of specialist from all other areas. Only if all of these happen, could the aptamers truly rival antibodies and serve better for human community.

References

1. Tuerk C, Gold L (1990) Systematic evolution of ligands by exponential enrichment: RNA ligands to bacteriophage T4 DNA polymerase. Science 249(4968):505–510
2. Ellington AD, Szostak JW (1990) In vitro selection of RNA molecules that bind specific ligands. Nature 346(6287):818–822. doi:10.1038/346818a0
3. Robertson DL, Joyce GF (1990) Selection in vitro of an RNA enzyme that specifically cleaves single-stranded DNA. Nature 344(6265):467–468. doi:10.1038/344467a0
4. Tolle F, Mayer G (2013) Dressed for success—applying chemistry to modulate aptamer functionality. Chem Sci 4(1):60–67. doi:10.1039/C2sc21510a
5. Jayasena SD (1999) Aptamers: an emerging class of molecules that rival antibodies in diagnostics. Clin Chem 45(9):1628–1650
6. Famulok M (1999) Oligonucleotide aptamers that recognize small molecules. Curr Opin Struct Biol 9(3):324–329. doi:10.1016/S0959-440x(99)80043-8
7. Gopinath SC (2007) Methods developed for SELEX. Anal Bioanal Chem 387(1):171–182. doi:10.1007/s00216-006-0826-2
8. Sun W, Du L, Li M (2010) Aptamer-based carbohydrate recognition. Curr Pharm Des 16 (20):2269–2278
9. Shangguan D, Li Y, Tang Z, Cao ZC, Chen HW, Mallikaratchy P, Sefah K, Yang CJ, Tan W (2006) Aptamers evolved from live cells as effective molecular probes for cancer study. Proc Natl Acad Sci USA 103(32):11838–11843. doi:10.1073/pnas.0602615103
10. Sefah K, Bae KM, Phillips JA, Siemann DW, Su Z, McClellan S, Vieweg J, Tan W (2013) Cell-based selection provides novel molecular probes for cancer stem cells. Int J Cancer 132 (11):2578–2588. doi:10.1002/ijc.27936

11. Van Simaeys D, Turek D, Champanhac C, Vaizer J, Sefah K, Zhen J, Sutphen R, Tan W (2014) Identification of cell membrane protein stress-induced phosphoprotein 1 as a potential ovarian cancer biomarker using aptamers selected by cell systematic evolution of ligands by exponential enrichment. Anal Chem 86(9):4521–4527. doi:10.1021/ac500466x
12. Jimenez E, Sefah K, Lopez-Colon D, Van Simaeys D, Chen HW, Tockman MS, Tan W (2012) Generation of lung adenocarcinoma DNA aptamers for cancer studies. PLoS ONE 7 (10):e46222. doi:10.1371/journal.pone.0046222
13. Mitchell P, Annemans L, White R, Gallagher M, Thomas S (2011) Cost effectiveness of treatments for wet age-related macular degeneration. Pharmacoeconomics 29(2):107–131. doi:10.2165/11585520-000000000-00000
14. Hamula CLA, Guthrie JW, Zhang HQ, Li XF, Le XC (2006) Selection and analytical applications of aptamers. Trac-Trends Anal Chem 25(7):681–691. doi:10.1016/j.trac.2006.05.007
15. Li N, Ebright JN, Stovall GM, Chen X, Nguyen HH, Singh A, Syrett A, Ellington AD (2009) Technical and biological issues relevant to cell typing with aptamers. J Proteome Res 8 (5):2438–2448. doi:10.1021/Pr801048z
16. Proske D, Blank M, Buhmann R, Resch A (2005) Aptamers—basic research, drug development, and clinical applications. Appl Microbiol Biotechnol 69(4):367–374. doi:10.1007/s00253-005-0193-5
17. King DJ, Ventura DA, Brasier AR, Gorenstein DG (1998) Novel combinatorial selection of phosphorothioate oligonucleotide aptamers. Biochemistry 37(47):16489–16493. doi:10.1021/bi981780f
18. Koshkin AA, Singh SK, Nielsen P, Rajwanshi VK, Kumar R, Meldgaard M, Olsen CE, Wengel J (1998) Locked Nucleic Acids (LNA): synthesis of the adenine, cytosine, guanine, 5-methylcytosine, thymine and uracil bicyclonucleoside monomers, oligomerisation, and unprecedented nucleic acid recognition. Tetrahedron 54(14):3607–3630. doi:10.1016/S0040-4020(98)00094-5
19. Koshkin AA, Rajwanshi VK, Wengel J (1998) Novel convenient syntheses of LNA [2.2.1] bicyclo nucleosides. Tetrahedron Lett 39(24):4381–4384. doi:10.1016/S0040-4039(98)00706-0
20. Wang RW, Zhu GZ, Mei L, Xie Y, Ma HB, Ye M, Qing FL, Tan WH (2014) Automated modular synthesis of aptamer-drug conjugates for targeted drug delivery. J Am Chem Soc 136(7):2731–2734. doi:10.1021/Ja4117395
21. Mallikaratchy P, Tang Z, Kwame S, Meng L, Shangguan D, Tan W (2007) Aptamer directly evolved from live cells recognizes membrane bound immunoglobin heavy mu chain in Burkitt's lymphoma cells. Mol Cell Proteomics 6(12):2230–2238. doi:10.1074/mcp.M700026-MCP200
22. Keefe AD, Pai S, Ellington A (2010) Aptamers as therapeutics. Nat Rev Drug Discovery 9 (7):537–550. doi:10.1038/nrd3141
23. Ng EW, Shima DT, Calias P, Cunningham ET Jr, Guyer DR, Adamis AP (2006) Pegaptanib, a targeted anti-VEGF aptamer for ocular vascular disease. Nat Rev Drug Discovery 5 (2):123–132. doi:10.1038/nrd1955
24. Jellinek D, Green LS, Bell C, Janjic N (1994) Inhibition of receptor binding by high-affinity RNA ligands to vascular endothelial growth factor. Biochemistry 33(34):10450–10456
25. Ruckman J, Green LS, Beeson J, Waugh S, Gillette WL, Henninger DD, Claesson-Welsh L, Janjic N (1998) 2′-Fluoropyrimidine RNA-based aptamers to the 165-amino acid form of vascular endothelial growth factor (VEGF165): inhibition of receptor binding and VEGF-induced vascular permeability through interactions requiring the exon 7-encoded domain. J Biol Chem 273(32):20556–20567
26. Carrigan MA, Ricardo A, Ang DN, Benner SA (2004) Quantitative analysis of a RNA-cleaving DNA catalyst obtained via in vitro selection. Biochemistry 43(36):11446–11459. doi:10.1021/Bi049898l

27. Hollenstein M, Hipolito CJ, Lam CH, Perrin DM (2009) A self-cleaving DNA enzyme modified with amines, guanidines and imidazoles operates independently of divalent metal cations (M-2). Nucleic Acids Res 37(5):1638–1649. doi:10.1093/Nar/Gkn1070
28. Kraemer S, Vaught JD, Bock C, Gold L, Katilius E, Keeney TR, Kim N, Saccomano NA, Wilcox SK, Zichi D, Sanders GM (2011) From SOMAmer-based biomarker discovery to diagnostic and clinical applications: a SOMAmer-based, streamlined multiplex proteomic assay. PLoS ONE 6(10):e26332. doi:10.1371/journal.pone.0026332
29. Vaught JD, Bock C, Carter J, Fitzwater T, Otis M, Schneider D, Rolando J, Waugh S, Wilcox SK, Eaton BE (2010) Expanding the chemistry of DNA for in vitro selection. J Am Chem Soc 132(12):4141–4151. doi:10.1021/ja908035g
30. Gold L, Ayers D, Bertino J, Bock C, Bock A, Brody EN, Carter J, Dalby AB, Eaton BE, Fitzwater T, Flather D, Forbes A, Foreman T, Fowler C, Gawande B, Goss M, Gunn M, Gupta S, Halladay D, Heil J, Heilig J, Hicke B, Husar G, Janjic J, Jarvis T, Jennings S, Katilius E, Keeney TR, Kim N, Koch TH, Kraemer S, Kroiss L, Le N, Levine D, Lindsey W, Lollo B, Mayfield W, Mehan M, Mehler R, Nelson SK, Nelson M, Nieuwlandt D, Nikrad M, Ochsner U, Ostroff RM, Otis M, Parker T, Pietrasiewicz S, Resnicow DI, Rohloff J, Sanders G, Sattin S, Schneider D, Singer B, Stanton M, Sterkel A, Stewart A, Stratford S, Vaught JD, Vrkljan M, Walker JJ, Watrobka M, Waugh S, Weiss A, Wilcox SK, Wolfson A, Wolk SK, Zhang C, Zichi D (2010) Aptamer-based multiplexed proteomic technology for biomarker discovery. PLoS ONE 5(12):e15004. doi:10.1371/journal.pone.0015004
31. Zichi D, Eaton B, Singer B, Gold L (2008) Proteomics and diagnostics: let's get specific, again. Curr Opin Chem Biol 12(1):78–85. doi:10.1016/j.cbpa.2008.01.016
32. Kimoto M, Cox RS 3rd, Hirao I (2011) Unnatural base pair systems for sensing and diagnostic applications. Expert Rev Mol Diagn 11(3):321–331. doi:10.1586/erm.11.5
33. Kimoto M, Yamashige R, Matsunaga K, Yokoyama S, Hirao I (2013) Generation of high-affinity DNA aptamers using an expanded genetic alphabet. Nat Biotechnol 31(5):453–457. doi:10.1038/nbt.2556
34. Henry AA, Romesberg FE (2003) Beyond A, C, G and T: augmenting nature's alphabet. Curr Opin Chem Biol 7(6):727–733
35. Keefe AD, Cload ST (2008) SELEX with modified nucleotides. Curr Opin Chem Biol 12 (4):448–456. doi:10.1016/j.cbpa.2008.06.028
36. Kuwahara M, Sugimoto N (2010) Molecular evolution of functional nucleic acids with chemical modifications. Molecules 15(8):5423–5444. doi:10.3390/molecules15085423
37. Piccirilli JA, Krauch T, Moroney SE, Benner SA (1990) Enzymatic incorporation of a new base pair into DNA and RNA extends the genetic alphabet. Nature 343(6253):33–37. doi:10.1038/343033a0
38. Benner SA, Allemann RK, Ellington AD, Ge L, Glasfeld A, Leanz GF, Krauch T, MacPherson LJ, Moroney S, Piccirilli JA et al (1987) Natural selection, protein engineering, and the last riboorganism: rational model building in biochemistry. Cold Spring Harb Symp Quant Biol 52:53–63
39. Benner SA, Yang ZY, Chen F (2011) Synthetic biology, tinkering biology, and artificial biology: what are we learning? C R Chim 14(4):372–387. doi:10.1016/j.crci.2010.06.013
40. Moran S, Ren RX, Kool ET (1997) A thymidine triphosphate shape analog lacking Watson-Crick pairing ability is replicated with high sequence selectivity. Proc Natl Acad Sci USA 94 (20):10506–10511
41. Moran S, Ren RX, Rumney S, Kool ET (1997) Difluorotoluene, a nonpolar isostere for thymine, codes specifically and efficiently for adenine in DNA replication. J Am Chem Soc 119(8):2056–2057. doi:10.1021/ja963718g
42. Malyshev DA, Dhami K, Lavergne T, Chen T, Dai N, Foster JM, Correa IR Jr, Romesberg FE (2014) A semi-synthetic organism with an expanded genetic alphabet. Nature 509 (7500):385–388. doi:10.1038/nature13314
43. Betz K, Malyshev DA, Lavergne T, Welte W, Diederichs K, Dwyer TJ, Ordoukhanian P, Romesberg FE, Marx A (2012) KlenTaq polymerase replicates unnatural base pairs by inducing a Watson-Crick geometry. Nat Chem Biol 8(7):612–614. doi:10.1038/Nchembio.966

44. Burmeister PE, Lewis SD, Silva RF, Preiss JR, Horwitz LR, Pendergrast PS, McCauley TG, Kurz JC, Epstein DM, Wilson C, Keefe AD (2005) Direct in vitro selection of a 2′-O-methyl aptamer to VEGF. Chem Biol 12(1):25–33. doi:10.1016/j.chembiol.2004.10.017
45. Eulberg D, Klussmann S (2003) Spiegelmers: biostable aptamers. ChemBioChem 4 (10):979–983. doi:10.1002/cbic.200300663
46. Lin Y, Qiu Q, Gill SC, Jayasena SD (1994) Modified RNA sequence pools for in-vitro selection. Nucleic Acids Res 22(24):5229–5234. doi:10.1093/nar/22.24.5229
47. Huang Y, Eckstein F, Padilla R, Sousa R (1997) Mechanism of ribose 2′-group discrimination by an RNA polymerase. Biochemistry 36(27):8231–8242. doi:10.1021/bi9626741
48. Burmeister PE, Wang C, Killough JR, Lewis SD, Horwitz LR, Ferguson A, Thompson KM, Pendergrast PS, McCauley TG, Kurz M, Diener J, Cload ST, Wilson C, Keefe AD (2006) 2′-Deoxy purine, 2′-O-methyl pyrimidine (dRmY) aptamers as candidate therapeutics. Oligonucleotides 16(4):337–351. doi:10.1089/oli.2006.16.337
49. Jellinek D, Green LS, Bell C, Lynott CK, Gill N, Vargeese C, Kirschenheuter G, McGee DP, Abesinghe P, Pieken WA et al (1995) Potent 2′-amino-2′-deoxypyrimidine RNA inhibitors of basic fibroblast growth factor. Biochemistry 34(36):11363–11372
50. O'Connell D, Koenig A, Jennings S, Hicke B, Han HL, Fitzwater T, Chang YF, Varki N, Parma D, Varki A (1996) Calcium-dependent oligonucleotide antagonists specific for L-selectin. Proc Natl Acad Sci USA 93(12):5883–5887
51. Pagratis NC, Bell C, Chang YF, Jennings S, Fitzwater T, Jellinek D, Dang C (1997) Potent 2′-amino-, and 2′-fluoro-2′-deoxyribonucleotide RNA inhibitors of keratinocyte growth factor. Nat Biotechnol 15(1):68–73. doi:10.1038/nbt0197-68
52. Lin Y, Nieuwlandt D, Magallanez A, Feistner B, Jayasena SD (1996) High-affinity and specific recognition of human thyroid stimulating hormone (hTSH) by in vitro-selected 2′-amino-modified RNA. Nucleic Acids Res 24(17):3407–3414
53. Wiegand TW, Williams PB, Dreskin SC, Jouvin MH, Kinet JP, Tasset D (1996) High-affinity oligonucleotide ligands to human IgE inhibit binding to Fc epsilon receptor I. J Immunol 157 (1):221–230
54. Kubik MF, Bell C, Fitzwater T, Watson SR, Tasset DM (1997) Isolation and characterization of 2′-fluoro-, 2′-amino-, and 2′-fluoro-/amino-modified RNA ligands to human IFN-gamma that inhibit receptor binding. J Immunol 159(1):259–267
55. Rusconi CP, Scardino E, Layzer J, Pitoc GA, Ortel TL, Monroe D, Sullenger BA (2002) RNA aptamers as reversible antagonists of coagulation factor IXa. Nature 419(6902):90–94. doi:10.1038/nature00963
56. Biesecker G, Dihel L, Enney K, Bendele RA (1999) Derivation of RNA aptamer inhibitors of human complement C5. Immunopharmacology 42(1–3):219–230
57. White R, Rusconi C, Scardino E, Wolberg A, Lawson J, Hoffman M, Sullenger B (2001) Generation of species cross-reactive aptamers using "toggle" SELEX. Mol Ther J Am Soc Genet Ther 4(6):567–573. doi:10.1006/mthe.2001.0495
58. Davis KA, Lin Y, Abrams B, Jayasena SD (1998) Staining of cell surface human CD4 with 2′-F-pyrimidine-containing RNA aptamers for flow cytometry. Nucleic Acids Res 26 (17):3915–3924
59. Richardson FC, Zhang C, Lehrman SR, Koc H, Swenberg JA, Richardson KA, Bendele RA (2002) Quantification of 2′-fluoro-2′-deoxyuridine and 2′-fluoro-2′-deoxycytidine in DNA and RNA isolated from rats and woodchucks using LC/MS/MS. Chem Res Toxicol 15 (7):922–926
60. Richardson FC, Tennant BC, Meyer DJ, Richardson KA, Mann PC, McGinty GR, Wolf JL, Zack PM, Bendele RA (1999) An evaluation of the toxicities of 2′-fluorouridine and 2′-fluorocytidine-HCl in F344 rats and woodchucks (Marmota monax). Toxicol Pathol 27 (6):607–617
61. Lato SM, Ozerova ND, He K, Sergueeva Z, Shaw BR, Burke DH (2002) Boron-containing aptamers to ATP. Nucleic Acids Res 30(6):1401–1407

62. Kang J, Lee MS, Copland JA 3rd, Luxon BA, Gorenstein DG (2008) Combinatorial selection of a single stranded DNA thioaptamer targeting TGF-beta1 protein. Bioorg Med Chem Lett 18(6):1835–1839. doi:10.1016/j.bmcl.2008.02.023
63. Kang J, Lee MS, Watowich SJ, Gorenstein DG (2007) Combinatorial selection of a RNA thioaptamer that binds to venezuelan equine encephalitis virus capsid protein. FEBS Lett 581 (13):2497–2502. doi:10.1016/j.febslet.2007.04.072
64. Kato Y, Minakawa N, Komatsu Y, Kamiya H, Ogawa N, Harashima H, Matsuda A (2005) New NTP analogs: the synthesis of 4′-thioUTP and 4′-thioCTP and their utility for SELEX. Nucleic Acids Res 33(9):2942–2951. doi:10.1093/nar/gki578
65. Klussmann S, Nolte A, Bald R, Erdmann VA, Furste JP (1996) Mirror-image RNA that binds D-adenosine. Nat Biotechnol 14(9):1112–1115. doi:10.1038/nbt0996-1112
66. Nolte A, Klussmann S, Bald R, Erdmann VA, Furste JP (1996) Mirror-design of L-oligonucleotide ligands binding to L-arginine. Nat Biotechnol 14(9):1116–1119. doi:10.1038/nbt0996-1116
67. Szeitner Z, Lautner G, Nagy SK, Gyurcsanyi RE, Meszaros T (2014) A rational approach for generating cardiac troponin I selective spiegelmers. Chem Commun 50(51):6801–6804. doi:10.1039/c4cc00447g
68. Leva S, Lichte A, Burmeister J, Muhn P, Jahnke B, Fesser D, Erfurth J, Burgstaller P, Klussmann S (2002) GnRH binding RNA and DNA spiegelmers: a novel approach toward GnRH antagonism. Chem Biol 9(3):351–359
69. Latham JA, Johnson R, Toole JJ (1994) The application of a modified nucleotide in aptamer selection: novel thrombin aptamers containing 5-(1-pentynyl)-2′-deoxyuridine. Nucleic Acids Res 22(14):2817–2822
70. Bock LC, Griffin LC, Latham JA, Vermaas EH, Toole JJ (1992) Selection of single-stranded DNA molecules that bind and inhibit human thrombin. Nature 355(6360):564–566. doi:10.1038/355564a0
71. Battersby TR, Ang DN, Burgstaller P, Jurczyk SC, Bowser MT, Buchanan DD, Kennedy RT, Benner SA (1999) Quantitative analysis of receptors for adenosine nucleotides obtained via in vitro selection from a library incorporating a cationic nucleotide analog. J Am Chem Soc 121(42):9781–9789
72. Vaish NK, Larralde R, Fraley AW, Szostak JW, McLaughlin LW (2003) A novel, modification-dependent ATP-binding aptamer selected from an RNA library incorporating a cationic functionality. Biochemistry 42(29):8842–8851. doi:10.1021/bi027354i
73. Masud MM, Kuwahara M, Ozaki H, Sawai H (2004) Sialyllactose-binding modified DNA aptamer bearing additional functionality by SELEX. Bioorg Med Chem 12(5):1111–1120. doi:10.1016/j.bmc.2003.12.009
74. Shoji A, Kuwahara M, Ozaki H, Sawai H (2007) Modified DNA aptamer that binds the (R)-isomer of a thalidomide derivative with high enantioselectivity. J Am Chem Soc 129 (5):1456–1464. doi:10.1021/ja067098n
75. Hollenstein M, Hipolito CJ, Lam CH, Perrin DM (2013) Toward the combinatorial selection of chemically modified DNAzyme RNase A mimics active against all-RNA substrates. ACS Comb Sci 15(4):174–182. doi:10.1021/co3001378
76. Benner SA (2004) Understanding nucleic acids using synthetic chemistry. Acc Chem Res 37 (10):784–797. doi:10.1021/ar040004z
77. Hirao I, Kimoto M, Yamashige R (2012) Natural versus artificial creation of base pairs in DNA: origin of nucleobases from the perspectives of unnatural base pair studies. Acc Chem Res 45(12):2055–2065. doi:10.1021/ar200257x
78. Hirao I, Kimoto M (2012) Unnatural base pair systems toward the expansion of the genetic alphabet in the central dogma. Proc Jpn Acad Ser B Phys Biol Sci 88(7):345–367
79. Sefah K, Yang Z, Bradley KM, Hoshika S, Jimenez E, Zhang L, Zhu G, Shanker S, Yu F, Turek D, Tan W, Benner SA (2014) In vitro selection with artificial expanded genetic information systems. Proc Natl Acad Sci USA 111(4):1449–1454. doi:10.1073/pnas.1311778111

80. Switzer C, Moroney SE, Benner SA (1989) Enzymatic incorporation of a new base pair into DNA and RNA. J Am Chem Soc 111(21):8322–8323. doi:10.1021/Ja00203a067
81. Morales JC, Kool ET (1998) Efficient replication between non-hydrogen-bonded nucleoside shape analogs. Nat Struct Biol 5(11):950–954. doi:10.1038/2925
82. Morales JC, Kool ET (1999) Minor groove interactions between polymerase and DNA: more essential to replication than Watson-Crick hydrogen bonds? J Am Chem Soc 121(10):2323–2324. doi:10.1021/ja983502+
83. Ohtsuki T, Kimoto M, Ishikawa M, Mitsui T, Hirao I, Yokoyama S (2001) Unnatural base pairs for specific transcription. Proc Natl Acad Sci USA 98(9):4922–4925. doi:10.1073/pnas.091532698
84. Hirao I, Ohtsuki T, Fujiwara T, Mitsui T, Yokogawa T, Okuni T, Nakayama H, Takio K, Yabuki T, Kigawa T, Kodama K, Yokogawa T, Nishikawa K, Yokoyama S (2002) An unnatural base pair for incorporating amino acid analogs into proteins. Nat Biotechnol 20(2):177–182. doi:10.1038/nbt0202-177
85. Hirao I, Harada Y, Kimoto M, Mitsui T, Fujiwara T, Yokoyama S (2004) A two-unnatural-base-pair system toward the expansion of the genetic code. J Am Chem Soc 126(41):13298–13305. doi:10.1021/ja047201d
86. Mitsui T, Kitamura A, Kimoto M, To T, Sato A, Hirao I, Yokoyama S (2003) An unnatural hydrophobic base pair with shape complementarity between pyrrole-2-carbaldehyde and 9-methylimidazo[(4,5)-b]pyridine. J Am Chem Soc 125(18):5298–5307. doi:10.1021/ja028806h
87. Kimoto M, Mitsui T, Harada Y, Sato A, Yokoyama S, Hirao I (2007) Fluorescent probing for RNA molecules by an unnatural base-pair system. Nucleic Acids Res 35(16):5360–5369. doi:10.1093/nar/gkm508
88. Hikida Y, Kimoto M, Yokoyama S, Hirao I (2010) Site-specific fluorescent probing of RNA molecules by unnatural base-pair transcription for local structural conformation analysis. Nat Protoc 5(7):1312–1323. doi:10.1038/nprot.2010.77
89. Kimoto M, Kawai R, Mitsui T, Yokoyama S, Hirao I (2009) An unnatural base pair system for efficient PCR amplification and functionalization of DNA molecules. Nucleic Acids Res 37(2):e14. doi:10.1093/nar/gkn956
90. McMinn DL, Ogawa AK, Wu YQ, Liu JQ, Schultz PG, Romesberg FE (1999) Efforts toward expansion of the genetic alphabet: DNA polymerase recognition of a highly stable, self-fairing hydrophobic base. J Am Chem Soc 121(49):11585–11586. doi:10.1021/Ja9925150
91. Ogawa AK, Wu YQ, McMinn DL, Liu JQ, Schultz PG, Romesberg FE (2000) Efforts toward the expansion of the genetic alphabet: Information storage and replication with unnatural hydrophobic base pairs. J Am Chem Soc 122(14):3274–3287. doi:10.1021/Ja9940064
92. Ogawa AK, Wu YQ, Berger M, Schultz PG, Romesberg FE (2000) Rational design of an unnatural base pair with increased kinetic selectivity. J Am Chem Soc 122(36):8803–8804. doi:10.1021/Ja001450u
93. Yu C, Henry AA, Romesberg FE, Schultz PG (2002) Polymerase recognition of unnatural base pairs. Angew Chem 41(20):3841–3844. doi:10.1002/1521-3773(20021018)41:20<3841:AID-ANIE3841>3.0.CO;2-Q
94. Wu YQ, Ogawa AK, Berger M, McMinn DL, Schultz PG, Romesberg FE (2000) Efforts toward expansion of the genetic alphabet: optimization of interbase hydrophobic interactions. J Am Chem Soc 122(32):7621–7632. doi:10.1021/Ja0009931
95. Matsuda S, Leconte AM, Romesberg FE (2007) Minor groove hydrogen bonds and the replication of unnatural base pairs. J Am Chem Soc 129(17):5551–5557. doi:10.1021/ja068282b
96. Leconte AM, Hwang GT, Matsuda S, Capek P, Hari Y, Romesberg FE (2008) Discovery, characterization, and optimization of an unnatural base pair for expansion of the genetic alphabet. J Am Chem Soc 130(7):2336–2343. doi:10.1021/ja078223d
97. Malyshev DA, Seo YJ, Ordoukhanian P, Romesberg FE (2009) PCR with an expanded genetic alphabet. J Am Chem Soc 131(41):14620–14621. doi:10.1021/ja906186f

98. Malyshev DA, Pfaff DA, Ippoliti SI, Hwang GT, Dwyer TJ, Romesberg FE (2010) Solution structure, mechanism of replication, and optimization of an unnatural base pair. Chemistry 16 (42):12650–12659. doi:10.1002/chem.201000959
99. Arens MQ, Buller RS, Rankin A, Mason S, Whetsell A, Agapov E, Lee WM, Storch GA (2010) Comparison of the eragen multi-code respiratory virus panel with conventional viral testing and real-time multiplex PCR assays for detection of respiratory viruses. J Clin Microbiol 48(7):2387–2395. doi:10.1128/JCM.00220-10
100. Yang ZY, Hutter D, Sheng PP, Sismour AM, Benner SA (2006) Artificially expanded genetic information system: a new base pair with an alternative hydrogen bonding pattern. Nucleic Acids Res 34(21):6095–6101. doi:10.1093/Nar/Gkl633
101. Yang ZY, Sismour AM, Sheng PP, Puskar NL, Benner SA (2007) Enzymatic incorporation of a third nucleobase pair. Nucleic Acids Res 35(13):4238–4249. doi:10.1093/Nar/Gkm395
102. Yang Z, Chen F, Chamberlin SG, Benner SA (2010) Expanded genetic alphabets in the polymerase chain reaction. Angew Chem 49(1):177–180. doi:10.1002/anie.200905173
103. Yang Z, Chen F, Alvarado JB, Benner SA (2011) Amplification, mutation, and sequencing of a six-letter synthetic genetic system. J Am Chem Soc 133(38):15105–15112. doi:10.1021/ja204910n
104. Sefah K, Shangguan D, Xiong X, O'Donoghue MB, Tan W (2010) Development of DNA aptamers using cell-SELEX. Nat Protoc 5(6):1169–1185. doi:10.1038/nprot.2010.66
105. Benner SA, Sismour AM (2005) Synthetic biology. Nat Rev Genet 6(7):533–543. doi:10.1038/nrg1637

Chapter 4
Cell-Specific Aptamer Characterization

Tao Chen, Cuichen Wu and Weihong Tan

Abstract The functional diversity of cell-specific aptamers has enabled their use for a broad spectrum of biomedical applications. A thorough characterization of aptamers would provide better and deeper understanding and facilitate the development of customized aptamer-based diagnostics and therapeutics with enhanced performance. In this chapter, key properties of cell-specific aptamers and their characterization are discussed.

Keywords Aptamer · Characterization · Binding affinity · Binding site density · Binding site distance · Binding strength

4.1 Introduction

Humans recognize objects and experience events by seeing, hearing, tasting, touching, and smelling (five senses). All these senses are inseparably interconnected and complementary to each other, providing comprehensive information to distinguish

T. Chen
Genentech Inc., 1 DNA Way, South San Francisco, CA 94080, USA

C. Wu · W. Tan
Center for Research at Bio/Nano Interface, Department of Chemistry and Department of Physiology and Functional Genomics, Shands Cancer Center, UF Genetics Institute and McKnight Brain Institute, University of Florida, Gainesville, FL 32611-7200, USA

W. Tan (✉)
Molecular Sciences and Biomedicine Laboratory, State Key Laboratory for Chemo/Biosensing and Chemometrics, College of Biology and College of Chemistry and Chemical Engineering, Collaborative Innovation Center for Chemistry and Molecular Medicine, Hunan University, Changsha 410082, People's Republic of China
e-mail: tan@chem.ufl.edu

W. Tan and X. Fang (eds.), *Aptamers Selected by Cell-SELEX for Theranostics*,
DOI 10.1007/978-3-662-46226-3_4

one thing from another. For example, to the eye, water and vinegar are both clear solutions, but the senses of taste or smell can certainly tell them apart.

Similarly, researchers understand aptamers by characterizing their critical properties (for conciseness, aptamers in this chapter refer to cell-specific aptamers unless stated otherwise). Even though a large quantity of aptamers has been selected against various cell lines, especially cancer cells, characterization of these aptamers is often restricted to binding affinity measurements, which fail to present a complete picture. In this chapter, we will describe aptamer binding affinity and its measurements. In addition, we will also discuss other key properties that help to define aptamers, including binding density, binding site distance, and binding strength, as well as the determination of these important parameters.

4.2 Aptamer Binding Affinity Measurements

4.2.1 Dissociation Constant (K_d)

The binding affinity of aptamers to their corresponding targets is typically evaluated by the dissociation constant (K_d), an equilibrium constant that assesses the tendency of an aptamer–target complex to dissociate into separate components (aptamer and target molecule on the cell surface). The dissociation constant is the inverse of the association constant (K_a), a mathematical constant that describes the binding affinity between aptamer and target molecules at equilibrium.

For a simple binding equilibrium between aptamer and target with a 1:1 stoichiometry, Eq. (1):

$$Aptamer + Target \rightleftharpoons Complex \tag{1}$$

The equilibrium can be described using the K_d in Eq. (2), where [Aptamer], [Target], and [Complex] are the concentrations of aptamer, target molecule, and aptamer–target complex, respectively.

$$K_d = \frac{[Aptamer][Target]}{[Complex]} \tag{2}$$

The dissociation constant has molarity unit, and the value of K_d can be understood as the aptamer concentration at which the concentration of target with aptamer bound equals the concentration of target without aptamer bound. Similar to interactions between antibody and antigen, a lower K_d value indicates tighter binding between the aptamer and its related target. For example, thrombin has two specific binding aptamers (15-mer and 29-mer), and the binding affinity of 29-mer aptamer (K_d = 0.5 nM) is much stronger than that of the 15-mer (K_d = ~100 nM) [1].

4.2.2 Methods for K_d Measurement

4.2.2.1 Methods Involving Physical Separation

The determination of K_d is usually performed with a fixed concentration of either the aptamer or target molecule and an elevated amount of the other component to achieve a binding equilibrium. Although it is difficult to specify a general way to determine every target/aptamer binding constant, the most common methods involve separation-based techniques, such as high-performance liquid chromatography (HPLC), capillary electrophoresis (CE), equilibrium dialysis, ultrafiltration, and gel electrophoresis. Due to the different interactions of free aptamer, target molecule, and aptamer–target complex with the stationary phase in liquid chromatography, zone separations can be used to calculate the equilibrium distribution of free aptamer, target, and aptamer–target complex [2]. Multiple chromatographic separation options are available to isolate the free aptamer from the aptamer–target complex, including size exclusion chromatography (SEC) and internal surface reversed-phase chromatography (ISRP) [3, 4]. However, the separation time (10–30 min/sample) and relatively high K_d (10^{-6} M) needed for accurate measurements limit the applicability of the method. Similar to HPLC, CE isolates the mixture of the bound and unbound aptamers by size and charge in an electric field. The merits of CE include both small sample volumes ($\sim$10 μL), and the improved separation speed and efficiency by using Joule heating [5]. Both dialysis and ultrafiltration separate the free aptamer from the aptamer–target complex based on size differentiation. Dialysis is applicable only for large targets (e.g., cells) because unbound aptamers, which are small in comparison, need to diffuse into the other compartment cell via a semipermeable membrane. The concentrations of free aptamer at different target concentrations are then calculated in the other dialysis compartment after equilibrium, resulting in the determination of K_d. Dialysis is a simple technique for K_d measurement, but it also suffers from experimental complications, such as long incubation time ($\sim$48 h), large volume environment, and nonspecific adsorption [6].

By using pressure, vacuum, or centrifugal force, the method of ultrafiltration can retain the aptamer–target complex in the membrane, allowing the equilibrium distribution to be measured for various concentrations of target [7]. The nitrocellulose membrane and "dot blot" apparatus are the most widely used components for ultrafiltration due to the capability to control both the pore sizes (as small as $\sim$2 kDa) and the degree of hydrophobic adsorption, as well as the minimal couple quantities required [8]. Other merits of nitrocellulose-based ultrafiltration are fast speed ($\sim$5 min/sample), high sensitivity (radioactive labeling allows pM K_d detection limits), and low cost. However, one major concern of this method is the incomplete retention of the aptamer–target complex by the nitrocellulose membrane, resulting in an overestimated K_d. Nonspecific adsorption of aptamer to the membrane is another problem leading to unreliable issues [9–11].

Due to the intermediate electrophoretic mobility of the aptamer–target complex compared to the polyanionic aptamer or the less charged target cell surface, gel

electrophoresis is a simple and straightforward separation method for determination of K_d with high sensitivity (0.1 pM K_d limit of detection) and low cost [12]. However, the long separation time ($\sim$3 h/sample) needs to be considered for association and dissociation rates of aptamer–target complex as well as gel casting and visualization [13].

4.2.2.2 Spectroscopic Methods

Other techniques widely used for K_d determination are spectroscopy-based measurements, including measurement of fluorescence intensity, fluorescence polarization, UV–Vis absorption, and circular dichroism (CD). Fluorescence methods measure the degree of emission increase or quenching of the aptamer upon target binding, which allows the determination of K_d in different buffer conditions without concern for the association or dissociation rates between aptamer and target [14]. Moreover, the experimental time of fluorescence methods is much shorter than the time for separation-based approaches, and the labeling of aptamers with fluorophores is a well-established technique [15, 16]. However, the fluorescence intensity and quantum yield of labeled dyes can be influenced by the microenvironment of the aptamer and target before and after binding, especially the fluorescence energy transfer during the binding process. One solution for this issue is the use of molecular aptamer beacons, in which the conformational change induces a fluorescent intensity difference. Unfortunately, not all aptamers can be designed to form the molecular beacons [17]. In fluorescence anisotropy, linearly polarized excitation light is used, and the vertical and horizontal components of the emitted light, I_v and I_h, are measured and used to calculate the polarization (P) [Eq. (3)], or the anisotropy (ε) [Eq. (4)].

$$P = \frac{I_v - I_h}{I_v + I_h} \tag{3}$$

$$\varepsilon = \frac{I_v - I_h}{I_v + 2I_h} \tag{4}$$

These quantities are highly dependent on the size of the fluorophore due to notational difference. If the aptamers are labeled, P and ε change exponentially upon binding to the cell. It is critical to choose a fluorophore whose lifetime matches its rotation rate [18].

UV–Vis spectroscopy also provides a simple, low cost, and label-free method to measure aptamer binding affinity. The maximum absorption of aptamer is the DNA occurs at $\lambda_{max} \sim 260$ nm. Thus, any change of the absorbance or λ_{max} induced by aptamer–target binding can be used to assess the K_d. However, UV–Vis absorption is not suitable for low K_d measurements ($\sim$μM K_d limit) [19]. CD is a powerful tool providing structural information of nucleic acids because of the differential absorption of left and right circularly polarized light by aptamers and targets; thus,

CD spectra may indicate a conformation change after the binding between aptamer and target, which can be used to determine their K_d value [20]. Although the signal change is not significant upon binding, due to the requirement of a high sample concentration (10^{-5} M), this technique still has merits in providing information of stoichiometry and conformational change [21].

4.2.2.3 Mass-Based and Other Methods

Mass-sensitive surface-based methods are also useful in certain types of aptamer K_d determinations. For example, the surface plasmon resonance (SPR) measures the differences of surface refractive index and the related resonance signal upon binding of the target to an aptamer immobilized on a metal film [22]. SPR is a label-free detection method to obtain both thermodynamic and kinetic information in a short time ($\sim$20 min), but requires a longer immobilization procedure (up to 3 h) [23, 24]. Another label-free method utilizes quartz crystal microbalance (QCM), in which the change in resonance frequency of a piezoelectric crystal is related to the mass accumulated from aptamer–target binding on the surface [25].

Isothermal titration calorimetry (ITC) is an alternative and accurate tool for the determination of not only K_d, but also the stoichiometry and thermodynamic parameters (ΔH^o and ΔS^o) of aptamer–target complex formation. ITC is a label-free and precise method to measure aptamer binding affinity [26]. Other methods, such as high-throughput affinity quantitative polymerase chain reaction (PCR) binding assay, in-line probing, and footprinting assays, are all recently emerging approaches to assess the equilibrium K_d of aptamer binding [27–29].

4.2.2.4 K_d Determination of Cell-Specific Aptamers

In cell selection or target molecules modified in carrier, flow cytometry provides a rapid and efficient platform to measure binding affinities. In particular, the mean fluorescence intensity of target cells bound to labeled aptamers is used to calculate the specific binding by subtracting the mean fluorescence intensity of nonspecific binding from unselected library DNAs [30, 31]. The equilibrium K_d of the aptamer–cell interaction is obtained by fitting the dependence of fluorescence intensity of specific binding on the concentration of the aptamers to Eq. (5) [32]

$$Y = B_{max} \frac{X}{K_d + X} \tag{5}$$

where Y, B_{max}, and X are the fluorescence intensity, maximum fluorescence intensity, and aptamer concentration, respectively.

Fluorescence correlation spectroscopy (FCS) is a bioanalytical tool for investigation of aptamer binding affinity at molecular level. Since the molecular interaction between cell membrane receptor and its aptamer can be directly observed with

FCS, the aptamer concentration that saturates the receptor binding sites can be used to calculate K_d of the aptamer for specific type of cancer cell. For example, when various concentrations of fluorescein isothiocyanate (FITC)-labeled sgc8 aptamers are incubated with HeLa cells, the different diffusion times of bound versus free aptamers can be used to assess the percentage of bound aptamer, followed by yielding the absolute number of total aptamers inside the confocal volume. A picomolar range dissociation constant (K_d = 790 ± 150 pM) of sgc8 aptamer has been measured for HeLa cells, which is in good agreement with the result determined by flow cytometry (K_d = 810 pM) [33].

4.2.3 K_d of Cell-Specific Aptamers Versus Antibodies

The K_ds of aptamers and antibodies to the surface biomarker of tumors usually vary, but are comparable and in the range of nM–pM. The K_d comparison between aptamers and antibodies for several common tumor biomarkers is shown in Table 4.1. The binding affinity parameters can be controlled on demand during selection of aptamers, but it is difficult to modify affinity parameters for antibodies [34].

4.3 Aptamer Binding Density Measurements

4.3.1 Significance of Aptamer Binding Density

Cellular membranes create an environment where many complicated enzymatic reactions and biochemical signaling procedures occur, such as the transportation of molecules into and out of cells and the conversion of metabolic energies into osmotic and electrical work. None of these physiological activities can be initiated or proceeded without the help of cellular membrane receptors. In other words, the specific ligand–receptor interactions embedded in lipid bilayer structure of the cellular membrane are the most significant source for the discovery, design, and screening of new therapeutic targets and drugs [35]. The specific binding of extracellular ligands to cellular receptors could provide researchers with ample information on cellular activities and their responses to the environment. Aptamers, which target cellular membrane surface biomarkers, are considered to be better molecular probes for surface biomarkers discovery compared to antibody-based recognition. This is due to the higher binding affinity (low K_d), specificity, and increased tumor penetration associated with the small size of aptamers, as well as the potentially reduced immunogenicity [32, 33, 36]. The density investigation of cellular receptors provided by the binding events of aptamers to specific receptors can help us to gain insight into membrane receptor characteristics, expression levels, and spatial distribution on the molecular level, as well as receptor clustering and molecular changes in living biological specimens.

Table 4.1 Comparison of binding affinity between aptamers and antibodies for cancer cell biomarkers

Biomarker	Expressed tumors	Antibody K_d (nM)	Aptamer K_d (nM)
Epithelial cell adhesion molecule (EpCAM)	Bladder, breast, colon, esophagus, lung, hepatocellular, ovarian, pancreas, prostate, etc.	0.2 [53]	22.8 [54]
Human epidermal growth factor 2 (HER2)	Breast, gastric, lung, bladder, colorectal, esophageal, ovarian cancers, etc.	0.56 [55]	18.9 [56]
IL-6 receptor (CD126)	Colon, ovarian and pancreatic cancers, multiple myeloma, hepatocellular carcinoma, etc.	5.5 [57]	20 [58]
Integrin $\alpha 3\beta\gamma$	Breast, pancreatic, leukemia, prostate, colorectal cancers, sarcoma, etc.	3.1 [59]	2 [60]
Mucin 1 (MUC1)	Ovarian, breast, lung, pancreatic cancer, prostate adenocarcinoma, multiple myeloma, etc.	1.7 [61]	0.135 [62]
Platelet derived growth factor receptor (PDGF-R)	Gastrointestinal stromal tumors, leukemia, multiple myeloma, dermatofibrosarcoma, melanoma, glioblastoma, etc.	0.9 [63]	0.1 [64]
Prostate-specific membrane antigen (PSMA)	Prostate, kidney, bladder cancer, etc.	18 [65]	2.1 [66]
Protein tyrosine kinase 7 (PTK7)	T-cell acute lymphoblastic leukemia, lung, gastric cancers, colon carcinoma, etc.	50 [67]	0.8 [32]
RET receptor tyrosine kinase (RTK)	Thyroid, breast, lung cancer, etc.	8.2 [68]	35 [69]
Vascular endothelial growth factor receptor (VEGF-R)	Ovarian, breast, cervical, lung cancers, thyroid, renal cell carcinoma, etc.	0.49 [70]	0.14 [71]

4.3.2 Approaches for Aptamer Binding Density Determination

Currently, only a few approaches have been used to estimate cell membrane receptor density, including liquid scintillation counting (LSC) and fluorescence subtraction. As a standard laboratory method in life science, LSC detects the radiation from radioactive nuclides, but it requires labeling with radioactive tags [37]. Fluorescence subtraction is a common and simple fluorescence method for density determination, but requires multiple steps to remove unbound ligands. The receptor density is estimated by measuring the fluorescence intensity in the supernatant, in which the free ligand concentration is estimated from a standard linear calibration curve [38]. However, due to the shorter half-life of the receptor–ligand complex compared to the time needed to separate bound and unbound ligands, this method sometimes causes an underestimate of the receptor density. The other concern is the low expression level of some receptors and interferences from other highly expressed receptors, resulting in an undetectable specific binding [33]. Thus, the development of a highly sensitive and effective approach for direct measurement of membrane receptor density on the cellular surface without radioactive labeling or tedious separation procedures is highly desired.

4.3.2.1 Fluorescence Correlation Spectroscopy (FCS) in Aptamer Binding Density Determination

FCS is an ideal bioanalytical and biophysical tool for investigating molecular interactions and internal dynamics at nanomolar levels in living cells [39, 40]. It is capable of analyzing even minute fluorescence intensity fluctuations caused by random motions, which are detected as the molecules or cells enter and leave the instrument's femtoliter-sized, optically defined observation volume excited by a focused laser beam (<1 fL, ~250 nm in diameter). When associated with fluorescent aptamers, FCS can be used to detect membrane receptors and estimate their density in the physiological environment. Different from conventional techniques (e.g., flow cytometry) for binding measurement, FCS can obtain binding affinity and receptor density information from a small number of cells (less than 50) rather than a large population. Moreover, FCS can eliminate the washing step that is necessary in other methods, because the diffusion time of the receptor–ligand complex is differentiated from that of unbound ligand fractions.

FCS measurements are performed by focusing an excitation laser beam onto the sample, following by monitoring the fluorescence fluctuations derived within the focal region of the laser beam. The FCS instrumental setup and scheme of aptamer–cellular receptor binding events inside FCS focus are shown in Fig. 4.1 [33]. The local concentration of fluorophores changes because of their diffusion into and out of the focal volume, resulting in a spontaneous change of fluorescence intensity fluctuations. The normalized intensity autocorrelation function, $G(\tau)$, can be

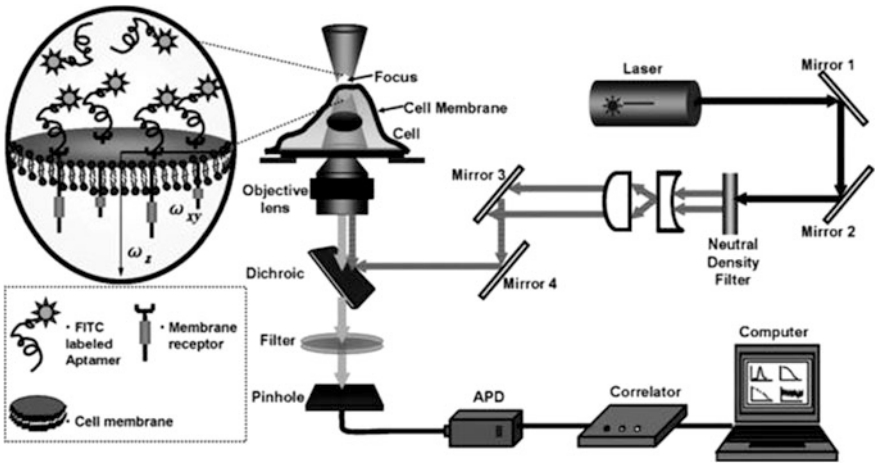

Fig. 4.1 Fluorescence correlation spectroscopy (FCS) instrumental setup and scheme of aptamer–receptor binding on the cell membrane inside the FCS focus. The enlarged diagram shows the geometry of the confocal volume with half-axes in length (ω_z) and width (ω_{xy}). Reprinted with the permission from Ref. [33]. Copyright 2009 John Wiley & Sons Ltd.

described in terms of the fluorescence intensity fluctuations at time t, $\delta I(t)$, and at time $(t + \tau)$, $\delta I(t + \tau)$, and the mean fluorescence intensity, $\langle I \rangle$ in Eq. (6).

$$G(\tau) = 1 + \frac{\langle \delta I(t)\, \delta I(t+\tau) \rangle}{\langle I \rangle^2} \tag{6}$$

The amplitude of $G(\tau)$ refers to the absolute number of molecules, N, occupying the observation volume. The mean diffusion time, τ_D, which indicates the average time for a molecule to diffuse through the observation volume, is considered as a key parameter in the FCS measurement, because free aptamers or bound aptamers on surface receptors will have different diffusion behavior. When the focal volume covers the cell surface, Eq. (6) can be converted to Eq. (7) that represents a linear combination of the autocorrelation functions of free and bound aptamers.

$$G(\tau) = \frac{1}{N}\left((1-r)\frac{1}{1+\frac{\tau}{\tau_D^{free}}}\frac{1}{\sqrt{1+\frac{\tau}{\left(\frac{\omega_z}{\omega_{xy}}\right)^2 \tau_D^{free}}}} + r\frac{1}{1+\frac{\tau}{\tau_D^{bound}}} \right) \tag{7}$$

In Eq. (7), N is the total absolute number of fluorescent molecules inside the focus, τ_D^{free} and τ_D^{bound} are the diffusion times for the free and bound labeled aptamers, and $(1 - r)$ and r are the fractions of free and bound aptamers diffusing with τ_D^{free} and τ_D^{bound}, respectively. The dimensions of the observation-volume element are defined

by the half-axes in length (ω_z) and width (ω_{xy}). Once the fluorophore-labeled aptamers in the confocal volume bind to membrane receptors, an increased diffusion time is observed in contrast to unbound free aptamers, because the specific receptor binding confines bound aptamers in the tiny focal volume. When FITC-modified sgc8 aptamers (targeting human protein tyrosine kinase-7 membrane receptor, PTK7) are used in HeLa cells, the diffusion time (τ_D) is 0.827 ms for bound aptamers, while τ_{D} free is only 0.235 ms for free aptamers, indicating that FCS can differentiate bound and free aptamers according to specific type of cancer cell (Fig. 4.2a).

The aptamer binding density can be calculated for each individual cell involved in an aptamer–receptor binding event. The absolute number of molecules, N, can be derived by fitting the autocorrelation function to a sum of bound aptamers on the membrane and free aptamers above the cell surface. The surface area on the membrane covered by the focus, in which all of the bound aptamers are located, is a circle with radius equal to ω_{xy}. Therefore, the aptamer binding density in the confocal volume can be estimated according to the total number of bound aptamers divided by the area covered as shown in Eq. 8.

$$\text{Density} = \frac{Nr}{\pi(\omega_{xy})^2} \tag{8}$$

HeLa cells were used as the model to determine sgc8 aptamer binding density on the membrane surface using Eq. 6. The 0.4 fL ellipsoid confocal volume from a 1.2 mW laser beam with half-axes of $\omega_{xy} = 0.22\,\mu\text{m}$ and $\omega_z = 1.56\,\mu\text{m}$ was projected onto each cell membrane. The circular area covered by the focus volume was estimated to be $\pi \times (\omega_{xy})^2 = \pi \times (0.22\,\mu\text{m})^2 = 0.15\,\mu\text{m}^2$. As determined from a previous binding affinity study, a 3.0 nM concentration of FITC-sgc8 can saturate all of the PTK7 binding sites on HeLa cells. Autocorrelation curves were obtained from the membranes of 50 individual cells, and an average of $N \times r = 84$ bound sgc8 aptamers was obtained with a variation of ±14, indicating that around 84

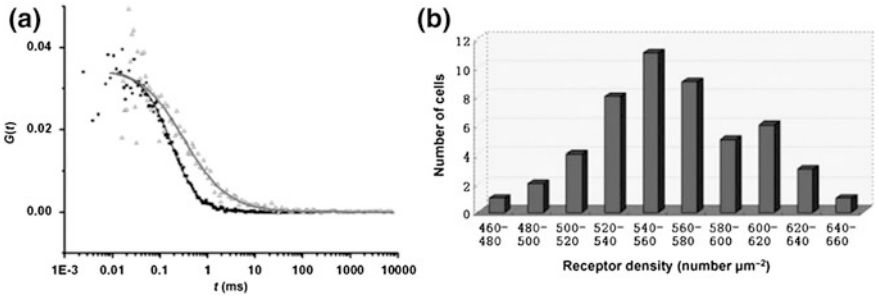

Fig. 4.2 **a** Autocorrelation functions of aptamer sgc8 (10 nM) free in solution (*black*) and aptamer sgc8 (10 nM) incubated with HeLa cells and bound to PTK7 membrane receptor on the cell surface (*gray*). **b** Distribution of PTK7 receptor density on HeLa cells, obtained from individual cell detection by using Eq. 5 (50 cells evaluated). Reprinted with the permission from Ref. [33]. Copyright 2009 John Wiley & Sons Ltd.

bound aptamers occupied the 0.15 μm^2 covered area in the confocal volume. The mean aptamer binding density on HeLa cells can be calculated by substituting these parameters into Eq. 8, to give 550 receptors/μm^2 with a variation of 90 receptors/μm^2 (Fig. 4.2b). Similarly, a higher aptamer binding density is obtained (1,300 ± 190 receptors/μm^2) on CCRF-CEM leukemia cells [33]. FCS measurement provides a simple, direct, and accurate estimation of aptamer binding density on the cellular membrane surface, which opens a door for the investigation of drug delivery and efficiency assessment in cancer therapeutics.

4.4 Aptamer Binding Site Distance Measurements

4.4.1 Receptors with Multiple Binding Sites

As emphasized above, receptors play a significant role in controlling signal transductions and modulating cellular functions. This is realized by regulatory networks created through transient or stable interactions between receptors and their ligands. The architecture of these networks exhibits a highly heterogeneous scale-free topology; i.e., most receptors have only one binding site for one ligand, whereas a few receptors have multiple binding sites for one or more ligands. For example, the sweet taste receptor, a heterodimer of two G protein (T1R2 and T1R3) coupled receptors, has at least three binding sites for different sweeteners: (1) receptor activity toward aspartame depends on residues in the amino terminal domain of T1R2; (2) receptor activity toward cyclamate depends on residues within the transmembrane domain of T1R3; and (3) receptor activity toward brazzein depends on the cysteine rich domain of T1R3 [41].

In the case of aptamers, receptors can be categorized into three types: (1) those with one aptamer binding site, which is the same as the antibody binding site; (2) those with one aptamer binding site, which is different from the antibody binding site; and (3) those with two (rarely more than two) aptamer binding sites. For the latter two types of receptors, it is important to determine the binding site distance between aptamer and antibody or between two aptamers. This binding site distance serves as another critical parameter to characterize aptamers. In addition, it also helps to better understand the interaction between aptamers and their receptors, shedding light on the design and development of high-performance (i.e., improved sensitivity and/or enhanced specificity) aptamer-based tools for cellular analysis.

4.4.2 The Determination of Binding Site Distance

Förster resonance energy transfer (FRET) is one of the most established methods for detection of both intra- and inter-molecular distances in the nanometer range for biological systems. The mechanism of FRET involves a donor fluorophore in an

excited electronic state, which may transfer its excitation energy to a nearby acceptor fluorophore (with an absorption spectrum that overlaps the emission spectrum of the donor) in a non-radiative fashion through long-range dipole–dipole interactions [42]. The FRET efficiency is inversely proportional to the sixth power of the distance between the donor and the acceptor, making FRET extremely sensitive to small changes in distance [42].

Many molecular rulers based on FRET have been developed to allow the measurement of dynamic distance changes in biological systems, in vitro as well as in vivo. Using single-molecule FRET, Blanchard et al. [43] directly monitored the time-dependent distances between donor (Cy3) and acceptor (Cy5) fluorophores attached to the elbow region of tRNA molecules on the ribosome, revealing the nature of the tRNA–ribosome interaction and providing an essential link between static structural studies of the ribosome and the mechanism of translation. Zhuang et al. explored the folding of Tetrahymena ribozyme, an intensely studied catalytic RNA of $\sim$400 nucleotides, which folds into its native structure through multiple intermediate states and pathways. Using FRET at the single-molecule level, they investigated P1 docking of ribozyme folding. According to their results, the distance between P1 and the ribozyme core decreased from $\sim$7 to 1–2 nm from the P1 undocked state to the P1 docked state, indicated by FRET values, which are different for these two distinct states [44].

In addition to FRET, localized surface plasmon resonance (LSPR) is another frequently used technique for measuring distances within biological systems. LSPR is an optical phenomena generated by a light wave trapped within conductive nanoparticles smaller than the wavelength of light. The phenomenon is a result of the interactions between the incident light and surface electrons in a conduction band [45]. This interaction produces coherent localized plasmon oscillations with a resonant frequency that strongly depends on the composition, size, geometry, dielectric environment, and particle–particle separation distance of nanoparticles [46]. Liu et al. [47] constructed an LSPR-based molecular ruler in which double-stranded DNA was attached to a gold nanoparticle, to measure nuclease activity and DNA footprinting. The change in plasmon resonance wavelength of individual gold nanoparticle-DNA conjugates depends on the length of the DNA and can be measured with subnanometer axial resolution. An average wavelength shift of approximately 1.24 nm is observed per DNA base pair.

4.4.3 Surface Energy Transfer (SET) Nanoruler for Measuring Binding Site Distances

Even though FRET and LSPR are commonly utilized for measuring the distance between two biological components, there are inherent limitations associated with each of these methods. The nature of the dipole–dipole mechanism effectively

constrains the length scales in FRET to distances on the order of <10 nm, and FRET generally poses restrictions for dipole–dipole interaction orientations [48]. LSPR performs very well in solution experiments. However, the high Raman scattering background from cells prevents LSPR applications to cellular systems (e.g., cell membranes). Bene et al. introduced a light scattering system to solve this problem. Nevertheless, this system requires close proximity (<10 nm) between the dye and the particle surface. Another issue is the need for small nanoparticles (<2 nm) due to insufficient overlap for fluorescence energy transfer and high probability of fluorescence quenching.

To overcome these limitations and construct an alternative system with large detection range and cellular system compatibility, we have developed a surface energy transfer (SET) nanoruler to measure the distance between two binding sites on membrane receptor PTK 7 [49]. SET is a dipole-SET process where energy transfer flows from a donor molecule to a nanoparticle surface at a much slower decay rate than FRET, with a $1/d$ [5] distance dependence. Although SET is similar to FRET, in that the interaction is dipole–dipole in nature, it is geometrically different from FRET, because an acceptor nanoparticle has a surface and an isotropic distribution of dipole vectors to accept energy from the donor, leading to a dipole–surface resonance mechanism. This arrangement effectively breaks the inherent detection barriers of FRET, increasing the probability of energy transfer of SET and ultimately enhancing the efficiency of SET over FRET. The validity of SET-based measurement tools for mapping distances in real biological systems has been demonstrated, showing its clear advantage over LSPR for live cell analysis.

In the effort to construct the SET nanoruler to measure the distance between two binding sites, PTK 7 highly expressed on CCRF-CEM cells was used as a proof of principle. PTK 7 receptor has two binding sites, one for sgc8 aptamer and another for anti-PTK 7 antibody. Sgc8 aptamer was selected for CCRF-CEM cells, and its molecular target on the cell membrane is the PTK 7 receptor. Gold nanoparticles were chosen as the energy acceptor and conjugated with sgc8 aptamer. Organic fluorophore Alexa Fluor 488 (Alexa488) was selected as the energy donor and modified onto anti-PTK 7 antibody. As a consequence of the co-localization of the two binding sites on PTK 7 receptor, binding of sgc8 aptamer and anti-PTK 7 antibody brought the fluorophore and gold nanoparticle into close proximity, effectively resulting in fluorescence energy transfer between them. As shown in Fig. 4.3, the distance, R, from the fluorophore on the antibody binding site to the center of the NP on the aptamer binding site, is equivalent to the distance between the two binding sites on the PTK7 receptor. In order to simplify the model, R was divided into two parts: the distance, r, from the fluorophore to the surface of the NP, and the distance from the surface of the particle to its center, which is the radius of the particle, $d/2$, with $R = r + (d/2)$. Therefore, as the size of the gold NP (d) is varied, the distance from the fluorophore to the particle surface (r) changes accordingly. Although some variations in position around the center point of the aptamer binding site can potentially occur, one million cells were counted each time

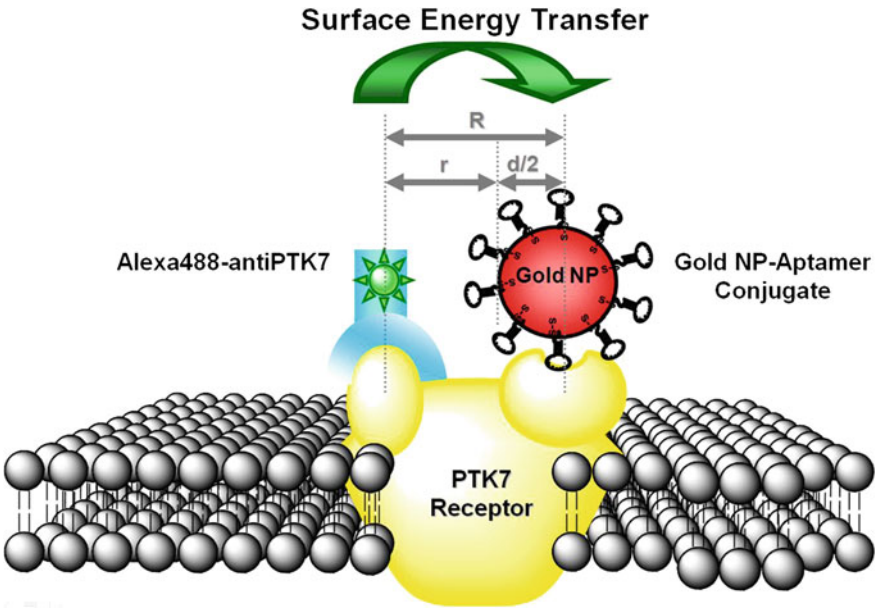

Fig. 4.3 SET nanoruler for measuring the distance between two binding sites in PTK 7 receptor on a live cell membrane. Reprinted with the permission from Ref. [49]. Copyright 2010 American Chemical Society

to cancel out these variances. In addition, a series of gold NPs of different sizes (5, 10, 13, 15, 18, 20, 25, 31, and 42 nm) were adopted to fit in the binding pockets to avoid steric effects. Therefore, by controlling the sizes of the gold NPs, the distance from the fluorophore molecule to the surface of gold NP could be manipulated, and the relationship between the size of the gold NPs and the change in the energy transfer efficiency could be evaluated.

The results of this study showed that the distance between the aptamer and antibody binding sites of PTK 7 receptor on CCRF-CEM cells in the natural physiological environment is 13.4 ± 1.4 nm (error within 10 %), which is beyond the detection capability of FRET. The SET nanoruler is more advantageous compared to LSPR in its suitability for cellular measurements. Moreover, only particles with diameter <2 nm can be used in LSPR, whereas the SET nanoruler has a much larger range for the choice of particle size. With all these built-in advantages, the SET nanoruler has the potential to become an alternative to FRET and LSPR for distance measurement, both short and long, in cellular systems. In addition, this distance can be between any two ligands/binding sites, including an aptamer and an antibody, as well as two aptamers, either the same or different.

4.5 Aptamer Binding Strength Measurements

4.5.1 AFM for Measuring Aptamer Binding Strength

Besides the binding constant, another more direct way to characterize the binding affinity between an aptamer and its target on a cell membrane is by measuring the force needed to separate the two after they bind. The larger the force needed, the higher the binding strength. In addition, the force needed is a straightforward parameter that can be used to compare the binding strengths between different aptamers as well as between aptamers and antibodies.

One of the best tools for measuring molecular forces is the atomic force microscope (AFM). This highly sensitive instrument has been designed to measure the small attractive and repulsive forces that a sharp tip experiences when it is brought near to or in contact with a surface, [50] which can include biomolecules, live cells, and bulk materials. In its simplest configuration, AFM measures the force on the sharp probe tip mounted at the end of a soft cantilever by monitoring the cantilever's deflection [51]. In addition, force sensing with high spatial resolution (atom scale) is well established for AFM, leading to its increased applications for bioanalysis and nanotechnology.

To demonstrate the concept and prove its feasibility, we used single-molecule AFM to measure the binding force between sgc8 aptamer and PTK 7 receptor [52]. As shown in Fig. 4.4a, amino-functionalized sgc8 aptamer was conjugated onto a N-hydroxysuccinimide ester (NHS)-bearing silicon nitride (Si_3N_4) tip. Instead of CCRF-CEM cells, HeLa cells (adherent cells) which also have high expression of PTK 7 receptors were used. The tip was suspended on a soft spring (also known as a soft cantilever) sensitive to small changes in forces that occur at the tip. With the

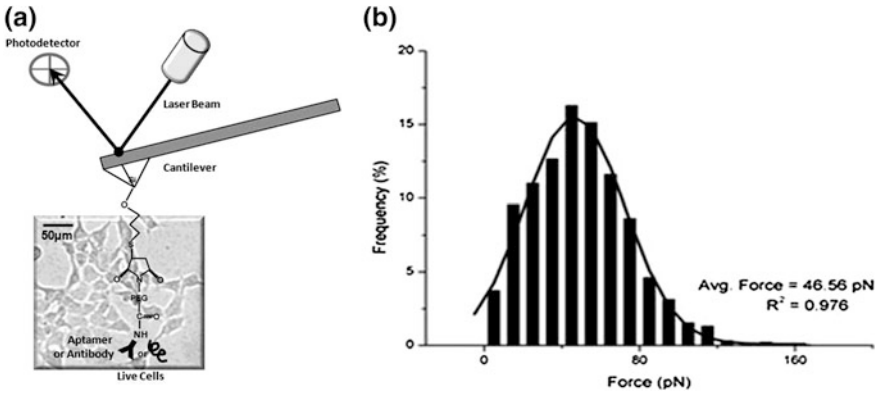

Fig. 4.4 **a** AFM for measuring the binding strength between sgc8 aptamer and PTK 7 receptor. **b** Histograms of binding forces between tips (functionalized with sgc8 aptamer) and Hela cells (highly expressed with PTK 7 receptor). Reprinted with the permission from Ref. [52]. Copyright 2012 Springer

deflection of the cantilever (denoted as x) measured by AFM and the spring constant (denoted as k) collected during tip calibration, the force between sgc8 aptamer and PTK 7 receptor was easily calculated using Hooke's law, $F = kx$.

To obtain statistical and representative data, about 1,500 force curves were recorded to construct force histograms, which were then fitted using Gaussian peak functions (Fig. 4.4b). A single standard deviation (σ) calculated from the Gaussian Curve was used to report the error. The single-molecule rupture force between sgc8 and PTK 7 receptor was found to be 46 ± 26 pN.

One more thing worth mentioning is that AFM not only provides rupture force/binding strength information, but also offers kinetic constants analysis—which reflects the stability of aptamer–receptor binding. An increase in the loading rate of AFM tip leads to a higher force between receptor and aptamer, which is directly linked to the kinetic dissociation constant (K_{off}). Enhancing the contact time between the tip and the sample allows an increase in the interaction probability, which can be related to the kinetic association constant (K_{on}).

4.5.2 Aptamers Versus Antibodies

Aptamers use 4 different nucleotides to create sequence diversity, and thus secondary/tertiary structure diversity, to recognize cell membrane receptors. These variable structures form distinct binding pockets that interact with receptors through non-covalent interactions, including hydrogen bonding, electrostatic interactions, and van der Waals forces. Antibodies are analogous to aptamers in that they also target specific receptors by non-covalent interactions using paratopes located on the extreme tips of antibodies. By contrast, the building blocks of antibody paratopes are 20 different amino acids, which generate more structural diversity.

Due to their similarity to target cell membrane receptors, yet very different structural properties, a natural question to ask is the following: "Will aptamers bind as robustly as antibodies?" To tackle this question, the binding strengths of the sgc8 aptamer–PTK 7 receptor pair and the anti-PTK 7 antibody–PTK 7 receptor pair were measured using AFM. The setup for measuring the rupture force between anti-PTK 7 antibody and PTK 7 receptor was the same as that used for sgc8 aptamer and PTK 7 receptor, except anti-PTK 7 was conjugated onto the tip. Based on these measurements, the single-molecule rupture force between anti-PTK 7 antibody and PTK 7 receptor is 68 ± 26 pN, slightly larger than that between sgc8 aptamer and PTK 7 receptor (46 ± 26 pN). Therefore, for the case of sgc8 aptamer and anti-PTK 7 antibody, the binding strengths are comparable for their common target—PTK 7 receptor. However, to draw a generalized conclusion, a large aptamer and antibody pool is needed.

4.6 Conclusion and Outlook

To accurately and precisely define cell-specific aptamers, a comprehensive characterization is required. An overall perspective will guide the selection of aptamers with improved properties and facilitate the development of aptamer-based molecular tools (especially for cell analysis) with enhanced performance. Typically, this full view of aptamers is achieved by systematically examining their critical properties, including binding affinity, binding site density, binding site distance, and binding strength. Apart from these four key parameters discussed in this chapter, other features, such as crystal structure, ion dependence, and buffer sensitivity, also contribute to the understanding of aptamers.

There are many different methods available for the determination of each property of aptamers. Therefore, it is important to choose a method that is suitable for the specific aptamer and its corresponding target. For instance, FRET is limited to short binding site distances (<10 nm), whereas SET is capable of measuring longer binding distances (>10 nm). In addition, the development of standard practices for aptamer characterization is highly desired and would have the potential to extend the application of aptamers beyond the small subset (e.g., sgc8) used in proof-of-concept.

References

1. Deng B, Lin Y, Wang C, Li F, Wang Z, Zhang H, Li X-F, Le XC (2014) Aptamer binding assays for proteins: the thrombin example—a review. Anal Chim Acta 837:1–15
2. Deng Q, German I, Buchanan D, Kennedy RT (2001) Retention and separation of adenosine and analogues by affinity chromatography with an aptamer stationary phase. Anal Chem 73 (22):5415–5421
3. Hage DS, Tweed SA (1997) Recent advances in chromatographic and electrophoretic methods for the study of drug-protein interactions. J Chromatogr B: Biomed Sci Appl 699(1–2):499–525
4. Hagestam IH, Pinkerton TC (1985) Internal surface reversed-phase silica supports for liquid chromatography. Anal Chem 57(8):1757–1763
5. Drabovich AP, Berezovski M, Okhonin V, Krylov SN (2006) Selection of smart aptamers by methods of kinetic capillary electrophoresis. Anal Chem 78(9):3171–3178
6. Cruz-Aguado JA, Penner G (2008) Determination of ochratoxin A with a DNA aptamer. J Agric Food Chem 56(22):10456–10461
7. Hall B, Arshad S, Seo K, Bowman C, Corley M, Jhaveri SD, Ellington AD (2001) In vitro selection of RNA aptamers to a protein target by filter immobilization. In: Current protocols in molecular biology. Wiley, New York
8. Ryan PC, Lu M, Draper DE (1991) Recognition of the highly conserved GTPase center of 23 S ribosomal RNA by ribosomal protein L11 and the antibiotic thiostrepton. J Mol Biol 221 (4):1257–1268
9. Carey J, Cameron V, De Haseth PL, Uhlenbeck OC (1983) Sequence-specific interaction of R17 coat protein with its ribonucleic acid binding site. Biochemistry 22(11):2601–2610

10. Hall K, Kranz J (1999) Nitrocellulose filter binding for determination of dissociation constants. In: Haynes S (ed) RNA-protein interaction protocols, vol 118. Humana Press, New York, pp 105–114
11. Oehler S, Alex R, Barker A (1999) Is nitrocellulose filter binding really a universal assay for protein–DNA interactions? Anal Biochem 268(2):330–336
12. Jaouen S, de Koning L, Gaillard C, Muselíková-Polanská E, Štros M, Strauss F (2005) Determinants of specific binding of HMGB1 protein to hemicatenated DNA loops. J Mol Biol 353(4):822–837
13. Tahiri-Alaoui A, Frigotto L, Manville N, Ibrahim J, Romby P, James W (2002) High affinity nucleic acid aptamers for streptavidin incorporated into bi-specific capture ligands. Nucleic Acids Res 30(10):e45
14. Flinders J, DeFina SC, Brackett DM, Baugh C, Wilson C, Dieckmann T (2004) Recognition of planar and nonplanar ligands in the malachite green–RNA aptamer complex. ChemBioChem 5(1):62–72
15. Nag A, Bhattacharyya K (1989) Fluorescence enhancement of p-toluidino naphthalenesulphonate in a micellar environment. J Photochem Photobiol A: Chem 47 (1):97–102
16. Nakayama K, Endo M, Fujitsuka M, Majima T (2006) Detection of the local structural changes in the dimer interface of BamHI initiated by DNA binding and dissociation using a solvatochromic fluorophore. J Phys Chem B 110(42):21311–21318
17. Tan W, Wang K, Drake TJ (2004) Molecular beacons. Curr Opin Chem Biol 8(5):547–553
18. Cruz-Aguado JA, Penner G (2008) Fluorescence polarization based displacement assay for the determination of small molecules with aptamers. Anal Chem 80(22):8853–8855
19. Guédin A, Lacroix L, Mergny J-L (2010) Thermal melting studies of ligand DNA interactions. In: Fox KR (ed) Drug-DNA interaction protocols, vol 613. Humana Press, New York, pp 25–35
20. Lin P-H, Chen R-H, Lee C-H, Chang Y, Chen C-S, Chen W-Y (2011) Studies of the binding mechanism between aptamers and thrombin by circular dichroism, surface plasmon resonance and isothermal titration calorimetry. Colloids Surf B: Biointerfaces 88(2):552–558
21. Jing M, Bowser MT (2011) Methods for measuring aptamer-protein equilibria: a review. Anal Chim Acta 686(1–2):9–18
22. Wang J, Lv R, Xu J, Xu D, Chen H (2008) Characterizing the interaction between aptamers and human IgE by use of surface plasmon resonance. Anal Bioanal Chem 390(4):1059–1065
23. Fägerstam LG, Frostell-Karlsson Å, Karlsson R, Persson B, Rönnberg I (1992) Biospecific interaction analysis using surface plasmon resonance detection applied to kinetic, binding site and concentration analysis. J Chromatogr A 597(1–2):397–410
24. Win MN, Klein JS, Smolke CD (2006) Codeine-binding RNA aptamers and rapid determination of their binding constants using a direct coupling surface plasmon resonance assay. Nucleic Acids Res 34(19):5670–5682
25. Sultan Y, Walsh R, Monreal C, DeRosa MC (2009) Preparation of functional aptamer films using layer-by-layer self-assembly. Biomacromolecules 10(5):1149–1154
26. Potty ASR, Kourentzi K, Fang H, Jackson GW, Zhang X, Legge GB, Willson RC (2009) Biophysical characterization of DNA aptamer interactions with vascular endothelial growth factor. Biopolymers 91(2):145–156
27. Yoshida W, Sode K, Ikebukuro K (2006) Homogeneous DNA sensing using enzyme-inhibiting DNA aptamers. Biochem Biophys Res Commun 348(1):245–252
28. Regulski E, Breaker R (2008) In-line probing analysis of riboswitches. In: Wilusz J (ed) post-transcriptional gene regulation, vol 419. Humana Press, New York, pp 53–67
29. Oh SS, Plakos K, Lou X, Xiao Y, Soh HT (2010) In vitro selection of structure-switching, self-reporting aptamers. Proc Nat Acad Sci 107(32):14053–14058
30. Davis KA, Abrams B, Lin Y, Jayasena SD (1996) Use of a high affinity DNA ligand in flow cytometry. Nucleic Acids Res 24(4):702–706

31. Davis KA, Abrams B, Lin Y, Jayasena SD (1998) Staining of cell surface human CD4 with 2′-F-pyrimidine-containing RNA aptamers for flow cytometry. Nucleic Acids Res 26(17):3915–3924
32. Shangguan D, Li Y, Tang Z, Cao ZC, Chen HW, Mallikaratchy P, Sefah K, Yang CJ, Tan W (2006) Aptamers evolved from live cells as effective molecular probes for cancer study. Proc Natl Acad Sci 103(32):11838–11843
33. Chen Y, Munteanu AC, Huang Y-F, Phillips J, Zhu Z, Mavros M, Tan W (2009) Mapping receptor density on live cells by using fluorescence correlation spectroscopy. Chem Eur J 15 (21):5327–5336
34. Nimjee SM, Rusconi CP, Sullenger BA (2005) Aptamers: an emerging class of therapeutics. Annu Rev Med 56(1):555–583
35. Takayama S, Shimosato H, Shiba H, Funato M, Che F-S, Watanabe M, Iwano M, Isogai A (2001) Direct ligand-receptor complex interaction controls brassica self-incompatibility. Nature 413(6855):534–538
36. Osborne SE, Ellington AD (1997) Nucleic acid selection and the challenge of combinatorial chemistry. Chem Rev 97(2):349–370
37. Colabufo NA, Berardi F, Calò R, Leopoldo M, Perrone R, Tortorella V (2001) Determination of dopamine D4 receptor density in rat striatum using PB12 as a probe. Eur J Pharmacol 427 (1):1–5
38. Huang Y-F, Chang H-T, Tan W (2008) Cancer cell targeting using multiple aptamers conjugated on nanorods. Anal Chem 80(3):567–572
39. Schwille P (2001) Fluorescence correlation spectroscopy and its potential for intracellular applications. Cell Biochem Biophys 34(3):383–408
40. Kim SA, Heinze KG, Schwille P (2007) Fluorescence correlation spectroscopy in living cells. Nat Meth 4(11):963–973
41. Cui M, Jiang P, Maillet E, Max M, Margolskee RF, Osman R (2006) The heterodimeric sweet taste receptor has multiple potential ligand binding sites. Curr Pharm Des 12(35):10
42. Zheng J (2006) Spectroscopy-based quantitative fluorescence resonance energy transfer analysis. In: Stockand JD, Shapiro MS (eds) Ion channels: methods and protocols, vol 337. Humana Press, New York
43. Blanchard SC, Kim HD, Gonzalez RL, Puglisi JD, Chu S (2004) tRNA dynamics on the ribosome during translation. Proc Natl Acad Sci USA 101(35):12893–12898
44. Zhuang X, Bartley LE, Babcock HP, Russell R, Ha T, Herschlag D, Chu S (2000) A single-molecule study of rna catalysis and folding. Science 288(5473):2048–2051
45. Willets KA, Van Duyne RP (2007) Localized surface plasmon resonance spectroscopy and sensing. Annu Rev Phys Chem 58(1):267–297
46. Petryayeva E, Krull UJ (2011) Localized surface plasmon resonance: nanostructures, bioassays and biosensing—a review. Anal Chim Acta 706(1):8–24
47. Liu GL, Yin Y, Kunchakarra S, Mukherjee B, Gerion D, Jett SD, Bear DG, Gray JW, Alivisatos AP, Lee LP, Chen FF (2006) A nanoplasmonic molecular ruler for measuring nuclease activity and DNA footprinting. Nat Nano 1(1):47–52
48. Persson BNJ, Lang ND (1982) Electron-hole-pair quenching of excited states near a metal. Phys Rev B 26(10):5409–5415
49. Chen Y, O'Donoghue MB, Huang Y-F, Kang H, Phillips JA, Chen X, Estevez MC, Yang CJ, Tan W (2010) A surface energy transfer nanoruler for measuring binding site distances on live cell surfaces. J Am Chem Soc 132(46):16559–16570
50. Stark RW (2007) Atomic force microscopy: getting a feeling for the nanoworld. Nat Nano 2 (8):461–462
51. Albers BJ, Schwendemann TC, Baykara MZ, Pilet N, Liebmann M, Altman EI, Schwarz UD (2009) Three-dimensional imaging of short-range chemical forces with picometre resolution. Nat Nano 4(5):307–310
52. O'Donoghue M, Shi X, Fang X, Tan W (2012) Single-molecule atomic force microscopy on live cells compares aptamer and antibody rupture forces. Anal Bioanal Chem 402(10):3205–3209

53. Munz M, Murr A, Kvesic M, Rau D, Mangold S, Pflanz S, Lumsden J, Volkland J, Fagerberg J, Riethmuller G, Ruttinger D, Kufer P, Baeuerle P, Raum T (2010) Side-by-side analysis of five clinically tested anti-EpCAM monoclonal antibodies. Cancer Cell Int 10(1):44
54. Song Y, Zhu Z, An Y, Zhang W, Zhang H, Liu D, Yu C, Duan W, Yang CJ (2013) Selection of DNA aptamers against epithelial cell adhesion molecule for cancer cell imaging and circulating tumor cell capture. Anal Chem 85(8):4141–4149
55. Rudnick SI, Lou J, Shaller CC, Tang Y, Klein-Szanto AJP, Weiner LM, Marks JD, Adams GP (2011) Influence of affinity and antigen internalization on the uptake and penetration of Anti-HER2 antibodies in solid tumors. Cancer Res 71(6):2250–2259
56. Liu Z, Duan J-H, Song Y-M, Ma J, Wang F-D, Lu X, Yang X-D (2012) Novel HER2 aptamer selectively delivers cytotoxic drug to HER2-positive breast cancer cells in vitro. J Transl Med 10(1):148
57. Kalai M, Montero-Julian FA, Grötzinger J, Fontaine V, Vandenbussche P, Deschuyteneer R, Wollmer A, Brailly H, Content J (1997) Analysis of the human interleukin-6/human interleukin-6 receptor binding interface at the amino acid level: proposed mechanism of interaction. Blood 89:1319–1333
58. Meyer C, Eydeler K, Magbanua E, Zivkovic T, Piganeau N, Lorenzen I, Grötzinger J, Mayer G, Rose-John S, Hahn U (2012) Interleukin-6 receptor specific RNA aptamers for cargo delivery into target cells. RNA Biol 9(1):67–80
59. Eble JA, Wucherpfennig KW, Gauthier L, Dersch P, Krukonis E, Isberg RR, Hemler ME (1998) Recombinant soluble human α3β1 integrin: purification, processing, regulation, and specific binding to laminin-5 and invasin in a mutually exclusive manner. Biochemistry 37 (31):10945–10955
60. Mi J, Zhang X, Giangrande PH, McNamara Ii JO, Nimjee SM, Sarraf-Yazdi S, Sullenger BA, Clary BM (2005) Targeted inhibition of αvβ3 integrin with an RNA aptamer impairs endothelial cell growth and survival. Biochem Biophys Res Commun 338(2):956–963
61. Lavrsen K, Madsen C, Rasch M, Woetmann A, Ødum N, Mandel U, Clausen H, Pedersen A, Wandall H (2013) Aberrantly glycosylated MUC1 is expressed on the surface of breast cancer cells and a target for antibody-dependent cell-mediated cytotoxicity. Glycoconj J 30(3):227–236
62. Ferreira CSM, Matthews CS, Missailidis S (2006) DNA aptamers that bind to MUC1 tumour marker: design and characterization of MUC1-binding single-stranded DNA aptamers. Tumor Biol 27(6):289–301
63. Fretto LJ, Snape AJ, Tomlinson JE, Seroogy JJ, Wolf DL, LaRochelle WJ, Giese NA (1993) Mechanism of platelet-derived growth factor (PDGF) AA, AB, and BB binding to alpha and beta PDGF receptor. J Biol Chem 268(5):3625–3631
64. Green LS, Jellinek D, Jenison R, Östman A, Heldin C-H, Janjic N (1996) Inhibitory DNA ligands to platelet-derived growth factor B-chain. Biochemistry 35(45):14413–14424
65. Smith-Jones PM, Vallabahajosula S, Goldsmith SJ, Navarro V, Hunter CJ, Bastidas D, Bander NH (2000) In vitro characterization of radiolabeled monoclonal antibodies specific for the extracellular domain of prostate-specific membrane antigen. Cancer Res 60(18):5237–5243
66. Lupold SE, Hicke BJ, Lin Y, Coffey DS (2002) Identification and characterization of nuclease-stabilized RNA molecules that bind human prostate cancer cells via the prostate-specific membrane antigen. Cancer Res 62(14):4029–4033
67. Yang M, Jiang G, Li W, Qiu K, Zhang M, Carter C, Al-Quran S, Li Y (2014) Developing aptamer probes for acute myelogenous leukemia detection and surface protein biomarker discovery. J Hematol Oncol 7(1):5
68. Vega QC, Worby CA, Lechner MS, Dixon JE, Dressler GR (1996) Glial cell line-derived neurotrophic factor activates the receptor tyrosine kinase RET and promotes kidney morphogenesis. Proc Natl Acad Sci 93(20):10657–10661
69. Cerchia L, Ducongé F, Pestourie C, Boulay J, Aissouni Y, Gombert K, Tavitian B, de Franciscis V, Libri D (2005) Neutralizing aptamers from whole-cell SELEX inhibit the RET receptor tyrosine kinase. PLoS Biol 3(4):e123

70. Witte L, Hicklin D, Zhu Z, Pytowski B, Kotanides H, Rockwell P, Böhlen P (1998) Monoclonal antibodies targeting the VEGF receptor-2 (Flk1/KDR) as an anti-angiogenic therapeutic strategy. Cancer Metastasis Rev 17(2):155–161
71. Green LS, Jellinek D, Bell C, Beebe LA, Feistner BD, Gill SC, Jucker FM, Janjić N (1995) Nuclease-resistant nucleic acid ligands to vascular permeability factor/vascular endothelial growth factor. Chem Biol 2(10):683–695

Chapter 5
Molecular Engineering to Enhance Aptamer Functionality

Da Han, Cuichen Wu and Weihong Tan

Abstract Rapid development of bioanalysis and biomedicine requires enhanced and multiple functionality of aptamers. The field of molecular engineering has advanced to a stage where more and more molecular functions can be rationally designed in a predictable manner. By combining these two fields together, aptamer-based molecular engineering is able to tune the functionalities of aptamers toward more complicated and effective biological and biomedical applications. In this chapter, we focus on introducing the substantial progress in the development of using smart ways to broaden the multifunctional and logical applications of aptamers.

Keywords Molecular engineering · Aptamer · Multifunctionality · Self-assembly · Logic system · Intelligent diagnosis · Cancer therapeutics

5.1 Introduction

The application of aptamers has greatly expanded since their inception approximately two decades ago. To meet the requirements of increasingly complicated biological and biomedical applications, aptamers with more functionality are needed. For example, one consideration when transitioning aptamers to clinical applications is the need to decrease their susceptibility to degradation when exposed to in vivo conditions. In addition, high signal-to-background ratios are essential for in vivo imaging, due to the great loss of signal when transmitting through tissues.

D. Han (✉)
Intel Corporation, Hillsboro, OR 97124, USA
e-mail: tan@chem.ufl.edu

D. Han · C. Wu · W. Tan
Departments of Chemistry Physiology and Functional Genomics, Center for Research at the Bio/Nano Interface, Shands Cancer Center, UF Genetics Institute and McKnight Brain Institute, University of Florida, Gainesville, FL 32611, USA

W. Tan and X. Fang (eds.), *Aptamers Selected by Cell-SELEX for Theranostics*,
DOI 10.1007/978-3-662-46226-3_5

Furthermore, in recent years, encoding aptamers with intelligent functions has attracted more and more attention because of the possible applications for future personalized diagnosis and therapy. Of these considerations, improvement of the physical behavior of aptamers under different conditions, possible chemical modifications, and better understanding of biological functions is the critical factors. Consequently, these studies have given use to a new subject area called "aptamer-based molecular engineering" to tune the functionalities of aptamers to realize more complicated applications. This chapter focuses on the engineering of aptamers with more functions.

5.2 Molecular Engineering of Multifunctional Aptamer Nanoassemblies for Biological and Biomedical Applications

Multifunctional systems have made significant contributions in disease diagnosis and drug delivery because of their increased biostability, specific targeting, high payload efficiency, and excellent internalization capabilities. Incorporation of aptamers adds target specificity with the advantages of automated synthesis, an established selection process, and high stability and reproducibility [1, 2]. Because of their biostability, enzymatic resistance, and excellent plasmonic properties, aptamer–nanoparticle hybrids, in particular aptamer-modified gold nanoparticles, have been widely used for investigations of cellular processes and in vivo assays.

Mirkin and his colleagues developed "nanoflares," [3], fluorophore-labeled aptamers conjugated to the AuNP surface. The flares fluoresce when they bind to specific intracellular targets. The dense shell of aptamers protected by the gold nanoparticle core shows better enzymatic resistance and increased stability compared to free aptamers. For example, 1–2 mM concentrations of intracellular ATP can be detected via an aptamer–AuNP hybrid [4]. The same strategy can be used for monitoring and regulation of mRNA gene expression in living cells by conjugation of molecular beacons (MBs) and antisense oligonucleotides onto the surfaces of gold nanoparticles [5, 6].

Carbon-based nanomaterials, such as graphene, with their excellent optical and electrical properties, have been used as in situ biosensors and delivery platforms. Because of π–π stacking between single-stranded aptamers and water-soluble graphene oxide, fluorescent aptamers are adsorbed and protected by graphene oxide (GO) in the absence of target molecules, resulting in a signal "OFF" state. Upon specific binding with targets, the aptamer undergoes a conformational change and leaves the GO surface, resulting in restoration of the signal from "OFF" to "ON." Lin et al. employed GO as the delivery carrier to transport protected aptamers into live cells for real-time monitoring of the variation of intracellular ATP concentration with detection limits as low as 10 μM [7]. These systems have greatly broadened the applications of aptamers in biology and biomedicine.

Although various nanomaterial-based aptamer systems have been created for cellular and in vivo assays, the cytotoxicity of nanomaterials cannot be neglected, especially at high concentrations for intracellular use. Thus, alternative platforms are still needed. DNA nanotechnology allows the self-assembly of one-dimensional nucleic acid molecules into two- and even three-dimensional multifunctional nanostructures through molecular recognition, such as hydrogen binding and π–π stacking [8–14]. Integration of aptamers with current DNA technology has led to novel aptamer nanoassemblies to enhance aptamer biological and biomedical performance.

5.2.1 Aptamer Nanoassembly to Enhance System Stability

As stated above, the stability of aptamers is critical in practical applications, especially in the complicated biomedical environments. For instance, when delivered systemically to a physiological environment, aptamer degradation or dissociation can be facilitated by ubiquitous nucleases, dilution to very low concentrations by large volumes of circulating blood, and strong shear force. Similar to aptamer–nanomaterial hybrids, aptamer-based nanostructures also show excellent biostability, particularly in the resistance of different enzymes, due to several features of aptamer particles: (1) long building blocks, which avoid the otherwise many nick sites sensitive to nuclease cleavage; (2) high density of DNA packed in each aptamer particle, reducing nuclease accessibility; and (3) extensive inter- and intrastrand weaving of long DNA building blocks, preventing denaturation or dissociation. Guided by this rule, we have developed a way to build aptamer particles for enhanced stability in cellular environments.

The design uses a bottom-up modular strategy to construct the aptamer-based nanoassembly (AptNA) (Fig. 5.1) [15, 16]. In this AptNA, the basic building unit consists of one X-shaped connector and several Y-shaped functional domains. The X-shaped core is assembled with four predesigned single-stranded DNAs (ssDNAs) and three different toehold sequences. For each Y-shaped functional domain, one type of featured oligonucleotide sequence is incorporated, including different targeting aptamers and therapeutic antisense oligonucleotides, as well as an acrydite group on the 5′-end. The building units are further photo-cross-linked to form size controllable nanoassemblies. Because of the precise design of the toehold sequences in each building unit, a precise ratio between different functional moieties (aptamers or antisense oligonucleotides), as well as programmable self-assembled functional domains, can be achieved throughout the entire nanoassembly. The stability of this aptamer-based nanoassembly was tested by treatment with DNase I (2 U/mL) for different times. The diameter of AptNAs did not show a significant change compared to the AptNAs without DNase I treatment even after 24 h, indicating that the aptamer nanoassemblies were stable against extremely high enzymatic environments.

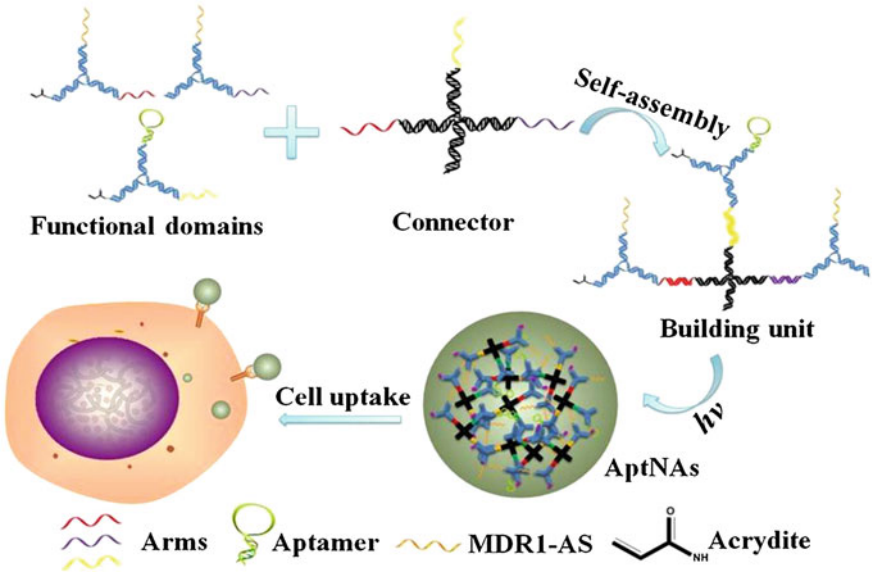

Fig. 5.1 Schematic of self-assembled and multifunctional nanoassembly structure. Multifunctional DNA sequences, including aptamers, acrydite-modified ssDNA, and antisense oligonucleotides, are assembled into Y-shaped functional domains. The basic building unit is formed by one X-shaped connector and multiple Y-shaped functional domains through predesigned hybridization. Finally, hundreds of these building units are photo-cross-linked into a multifunctional and programmable nanoassembly (Reprinted with the permission from Ref. [15], copyright 2013 American Chemical Society)

5.2.2 Biaptamer System to Enhance the Affinity and Selectivity

In biology, multivalent interactions can provide higher binding affinity and selectivity in target recognition compared to monovalent interactions, mostly due to the "cooperative" property, as seen, for example, in the binding of galactose-terminated oligosaccharides to C-type mammalian hepatic lectins [17, 18]. In another example, recombinant antibody technology is used to construct bivalent and trivalent single-chain fragment variables (scFv) by linking the antigen-binding V_H and V_L domains with a flexible polypeptide linker [19]. Learning from these and other examples, aptamers have also been engineered toward multivalency to enhance their affinity and selectivity. In contrast to antibodies, aptamers have some intrinsic advantages, such as low molecular weights, predictable secondary structures, high stability, and reproducibility [1]. In addition, the advantages of aptamer molecular assembly are facile conjugation of aptamers and reversible regulation of aptamer functions via their complementary sequences [20].

Kim et al. [21] designed an aptamer assembly to enhance enzymatic inhibition by linking two different functional aptamers. Thrombin, a protease that hydrolyzes fibrinogen and activates platelets and blood coagulation factors, was chosen as the model to demonstrate the functionality of the two-aptamer assembly [22]. Two well-known thrombin aptamers have been reported, one is a 15-mer (15Apt) that binds to exosite 1, resulting in the thrombin inhibitory function, and the other is a 27-mer (27Apt) that binds to exosite 2 but without any inhibition to thrombin function [23]. The dissociation constant (K_d) of 27Apt ($\sim$0.5 nM) is much lower than that of 15Apt ($\sim$100 nM), indicating the higher binding affinity of 27Apt compared to 15Apt [24]. The 15Apt monovalent inhibitor is easily dissociated by competition with thrombin substrate, and the released 15Apt diffuses out of the binding site, causing low inhibition. However, when linked to 27Apt to form a bivalent ligand, the 15Apt is confined and can rapidly return to the binding site even after dissociation (Fig. 5.2). Molecular assembly of these two thrombin aptamers with a specific linker length provides stronger binding affinity, enhanced inhibitory function, intrinsic high selectivity, and low cytotoxicity [25].

To design this bivalent aptamer inhibitor for thrombin, the linker length was first optimized. In contrast to monovalent 15Apt inhibitor, the bivalent aptamer ligands with 8 hexaethyleneglycol spacers showed the longest clotting time, indicating the best inhibitory effect to thrombin. Because of the bivalent interaction realized by molecular assembly, 8-spacer-linked biaptamers (Bi-8S) achieve a ninefold increase of clotting inhibition over 15Apt only (Fig. 5.3a). Real-time light scattering to monitor the coagulation process further confirmed the inhibitory function of Bi-8S, which decreased the net rate of the coagulation reaction. Based on the binding kinetic studies (Fig. 5.3b), monovalent 15Apt and bivalent aptamers show relative k'_{off} values (dissociation rate) of 1.5 and 0.029 %/s, respectively, while the relative k'_{on} values (association rate) of 15Apt and Bi-8S are similar, 0.00424 and

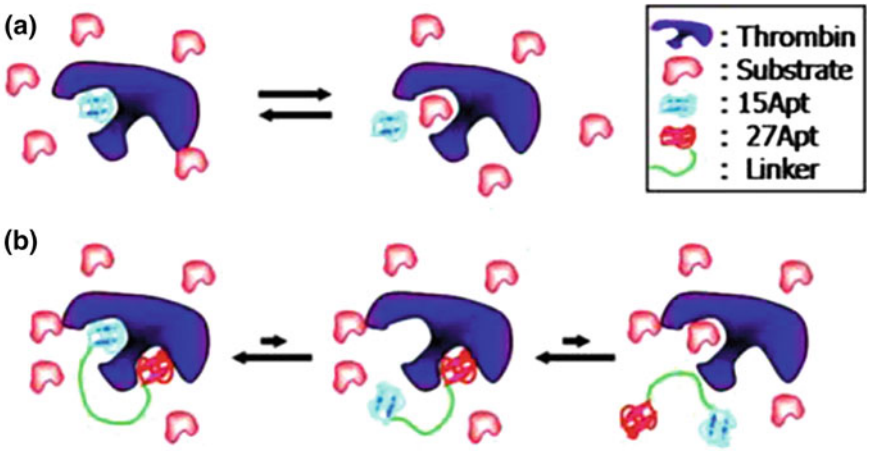

Fig. 5.2 Schematics of monovalent and bivalent aptamer inhibitors

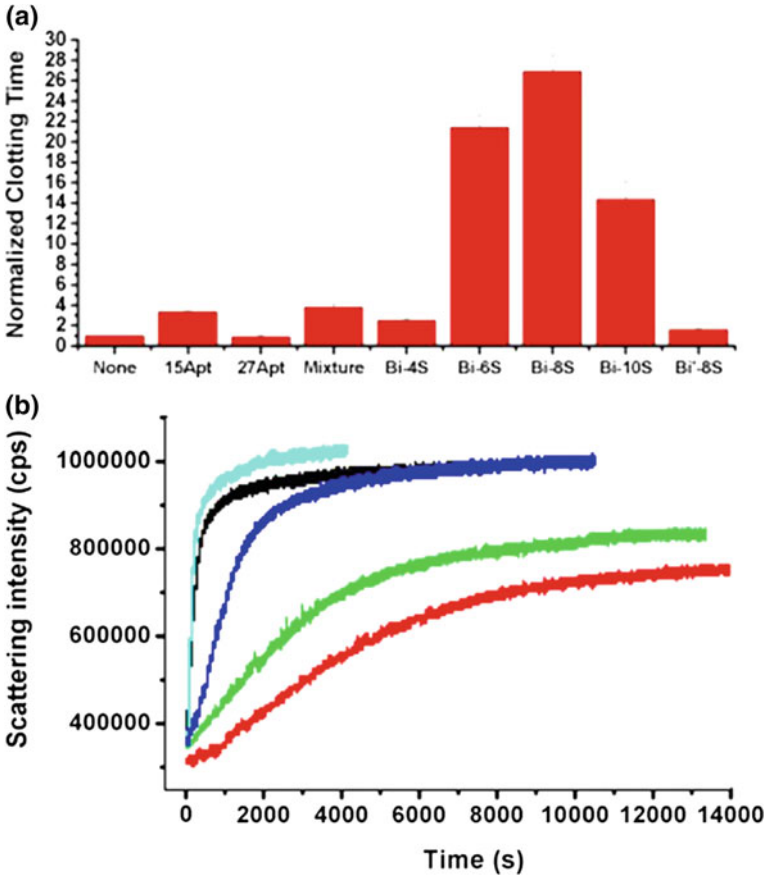

Fig. 5.3 **a** Optimization of bivalent aptamers with different linker lengths based on the normalized clotting times of thrombin. In bivalent aptamer Bi-xS, x means the number of hexaethyleneglycol spacers. **b** Real-time monitoring of light scattering generated by the coagulation process in the presence of monovalent 15Apt or different bivalent aptamers (*Cyan* Bi-4S; *Black* 15Apt; *Blue* Bi-10S; *Green* Bi-6S; *Red* Bi-8S)

0.00498 %/s. Thus, the overall association constant ($K'_a = \frac{k'_{on}}{k'_{off}}$) of Bi-8S is $\sim$51.7 times higher than that of 15Apt to thrombin [21]. Therefore, this high-performance bivalent ligand can be applied as a potential anticoagulant.

5.2.3 Aptamer Micelle Flares to Enhance Cell Internalization

Investigation of the expression and dynamics of intracellular biological molecules is significant for understanding physiological processes, diagnosing disease stages,

and identifying therapeutic targets. The prerequisite of successful molecular imaging in live cells is the development of a delivery of platform with ultrasensitive molecular probes for specific targets of interest and high efficiency. Since the appearance of MBs, nucleic acid molecular probes have provided an opportunity for intracellular imaging of targets ranging from proteins to RNAs and even small molecules [1, 26]. For example, Tyagi and Kramer [27] designed fluorescent-labeled MBs to visualize the distribution and dynamics of specific mRNAs in live cells and even in vivo. Tan et al. utilized a series of unnatural nucleic acid bases, including locked nucleic acids (LNA), L-DNA, and 2′-O-methylribonucleotides, and hybrid molecular probes, for intracellular mRNA monitoring over a long period (over 24 h) and in real-time [28–30]. However, nucleic acid molecular probes suffer from the issues of insufficient probe introduction and uneven distribution of probes inside live cells [31]. Although this delivery issue has been partially resolved by newly developed nanomaterials, such as gold nanoparticles (AuNPs) and GO [3, 7], the challenges of uneven distribution and cytotoxicity of nanomaterials still remain; for example, GO-based nanosheets have been reported to be preferentially internalized into the lysosomes and endosomes of live cells [32].

Due to their excellent biocompatibility and controllability, and their efficient cellular internalization, nucleic acid-based micelle structures have gained increasing attention in the fields of intracellular detection and drug delivery [33, 34]. As shown in Fig. 5.4a, DNA micelles consist of amphiphilic DNA–diacyllipid conjugates synthesized with hydrophilic ssDNA heads and hydrophobic lipid tails. By incorporating functional nucleic acids (NA), such as aptamers or MBs, the DNA micelles can be termed as aptamer or MB micelle flares [35, 36]. Since the amphiphilic DNA–diacyllipid conjugates can self-assemble into a uniform spherical nanostructure, and the fluorescent signal attached on the micelles is switched from "OFF" to "ON" upon targeting binding, this micelle nanostructure can be applied for biosensing and bioimaging. Because of the similar lipid composition of DNA micelles and phospholipid bilayers in live cell membranes, DNA micelles can interact with cell membranes and enter live cells without an auxiliary agent.

The DNA micelle flares designed by the Tan group are self-assembled from conjugates containing an aptamer switch probe (ASP) with TAMRA (tetramethylrhodamine) and DABYCL (4-(4-dimethylaminophenylazo)-benzoic acid) dye/quencher pair [37], a PEG linker to a short DNA sequence complementary to part of the ASP, and a diacyllipid tail. The switchable ATP aptamer micelle flares (SAMFs) are designed for self-delivery and monitoring of intracellular ATP (adenosine triphosphate) concentration. As shown in Fig. 5.4a, the SAMFs maintain the quenched fluorescent signal (OFF state) in the absence of ATP targets. However, the fluorescent signal of SAMFs is restored upon ATP binding inside live cells.

The internalization mechanism of DNA micelles was clarified with the SAMFs and HeLa cancer cells. Different incubation times were used with confocal fluorescence measurements (Fig. 5.4b). SAMFs were initially distributed on the cell membrane and produced a fluorescence signal at 0.5 h. Then, the fluorescent signal accumulated in the cytoplasm from 1 to 2 h. Finally, SAMFs were mostly distributed in the cytoplasm outside the the nucleus at 4 h. During this time, the control

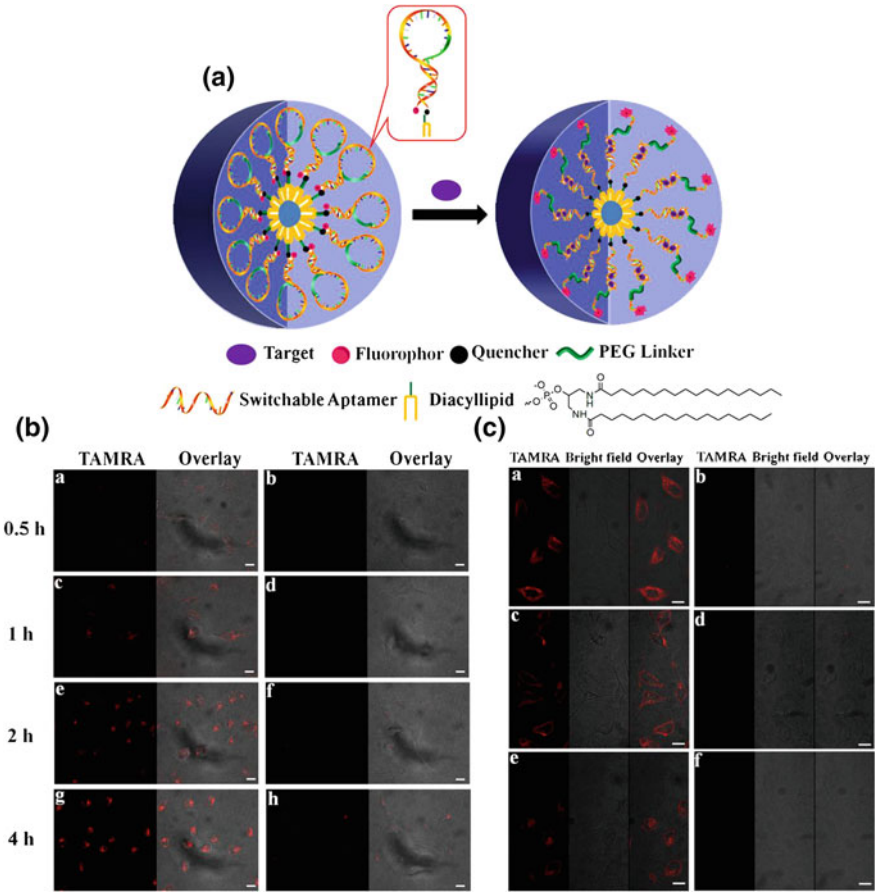

Fig. 5.4 **a** Schematic of aptamer micelle flares. In the absence of target, the aptamer probe maintains the loop–stem structure and fluorescence is quenched due to the close proximity between fluorophore and quencher. The conformation of the switchable aptamer is altered upon target binding, resulting in restoration of the fluorescence signal. **b** Time-dependent fluorescence imaging of SAMFs and CSMFs in HeLa cells. Confocal laser scanning microscopy images of HeLa cells incubated with SAMFs or CSMFs for 0.5 h (**a**, **b**), 1 h (**c**, **d**), 2 h (**e**, **f**), and 4 h (**g**, **h**). *Scale bars* 20 μm. **c** Confocal microscopy fluorescence imaging of HeLa cells treated (**a**, **b**) with 100 μM etoposide, (**c**, **d**) with 3 μg/mL oligomycin, and (**e**, **f**) without treatment, followed by incubation with 1-μM SAMFs (*left*) or CSMFs (*right*). *Scale bar* 50 μm. (Reprinted with the permission from Ref. [36], copyright 2013 American Chemical Society)

DNA micelle flares (CSMFs) showed a weak increase of fluorescence signal from 0.5 to 4 h, probably resulting from nonspecific opening of the hairpins by protein binding [36]. In the further colocalization assay, except for a fraction of SAMFs colocalized with lysosomes, most amphiphilic SAMFs were distributed in the cellular plasma. The possible internalization mechanism of SAMFs into live cells was proposed based on the time-dependent fluorescence measurements and

colocalization assay. SAMFs are initially in close proximity to the cell membrane, and then, they disintegrate and fuse with the cell membrane. Partially disintegrated SAMFs permeate the cell through the process of endocytosis, while most fused SAMFs flip and diffuse from the cell membrane to the cytoplasm. This occurs during a process of membrane recycling due to the thermodynamically unfavorable structure with the hydrophobic tail pointing into the aqueous solution [33, 36].

Although the diameter of DNA micelles can be tuned by changing the length of DNA sequences, the size of SAMFs is around 30 nm, as confirmed by DLS and TEM, because of the hairpin-shaped ASP. In contrast to other analogues, the aptamer probe in the SAMFs still maintains its high specificity and selectivity for ATP molecules with a detection range of 0.1–3.0 mM. The cellular permeability of DNA micelle flares was verified by incubating SAMFs, CSMFs, and ASPs (without diacyllipid) with HeLa cells. SAMFs showed an intense fluorescent signal in contrast to both CSMFs and ASPs, indicating not only the internalization of SAMFs into HeLa cells, but also the sensitive detection of target ATPs inside cells. Moreover, SAMFs displayed a 2.3-fold fluorescence enhancement relative to the cells treated with CSMFs in the flow cytometric experiments. Finally, the ability of SAMFs to respond to intracellular ATP concentration variation was demonstrated (Fig. 5.4c). Two small molecules, etoposide and oligomycin, were used to stimulate or suppress the intracellular ATP concentration, followed by treatment with same amount of SAMFs and CSMFs. The confocal imaging of etoposide-treated HeLa cells showed increased fluorescence in contrast to untreated HeLa cells, while oligomycin-treated HeLa cells displayed the decreased fluorescence intensity. Their corresponding fluorescence intensities were reported relative to the ATP concentration in the untreated HeLa cells (set to 100). The intracellular ATP concentration in HeLa cells treated with etoposide increased from 100 to 135, while that treated with oligomycin decreased from 100 to 84, in good agreement with confocal results.

5.3 Molecular Engineering of a Switchable Aptamer System for Sensing and Cancer Therapy

Although aptamers generated from SELEX have good selectivity for their specific targets, challenges with molecularly engineered target responsive aptamers for bioassay applications still remain, for example, unpredictable structural alterations in complex biological fluids [38]. Other strategies, such as use of an intermolecular complementary competitor, can be used to verify the binding between aptamer and target. However, this approach requires optimization of competitor length to avoid conformational changes that would probably affect the aptamer's recognition of the target [39, 40].

To develop highly selective aptamer probes for biosensing and bioimaging, the Tan group designed an ASP-based intramolecular displacement [37]. An ASP

consists of an aptamer, a short DNA sequence complementary to part of the aptamer, and a PEG (polyethylene glycol) linker connecting the two. In addition, a fluorophore and a quencher are attached at the two ends of the ASP, respectively. Due to the flexible PEG linker, the short complementary DNA sequence can hybridize to part of the aptamer sequence in the absence of target, resulting in quenching of the fluorophore. However, the conformation of the ASP is altered upon target binding, causing the quencher to move away from the fluorophore, thereby restoring the fluorescence signal (Fig. 5.5a). The ASP is able to switch the fluorescence signal from OFF to ON before and after addition of target. Thus, this strategy offers a robust probe construction by integrating aptamer, competitor, and signaling moieties together, in contrast to simple target responsive aptamers, and can be applied to any aptamer design [37]. For example, the ATP–ASP (1.0 μM) showed a 30-fold fluorescence enhancement after introducing 3.5 mM ATP compared to its analogues, GTP, UTP, and CTP, indicating the excellent selectivity of ASP to its corresponding target (Fig. 5.5b). As shown in Fig. 5.5c, the kinetic assay further demonstrated the higher recognition affinity, better selectivity, and faster hybridization/dehybridization rate in contrast to commonly used aptamer probes [29, 37, 41]. The generality of ASP strategy has also be demonstrated in the design of a human α-thrombin aptamer switch probe (Tmb-ASP). A fluorescence enhancement of up to 17.6 was obtained by introducing 300 nM thrombin into Tmb-ASP. Moreover, the selectivity of Tmb-ASP was also verified with different protein interferences, such as IgG, IgM, and BSA [37].

A major reason for using aptamers in cancer therapy is the high selectivity of aptamers to cancer cells. The selectivity is usually controlled at two levels. The first

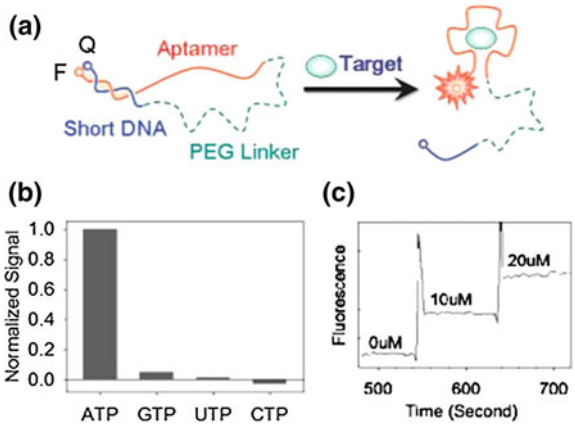

Fig. 5.5 **a** Schematic of aptamer switch probe (*ASP*). **b** Selectivity of ATP–ASP toward to ATP and its analogues. **c** Kinetic response of ATP–ASP to low concentrations of ATP (Reprinted with the permission from Ref. [37], copyright 2008 American Chemical Society)

level controls the spatial localization of aptamers. This approach has been actively pursued by specifically linking drugs with aptamers and has effectively improved drug selectivity and efficiency. But the tendency to cause damage to surrounding normal tissues was still present. To achieve greater selectivity, a molecular activation layer was added to further control the specificity of the drugs linked with aptamers. At this level, the probe initially stays in the nontoxic state and can only be activated when it interacts with its corresponding trigger at the tumor site. Toward this goal, the switchable aptamer system has some intrinsic advantages because the release of drugs can be controlled by activation of external biomarkers.

Several research groups have developed activatable aptamer-based methods which can be triggered by cancer biomarkers [42], membrane proteins, extracellular proteases [43], or cellular environments (e.g., pH) [44] or by other external stimuli, including artificial molecular switches [45]. For example, combination of a photosensitizer and ASP results in a switchable aptamer system which offers a reliable and versatile approach to the molecular mediation of singlet oxygen generation [46]. Specifically, a photosensitizer and a quencher are covalently attached at the two termini of the coupled ASP. The conformation of the ASP can then be altered upon target binding. In the absence of a target molecule, the short DNA hybridizes with a small section of the aptamer, placing the photosensitizer and quencher in close proximity. This action turns off the fluorescence of the photosensitizer, as well as the singlet oxygen generation. Conversely, when ASP meets its target, the recognition and binding between aptamer and target molecule destabilize the intramolecular DNA hybridization and drive the quencher away from the photosensitizer, resulting in restoration of fluorescence and the generation of cytotoxic singlet oxygen capable of oxidizing the cell membrane components and inducing cell death. This approach holds the potential to improve the selectivity and efficiency of photodynamic therapy.

Similarly, a switchable aptamer system was engineered by combining two functional DNA groups, such that one group is an aptamer capable of recognizing the target cell, while a complementary group acts as a drug delivery carrier (shown in Fig. 5.6) [47]. Because of the binding of aptamer (sgc8) to the cancer cell membrane, the guanine-rich ssDNA segments are induced to form a G-quadruplex structure that can be used as drug delivery carrier for a photosensitizer (TMPyP4). This novel G-quadruplex–aptamer–drug platform takes advantage of the target recognition function of the DNA aptamer and the drug-loading ability of the G-quadruplex. In this way, increased toxicity to the target cells was achieved during photodynamic therapy, while the cytotoxicity of the photosensitizer to the nontarget cells was minimized.

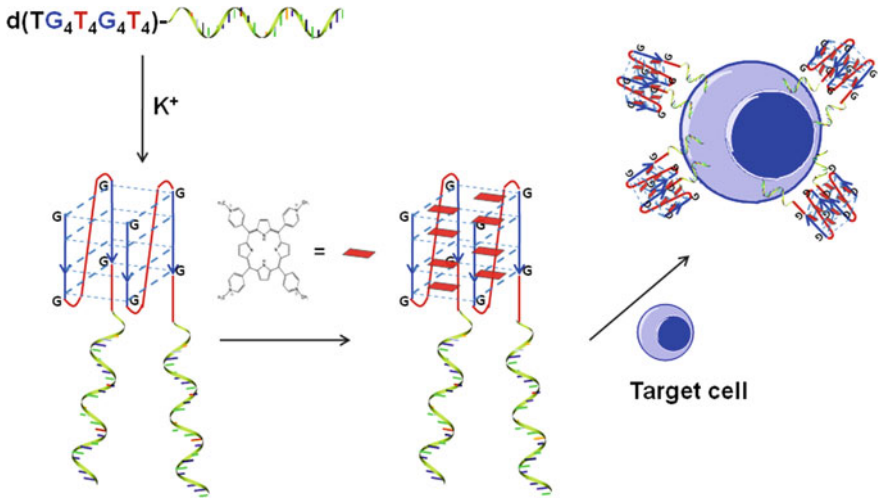

Fig. 5.6 Scheme of G-quad-aptamer system. This design utilizes the G-quadruplex as the drug carrier and the aptamer as the targeting molecule to deliver TMPyP4, which is known to bind and stabilize different types of quadruplexes. The green strand represents the aptamer (Reprinted with the permission from Ref. [47], copyright 2011 John Wiley and Sons)

5.4 Molecular Engineer of Logical Aptamer Systems for Intelligent Diagnosis and Therapy

5.4.1 Coding Aptamers with Logical Functions

Today's world is completely driven by silicon-based computers because of their unprecedented computing power, seamless coupling ability, and incredible adaptability. Meanwhile, within the computational field, computational power is increasingly exponentially, but this requires continuous miniaturization of critical components. As a result of the physical limitations of conventional silicon chips, the development of more powerful microprocessors is heading toward a barrier [48]. To address the challenge ahead, researchers have been pursuing the idea of constructing computers in which computations are performed by individual molecules, allowing for a continuous exponential increase in performance and decrease in size for microprocessors.

NA are extremely effective for miniaturization of information storage because only approximately 50 atoms are used for one bit of information [49, 50]. In addition, easy chemical synthesis, combinatorial structures, and Watson-Crick complementarity principle provide sufficient theoretical and experimental bases for the rational design of logical devices. Therefore, researchers have challenged themselves to use DNA or RNA to build logical devices for molecular computation. As early as 1994, Adleman [51] used DNA to solve a computational problem. He encoded the Hamiltonian path problem into different ssDNA sequences and applied

biotechnologies (such as ligation, PCR, sequencing) to decode the answers to the correct Hamiltonian path.

After confronting various barriers, it has become increasingly clear that the ability to interact with naturally occurring biomolecules, together with such unique properties as programmability, nanometric size, and autonomous operation, can be used for practical applications of NA-based logical devices. This has allowed biological properties to be interfaced to other materials, thereby opening up a novel and exciting direction in biological and biomedical applications.

As special single-stranded oligonucleotides, aptamers can extend the recognition capabilities of NA from Watson-Crick base-pairing to interact with various targets, such as small molecules, proteins, and even viruses or cells. In addition, the affinity and specificity of an aptamer can be tuned through the selection process or by post-selection sequence optimization in order to meet the specific performance requirements of a given application. Finally, some aptamers are not only able to recognize the target proteins but can also regulate protein functions [52]. Such aptamers are regarded as potential drugs with protein regulation functions or as drug carriers for many diseases and are already in the pipeline for clinical use, including PDGF and VEGF aptamers for controlling age-related macular degeneration [53], demonstrating their reliability for biomedical applications. Since an aptamer is essentially a single-stranded oligonucleotide, it is conveniently coded in logic circuit design, just as previous NA-based circuits. Therefore, aptamers can be directly used as building blocks to fabricate seamless logic-based aptamer circuits with enhanced capabilities and an extended scope of applications in future intelligent diagnosis and therapy.

5.4.2 Logical Aptamer System for Intelligent Therapy

Kolpashchikov and Stojanovic [54] were the first to include aptamers in DNA logical circuits. They constructed deoxyribozyme-based logic gates that could perform Boolean calculations on the input molecules to control the functional binding state of aptamers. Similar examples include the use of the binding between targets and aptamers to control the power release of biofuel cells according to the built-in Boolean NAND logic [55]. These two examples mainly demonstrated the feasibility of incorporating aptamer–small molecule interactions into logical molecular circuits.

To address the question of using aptamer-based circuits for future intelligent therapy, the Tan group has developed a logical circuit based on DNA-protein interactions with accurate threshold control, enabling autonomous, self-sustained, and programmable manipulation of protein activity in vitro (Fig. 5.7) [56]. In general, a programmable and autonomous circuit with threshold control is constructed of three DNA modules: an input convertor that converts the protein input to DNA input for downstream cascade reactions; a threshold controller that sets the threshold concentration for the system to maintain regular protein activity;

and an inhibitor generator that inhibits excessively high protein activity once it surpasses the threshold. This circuit can intelligently sense the activity (i.e., the concentration) of protein and initiate the inhibitory function via a threshold control loop when excessively high protein activity occurs. By setting the threshold value according to each practical situation, the circuit may be usable as a smart drug delivery system in the design of personalized medicine.

To demonstrate such intelligent regulatory function with thrombin as a model, two antithrombin aptamers are employed to build an aptamer circuit to smartly control coagulation: a 29-mer (TA-29) that binds to the heparin exosite without inhibitory function, and a 15-mer (TA-15) that binds to the fibrinogen exosite with strong inhibitory function. In the detailed design (Fig. 5.7b), the circuit includes a series of aptamer and DNA displacement reactions, in which a ssDNA can be displaced from the initial duplex by an even stronger binder, either a protein molecule or a better matched DNA strand.5,30,31. The circuit starts with the introduction of thrombin. In the input convertor, thrombin reacts with duplex

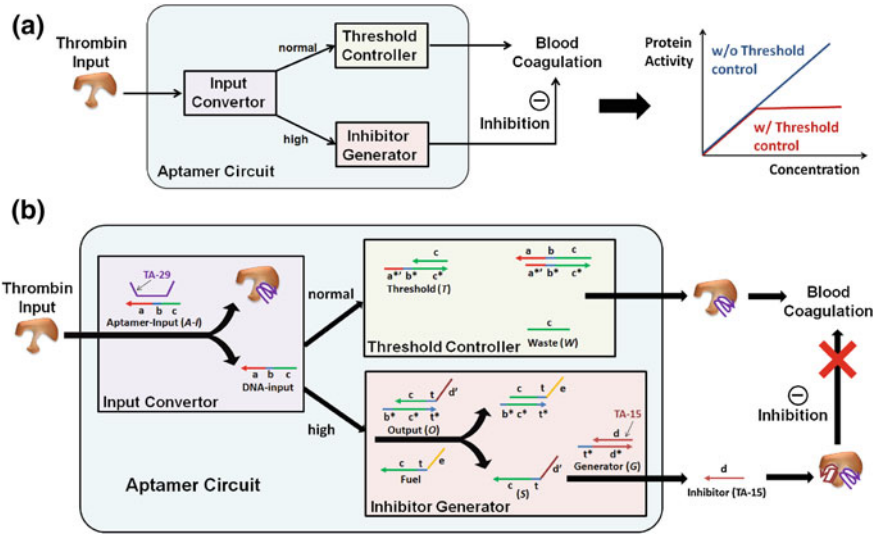

Fig. 5.7 Working Scheme of molecular circuit. **a** Diagram illustrating circuitry. The circuit consists of three modules, **Input Convertor**, **Threshold Controller,** and **Inhibitor Generator**, which can be programmed with threshold control for smart manipulation of protein activity. **b** Working scheme for molecular circuit, driven by a series of DNA displacement reactions. Colored lines indicate DNA strands with different domains. TA-29 and TA-15 are two thrombin aptamers with different functions, including recognition and inhibition, respectively. All **x** domains are complementary to **x***; **b*** and **t*** are short toehold domains with 5-nt; **a*′b*** is a long toehold domain with 10-nt; **c*** and **d*** are recognition domains with 15-nt. ***A-I***, ***T***, ***O,*** and ***G*** are initially presented as duplex components, along with ssDNA ***fuel*** (Reprinted with the permission from Ref. [56], copyright 2012 American Chemical Society)

Aptamer-Input (A-I), which contains TA-29 partially hybridized with a piece of ssDNA. This ssDNA, termed as DNA input, is released from A-I by competitive binding of thrombin to TA-29, converting the protein input to DNA input for the following cascade reactions.

The DNA input then enters the threshold controller module and rapidly reacts with duplex threshold (T) via an exposed toehold a*′b* to generate inert ssDNA Waste (W1) without further reaction. Through this bypass route, thrombin only binds with TA-29 and thus can still perform its normal catalytic function in blood coagulation. However, after T is depleted, the excess DNA input continues to the inhibitor generator module, in which DNA input reacts with duplex output (O) via exposed toehold b*, thereby triggering the amplification reaction of O with fuel (F), i.e., signals that help to catalytically produce the output. The released product, which is denoted as S (ctd') with effective toehold t, then cascades to duplex generator (G), followed by the release of the Inhibitor TA-15 to inhibit thrombin coagulation.

The Tan group also designed an aptamer-based DNA logical circuit constructed on cell membranes capable of selective recognition of cancer cells, controllable activation of a photosensitizer, and amplification of the photodynamic therapeutic (PDT) effect [57]. Here, the aptamers are able to selectively recognize target cancer cells and bind to the specific proteins on the cell membranes. An overhanging catalyst sequence on the aptamer then triggers a toehold-mediated catalytic strand displacement to activate the photosensitizer for amplified PDT. The specific binding-induced activation allows the DNA circuit to distinguish diseased cells from healthy cells, reducing damage to nearby healthy cells, while resulting in a high local concentration of singlet oxygen around diseased cells (Fig. 5.8).

To further demonstrate the feasibility of engineering logical aptamer systems for intelligent therapy, You et al. [58] also designed an aptamer-based logical robot capable of autonomously analyzing multiple cell molecular signature inputs and realizing targeted therapeutic effects. Structurally, this logic robot consists of an oligonucleotide backbone as the scaffold, several structure-switchable aptamers as "capture toes," and a logic-gated DNA duplex as the "effector toe" (Fig. 5.9). The "capture toes" have two functions: first targeting each cell surface marker and then generating the respective barcode oligonucleotide for activation of the "effector toe." Finally, the "effector toe" analyzes these barcode oligonucleotides and autonomously makes decisions in generating a therapeutic effect.

The functions of the "capture toes" were achieved on the basis of structure-switchable aptamers [59]. In the absence of target, the aptamer binds to a piece of complementary DNA (cDNA) to form a duplex structure. However, when a target is introduced, the structures are induced to switch from aptamer/cDNA duplex to aptamer/target complex and release the cDNA as an output. Three aptamers, Sgc8c, Sgc4f, and TC01, were chosen to, respectively, target three overexpressed markers (PTK7 for Sgc8c; Sgc4f and TC01 targets not yet identified) on the surface of cancer cells, such as human acute lymphoblastic leukemia cells (CCRF-CEM). Several 11–19 nt-long candidate strands were tested for each aptamer, and three 15 nt-long cDNA strands were chosen: cS15 for Sgc8c aptamer, cF15 for Sgc4f

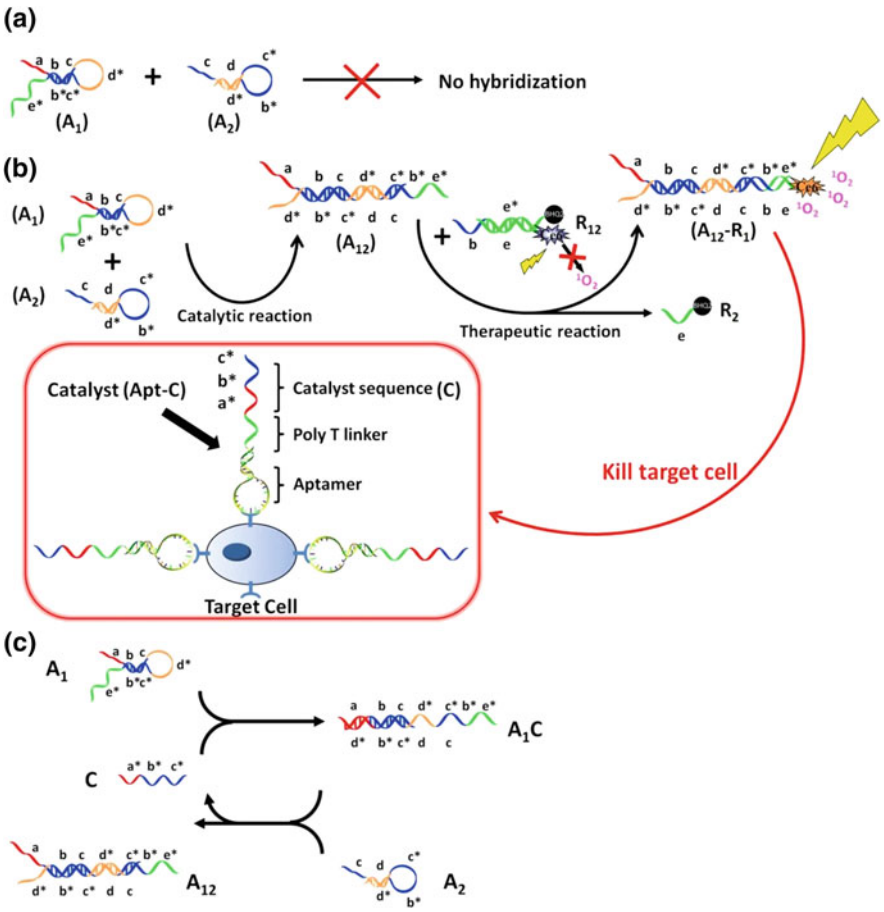

Fig. 5.8 Working Scheme of DNA aptamer circuit on cell membrane. **a** Scheme of the circuit without catalyst. **b** Scheme of the circuit on cell membrane. The circuit involves two individual steps. In the catalytic step, target cell labeled with **Apt-C** catalyzes DNA hairpins $\mathbf{A_1}$ and $\mathbf{A_2}$ to form duplex $\mathbf{A_{12}}$. In the therapeutic step, $\mathbf{A_{12}}$ can open duplex $\mathbf{R_{12}}$ and displace quencher-labeled single strand $\mathbf{R_2}$ to form $\mathbf{A_{12}}$-$\mathbf{R_1}$. Subsequently, Ce6-labeled $\mathbf{R_1}$ generates singlet oxygen ($^1\mathbf{O_2}$) to kill cancer cells by irradiation at 404 nm. **c** Scheme of detailed reaction of DNA hairpins $\mathbf{A_1}$ and $\mathbf{A_2}$ catalyzed by **C** sequence. Different domains are labeled with different colors. All **x** domains are complementary to **x*** (Reprinted with the permission from Ref. [57], copyright 2013 American Chemical Society)

aptamer, and cT15 for TC01 aptamer. These cDNA strands strongly bound with their respective aptamer in the absence of target. Furthermore, they did not prohibit the binding of the aptamers to their corresponding cellular targets and could be freed after cellular binding.

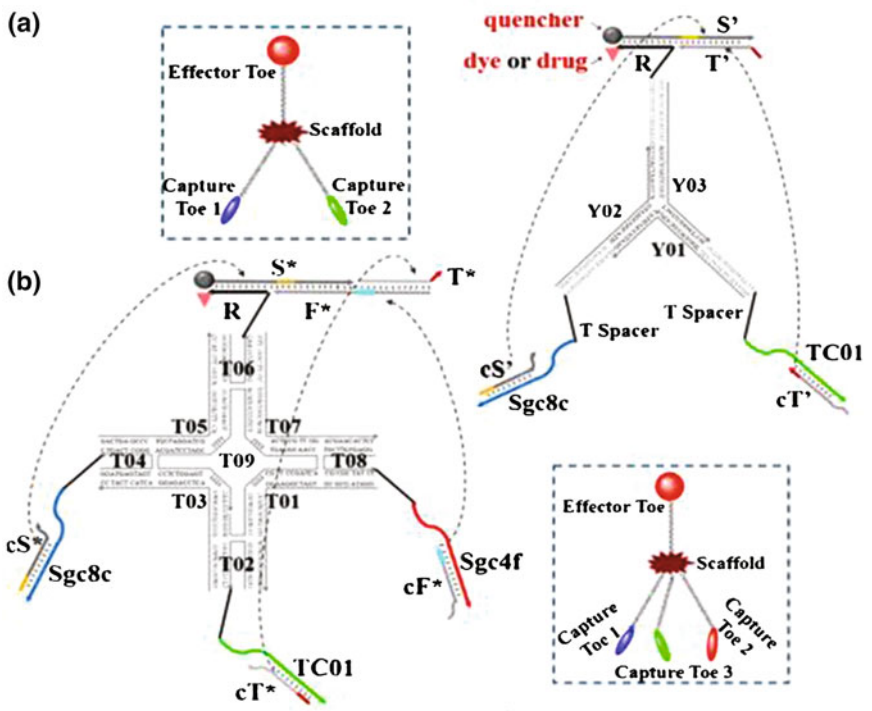

Fig. 5.9 Symbols and construction schemes are shown for **a** two-input trivalent "Y"-shaped Nano-Claw and **b** three-input tetravalent "X"-shaped Nano-Claw (Reprinted with the permission from Ref. [58], copyright 2014 American Chemical Society)

5.4.3 Logical Aptamer System for Intelligent Diagnosis

Pioneer work started with the application of intelligent sensing of cancer cells via biomarkers on cell membranes. Douglas et al. [60] developed a DNA aptamer-based nanorobot with the ability to detect antigen information on cell membranes and autonomously release the payloads according to the different combinations of cell surface inputs (Fig. 5.10a). Specifically, this nanorobot was assembled by the DNA origami method [61] in the shape of a hexagonal barrel with dimensions of 35 nm × 35 nm × 45 nm. The nanobarrel was noncovalently fastened in the front by "staples" modified with DNA aptamer-based "locks" that could be specifically opened via DNA–protein binding to cell surface proteins. Then, the payloads, which were either labeling antibodies or gold nanoparticles, were selectively released to realize intelligent sensing and delivery. A similar idea was implemented by Stojanovic and coworkers, who built DNA-based logical devices on cell membranes for intelligent sensing (Fig. 5.10b) [62]. First, the DNA probes were conjugated with antibodies independently targeting specific antigens on cell

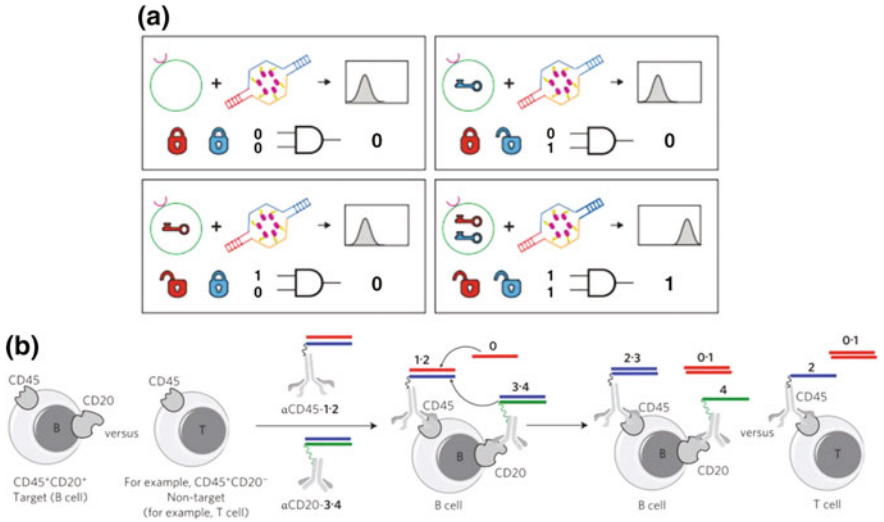

Fig. 5.10 Aptamer-based logical circuits for intelligent diagnosis. **a** Illustration and truth table showing how this aptamer-based nanorobot works (reprinted by permission from Ref. [60], copyright 2012, AAAS). **b** Scheme of DNA-based logical circuit operating on a target B cell with a C45+CD20+ phenotype and on a nontarget cell with a CD45+CD20− phenotype (e.g., a T cell) (Ref. [62], reprinted by permission from Macmillan Publishers Ltd., Nature Nanotechnol., copyright 2013)

membranes. The cell-bound probes would then undergo a cascade of reactions for fundamental logical operations including AND, OR, and NOT, through toehold-mediated displacement reaction [63]. This DNA-based logical device provides a reliable method for analysis of complex cell membrane information and the accurate identification of stem cells.

5.5 Conclusions

The field of molecular engineering clearly has advanced to a stage where more and more aptamer functions can be rationally designed in a predictable manner in vitro. With respect to device construction, aptamer systems can be integrated at the nucleic acid level and coupled with other entities such as proteins or nanomaterials. Operationally, the behavior of these aptamer systems can be either static or dynamic, in which the output may be produced, degraded, or modified reversibly or irreversibly in response to design principles. Furthermore, it should not be forgotten that the efforts of using programs to aid in system design greatly improve experimental implementation efficiencies, such as the aptamer logical circuit design. Combining these points, both the quality and quantity of an aptamer's new functionality have experienced a dramatic increase in the last 10 years. However, this

does not mean that these devices have reached a mature state. Some limitations still need to be overcome prior to translation of an aptamer's new functions into real-world biological and biomedical applications. For example, the performance of some aptamer systems with new functions may be less effective in a complex environment, especially in living systems, thus depressing the effectiveness of aptamers in vivo. To overcome these challenges, on a fundamental level, more studies need to be performed to understand the properties of aptamers, including their biological functions inside cells. Another direction includes discovering more new materials or molecules and then combining these new materials or molecules with aptamers to enhance their functionality. It is difficult to predict how far these aptamer systems with new functions can go, as new technologies will continue to emerge. However, it is certain that highly sophisticated architectures and attractive functionalities will continue to be designed, and they will find widespread applications in biology, biotechnology, and biomedicine.

References

1. Liu J, Cao Z, Lu Y (2009) Functional nucleic acid sensors. Chem Rev 109(5):1948–1998
2. Xing H et al (2012) DNA aptamer functionalized nanomaterials for intracellular analysis, cancer cell imaging and drug delivery. Curr Opin Chem Biol 16(3–4):429–435
3. Seferos DS et al (2007) Nano-flares: probes for transfection and mRNA detection in living cells. J Am Chem Soc 129(50):15477–15479
4. Zheng D et al (2009) Aptamer nano-flares for molecular detection in living cells. Nano Lett 9 (9):3258–3261
5. Rosi NL et al (2006) Oligonucleotide-modified gold nanoparticles for intracellular gene regulation. Science 312(5776):1027–1030
6. Jayagopal A et al (2010) Hairpin DNA-functionalized gold colloids for the imaging of mRNA in live cells. J Am Chem Soc 132(28):9789–9796
7. Wang Y et al (2010) Aptamer/graphene oxide nanocomplex for in situ molecular probing in living cells. J Am Chem Soc 132(27):9274–9276
8. Li Y et al (2004) Controlled assembly of dendrimer-like DNA. Nat Mater 3(1):38–42
9. Goodman RP et al (2005) Rapid chiral assembly of rigid DNA building blocks for molecular nanofabrication. Science 310(5754):1661–1665
10. Aldaye FA, Palmer AL, Sleiman HF (2008) Assembling materials with DNA as the guide. Science 321(5897):1795–1799
11. Yin P et al (2008) Programming DNA tube circumferences. Science 321(5890):824–826
12. Afonin KA et al (2010) In vitro assembly of cubic RNA-based scaffolds designed in silico. Nat Nano 5(9):676–682
13. Gu H et al (2010) A proximity-based programmable DNA nanoscale assembly line. Nature 465(7295):202–205
14. Severcan I et al (2010) A polyhedron made of tRNAs. Nat Chem 2(9):772–779
15. Wu C et al (2013) Building a multifunctional aptamer-based DNA nanoassembly for targeted cancer therapy. J Am Chem Soc 135(49):18644–18650
16. Zhu GZ et al (2013) Noncanonical self-assembly of multifunctional DNA nanoflowers for biomedical applications. J Am Chem Soc 135(44):16438–16445
17. Lee YC, Lee RT (1995) Carbohydrate-protein interactions: basis of glycobiology. Acc Chem Res 28(8):321–327

18. Mammen M, Choi S-K, Whitesides GM (1998) Polyvalent interactions in biological systems: implications for design and use of multivalent ligands and inhibitors. Angew Chem Int Ed 37 (20):2754–2794
19. Kortt AA et al (2001) Dimeric and trimeric antibodies: high avidity scFvs for cancer targeting. Biomol Eng 18(3):95–108
20. Rusconi CP et al (2002) RNA aptamers as reversible antagonists of coagulation factor IXa. Nature 419(6902):90–94
21. Kim Y, Cao Z, Tan W (2008) Molecular assembly for high-performance bivalent nucleic acid inhibitor. Proc Natl Acad Sci 105(15):5664–5669
22. Hirsh J (2003) Current anticoagulant therapy—unmet clinical needs. Thromb Res 109:S1–S8
23. Tasset DM, Kubik MF, Steiner W (1997) Oligonucleotide inhibitors of human thrombin that bind distinct epitopes. J Mol Biol 272(5):688–698
24. Deng B et al (2014) Aptamer binding assays for proteins: the thrombin example—a review. Anal Chim Acta 837:1–15
25. Nimjee SM et al (2005) The potential of aptamers as anticoagulants. Trends Cardiovasc Med 15(1):41–45
26. Wang K et al (2009) Molecular engineering of DNA: molecular beacons. Angew Chem Int Ed 48(5):856–870
27. Tyagi S, Kramer FR (1996) Molecular beacons: probes that fluoresce upon hybridization. Nat Biotech 14(3):303–308
28. Wang L et al (2005) Locked nucleic acid molecular beacons. J Am Chem Soc 127 (45):15664–15665
29. Yang CJ et al (2006) Hybrid molecular probe for nucleic acid analysis in biological samples. J Am Chem Soc 128(31):9986–9987
30. Wu Y et al (2008) Nucleic acid beacons for long-term real-time intracellular monitoring. Anal Chem 80(8):3025–3028
31. Tyagi S (2009) Imaging intracellular RNA distribution and dynamics in living cells. Nat Meth 6(5):331–338
32. Sharifi S et al (2012) Toxicity of nanomaterials. Chem Soc Rev 41(6):2323–2343
33. Liu H et al (2010) DNA-based micelles: synthesis, micellar properties and size-dependent cell permeability. Chem Eur J 16(12):3791–3797
34. Wu Y et al (2010) DNA aptamer–micelle as an efficient detection/delivery vehicle toward cancer cells. Proc Natl Acad Sci 107(1):5–10
35. Chen T et al (2013) DNA micelle flares for intracellular mRNA imaging and gene therapy. Angew Chem Int Ed 52(7):2012–2016
36. Wu C et al (2013) Engineering of switchable aptamer micelle flares for molecular imaging in living cells. ACS Nano 7(7):5724–5731
37. Tang Z et al (2008) Aptamer switch probe based on intramolecular displacement. J Am Chem Soc 130(34):11268–11269
38. Lin CH, Patei DJ (1997) Structural basis of DNA folding and recognition in an AMP-DNA aptamer complex: distinct architectures but common recognition motifs for DNA and RNA aptamers complexed to AMP. Chem Biol 4(11):817–832
39. Nutiu R, Li Y (2003) Structure-switching signaling aptamers. J Am Chem Soc 125 (16):4771–4778
40. Li N, Ho C-M (2008) Aptamer-based optical probes with separated molecular recognition and signal transduction modules. J Am Chem Soc 130(8):2380–2381
41. Bonnet G, Krichevsky O, Libchaber A (1998) Kinetics of conformational fluctuations in DNA hairpin-loops. Proc Natl Acad Sci 95(15):8602–8606
42. Wang J et al (2012) Assembly of aptamer switch probes and photosensitizer on gold nanorods for targeted photothermal and photodynamic cancer therapy. ACS Nano 6(6):5070–5077
43. Zheng G et al (2007) Photodynamic molecular beacon as an activatable photosensitizer based on protease-controlled singlet oxygen quenching and activation. Proc Natl Acad Sci USA 104 (21):8989–8994

44. McDonnell SO et al (2005) Supramolecular photonic therapeutic agents. J Am Chem Soc 127 (47):16360–16361
45. Zhu Z et al (2008) Regulation of singlet oxygen generation using single-walled carbon nanotubes. J Am Chem Soc 130(33):10856–10857
46. Tang ZW et al (2010) Aptamer-target binding triggered molecular mediation of singlet oxygen generation. Chem Asian J 5(4):783–786
47. Wang KL et al (2011) Self-assembly of a bifunctional DNA carrier for drug delivery. Ange Chem Int Ed 50(27):6098–6101
48. Ball P (2000) Chemistry meets computing. Nature 406(6792):118–120
49. Goldman N et al (2013) Towards practical, high-capacity, low-maintenance information storage in synthesized DNA. Nature 494(7435):77–80
50. Church GM, Gao Y, Kosuri S (2012) Next-generation digital information storage in DNA. Science 337(6102):1628
51. Adleman LM (1994) Molecular computation of solutions to combinatorial problems. Science 266(5187):1021–1024
52. Vuyisich M, Beal PA (2002) Controlling protein activity with ligand-regulated RNA aptamers. Chem Biol 9(8):907–913
53. Lee JF, Stovall GM, Ellington AD (2006) Aptamer therapeutics advance. Curr Opin Chem Biol 10(3):282–289
54. Kolpashchikov DM, Stojanovic MN (2005) Boolean control of aptamer binding states. J Am Chem Soc 127(32):11348–11351
55. Zhou M et al (2010) Aptamer-controlled biofuel cells in logic systems and used as self-powered and intelligent logic aptasensors. J Am Chem Soc 132(7):2172–2174
56. Han D et al (2012) A logical molecular circuit for programmable and autonomous regulation of protein activity using DNA aptamer-protein interactions. J Am Chem Soc 134 (51):20797–20804
57. Han D et al (2013) Engineering a cell-surface aptamer circuit for targeted and amplified photodynamic cancer therapy. ACS Nano 7(3):2312–2319
58. You MX et al (2014) DNA "nano-claw": logic-based autonomous cancer targeting and therapy. J Am Chem Soc 136(4):1256–1259
59. Nutiu R, Li YF (2003) Structure-switching signaling aptamers. J Am Chem Soc 125 (16):4771–4778
60. Douglas SM, Bachelet I, Church GM (2012) A logic-gated nanorobot for targeted transport of molecular payloads. Science 335(6070):831–834
61. Rothemund PWK (2006) Folding DNA to create nanoscale shapes and patterns. Nature 440 (7082):297–302
62. Rudchenko M et al (2013) Autonomous molecular cascades for evaluation of cell surfaces. Nat Nanotechnol 8(8):580–586
63. Zhang DY, Winfree E (2009) Control of DNA strand displacement kinetics using toehold exchange. J Am Chem Soc 131(47):17303–17314

Chapter 6
Aptamers-Guided DNA Nanomedicine for Cancer Theranostics

Guizhi Zhu, Liping Qiu, Hongmin Meng, Lei Mei and Weihong Tan

Abstract The past two decades have witnessed the booming of DNA aptamers, and particularly the development of aptamers for the specific recognition of versatile disease-related molecular biomarkers and living cells, as well as the application of aptamers for molecular and cellular engineering, bioanalysis, and disease therapy. Owing to the predictable Watson-Crick base-pairing, DNA can be easily designed and engineered to construct sophisticated molecular devices and nanostructures, which, at the same time, can be integrated with many biofunctionalities, including DNA aptamers for specific target recognition, bioimaging agents for biosensing, as well as drug-loading moieties for targeted drug delivery. The ability of many aptamers to mediate internalization into mammalian cells additionally empowered aptamer-incorporated DNA devices to be utilized for intracellular delivery of biosensors and drug carriers, and eventually sensing intracellular biomolecular behaviors in real-time or modulating intracellular biological activities for therapeutic purposes. In this chapter, we discuss the development of aptamer-integrated DNA nanodevices for versatile applications in bioanalysis and disease therapy, with an emphasis on cancer theranostics.

Keywords Aptamer · DNA nanotechnology · DNA engineering · Biosensor · Targeted drug delivery

G. Zhu
Laboratory of Molecular Imaging and Nanomedicine, National Institute of Biomedical Imaging and Bioengineering, National Institutes of Health, Bethesda, MD 20892-3759, USA

L. Qiu · W. Tan
Molecular Sciences and Biomedicine Laboratory, State Key Laboratory for Chemo/Biosensing and Chemometrics, College of Biology and College of Chemistry and Chemical Engineering, Collaborative Innovation Center for Chemistry and Molecular Medicine, Hunan University, Changsha 410082, China

L. Qiu · H. Meng · L. Mei · W. Tan (✉)
Departments of Chemistry, Physiology and Functional Genomics, Center for Research at the Bio/Nano Interface, Shands Cancer Center, UF Genetics Institute and McKnight Brain Institute, University of Florida, Gainesville, FL 32611-7200, USA
e-mail: tan@chem.ufl.edu

W. Tan and X. Fang (eds.), *Aptamers Selected by Cell-SELEX for Theranostics*,
DOI 10.1007/978-3-662-46226-3_6

6.1 Introduction

DNA has been extensively studied to develop nanodevices, owing to the remarkable features of DNA, such as biodegradability and sequence programmability. Various DNA nanodevices have been developed, including DNA origami [1], tetrahedra [2], nanotrains, nanoflowers, and so forth. Molecular DNA can also serve as recognition probes against a wide range of targets. These probes are generally termed as aptamers. The combination of aptamers and DNA nanodevices can thus merge the specific recognition capability of aptamers with the ability of DNA nanodevices for sensitive bioanalysis and disease-related biomarker detection, as well as targeted delivery of therapeutics.

Nucleic acid aptamers, single-stranded (SS) oligonucleotides with unique intramolecular conformations and specific recognition abilities to targets, are isolated from large libraries containing 10^{13}–10^{16} random nucleic acid sequences through SELEX [3, 4]. Since the pioneering isolations of aptamers against organic dyes [3] and T4 DNA polymerase [4] in 1990, a wide variety of aptamers have been identified. The targets of aptamers range from small molecules [3, 5, 6], to biomacromolecules such as proteins [4, 7–13], virus-infected cells [14], stem cells [15], and mammalian cancer cells [16–23], as well as implanted tumors [24]. A wide variety of targets of high interest in clinical diagnosis and therapy were used as targets for aptamer identification, which resulted in an array of aptamers that have the potential for rapid and sensitive diagnosis, agonist therapeutics, targeted delivery of therapeutics, and as templates for disease biomarker discovery and high-throughput drug screening. In addition, the elucidation of molecular structures of some aptamer-target complexes [25–28] will not only help our understanding of aptamer-target interaction, but also facilitate drug design and screening, and the discovery of new drugable sites on disease biomarkers.

Particularly, cell-SELEX has been developed to use living cancer cells as targets during aptamer screening, with the long-term goal of screening molecular probes for cancer theranostics (diagnosis and therapy), which has been discussed in previous chapters. Cell-SELEX provides a unique set of capabilities: Identification of aptamers that recognize molecules needing cofactors or post-translational modification to form functional conformations on the cell membrane; aptamer identification without prior knowledge of the molecular differences between targets and non-targets; simultaneous generation of a collection of aptamers, which may have different molecular targets; further application of the resultant aptamers for disease biomarker identification, which could, in turn, help elucidate protein expression patterns on diseased cell surfaces, decipher the pathogenesis, and open new avenues to therapy. Using cell-SELEX, aptamers were identified against cells of a panel of cancers, including acute lymphocytic leukemia (ALL) T cell leukemia [16], liver cancer [18], acute myeloid leukemia (AML) [19], lung cancer [20, 23], ovarian cancer [22], B cell lymphoma [29], colorectal cancer [30], and breast cancer [31]. These aptamers were then able to serve as excellent probes for early detection of cancer cells or cancer-related biomarkers, as well as targeted delivery of

therapeutics into cancer cells. In addition, the ability to evolve aptamers to target diseased cells through cell-SELEX without prior knowledge of exact molecular targets provides a novel way to identify disease-associated biomarkers and is poised to increase our understanding of molecular oncology and guide targeted therapy.

Compared with other molecular recognition moieties, such as antibodies, aptamers hold many unique properties or advantages for biomedical applications. Briefly, aptamers can be developed against a wide range of targets, including those toxic to organisms and therefore inaccessible for antibody development. The latter capability makes it feasible to generate aptamers to toxic therapeutics and to utilize the complexes of resultant aptamers and therapeutics for targeted transport of toxic drugs. Moreover, aptamer identification through in vitro SELEX is usually more efficient and cost-effective than antibody development. The advancement of automated nucleic acid synthesis enables easy, cost-effective chemical synthesis and modification of functional moieties, as well as scale-up on a commercial level. The binding affinities of aptamers to their targets (K_d's are typically in the high picomolar to low nanomolar range) are comparable to, or sometimes stronger than, those of other molecular recognition elements, such as antibodies. O'Donoghue et al. [32] Other advantages include high stability and long shelf-life, rapid tissue penetration due to relatively small molecular weights, low immunogenicity [33], and ease of antidote development [34, 35]. This collection of advantages makes aptamers more than attractive for clinical or biomedical applications, such as disease diagnosis and therapy.

Nucleic acid aptamers are easy to be molecularly/nano-engineered and chemically modified, which, combined with the predictable Watson-Crick base-pairing of nucleic acids, has made aptamers (examples list in Table 6.1) easily incorporated into nucleic acid nanodevices. Nucleic acids have been used as building block materials to construct various nucleic acid nanostructures for applications in biomedicine and biotechnology.

Nucleic acids hold unique features and have been extensively exploited for applications in the field of molecular medicine and nanomedicine. Owing to Watson-Crick base-pairing, the resultant programmability of nucleic acids allows nucleic acid nanostructures to be self-assembled through versatile approaches, including nucleic acid-hybridization-dependent assembly and non-hybridization-dependent nucleic acid nanocomplexation. More attractively, the incorporation of molecular functionalities into nucleic acid nanodevices allows them to specifically recognize molecular targets, which is particularly significant for the development of bionanotechnology. In particular, the functionalities can range from nucleic acid functionalities, such as aptamers, molecular beacons, DNA antisense, and siRNA, through predicable molecular design and simple self-assembly, to relatively general or non-nucleic acid functionalities, such as fluorophores, radiotracers, and chemical therapeutics, through physical interaction, chemical conjugation, or biochemical conjugation via enzymatic reaction. For instance, aptamers have been incorporated into nucleic acid nanosensors for sensitive monitoring of biomolecules, and aptamer-modified nanostructures have also been developed as drug nanocarriers to selectively deliver therapeutics into target diseased cells.

Table 6.1 Examples of nucleic acid aptamers having potential to be incorporated into DNA nanodevices for disease theranostics (diagnosis and therapy)

Aptamers	Molecular targets	Associated pathogenesis	Refs
Macugen	Vascular endothelial growth factor	Age-related macular degeneration	Gragoudas et al. [36]
AS1411	Nucleolin	Cancer development	Bates et al. [37]
sgc8	Protein tyrosine Kinase 7	Cancer development	Shangguan et al. [38]
A20	Prostate-specific membrane antigen	Cancer development	Lupold et al. [39]
TTA1	Tenascin C	Cancer development	Daniels et al. [8]
S1.3/S2.2	Mucin 1	Cancer development	Ferreira et al. [40]
IGEL1.2	Immunoglobulin E	Allergy	Wiegand et al. [41]
Apt-αvβ3	αvβ3 integrin	Cancer development	Mi et al. [42]
TBA (thrombin binding aptamer)	α-thrombin	Thrombosis	Bock et al. [10]
B28	HIV gp120	Viral infection	Khati et al. [13]
(NA)	NF-κB	Cancer development	Lebruska and Maher [43]
E2F-E1	E2F transcription factor	Cancer development	Martell et al. [44], Ishizaki et al. [45]
A30	HER3	Cancer development	Chen et al. [12]

NA not available

In this chapter, we will discuss the biomedical applications of aptamers generated by cell-SELEX for specific recognition of diseased cells. Specifically, from the molecular engineering and nanoengineering perspectives, we will cover the engineering of aptamer-incorporated molecular biosensors, nanosensors, and drug nanocarriers; and from the biomedical application perspective, we will cover the applications of the corresponding DNA devices in bioanalysis, bioimaging, and targeted drug delivery. We will also cover a novel approach to the self-assembly of DNA nanostructures, through the self assembly of a high concentration of DNA generated during rolling circle replication, in contrast to conventional assembly of DNA nanomaterials through DNA hybridization.

6.2 Building DNA Biosensors on Target Living Cell Surfaces

The cell membrane serves as the interface between the intracellular and extracellular environments. On one hand, intracellular biological activities can be regulated via signal transduction resulting from the interaction of membrane-bound receptors

and signaling molecules, including hormones, neurotransmitters, or therapeutics from complex extracellular environments; on the other hand, extracellular biological behavior can also be influenced by intracellular molecular role players by means of such secretion of intracellular biomolecules, regulation of cellular biophysics through intracellular organization of cytoskeletons, etc. [46]. In situ, analysis and regulation of these key biomolecular role players is necessary for both a complete, comprehensive understanding of biological pathways with high spatiotemporal resolution and specific biological and therapeutic applications.

To sense biomolecular behavior in situ on the cell membrane, one approach is to build biosensors in situ in the local microenvironment on cell surfaces. Previous tactics to accomplish these goals include cell-surface engineering through genetic approaches and chemical modification. Cell-surface modification with proteins has been achieved through genetic engineering, whereby cells are transformed with plasmids or transfected with viruses that express proteins of interest and secrete them onto cell surfaces. While this approach can be hampered by complex manipulation, prolonged protein expression and secretion, or difficult construction of nanostructures using these proteins [47], an alternative approach, chemical modification of cell surfaces with such moieties as proteins, DNA, or nanomaterials has provided a new direction for cell-surface engineering. For example, using Staudinger ligation, mammalian cell surfaces were modified with DNA and imparted specific recognition capability to cells, enabling programmed assembly of three-dimensional microtissues [48].

Beyond these strategies, DNA, as a novel biomaterial in addition to the carrier of genetic information, combined with nucleic acid functionalities, such as aptamers, offers a simple method to engineer nanodevices in situ on target cell surfaces. Because of Watson-Crick base-pairing and programmability, DNAs have been explored as novel biomaterials for the construction of DNA nanostructures [49]. Herein, we will discuss a few examples of the construction of molecular biosensors and nanosensors on target living cells for in situ bioanalysis.

6.2.1 Using Chimeric DNA-Lipid to Build Cell Membrane-Anchored DNA Aptamer Biosensors

The cellular microenvironment includes the local surroundings with which cells interact by processing various physical and chemical signals. The microenvironment is of significance in regulating many cell functions, such as metabolism, signaling, and apoptosis. It even affects the differentiation fate of stem cells [50, 51]. The ability for real-time monitoring of the cellular microenvironment can provide valuable information for studying many important biological processes [50, 52]. On the other hand, because of the rapid fluctuation of molecules and ions in the cell membrane-surrounding environment, as well as the quick diffusion of the released molecules and ions into the bulk medium, it is always challenging to capture and to

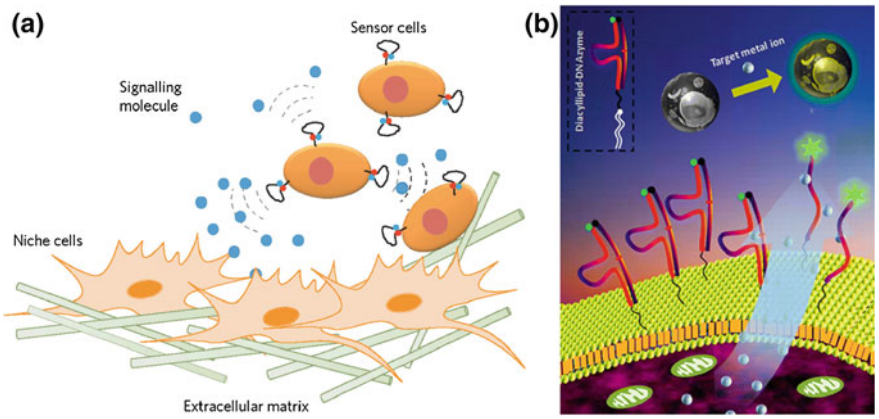

Fig. 6.1 Schematic representation of two cell-surface DNA biosensors. **a** Fluorescent aptamers were immobilized on the cell membrane via covalent chemistry and used for monitoring a protein target in the cellular microenvironment. Reprinted by permission from Macmillan Publishers Ltd: Ref. [54], copyright 2011. **b** Fluorescent DNAzymes anchored on the cell membrane by hydrophobic interactions and used for monitoring target metal ion in real time. Reproduced from Ref. [60] by permission of the royal society of chemistry

measure the analytes using conventional detection techniques, for example, enzyme-linked immunosorbent assay (ELISA), fluorescence, inductively coupled plasma-atomic emission spectrometry, and mass spectrometry.

To overcome this challenge, biosensing elements have been engineered onto the cell membrane and have shown their capability for investigating cell functions with high spatial and temporal resolution [53–56]. Thus far, cell-surface sensors have been designed for signaling proteins, enzymes, or metabolites by using fluorescent proteins, polymers, nanoparticles, or aptamers as the sensing units. Among which, DNA probes have been attractive biosensing elements, due to their intrinsic advantages of high stability, easy synthesis, flexible design, reproducibility, and convenient modification with various functional groups. Moreover, based on an in vitro selection technique termed as SELEX, various functional DNA probes, primarily aptamers [57, 58] and DNAzymes [59], have been selected from random DNA libraries on the basis of either their specific affinity to target cargos or their ability to induce catalytic reactions in the presence of target molecules. As aptamers and DNAzymes appear, the application of DNA probes in biosensing areas has expanded quickly from gene test to the analysis of small molecules, metal ions, peptides, proteins, and even whole viruses, bacteria, and cells.

By using functional DNAs as the sensing blocks, the Karp group at Harvard University engineered a modified aptamer which can specifically bind to platelet-derived growth factor (PDGF) onto the membranes of mesenchymal stem cells through covalent chemistry (Fig. 6.1). For signal transduction, the aptamer was labeled with a fluorescence emitter and a fluorescence quencher. In the absence of target, the fluorophore did not emitting, due to the quenching of fluorescence.

However, upon binding with PDGF, the conformational change of the aptamer resulted in the partition of the dye and quencher, thus restoring the fluorescence and producing a detectable signal. In this way, the cell-surface aptamer sensor was able to detect both the exogenously added and the neighboring cell-secreted PDGF with high spatiotemporal resolution.

In order to engineer biosensing elements onto the cell membrane without affecting the cell physiology, our research group has developed a simple, efficient, noninvasive, and universal strategy for construction of cell-surface sensors by using diacyllipid-DNA conjugates as the building and sensing elements (Fig. 6.1) [60]. The diacyllipid-DNA conjugate, which was first synthesized in our lab, was prepared by directly incorporating a diacyllipid phosphoramidite tail on the 5′-end of the DNA sequence in an automated DNA synthesizer [61]. We have demonstrated that the diacyllipid-DNA conjugate can efficiently self-assemble onto the cell membrane based on the hydrophobic interaction between the lipophilic tail and the cellular phospholipid layer [61, 62]. The membrane-anchored DNA biosensors could be simply fabricated by directly incubating the cells with the diacyllipid-DNA probes and then washing away the free probes. To verify the performance of this cell membrane-anchored sensor, we engineered specific DNAzymes on the cell membrane for metal ion assay in the extracellular microspace. The cell-surface DNAzymes showed excellent performance for reporting and quantifying both exogenous and cell-extruded target metal ions in real time. Furthermore, with the variety and power of DNA probes, this membrane-anchored sensor could also be used for detection of various targets by inserting different DNA probes, providing potentially useful tools for versatile applications in cell biology, biomedical research, drug discovery, and tissue engineering.

6.2.2 *Using Aptamers to Build Fluorescent DNA Nanobiosensors on Target Living Cell Surfaces*

Aptamer-tethered DNA nanodevices (aptNDs) were built in situ on cell surfaces by either anchoring of preformed fluorescent aptNDs or the in situ self-assembly of fluorescent aptNDs. Fluorescence has been attractive for noninvasive biosensing in living cells, and the ability to modify DNA with fluorophores enables versatile application of fluorescence in DNA-based biosensors.

To construct aptNDs, the Tan group first designed two partially complementary hairpin monomers, namely M1 and M2, in which the stored energy in each loop was protected by the corresponding stem, preventing their hybridization and polymerization in the absence of an initiator trigger probe. Aptamers sgc8 and TDO5 were chosen to construct our model aptNDs. Sgc8 binds to target protein PTK7, which is overexpressed on target CEM cells, but not on nontarget Ramos cells. TDO5 binds to the μ heavy chain of immunoglobulin M overexpressed on

Ramos cells, but not on CEM cells. A DNA initiator probe was modified on the 5′-ends of the aptamers, resulting in the self-assembly of nanodevices in a cascading manner from M1 and M2 via HCR. The resultant aptNDs carried multiple monomers and were implemented for chemical labeling (covalent) of multiple copies of fluorophores or physical association (noncovalent) with multiple dsDNA-intercalating fluorophores on these nanosensors.

Corresponding to the different types of fluorescence signal transduction widely used in bioanalysis, three different types of aptNDs were constructed and selectively anchored on target cell surfaces: (1) a chemically modified fluorescent aptND, in which fluorophores were chemically modified on the ends of DNA monomers; (2) a label-free fluorescent aptND, in which fluorogenic molecules were physically associated with dsDNA boxcars; and (3) a FRET aptND, in which two fluorophores were chemically modified on monomers and physically associated with boxcars, respectively, to enable energy transfer between the two (Fig. 6.2a) [63].

Chemically modified fluorescent aptNDs were built by modifying DNA monomers with fluorophores (FITC as a model). Flow cytometry analysis of cells incubated with the resultant aptNDs indicated that these aptNDs were anchored selectively on their corresponding target cell surfaces. In addition, since a single nanodevice was loaded with multiple fluorophore copies, cells having anchored aptNDs displayed enhanced fluorescence intensities compared with the corresponding cells labeled with aptamers. Likewise, label-free fluorescent aptNDs were built on target cell surfaces using aptNDs loaded with fluorogenic dsDNA-intercalating dyes (EvaGreen (EG) as a model), taking advantage of the structural feature of aptNDs that consist of long dsDNA sections. Again, these aptNDs were evaluated by flow cytometry and demonstrated to be selectively anchored on cell surfaces. We also studied construction of FRET nanodevices on living cell surfaces. The programmability of aptNDs and ease of chemical modification on DNA allowed the tandem positioning of multiple FRET components by both covalent and noncovalent means. In this nanodevice, EG (energy donor) was intercalated into dsDNA of aptNDs, and Cy3 (energy acceptor) was chemically modified on the 3′-ends of monomers, M1 and M2. The intercalated EG was designed to absorb short-wavelength light and then transfer the energy to densely positioned and evenly distributed Cy3 on the proximate aptNDs. Fluorescence spectrometry and flow cytometry both demonstrated the efficient energy transfer on aptNDs and the immobilization of these DNA structures on cell surfaces.

In addition to building preformed nanodevices on cell surfaces, in situ nanodevice assembly would be highly desirable, especially in situations where it is difficult to transport preformed devices to, or anchor them on, target cells. Construction of such devices may also be hindered by the absence of local stimuli. Motivated by this, we further exploited the in situ self-assembly of fluorescent aptNDs on target living cell surfaces (Fig. 6.2b).

Overall, owing to the specific recognition ability of aptamers and the programmability of DNA, we have built fluorescent DNA nanodevices on target living

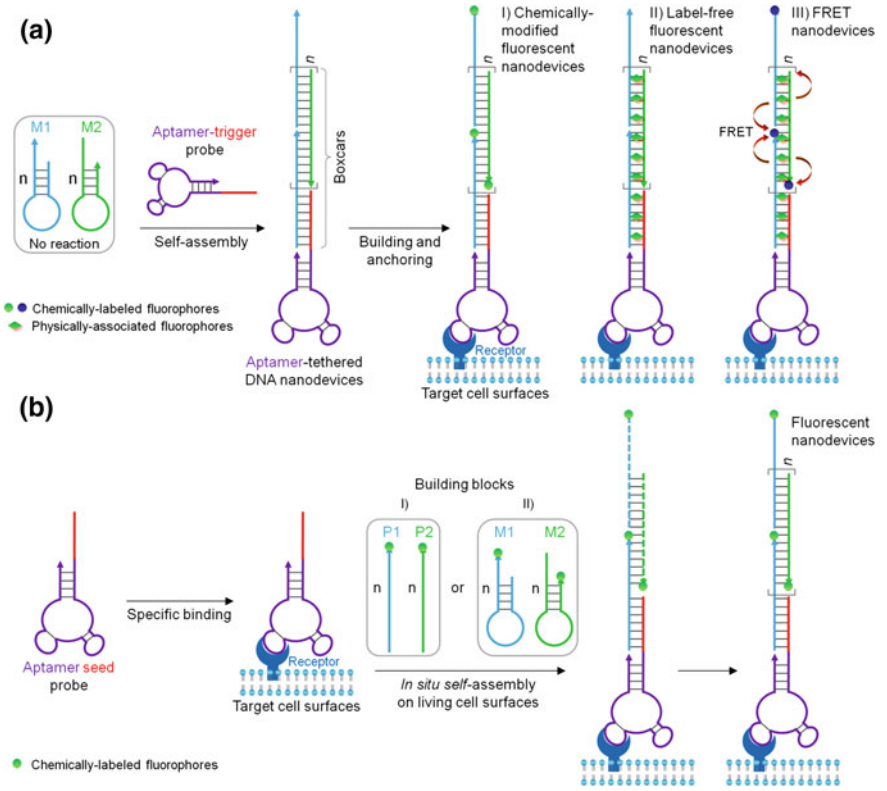

Fig. 6.2 Schematic illustration of the construction of fluorescent DNA nanodevices on target living cell surfaces. **a** Three types of fluorescent DNA nanodevices, preformed via HCR-based self-assembly upon initiation by aptamer-tethered trigger probes, are anchored on target cell surfaces, or **b** aptamer seed probes initiate in situ self-assembly of fluorescent DNA nanodevices on target cell surfaces by either (*I*) cascading alternative hybridization of two partially complementary monomers or (*II*) HCR. Reprinted with the permission from Ref. [63] copyright 2013 wiley

cell surfaces in order to achieve the long-term goal of pinpoint bioanalysis or biomanipulation on target living cell membranes in the complex extracellular environment. The features of repetitive and alternating DNA building blocks in these nanodevices provide an excellent platform for positioning of multi-component molecular arrays through either chemical modification or physical interaction. This approach could be useful for real-time tracking of analytes in extracellular environments, cell-surface engineering, targeted drug delivery, and manipulation of biological pathways.

6.3 Aptamers Guide and Deliver DNA Biosensors into Living Cells for Real-Time Monitoring of Bioactivities

The intracellular environment holds most of the molecular machineries and is the site for the majority of molecular biological activities. Knowledge of the involved molecular role players is essential to the elucidation of these biological activities. Biosensors comprise a class of smart devices that can be used to accomplish this task. However, the cell membrane presents a physical barrier for many biosensors to penetrate living cells. Fortunately, many aptamers are capable of being internalized into living cells, without compromising cellular integrity. Hence, aptamers have been engineered into various molecular biosensors or nanosensors, allowing them to be delivered into cells and executing intracellular biosensing in intact cytoplasmic environments, providing a potential robust approach to "watching" the biological activities in their native state.

6.3.1 Aptamer-Mediated Targeted Delivery of DNA Biosensors for Intracellular Monitoring of mRNA

Cells, as the building blocks of life, occupy the midpoint of micro- and macrostructure and provide critical insight into the basic processes of life at the molecular level [64, 65]. The ability for real-time monitoring of specific bioactive molecules in living cells enables us to obtain a better understanding of cellular dynamic functions [66, 67]. To implement live-cell monitoring, the first task is to construct effective biosensors for signaling the presence of the analytes, and then send them into the target living cells. While many excellent biosensors have been fabricated [68, 69], the development of their cellular delivery methods has lagged far behind. Taking live-cell messenger-RNA (mRNA) detection for example, mRNAs are specific RNAs that convey genetic information from DNA in the nuclei to guide protein synthesis in the cytoplasm. The expression level and subcellular distribution of specific mRNA can be modulated by cells when responding to their internal genetic programs or external stimuli. Therefore, intracellular mRNA monitoring can yield valuable information for biological study, medical diagnosis, adaptive therapy, and drug discovery. So far, in situ hybridization is the commonly used technique for studying intracellular events [70]. However, since this method presents a static map in fixed cells and the cellular structure may be affected by the fixing process, live-cell imaging is a more desirable approach. Of the several current live-cell imaging methods, molecular beacons (MBs) may be the most attractive, since they are easy to make, simple to use, convenient to modify with various functional groups, and they do not involve the complicated genetic manipulations of GFP-tagged methods [71] or require removal of unbound probes [72]. To visualize and

track mRNA in living cells, one critical issue must be addressed: delivering MBs into the cytoplasm with high efficiency.

Since MBs are negatively charged hydrophilic macromolecules, they cannot permeate the lipophilic cell membrane [73]. To solve the problem of MB delivery, several solutions have been attempted, including microinjection, electroporation, reversible permeabilization, transfection using liposomes and cationic polymers, and peptide-assisted delivery, to name just a few. Despite wide investigation, all of these methods have their limitations. For example, microinjection is tedious and low-throughput, while oligonucleotide probes sequester in the nucleus rapidly and completely by a single pulse [74]. Electroporation and reversible permeabilization using streptolysin O are invasive and may generate a variation in the intracellular amount of the probes, since probes enter cells by passive diffusion [75]. Methods based on transfection with liposomes or cationic polymers are reported to deliver the probes via the endocytic pathway, followed by additional problems common to endosomes or lysosomes, such as rapid degradation, low efficiency, and high background [76]. Although peptide-assisted delivery can deliver probes in a non-endocytic way, its application was limited by the complicated conjugation between the peptide and the DNA [77]. Moreover, most of these methods show no cell specificity.

Delivery strategies with the advantages of high-throughput, non-invasive, low cost, and simple synthesis are being sought. Aptamers have become attractive targeting ligands; in particular, those aptamers which can internalize into cells have been widely used for cell-targeted drug delivery [78]. The Tan group developed a self-delivered MB for detecting mRNA in living cells through hybridization between the cell-type specific internalizing aptamer AS1411 and the MB (Fig. 6.3) [79]. Aptamer AS1411 can specifically recognize nucleolin, which is overexpressed on the cancer cell membrane [80]. Since nucleolin can transport between the cell membrane and the nucleus, AS1411 can be delivered into the cells. In this design, the MB was integrated with AS1411 via hybridization with the extended cDNA sequence of AS1411; thus, the MB was efficiently delivered into the cytoplasm of targeted cells using the aptamer as the guidance system. To control the detection activity of the MB, two light-sensitive caging groups were inserted in the cDNA sequence of AS1411, disabling the MB's ability to sense the presence of the target in the absence of activation by a single light pulse. In this way, the MB was able to detect target mRNA with high spatial and temporal resolution. By using cell-internalizing aptamers as the guidance system, many biosensors can be efficiently delivered into the target cells and perform live-cell monitoring of specific biomolecules in real time.

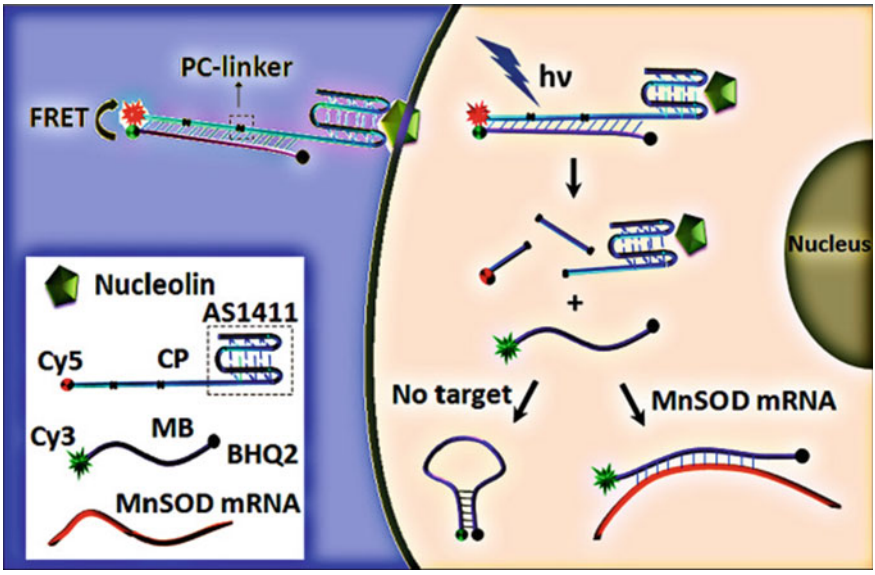

Fig. 6.3 Schematic illustration of the targeted, self-delivered, and photocontrolled molecular beacon for mRNA detection in living cells. Reprinted with the permission from Ref. [79] copyright 2012 American chemical society

6.3.2 Aptamer-Incorporated DNA Dendrimers as Efficient Nanocarriers of Functional Nucleic Acids for Intracellular Molecular Sensing

Dendritic molecules are highly branched, globular, monodisperse, and nanosized structures, which have attracted much attention in biomedicine and biotechnology [81]. Because of their biocompatibility, programmability, and easy synthesis, nucleic acids are excellent candidates for fabrication of dendritic structures, as theorized by Nilsen et al. [82]. These dendrimer-like DNA structures were first produced in 2004 by Li et al. [83] using enzymatic ligation.

The Liu group then reported an enzyme-free method to swiftly prepare large DNA dendrimers in high yield. DNA dendrimers were prepared from Y-shaped DNA using an enzyme-free and step-by-step assembly strategy. To prepare the Y-DNA, equal moles of three or four oligonucleotides were first mixed together. Different generations of DNA dendrimer (G_n) were then prepared from Y-DNAs. The sequences of Y-DNA were carefully designed to guarantee that the hybridization of sticky ends would only occur between Y_n and Y_{n+1}. To achieve pH responsiveness in a DNA dendrimer, they incorporated a type of DNA molecular motor into the scaffold between the core and the first layer. This DNA molecular motor is composed of a cytosine-rich strand and an optimized complementary sequence X. Under basic or neutral conditions, it forms an extended duplex, but

under slightly acidic conditions, it folds into a constrained four-stranded i-motif structure between cytosine residues. Upon a change in pH value, the i-motif DNA undergoes conformational changes and generates several nanometers of linear motion, which were expected to allow for tunable dimensions of the DNA dendrimer.

The Tan group recently developed a DNA dendrimer scaffold as an efficient nanocarrier to deliver functional nucleic acids (FNAs) and to conduct in situ monitoring of biological molecules in living cells. A histidine-dependent DNAzyme and an ATP-binding aptamer were chosen as the model FNAs. The DNAzyme or aptamer was incorporated in the second layer (Y_1) of the DNA dendrimer, which contained four different single strands and served as the signal reporter part of the sensing system (Fig. 6.4) [84].

In their design of the L-histidine-responsive DNA dendrimer sensing system, the 3′-end of the Y_{1b} strand was functionalized with a quencher (BHQ-1), while the 5′-end of the substrate strand X was labeled with carboxyfluorescein (FAM). The four oligonucleotides Y_{1a}, the Y_{1b} enzyme strand of DNAzyme $Y_{1c\text{-}L\text{-}histidine}$, and its substrate strand $X_{L\text{-}histidine}$ hybridize to form the Y-shaped structure $Y_{1\text{-}L\text{-}histidine}$, which brings the quencher and fluorophore into close proximity, thereby effectively quenching FAM fluorescence. In the presence of L-histidine, the substrate strand X is cleaved, resulting in a shorter DNA strand which shows a lower melting temperature (12.7 °C) with Y_{1b} than that of the original full-length substrate strand (44.3 °C). Thus, the shorter DNA strand containing FAM is then released from the sensing system at room temperature and away from the quencher BHQ-1, causing fluorescence recovery to sense L-histidine.

They also employed a similar strategy to design an aptamer-based DNA dendrimer sensing system. Here, DNA dendrimer served as a transporter of DNA aptamer into living cells. The ATP aptamer strand was modified with the FAM on its 5′-end (denoted X_{ATP}). The 3′-end of the Y_{1b} strand was functionalized with a quencher (Black Hole Quencher-1, BHQ-1), and the $Y_{1c\text{-}ATP}$ strand was designed to partly hybridize with X_{ATP}. In the absence of the target, the four oligonucleotides Y_{1a}, Y_{1b}, $Y_{1c\text{-}ATP}$, and anti-ATP aptamer strand X_{ATP} hybridize to form $Y_{1\text{-}ATP}$, bringing the fluorophore and quencher into close proximity, thereby effectively quenching the fluorescence of FAM. However, as a result of the strong binding affinity between ATP-binding ATP aptamer and ATP, the introduction of the target ATP into the DNA dendrimer sensing system induces formation of an ATP-aptamer complex, releasing the aptamer from the dendrimer, causing fluorescence recovery of the sensing system to sense ATP (Fig. 6.5).

Further, intracellular monitoring of histidine and ATP demonstrated that these FNA-embedded dendrimeric sensing systems could successfully self-deliver into living cells while maintaining their target recognition capabilities. Instead of incorporating potentially biohazardous inorganic materials for efficient FNA delivery, the proposed nanocarrier employs naturally occurring DNA molecules as building blocks, exhibiting excellent biocompatibility. Moreover, such nanocarriers

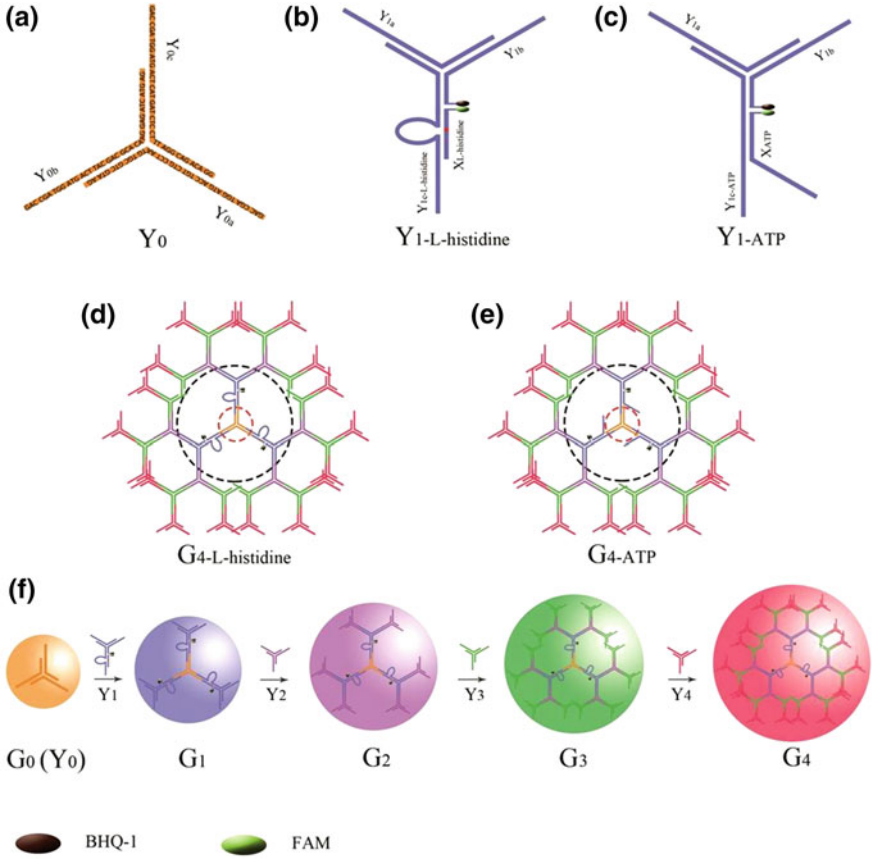

Fig. 6.4 **a** Y_0 was assembled from three different single strands: Y_{0a}, Y_{0b}, and Y_{0c}. The other Y-DNA scaffolds were prepared according to same strategy, except for Y_1. **b** $Y_{1\text{-L-histidine}}$ was achieved by the assembly of Y_{1a}, Y_{1b}, $Y_{1c\text{-L-histidine}}$, and $X_{\text{L-histidine}}$. **c** $Y_{1\text{-ATP}}$ was achieved by the assembly of Y_{1a}, Y_{1b}, $Y_{1c\text{-ATP}}$, and X_{ATP}. **d** $G_{4\text{-L-histidine}}$ was assembled from Y_0, $Y_{1\text{-L-histidine}}$, Y_2, Y_3, and Y_4. **e** $G_{4\text{-ATP}}$ was assembled from Y_0, $Y_{1\text{-ATP}}$, Y_2, Y_3, and Y_4. **f** The preparation of the first to fourth generation of DNA dendrimers. Reprinted with the permission from Ref. [84] copyright 2014 American chemical society

possess several other advantages, such as easy preparation, enhanced enzyme-resistance, high stability at very low concentrations (no CMC effect), and good self-delivery capability. These advantages, coupled with the fact that DNAzymes and aptamers for any target can be selected via in vitro selection, make this DNA dendrimeric nanocarrier a promising new platform for efficient intracellular monitoring of targets of interest and, hence, for wide applications in biomedicine.

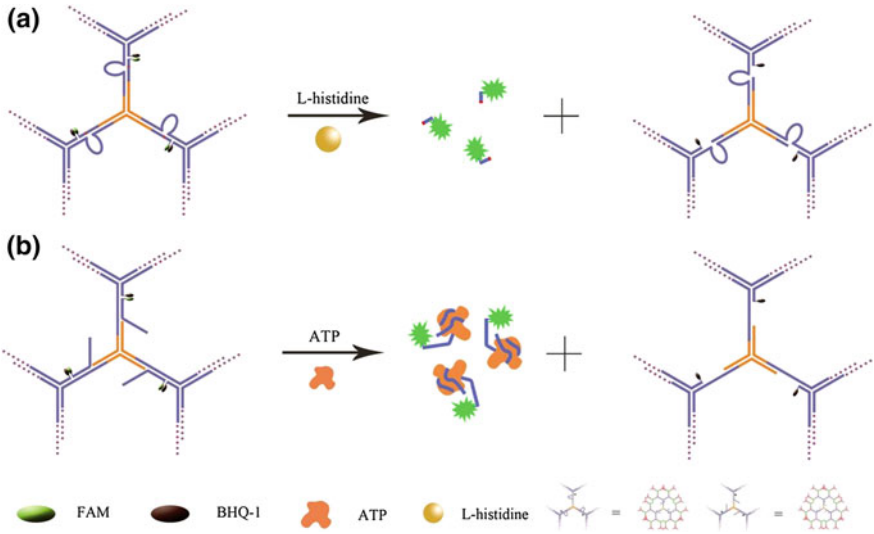

Fig. 6.5 **a** Schematic of DNAzyme-based dendrimeric sensing system for L-histidine. **b** Schematic of aptamer-based dendrimeric sensing system for ATP. Reprinted with the permission from Ref. [84] copyright 2014 American chemical society

6.4 Aptamers Guide and Deliver DNA Drug Nanocarriers into Diseased Cells for Targeted Therapy

Conventional cancer therapeutic modalities, such as chemotherapy and radiotherapy, are predominant in current clinical cancer therapy. However, these therapeutic modalities usually lack specificity and consequently induce cytotoxicity in both cancerous and healthy cells, causing side effects [85], limited maximal tolerated dosage (MTD) and reduced therapeutic efficacy [86, 87]. A therapeutic [88] platform with cancer cell-selective drug delivery is expected to overcome these limitations. Toward this end, DNA nanotechnology, by its programmability, has been extensively studied for the rational assembly of one-, two-, and three-dimensional nanodevices [49, 89–91] for the passive targeted delivery of theranostic agents by the enhanced permeation and retention (EPR) effect [1, 2, 92–98]. Because of the leaky blood vasculature in tumors, nanomaterials with diameters as small as a few hundred nanometers are more likely to penetrate through to tumor tissues, be taken up by cancer cells, and remain in tumor tissues for an enhanced retention time resulting from the weakened lymphatic drainage in tumor tissues [99–101]. Additionally, these nanodevices can also be appended with aptamers for active targeting to guide the delivery of theranostic agents to the specific target diseased cells. Recent biotechnological advancements have led to a variety of targeted drug delivery systems based on aptamer-DNA nanodevices [93, 94].

By molecular- and nano-engineering, scientists have developed various aptamer-integrated DNA nanodevices to serve as drug carriers for targeted delivery of therapeutics and the subsequent regulation of biological activities in target cells [102]. Herein, we will mainly discuss aptamer-incorporated two-dimensional DNA nanotrains, spherical DNA nanoflowers, and DNA origami for targeted delivery of imaging agents and chemotherapeutics, as well as immunotherapeutics for disease theranostics.

6.4.1 *Aptamer-Tethered DNA Nanotrains for Targeted Delivery of Molecular Imaging Agents and Drugs for Cancer Theranostics*

While chemotherapeutic drugs lack specificity and can cause side effects, a theranostic [88] platform with the ability of targeted drug delivery is expected to solve these problems. Toward this end, a variety of drug delivery systems based on aptamer-drug conjugates or aptamer-nanomaterial assemblies [14, 93, 94, 103–106] have been reported. DNA nanotechnology has also been utilized to develop targeted delivery systems for theranostic agents [1, 2, 92–98]. However, these strategies have unique limitations that could hamper the transition to clinical application, including (1) complicated design, laborious, and uneconomical preparation of DNA to construct these sophisticated DNA nanodevices, or laborious and inefficient preparation of aptamer-drug conjugates [1, 93, 95, 96, 98, 103]; (2) limited drug payload capacity and the resultant high cost, hampering production scale-up [1, 93, 95, 96, 98, 103, 104, 106]; (3) poor biodegradability, leading to chronic accumulation of many inorganic nanomaterials in vivo [107, 108]; and (4) limited universality [104].

We have designed and engineered a DNA nanodevice, termed as aptamer-tethered DNA nanotrain (aptNTr), to circumvent these limitations [109]. An aptNTr is a long linear DNA nanostructure self-assembled simply from two short DNA strands upon initiation of aptamer-tethered trigger probes, through a hybridization chain reaction (HCR) [91] (Fig. 6.6). Each nanotrain is tethered with an aptamer moiety on one end for molecular targeting of cognate cancer cells and operating like locomotives to guide a series of tandem dsDNA "boxcars" toward target cells. Two hairpin monomers (M1 and M2) were designed, such that the stored energy in the loops is protected by the corresponding stems, preventing their polymerization in the absence of an initiation probe. To construct aptNTrs, aptamer sgc8 was chosen as a model. Sgc8 can bind to target protein PTK7, which is overexpressed on target CEM cell membranes, but not on nontarget Ramos cells [16, 38]. To initiate NTr self-assembly, a DNA trigger probe was modified on the 5′-end of sgc8. Introduction of sgc8-trigger to a mixture of M1 and M2 initiated the autonomous polymerization of these building blocks through mutual hybridization, resulting in

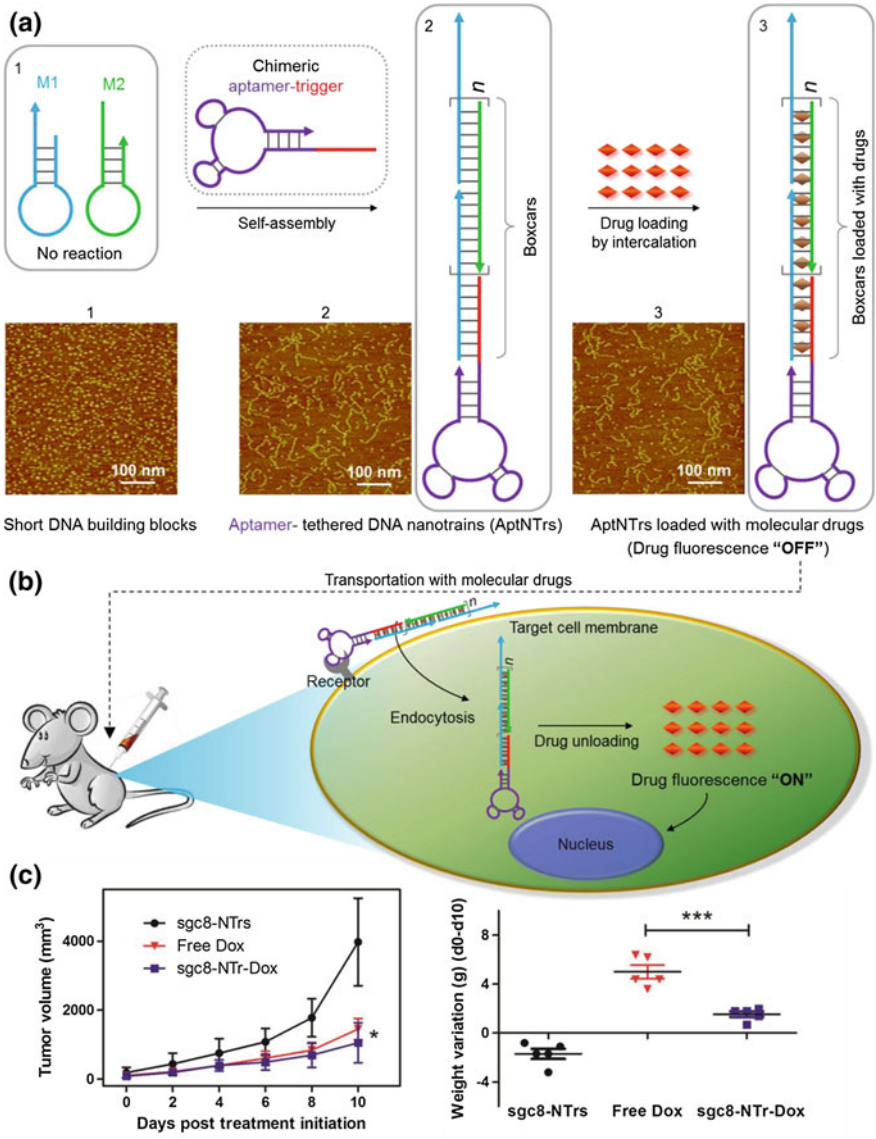
(a)
1
M1
M2
No reaction
Chimeric
aptamer-trigger
Self-assembly
2
n
Boxcars
Drug loading
by intercalation
3
n
Boxcars loaded with drugs
1
100 nm
2
100 nm
3
100 nm
Short DNA building blocks
Aptamer- tethered DNA nanotrains (AptNTrs)
AptNTrs loaded with molecular drugs
(Drug fluorescence "OFF")
(b)
Transportation with molecular drugs
Target cell membrane
Receptor
Endocytosis
Drug unloading
Drug fluorescence "ON"
Nucleus
(c)
Tumor volume (mm3)
4000
2000
0
sgc8-NTrs
Free Dox
sgc8-NTr-Dox
*
0
2
4
6
8
10
Days post treatment initiation
Weight variation (g) (d0-d10)
8
4
0
-4
***
sgc8-NTrs
Free Dox
sgc8-NTr-Dox

◀**Fig. 6.6** Schematic illustration of the self-assembled aptamer-tethered DNA nanotrains (aptNTrs) for cancer theranostics. **a** Self-assembly of aptNTrs from short DNA building blocks (*1*) upon initiation from a aptamer-tethered trigger probe. The resultant nanotrains (*2*) were tethered with aptamers on one end working as locomotives, with multiple repetitive "boxcars" on the other end to be loaded with molecular drugs (*3*). AFM images (*1–3*) show the corresponding morphologies. **b** Drugs were specifically transported to target cancer cells via aptNTrs, where they were unloaded and induced cytotoxicity to target cells. The fluorescence of drugs loaded onto nanotrains was quenched (fluorescent "OFF"), but was recovered upon drug unloading (fluorescent "ON"). **c**, **d** CEM xenograft mouse tumor model was developed by subcutaneous injection of CEM cells in the back of NOD. Cg-Prkdc (scid) IL2 mice. Mice were divided into three groups that were, respectively, treated by intravenous injections of (i) sgc8-NTrs, (ii) free Dox, and (iii) sgc8-NTr-Dox, with 2 mg/kg Dox or Dox equivalent dosages in (ii) and (iii) and accordingly 23 mg/kg sgc8-NTrs in (i). **c** Tumor volume up to day 10 after treatment initiation (mean ± S.D.; $n = 5$). Asterisk on day 10 represents significant differences between tumor volumes of free Dox- and sgc8-NTr-Dox-treated mice ($*p < 0.05$, $n = 5$; Student's t-test). **d** Mouse body weight loss at day 10 compared with day 0, after treatment initiation (mean ± S.D.; $n = 5$). Asterisk represents significant differences between weight loss of free Dox- and sgc8-NTr-Dox-treated mice ($***p < 0.001$, $n = 5$; One-way ANOVA with Newman-Keuls post hoc test). Reprinted from Ref. [109] by permission of PNAS

the self-assembly of sgc8-NTrs. By flow cytometry, these nanodevices were demonstrated to selectively recognize target cancer cells, but not nontarget cells.

Importantly, the periodically aligned boxcars provided a large number of spatially addressable sites for high-capacity loading of therapeutics or bioimaging agents. The aptamer-initiated nanotrain formation was demonstrated using atomic force microscopy (AFM). Chemotherapeutic drugs were loaded on these nanotrains, with several widely used anthracycline anticancer drugs, including Doxorubicin (Dox), Daunorubicin (DNR), and Epirubicin (EPR), as drug cargo models. Since it is well known that these drugs can preferentially intercalate into double-stranded 5′-GC-3′ or 5′-CG-3′, resulting in the quenching of drug fluorescence [104, 106, 110], M1 and M2 were designed such that all their sequences would form drug intercalation sites (ACG/CGT) in nanotrains. Sgc8-NTr-Dox complexes showed negligible drug diffusion from sgc8-NTrs, indicating the high stability of sgc8-NTr-Dox complexes. Using confocal microscopy, aptNTrs were shown to selectively deliver drugs into target cancer cells, further verified by an in vitro MTS cell viability assay which indicated that sgc8-NTr-Dox induced cytotoxicity comparable to that induced by free drugs in target cells, but not in nontarget cells.

Next, the in vivo therapeutic efficacy (both anticancer potency and side effects) of Dox delivered by this nanodevice was evaluated using a CEM subcutaneous xenograft mouse tumor model. Mice were divided into three groups for comparative efficacy studies, in which the following regimens were administered by intravenous injections every other day: (i) sgc8-NTrs, (ii) free Dox, and (iii) sgc8-NTr-Dox. Compared with blank drug carriers (sgc8-NTrs), both sgc8-NTr-Dox and free Dox caused significant inhibition of tumor growth, with slightly stronger potency of sgc8-NTr-Dox than free Dox. This may be attributed to specific targeting ability and larger molecular weight of aptNTrs that endowed them with relatively long drug clearance time from blood, relatively high concentration of accumulated drug

and long drug retention times in tumor. Consistently, both sgc8-NTr-Dox and free Dox led to longer mouse survival time than sgc8-NTrs. These results demonstrated the potent anticancer efficacy of drugs delivered via aptNTrs. Moreover, mice treated with free Dox lost significantly more weight than those treated with sgc8-NTr-Dox, while those treated with sgc8-NTrs showing slight body weight increase, indicating the reduction of drug side effects using aptNTrs, as well as the biocompatibility of aptNTrs. Overall, these data demonstrated the potent antitumor efficacy and the reduced side effects of drugs delivered via aptamer-tethered DNA nanotrains as the drug nanocarriers.

In addition, this drug delivery system allows cost reduction of DNA preparation in reproducing this type of drug carriers, due to (a) the use of short DNAs in aptNTrs leading to a relatively high DNA synthesis yield compared with the use of long strands, and (b) the maximal contribution of DNA in aptNTrs to cargo loading resulting in the use of a relatively low amount of DNA to deliver a specific amount of cargo. Moreover, bioimaging agents coupled on nanotrains and drug fluorescence dequenching upon release allowed for real-time signaling of behaviors of nanotrains and drugs at target cells, making it an excellent platform for cancer theranostics. Moreover, the aptamer module in these nanostructures can be easily changed, so that this system can also apply to other nucleic acid-based systems and some other theranostic agents, ensuring wide applicability. Furthermore, the degradability of DNA would prevent a chronic accumulation of nanomaterials with molecular weight above the renal filtration cutoff, and the long linear nanostructure of this drug transporter is expected to increase circulation time in vivo, as shown in studies using filomicelles [111]. Collectively, aptNTrs are uniquely attractive for cancer theranostics.

6.4.2 Noncanonically Self-assembled Aptamer-Incorporated DNA Nanoflowers for Cancer Theranostics

DNA has emerged as a building block material for the construction of DNA nanodevices, typically relying on bottom-up assembly through Watson-Crick base-pairing between short DNA building blocks. However, these approaches have intrinsic drawbacks, including: (1) complicated design of the myriad of different DNA strands needed to assemble relatively large and sophisticated nanodevices; (2) the bulky preparation of a large amount of DNA; (3) the limited compaction resulted from steric hindrance of DNA strands, yet highly compact DNA is typically favored for applications in nanotherapeutics and bioimaging nanoassemblies; (4) the extensive intrinsic nicks of phosphodiester bonds in DNA building blocks, which provide potential cleavage sites for many exonucleases [112–114]; and (5) dissociation that accompanies denaturation or extremely low concentrations. Therefore, it would be desirable to assemble densely compacted multifunctional DNA nanostructures using elongated less-nicked building blocks made from a low amount of only a few DNA strands, without relying on Watson-Crick base-pairing.

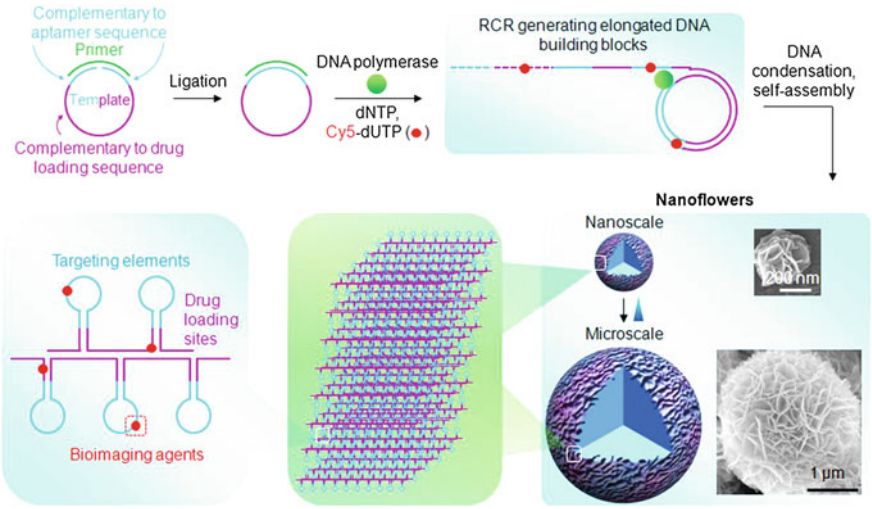

Fig. 6.7 Schematic illustration of noncanonical self-assembly of multifunctional DNA nanoflowers (NFs). The designer linear ssDNA template was first ligated to form a circular template, which then served as the template for RCR using Φ29 DNA polymerase and a primer. RCR generated a large amount of elongated non-nicked concatemer DNA with each unit complementary to the template. These DNAs then served as building blocks to self-assemble monodisperse, densely packed, and hierarchical DNA NFs. NF sizes were tunable with diameters ranging from approximately 200 nm to several micrometers, as shown by the representative SEM images. NF assembly does not rely on Watson-Crick base-pairing between DNA building blocks, enabling tailored design of the template to carry multiple complements of functional nucleic acids, e.g., aptamers and drug-loading sites. Functionalities could also be incorporated via primers or modified deoxynucleotides, such as Cy5-dUTP for bioimaging as shown here as an example. The multifunctional NFs were applied for selective target cancer cell recognition, bioimaging, and targeted drug delivery. Reprinted with the permission from Ref. [81] copyright 2013 American chemical society

Toward this end, the Tan group developed the noncanonical self-assembly of hierarchical DNA nanodevices, termed as nanoflowers (NFs), with densely packed DNA and built-in multiple functionalities (Fig. 6.7) [81]. Using only a low amount of two DNA strands (one designer template and one primer), long DNA building blocks were generated through Rolling Cycle Replication (RCR), an isothermal enzymatic reaction catalyzed by Φ29 DNA polymerase. Since the templates for RCR can be tailor-designed, various structural and functional moieties can be incorporated into templates and subsequently built into RCR products. The RCR template was designed such that the resultant RCR products consist of a series of aptamers (sgc8 as a model) and drug-loading sites for Dox. The concatemer aptamers in elongated ssDNA were expected to enhance the binding affinity of the resultant NFs to target cells through multivalent binding, and the tremendous drug-association sequences in NFs were expected to endow NFs with high drug payload capacity. The above-generated DNA then served as building blocks to assemble NFs. RCR products obtained after reaction for n hours were denoted as RCR_n, and

scanning electron microscopy (SEM) indicated that NFs were formed in RCR_{10} with diameters of about 200 nm and petal-like structures on the surfaces. The ability to build monodisperse nanodevices with hundreds of nanometers is highly significant, especially for biomedical applications such as passive targeted drug delivery via the enhanced permeation and retention (EPR) effect. The one-step self-assembly of small monodisperse NFs prevented the otherwise physical cutting for aggregate partition or physical compaction for size reduction, which could be difficult to precisely manipulate and could damage DNA functionalities in NFs [115, 116]. Detailed examination indicated that NF assembly underwent a progressive process, with NF size increasing with the increase of RCR reaction time, which allowed for fine-tuning the sizes of DNA NFs for versatile applications. In our study, we have observed NFs with diameters up to 4 μm. It was also demonstrated that NFs were self-assembled noncanonically. The sparsity of nick sites in the elongated building blocks and the compactness of DNA in NFs increased the resistance of NFs to nuclease degradation, denaturation, or dissociation at low concentrations. The exceptional biostability was demonstrated by the maintenance of NF structural integrity during treatment with nucleases, human serum, high temperature, urea, or dilution, making NFs amenable for versatile future applications, especially in biomedical situations.

By rational design of RCR templates, the elongated DNA building blocks can carry a large amount of concatemer structural and functional moieties, which are further compacted into NFs. For example, during the de novo generation of NF building blocks, functionalities can also be incorporated via (1) chemically functionalized deoxynucleotides that can be utilized as substrates in RCR and (2) customized design of templates and primers. In this study, we used both of these approaches to incorporate different fluorescent bioimaging agents, aptamers, and drug-loading sites. NFs were equipped with functionalities including aptamers, fluorophores, and drug-loading sites. The resultant NFs were then capable of selective cancer cell recognition, cell bioimaging, and targeted anticancer drug delivery. Specifically, for fluorescent molecular imaging, FITC was chemically modified on one end of the RCR primer, such that multiple copies of fluorophores could be integrated into one NF composed of many copies of DNA building blocks. Bioimaging agents were incorporated enzymatically via chemically modified deoxynucleotides, a Cyanine 5 (Cy5)-modified dUTP, which can work as a substrate for many DNA polymerases, including Φ29 [117, 118]. The fluorescence of these resultant NFs was validated through fluorescence microscopy. The incorporation of fluorophores into NFs provides the basis for further applications of NFs in bioimaging. Moreover, by design of RCR templates, aptamer sgc8 and drug-loading sequences (ds(CG) and ds(GC)) for Dox were incorporated into NFs. Using flow cytometry, $NF_{0.2}$s incorporated with FITC, drug-loading sites, and sgc8 were demonstrated to selectively recognize target HeLa cells and CEM cells, but not nontarget Ramos cells. This provides the basis for potential applications in cancer imaging and active cancer therapy. Using confocal microscopy, the fluorophore-incorporated NFs were able to elucidate that NFs could be internalized into target cancer cells, providing the basis for efficient drug delivery mediated by NFs as

aptamer-guided drug carriers. These DNA NFs possessed high drug-loading capacity, via either association with specific drug-loading sequences or physical encapsulation, owing to high density of DNA drug-loading sequences and internal hierarchical structures. NF-drug complexes were then evaluated for targeted drug delivery in vitro using an MTS assay, and these nanodevices were demonstrated to have the capability of intracellular imaging and targeted drug delivery.

References

1. Jiang Q, Song C, Nangreave J, Liu X, Lin L, Qiu D, Wang Z-G, Zou G, Liang X, Yan H, Ding B (2012) DNA origami as a carrier for circumvention of drug resistance. J Am Chem Soc 134:13396–13403
2. Lee H, Lytton-Jean AKR, Chen Y, Love KT, Park AI, Karagiannis ED, Sehgal A, Querbes W, Zurenko CS, Jayaraman M, Peng CG, Charisse K, Borodovsky A, Manoharan M, Donahoe JS, Truelove J, Nahrendorf M, Langer R, Anderson DG (2012) Molecularly self-assembled nucleic acid nanoparticles for targeted in vivo siRNA delivery. Nat Nano 7:389–393
3. Ellington AD, Szostak JW (1990) In vitro selection of RNA molecules that bind specific ligands. Nature 346:818–822
4. Tuerk C, Gold L (1990) Systematic evolution of ligands by exponential enrichment: RNA ligands to bacteriophage T4 DNA polymerase. Science 249:505–510
5. Huizenga DE, Szostak JW (1995) A DNA aptamer that binds adenosine and ATP. Biochemistry 34:656–665
6. Hermann T, Patel DJ (2000) Adaptive recognition by nucleic acid aptamers. Science 287:820–825
7. Mallikaratchy P, Stahelin RV, Cao Z, Cho W, Tan W (2006) Selection of DNA ligands for protein kinase C-delta. Chem Commun 30:3229–3231
8. Daniels DA, Chen H, Hicke BJ, Swiderek KM, Gold L (2003) A tenascin-C aptamer identified by tumor cell SELEX: systematic evolution of ligands by exponential enrichment. Proc Natl Acad Sci 100:15416–15421
9. Parekh P, Tang Z, Turner PC, Moyer RW, Tan W (2010) Aptamers recognizing glycosylated hemagglutinin expressed on the surface of vaccinia virus-infected cells. Anal Chem 82:8642–8649
10. Bock LC, Griffin LC, Latham JA, Vermaas EH, Toole JJ (1992) Selection of single-stranded DNA molecules that bind and inhibit human thrombin. Nature 355:564–566
11. Hu J, Wu J, Li C, Zhu L, Zhang WY, Kong G, Lu Z, Yang CJ (2011) A G-quadruplex aptamer inhibits the phosphatase activity of oncogenic protein Shp2 in vitro. ChemBioChem 12:424–430
12. Chen C-HB, Chernis GA, Hoang VQ, Landgraf R (2003) Inhibition of heregulin signaling by an aptamer that preferentially binds to the oligomeric form of human epidermal growth factor receptor-3. Proc Natl Acad Sci 100:9226–9231
13. Khati M, Schüman M, Ibrahim J, Sattentau Q, Gordon S, James W (2003) Neutralization of infectivity of diverse R5 clinical isolates of human immunodeficiency virus type 1 by gp120-binding 2′F-RNA aptamers. J Virol 77:12692–12698
14. Keefe AD, Pai S, Ellington A (2010) Aptamers as therapeutics. Nature Rev Drug Discov 9:537–550
15. Guo K-T, SchÄfer R, Paul A, Gerber A, Ziemer G, Wendel HP (2006) A new technique for the isolation and surface immobilization of mesenchymal stem cells from whole bone marrow using high-specific DNA aptamers. Stem Cells 24:2220–2231

16. Shangguan D, Li Y, Tang Z, Cao Z, Chen HW, Mallikaratchy P, Sefah K, Yang CJ, Tan W (2006) Aptamers evolved from live cells as effective molecular probes for cancer study. Proc Natl Acad Sci USA 103:11838–11843
17. Tang Z, Shangguan D, Wang K, Shi H, Sefah K, Mallikaratchy P, Chen HW, Li Y, Tan W (2007) Selection of aptamers for molecular recognition and characterization of cancer cells. Anal Chem 79:4900–4907
18. Shangguan D, Meng L, Cao ZC, Xiao Z, Fang X, Li Y, Cardona D, Witek RP, Liu C, Tan W (2008) Identification of liver cancer-specific aptamers using whole live cells. Anal Chem 80:721–728
19. Sefah K, Tang Z, Shangguan D, Chen H, Lopez-Colon D, Li Y, Parekh P, Martin J, Meng L, Phillips JA, Kim Y, Tan W (2009) Molecular recognition of acute myeloid leukemia using aptamers. Leukemia 23:235–244
20. Chen HW, Medley CD, Sefah K, Shangguan D, Tang Z, Meng L, Smith JE, Tan W (2008) Molecular recognition of small-cell lung cancer cells using aptamers. ChemMedChem 3:991–1001
21. Bayrac AT, Sefah K, Parekh P, Bayrac C, Gulbakan B, Oktem HA, Tan W (2011) In vitro selection of DNA aptamers to glioblastoma multiforme. ACS Chem Neurosci 2:175–181
22. Simaeys DV, López-Colón D, Sefah K, Sutphen R, Jimenez E, Tan W (2010) Study of the molecular recognition of aptamers selected through ovarian cancer cell-SELEX. Plos One 5
23. Zhao Z, Xu L, Shi X, Tan W, Fang X, Shangguan D (2009) Recognition of subtype non-small cell lung cancer by DNA aptamers selected from living cells. Analyst 134:1808–1814
24. Mi J, Liu Y, Rabbani ZN, Yang Z, Urban JH, Sullenger BA, Clary BM (2010) In vivo selection of tumor-targeting RNA motifs. Nat Chem Biol 6:22–24
25. Padmanabhan K, Padmanabhan KP, Ferrara JD, Sadler JE, Tulinsky A (1993) The structure of alpha-thrombin inhibited by a 15-mer single-stranded DNA aptamer. J Biol Chem 268:17651–17654
26. Long SB, Long MB, White RR, Sullenger BA (2008) Crystal structure of an RNA aptamer bound to thrombin. RNA-Publ. RNA Soc. 14:2504–2512
27. Lebars I, Legrand P, Aime A, Pinaud N, Fribourg S, Di Primo C (2008) Exploring TAR-RNA aptamer loop-loop interaction by X-ray crystallography, UV spectroscopy and surface plasmon resonance. Nucleic Acids Res 36:7146–7156
28. Huang DB, Vu D, Cassiday LA, Zimmerman JM, Maher LJ, Ghosh G (2003) Crystal structure of NF-kappa B (p50)(2) complexed to a high-affinity RNA aptamer. Proc Natl Acad Sci USA 100:9268–9273
29. Mallikaratchy P, Tang Z, Kwame S, Meng L, Shangguan D, Tan W (2007) Aptamer directly evolved from live cells recognizes membrane bound immunoglobin heavy mu chain in Burkitt's lymphoma cells. Mol Cell Proteomics 6:2230–2238
30. Sefah K, Meng L, Lopez-Colon D, Jimenez E, Liu C, Tan W (2010) DNA aptamers as molecular probes for colorectal cancer study. Plos One 5
31. Zhang K, Sefah K, Tang L, Zhao Z, Zhu G, Ye M, Sun W, Goodison S, Tan W (2012) A novel aptamer developed for breast cancer cell internalization. ChemMedChem 7:79–84
32. O'Donoghue M, Shi X, Fang X, Tan W (2012) Single-molecule atomic force microscopy on live cells compares aptamer and antibody rupture forces. Anal Bioanal Chem 402:3205–3209
33. Group TES (2002) Preclinical and phase 1A clinical evaluation of an anti-VEGF pegylated aptamer (EYE001) for the treatment of exudative age-related macular degeneration. Retina 2:143–152
34. Rusconi CP, Roberts JD, Pitoc GA, Nimjee SM, White RR, Quick G, Scardino E, Fay WP, Sullenger BA (2004) Antidote-mediated control of an anticoagulant aptamer in vivo. Nat Biotech 22:1423–1428
35. Oney S, Lam RTS, Bompiani KM, Blake CM, Quick G, Heidel JD, Liu JY-C, Mack BC, Davis ME, Leong KW, Sullenger BA (2009) Development of universal antidotes to control aptamer activity. Nat Med 15:1224–1228
36. Gragoudas ES, Adamis AP, Cunningham ET, Feinsod M, Guyer DR (2004) Pegaptanib for neovascular age-related macular degeneration. N Engl J Med 351:2805–2816

37. Bates PJ, Laber DA, Miller DM, Thomas SD, Trent JO (2009) Discovery and development of the G-rich oligonucleotide AS1411 as a novel treatment for cancer. Exp Mol Pathol 86:151–164
38. Shangguan D, Cao Z, Meng L, Mallikaratchy P, Sefah K, Wang H, Li Y, Tan W (2008) Cell-specific aptamer probes for membrane protein elucidation in cancer cells. J Proteome Res 7:2133–2139
39. Lupold SE, Hicke BJ, Lin Y, Coffey DS (2002) Identification and characterization of nuclease-stabilized RNA molecules that bind human prostate cancer cells via the prostate-specific membrane antigen. Cancer Res 62:4029–4033
40. Ferreira CSM, Matthews CS, Missailidis S (2006) DNA aptamers that bind to MUC1 tumour marker: design and characterization of MUC1-binding single-stranded DNA aptamers. Tumor Biology 27:289–301
41. Wiegand T, Williams P, Dreskin S, Jouvin M, Kinet J, Tasset D (1996) High-affinity oligonucleotide ligands to human IgE inhibit binding to Fc epsilon receptor I. J Immunol 157:221–230
42. Mi J, Zhang X, Giangrande PH, McNamara Ii JO, Nimjee SM, Sarraf-Yazdi S, Sullenger BA, Clary BM (2005) Targeted inhibition of αvβ3 integrin with an RNA aptamer impairs endothelial cell growth and survival. Biochem Biophys Res Commun 338:956–963
43. Lebruska LL, Maher LJ (1999) Selection and characterization of an RNA decoy for transcription factor NF-κB†. Biochemistry 38:3168–3174
44. Martell RE, Nevins JR, Sullenger BA (2002) Optimizing aptamer activity for gene therapy applications using expression cassette SELEX. Mol Ther 6:30–34
45. Ishizaki J, Nevins JR, Sullenger BA (1996) Inhibition of cell proliferation by an RNA ligand that selectively blocks E2F function. Nat Med 2:1386–1389
46. Geiger B, Bershadsky A, Pankov R, Yamada KM (2001) Transmembrane crosstalk between the extracellular matrix and the cytoskeleton. Nat Rev Mol Cell Biol 2:793–805
47. Mahal LK, Bertozzi CR (1997) Engineered cell surfaces: fertile ground for molecular landscaping. Chem Biol 4:415–422
48. Gartner ZJ, Bertozzi CR (2009) Programmed assembly of 3-dimensional microtissues with defined cellular connectivity. Proc Natl Acad Sci USA 106:4606–4610
49. Pinheiro AV, Han D, Shih WM, Yan H (2011) Challenges and opportunities for structural DNA nanotechnology. Nature Nanotech 6:763–772
50. Elbrink J, Bihler I (1975) Membrane transport: its relation to cellular metabolic rates. Science 188:1177–1184
51. Joyce JA, Pollard JW (2008) Microenvironmental regulation of metastasis. Nat Rev Cancer 9:239–252
52. Ali MM, Kang DK, Tsang K, Fu M, Karp JM, Zhao W (2012) Cell-surface sensors: lighting the cellular environment. Wiley Interdisc Rev Nanomed Nanobiotechnol 4:547–561
53. Tanaka M, Sackmann E (2005) Polymer-supported membranes as models of the cell surface. Nature 437:656–663
54. Zhao W, Schafer S, Choi J, Yamanaka YJ, Lombardi ML, Bose S, Carlson AL, Phillips JA, Teo W, Droujinine IA (2011) Cell-surface sensors for real-time probing of cellular environments. Nat Nanotechnol 6:524–531
55. Tokunaga T, Namiki S, Yamada K, Imaishi T, Nonaka H, Hirose K, Sando S (2012) Cell surface-anchored fluorescent aptamer sensor enables imaging of chemical transmitter dynamics. J Am Chem Soc 134:9561–9564
56. Giepmans BN, Adams SR, Ellisman MH, Tsien RY (2006) The fluorescent toolbox for assessing protein location and function. Science 312:217–224
57. Sefah K, Shangguan D, Xiong X, O'Donoghue MB, Tan W (2010) Development of DNA aptamers using Cell-SELEX. Nat Protoc 5:1169–1185
58. Iliuk AB, Hu L, Tao WA (2011) Aptamer in bioanalytical applications. Anal Chem 83:4440–4452

59. Qiu L, Zhang T, Jiang J, Wu C, Zhu G, You M, Chen X, Zhang L, Cui C, Yu R (2014) Cell membrane-anchored biosensors for real-time monitoring of the cellular microenvironment. J Am Chem Soc 136(38):13090–13093
60. Willner I, Shlyahovsky B, Zayats M, Willner B (2008) DNAzymes for sensing, nanobiotechnology and logic gate applications. Chem Soc Rev 37:1153–1165
61. Liu H, Kwong B, Irvine DJ (2011) Membrane anchored immunostimulatory oligonucleotides for in vivo cell modification and localized immunotherapy. Angew Chem 123:7190–7193
62. Xiong X, Liu H, Zhao Z, Altman MB, Lopez-Colon D, Yang CJ, Chang LJ, Liu C, Tan W (2013) DNA aptamer-mediated cell targeting. Angew Chem Int Ed 52:1472–1476
63. Zhu G, Zhang S, Song E, Zheng J, Hu R, Fang X, Tan W (2013) Building fluorescent DNA nanodevices on target living cell surfaces. Angew Chem Int Ed 52:5490–5496
64. Einhorn TA (1998) The cell and molecular biology of fracture healing. Clin Orthop Relat Res 355:S7–S21
65. Bao G, Suresh S (2003) Cell and molecular mechanics of biological materials. Nat Mater 2:715–725
66. Tyagi S (2009) Imaging intracellular RNA distribution and dynamics in living cells. Nat Methods 6:331–338
67. Bratu DP, Cha B-J, Mhlanga MM, Kramer FR, Tyagi S (2003) Visualizing the distribution and transport of mRNAs in living cells. Proc Natl Acad Sci 100:13308–13313
68. Cui Y, Wei Q, Park H, Lieber CM (2001) Nanowire nanosensors for highly sensitive and selective detection of biological and chemical species. Science 293:1289–1292
69. Medintz IL, Uyeda HT, Goldman ER, Mattoussi H (2005) Quantum dot bioconjugates for imaging, labelling and sensing. Nat Mater 4:435–446
70. MacCumber MW, Ross CA, Glaser BM, Snyder SH (1989) Endothelin: visualization of mRNAs by in situ hybridization provides evidence for local action. Proc Natl Acad Sci 86:7285–7289
71. Wang S, Hazelrigg T (1994) Implications for bcd mRNA localization from spatial distribution of exu protein in Drosophila oogenesis. Nature 369:400–403
72. Tan W, Wang K, Drake TJ (2004) Molecular beacons. Curr Opin Chem Biol 8:547–553
73. Boussif O, Lezoualc'h F, Zanta MA, Mergny MD, Scherman D, Demeneix B, Behr J-P (1995) A versatile vector for gene and oligonucleotide transfer into cells in culture and in vivo: polyethylenimine. Proc Natl Acad Sci 92:7297–7301
74. Santangelo PJ, Nix B, Tsourkas A, Bao G (2004) Dual FRET molecular beacons for mRNA detection in living cells. Nucleic Acids Res 32:e57–e57
75. Chen AK, Behlke MA, Tsourkas A (2008) Efficient cytosolic delivery of molecular beacon conjugates and flow cytometric analysis of target RNA. Nucleic Acids Res 36:e69–e69
76. Fang X, Liu X, Schuster S, Tan W (1999) Designing a novel molecular beacon for surface-immobilized DNA hybridization studies. J Am Chem Soc 121:2921–2922
77. Nitin N, Santangelo PJ, Kim G, Nie S, Bao G (2004) Peptide-linked molecular beacons for efficient delivery and rapid mRNA detection in living cells. Nucleic Acids Res 32:e58–e58
78. Dhar S, Kolishetti N, Lippard SJ, Farokhzad OC (2011) Targeted delivery of a cisplatin prodrug for safer and more effective prostate cancer therapy in vivo. Proc Natl Acad Sci 108:1850–1855
79. Qiu L, Wu C, You M, Han D, Chen T, Zhu G, Jiang J, Yu R, Tan W (2013) A targeted, self-delivered, and photocontrolled molecular beacon for mRNA detection in living cells. J Am Chem Soc 135:12952–12955
80. Cao Z, Tong R, Mishra A, Xu W, Wong GCL, Cheng J, Lu Y (2009) Reversible cell-specific drug delivery with aptamer-functionalized liposomes. Angew Chem Int Ed 48:6494–6498
81. Zhu G, Hu R, Zhao Z, Chen Z, Zhang X, Tan W (2013) Noncanonical self-assembly of multifunctional DNA nanoflowers for biomedical applications. J Am Chem Soc 135:16438–16445
82. Nilsen TW, Grayzel J, Prensky W (1997) Dendritic nucleic acid structures. J Theor Biol 187:273–284

83. Li Y, Tseng YD, Kwon SY, d'Espaux L, Bunch JS, McEuen PL, Luo D (2004) Controlled assembly of dendrimer-like DNA. Nat Mater 3:38–42
84. Meng H-M, Zhang X, Lv Y, Zhao Z, Wang N-N, Fu T, Fan H, Liang H, Qiu L, Zhu G, Tan W (2014) DNA dendrimer: an efficient nanocarrier of functional nucleic acids for intracellular molecular sensing. ACS Nano 8:6171–6181
85. Minotti G, Menna P, Salvatorelli E, Cairo G, Gianni L (2004) Anthracyclines: molecular advances and pharmacologic developments in antitumor activity and cardiotoxicity. Pharmacol Rev 56:185–229
86. Cardinale D, Colombo A, Lamantia G, Colombo N, Civelli M, De Giacomi G, Rubino M, Veglia F, Fiorentini C, Cipolla CM (2010) Anthracycline-induced cardiomyopathy: clinical relevance and response to pharmacologic therapy. J Am Coll Cardiol 55:213–220
87. Andrew MacKay J, Chen M, McDaniel JR, Liu W, Simnick AJ, Chilkoti A (2009) Self-assembling chimeric polypeptide-doxorubicin conjugate nanoparticles that abolish tumours after a single injection. Nat Mater 8:993–999
88. Lammers T, Aime S, Hennink WE, Storm G, Kiessling F (2011) Theranostic nanomedicine. Acc Chem Res 44:1029–1038
89. Seeman NC (2010) Nanomaterials Based on DNA. Annu Rev Biochem 79:65–87
90. Bath J, Turberfield AJ (2007) DNA nanomachines. Nat Nanotech 2:275–284
91. Dirks RM, Pierce NA (2004) Triggered amplification by hybridization chain reaction. Proc Natl Acad Sci USA 101:15275–15278
92. Luo D, Saltzman WM (2000) Synthetic DNA delivery systems. Nat Biotech 18:33–37
93. Douglas SM, Bachelet I, Church GM (2012) A logic-gated nanorobot for targeted transport of molecular payloads. Science 335:831–834
94. Tan W, Wang H, Chen Y, Zhang X, Zhu H, Yang C, Yang R, Liu C (2011) Molecular aptamers for drug delivery. Trends Biotechnol 29:634–640
95. Schüller VJ, Heidegger S, Sandholzer N, Nickels PC, Suhartha NA, Endres S, Bourquin C, Liedl T (2011) Cellular immunostimulation by CpG-sequence-coated DNA origami structures. ACS Nano 5:9696–9702
96. Li J, Pei H, Zhu B, Liang L, Wei M, He Y, Chen N, Li D, Huang Q, Fan C (2011) Self-assembled multivalent DNA nanostructures for noninvasive intracellular delivery of immunostimulatory CpG oligonucleotides. ACS Nano 5:8783–8789
97. Tan SJ, Kiatwuthinon P, Roh YH, Kahn JS, Luo D (2011) Engineering nanocarriers for siRNA delivery. Small 7:841–856
98. Chang M, Yang C-S, Huang D-M (2011) Aptamer-conjugated DNA icosahedral nanoparticles as a carrier of doxorubicin for cancer therapy. ACS Nano 5:6156–6163
99. Zhao F, Zhao Y, Liu Y, Chang X, Chen C, Zhao Y (2011) Cellular uptake, intracellular trafficking, and cytotoxicity of nanomaterials. Small 7:1322–1337
100. Peer D, Karp JM, Hong S, Farokhzad OC, Margalit R, Langer R (2007) Nanocarriers as an emerging platform for cancer therapy. Nat Nano 2:751–760
101. Petros RA, DeSimone JM (2010) Strategies in the design of nanoparticles for therapeutic applications. Nat Rev Drug Discov 9:615–627
102. Zhu G, Zheng J, Song E, Donovan M, Zhang K, Liu C, Tan W (2013) Self-assembled, aptamer-tethered DNA nanotrains for targeted transport of molecular drugs in cancer theranostics. Proc Natl Acad Sci USA 110:7998–8003
103. Huang Y-F, Shangguan D, Liu H, Phillips JA, Zhang X, Chen Y, Tan W (2009) Molecular assembly of an aptamer-drug conjugate for targeted drug delivery to tumor cells. ChemBioChem 10:862–868
104. Bagalkot V, Farokhzad OC, Langer R, Jon S (2006) An aptamer-doxorubicin physical conjugate as a novel targeted drug-delivery platform. Angew Chem Int Ed 45:8149–8152
105. Yang L, Zhang X, Ye M, Jiang J, Yang R, Fu T, Chen Y, Wang K, Liu C, Tan W (2011) Aptamer-conjugated nanomaterials and their applications. Adv Drug Deliv Rev 63:1361–1370
106. Meng L, Yang L, Zhao X, Zhang L, Zhu H, Liu C, Tan W (2012) Targeted delivery of chemotherapy agents using a liver cancer-specific aptamer. PLoS One 7:e33434

107. Luo Y-L, Shiao Y-S, Huang Y-F (2011) Release of photoactivatable drugs from plasmonic nanoparticles for targeted cancer therapy. ACS Nano 5:7796–7804
108. Ruggiero A, Villa CH, Bander E, Rey DA, Bergkvist M, Batt CA, Manova-Todorova K, Deen WM, Scheinberg DA, McDevitt MR (2010) Paradoxical glomerular filtration of carbon nanotubes. Proc Natl Acad Sci 107:12369–12374
109. Zhu G, Zheng J, Song E, Donovan M, Zhang K, Liu C, Tan W (2013) Self-assembled, aptamer-tethered DNA nanotrains for targeted transport of molecular drugs in cancer theranostics. In: Proceedings of the national academy of sciences
110. Zhu G, Meng L, Ye M, Yang L, Sefah K, O'Donoghue MB, Chen Y, Xiong X, Huang J, Song E, Tan W (2012) Self-assembled aptamer-based drug carriers for bispecific cytotoxicity to cancer cells. Chem Asian J 7:1630–1636
111. Geng Y, Dalhaimer P, Cai S, Tsai R, Tewari M, Minko T, Discher DE (2007) Shape effects of filaments versus spherical particles in flow and drug delivery. Nat Nanotech 2:249–255
112. Tamkovich SN, Cherepanova AV, Kolesnikova EV, Rykova EY, Pyshnyi DV, Vlassov VV, Laktionov PP (2006) Circulating DNA and DNase Activity in Human Blood. Ann N Y Acad Sci 1075:191–196
113. Hamblin GD, Carneiro KMM, Fakhoury JF, Bujold KE, Sleiman HF (2012) Rolling circle amplification-templated DNA nanotubes show increased stability and cell penetration ability. J Am Chem Soc 134:2888–2891
114. Keum J-W, Bermudez H (2009) Enhanced resistance of DNA nanostructures to enzymatic digestion. Chem Commun 7036–7038
115. Lee JB, Hong J, Bonner DK, Poon Z, Hammond PT (2012) Self-assembled RNA interference microsponges for efficient siRNA delivery. Nat Mater 11:316–322
116. Lee JB, Peng S, Yang D, Roh YH, Funabashi H, Park N, Rice EJ, Chen L, Long R, Wu M, Luo D (2012) A mechanical metamaterial made from a DNA hydrogel. Nat Nano 7:816–820
117. Shalon D, Smith SJ, Brown PO (1996) A DNA microarray system for analyzing complex DNA samples using two-color fluorescent probe hybridization. Genome Res 6:639–645
118. Credo GM, Su X, Wu K, Elibol OH, Liu DJ, Reddy B, Tsai T-W, Dorvel BR, Daniels JS, Bashir R, Varma M (2012) Label-free electrical detection of pyrophosphate generated from DNA polymerase reactions on field-effect devices. Analyst 137:1351–1362

Chapter 7
Properties of Nucleic Acid Amphiphiles and Their Biomedical Applications

Haipeng Liu

Abstract Nucleic acid-based amphiphiles, which consist of nucleic acids covalently linked to lipophilic lipid molecules, have demonstrated unique physicochemical and biological properties and are emerging as new types of materials in biomedical applications. These types of hybrid materials combine the functions and properties from both hydrophilic nucleic acids and hydrophobic lipid tails and thus are developed to carry therapeutic drugs, to penetrate cell membranes, to decorate the cell surface, and to interact with endogenous proteins. These functional amphiphiles have demonstrated potentials in extending the usage of traditional nucleic acids. In this chapter, we highlight the recent advances with an emphasis on their synthesis, self-assemble properties, and biomedical applications. Specifically, we focus on illustrating the structure–function relationship which provides the foundation for rational design of nucleic acid amphiphiles in future applications in the biomedical field.

Keywords Nucleic acids · Amphiphiles · Self-assembly · Membrane · Sensor · Biomedical · Vaccine adjuvant

7.1 Introduction

Nucleic acids are versatile biomaterials that are helping researchers understand disease pathways and biological mechanisms and are extensively explored as novel theranostics. Synthetic nucleic acids, such as plasmid DNA, [1] siRNA, [2] antisense DNA, [3] molecular beacons, [4] aptamers [5], and DNAzymes [6], are powerful tools for dissecting, detecting, regulating, or inhibiting biological functions at molecular and cellular levels. However, despite the high therapeutic

H. Liu (✉)
Department of Chemical Engineering and Materials Science, Wayne State University, Detroit, MI 48202, USA
e-mail: haipeng.liu@wayne.edu

W. Tan and X. Fang (eds.), *Aptamers Selected by Cell-SELEX for Theranostics*,
DOI 10.1007/978-3-662-46226-3_7

potential of nucleic acids, their application in clinical settings is still limited due to the challenges in the delivery of synthetic nucleic acids to disease sites and cross cell membranes [7]. This is part because of the genetic role of nucleic acids. In nature, foreign nucleic acids pose a biosecurity threat to cells by allowing the expression of potential pathogenic proteins. Thus, almost all living organisms develop their own defense mechanisms to prevent the entrance, replication, and genome incorporation of foreign nucleic acids. For example, cellular membranes are negatively charged and act as a natural barrier to prevent the entrance of polyanionic nucleic acids; once inside the cells, rapid enzymatic degradation of nucleic acids efficiently prevents them from integrating to the genome. Furthermore, in vivo application of nucleic acids as theranostics often requires the tissue/organ-specific delivery to maximize the therapeutic/diagnostic efficacy and minimize the side effects. Thus, a series of barriers need to be overcome in order for synthetic nucleic acids to function in vitro and in vivo [7].

Numerous delivery carriers, including non-viral vectors such as polymers, liposomes, lipids, peptides, and viral-based vectors have been suggested for overcoming the delivery barriers of nucleic acids. Historically, transfection agents, such as cationic materials that can form polyelectrolyte complexes with negatively charged nucleic acids via ionic interactions have been developed to bring in nucleic acids to cells, a process called transfection. The cationic agents can condense nucleic acids into nanosized particles via charge–charge interaction and provide excellent protection of nucleic acids from enzymatic degradation. However, cationic agents are not ideal for systemic delivery because they often exhibit limited organ/tissue selectivity, severe cytotoxicity, and immunogenicity, limiting their clinical applications.

Recently, it has been demonstrated that nucleic acids, especially synthetic short oligonucleotides, when covalently conjugated to lipophilic molecules, can confer increased nuclease resistance, [8] improved duplex stability, and [8] prolonged half-lives after administration [9] and are able to penetrate the cellular membrane efficiently [10]. Moreover, lipophilic nucleic acids are known to self-assemble into a wide range of different types of nanosized structures, making them interesting candidates as new types of nanomaterials in the emerging field of nano/biotechnology [11].

Additionally, due to the strong plasmid membrane affinity, lipophilic nucleic acids are engineered as cell membrane-anchored biochemical sensors that allow real-time monitoring of the interactions of cells with their microenvironment [12, 13] or as cell membrane-anchored targeting ligands to direct the engagement of immune cells and disease cells [14]. This type of live cell membrane surface engineering can be used to improve the diagnostics or enhance cell-based therapies without complex manipulation and thus has potential application in immunotherapy for diseases such as cancer.

Finally, clinical validated method of using nucleic acids requires the organ-specific targeting. Lipophilic modification results in extensive interaction with serum proteins which enable the efficient delivery of nucleic acids compounds without the requirement of an additional delivery vehicle [9, 15–17]. This self-delivering

approach has been applied in siRNA delivery to the liver to silence an endogenous gene [16] and in vaccine adjuvant delivery to the lymph node in mounting a potent immune response [17].

7.2 Synthesis of Lipophilic Nucleic Acids

Lipophilic nucleic acids are composed of a nucleic acid, a linker, and a lipophilic tails. Depending on the aims of the study, these components can be tailored to realize desired properties. Lipophilic modifications of nucleic acids usually can be achieved by conjugating at least one lipophilic moiety either at 3′-terminal or at 5′-terminal of the nucleic acids or within the sequence. There are generally two conjugation strategies to achieve covalent linkage between lipids and nucleic acids: solid-phase coupling or solution-phase synthesis. Solution-phase synthesis requires the conjugation reaction between two dramatically different molecules: highly hydrophobic lipids and highly hydrophilic nucleic acids. This has posed a challenge in identifying proper conjugation chemistry as well as suitable solvent systems. Compared with solution-phase coupling, solid-phase synthesis has the advantages of simple setups, high yield, easy purification, and compatibility with traditional solid-phase DNA synthesis and thus is gaining more popular among researchers. However, the solid-phase conjugation is limited by the availability of appropriate reagents as well as compatibility in the automated DNA synthesis and subsequent deprotection. It is worth to point out that traditionally cholesterol is one of the most commonly used lipophilic modifications for modifying oligonucleotides [8, 9]. Using solid-phase synthesis, both 3′- and 5′-terminals of nucleic acids can be easily modified with cholesterol [8, 9]. Similar method has been used to link steroids with oligonucleotides [18]. Other lipophilic/hydrophobic molecules, such as synthetic single-chain fatty acids, [19–21] lipids [19, 21–24], or polymers [25], have been synthesized and incorporated into synthetic nucleic acids. Several lipophilic groups (e.g., cholesterol, palmitate, and tocopherol) are also commercially available [26]. It has been demonstrated that traditional reverse-phase HPLC can be used to purify lipophilic oligonucleotides. However, less hydrophobic columns such as C8 or C4 columns are superior to C18 columns for this purpose since oligos are strongly lipophilic [19]. To date, methods for synthesis and purification of lipophilic nucleic acids are well documented in the literature [18–26].

7.3 Self-assembly Properties of Amphiphilic Nucleic Acids

The interest in amphiphilic nucleic acids was further simulated by the self-organization properties of these molecules which combine the characteristics of lipids and functionalities of nucleic acids. Physically linking lipophilic moieties to nucleic acids creates a new type of amphiphilic molecules that are capable of self-assembly,

a process in which highly organized structures are formed spontaneously. Lipophilic modifications lead to amphiphilic nucleic acids which self-assemble into well-defined spherical nucleic acids without tedious manipulation [19, 24, 27]. Depending on both the nature of lipophilic moieties and nucleic acids, lipophilic nucleic acids have been reported to give aggregates including micelles [19, 24, 28] and vesicles [29, 30]. Dentinger et al. [29] reported the vesicular aggregation formation of alkylamine-modified oligonucleotide. The vesicular aggregates stabilize hydrophobic dyes and upon exposure to the complementary oligo, the aggregates are disrupted and release lipophilic dye, suggesting the DNA vesicular aggregates might be used for DNA-mediated smart materials in drug delivery [29]. Teixeira et al. [30] synthesized poly(butadiene)–oligonucleotide conjugates that are capable of self-assembling into nanometer-sized vesicular structures. Polybutadiene was selected in this case due to its low glass transition temperature. Driven by the hydrophobic interaction, the nucleo-copolymer undergo self-assembly in aqueous solution. In the literature, however, the vast majority of nucleic acid amphiphiles self-assemble into micellar structures with a lipid core and a DNA corona [19, 24, 28]. These hierarchical architectures are results of intermolecular hydrophobic interaction. Using solid-phase synthesis, Liu et al. [19] successfully constructed a series of hybrid molecules consisting oligodeoxynucleotides and a diacyl lipid intervened with a pyrene molecule as fluorescence reporter (Fig. 7.1). The authors thoroughly studied the self-assembly of a diacyl lipid–DNA conjugates and found those amphiphiles self-assemble into nanosized micelles with a DNA corona and a lipid core independent of the length and sequences of the oligos. The introduction of fluorescent pyrene in the system has greatly facilitated the evaluation of micellar aggregation via fluorescent spectroscopy measurement. Amphiphiles with different DNA lengths

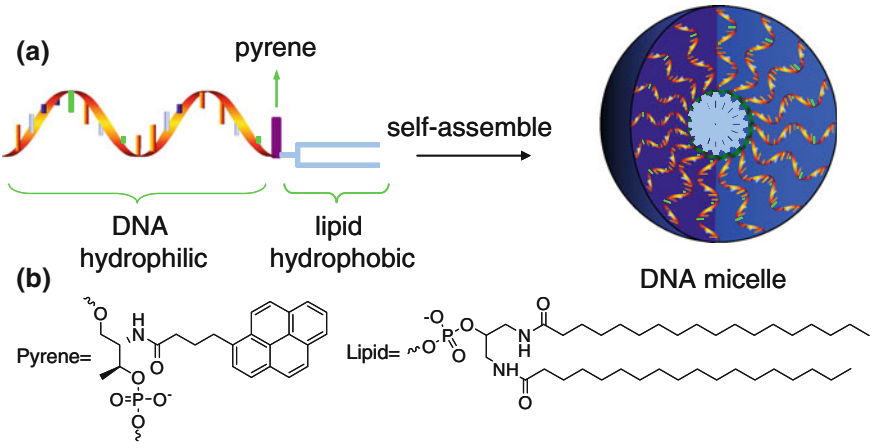

Fig. 7.1 Design and self-assembly of DNA micelles. **a** Oligonucleotide micelles contain a DNA corona, a pyrene fluorescent dye (fluorescence reporter), and a lipid core. **b** Molecular structure of pyrene and lipid used for the design. Reproduced from Ref. [19] by permission of John Wiley & Sons Ltd

(random sequences, 5–50 mer) were prepared. In the aggregation state, the pyrene units, which were designed to be close to the lipid tails, are spatially proximate to each other and give excimer-type fluorescence for all oligos as shown in fluorescent spectra in Fig. 7.2a. All four DNA micelles used in this study revealed a broad emission of pyrene excimer at 480 nm with an excitation at 350 nm in aqueous solution, suggesting the presence of a self-assembled aggregation state. Adding an organic solvent disrupted the micelle structure and gave monomer-type fluorescence (Fig. 7.2b). Agarose gel electrophoresis was also used to characterize the aggregation of lipophilic oligos. As shown in Fig. 7.2c, each DNA assembly migrated as a single, sharp band with expected mobility and fluorescent color, suggesting that the micelle aggregations were stably formed and the aggregates have uniform sizes. Upon adding 0.8 % (w/v) sodium dodecyl sulfate (SDS) to the gel, the micelle structure was immediately disrupted and all DNA migrated as faster bands showing monomeric pyrene fluorescence, indicating that the diacyl lipid DNAs are migrating as individual molecule. These studies demonstrated the amphiphilic DNA is capable of self-assembly and revealed that the diacyl lipid DNA's self-assemble properties were

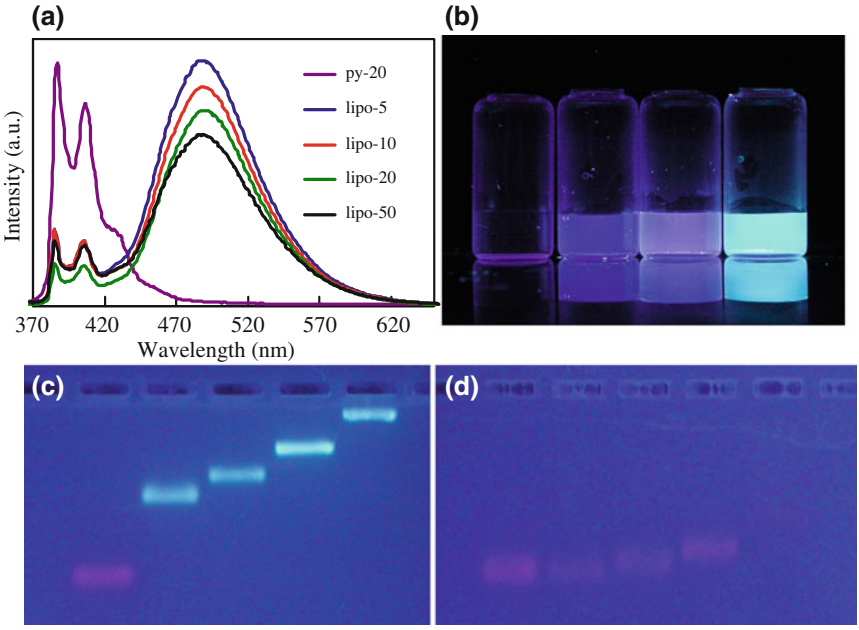

Fig. 7.2 Fluorescence characterization of DNA micelles. **a** Fluorescence spectra scans of lipophilic oligonucleotides in PBS. **b** Photographic image of micelle aggregation in different solvent systems. From *left* to *right* ddH_2O, Py-20 (same sequence as lipo-20, but no lipid was coupled) in PBS buffer, lipo-20 in PBS, and acetone mixture (v/v 50:50) and lipo-20 in PBS buffer. Samples were illuminated by a UV transilluminator (312 nm) and photographed by a digital camera. **c** and **d** 4 % agarose gel analysis of amphiphilic DNA. From *left* to *right* Py-20, lipo-5, lipo-10, lipo-20, and lipo-50. **c** Gel ran in 1xTBE buffer. **d** Gel ran in 1xTBE buffer containing 0.8 % SDS. Reproduced from Ref. [19] by permission of John Wiley & Sons Ltd

independent of oligo length and sequence. The micelles can be visualized under atomic force microscope (AFM). Figure 7.3a showed the images of self-assembled structures of lipo-20 measured by typing-mode AFM in aqueous solution. Uniformed spherical structures with diameters around 10–12 nm were observed under AFM. The hydrodynamic diameters in PBS buffer, as measured by DLS, for lipo-5, lipo-10, lipo-20, and lipo-50, were 7.8, 9.5, 14.6, and 36.4 nm, respectively (Fig. 7.3b–e). These values agree well with the sizes of micelle aggregations, but they are far less than those in previously reported DNA vesicles. The fact that amphiphiles with different DNA lengths (random sequences, 5–50 mer) were found to form micelles whose sizes were linearly proportional to DNA length suggests a predictable relationship between micelle size and length of the oligo. Finally, the oligo micelles showed very low critical micelle concentration (CMC, estimated to be below 10 nm in PBS), suggesting the aggregates are stable under these experiment conditions.

Micelles formed by linking oligonucleotides with other lipid-like molecules are also reported in the literature. Pokholenko et al. constructed the lipophilic oligonucleotide micelles by covalent conjugate double- or triple-hydrocarbon chain to oligonucleotides; [24] these micelles feature a lipophilic core, which was subsequently used for loading and delivery of hydrophobic drugs.

Self-assembled oligo micelles also showed enhanced stability toward enzymatic digestion [31]. Similar phenomenon has been reported for other lipophilic modifications [32] or nucleic acids aggregations [33]. Although details about mechanisms are still not clear, the enhanced stability would be beneficial in using nucleic acids in vivo, where enzymatic degradation posts a major barrier.

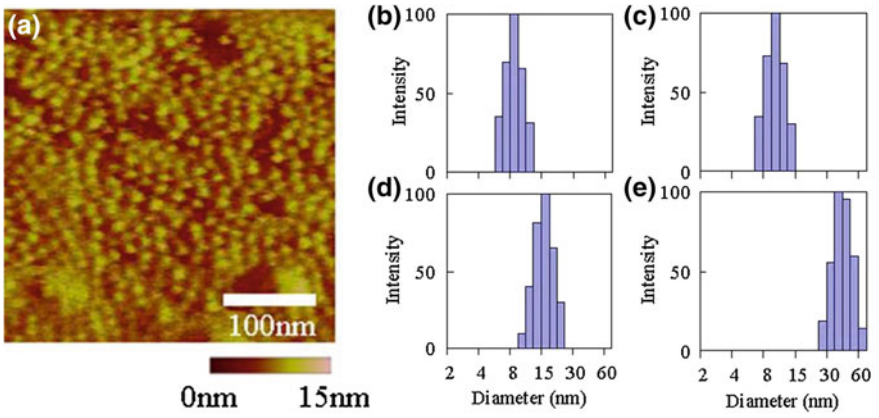

Fig. 7.3 Size analysis of DNA micelles. **a** AFM topography image of the self-assembled micelle (lipo-20) deposit on a mica surface. The sample was pipetted onto a freshly cleaved mica surface and imaged by tapping-mode AFM in PBS buffer. Dynamic light scattering (*DLS*) data of lipo-5 (**b**), lipo-10 (**c**), lipo-20 (**d**), and lipo-50 (**e**). Reproduced from Ref. [19] by permission of John Wiley & Sons Ltd

7.4 Biological Applications of Lipophilic Nucleic Acids

One of the most interesting features of nucleic acid amphiphiles lies in their biological applications. A great number of articles have been published demonstrating the activity of oligonucleotides in a variety of diseases in clinical and also in preclinical studies. Conjugation of various pendant moieties to oligonucleotides can be utilized to improve the physicochemical properties. The rationales for conjugating lipophilic groups to nucleic acids include (1) lipophilic pendants can be employed as uptake-enhancing agents for synthetic nucleic acids such as siRNA. This feature relies on the hydrophobic interactions between the lipids and cellular membranes. (2) Lipophilic oligonucleotides can self-assemble into spherical nucleic acids, a unique nanosized structure with a dense DNA monolayer that is capable of cellular uptake without any helper reagents [33]. (3) Due to the spontaneous association to form well-defined nanostructure with organized multiple ligands, lipophilic nucleic acids exhibit high-affinity molecular recognition in biological systems. Such multivalent system has been explored as a general strategy to enhance the ligand–target interactions [10]. (4) Lipophilic nucleic acids are also able to bind to various endogenous proteins and activate a delivery process to target the nucleic acids to specific locations after administration. Here, we summarize recent literature examples with demonstrated biological activities.

7.4.1 Interaction with Membrane Bilayers

One of the unique features of lipophilic nucleic acids is that they are able to inset into plasmid membranes. This feature has been used to enhance the incorporation of oligo onto liposome surface, as well as to engineer cell surface with functional nucleic acids. Lipophilic nucleic acids enable rapid, efficient, and stable insertion into live cell membranes. DNA derivatives with lipophilic moieties, such as cholesterol [8, 34], dendrimers [35], polymers [36], or lipids [19, 24, 28], have been intensively investigated for their membrane affinity. A hydrophobic anchor allows incorporation of nucleic acids into lipid bilayers, overcoming the membrane barrier and facilitating their uptake by cells. Often, there exists a partitioning balance between the self-assembled nanostructure (e.g., micelles) and membrane insertion. Less hydrophobic anchors are able to rapidly insert into membrane bilayers; however, their membrane stability is compromised. In contrast, more hydrophobic anchors have increased thermodynamic stability when inserted into cell membranes, but these amphiphiles also form stable aggregates which reduce the membrane partition [28, 37].

Due to the importance of cellular uptake of nucleic acids, a variety of lipophilic nucleic acids conjugates have been examined for controlling the interactions. Within different pendants, cholesterol-modified oligonucleotides have received the most attention. However, studies have shown that cholesterol-modified oligos were not

stably inserted into lipid bilayers, most likely due to its relative rigid structure and hydrophobicity [37, 38]. Thus, when incubated with lipid bilayers, cholesterol–oligos can insert into membranes, but can also flip back and come off the membrane bilayer after insertion. For cell surface engineering purposes, it is desired to have a stable insertion. Long-chain hydrocarbons have been shown to stably anchor to the lipid bilayer of the cell membrane through hydrophobic interactions [19, 39]. Besides the hydrophobic anchors, the length or the molecular weight of the oligonucleotides also affect the partition between micelle aggregates and membrane insertion. Using fluorescence techniques, we have extensively evaluated the structure-based membrane affinity of diacyl lipid-modified oligonucleotides [19]. Our results indicated that attachment of two long-chain hydrocarbons (18 carbons) to oligos allows stable incorporation into lipid bilayers and cell membranes. Interestingly, the molecular weights of amphiphilic DNA (and thus the sizes of the micellar aggregates) greatly affect the membrane incorporation kinetics and density. Small micelles have faster incorporation rate and thus higher membrane density, while large DNA micelles show slow partition rate and lower membrane density [19].

Fast, stable decoration of cell surface with lipophilic nucleic acids can be explored in several applications. For example, a lipophilic aptamer anchored on immune effector cell surface could act as targeting ligands that specifically recognize their target cells. Additionally, this approach allows multiple copies of ligand decoration and enhances the binding affinity via multivalency. The artificial aptamer ligands enable the engagement of immune cells and their target cells and enhance the cytotoxic killing. Xiong et al. [14] successfully used this strategy for DNA aptamer-mediated cell targeting. Figure 7.4a illustrates the concept of using cell surface-anchored aptamer for cell-specific targeting. In this approach, cell membrane-anchored aptamer can be divided into three distinct segments: The first segment is an aptamer sequence selected by a process called cell-systematic evolution of ligands by exponential enrichment (SELEX) [40]. Two different aptamers, Sgc8, which targets protein tyrosine kinase 7 on CCRF-CEM cell membrane, [41] and TD05, which targets the immunoglobulin heavy mu chain on Ramos cells surface, [42] were used for testing the principle. These aptamers exhibit high affinity (K_{dSgc8}: 0.8 nm, K_{dTD05}: 74 nm) and excellent selectivity toward their target cells, which is required for mimicking native cell surface ligand–receptor interactions. In addition, because multiple aptamers are anchored on each cell surface, multivalent interaction with target proteins can greatly improve the cell binding. The second segment is a PEG linker. Here, PEG allows DNA aptamer to extend out from the cell surface, minimizing non-specific interactions between the cell surface molecules and the aptamer, facilitating the conformational folding of aptamer. The third segment, a synthetic diacyl lipid tail with two stearic acids, is conjugated at the 5′-terminal as the membrane anchor. This design allows aptamers to firmly insert into cell membrane and retain their biologic functions. Additionally, aptamer density on the cell surface can be controlled by simply varying the incubation time or initial DNA concentration. The aptamers could fold properly to recognize their targets after anchoring on the cell membrane, as demonstrated by a homotypic cell aggregation experiment. In this experiment, when TDO5, an aptamer sequence which specifically recognizes Ramos

cells (a B-cell lymphoma cell line), was used to treat Ramos cells, we observed extensive aggregation of the Ramos cells, indicating that the lipophilic aptamer can firstly insert into Ramos cell surface and bind to adjacent Ramos cells. Notably, no aggregates were observed when a random sequence was used, suggesting a sequence-specific cell aggregation. Similarly, heterotypic cell targeting can be achieved by a two-step method. First, capture cell surfaces were decorated with lipo-aptamer. After removing the unmodified DNA, target cells were incubated with capture cells at 10:1 ratio. Heterotypic cell adhesions were observed with flower-like aggregates: an aptamer-modified cell in the center and 3–6 target cells adhere around (Fig. 7.4b). Controlled cell aggregation could also be realized in mixed cell populations (Fig. 7.4c, d). Aptamer anchored on cell surface retain their specificity as demonstrated by specific recognition of target cells in multi-cell mixtures. Flow cytometer analysis indicated that 40–90 % of the modified cells bind to target cells, depending on the aptamer densities on the cell surface.

This aptamer-mediated cell targeting strategy enables interaction between two types of cells with specificity and thus could be explored as a general approach for enhancing the immune recognition in immunotherapies. In a typical immune response, the affinity between T-cell receptor (TCR) and peptide–MHC is the key factor which determines tolerance or non-tolerance. While TCR specific for self-antigens (tolerant) tend to have low affinity, TCR specific for non-self-antigens (non-tolerant) tend to have higher affinity [43]. Thus, aptamer anchored on the immune effector cell surface can act as an artificial ligand to enhance the engagement between effector cells and target cells. To demonstrate the working principle, natural killer cells were modified with lipo-KK1B10, [44] an aptamer that specifically recognizes K562 cells and were mixed with K562 cells. A 50 % enhancement of binding was observed for aptamer-modified NK cells. Moreover, the killing efficiency was significantly improved: Compared with unmodified NK cells, which killed 21 % of the K562 cells, the aptamer-modified NK cells killed about 30 % of K562 cells. The incremental killing efficiency correlates well with targeting efficiency. These results demonstrated the feasibility of using cell-surface-anchored aptamer for enhancing cytotoxicity. To test whether this strategy could be applied to T lymphocyte-mediated cytotoxic assay, the same group tested the specific killing efficiency with a $CD8^+$ cytotoxic T-lymphocyte clone preactivated with universal T cell-activating agents. In nature, $CD8^+$ T cells recognize target cells via the binding between TCR and peptide–MHC I complex. Encouragingly, the aptamer modified on $CD8^+$ T-cell surface not only engaged the binding between $CD8^+$ T cells and target tumor cells, but also mediated aptamer-sequence-dependent cell killing. Thirty percentage of the Ramos cells were dead in the aptamer-modified CTL group in 6 h, as compared to only 5 % in the random sequence modified or unmodified CTL groups. Notably, the cytotoxic killing was achieved by aptamer-mediated cell–cell engagement, without the need of traditional binding between T-cell receptor and MHC I–peptide complex. As therapeutic treatment based on introduction of living cells is in clinical use and preclinical development for a wide variety of diseases, this cell surface-anchored aptamer strategy is expected to find potential in future cell-based delivery and therapy [45].

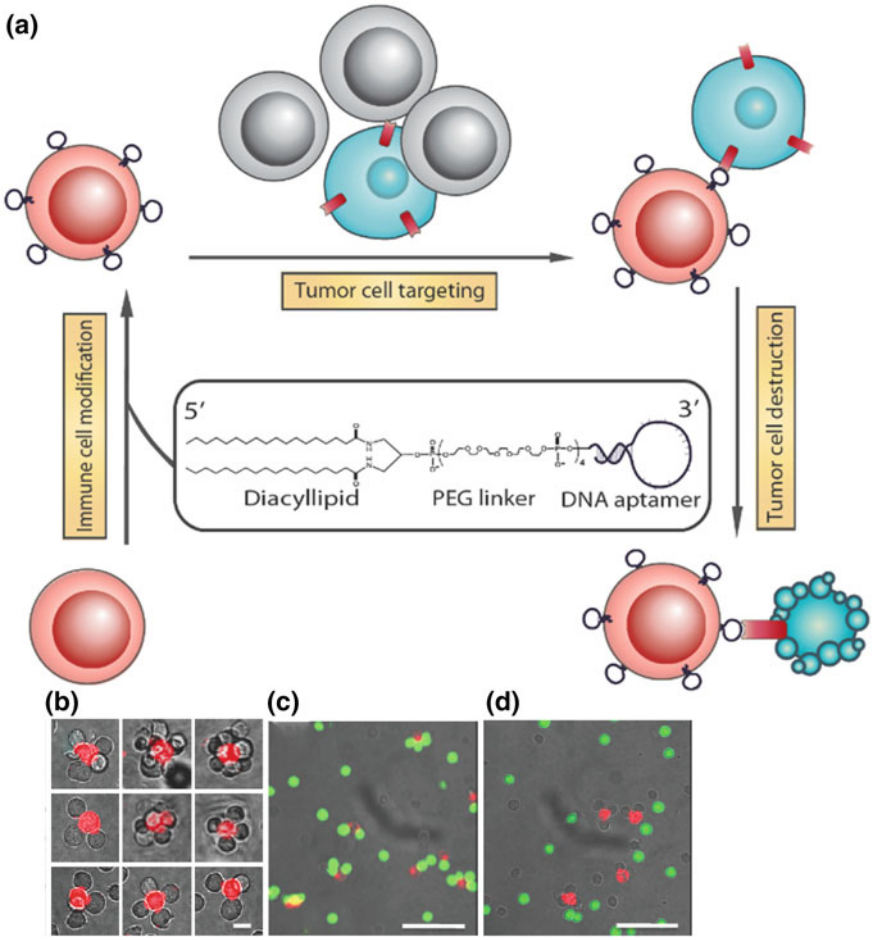

Fig. 7.4 Aptamer-mediated cell targeting. **a** Diacyl lipid aptamer-modified immune cells (*red*) can recognize targeting cancer cells (*blue*) in the presence of normal cells (*gray*) and induce cytotoxic killing of cancer cells. **b** Confocal microscope image of cell aggregates when 1:10 mixture of lipo-sgc8-TMR-modified Ramos (*red*) and CEM cells (*gray*). *Scale bar* 20 μm. **c**, **d** Aptamer-specific cell assembly. **c** Lipo-TD05-TMR-modified K562 cells (*red*) only bind to Ramos cells (*green*) but not unlabeled CEM cells. *Scale bar* 50 μm. **d** Lipo-Sgc8-TMR-modified K562 cells (*red*) bind to CEM cells (*gray*) in the presence of Ramos cells (*green*). Reproduced from Ref. [14] by permission of John Wiley & Sons Ltd

Cell surface-anchored nucleic acids have also been engineered as cell surface sensors for real-time monitoring of the cellular microenvironment. Nucleic acids are extensively used as biological sensors due to the advantages such as low costs, high stability, and high sensitivities [46]. However, nucleic acids as a single element are difficult to track the cellular microenvironment in a complicated biological system. For example, no nucleic acids are capable of monitoring what happen to the cells as

they circulate in the body. Thus, the cell membrane-anchored nucleic acid technology greatly expands the use of nucleic acids as biological sensor.

Recently, several groups have developed cell surface sensors based on nucleic acids. Qiu et al. [13] engineered a DNAzyme on the surface of cells and successfully used it for metal ion sensing. A diacyl lipid-tagged DNAzyme (sensing element) was used to decorate the cell surface via spontaneous membrane insertion. Under optimized conditions, approximately 1.65×10^6 DNAzymes were inserted on each CCRF-CEM cell in 30 min. This measurement demonstrates high-density sensors can be anchored on each cells. Importantly, the vast majority of the DNA probe appeared on the cell surface with minimal internalization after incubating at 37 °C for 2 h, suggesting a stable membrane decoration. The cell surface-decorated nucleic acid sensor was first evaluated for its ability to detect Mg^{2+}. Thus, a Mg^{2+}-specific DNAzyme (Mg-DNAzyme) was used to anchor on CEM cell surface. After washing away the free DNA, CEM cells were resuspended in buffer solutions containing different concentrations of Mg. Here, the Mg^{2+} acts as the coenzyme when present in the DNAzyme, cleaves the substrate oligo, and results in a fluorescence output. Both flow cytometry analysis and confocal microscopy showed a Mg^{2+} concentration-dependent fluorescence enhancement (Fig. 7.5). When exogenous Mg^{2+} was added, the fluorescence signal increased significantly, suggesting a change in the cellular environment. Moreover, the DNAzyme can sense the cellular Mg^{2+} extrusion process. When α1-adrenoceptor, a hormone which stimulates the efflux of Mg^{2+} from the cell, was added, the fluorescence signal of the cells increased rapidly. In contrast, CEM cells decorated with the same DNAzyme respond little without the hormone stimulation. One of the major advantages of using nucleic acids as sensor is that unlimited functional DNAzymes can be developed using an in vitro process known as SELEX [40]. Thus, this approach might be explored as a multiplex sensing platform to simultaneously monitor multiple key stimuli without complex manipulation. As a principle of demonstration, the same group successfully achieved detecting two different ions using the cell surface DNAzymes.

In a similar approach, Ke et al. described a cell surface-anchored ratiometric fluorescent probe for extracellular pH sensing. The authors used a membrane-anchored DNA to decorate cell surface with two fluorescent dyes. The resulting lipid–DNA probe showed sensitive and reversible response to pH change in the range of 6.0–8.0, which is suitable for most extracellular studies. This diacyl lipid DNA-based cell membrane anchoring strategy might be engineered for analysis of a wide range of targets and fulfill the need for real-time monitoring of the cell surface environment.

The above examples demonstrated the effectiveness of using membrane-anchored nucleic acids in vitro, either in cell targeting or in sensing applications. However, most in vivo application cannot be predicted by in vitro results. In an attempt to expand this technology in vivo, Liu et al. [47] directly decorated tumor cells with the diacyl lipid immunostimulatory oligonucleotide for augmenting the anti-tumor immune response. Intratumoral injection of diacyl lipid-modified CpG DNA, single-stranded oligonucleotides containing unmethylated cytosine–guanine

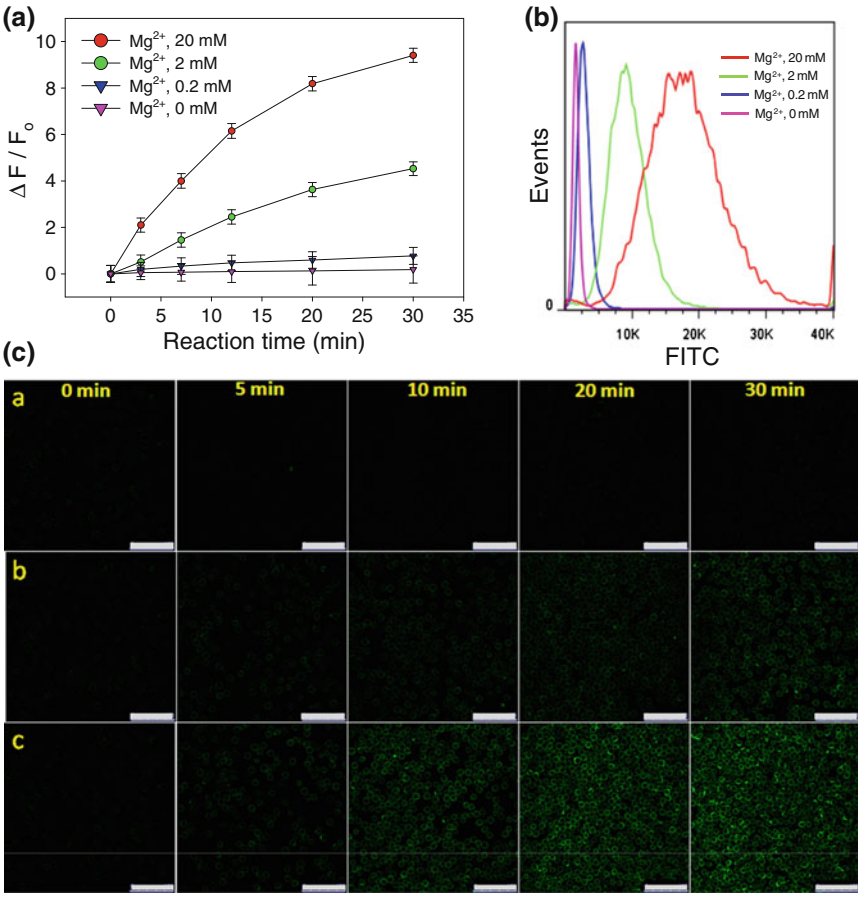

Fig. 7.5 Analysis of the cell surface Mg sensor for externally added Mg^{2+}. **a** Flow cytometry analysis of the kinetics of CEM cells modified with Mg-DNAzyme and then treated with Mg^{2+} of different concentrations. **b** Flow cytometry assay of CEM cells modified with Mg-DNAzyme and then treated with Mg^{2+} of different concentrations at RT for 30 min. **c** Confocal images of the Mg-DNAzyme-modified cells treated different concentrations of Mg^{2+} at RT for different time spans. Reprinted with the permission from Ref. [13]. Copyright 2014 American Chemical Society

motifs that bind Toll-like receptor-9 (TLR-9) and serve as potent molecular adjuvants can directly label tumor cells, leading to greatly prolonged local retention time of oligos at the injection site (Fig. 7.6). Directly decorating tumor cells with immunostimulatory DNA promotes the close association of oligonucleotides with tumor antigen or tumor cells. Membrane-anchored CpG oligonucleotide can overcome two fundamental limitations of direct injection of unmodified CpG into tumors. First, membrane anchored CpG DNA quickly insert into the tumor cell membranes following introtumoral injection, preventing the rapid diffusion of CpG DNA from the injection sites and prolonging the stimulation of local immune cells.

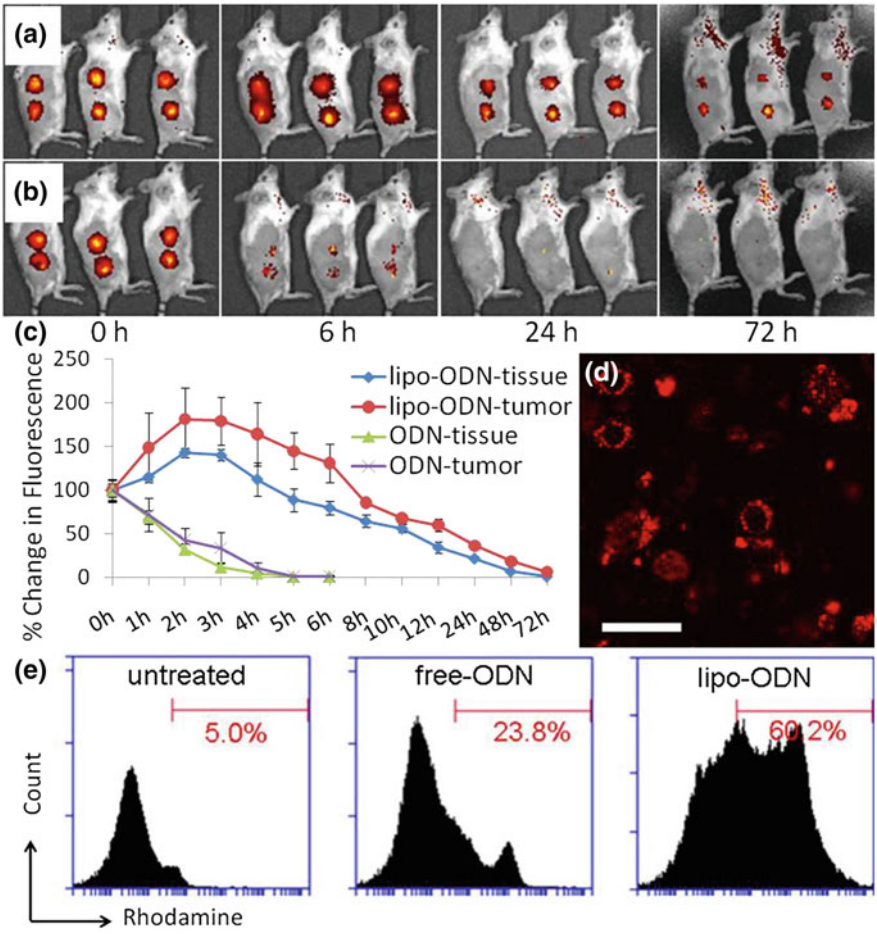

Fig. 7.6 In situ cell modification with amphiphilic oligonucleotide. **a–c** In vivo kinetics of fluorescence decay of dye-labeled amphiphilic ODN (**a**) and non-lipidated ODN (**b**). **c** Quantification of total fluorescence over time from ODN fluorescence at the injection sites. **d**, **e** Representative confocal image of tumor cells recovered from an intratumoral injection site (**d**) and flow cytometric analysis of recovered tumor cells (**e**) 3 h after injection. *Scale bar* 50 µm. Reproduced from Ref. [47] by permission of John Wiley & Sons Ltd

Second, the unique property of membrane-anchored ODNs allows the physical association between the CpG ODNs and tumor cells, a key element for codelivery of both antigens and adjuvants. In situ modification of tumor cells will be beneficial for the local stimulation of antigen-presenting cells such as dendritic cells responding to apoptotic tumor cells. In a murine melanoma tumor model, cell membrane-anchored CpG ODNs with nuclease-resistant phosphorothioate backbone exhibited significantly enhanced immunostimulatory activity and improved anti-tumor efficacy compared to soluble CpG.

7.4.2 Enhance Membrane Permeability

The development of disease diagnosis and gene therapy using nucleic acids holds great potential in future medicine. For example, double-stranded RNA molecules are utilized for RNA interference to the destruction of specific mRNA molecules; nucleic acid probes have been used to visualize and detect specific messenger RNA (mRNAs) in living cells. In previous section, we discussed the interaction between lipophilic nucleic acids and cell membranes, focusing on the insertion of lipophilic moieties into membrane bilayers. However, stable nanostructures assembled from nucleic acids, though they lack the membrane insertion capability, are able to cross the cell membrane. The fact that amphiphilic nucleic acids can self-assemble into stable nanosized structures offers the possibility to obtain new supramolecular systems with new biophysical characteristics for numerous applications ranging from biosensor to drug delivery systems. Early studies have demonstrated that nucleic acid aggregates, which are composed of a densely packed nucleic acids in a spherical geometry, were efficiently taken up by cells and were highly effective as gene regulation agents in siRNA, antisense, or mRNA regulation pathways. In contrast, linear nucleic acids would not efficiently enter cells without an effective carrier. Studies of the mechanism for cell uptake revealed that nucleic acid aggregates can complex with scavenger proteins and facilitate endocytosis. However, early studies include nucleic acids packed onto inorganic nanoparticles such as gold (AuNPs) or cross-linked spherical nucleic acids using gold nanoparticles as a template [33]. These methods are time-consuming and tedious. In contrast, nanostructures formed via self-assembly are easy to fabricate, possess self-delivery capability, are highly biocompatible, and are sufficiently stable in cellular environment.

Tan group first described the ability to enhance cell membrane permeability of the self-assembled DNA micelles. The attachment of a diacyl lipid tail onto the end of nucleic acid aptamers not only greatly enhance the aptamer's affinity toward recognizing target proteins, but also provides these novel nanostructures with an internalization pathway for cellular entrance. The aptamer strand acts as recognition ligands as well as the building block for the nanostructures. These aptamer DNAs were linked to lipid anchor via a short PEG linker. Similar to previous design, the PEG linker provides a spacer that greatly perseveres the aptamer's binding capability. Meanwhile, PEG linker also greatly stabilizes the micellar nanostructure by minimizing the charge–charge interaction of nucleic acids. Further studies showed that densely packing DNA on such an assembly creates multivalent aptamers, leading to greatly improved binding affinity toward target cells. Most importantly, the self-assembled micellar structure closely mimics the spherical nucleic acids, leading to a unique pathway to cross cell membrane without the need of transfection reagents and paving the way for the construction of aptamer–micelles with applications in diagnosis and targeted therapies. In this work, aptamer micelles have been shown to be able carry hydrophobic drugs in their lipophilic cores. Aptamer–micelles thus can act as nanosized carrier for targeted drug delivery.

The drug-encapsulated aptamer–micelles quickly internalize into target cells with high specificity even though individual aptamer lacks the binding ability at this temperature. The engineered aptamer–micelles represent a new class of nanomaterials that can be used for potential detection/delivery application in biological living systems.

In a similar approach, DNA micelle flares were designed to target intracellular mRNA for imaging and gene therapy [31]. Molecular beacon micelle flares (MBMFs) were assembled by covalently conjugating the hairpin molecular beacon to diacyl lipid. The molecular interactions allow the conjugate to self-assemble into micellar nanostructures which penetrate the cell membrane and bind to target mRNA. Once internalized, the molecular beacons function as a flare upon hybridizing to target mRNA, bursting a significant enhancement of fluorescence (Fig. 7.7). Under optimized condition, confocal laser scanning microscopy results revealed that MBMFs, but not unmodified molecular beacons, penetrated the cell membranes and bond to target mRNA, displaying enhanced fluorescence. This observation demonstrated that the need of diacyl lipid for efficient intracellular delivery of molecular beacons to cells. When non-complementary sequences were used for MBMFs, significant reduction of fluorescence was observed, demonstrating the selectivity of this approach. Furthermore, in a controlled cell line in which little mRNA was expressed, very low fluorescence was observed, suggesting

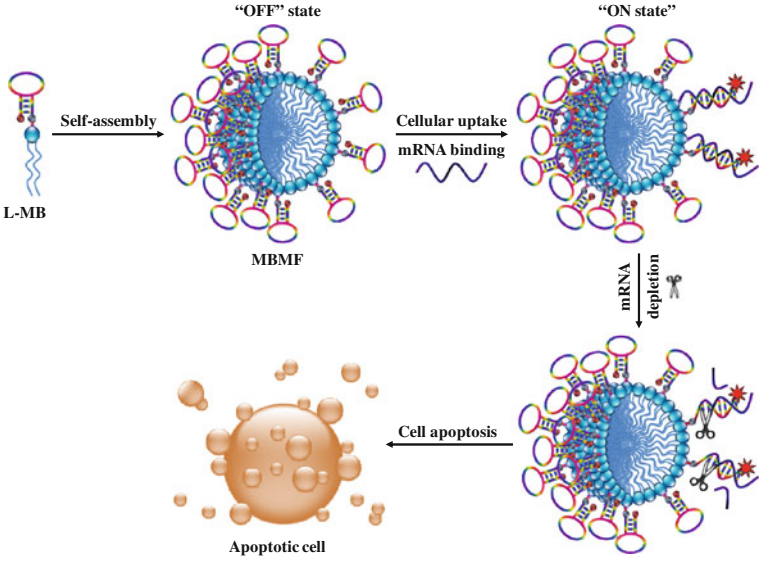

Fig. 7.7 Schematic illustration of molecular beacon micelle flares (*MBMFs*) for intracellular mRNA detection and gene therapy. Diacyl lipid-molecular beacon conjugates self-assemble into stable MBMFs and penetrate living cell membranes. Upon hybridization with target mRNA, the beacons are turned on, resulting in a fluorescent readout as well as RNAse H activity. This strategy can be used for gene regulation or therapy. Reproduced from Ref. [31] by permission of John Wiley & Sons Ltd

that MBMF approach can also differentiate cell lines with distinct mRNA expression levels. Flow cytometric analysis also correlated well with confocal results. Taken together, the above results strongly support the fact that nanostructured MBMFs are able to self-delivery into cells and are excellent candidate for intracellular mRNA detection.

In an attempt to use MBMFs for imaging-guided gene therapy, the same group tested the idea of using MBMFs to hybridize with target mRNA and block the production of a vital protein (Fig. 7.8). MBMFs can act either by providing a translation block, preventing translation from targeted mRNA, or by forming a DNA/RNA hybrid, causing it to be degraded by enzyme RNAse H. A model gene, Raf genes which code for serine threonine-specific protein kinases, was selected as target [31]. A phosphrothioate backbone (to enhance the stability)-modified MBMF was shown to markedly inhibit A549 cell proliferation in a dose-dependent manner, suggesting that MBMFs might be applied as antisense therapy for cancer.

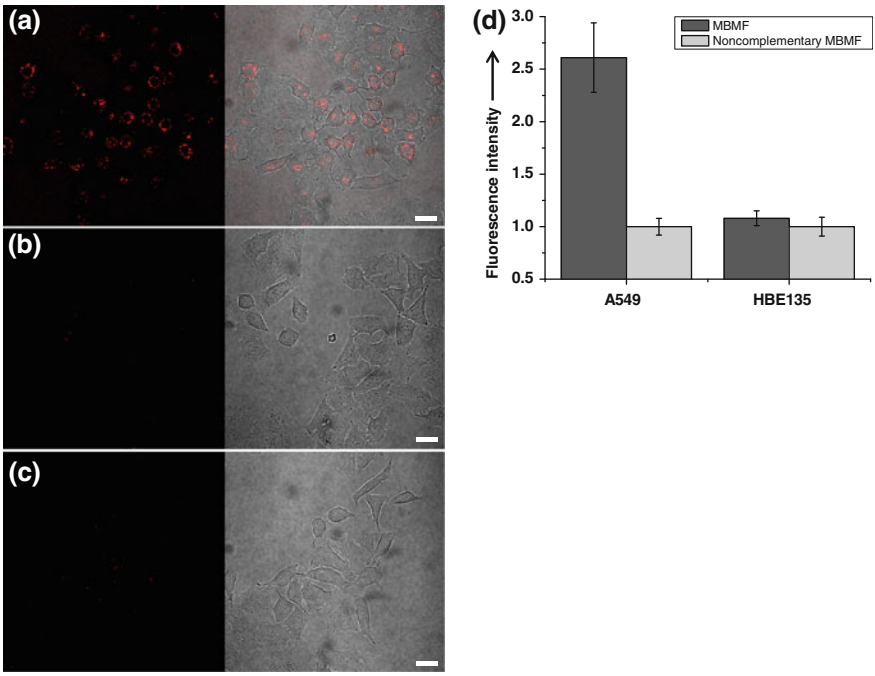

Fig. 7.8 Analysis of MBMFs in living cells. Confocal laser scanning microscopy images of A549 cells treated with 300 nm **a** MBMFs, **b** non-complementary MBMFs, and **c** MBs. Only MBMF-treated cells are fluorescent under this concentration. *Scale bars* 20 μm. **d** Flow cytometry results of A549 and HBE135 cells treated with 300 nm MBMFs and non-complementary MBMFs. MBMFs showed a cell-type-dependent response. Reproduced from Ref. [31] by permission of John Wiley & Sons Ltd

7.4.3 Interaction with Proteins

Depending on their pendants, lipophilic modified oligonucleotides can bind to various endogenous proteins. A major limitation of oligonucleotide therapeutics is short half-life. Most therapeutic oligos are rapidly degraded by enzymes or cleared from circulation through renal filtration. Some endogenous proteins (e.g., albumin, immunoglobulins) have exceptionally long half-lives due to an active recycling mechanisms mediated by the neonatal Fc receptor, which ultimately prevents the endosomal/lysosomal degradation [48, 49]. Drugs that bind to endogenous protein are known to have enhanced solubility and in vivo stability and have long circulatory half-life [49]. Oligos that are engineered to interact with long-lived serum proteins such as serum albumin or immunoglobulins (IgGs) can dramatically extend their half-lives in vivo [50]. Increased persistence of nucleic acids enables less frequent drug administration and expends the therapeutic window. Additionally, oligonucleotides that bind to protein can lead to the change of the in vivo pharmacokinetics and biodistribution after administration [50]. For this purpose, endogenous proteins can be harnessed as delivery devices to target nucleic acids to the tissue of interest.

Several studies have shown improved efficacy of cholesterol-conjugated antisense oligonucleotides and small interfering RNA in vivo [9, 15, 16]. For example, cholesterol modification promoted the plasma protein binding and modulated the in vivo liver cell uptake [9]. It was concluded that the interaction of the oligonucleotides with plasma proteins leads to improved therapeutic benefit. In a separate study, cholesterol-conjugated siRNAs facilitated cellular uptake as well as silence gene expression in vivo [16]. Subsequent studies also revealed the mechanisms of action of lipophilic siRNAs in vivo [15]. Wolfrum et al. [15] showed that efficient and selective uptake of lipophilic siRNAs depends on interactions with lipoprotein particles, transmembrane proteins, and lipoprotein receptors. Both high-density lipoprotein (HDL) and low-density lipoprotein (LDL) play an important role in lipophilic siRNA transport and organ uptake. While HDL transports siRNA to liver, gut, kidney, and steroidogenic organs, LDL directs the delivery of siRNA primarily to the liver [15]. These findings demonstrated that conjugation to lipophilic molecules provides nucleic acids with prolonged circulation time, favorable pharmacokinetics, effective tissue targeting, enhanced cellular uptake, and improved therapeutic efficacy.

Recently, diacyl lipid-modified immunostimulatory oligonucleotides have been shown to be able to target lymph nodes after s.c. injection [17]. This is of particular interest in the field of vaccine/adjuvant delivery. Subunit vaccines require the co-delivery of strong adjuvants to overcome the relatively weak immunogenicity associated with antigen fragments. One of the major challenges is to deliver the vaccine components to the lymph node, where all the immune cells interact [51]. Liu et al. [17] described a new strategy to target molecular vaccines, including an immunostimulatory oligonucleotide, to the secondary lymphoid organs following administration. In cancer staging, to visualize sentinel lymph nodes, surgeons often

inject colored dyes (e.g., isosulfan blue) at the tumor bed, from which they are transported into lymphatics and accumulate in the draining lymph nodes. A clinical design for effective sentinel LN mapping dyes is to choose compounds that bind tightly to serum albumin [52]. Albumin binding prevents small-molecule dyes from rapidly diffusing into the blood circulation and redirect them to lymphatics and draining LNs, where they are filtered by immune cells and accumulate, permitting LN visualization. Inspired by this 'albumin-hitchhiking' method, the authors developed molecular conjugates that similarly bind to albumin and follow s.c. injection, exhibit dramatic increases in lymph node accumulation via in situ binding, and transport with endogenous albumin (Fig. 7.9). In this approach, long, diacyl lipids which have strong affinity toward albumin are required to associate with albumin in the presence of many other serum proteins. Using PEG

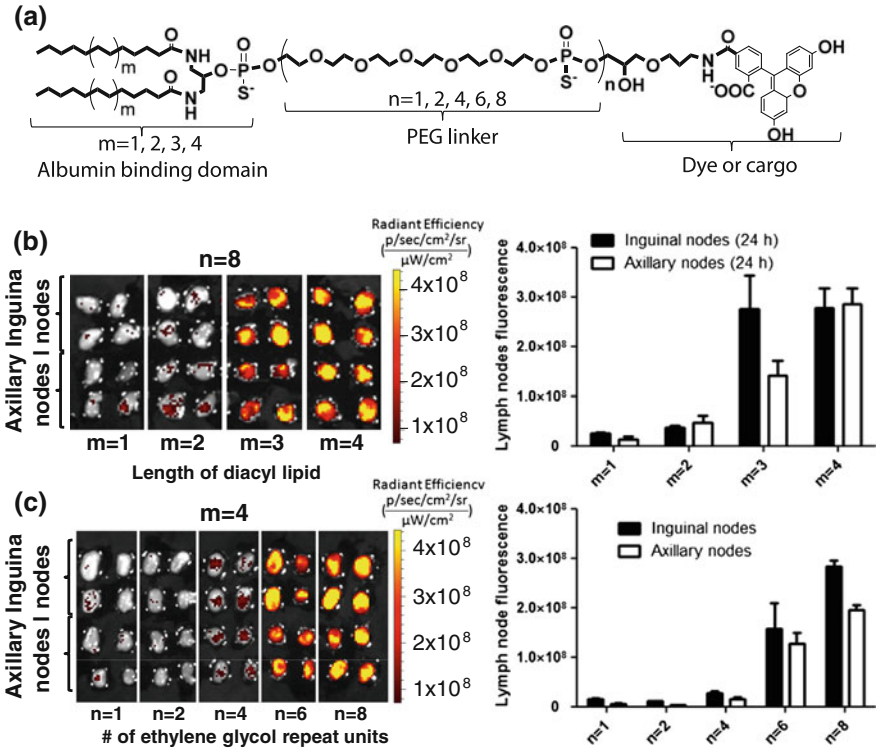

Fig. 7.9 Target LN by albumin-hitchhiking vaccines. **a** Schematic of the design of albumin-binding amphiphiles. Vaccine amphiphile contains a lipophilic albumin-binding diacyl lipid tail, a PEG solubilizing linker, and a vaccine cargo. **b** and **c** Fluorescent amphiphiles were injected s.c. at the tail base, draining LNs were isolated and imaged 24 h post-injection. Albumin-binding amphiphiles accumulate in lymph nodes in a lipid- (**b**, fixed PEG length 48 EG units) and PEG (**c**, fixed C18 diacyl lipid tails)-molecular weight-dependent manner. Reprinted by permission from Macmillan Publishers Ltd: Ref. [17], copyright 2014

amphiphiles, the authors have demonstrated generalized structure-based design rules for lymph node accumulation of amphiphiles after s.c. injection. (1) The lymph node accumulation after subcutaneous injection was directly linked to the structure of albumin-binding lipid domain: while long diacyl lipids (≥16 carbons, which exhibit a high affinity for albumin) showed intense accumulation in LN, short diacyl lipids (≤14 carbons) with low affinity displayed significantly reduced retentions (Fig. 7.9b). (2) The molecular weight of PEG was found to be critical in determining the lymph node accumulation (Fig. 7.9c). It was determined that the molecular weight of PEG molecules controls the partition between cell membrane insertion at the local injection sites and albumin binding: Amphiphiles with long PEG blocks showed preferential albumin binding when incubated with cells in the presence of albumin in vitro, which would reduce plasma membrane insertion. The same design rules can be applied to CpG oligonucleotide, a molecular adjuvant which activates the innate immunity. By these optimized molecular design, vaccine amphiphiles bind to albumin tightly in the presence of other serum proteins and efficiently accumulate in the lymph nodes following subcutaneous injection, achieving 8–15-fold greater retention than vaccines that do not bind albumin. Importantly, vaccine amphiphiles outperformed incomplete Freund's adjuvant (IFA) and poly(ethylene glycol) (PEG)-coated liposomes (100 nm diameters), two frequently used particulate delivery systems known to enhance vaccine accumulation in LNs, [53] suggesting albumin-binding amphiphile is superior to particulate carriers for LN targeting.

Subsequent immunization with the 'albumin-hitchhiking' molecular vaccines showed massive antigen-specific T-cell priming and improved anti-tumor efficacy. Administration of low dose of albumin-binding CpG and albumin-binding peptide antigens resulted in dramatically increased antigen-specific $CD8^+$ T-cell expansion relative to unmodified CpG and ovalbumin vaccines, as illustrated by substantial increases in the frequency of antigen-specific cytokine production in a variety of peptides (Fig. 7.10a). Importantly, the immune responses correlated well with lymph node accumulation, demonstrating that the lymph node accumulation of synthetic TLR adjuvants is critical in eliciting cytotoxic CD8 T-cell responses. In an animal therapeutic cervical tumor model, albumin-hitchhiking vaccine significantly delayed the s.c. implanted TC-1 (a mice cervical cancer model) tumor growth when compared to soluble vaccines, suggesting these vaccines have superior anti-tumor efficacy (Fig. 7.10b).

One of the benefits associated with albumin-hitchhiking vaccines is that it greatly enhances the vaccines' safety profiles. Albumin binding changes the biodistribution of vaccines. After s.c. injection, albumin-binding vaccines accumulate in LNs and reduce systemic exposure. In contrast, soluble vaccines quickly diffuse into blood circulation and access the APCs in the distal lymphoid organs; such systemic dissemination often results in systemic toxicity. Liu et al. also evaluated the toxicity profile of albumin-binding CpG oligonucleotide. Despite obvious lymphadenopathy of local draining LNs indicating local activity of lipo-CpG,

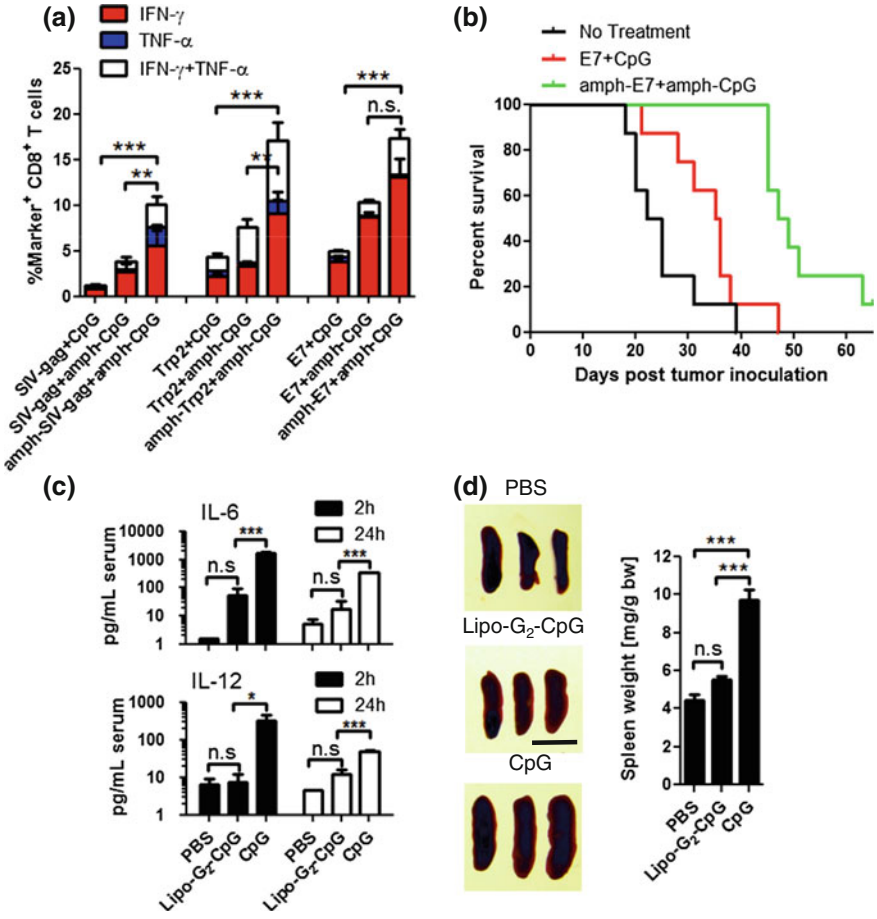

Fig. 7.10 Albumin-binding vaccines elicit massive antigen-specific T-cell response, maximize the antitumor efficacy, and reduce the systemic toxicity. **a** Mice were immunized with soluble vaccine or albumin-binding vaccines, antigen-specific CD8 T-cell responses were measured 6 days post-vaccination. **b** Mice survival curve in a cervical tumor model. **c**, **d** Serum inflammatory cytokines (**c**) and splenomegaly (**d**) after repeated injection of unmodified CpG or diacyl lipid-modified CpG. Reprinted by permission from Macmillan Publishers Ltd: Ref. [17], copyright 2014

repeated s.c. injections of high doses of albumin-binding CpG showed greatly reduced systemic inflammation relative to free CpG, as characterized by serum inflammatory cytokines (Fig. 7.10c, d) and leukocyte activation in the spleen (splenomegaly). These results suggest that the efficient LN targeting achieved by albumin-binding lipo-CpG also greatly reduces acute systemic side effects that have made CpG less attractive as a prophylactic vaccine adjuvant.

7.5 Conclusion and Future Outlook

Recent progress in the design of amphiphilic nucleic acids has provided new insights in using this new type of material in bio/nanotechnology and medicine. As discussed in the diverse examples here, novel nucleic acid amphiphiles are promising as bioactive drug carrier, or as theranostics (e.g., vaccine adjuvant) for disease including cancer, thanks to the versatile functions of both blocks in the nucleic acid amphiphiles. While this review outlines the current research on nucleic acid amphiphiles, it underscores the promise of designing future innovative nucleic acids for biomedical applications. As we gain more knowledge in human diseases, new nucleic acid-based amphiphiles will be emerged. For example, nucleic acid amphiphiles might be used to regulate stem cell differentiation. Nucleic acid amphiphiles might also be developed to modulate the immune system. Nevertheless, as nucleic acid amphiphiles open new perspectives toward the design and tailoring with desired features and functions, we will continue to witness rapid development of this type of materials in the biomedical field.

References

1. Kutzler MA, Weiner DB (2008) DNA vaccines: ready for prime time? Nat Rev Genet 9:776–788
2. Okamura K, Lai EC (2008) Endogenous small interfering RNAs in animals. Nat Rev Mol Cell Biol 9:673–678
3. Crooke ST (2004) Progress in antisense technology. Annu Rev Med 55:61–95
4. Wang K, Tang Z et al (2004) Molecular engineering of DNA: molecular beacons. Angew Chem Int Ed 48:856–870
5. Keefe AD, Pai S, Ellington A (2010) Aptamers as therapeutics. Nat Rev Drug Discov 9:537–550
6. Achenbach JC, Chiuman W, Cruz RP, Li Y (2004) DNAzymes: from creation in vitro to application in vivo. Curr Pharm Biotechnol 5:321–336
7. Whitehead KA, Langer R (2009) Anderson DG knocking down barriers: advances in siRNA delivery. Nat Rev Drug Discov 8:129–138
8. Letsinger RL, Zhang G, Sun DK, Ikeuchi T, Sarin PT (1989) Cholesteryl conjugated oligonucleotides: synthesis, properties, and activity as inhibitors of replication of human immunodeficiency virus in cell culture. Proc Natl Acad Sci USA 86:6553–6556
9. Bijsterbosch MK, Rump ET, De Vrueh RL, Dorland RR, Veghel R, Tivell KL, Biessen EA, Berkel TJ, Manoharan M (2000) Modulation of plasma protein binding and in vivo live cell uptake of phosphorothioate oligodeoxynucleotides by cholesterol conjugation. Nucleic Acids Res 28:2717–2725
10. Wu Y, Sefan K, Liu H et al (2010) DNA aptamer-micelle as an efficient detection/delivery vehicle toward cancer cells. PNAS 107:5–10
11. Kwak M, Herrmann A (2011) Nucleic acid amphiphiles: synthesis and self-assembled nanostructures. Chem Soc Rev 40:5745–5755
12. Ke G, Zhu Z, Wang W et al (2014) A cell-surface-anchored ratiometric fluorescent probe for extracellular pH sensing. ACS Appl Mater Interfaces 6:15329–15334
13. Qiu L, Zhang T, Jiang J et al (2014) Cell membrane-anchored biosensors for real-time monitoring of cellular microenvironment 136:13090–13093
14. Xiong X, Liu H, Zhao Z et al (2013) DNA aptamer-mediated cell targeting. Angew Chem Int Ed Engl 52:1472–1476

15. Wolfrum C, Shi S, Jayaprakash KN et al (2007) Mechanisms and optimization of in vivo delivery of lipophilic siRNAs. Nat Biotechnol 25:1149–1157
16. Soutschek J, Akinc A, Bramlage B et al (2004) Therapeutic silencing of an endogenous gene by systemic administration of modified siRNAs. Nature 432:173–178
17. Liu H, Moynihan KD, Zheng Y et al (2014) Structure-based programming of lymph-node targeting in molecular vaccines. Nature 507:519–522
18. Bhatia D, Li Y, Ganesh KN (1999) Steroid—DNA conjugates: improved triplex formation with 5-amido-(7-deoxycholic acid)-dU incorporated oligonucleotides. Bioorg Med Chem Lett 9:1789–1794
19. Liu H, Zhu Z, Kang H et al (2010) DNA-based micelles: synthesis, micellar properties and size-dependent cell permeability. Chem-Eru J 16:3791–3797
20. Anaya M, Kwak M, Musser AJ et al (2010) Tunable hydrophobicity in DNA micelles: design, synthesis, and characterization of a new family of DNA amphiphiles. Chem-Eru J 16:12852–12859
21. Borisenko GG, Zaitseva MA, Chuvilin AN, Pozmogova GE (2009) DNA modification of live cell surface. Nucleic Acids Res 37:e28
22. Brush CK (1995) Lipo-phosphoramidites. US Patent 5,420,330
23. Chan YH, Lenz P, Boxer SG (2007) Kinetics of DNA-mediated docking reactions between vesicles tethered to supported lipid bilayers. Proc Natl Adad Sci USA 104:18913–18918
24. Pokholenko O, Gissot A, Vialet B et al (2013) Lipid oligonucleotide conjugates as responsive nanomaterials for drug delivery. J Mater Chem B 1:5329–5331
25. Zimmermann J, Kwak M, Musser AJ, Herrmann A (2011) Amphiphilic DNA block copolymer: nucleic acid-polymer hybrid materials for diagnostics and biomedicine. Methods Mol Biol 751:239–266
26. http://www.linktech.co.uk/products/modifiers/hydrophobic_group_cholesterol_palmitate_modification
27. Schade M, Berti D, Huster D et al (2014) Lipophilic nucleic acids—a flexible construction kit for organization and functionalization of surfaces. Adv Colloid Interface Sci 208:235–251
28. Gosse C, Boutorine A, Aujard C, Chami M, Kononov A, Cogne-Laage E, Allemand JF, Li J, Jullien L (2004) Micelles of lipid-oligonucleotide conjugates: implications for membrane anchoring and base pairing. J Phys Chem B 108:6485–6497
29. Dentinger PM, Simmons BA, Cruz E, Sprague M (2006) DNA-mediated delivery of lipophilic molecules via hybridization to DNA-based vesicular aggregates. Langmuir 22:2935–2937
30. Teixeira F, Rigler JP, Vebert-Nardin C (2007) Nucleo-copolymers: oligonucleotide-based amphiphilic diblock copolymers. Chem Comm 1130–1132
31. Chen T, Wu C, Jimenez E et al (2013) DNA micelle flares for intracellular mRNA imaging and gene therapy. Angew Chem Int Ed 52:2012–2016
32. Rattanakiat S, Nishikawa M, Takakura Y (2012) Self-assembling CpG DNA nanoparticles for efficient antigen delivery and immunostimulation. Eur J Pharm Sci 47:352–358
33. Cutler JI, Auyeung E, Mirkin CA (2012) Spherical nucleic acids. J Am Chem Soc 134: 1376–1391
34. Kabanov AV, Vinogradov SV, Ovchareko AV (1990) A new class of antivirals: antisense oligonucleotides combined with a hydrophobic substituent effectively inhibit influenza virus reproduction and synthesis of virus-specific proteins in MDCK cells. FEBS Lett 259:327–330
35. Skobridis K, Husken D, Nicklin P, Haner R (2005) Hybridisation and cellular uptake properties of lipophilic oligonucleotide-dendrimer conjugates. ARKIVOC 6:459–469
36. Li Z, Zhang Y, Fullhart P, Mirkin CA (2004) Reversible and chemically programmable micelle assembly with DNA block-copolymer amphiphiles. Nano Lett 4:1055–1058
37. Weber RJ, Liang SI, Selden NS, Desai TA, Gartner ZJ (2014) Efficient targeting of fatty-acid modified oligonucleotides to live cell membranes through step-wise assembly. Biomacromolecules published online 17 Oct 2014
38. Pfeiffer I, Hook F (2004) Bivalent cholesterol-based coupling of oligonucleotides to lipid membrane assemblies. J Am Chem Soc 126:10224–10225

39. Selden NS, Todhunter ME, Jee NY, Liu JS, Broaders KE, Gartner ZJ (2012) Chemically programmed cell adhesion with membrane-anchored oligonucleotides. J Am Chem Soc 134:765–768
40. Sefah K, Shangguan D, Xiong X, O'Donoghue MB, Tan W (2010) Development of DNA aptamers using cell-SELEX. Nat Protoc 5:1169–1185
41. Shangguan D, Li Y, Tang Z, Cao Z, Chen HW, Mallikaratchy P, Sefah K, Yang CJ, Tan W (2006) Aptamers evolved from live cells as effective molecular probes for cancer study. Proc Natl Adad Sci USA 103:11838–11843
42. Tang Z, Shangguan D, Wang K, Shi H, Sefah K, Mallikratchy P, Chen H, Li Y, Tan W (2007) Selection of aptamers for molecular recognition and characterization of cancer cells. Anal Chem 79:4900–4907
43. Kammertoens T, Blankenstein T (2013) It's the peptide-MHC affinity, stupid. Cancer Cell 23:429–431
44. Sefah K, Tang Z, Shangguan D, Chen H, Lepez-Colon D, Li Y, Parekh P, Martin J, Meng L, Philips JA, Kim YM, Tan W (2009) Molecular recognition of acute myloid leukemia using aptamers. Leukemia 23:235–244
45. Stephan MT, Irvine DJ (2011) Enhancing cell therapies from the outside in: cell surface engineering using synthetic nanomaterials. Nanotoday 6:309–325
46. Liu J, Cao Z, Lu Y (2009) Functional nucleic acid sensors. Chem Rev 109:1948–1998
47. Liu H, Kwong B, Irvine DJ (2011) Membrane anchored immunostimulatory oligonucleotides for in vivo cell modification and localized immunotherapy. Angew Chem Int Ed 50:7052–7055
48. Dennis MS, Zhang M, Meng G, Kadhodayan M et al (2002) Albumin binding as a general strategy for improving the pharmacokinetics of proteins. J Biol Chem 227:35035–35043
49. Roopenian DC, Akilesh S (2007) FcRn: the neonatal Fc receptor comes of age. Nat Rev Immunol 7:715–725
50. Juliano RL, Ming X, Nakaguwa O (2012) The chemistry and biology of oligonucleotide conjugates. Acc Chem Res 45:1067–1076
51. Pal I, Ramsey JD (2011) The role of the lymphatic system in vaccine trafficking and immune response. Adv Drug Deliv Rev 63:909–922
52. Tsopelas C, Sutton R (2002) Why certain dyes are useful for localizing the sentinel lymph node. J Nucl Med 43:1377–1382
53. Bachmann MF, Jennings GT (2010) Vaccine delivery: a matter of size, geometry, kinetics and molecular patterns. Nat Rev Immunol 10:787–796

Chapter 8
Aptamer-Based Hydrogels and Their Applications

Chun-Hua Lu, Xiu-Juan Qi, Juan Li and Huang-Hao Yang

Abstract Hydrogels are water-retainable materials that can absorb a large amount of water. Different stimuli can be used to stimulate the hydrogels with a variety of physical and chemical changes, thus leading to numerous applications in bioanalysis and biomedicine. Aptamers are special types of single-stranded DNA generated by a process called systematic evolution of ligands by exponential enrichment (SELEX). They are able to specifically recognize a wide range of targets which vary from ions, small molecules, to proteins, and even whole cells. Aptamer incorporation has greatly expanded the applications of hydrogels. Due to their unique properties, such as biocompatibility, selective binding, and molecular recognition, these aptamer-based hydrogels can be utilized for target-responsive hydrogel engineering. In this chapter, we discuss a variety of applications of aptamer-based hydrogels, especially in sensing, target capture and separation, control of target release and in vivo applications.

Keywords Biosensors · Cancer therapy · Colorimetric · Controlled release · Drug delivery · Gel–sol transition · Nucleic acids · Polyacrylamide chains · Thrombin · Visual detection

8.1 Introduction

Hydrogels are water-retainable materials that can absorb a large amount of water (containing up to 99 wt% water). Due to their significant water content, hydrogels possess a degree of flexibility that is similar to natural tissue. There are two mech-

C.-H. Lu · X.-J. Qi · J. Li · H.-H. Yang (✉)
The Key Lab of Analysis and Detection Technology for Food Safety of the MOE, College of Chemistry, Fuzhou University, Fuzhou 350108, China
e-mail: hhyang@fzu.edu.cn

W. Tan and X. Fang (eds.), *Aptamers Selected by Cell-SELEX for Theranostics*,
DOI 10.1007/978-3-662-46226-3_8

anisms of hydrogel formation: covalent cross-linking and noncovalent cross-linking. The type and degree of cross-linking, as well as the components of materials, define the properties of a hydrogel. Different stimuli can be used to stimulate the hydrogels with a variety of physical and chemical changes, including pH [1], temperature [2], ionic strength [3], electric field strength [4], supramolecular receptor-ion complex formation [5–7], exposure to light [8, 9] or ultrasound [10], and magnetic stimuli [11, 12]. These stimuli-responsive hydrogels have attracted attention because of their potential in drug delivery systems [13–16], sensors [17–21], cancer therapy [22], the use of stimuli regulated hydrogels as pumps or valves in microdevices [23–25], cell culture substrates [26, 27], and tissue engineering [28, 29]. Although a number of smart hydrogels have been prepared, the search for other stimuli is ongoing. Molecular recognition motifs, such as metal ions [30], oligonucleotides [31], antibodies [32], and enzymes [33], can be used to expand the range of stimuli.

One specific class of hydrogels consists of those based on DNA, which bring with them the unique features of nucleic acids [34–38]. Based on Watson-Crick base pairing of purine and pyrimidine groups [39–42], double helix formation makes oligonucleotides programmable and predictable polymers in materials science [43]. Self-assembly of single-stranded DNA into supramolecular nanostructures and metal ion-assisted cooperative stabilization of duplex DNA are further interactions characterizing DNA biopolymers [44–50].

Three different strategies can be used to develop DNA-based hydrogels. The first involves cross-linking of nucleic acid units by self-assembly or hybridization to form the hydrogel. Examples include hybridization of Y-shaped duplex units and double-stranded DNA to form a three-dimensional DNA hydrogel [51, 52], enzyme-catalyzed assembly of branched DNA nanostructures [53], and formation of an i-motif at acidic pH as the cross-linking bridge [54]. The second method involves modification of hydrophilic polymer chains with nucleic acids as chain branches and subsequent formation of the DNA hydrogel by cross-linking the branches. For example, polyacrylamide chains functionalized with nucleic acids form hydrogels by hybridization between the nucleic acids [31] or by G-quadruplex formation in the presence of K^+ [55]. As a third method, polymerization of organic monomer and cross-linker to form polymer networks with tethered or entrapped functional nucleic acids [56–58].

Switchable DNA hydrogel transitions can be induced by various stimuli, including the formation and separation of DNA hydrogels by strand displacement [59], temperature control [60], formation and dissociation of i-motif [54] or G-quadruplex [55], and by use of metal ions-ligand complexes [30]. The separation of cross-linking bridges of DNA hydrogels by photochemical isomerization of azobenzenes groups conjugated to the DNA [61], formation of aptamer-substrate complexes [62, 63], and enzymatic [51] or DNAzyme-catalyzed cleavage of the hydrogel bridging units [64] were also reported. A variety of applications have been

demonstrated with stimuli-responsive DNA hydrogels, including sensing [58], removal of hazardous metal ions [57], inscription of structural information [65], switchable fluorescence properties [52], and catalytic DNAzyme functions [55].

Among the DNA-based hydrogels, those containing aptamers are especially attractive. Aptamers are single-stranded DNAs generated by a process called systematic evolution of ligands by exponential enrichment (SELEX) [66, 67]. Due to their unique secondary and tertiary structures, aptamers are able to specifically recognize a wide range of targets, including ions, small molecules, proteins, and even whole cells [66–76]. Aptamers are often called chemical antibodies because of their comparable dissociation constants (K_ds) [77]. Since their discovery in the 1990s [78], aptamers have been developed as specific, high-affinity probes for bioanalytical and cancer-related research. Aptamers can be chemically conjugated with various signal-generating components for acoustic [79–81], electrochemical [82–85], and optical [86–88] sensing. The high affinity, easy fabrication, low cost, and easy modification of aptamers have made them excellent components in DNA hydrogel engineering. Due to their low K_d values, aptamers can specifically recognize their substrates even at very low concentrations and undergo changes upon binding or dissociation of substrates. These structural changes can stimulate specific physical or chemical interactions within hydrogel systems or circumambient solution systems. Entrapment of drugs [89, 90], nanoparticles [91–93], and dyes [57, 58] has greatly expanded the applications of aptamer-based hydrogels [94], allowing capabilities such as visual detection [56–58, 62, 95, 96], controlled drug release [97–101], and cancer therapy [89, 90, 102]. Furthermore, the availability of a wider range of aptamers will make aptamer-based hydrogel systems even more versatile in the future.

In this chapter, emphasis is placed on aptamer-based hydrogels, with selected examples to illustrate the most recent developments in their applications.

8.2 Aptamer-Based Hydrogels for Sensing and Detection

To act as a sensor, an aptamer-based hydrogel should produce an output signal when stimulated by the target. The following section discusses three kinds of aptamer-based hydrogel sensors.

8.2.1 Target Stimulated Gel–Sol Transitions

The use of aptamers for target-responsive reconfiguration of DNA nanostructures has been developed using gold nanoparticles [103–106], quantum dots [107], and magnetic nanoparticles [108]. Therefore, combined aptamer into the DNA duplex

structure as cross-linker to form a hydrogel, it is easy to design an aptamer sensor based on gel–sol transition. In one of the first reports, Yang et al. showed that a gel–sol transition can be achieved using an aptamer-based hydrogel [91] responsive to adenosine, Fig. 8.1a. Two acrydite-modified oligonucleotides, strand (**1**) and strand (**2**), were copolymerized with acrylamide and incorporated into polyacrylamide chains P-1 and P-2, respectively. When these two oligonucleotide-conjugated polyacrylamide chains were mixed, a fluid state was obtained. The fluid system could undergo a sol-gel transition by the addition of cross-linking oligonucleotides, (**3**), which containing three functional domains: domain I complementary with strand (**1**), domain II complementary to the last five nucleotides of strand (**2**), and domain III as the aptamer sequence with seven nucleotides complementary with strand (**2**). Upon adding (**3**), the system formed a rigid hydrogel. In the presence of target adenosine molecules, the aptamer competitively bound to target, and the five remaining

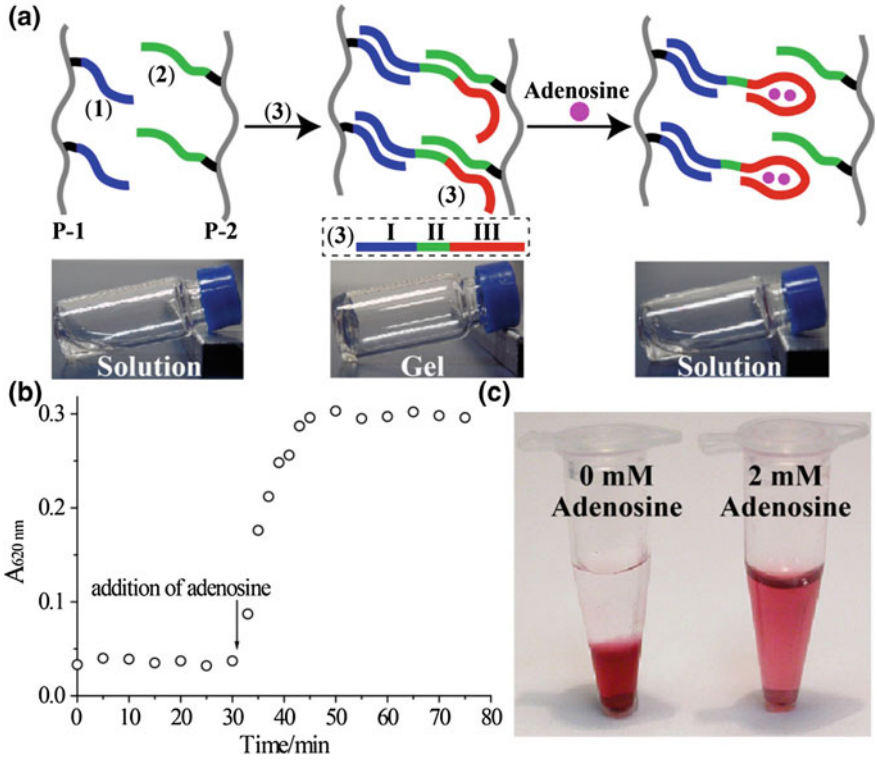

Fig. 8.1 **a** Hydrogel cross-linked by DNA containing adenosine-binding aptamer undergoes a gel–sol transition upon adding target adenosine. **b** Absorption measurements of gold nanoparticles upon addition of adenosine. The gold nanoparticles were preloaded inside the hydrogel during its formation. **c** Photograph of hydrogel having entrapped gold nanoparticles without and with target adenosine. Reprinted with the permission from Ref. [91]. Copyright 2008 American Chemical Society

nucleotides could not remain hybridized with strand (**2**), leading to the dissolution of the hydrogel within 15 min, Fig. 8.1b. Because of their unique optical properties, gold nanoparticles could be used as an indicator to monitor the gel–sol transition, Fig. 8.1c. The aptamer-based hydrogel was very selective for adenosine. Analogues, such as cytidine, uridine, and guanosine, did not result in a gel–sol transition, even at high concentrations. In order to demonstrate the generality of the method, the authors also designed a thrombin-binding aptamer-based hydrogel and similar phenomena were observed. It should be noted that the thrombin-induced gel–sol transition was much slower due to the larger size of thrombin, leading to slow diffusion of thrombin into the gel. The generality of this method was further developed by using cocaine as trigger for the dissociation of the aptamer-based hydrogel [62].

While gold nanoparticles could be used as indicator in the above method, a high concentration of target was needed for gel dissolution, thus limiting the usefulness of the method in analysis field. To solve this problem, Zhu et al. [62] designed a colorimetric method based on a cocaine-binding aptamer-based hydrogel using an enzyme as a tool for signal amplification. Figure 8.2 illustrates the working principle of this gel–sol transition system. Two acrydite-modified DNA strands, (**4**) and (**5**), were grafted onto linear polyacrylamide polymers to form polymer strands P-4 and P-5, respectively. Strands (**4**) and (**5**) were partially complementary to strand (**6**), which contained the cocaine aptamer sequence. Upon adding strand (**6**), (**4**) and (**5**) were hybridized with (**6**), thus leading to the cross-linking of P-4 and P-5. As the hybridization proceeded, the polymers were transformed into the gel state. However, instead of gold nanoparticles, the enzyme amylase, which catalyzes the hydrolysis of amylose to maltose, was entrapped in the aptamer-based hydrogel. In

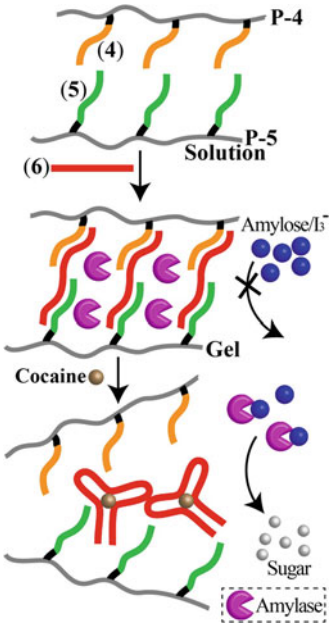

Fig. 8.2 Visual detection of cocaine using an aptamer-based hydrogel with an enzymatic signal amplification step. In the presence of cocaine, the entrapped amylase was released into the surrounding solution to digest amylose, thus decreasing the intensity of the blue amylose/I_3^- color. Reprinted with the permission from Ref. [62]. Copyright 2010 Wiley-VCH

the buffer solution outside the hydrogel, amylose with iodine yielded a dark blue color. Since amylase was entrapped in the hydrogel, it was isolated from amylose. In the presence of cocaine, the cross-linker strand (**6**) was bound to target, leading to the dissolution of the hydrogel and release amylase into the solution, where it hydrolyzed amylose and the dark blue color disappeared. It should be noted that in this method, the enzyme amylase was used for signal amplification. Therefore, as long as sufficient amylase was released to the solution to cause the color fading, the hydrogel did not have to dissolve completely. The authors demonstrated that by using this method, they were able to detect less than 20 ng of cocaine with the naked eye within 10 min.

A related study was also developed by the same group for quantitative analysis of the target molecule [95]. The authors proposed the concept of a target-responsive "sweet" aptamer-based hydrogel encapsulating glucoamylase, which allowed efficient conversion of the target recognition event into a cascaded glucose production reaction for subsequent portable personal glucose meter (PGM) readout. As shown in Fig. 8.3a, before adding cocaine aptamer to cross-link the polymer strands

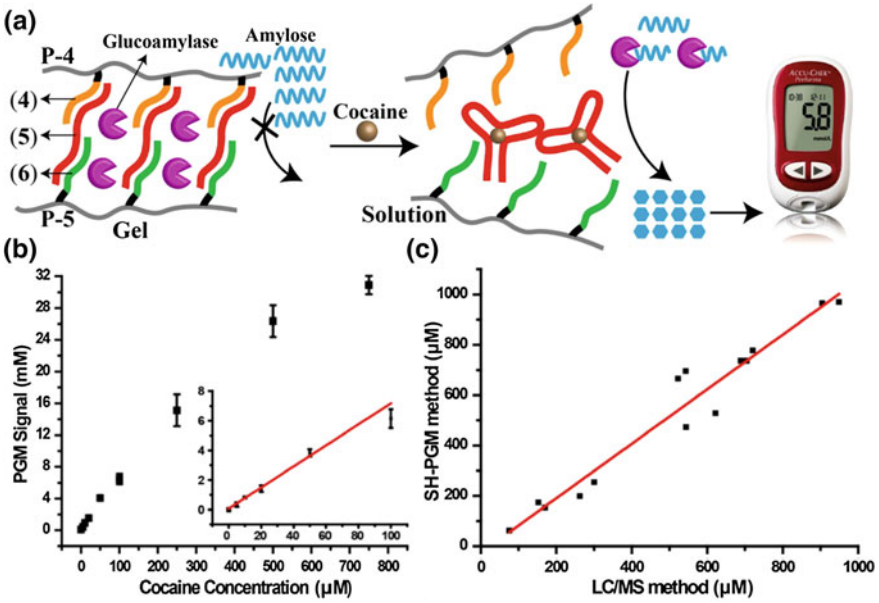

Fig. 8.3 **a** Schematic representation of the target-responsive "sweet" aptamer-based hydrogel. The entrapped glucoamylase was released upon adding target cocaine, thus catalyzing the hydrolysis of amylose to produce a large amount of glucose for quantitative readout by the glucometer. **b** Resulting calibration curve corresponding to analysis of different concentrations of cocaine according to **a**. The concentrations of cocaine were ranged from 0 to 750 μM. *Inset* calibration curve of lower concentration range of cocaine. **c** Comparison of the cocaine-binding aptamer-based hydrogel with the standard LC/MS method based on 14 samples in urine. Reprinted with the permission from Ref. [95]. Copyright 2013 American Chemical Society

(**4**) and (**5**) (P-4 and P-5), glucoamylase was mixed into the polymer solution. Strands (**4**) and (**5**) were complementary to adjacent areas of strand (**6**), containing the cocaine aptamer sequence. Upon adding (**6**) to form the hydrogel, glucoamylase was trapped in the hydrogel. In the presence of target cocaine, strand (**6**) preferentially bound to the cocaine, leading to a gel–sol transition of the hydrogel and release of glucoamylase, which catalyzed the hydrolysis of amylose to produce a large amount of glucose for quantitative readout by the PGM. The method enabled selective analysis of cocaine with a detection limit corresponding to 3.8 μM in buffer solution, Fig. 8.3b. Furthermore, the authors also demonstrated the wide applicability of this method in complex body fluids (the detection limits of cocaine were 4.4 μM in urine and 7.7 μM in 50 % human plasma). In order to verify the accuracy and reliability of the method, they compared it with a LC/MS method for cocaine detection, Fig. 8.3, and obtained similar results. Since different aptamers can be used for construction, it is possible to design an inexpensive, rapid, portable, and quantitative hydrogel detection method for a range of nonglucose targets. Furthermore, the authors integrated Au core/Pt shell nanoparticles (Au@PtNPs) into the aptamer-based hydrogel with a volumetric bar-chart chip (V-chip) to develop a novel method for quantitative point-of-care testing (POCT) [96]. As illustrated in Fig. 8.4a, b, cocaine-binding aptamer-based hydrogel was formed in the gel reservoir, and Au@PtNPs, which can catalyze the decomposition of H_2O_2 to O_2, were preloaded inside the hydrogel during formation. In the presence of target cocaine, the hydrogel dissociated, thus leading to the release of entrapped

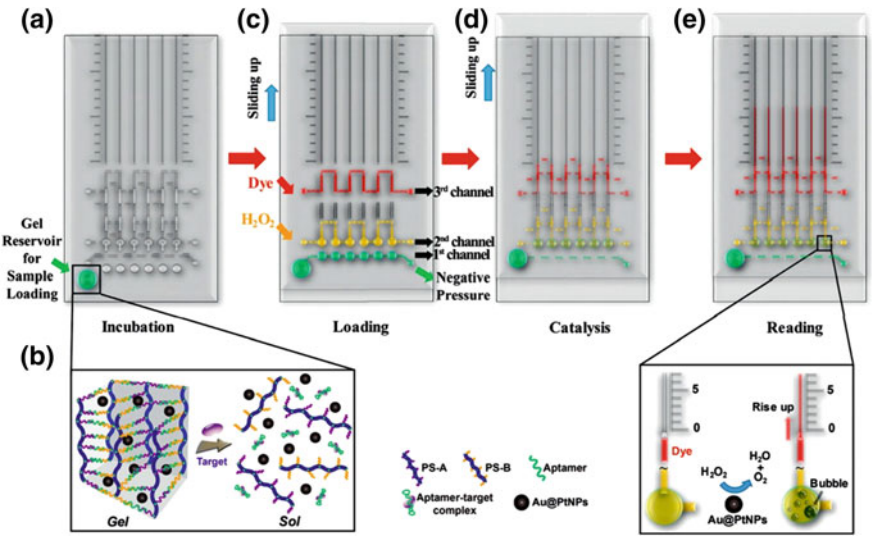

Fig. 8.4 Au core/Pt shell nanoparticles entrapped in an aptamer-based hydrogel with a volumetric bar-chart chip for visual quantitative detection of cocaine. Reprinted with the permission from Ref. [96]. Copyright 2014 Wiley-VCH

Au@PtNPs into the supernatant solution. By sliding up the V-chip, three connected horizontal channels were formed, Fig. 8.4c. Under negative pressure, the supernatant containing the released Au@PtNPs was drawn into the first channel (green). H_2O_2 and the indicator red ink were injected into the second channel (yellow) and third channel (red), respectively. By further sliding up the V-chip, the supernatant, H_2O_2, and red ink were loaded in six independent parallel connected vertical channels, Fig. 8.4d. The contact between Au@PtNPs and H_2O_2 led to the catalytic decomposition of H_2O_2 to generate O_2, which pushed the red ink into the top thinner channel, Fig. 8.4e, f. The distance that each ink bar moved within a fixed time interval was proportional to the target cocaine concentration. The V-chip method enabled visual detection of cocaine with a detection limit corresponding to 0.06 μM. With the advantages of low cost, speed, portability, and quantitative visual detection, the V-chip method has potential application in POCT of health care, environmental safety and food quality assurance.

Manipulation of an aptamer-based hydrogel by target to stimulate a gel–sol transition also allowed design of logic gate systems. Using cocaine aptamer and ATP aptamer as cross-linkers to form the aptamer-based hydrogel, two kinds of logic gates (AND and OR) were demonstrated [92]. Figure 8.5a shows the AND logic gate. Similar to the aptamer-based hydrogels described above, two acrydite-

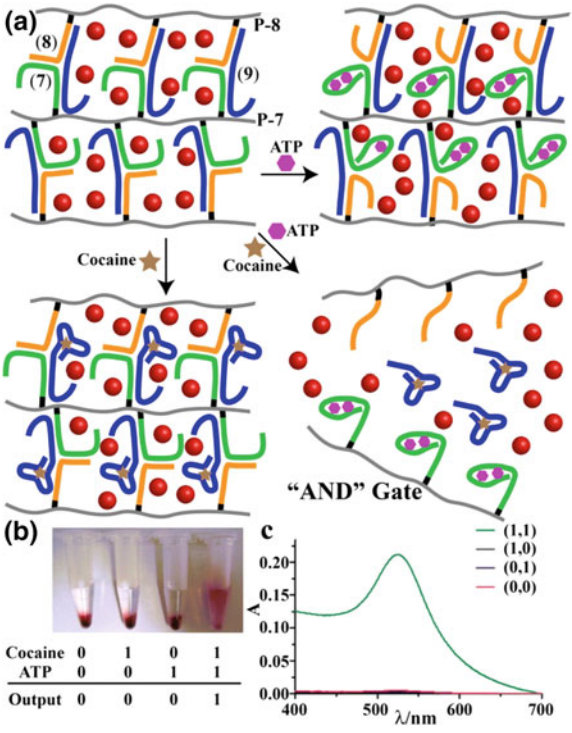

Fig. 8.5 **a** AND gate system based on cocaine- and ATP-binding aptamer-based hydrogel. The hydrogel dissociated only when both cocaine and ATP were present. **b** Photograph of hydrogel with entrapped BSA-GNPs without and with target adenosine and/or ATP. **c** UV-VIS spectra of the BSA-GNPs of the AND gate system. Reprinted with the permission from Ref. [92]. Copyright 2011 Royal Society of Chemistry

modified DNA strands were copolymerized with linear polyacrylamide chains to form polymer strands P-7 and P-8, respectively. Strand (**7**) was designed to contain an ATP aptamer sequence, which could partially hybridize with strand (**8**). A cross-linker (**9**), containing a cocaine aptamer sequence, was designed to partially hybridize with strands (**7**) and (**8**). Upon mixing P-7, P-8 and (**9**), the polymers transformed into a hydrogel as the hybridization proceeded. These three strands formed a Y-shaped structure inside the hydrogel, with each strand containing two complementary domains for the other two strands. In order to visualize the gel–sol transition, the authors entrapped BSA-modified gold nanoparticles (BSA-GNPs) into the hydrogel as indicator. As shown in Fig. 8.5b, c, in the presence of ATP as input, the ATP aptamer domain in P-7 dissociated from P-8, forming the ATP/aptamer complex. However, since strand (**9**) was still hybridized with both P-7 and P-8, the hydrogel remained intact. Similarly, in the presence of cocaine as input, the cocaine aptamer sequence in (**9**) separated from P-8, but hybridization of P-7 and P-8 maintained the hydrogel structure. However, if both of cocaine and ATP were introduced as inputs, the hydrogel underwent a gel–sol transition, and the entrapped BSA-GNPs were released into the buffer solution. As a result, the buffer solution turned from colorless to red, a color change that could be easily detected with the naked eye. Using a similar approach, an OR logic gate was constructed by including both cocaine and ATP aptamer sequences in a cross-linker, which could hybridize with two polymer strands.

Use of pure DNA molecules as building blocks for hydrogel construction has attracted substantial attention directed to the formation of smart devices and precisely addressable structures at the nanometer scale for sensing or drug delivery and controlled release [109–114]. An aptamer-functionalized pure DNA hydrogel was designed as a target-responsive material for thrombin detection [93]. As shown in Fig. 8.6a, this pure DNA hydrogel was constructed with two different building blocks: Y-shaped DNA (Y-DNA) and linker DNA (L-DNA), which included two DNA strands (**10**) and (**11**) with two different thrombin-binding aptamer sequences in (**10**). The single-stranded tethers of Y-DNA and L-DNA were designed to hybridize with each other, thus leading to formation of the DNA hydrogel by cross-linking hybridization between Y-DNA and L-DNA. In the presence of target thrombin, (**10**) in L-DNA underwent a structural change and dissociated from L-DNA to bind thrombin. A visual detection method for thrombin was designed by entrapping gold nanoparticles into the DNA hydrogel. Upon addition of target thrombin, the DNA hydrogel system dissolved, and gold nanoparticles were released into the buffer solution for visual detection with an LOD of 1 μM, Fig. 8.6b. Furthermore, by using polyethyleneimine-modified quantum dots (PEI-QDs) as fluorescence agent, the hydrogel system was also used for fluorescence detection of thrombin. Along with a gel–sol transition in the presence of target, the released gold nanoparticles from the hydrogel approached the positively charged PEI-QDs, leading to fluorescence resonance energy transfer (FRET) with quenching of the QD fluorescence dependent on the thrombin concentration. The method enabled the fluorescence detection of thrombin with an LOD of 67 nM, Fig. 8.6c.

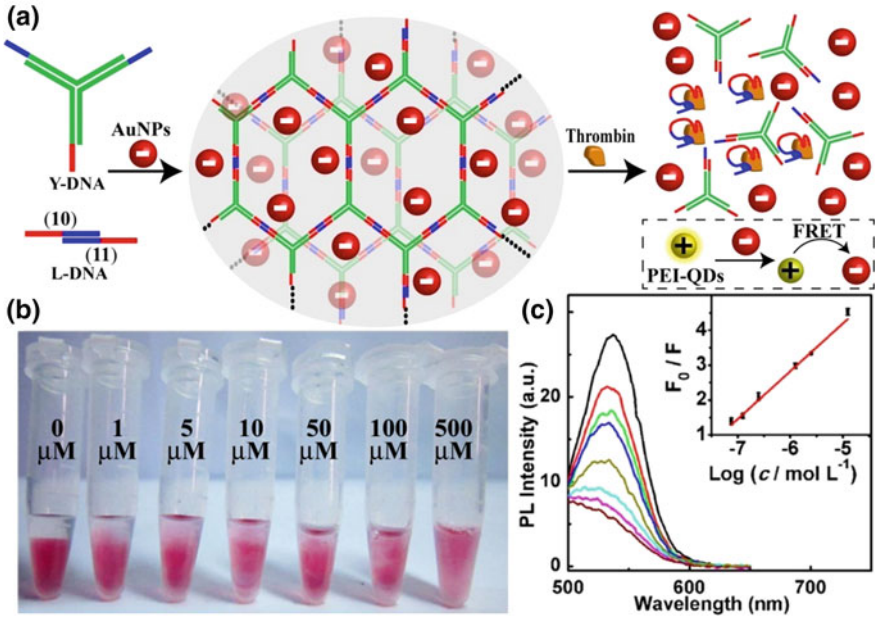

Fig. 8.6 **a** Schematic representation of the aptamer-functionalized pure DNA hydrogel for colorimetric and fluorescent detection of thrombin. **b** Photograph of hydrogel response to different concentrations of thrombin. **c** Fluorescence spectra corresponding to analysis of different concentrations of thrombin (0–250 μM). *Inset* resulting calibration curve. Reprinted with the permission from Ref. [93]. Copyright 2013 American Chemical Society

8.2.2 Stimuli-Responsive Hydrogels with Volume Changes

As described above, aptamer-based hydrogel sensors involving a gel–sol transition in the presence of target have straightforward designs. Sensors using DNA hydrogels can also be constructed based on a trigger-stimulated network structural change. Hydrogel scan undergo volume changes (expansion or shrinkage) in aqueous solution when triggered by a small change in the environmental parameters such as pH, temperature, and ionic strength [115]. Sensors producing volume changes have also been reported for aptamer-based hydrogels.

Aptamer-based hydrogel diffraction gratings are versatile biosensors which recognize target biomolecules and transduce the recognition event into optical signals [116], Fig. 8.7a. In order to incorporate thrombin-binding aptamer (**12**) into a hydrogel by photopolymerization, the aptamer and its partially complementary DNA (**13**) were first reacted with N-succinimidyl-acrylate (NSA) to obtain double bonds on the DNA. The aptamer-based hydrogel diffraction gratings were then fabricated by microcontact printing with photopolymerization using poly(dimethylsiloxane) (PDMS) stamps and the precursor solution, containing monomer, cross-linker, photoinitiator, and two monomer-modified DNA strands, as "ink." Since the

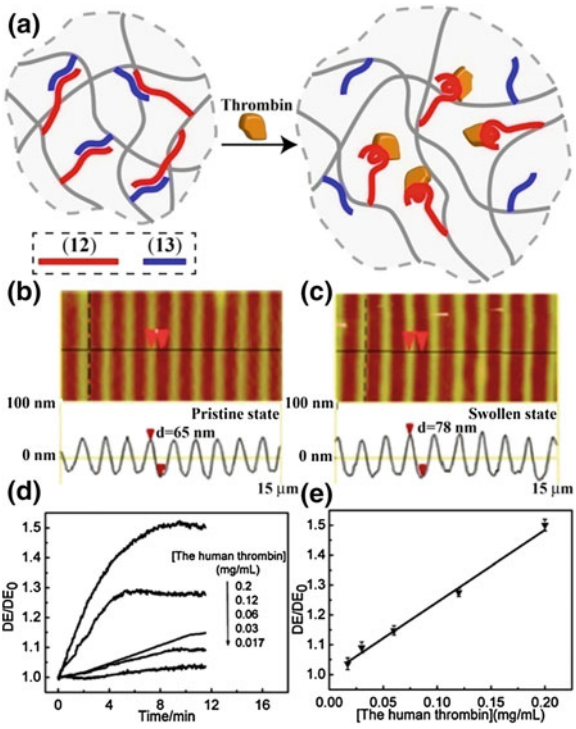

Fig. 8.7 **a** Schematic representation of an aptamer-based hydrogel diffraction grating. In the presence of thrombin, the duplex (**12**)/(**13**) structure was separated and aptamer sequence (**12**) was bound to thrombin, thus leading swelling of the hydrogel grating. Cross-sectional analysis by AFM was used to monitor the volume increase. **b** Pristine grating. **c** Grating in a thrombin solution (0.06 mg mL^{-1}) for 10 min. **d** Time-dependent DE/DE_0 changes upon analyzing different concentrations of thrombin (range from 0.07 to 0.2 mg mL^{-1}). **e** Resulting calibration curve according to (**d**). Reprinted with the permission from Ref. [116]. Copyright 2013 Royal Society of Chemistry

two DNA strands formed a duplex DNA structure inside the hydrogel, the cross-linking density of the hydrogel was high (Fig. 8.7a). In the presence of target thrombin, the duplex DNA structure dissociated and the cross-linking density inside the hydrogel was decreased. Therefore, the hydrogel could swell and increase in volume. As shown in Fig. 8.7b, c, in the presence of thrombin, the depth of gratings increased due to the separation between the aptamer (**12**) and its partially complementary DNA (**13**). Optical sensing was carried out by immersing the gratings in different concentrations of thrombin. As shown in Fig. 8.7d, e, as the concentration of thrombin increased, the first-order diffraction efficiency (DE) relative to its initial value (DE_0) increased. The lowest measured concentration of thrombin by this optical sensing detection corresponded to 0.017 mg/mL. Furthermore, the aptamer-based hydrogel gratings developed in this study showed excellent sensitivity to human thrombin with a reasonably rapid responsive rate.

Volume change in the presence of target was further implemented to develop a quartz crystal microbalance (QCM) sensor [117] based on single-stranded DNA cross-linked polymeric hydrogel for rapid, sensitive, and specific detection of avian influenza virus (AIV) H5N1 surface protein. As shown in Fig. 8.8, two acrydite-modified DNA strands, (**14**) and (**15**), were each copolymerized with linear polyacrylamide chains. (**14**) was the aptamer and (**15**) was hybridized with one end of the aptamer. When the chains were mixed, (**14**) and (**15**) hybridized to form a cross-linked hydrogel, which was immobilized on the gold electrode of the QCM by a self-assembled monolayer (SAM) method. Based on the carboxylic acid-modified gold electrode and the amino group in the polymer strands, 1-ethyl-3-(3-dimethylaminopro-pyl)carbodiimide (EDC) and N-hydroxysuccinimideester (NHS) were used to cross-link the hydrogel on the gold electrode surface. In the absence of target H5N1 virus, the hydrogel remained in its shrunken state. However, in the presence of H5N1 virus, bonding between (**14**) and the target dissociated the cross-links, allowing the hydrogel to swell, and the volume change was monitored by frequency shifts of the QCM. With optimized conditions, the QCM sensor enabled analysis of target H5N1 virus with a detection limit corresponding to 0.0128 HAU (HA unit). Compared to the anti-H5 antibody-coated QCM immunosensor, the aptamer-based hydrogel QCM sensor lowered the detection limit and reduced the detection time.

Aptamer sensors have been incorporated into colloidal photonic crystal hydrogel (CPCH) films that have been used to construct sensors for visual detection of heavy metal ions, such as Hg^{2+} and Pb^{2+} [118]. Colloidal crystals, which assembled from monodisperse nanoparticles, have been used to construct sensors [119–123]. Due to periodic variation in the refractive index, colloidal crystals give rise to interesting optical properties, such as photonic band gaps (PBGs). Therefore, the aptamer sensor based on CPCH films could be underwent a shrinkage changes upon adding targets, leading to a change in the PBGs accompanied by a visually perceptible color change. As illustrated in Fig. 8.9a, the 3′ and 5′ ends of Hg^{2+} or Pb^{2+} binding aptamers were cross-linked to the CPCH networks to construct the aptamer sensor-

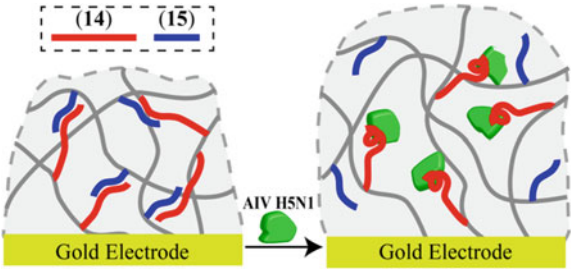

Fig. 8.8 Schematic representation of the aptamer-based hydrogel immobilized on the QCM gold electrode surface. In the presence of target AIV H5N1, the cross-linker (**14**)/(**15**) duplex structure was separated, leading to the swelled hydrogel. Reprinted with the permission from Ref. [117]. Copyright 2013 Elsevier

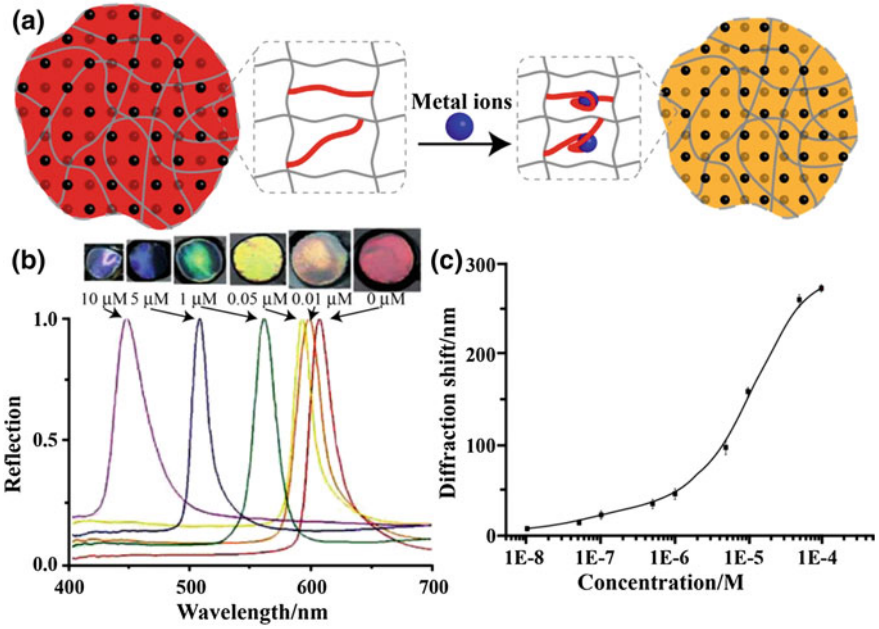

Fig. 8.9 **a** Schematic representation of aptamer sensor-based CPCHs for the detection of heavy metal ions. **b** Effect of the Hg^{2+} concentration on the diffraction wavelength of CPCHs. *Top* Diffraction color changes from *red* to *blue* with an increasing Hg^{2+} concentration. **C** Diffraction blue shifts as a function of the Hg^{2+} concentrations with range from 10 nM to 100 μM. Reprinted with the permission from Ref. [118]. Copyright 2012 Royal Society of Chemistry

based CPCHs. In the absence of target metal ions, the aptamer adopted a random coil structure, but when target was present, the aptamer bound to the ions and formed a metal ion/aptamer complex structure. This led to CPCH shrinkage and a decrease in the lattice spacing, which was observed as a blue shift of the structural colors or as a corresponding blue shift in the Bragg diffraction peak position. The shift value could be used for quantitative analysis of the target metal ions. As shown in Fig. 8.9b, with the increase concentration of Hg^{2+}, the degree of shrinkage of aptamer sensor-based CPCHs intensified, consistent with more aptamers inside CPCHs were form Hg^{2+}/aptamer complex structure. According to the shrinkage of the CPCHs, the color and the diffraction peak underwent a blue shift. Based on the diffraction blue shift, Hg^{2+} could be visually detected with a detection limit corresponded to 10 nM, Fig. 8.9c. Also, by using the same approach, the Pb^{2+} ions binding aptamer sensor-based CPCHs could be used to visual detection of Pb^{2+} with a detection limit of 1 nM. These CPCH sensors showed good durability over tens of cycles and could be rehydrated from dried gels for storage and aptamer protection.

A new type of aptamer-based hydrogel was developed for specific, ultrasensitive, and visual detection of proteins [124]. The remarkable feature of this kind of

hydrogel was that volume changes were visible to the naked eye down to femtomolar concentrations of proteins. As outlined in Fig. 8.10a, two different polymerizable methacrylamide-modified thrombin-binding aptamers were first mixed with thrombin to form aptamer–thrombin–aptamer imprinted complexes. Then, the complexes were mixed with a solution containing ammonium persulfate (APS), acrylamide, bis-acrylamide, and *N*,*N*,*N*′,*N*′-tetramethylethylenediamine (TEMED) to initiate free radical polymerization. Thus, the two aptamers were incorporated into the hydrogel network by copolymerization, and the thrombin acted as the cross-linker imprinted in the hydrogel, as shown in Fig. 8.10b, left. Removal of the imprinted thrombin dissolved partial cross-links, resulting in a swelling response of the hydrogel (increased length of hydrogel), Fig. 8.10b, right. The hydrogel length changes were reversible by reintroducing target thrombin into the hydrogel, with shortening dependent on the amount of thrombin introduced, Fig. 8.10c. The shrinkage of hydrogel can be observed by the naked eye with a detection limit in the

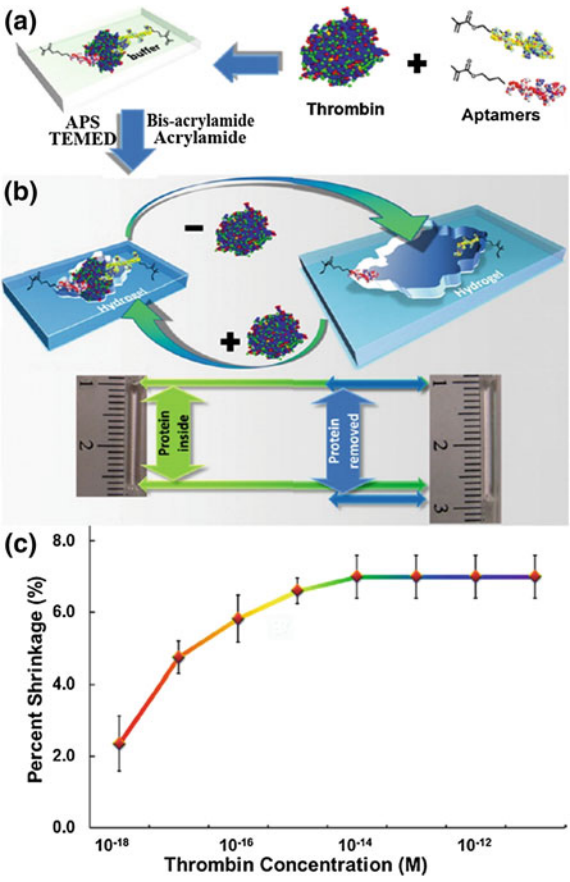

Fig. 8.10 **a** Schematic representation of the thrombin-bioimprinted aptamer hydrogel. **b** Visualization of the volume change responses by the hydrogel. **c** Binding isotherm of thrombin-imprinted hydrogels: the volume response of the hydrogel could be observed down to the femtomolar range and became saturated at picomolar concentrations. Reprinted with the permission from Ref. [124]. Copyright 2013 American Chemical Society

femtomolar range. This type of hydrogel sensor has the advantages of low cost, easy to use, and portable detection of molecules of interest for biomedicine, environmental science, and biosecurity, such as detection of apple stem pitting virus (ASPV) [125].

8.2.3 Aptamer Sensors Embedded Inside DNA Hydrogels

Although aptamer-based hydrogels undergoing a gel–sol transition or volume change can be used to fabricate the sophisticated sensors, one may find that a relatively large amount of target is needed to trigger hydrogel response. To solve this drawback, one method embeds sensors inside the DNA hydrogel and uses an optical signal as output. In addition, besides using gold nanoparticles as the indicating agent, fluorescent molecules, including fluorophore/quencher pairs and DNA staining dyes, have been used to transduce optical signals.

There are two methods to embed aptamer sensors into DNA hydrogels: immobilization of sensors on the polymer chains and entrapment of sensors within the hydrogel network. One of the first systems reported by Liu and co-workers involved immobilizing an acrydite-modified mercury (Hg^{2+})-binding aptamer sequence in a polyacrylamide DNA hydrogel [57]. According to this principle, the hydrogel was cross-linked by bis-acrylamide and the acrydite-modified aptamer was immobilized on the polymer chains. The Hg^{2+} aptamer is a thymine-rich sequence, which remains in a random coil structure in the absence of Hg^{2+} ions. However, when Hg^{2+} is present, it mediates the T bases to form T-Hg^{2+}-T base pairs [126, 127], thus producing a change to a hairpin structure. The output signal was generated by adding a DNA-binding dye called SYBR Green I (SG), which produced a yellow fluorescence when bound to unfolded DNA, but changed to green fluorescence when bound to duplex (hairpin structure) DNA [128], as shown in Fig. 8.11a. Therefore, the aptamer immobilized within the hydrogel networks could actively adsorb Hg^{2+} and optical sensing of Hg^{2+}. As shown in Fig. 8.11b, as the concentration of Hg^{2+} increased, the hydrogel fluorescence gradually changed from yellow to green as more hairpin structures were formed. The detection limit for Hg^{2+} was 10 nM. Furthermore, the sensor was resistant to nuclease and could be rehydrated from dried hydrogels for storage and nucleic acid protection. However, in this study, in the absence of Hg^{2+}, the random coil aptamer stained by SG gave a high yellow fluorescence background. In the further study, the same group introduced 20 % positively charged allylamine monomer into the hydrogel to reduce the fluorescence background [58]. Due to the repulsion between positively charged SG and the hydrogel matrix, as well as the strong binding between SG and aptamer/Hg^{2+} complex, the signal-to-background ratio was improved by sixfold and the detection limit for Hg^{2+} was lowered to 1.1 nM.

A similar approach to analyze lead ions (Pb^{2+}) was demonstrated by immobilizing a guanine-rich Pb^{2+} aptamer, which formed a quadruplex with Pb^{2+} inside a hydrogel [129]. Using thiazole orange (TO) as staining dye, in the absence of Pb^{2+},

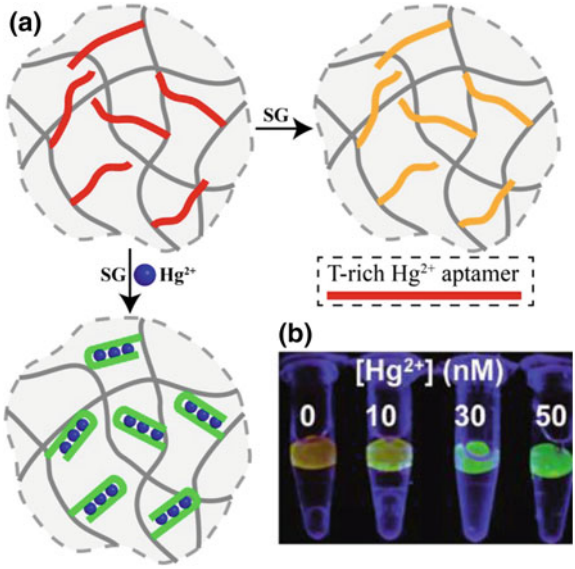

Fig. 8.11 **a** Schematic representation of the SYBR Green I-stained Hg^{2+} aptamer-based hydrogel. In the absence of Hg^{2+}, the hydrogel displayed yellow fluorescence. In the presence of Hg^{2+}, the fluorescence of the hydrogel turned to green. **b** Photograph of hydrogel response to different concentrations of Hg^{2+}. Reprinted with the permission from Ref. [57]. Copyright 2010 American Chemical Society

the TO-stained aptamer produced yellow fluorescence. When Pb^{2+} was present, it induced the aptamer sequence to form a quadruplex, thus leading to the green fluorescence for visual detection of Pb^{2+} with a detection limit of 20 nM. The authors also demonstrated simultaneous detection of both Hg^{2+} and Pb^{2+} in the same sample by using differently shaped DNA hydrogels to distinguish the two different aptamer sensors. In addition to bulk DNA hydrogels, Liu and co-workers incorporated aptamer sensors into hydrogel microparticles [130]. The aptamer-based hydrogel microparticles with sizes between 10 and 50 μm were synthesized using an emulsion polymerization technique, and the acrydite-modified aptamer was incorporated by copolymerization. The kinetics of signal generation from hydrogel microparticles was much fast than that from bulk DNA hydrogel sensors due to the short diffusion distance. This hydrogel microparticle sensor enabled analysis of Hg^{2+} with a detection limit of 10 nM within 2 min and analysis of adenosine with LOD of 50 μM.

In addition to being immobilized on the polymer networks, aptamer sensors can be entrapped within the hydrogel [131, 132]. Brennan and co-authors developed a method that entrapped ATP aptamer sensor inside a sol-gel-derived silica hydrogel [131]. As shown in Fig. 8.12, two kinds of ATP aptamer sensors were entrapped: a sensor constructed from three strands of DNA (ATP aptamer, complementary fluorophore-labeled DNA strand, and another complementary DNA modified with a

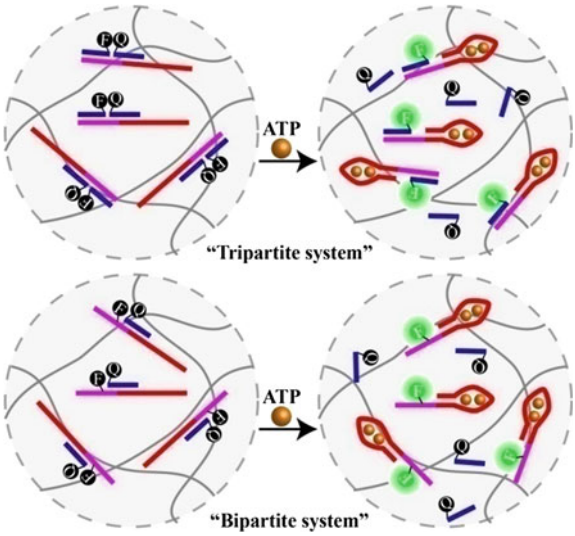

Fig. 8.12 Schematic representation of entrapping DNA sensor into hydrogel and the gel fluorescence was intensified upon adding target ATP. The DNA sensors were constructed by three DNA strands system (tripartite system) or two DNA strands system (bipartite system). Reprinted with the permission from Ref. [131]. Copyright 2005 American Chemical Society

quencher), and a sensor having two DNA strands, where the fluorophore was covalently tethered to the aptamer rather than bound to a complementary DNA. In both systems, fluorescence was initially quenched by the close proximity of the quencher molecule, but binding of ATP to the aptamer, induced a conformational change in the DNA structure. The quencher-modified strand was separated from the fluorophore group, leading to the restoration of the fluorescent signal of the fluorophore. The authors demonstrated that both of these systems could be used for selective and sensitive detection of ATP. Although this type of aptamer-based hydrogel could be easily fabricated by simply entrapping the aptamer sensor into the silica hydrogel, the sensor may leach out of the gel matrix due to noncovalent interactions between DNA and the gel matrix.

8.3 Aptamer-Based Hydrogels for Target Molecule Capture and Release

Different external stimuli, such as pH value [133], temperature [134], electric fields [135], and saccharide levels [136], have been used to stimulate hydrogel structural changes. However, in the DNA hydrogel separation platforms, such external stimuli may adversely affect the structural and functional integrity of the target

biomacromolecules. To solve this problem, the strand displacement technique has been used as a new method to manipulate hydrogel structural changes at constant temperature and under unchanged buffer condition [137–140].

A DNA-induced sol-gel transition hydrogel was combined with a protein-binding aptamer to capture and release target proteins [111]. As illustrated in Fig. 8.13, two acrydite-modified DNA strands, (**16**) and (**17**), were grafted onto separate polymer chains. A third DNA strand, (**18**) containing thrombin-binding aptamer, could hybridize with both (**16**) and (**17**) to cross-link the polymer chains and form the hydrogel. Before forming the DNA hydrogel, strand (**18**) could capture thrombin to form the thrombin/(**18**) complex, which was largely retained in the hydrogel, even when immersed in buffer solution for a week. Strand (**18**) also contained a toehold, which acted as a recognition tag for strand displacement. To release thrombin, a fourth DNA strand (**19**) which was fully complementary to strand (**18**) was added to the hydrogel. After forming the duplex structure (**18**)/(**19**), the DNA hydrogel was dissolved and the thrombin was released from strand (**18**). A related method for separation of ATP from a complex mixture was developed by the same group [141]. In the study, the two acrydite-modified DNAs were copolymerized with acrylamide monomer into polymer chains, respectively. A cross-linker DNA containing the ATP-binding aptamer sequence could hybridize with both polymer chains to form the DNA hydrogel. The aptamer sequence in the cross-linker DNA acted as a hook that could fish target ATP molecule from a pool of different molecules (ATP and GTP). The results demonstrated that this kind of DNA-induced hydrogel has the ability to recognize and extract the specific target from a dual-molecule pool with a high degree of specificity. Upon adding the fully complementary sequence of the cross-linker DNA, the cross-linker DNA was

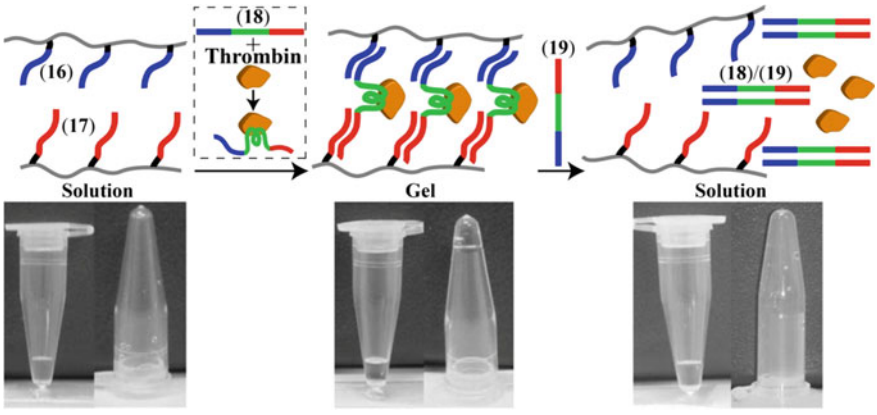

Fig. 8.13 Schematic representation of the aptamer-based hydrogel for capture and release of thrombin. *Bottom* Photograph of different states of the system. *Left* Liquid state before adding thrombin/(**18**) complex. *Middle* Hydrogel state after adding thrombin/(**18**) complex. *Right* Return to liquid state upon adding strand (**19**) to dissociate the hydrogel. Reprinted with the permission from Ref. [111]. Copyright 2007 Wiley-VCH

hybridized with its fully complementary sequence and dissociated from the polymer chains, leading to dissolution of the DNA hydrogel and release of the target ATP. The results showed that about 86% of the original quantity of target ATP could be retained and released from the hydrogel. In order to demonstrate the generality of the method, the authors also successfully designed a thrombin-binding aptamer-based hydrogel for the capture and release of target thrombin protein from a dual-protein pool of thrombin and bovine serum albumin (BSA).

Theoretically, the above-mentioned aptamer-based hydrogels can be used to capture a large target. However, due to the pore size restriction of the hydrogel, large targets, such as cells (usually larger than 10 μm), are not easily entrapped inside hydrogels. The Wang group developed a novel approach that tethered DNA aptamers on a hydrogel surface to capture and release cancer cells using a strand displacement technique [142, 143]. As illustrated in Fig. 8.14, three DNA strands were used to construct the DNA hydrogel. After silanization of the glass, the primary strand, (**20**), was initially conjugated to a polyacrylamide hydrogel formed as a coating on a silanized glass surface. Strand (**20**) was able to hybridize with strand (**21**) containing the aptamer sequence with high binding affinity and specificity for target CCRF-CEM cells [74]. The hybridization between (**20**) and (**21**) led to the immobilization of aptamer on the hydrogel surface. When incubated in a suspension of CCRF-CEM cells, the cells were captured on the hydrogel surface *via* polyvalent aptamer–receptor interactions. Upon adding the fully complementary sequence (**22**) of strand (**21**), the system underwent a strand displacement procedure and the hydrogel was triggered to dissociate strand (**21**) from strand (**20**) to form the (**21**)/(**22**) duplex structure. The formation of duplex (**21**)/(**22**) disturbed the polyvalent interaction between aptamer sequence and cells, thus leading to cell release from the hydrogel surface and regeneration of the hydrogel for a new round of cell capture and release. After incubation, 2,519 ± 284 CCRF-CEM cells/mm^2 were observed on the hydrogel surface, while only 6 ± 4 cells/mm^2 of control cells were observed. The authors also used a live/dead cell assay to verify the viability of the released cells. The

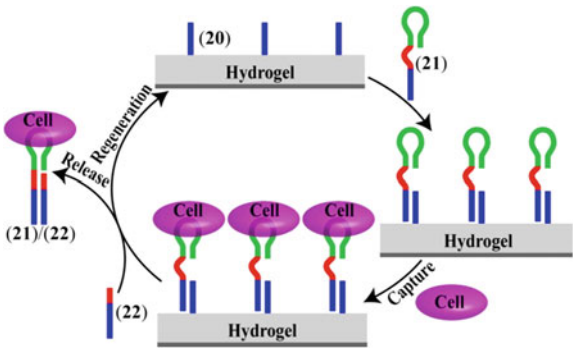

Fig. 8.14 Schematic representation of an aptamer-based hydrogel for cell capture and release by a strand displacement technique. Reprinted with the permission from Ref. [142]. Copyright 2012 American Chemical Society

nondestructive cell capture and release made the hydrogel fundamentally unique and suitable for numerous biological and biomedical applications.

Besides using strand displacement to release target cells from DNA hydrogel, the Wang group implemented restriction endonuclease as a new manner to manipulate the release of cells [144]. The results showed that the release efficiency of target cells reached about 99 %, and about 98 % of the released cell maintained viability. Furthermore, an aptamer could be applied to functionalize hydrogel for mimicking the adhesion sites of the extracellular matrix and maintaining cells viability after adhesion [145]. Therefore, aptamer-functionalized hydrogels are promising biomaterials for the development of artificial extracellular matrixes.

8.4 Aptamer-Based Hydrogels for Controlling Target Molecular Release

Hydrogels are attractive polymeric materials for design of sustained-release systems [146–149]. For example, for drug delivery, sustained release not only improves the efficacy of the drug, but also minimizes side effects [148]. Although the above section mentioned that aptamer-based hydrogels could release entrapped target, that application involved a gel–sol transition and the rate of target release was rapid and usually complete within a few minutes. Thus, there is a clear need to develop novel methods to improve and control the target release rate of DNA hydrogels.

For the aptamer-based hydrogel, sustained release of the target depends on several factors, including the pore size of the polymer network, the diffusion rate of the entrapped target molecule, and the affinity between the aptamer and target molecule. The Wang group developed a method to demonstrate that hydrogel functionalization with a DNA aptamer was applicable to a sustained-release system [97]. As shown in Fig. 8.15a, the acrydite-modified aptamer sequence was first mixed with its target, platelet-derived growth factor-BB, PDGF-BB, allowing for sufficient molecular recognition and the formation of the aptamer/PDGF-BB complex, which was then mixed with a solution containing APS, acrylamide, bis-acrylamide, and TEMED, to initiate free radical polymerization. Therefore, the aptamer/PDGF-BB complex was incorporated into the DNA hydrogel networks. The PDGF-BB entrapped aptamer-based hydrogel was subjected to sustained-release tests by immersion in a release medium. In order to evaluate the sustained-release system, the authors prepared three kinds of DNA hydrogels: the native hydrogel without aptamer units, a hydrogel with high-affinity immobilized aptamer, and a hydrogel with low-affinity immobilized aptamer. As shown in Fig. 8.15b, in the first 24 h, about 70 % of the PDGF-BB was released from the native gel. The low-affinity aptamer-based hydrogel released about 40 % of PDGF-BB in the first 24 h, while only 10 % of PDGF-BB was released from the high-affinity aptamer-based hydrogel in the same time period. The results demonstrated that the release rate could be controlled by using aptamers with different PDGF-BB binding

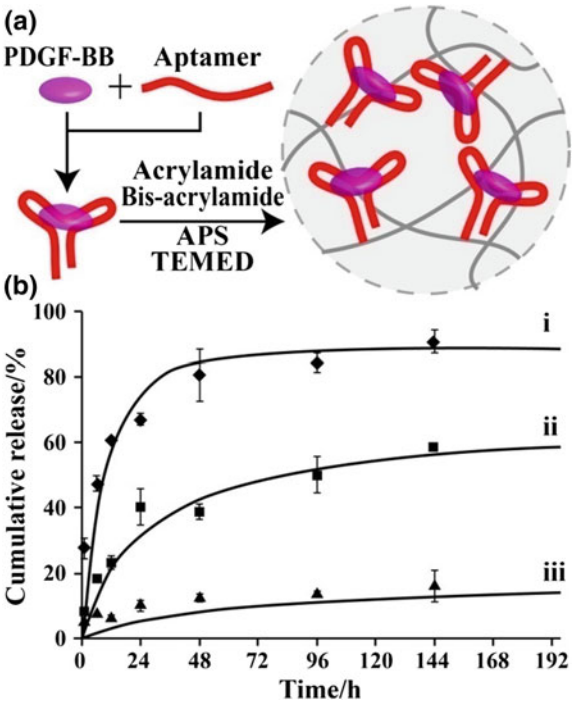

Fig. 8.15 **a** Schematic representation of aptamer-based hydrogel for sustained PDGF-BB release. The release rate of target could be tuned by using aptamers with different binding affinities. **b** Cumulative release of PDGF-BB from different kind of hydrogels: native hydrogel (*curve i*), low-affinity aptamer hydrogel (*curve ii*), and high-affinity aptamer hydrogel (*curve iii*). Reprinted with the permission from Ref. [97]. Copyright 2010 Royal Society of Chemistry

affinities. By tuning the binding affinities of aptamers, the same group demonstrated a novel strategy for synthesizing in situ injectable hydrogels to control the release of PDGF-BB [98]. A series of PDGF-BB aptamers with different binding affinities were designed, either by randomizing the nonessential nucleotide tail or mutating the essential nucleotides. After modifying on streptavidin-coated polystyrene particles, the aptamers were mixed with PDGF-BB to obtain the aptamer/PDGF-BB complex, and the functionalized particles were incorporated into poloxamer hydrogels for in situ injection. The release tests showed that PDGF-BB was rapidly released from the native poloxamer hydrogel (without aptamer-functionalized particles). In turn, release of PDGF-BB from the aptamer-functionalized poloxamer hydrogels was significantly prolonged, and the rate could be modulated by adjusting the affinity of the aptamer.

Delivery systems with a pulsatile release pattern are receiving increasing interest for the development of drugs for which conventional controlled sustained-release systems are not ideal [150–152]. Soontornworajit et al. developed a pulsatile protein release system by adding a single-stranded DNA to a hybrid particle–hydrogel composite [99]. As illustrated in Fig. 8.16a, biotinylated PDGF-BB aptamers, (**23**), were linked on the streptavidin-coated polystyrene particles, and the complex was entrapped inside the agarose hydrogel to form a hybrid particle–hydrogel composite. A controlled-release test was carried out to check whether the composite

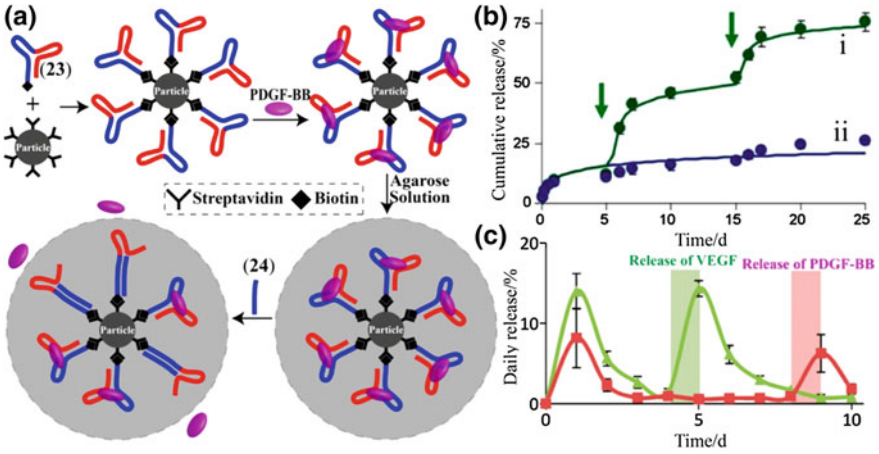

Fig. 8.16 **a** Schematic representation of the preparation of hybrid particle–hydrogel composite for pulsatile protein release using a strand displacement technique. **b** Time-dependent cumulative release of PDGF-BB upon adding the complementary DNA strand (**24**), *curve i*, and scrambled DNA strand, *curve ii*. The *arrows* indicate the time point of adding DNA strand. Reprinted with the permission from Ref. [99]. Copyright 2010 Royal Society of Chemistry. **c** Profiles of daily release of VEGF and PDGF-BB regulated via the corresponding complementary DNA. Pulsatile release of VEGF was triggered on day 4 and release of PDGF-BB was triggered on day 8. Reprinted with the permission from Ref. [100]. Copyright 2012 American Chemical Society

could prevent rapid release of target proteins. Compared to the native agarose gel (without functionalized particles), which released 70 % of the protein in the first 24 h, the aptamer retained the protein inside the hydrogel, resulting in only about 8 % release. As shown in Fig. 8.16b, by adding partially complementary DNA strand, (**24**), at two time points, pulsatile protein release occurred with about 35 and 23 % release, respectively. In turn, adding scrambled DNA would not release the proteins. The results demonstrated that the composite could release proteins in a pulsatile manner through the intermolecular hybridization mechanism. In the further study, the system was designed for the controllable pulsatile release of multiple proteins [100]. Two aptamers, one binding to PDGF-BB and the other binding to vascular endothelial growth factor (VEGF), were used to functionalize two sets of streptavidin-coated polystyrene particles, which were incorporated into the agarose solution to form the hydrogel. As shown in Fig. 8.16c, the hydrogel was treated with complementary DNA at two different time points, first with the complementary DNA of VEGF aptamer and then with the complementary DNA of PDGF-BB aptamer. The results showed that the two complementary DNAs triggered pulsatile release of only their individual target proteins without affecting the other protein.

8.5 Aptamer-Based Hydrogels for In Vivo Applications

Strategies for controlled drug release with polymeric materials have been intensively investigated for applications such as biomedicine and tissue engineering [153, 154]. As discussed above, for hydrogels many stimuli, such as changes in pH [1], temperature [2], and ionic strength [3], can be used to trigger physical or chemical changes. However, in physiological conditions, the stimuli are more subtle, especially for biochemical signals or subnanomolar-level biomarkers. By light irradiation or exposure to electrical or magnetic fields, the responsive hydrogel can be applied in sensors [21, 155] and drug delivery [156–158]. In a related study, a light-driven hydrogel was investigated for controlled release of doxorubicin (DOX) [89]. As illustrated in Fig. 8.17, a near-infrared (NIR) light-responsive drug delivery platform based on Au–Ag nanorods (Au–Ag NRs) coated with DNA cross-linked core–shell nanogels was fabricated. In one part, the methacryl group-modified NRs could initiate the growth of linear polymer chains P-A through photocopolymerization with acrydite-modified strand (**25**) and acrylamide monomer. In another part, acrydite-modified strand (**26**) and acrydite-modified aptamer sequence (**27**) were incorporated to obtain polymer chains P-B. The cross-linker DNA strand (**28**), which hybridized with both strands (**25**) and (**26**), could cross-link P-A and P-B, resulting in the formation of core–shell nanogels. The aptamer sequence (**27**) was selected for the binding CCRF-CEM (T cell acute lymphoblastic leukemia cell line) cells. Flow cytometry results showed that the aptamers on the core–shell nanogels maintained their specific binding and high affinity for the target cancer cells. In order to establish the drug delivery system, a chemotherapeutic agent, DOX, was incorporated in the nanogels. Although free DOX was toxic to both target CCRF-CEM cells and control Ramos cells, the DOX-incorporated nanogels did not show obvious toxicity. The Au–Ag NRs used in the study could absorb light energy in the NIR range and convert it to heat. Therefore, upon irradiating with NIR light, the elevated temperature led the dissociation of the hybridization inside the nanogels and the entrapped drug DOX was released to

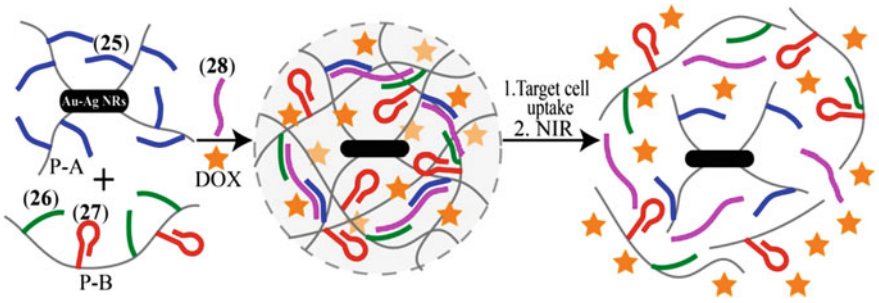

Fig. 8.17 Schematic representation of aptamer-based core–shell DNA nanogel and the nanogel for targeted therapy. Reprinted with the permission from Ref. [89]. Copyright 2011 American Chemical Society

generate a therapeutic effect. The cell viability results showed that after irradiation, the drug release process caused 67 ± 5 % CCRF-CEM cell death, while less than 10 % of control Ramos cells died. This study demonstrated that aptamer-functionalized core–shell nanogels could be used as drug carriers for targeted drug delivery with remote control by NIR light.

A DNA nanogel fabricated from various functional DNA strands could apply for targeted cancer therapy [90]. As illustrated in Fig. 8.18, the three functional domains (Y-shaped DNA) and the connector (X-shaped DNA) were mixed to form the building unit from stoichiometric amounts of each of these components. Different functional elements could be incorporated into the domains, including aptamer, acrydite-modified DNA, antisense oligonucleotide, and intercalated chemical anticancer drug DOX. Since two of the functional domains of each building unit were modified with acrydite groups, the acrydite-modified building units were further photo-cross-linked into a multifunctional and programmable aptamer-based DNA nanogel. The nanogel diameters could be tuned by simply changing the concentrations of the building units. The aptamer moieties of the nanogels could act as a guide to target specific cancer cells. By incorporating sgc8 aptamer, which targets CCRF-CEM cancer cells, into the functional domain, the DOX-loaded aptamer-based DNA nanogel showed a specific cytotoxic effect against CCRF-CEM cells. Moreover, by functionalization with therapeutic antisense DNA, which was explored to overcome the obstacle of multidrug resistance in chemotherapy, the multifunctional nanogel could be constructed to selectively kill drug-resistant cancer cells.

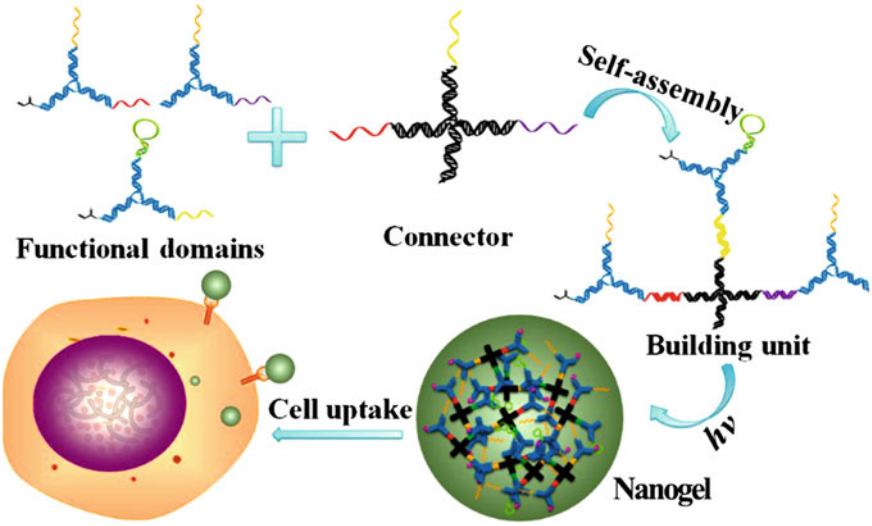

Fig. 8.18 Schematic representation of multifunctional self-assembled building units and photo-cross-linked aptamer-based DNA nanogel. Reprinted with the permission from Ref. [90]. Copyright 2013 American Chemical Society

Many cellular processes depend on the concentrations of small molecules and ions in the cellular environment, including cations, anions, pH values, amino acids, sugars, and ATP [159, 160]. Quantitation of ions or metabolites is important in understanding cell metabolism [161]. Probes encapsulated by biologically localized embedding (PEBBLE) forma class of nanosensors designed for in vivo biological sensing applications [162]. Ratiometric detection is commonly used for nano-PEBBLEs, in which a target-induced responsive dye and a reference dye are entrapped in the polymeric matrix [163]. A related study described a new type of aptamer-based nano-PEBBLE, in which a target-responsive DNA sequence was embedded in porous polyacrylamide nanoparticles for in vivo sensing of metabolite ATP [102]. In the study, the aptamer-switch probes were embedded in the polyacrylamide nanoparticle prepared by inverse microemulsion polymerization, Fig. 8.19. The switch probes included an ATP-binding aptamer sequence, together with a short DNA which could partially hybridize with the aptamer sequence, and a fluorophore/quencher pair at the two ends of the probes. In the absence of the target molecule, the close proximity of two ends by formation of a hairpin structure quenched the fluorescence. The authors demonstrated that the switch probes embedded in nanoparticles were resistant to treatment with DNase I and the nanoparticles could protect probes against nucleases. The functionalized nanoparticles were delivered to yeast cells by electroporation to visualize and measure the distribution of adenine–nucleotide concentrations in the cytoplasm of the cells by a ratiometric method. In the cytoplasm, upon binding to the adenine, the switch probes underwent a structural change, and the quencher moved far from the fluorophore, leading to restoration of fluorescence. The results showed that the total adenine in the cell cytoplasm of yeast cell was over 2.9 mM. In general, the system can be extended to any metabolites of interest in live cells by selecting the corresponding aptamers and embedding them into the nanoparticles.

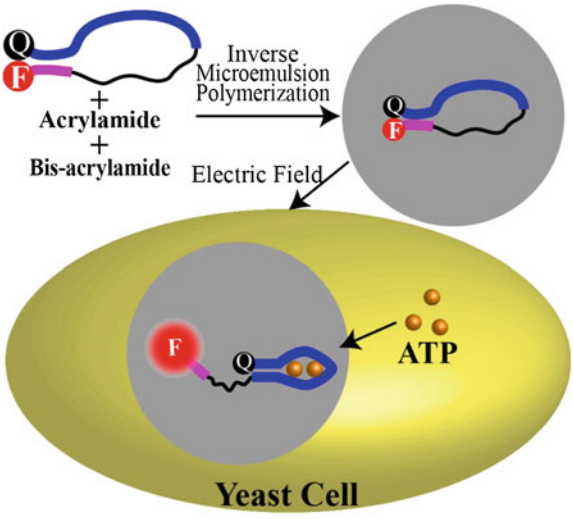

Fig. 8.19 Schematic representation of switch probes embedded in polyacrylamide nanoparticles and their intracellular ATP sensing. Reprinted with the permission from Ref. [102]. Copyright 2010 American Chemical Society

8.6 Conclusion

Aptamers have become useful and important tools for biotechnological and therapeutic applications. Since aptamers mimic and extend many properties of antibodies, such as high target-binding ability, low immunogenicity, wide temperature range stability, and easy modification, they have the potential to play an important role in biorecognition. In addition, due to the remarkable properties of DNA and easy preparation under physiological conditions, DNA hydrogels have attracted more and more attention in bioapplications. Different stimuli can be used to trigger the transitions of DNA hydrogels, including complementary DNA, pH, temperature, light, and metal ions. Incorporation of aptamers into traditional DNA hydrogels has greatly expanded the range of applications. Compared to traditional DNA hydrogels, aptamer-based hydrogels have several advantages: (1) Versatile aptamer-based hydrogels can be fabricated due to a wide range of targets recognized by aptamers. (2) The targets are easily entrapped in aptamer-based hydrogels and can be implemented as cargo delivery systems. (3) In addition to burst release of entrapped proteins or drugs, aptamer-based hydrogels can control sustained release of the entrapped species. (4) The ability to recognize and capture target proteins or drugs indicates potential therapeutic applications for aptamer-based hydrogels.

Although different kinds of aptamer-based hydrogels have been well developed, several challenges still need to be addressed. First, rapid and sensitive detection of heavy metal ions and hazardous materials in the environment is very important. However, to improve the sensitivity of functional hydrogels is a challenge. By using cascade reactions (for example, by incorporating enzymes or DNAzymes), signal amplification can be achieved. Second, besides using polyacrylamide, silica, poloxamer, and agarose as the hydrogel networks, the development of low-toxicity or nontoxic and biocompatible hydrogels for in vitro and in vivo applications remains a challenge. Third, development of methods for preparation of nanogels and delivery of nanogels into cells will greatly expand the scope of in vivo applications. Fourth, fabrication of bifunctional hydrogels is a new direction which can be used for precise control of protein or drug release. For example, incorporation of N-isopropylacrylamide (NIPAM) into the polyacrylamide gel will give the hydrogel additional thermo-sensitive property. In addition, light-sensitive properties can be regulated by incorporating azobenzenes, and pH-sensitive properties can be achieved by i-motif structure. In bifunctional hydrogels, hydrogel transitions can be triggered only in the presence of both stimuli, thus leading to more accurate operation of hydrogel systems.

References

1. Richter A, Paschew G, Klatt S, Lienig J, Arndt KF, Adler HJ (2008) Review on hydrogel-based Ph sensors and microsensors. Sensors 8:561–581
2. Jeong B, Kim SW, Bae YH (2002) Thermosensitive sol-gel reversible hydrogels. Adv Drug Deliv Rev 54:37–51
3. Ulijn RV, Bibi N, Jayawarna V, Thornton PD, Todd SJ, Mart RJ, Smith AM, Gough JE (2007) Bioresponsive hydrogels. Mater Today 10:40–48
4. Kulkarni RV, Biswanath SA (2007) Electrically responsive smart hydrogels in drug delivery: a review. J Appl Biomater Biomech 5:125–139
5. Murata K, Aoki M, Nishi T, Ikeda A, Shinkai S (1991) New cholesterol-based gelators with light-and metal-responsive functions. J Chem Soc Chem Commun 24:1715–1718
6. Maitra U, Mukhopadhyay S, Sarkar A, Rao P, Indi SS (2001) Hydrophobic pockets in a nonpolymeric aqueous gel: observation of such a gelation process by color change. Angew Chem Int Ed 40:2281–2283
7. Beck JB, Rowan SJ (2003) Multistimuli, multiresponsive metallo-supramolecular polymers. J Am Chem Soc 125:13922–13923
8. Zhao Y (2009) Photocontrollable block copolymer micelles: what can we control? J Mater Chem 19:4887–4895
9. Zhao Y (2012) Light-responsive block copolymer micelles. Macromolecules 45:3647–3657
10. Sambri L, Cucinotta F, Paoli GD, Stagni S, Cola LD (2010) Ultrasound-promoted hydrogelation of terpyridine derivatives. New J Chem 34:2093–2096
11. Satarkar NS, Hilt JZ (2008) Magnetic hydrogel nanocomposites for remote controlled pulsatile drug release. J Control Rel 130:246–251
12. Ozay O, Ekici S, Baran Y, Aktas N, Sahiner N (2009) Removal of toxic metal ions with magnetic hydrogels. Water Res 43:4403–4411
13. Peppas NA, Bures P, Leobandung W, Ichikawa H (2000) Hydrogels in pharmaceutical formulations. Eur J Pharm Biopharm 50:27–46
14. Byrne ME, Park K, Peppas NA (2002) Molecular imprinting within hydrogels. Adv Drug Delivery Rev 54:149–161
15. Peppas NA, Langer R (2004) Origins and development of biomedical engineering within chemical engineering. AIChE J 50:536–546
16. Hilt JZ, Byrne ME (2004) Configurational biomimesis in drug delivery: molecular imprinting of biologically significant molecules. Adv Drug Delivery Rev 56:1599–1620
17. Holtz JH, Asher SA (1997) Polymerized colloidal crystal hydrogel films as intelligent chemical sensing materials. Nature 389:829–832
18. Holtz JH, Holtz JSW, Munro CH, Asher SA (1998) Intelligent polymerized crystalline colloidal arrays: novel chemical sensor materials. Anal Chem 70:780–791
19. Zhang L, Seitz RW (2002) A pH sensor based on force generated by pH-dependent polymer swelling. Anal Bioanal Chem 373:555–559
20. Herber S, Olthuis W, Bergveld P (2003) A swelling hydrogel-based P_{CO2} sensor. Sens Actuators, B 91:378–382
21. Hilt JZ, Gupta AK, Bashir R, Peppas NA (2003) Ultrasensitive biomems sensors based on microcantilevers patterned with environmentally responsive hydrogels. Biomed Microdevices 5:177–184
22. Xu K, Lee F, Gao SJ, Chung JE, Yano H, Kurisawa M (2013) Injectable hyaluronic acid-tyramine hydrogels incorporating interferon-α2a for liver cancer therapy. J Control Release 166:203–210
23. Beebe DJ, Moore JS, Bauer JM, Yu Q, Liu RH, Devadoss C, Jo BH (2000) Functional hydrogel structures for autonomous flow control inside microfluidic channels. Nature 404:588–590
24. Kapur TA, Shoichet MSJ (2004) Immobilized concentration gradients of nerve growth factor guide neurite outgrowth. Biomed Mater Res A 68A:235–243

25. Kim D, Beebe D (2007) Hydrogel-based reconfigurable components for microfluidic devices. Lab Chip 7:193–198
26. Schmidt S, Zeiser M, Hellweg T, Duschl C, Fery A, Möhwald H (2010) Adhesion and mechanical properties of PNIPAM microgel films and their potential use as switchable cell culture substrates. Adv Funct Mater 20:3235–3243
27. McCain ML, Agarwal A, Nesmith HW, Nesmith AP, Parker KK (2014) Micromolded gelatin hydrogels for extended culture of engineered cardiac tissues. Biomaterials 35:5462–5471
28. Rowley JA, Madlambayan G, Mooney DJ (1999) Alginate hydrogels as synthetic extracellular matrix materials. Biomaterials 20:45–53
29. Lee KY, Mooney D (2001) Hydrogels for tissue engineering. J Chem Rev 101:1869–1879
30. Guo W, Qi XJ, Orbach R, Lu CH, Freage L, Mironi-Harpaz I, Willner I (2014) Reversible Ag^{+}-crosslinked DNA hydrogels. Chem Commun 50:4065–4068
31. Nagahara S (1996) A reversibly antigen-responsive hydrogel formation via hybridization of oligonucleotides derivatized in water-soluble vinyl polymers. Polym Gels Networks 4:111–127
32. Miyata T, Asami N, Uragami T (1999) A reversibly antigen-responsive hydrogel. Nature 399:766–799
33. Wang C, Stewart RJ, Kopecek J (1999) Hybrid hydrogels assembled from synthetic polymers and coiled-coil protein domains. Nature 397:417–420
34. Liu J (2011) Oligonucleotide-functionalized hydrogels as stimuli responsive materials and biosensors. Soft Matter 7:6757–6767
35. Peng L, Wu C, You M, Han D, Chen Y, Fu T, Ye M, Tan W (2013) Engineering and applications of DNA-grafting polymer materials. Chem Sci 4:1928–1938
36. Khimji I, Kelly EY, Helwa Y, Hoang M, Liu J (2013) Visual optical biosensors based on DNA-functionalized polyacrylamide hydrogels. Methods 64:292–298
37. Xiong X, Wu C, Zhou C, Zhu G, Chen Z, Tan W (2013) Responsive DNA-based hydrogels and their applications. Macromol Rapid Commun 34:1271–1283
38. Yang D, Hartman MR, Derrien TL, Hamada S, An D, Yancey KG, Cheng R, Ma M, Luo D (2014) DNA materials: bridging nanotechnology and biotechnology. Acc Chem Res 47:1902–1911
39. Watson JD, Crick FHC (1953) Molecular structure of nucleic acids—A structure for deoxyribose nucleic acid. Nature 171:737–738
40. Sinden RR, Pearson CE, Potaman VN, Ussery DW (1998) DNA: structure and function. Adv Gen Biol 5A:1–141
41. Hannon MJ (2007) Supramolecular DNA recognition. Chem Soc Rev 36:280–295
42. Stulz E, Clever G, Shionoya M, Mao C (2011) DNA in a modern world. Chem Soc Rev 40:5633–5635
43. Storhoff JJ, Mirkin CA (1999) Programmed materials synthesis with DNA. Chem Rev 99:1849–1862
44. Sen D, Gilbert W (1988) Formation of parallel four-stranded complexes by guanine-rich motifs in DNA and its implications for meiosis. Nature 334:364–366
45. Miyake Y, Togashi H, Tashiro M, Yamaguchi H, Oda S, Kudo M, Tanaka Y, Kondo Y, Sawa R, Fujimoto T, Machinami T, Ono A (2006) MercuryII-mediated formation of Thymine-HgII-Thymine base pairs in DNA duplexes. J Am Chem Soc 128:2172–2173
46. Li T, Dong S, Wang E (2009) Label-free colorimetric detection of aqueous mercury ion (Hg^{2+}) using Hg^{2+}-modulated G-quadruplex-based DNAzymes. Anal Chem 81:2144–2149
47. Zhu Z, Su Y, Li J, Li D, Zhang J, Song S, Zhao Y, Li G, Fan C (2009) Highly sensitive electrochemical sensor for mercury(II) ions by using a mercury-specific oligonucleotide probe and gold nanoparticle-based amplification. Anal Chem 81:7660–7666
48. Park KS, Jung C, Park HG (2010) "Illusionary" polymerase activity triggered by metal ions: use for molecular logic-gate operations. Angew Chem Int Ed 49:9757–9760
49. Collie GW, Parkinson GN (2011) The application of DNA and RNA G-quadruplexes to therapeutic medicines. Chem Soc Rev 40:5867–5892

50. Wang F, Lu CH, Willner I (2014) From cascaded catalytic nucleic acids to enzyme-DNA nanostructures: controlling reactivity, sensing, logic operations, and assembly of complex structures. Chem Rev 114:2881–2941
51. Xing Y, Cheng E, Yang Y, Chen P, Zhang T, Sun Y, Yang Z, Liu D (2011) Self-assembled DNA hydrogels with designable thermal and enzymatic responsiveness. Adv Mater 23:1117–1121
52. Guo W, Orbach R, Mironi-Harpaz I, Seliktar D, Willner I (2013) Fluorescent DNA hydrogels composed of nucleic acid-stabilized silver nanoclusters. Small 9:3748–3752
53. Um SH, Lee JB, Park N, Kwon SY, Umbach CC, Luo D (2006) Enzyme-catalysed assembly of DNA hydrogel. Nat Mater 5:797–801
54. Cheng E, Xing Y, Chen P, Yang Y, Sun Y, Zhou D, Xu L, Fan Q, Liu D (2009) A pH-triggered, fast-responding DNA hydrogel. Angew Chem Int Ed 48:7660–7663
55. Lu CH, Qi XJ, Orbach R, Yang HH, Mironi-Harpaz I, Seliktar D, Willner I (2013) Switchable catalytic acrylamide hydrogels crosslinked by Hemin/G-quadruplexes. Nano Lett 13:1298–1302
56. Baeissa A, Dave N, Smith BD, Liu J (2010) DNA-functionalized monolithic hydrogels and gold nanoparticles for colorimetric DNA detection. ACS Appl Mater Interfaces 2:3594–3600
57. Dave N, Chan MY, Huang PJJ, Smith BD, Liu J (2010) Regenerable DNA-functionalized hydrogels for ultrasensitive instrument-free mercury(II) detection and removal in water. J Am Chem Soc 132:12668–12673
58. Joseph KA, Dave N, Liu J (2011) Electrostatically directed visual fluorescence response of DNA-functionalized monolithic hydrogels for highly sensitive Hg^{2+} detection. ACS Appl Mater Interfaces 3:733–739
59. Liedl T, Dietz H, Yurke B, Simmel F (2007) Controlled trapping and release of quantum dots in a DNA-switchable hydrogel. Small 3:1688–1693
60. Guo W, Lu CH, Qi XJ, Orbach R, Fadeev M, Yang HH, Willner I (2014) Switchable bifunctional stimuli-triggered poly-N-isopropylacrylamide/DNA hydrogels. Angew Chem Int Ed 53:10134–10138
61. Peng L, You M, Yuan Q, Wu C, Han D, Chen Y, Zhong Z, Xue J, Tan W (2012) Macroscopic volume change of dynamic hydrogels induced by reversible DNA hybridization. J Am Chem Soc 134:12302–12307
62. Zhu Z, Wu C, Liu H, Zou Y, Zhang X, Kang H, Yang CJ, Tan W (2010) An aptamer crosslinked hydrogel as a colorimetric platform for visual detection. Angew Chem Int Ed 49:1052–1056
63. Zhou L, Chen C, Ren J, Qu X (2014) Towards intelligent bioreactor systems: triggering the release and mixing of compounds based on DNA-functionalized hybrid hydrogel. Chem Commun 50:10255–10257
64. Lin H, Zou Y, Huang Y, Chen J, Zhang WY, Zhuang Z, Jenkins G, Yang CJ (2011) DNAzyme crosslinked hydrogel: a new platform for visual detection of metal ions. Chem Commun 47:9312–9314
65. Lee JB, Peng S, Yang D, Roh YH, Funabashi H, Park N, Rice EJ, Chen L, Long R, Wu M, Luo D (2012) A mechanical metamaterial made from a DNA hydrogel. Nat Nanotechnol 7:816–820
66. Ellington AD, Szostak JW (1990) In vitro selection of RNA molecules that bind specific ligands. Nature 346:818–822
67. Tuerk C, Gold L (1990) Systematic evolution of ligands by exponential enrichment: RNA ligands to bacteriophage T4 DNA polymerase. Science 249:505–510
68. Sassanfar M, Szostak JW (1993) An RNA motif that binds ATP. Nature 364:550–553
69. Geiger A, Burgstaller P, von der Eltz H, Roeder A, Famulok M (1996) RNA aptamers that bind L-arginine with sub-micromolar dissociation constants and high enantioselectivity. Nucleic Acids Res 24:1029–1036
70. Jenison RD, Gill SC, Pardi A, Polisky B (1994) High-resolution molecular discrimination by RNA. Science 263:1425–1429

71. Haller AA, Sarnow P (1997) In vitro selection of a 7-methyl-guanosine binding RNA that inhibits translation of capped mRNA molecules. Proc Natl Acad Sci USA 94:8521–8526
72. Mannironi C, DiNardo A, Fruscoloni P, Tocchini-Valentini GP (1997) In vitro selection of dopamine RNA ligands. Biochemistry 36:9726–9734
73. Rajendran M, Ellington AD (2002) Selecting nucleic acids for biosensor applications. Comb Chem High Throughput Screening 5:263–270
74. Shangguan D, Li Y, Tang ZW, Cao ZHC, Chen HW, Mallikaratchy P, Sefah K, Yang CYJ, Tan WH (2006) Aptamers evolved from live cells as effective molecular probes for cancer study. Proc Natl Acad Sci USA 103:11838–11843
75. Tang ZW, Shangguan D, Wang KM, Shi H, Sefah K, Mallikratchy P, Chen HW, Li Y, Tan WH (2007) Selection of aptamers for molecular recognition and characterization of cancer cells. Anal Chem 79:4900–4907
76. Rajendran M, Ellington AD (2008) Selection of fluorescent aptamer beacons that light up in the presence of zinc. Anal Bioanal Chem 390:1067–1075
77. Cho EJ, Lee JW, Ellington AD (2009) Applications of aptamers as sensors. Annu Rev Anal Chem 2:241–264
78. Keefe AD, Pai S, Ellington A (2010) Aptamers as therapeutics. Nat Rev Drug Discov 9:537–550
79. Liss M, Petersen B, Wolf H, Prohaska E (2002) An aptamer-based quartz crystal protein biosensor. Anal Chem 74:4488–4495
80. Minunni M, Tombelli S, Gullotto A, Luzi E, Mascini M (2004) Development of biosensors with aptamers as bio-recognition element: the case of HIV-1 Tat protein. Biosens Bioelectron 20:1149–1156
81. Schlensog MD, Gronewold TMA, Tewes M, Famulok M, Quandt E (2004) A Love-wave biosensor using nucleic acids as ligands. Sens Actuators, B 101:308–315
82. Xu DK, Xu DW, Yu XB, Liu ZH, He W, Ma ZQ (2005) Label-free electrochemical detection for aptamer-based array electrodes. Anal Chem 77:5107–5113
83. Ferapontova EE, Olsen EM, Gothelf KV (2008) An RNA aptamer-based electrochemical biosensor for detection of theophylline in serum. J Am Chem Soc 130:4256–4258
84. Lu Y, Li X, Zhang L, Yu P, Su L, Mao L (2008) Aptamer-based electrochemical sensors with aptamer-complementary DNA oligonucleotides as probe. Anal Chem 80:1883–1890
85. Pan CF, Guo ML, Nie Z, Xiao XL, Yao SZ (2009) Aptamer-based electrochemical sensor for label-free recognition and detection of cancer Cells. Electroanalysis 21:1321–1326
86. Lee M, Walt DR (2000) A fiber-optic microarray biosensor using aptamers as receptors. Anal Biochem 282:142–146
87. McCauley TG, Hamaguchi N, Stanton M (2003) Aptamer-based biosensor arrays for detection and quantification of biological macromolecules. Anal Biochem 319:244–250
88. Kirby R, Cho EJ, Gehrke B, Bayer T, Park YS, Neikirk DP, McDevitt JT, Ellington AD (2004) Aptamer-based sensor arrays for the detection and quantitation of proteins. Anal Chem 76:4066–4075
89. Kang HZ, Trondoli AC, Zhu GZ, Chen Y, Chang YJ, Liu HP, Huang YF, Zhang XL, Tan WH (2011) Near-infrared light-responsive core-shell nanogels for targeted drug delivery. ACS Nano 5:5094–5099
90. Wu C, Han D, Chen T, Peng L, Zhu G, You M, Qiu L, Sefah K, Zhang X, Tan W (2013) Building a multifunctional aptamer-based DNA nanoassembly for targeted cancer therapy. J Am Chem Soc 135:18644–18650
91. Yang H, Liu H, Kang H, Tan W (2008) Engineering target-responsive hydrogels based on aptamer-target interactions. J Am Chem Soc 130:6320–6321
92. Yin BC, Ye BC, Wang H, Zhu Z, Tan W (2012) Colorimetric logic gates based on aptamer-crosslinked hydrogels. Chem Commun 48:1248–1250
93. Zhang L, Lei J, Liu L, Li C, Ju H (2013) Self-assembled DNA hydrogel as switchable material for aptamer-based fluorescent detection of protein. Anal Chem 85:11077–11082

94. Liu J, Liu H, Kang H, Donovan M, Zhu Z, Tan W (2012) Aptamer-incorporated hydrogels for visual detection, controlled drug release, and targeted cancer therapy. Anal Bioanal Chem 402:187–194
95. Yan L, Zhu Z, Zou Y, Huang Y, Liu D, Jia S, Xu D, Wu M, Zhou Y, Zhou S, Yang CJ (2013) Target-responsive "sweet" hydrogel with glucometer readout for portable and quantitative detection of non-glucose targets. J Am Chem Soc 135:3748–3751
96. Zhu Z, Guan Z, Jia S, Lei Z, Lin S, Zhang H, Ma Y, Tian Z, Yang CJ (2014) Au@Pt nanoparticle encapsulated target-responsive hydrogel with volumetric bar-chart chip readout for quantitative point-of-care testing. Angew Chem Int Ed 53:12503–12507
97. Soontornworajit B, Zhou J, Shaw MT, Fan TH, Wang Y (2010) Hydrogel functionalization with DNA aptamers for sustained PDGF-BB release. Chem Commun 46:1857–1859
98. Soontornworajit B, Zhou J, Zhang Z, Wang Y (2010) Aptamer-functionalized in situ injectable hydrogel for controlled protein release. Biomacromolecules 11:2724–2730
99. Soontornworajit B, Zhou J, Wang Y (2010) A hybrid particle-hydrogel composite for oligonucleotide-mediated pulsatile protein release. Soft Matter 6:4255–4261
100. Battig MR, Soontornworajit B, Wang Y (2012) Programmable release of multiple protein drugs from aptamer-functionalized hydrogels via nucleic acid hybridization. J Am Chem Soc 134:12410–12413
101. Battig MR, Huang Y, Chen N, Wang Y (2014) Aptamer-functionalized superporous hydrogels for sequestration and release of growth factors regulated via molecular recognition. Biomaterials 35:8040–8048
102. Nielsen LJ, Olsen LF, Ozalp VC (2010) Aptamers embedded in polyacrylamide nanoparticles: a tool for in vivo metabolite sensing. ACS Nano 4:4361–4370
103. Pavlov V, Xiao Y, Shlyahovsky B, Willner I (2004) Aptamer-functionalized Au nanoparticles for the amplified optical detection of thrombin. J Am Chem Soc 126:11768–11769
104. Huang CC, Huang YF, Cao Z, Tan W, Chang HT (2005) Aptamer-modified gold nanoparticles for colorimetric determination of platelet-derived growth factors and their receptors. Anal Chem 77:5735–5741
105. Liu JW, Lu Y (2006) Fast colorimetric sensing of adenosine and cocaine based on a general sensor design involving aptamers and nanoparticles. Angew Chem Int Ed 45:90–94
106. Liu J, Lu Y (2006) Smart nanomaterials responsive to multiple chemical stimuli with controllable cooperativity. Adv Mater 18:1667–1671
107. Liu JW, Lee JH, Lu Y (2007) Quantum dot encoding of aptamer-linked nanostructures for one-pot simultaneous detection of multiple analytes. Anal Chem 79:4120–4125
108. Yigit MV, Mazumdar D, Kim HK, Lee JH, Odintsov B, Lu Y (2007) Smart "turn-on" magnetic resonance contrast agents based on aptamer-functionalized superparamagnetic iron oxide nanoparticles. ChemBioChem 8:1675–1678
109. Lin DC, Yurke B, Langrana NA (2004) Mechanical properties of a reversible, DNA-crosslinked polyacrylamide hydrogel. J Biomech Eng 126:104–110
110. Murakami Y, Maeda M (2005) Hybrid hydrogels to which single-stranded (ss) DNA probe is incorporated can recognize specific ssDNA. Macromolecules 38:1535–1537
111. Wei B, Cheng I, Luo KQ, Mi Y (2008) Capture and release of protein by a reversible DNA-induced sol-gel transition system. Angew Chem Int Ed 47:331–333
112. Tang H, Duan X, Feng X, Liu L, Wang S, Li Y, Zhu D (2009) Fluorescent DNA-poly (phenylenevinylene) hybrid hydrogels for monitoring drug release. Chem Commun 6:641–643
113. Roh YH, Ruiz RCH, Peng S, Lee JB, Luo D (2011) Engineering DNA-based functional materials. Chem Soc Rev 40:5730–5744
114. Okay O (2011) DNA hydrogels: new functional soft materials. J Polym Sci B Polym Phys 49:551–556
115. Tokarev I, Minko S (2009) Stimuli-responsive hydrogel thin films. Soft Matter 5:511–524
116. Wang X, Wang X (2013) Aptamer-functionalized hydrogel diffraction gratings for the human thrombin detection. Chem Commun 49:5957–5959

117. Wang R, Li Y (2013) Hydrogel based QCM aptasensor for detection of avian influenza virus. Biosens Bioelectron 42:148–155
118. Ye BF, Zhao YJ, Cheng Y, Li TT, Xie ZY, Zhao XW, Gu ZZ (2012) Colorimetric photonic hydrogel aptasensor for the screening of heavy metal ions. Nanoscale 4:5998–6003
119. Lopez C (2003) Materials aspects of photonic crystals. Adv Mater 15:1679–1704
120. Kamenjicki M, Kesavamoorthy R, Asher SA (2004) Photonic crystal devices. Ionics 10:233–236
121. Li M, He F, Liao Q, Liu J, Xu L, Jiang L, Song Y, Wang S, Zhu D (2008) Ultrasensitive DNA detection using photonic crystals. Angew Chem Int Ed 47:7258–7262
122. Meade SO, Chen MY, Sailor MJ, Miskelly GM (2009) Multiplexed DNA detection using spectrally encoded porous SiO_2 photonic crystal particles. Anal Chem 81:2618–2625
123. Ge JP, He L, Hu YX, Yin YD (2011) Magnetically induced colloidal assembly into field-responsive photonic structures. Nanoscale 3:177–183
124. Bai W, Gariano NA, Spivak DA (2013) Macromolecular amplification of binding response in superaptamer hydrogels. J Am Chem Soc 135:6977–6984
125. Bai W, Spivak DA (2014) A double-imprinted diffraction-grating sensor based on a virus-responsive super-aptamer hydrogel derived from an impure extract. Angew Chem Int Ed 53:2095–2098
126. Ono A, Togashi H (2004) Highly selective oligonucleotide-based sensor for mercury(ii) in aqueous solutions. Angew Chem Int Ed 43:4300–4302
127. Tanaka Y, Oda S, Yamaguchi H, Kondo Y, Kojima C, Ono A (2007) ^{15}N–^{15}N J-coupling across Hg^{II}: direct observation of Hg^{II}-mediated T–T base pairs in a DNA duplex. J Am Chem Soc 129:244–245
128. Wang J, Liu B (2008) Highly sensitive and selective detection of Hg^{2+} in aqueous solution with mercury-specific DNA and SYBR Green I. Chem Commun 39:4759–4761
129. Jacobi ZE, Li L, Liu J (2012) Visual detection of lead(II) using a label-free DNA-based sensor and its immobilization within a monolithic hydrogel. Analyst 137:704–709
130. Helwa Y, Dave N, Froidevaux R, Samadi A, Liu J (2012) Aptamer-functionalized hydrogel microparticles for fast visual detection of mercury(II) and adenosine. ACS Appl Mater Interfaces 4:2228–2233
131. Rupcich N, Nutiu R, Li Y, Brennan JD (2005) Entrapment of fluorescent signaling DNA aptamers in sol-gel-derived silica. Anal Chem 77:4300–4307
132. Hui CY, Li Y, Brennan JD (2014) Fluorescence analysis of the properties of structure-switching DNA aptamers entrapped in sol-gel-derived silica materials. Chem Mater 26:1896–1904
133. Siegel RA, Firestone BA (1988) pH-Dependent equilibrium swelling properties of hydrophobic polyelectrolyte copolymer gels. Macromolecules 21:3254–3259
134. Yoshida R, Uchida K, Kaneko Y, Sakai K, Kikuchi A, Sakurai Y, Okano T (1995) Comb-type grafted hydrogels with rapid deswelling response to temperature changes. Nature 374:240–242
135. Osada Y, Okuzaki H, Hori H (1992) A polymer gel with electrically driven motility. Nature 355:242–244
136. Kokufata E, Zhang YQ, Tanaka T (1991) Saccharide-sensitive phase transition of a lectin-loaded gel. Nature 351:302–304
137. Mao C, Sun W, Shen Z, Seeman NC (1999) A nanomechanical device based on the B–Z transition of DNA. Nature 397:144–146
138. Yurke B, Turberfield AJ, Mills AP, Simmel FC, Neumann JL (2000) A DNA-fuelled molecular machine made of DNA. Nature 406:605–608
139. Yan H, Zhang X, Shen Z, Seeman NC (2002) A robust DNA mechanical device controlled by hybridization topology. Nature 415:62–65
140. Feng L, Park SH, Reif JH, Yan H (2003) A two-state DNA lattice switched by DNA nanoactuator. Angew Chem Int Ed 42:4342–4346
141. He X, Wei B, Mi Y (2010) Aptamer based reversible DNA induced hydrogel system for molecular recognition and separation. Chem Commun 46:6308–6310

142. Zhang Z, Chen N, Li S, Battig MR, Wang Y (2012) Programmable hydrogels for controlled cell catch and release using hybridized aptamers and complementary sequences. J Am Chem Soc 134:15716–15719
143. Zhang ZL, Li S, Chen N, Yang C, Wang Y (2013) Programmable display of DNA-protein chimeras for controlling cell-hydrogel interactions via reversible intermolecular hybridization. Biomacromolecules 14:1174–1180
144. Li S, Chen N, Zhang Z, Wang Y (2013) Endonuclease-responsive aptamer-functionalized hydrogel coating for sequential catch and release of cancer cells. Biomaterials 34:460–469
145. Chen N, Zhang Z, Soontornworajit B, Zhou J, Wang Y (2012) Cell adhesion on an artificial extracellular matrix using aptamer-functionalized PEG hydrogels. Biomaterials 33:1353–1362
146. Langer R (1998) Drug delivery and targeting. Nature 392:5–10
147. Putney SD, Burke PA (1998) Improving protein therapeutics with sustained-release formulations. Nat Biotechnol 16:153–157
148. Hoare TR, Kohane DS (2008) Hydrogels in drug delivery: progress and challenges. Polymer 49:1993–2007
149. Jia XQ, Kiick KL (2009) Hybrid multicomponent hydrogels for tissue engineering. Macromol Biosci 9:140–156
150. Bussemer T, Otto I, Bodmeier R (2001) Pulsatile drug-delivery systems. Crit Rev Ther Drug Carrier Syst 18:433–458
151. Richards Grayson AC, Choi IS, Tyler BM, Wang PP, Brem H, Cima MJ, Langer R (2003) Multi-pulse drug delivery from a resorbable polymeric microchip device. Nat Mater 2:767–772
152. De Geest BG, De Koker S, Immesoete K, Demeester J, De Smedt SC, Hennink WE (2008) Self-exploding beads releasing microcarriers. Adv Mater 20:3687–3691
153. Hoffman AS (2002) Hydrogels for biomedical applications. Adv Drug Delivery Rev 54:3–12
154. Stuart MAC, Huck WTS, Genzer J, Muller M, Ober C, Stamm M, Sukhorukov GB, Szleifer I, Tsukruk VV, Urban M, Winnik F, Zauscher S, Luzinov I, Minko S (2010) Emerging applications of stimuli responsive polymer materials. Nat Mater 9:101–113
155. Bashir R, Hilt JZ, Elibol O, Gupta A, Peppas NA (2002) Micromechanical cantilever as an ultrasensitive pH microsensor. Appl Phys Lett 81:3091–3093
156. Yavuz MS, Cheng YY, Chen JY, Cobley CM, Zhang Q, Rycenga M, Xie JW, Kim C, Song KH, Schwartz AG, Wang LHV, Xia YN (2009) Gold nanocages covered by smart polymers for controlled release with near-infrared light. Nat Mater 8:935–939
157. Satarkar NS, Biswal D, Hilt JZ (2010) Hydrogel nanocomposites: a review of applications as remote controlled biomaterials. Soft Matter 6:2364–2371
158. Kang HZ, Liu HP, Zhang XL, Yan JL, Zhu Z, Peng L, Yang HH, Kim YM, Tan WH (2011) Photoresponsive DNA-cross-linked hydrogels for controllable release and cancer therapy. Langmuir 27:399–408
159. Sasaki K, Shi ZY, Kopelman R, Masuhara H (1996) Three-dimensional pH microprobing with an optically-manipulated fluorescent particle. Chem Lett 25:141–142
160. Clark HA, Barker SLR, Brasuel M, Miller MT, Monson E, Parus S, Shi ZY, Song A, Thorsrud B, Kopelman R, Ade A, Meixner W, Athey B, Hoyer M, Hill D, Lightle R, Philbert MA (1998) Subcellular optochemical nanobiosensors: probes encapsulated by biologically localised embedding (PEBBLEs). Sens Actuators, B 51:12–16
161. Bermejo C, Ewald JC, Lanquar V, Jones AM, Frommer WB (2011) In vivo biochemistry: quantifying ion and metabolite levels in individual cells or cultures of yeast. Biochem J 438:1–10
162. Buck SM, Xu H, Brasuel M, Philbert MA, Kopelman R (2004) Nanoscale probes encapsulated by biologically localized embedding (PEBBLEs) for ion sensing and imaging in live cells. Talanta 63:41–59
163. Clark HA, Kopelman R, Tjalkens R, Philbert MA (1999) Optical nanosensors for chemical analysis inside single living cells. 2. Sensors for pH and calcium and the intracellular application of PEBBLE sensors. Anal Chem 71:4837–4843

Chapter 9
Cell-Specific Aptamers for Disease Profiling and Cell Sorting

Kwame Sefah, Joseph Phillips and Cuichen Wu

Abstract The molecular recognition of medically relevant cell-surface proteins and other biomarkers by molecular probes plays a major role in this current era of molecular medicine. Molecular probes have served as platforms for diagnosis, prognostic indication and targeted radio- or chemotherapy in cancer medicine. Since cancer is generally a heterogeneous disease, the elucidation of new disease specific molecular features will facilitate our understanding of cancer. The development of new molecular probes to detect disease specific features will improve our ability to specifically target and treat cancers. Cell-specific aptamers have emerged as unique candidates for molecular identification of cancer cells. Single runs of cell-SELEX can generate panels of aptamers that target disease specific molecular markers with high affinity and selectivity. We have shown that these panels can be used for molecular profiling of cancer and aid in the diagnosis of cancer. The ability to detect diseased cells in biological fluids is important for early detection, monitoring disease progression or remission, and tracking drug efficacy. Our research has shown that aptamers can be used to purify cells from a flowing suspension of biological fluid. When integrated into microfluidic devices, aptamers can be used for enrichment of rare tumor cells and multiplexed cell sorting of heterogeneous cell mixtures. For these reasons, aptamers have emerged as unique candidates for molecular recognition and cell-isolation and their future contributions will be a key factor in molecular medicine.

K. Sefah (✉) · J. Phillips
Roche Molecular Systems, 700 Nickerson Road, Marlborough, MA 01752, USA
e-mail: Skwame15@gmail.com

J. Phillips
e-mail: japhillips99@gmail.com

C. Wu
Departments of Chemistry, Physiology and Functional Genomics, Center for Research at the Bio/Nano Interface, Shands Cancer Center, UF Genetics Institute and McKnight Brain Institute, University of Florida, Gainesville, FL 32611, USA
e-mail: cwu@chem.ufl.edu

W. Tan and X. Fang (eds.), *Aptamers Selected by Cell-SELEX for Theranostics*,
DOI 10.1007/978-3-662-46226-3_9

Keywords Aptamers · Molecular profiling · Cell isolation · Flow cytometry · Microfluidic channel

9.1 Introduction

The availability of molecular probes for the recognition of medically relevant cell-surface proteins and biomarkers has had and will continue to have a major impact in this era of molecular medicine. Tailored molecular probes have the ability to improve every aspect of medicine, including early detection, diagnostic resolution, and disease treatment options. Generally antibodies have been the probe of choice as they are able to detect molecular markers with high affinity and specificity. In fact, antibodies have been utilized successfully in many aspects of medicine including diagnosis, therapy, and prognosis of diseases. One major challenge for antibody technology is that there are not enough antibodies to target all the necessary disease-specific markers and creating new antibodies is a relatively long, technically cumbersome process involving animals with a generally low success rate. Further, many of the molecular markers that antibodies do recognize are also expressed on healthy cells and this may lead to deleterious effects when implementing such antibody-mediated drugs schemes or interventions. Ideally, technology for generating molecular probes should target disease specific molecular markers, generate high affinity and highly selective probes, be relatively fast with a high success rate, and produce multiple probes simultaneously. One promising technology for producing molecular probes that target diseased cells is the systematic evolution of ligands by exponential enrichment (SELEX) or Cell-SELEX.

Cell-SELEX generates molecular probes called aptamers that can target diseased cells specifically and with high affinity. Aptamers are single-stranded nucleic acids (DNA or RNA) that can bind with high affinity and selectivity to proteins, peptides, and other small molecules [1–3]. The dissociation constants of aptamers to their targets can range from picomolar to micromolar (See section on aptamers for details). Aptamer selection via cell-SELEX uses complex cellular targets, such as live cancer cells, red blood cells, or bacteria surface proteins, has been used to generate useful aptamers for cell recognition. Our research has focused on using cell-SELEX to generate cancer cell-specific aptamers and use them to develop novel technologies in the field of molecular medicine [4–9]. Two major areas that we have applied aptamer technology to are cancer cell-sorting/enrichment and molecular profiling of cancer cells. New technologies in these areas can be directly translated into novel methods for early detection of cancer, cancer diagnostic assays, and monitoring of disease progression and therapeutic response.

9.2 Cell-Sorting/Enrichment

Biological cells are mostly of heterogeneous population. In order to obtain single species for analysis, and obtain accurate biological information, it is important to track and isolate these cells into individual sub-populations based on their unique biological features. Therefore cell sorting of heterogeneous subpopulations of tumor and tumor-associated cells has been a long established strategy in cancer research. This technology has many important applications including detecting circulating tumor cells, separating stem cells from tissues, cell and protein engineering, and diagnosing the hematologic malignancies [10–15]. Sorting can be performed based on a myriad of cell properties, for example, size, shape, surface antigen expression, protein expression, and metabolic activity. Cell size and shape can be roughly discerned using FACS methods and more novel microfluidic methods [16]. Many cell properties can be detected using fluorescent probes and therefore FACS methods are popular. There are important situations in which FACS methods are not possible or efficient, e.g. point-of-care diagnostics, therefore other methods have gained in popularity. Our research has focused on microfluidic methods of tumor cell enrichment and cell sorting based on cell-surface protein/antigen expression, due to the nature of cell-SELEX aptamer selection which targets the surface of live cells.

To show proof-of-concept of tumor cell-enrichment, simple microfluidic channels were constructed by sandwiching parafilm between a cover glass and microscope slide. The channel was then coated with streptavidin by allowing the protein solution to fill the channel by capillary action. Excess streptavidin was then rinsed away by drawing solutions through the channel using filter paper as a wick. Biotinylated aptamers were then introduced and excess rinsed via wicking. Mixtures of fluorescent labeled target and non-target tumor cells were then introduced into the channel via wicking. After a final rinse step, the channel surface was imaged using a fluorescent microscope. Based on image analysis, the percent of target and non-target cells captured and purity of captured cells could be calculated. With this rudimentary device, we achieved 95 % purity and ~15 % efficiency of target cell capture [17]. To further improve the device capabilities, a PDMS version was created in which the channel height was reduced by four times to ~25 μm, on the same order as the cell diameter. The PDMS channel was reversibly attached to a large cover glass and operated via syringe pump. This PDMS device achieved 97 % purity and 80 % efficiency of target cell capture see Figure Enrichment. The increase in efficiency of target cell capture of the PDMS device could not be explained based on the difference in channel geometry compared to the parafilm-based device. One plausible explanation for this effect is based on mathematical modeling of particle velocities in microfluidic flows at low Reynolds number. Modeling predicts that if the particle diameter is on the order of the channel height, then the particle could exhibit significant velocity perpendicular to the fluid flow direction. In this case, we estimated that the tumor cells could be moving at 1–50 μm/s, fast enough to traverse the 25 μm channel height while passing through

the device. This basic research exhibiting the selective and efficient aptamer-based capture of tumor cells from a flowing suspension has been implemented in other microfluidic cell detection systems, including microcapillary [18], paper-based lateral flow devices [19], and Differential Mobility Cytometry [20]. Other research that has improved the efficiency of target cell capture to >90 % includes improving the device architecture by adding arrays of micropillars [21] and implementing multivalent aptamer technology like aptamer-conjugated gold nanoparticles [22] and linear-repeating aptamer arrays generated by rolling circle amplification [23], (Figs. 9.1 and 9.2).

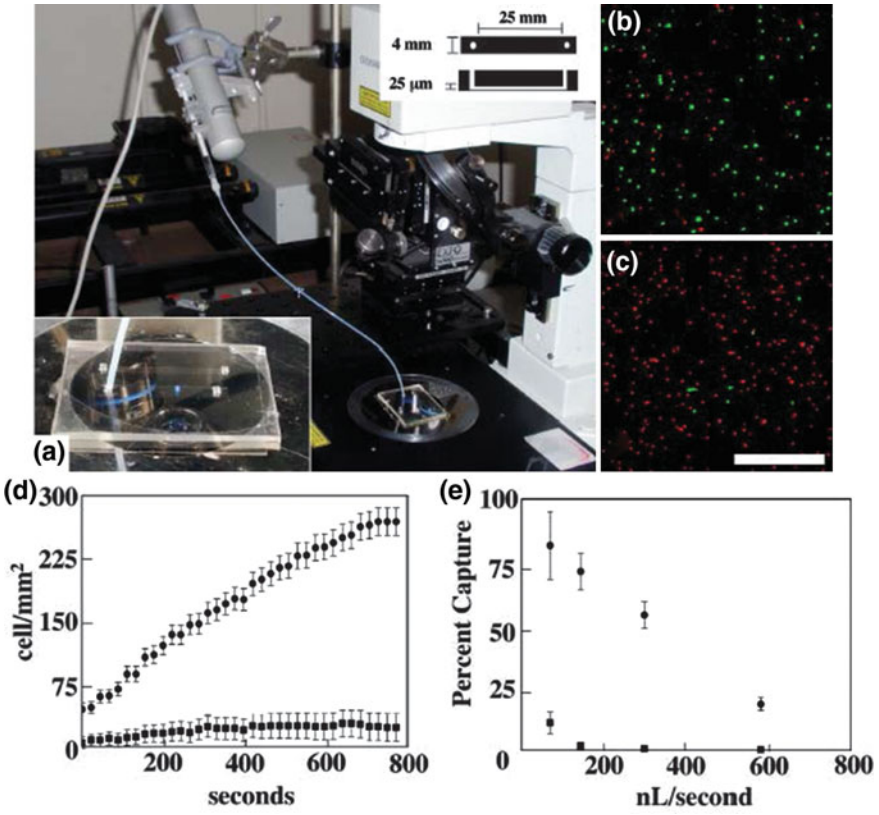

Fig. 9.1 Image of basic PDMS device on confocal microscope (**a**). The *bottom left* inlay shows the device, and the *top right* inlay shows *top-down* and *sideways views* with dimensions. Representative images of original mixture of cells before cell capture assay (**b**) and channel surface after the cell capture assay performed at 154 nL/s flow rate (**c**) with target and control cells stained *red* and *green*, respectively. Cell-surface density measured over the course of the cell capture experiment showing linear increase in target cells captured over time (**d**). Target cell capture efficiency decreases with increased fluid flow rate (**e**). Bar = 500 µm (Reprinted with the permission from Ref. [17], Copyright 2009 American Chemical Society)

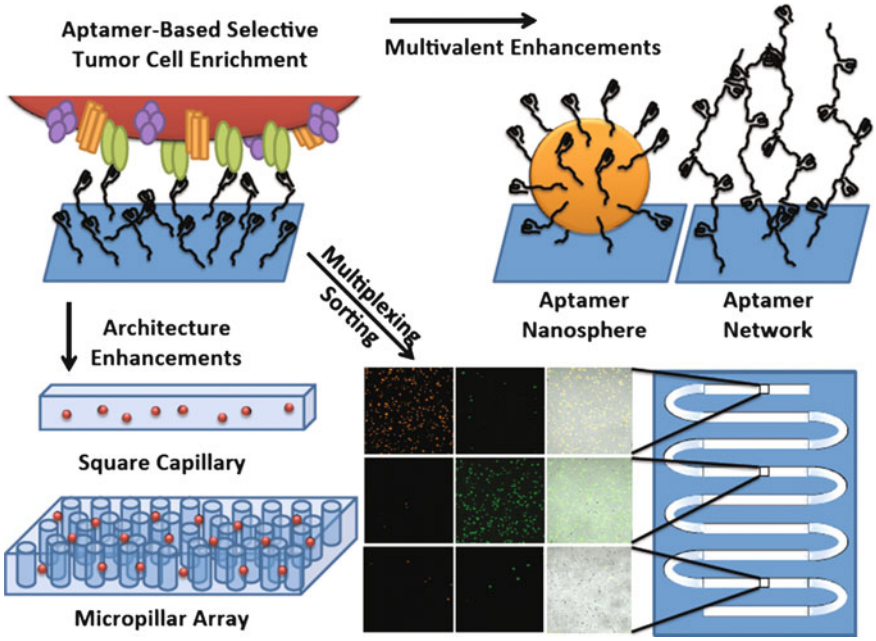

Fig. 9.2 Evolution of aptamer-based microfluidic devices for tumor cell enrichment (Reproduced with the permission from Ref. [18], The Royal Society of Chemistry, Adapted from Refs. [21, 22, 24], Copyright 2009, 2012, 2013 American Chemical Society)

To further demonstrate the capability and feasibility of tumor cell-sorting using aptamer platform, we created an S-shaped PDMS channel with multiple regions for cell-capture. The channel had fluid ports positioned at each bend which allowed us to immobilize one of three different biotinylated aptamers within each long stretch of the channel. We mixed 3 different tumor cell types together and were able to selectively capture each target cell within the region associated with its specific aptamer. We achieved ~97 % purity for two tumor cell lines and ~88 % purity for the third tumor cell line [24]. We also released cells from each region of the device and cultured them for several days. Results from flow cytometry experiments on the cultured cells showed that sorted cells had ~96.5 % purity. The level of multiplex sorting in this type of device is only limited to the surface area of the device.

After the initial proof-of-concept of capturing tumor cells from a flowing suspension using aptamer-based microfluidic devices, improvements in device design and implementation of molecular engineering of multivalent structures have produced devices that can achieve >90 % capture efficiency. These devices can take whole blood as sample matrix and operate at flow rates that are useful for point-of-care applications. Sorting of cells can be achieved without the use of lasers or any other sophisticated equipment. Since aptamers can be created for any diseased cell, we believe that these types of devices should be useful for detecting tumor cells in in various bodily fluids.

9.2.1 Summary

After the initial proof-of-concept of capturing tumor cells from a flowing suspension using aptamer-based microfluidic devices, improvements in device design and implementation of molecular engineering of multivalent structures have produced devices that can achieve >90 % capture efficiency. These devices can take whole blood as sample matrix and operate at flow rates that are useful for point-of-care applications. Sorting of cells can be achieved without the use of lasers or any other sophisticated equipment. Since aptamers can be created for any diseased cell, we believe that these types of devices should be useful for detecting tumor cells in various bodily fluids.

9.3 Disease (Molecular) Profiling

As personalized medicine is becoming increasingly important in the effective management of diseases, especially cancers, there is the need to intensify efforts to identify unique disease signatures of therapeutic importance. This is necessary because even tumors arising from the same source have varied molecular characteristics as the disease progressed. Therefore molecular profiling of individual disease will allow us to measure the expression of multiple genes on tissues or biological samples and this will present individual molecular portraits of specific disease. This will allow us to capture the biological complexity of diseases more comprehensively, and utilize these features for design of effective therapeutic regimen. Simply put, molecular profiling will allow us to define diseases more carefully, for example; giving a molecular classification between healthy and disease cells (good diagnostic performance), or molecular markers to determine outcome after intervention (predictive performance), or for monitoring prognosis. This type of technology is integral to better understanding the unique molecular characteristics of a patient's disease rather than using the morphological features, which is the common gold standard practice for most tumors. It is anticipated that molecular profiling will become a valuable tool for oncologists when making treatment decisions for patients with difficult-to-treat and/or rare and aggressive cancers.

In theory, the expression of molecular targets of therapeutic and diagnostic importance is not in doubt. Many studies have demonstrated that each disease has unique sets of genes that are expressed and can be targeted for use in diagnosis and therapy. These biomarkers provide unique features about each patient's diseases, from which more tailored treatments can be most effective. Similarly, biomarkers can also provide information about which treatment regimen might not be suitable for a patient's disease based on the molecular profile and thus prevent excessive use of ineffective drugs. This observation of over treatment is well documented in breast cancer [25]. If an exhaustive set of biomarkers were known, physicians could

prescribe more defined treatment options for patients and further monitor these treatments with certainty. For instance, by gene expression patterns, it is now clear that breast cancer can be sub-typed into more than five different diseases [25]. In fact, breast cancer was the first cancer in which molecular profiling was approved for clinical use [26, 27]. Profiles such as the 21-gene recurrence score (Oncotype Dx), 70-gene signature, 76-gene signature, and wound-response gene profile of predicting breast cancer survival have shown great promise [28–31]. Other profiling technology such as Lymphochip has shown great success in treating lymphomas [32, 33]. The potential of molecular profiling is not limited to lymphomas and breast cancer. Progress has been made in others such as acute leukemia, prostate and lung cancers [34–39]. Generally, this technology has been developed using different cellular product platforms including RNA profiling, DNA profiling, and proteomic profiling [40–42]. While RNA and DNA profiling are undoubtedly promising, the scope of this book will only deal with proteomic profiling, and specifically using cell surface expressed proteins.

While there are many gene products that differ between disease state and normal cells and could serve as potential biomarkers for disease management, surface expressed genes are good candidates for effective and reliable targeted therapy. Membrane proteins are uniquely important because they play a critical role in how the cell interacts with its environment. Most FDA-approved clinically proven cancer drugs target cell-surface proteins and inhibit their functions [43]. Discovery of tumor-specific membrane proteins is a significant challenge. Using whole-proteome analysis, the most under-represented group is membrane proteins and roughly 30 % of proteins consist of membrane proteins, but less than 5 % of this total are recognized by mass spectroscopy, a major limitation for drug development [44]. The hydrophobic properties of membrane proteins further complicate their analysis as they are insoluble in non-detergent buffers. In addition, membrane proteins are typically lower in abundance when compared with soluble proteins. Therefore any technology that can overcome these limitations and generate reagents that can target membrane proteins for disease management will have significant impact in biological mechanism studies, biomarker discovery, and drug development.

9.3.1 How Do We Isolate and Identify These Genes?

Generally mass spectroscopy has been used to identify these genes and even predict the importance of these targets in drug development. Methods that can both identify genes and provide probes to target their gene products are ideal. The probes should identify the surface molecules with high specificity and affinity. For targeted therapies, these probes could serve as delivery tools to target these gene products and deliver drug payload capable of killing cancer cells or inhibiting their growth. Traditionally, antibodies have been generated and used to perform these functions and most of the current targeted therapies have antibodies as the central reagent.

While this has been successful, there are many important targets that do not have specific antibodies. Further, most of the antibody tumor targets are also expressed on normal cells, therefore limiting their utility. Thus there is a great need to generate more probes but generating high affinity tumor specific antibodies is not easy. As a result, researchers found different ways to complement antibody-mediated molecular target identification. In the past two decades, attention has been focused on the use of another powerful technology called Systematic Evolution of Ligands by EXponential enrichment (SELEX), which can generate molecular probes called aptamers. Aptamers are short nucleic acid strands that are selected from a library and they identify their targets with high affinity and specificity. It has been clearly demonstrated that aptamers can uniquely identify surface gene products of diagnostic and therapeutic importance [45–47]. By using cell-SELEX, many aptamers have been generated for cell surface molecules [4, 7, 48]. While the identity of some of these molecules are yet to be identified, their unique characteristics and sensitivity to identify specific diseases have adequately been demonstrated. Some of these aptamers have been used as baits for biomarker discovery [49–51], profiling clinical samples [52], and used for diagnostics even though their specific targets may not be known. We believe that cell-SELEX can adequately profile any diseased cell by using multiple aptamers that target cell surface molecules.

9.3.2 Why Is Aptamer-Mediated Molecular Profiling Important?

For molecular profiling to be effective, we must possess many molecular probes that can recognize specific cell surface markers important to disease diagnosis or therapy. With the correct probes, one can fully define the molecular identity of specific diseases and define the prognosis with certainty. The aptamer technology is important for molecular profiling because:

(i) SELEX produces multiple aptamers targeting different expressed genes of importance.
(ii) Negative selection against healthy cells can produce aptamers that are highly selective for diseased cells.
(iii) Aptamers can be engineered to suit specific needs or intended use.

While the molecular profiling procedure has not been well established for aptamers, the potential for aptamers to revolutionize this technology has adequately been demonstrated and the Tan group has played a leading role. Some of these aptamer-based profiles are discussed below.

One of the earliest demonstration of aptamers as potential molecular profiling reagents was reported by Shangguan et al. [52]. In this study, the authors used aptamers that had previously been generated for leukemia cells using CCRF-CEM as the target cell and Ramos as negative cell line [4]. The selection generated a

Table 9.1 Using aptamers to recognize cancer cells [4]

	Cell line	sgc8	sgc3	sgc4	sgd2	sgd3
Cultured cell lines	CCRF-CEM, Pre T ALL	+++	++	++++	++++	++
	Molt-4, pre T ALL	++++	+++	++++	++++	++++
	Sup-T1, Pre-T ALL.	++++	+	++++	++++	++
	Jurkat, Pre-T ALL	++++	+++	++++	++++	++++
	SUP-B15, pre-B ALL, Ph+	+	0	++	+	0
	U266, plasmacytoma	0	0	0	0	0
	Ramos, Burkitt lymphoma	0	0	++++	++++	0
	Toledo, B cell lymphoma	0	0	++++	++++	+
	Mo2058, B cell lymphoma	0	++	++	0	+
	NB-4 (AML, APL)	0	0	+++	++++	0
Cells from Patients	T cell ALL	++	+++	+++	+++	+++
	Large B Cell lymphoma	0	0	0	0	0

Note A threshold based on fluorescence intensity of FITC in the flow-cytometric analysis was chosen so that 99 % of cells incubated with the FITC-labeled unselected DNA library would have fluorescence intensity below it. When the FITC-labeled aptamer was allowed to interact with the cells, the percentage of the cells with fluorescence above the set threshold was used to evaluate the binding capacity of the aptamer to the cells. 0, <10 %; +, 10–35 %; ++, 35–60 %; +++, 60–85 %; ++++, >85 %; *AML* acute myeloid leukemia; *APL* acute promyelocytic leukemia (Reprinted with the permission from Ref. [4], Copyright 2006 National Academy of Sciences, USA)

panel of aptamers that showed specific features unique to individual aptamers. Based on the initial cell culture studies (Table 9.1) and limited clinical samples obtained from the pathology department of Shands hospital at the University of Florida, the authors showed that, these aptamers could be used to profile leukemia clinical samples.

The observation was important since diagnosis of leukemia is commonly based on morphologic evaluation and immunophenotype analysis and not molecular profiling. Current antibodies for leukemia are not specific for only diseased cells and therefore not intended for comprehensive recognition of molecular features of specific disease, especially subtyping. The lack of disease-specific markers is a shortfall not only in leukemia, but also in many other cancers. Thus in subsequent and more comprehensive clinical samples studies, the authors used the leukemia aptamers to profile leukemia patients' samples [52]. The selected aptamers could group real leukemia patient samples into different categories, T-cell acute lymphoblastic leukemia (T-ALL), B-cell acute lymphoblastic leukemia (B-ALL), acute myeloid leukemia (AML), and other lymphomas of mature lymphocytes based on surface markers. These results as shown in Table 9.2, clearly demonstrate an effective detection of targets on the cell membranes by the aptamers. This recognition was not due to non-specific interactions or random binding. All the lymphoma cases showed no or very low binding, in agreement with the fact that the mature lymphoma cells often do not share the same receptors with the immature leukemia cells. Moreover, the aptamers had much stronger binding with the T-ALL cases than others did, an expected outcome since the aptamers were selected to

Table 9.2 Aptamer profiling of cancer cells [52]

Cells lines		sgc8	sgc3	sgc4	sgd2	sgd3	sgd5
Cultured cell lines							
T-ALL	CCRF-CEM	+++	++	++++	++++	++	0
	Molt-4	++++	+++	++++	++++	++++	0
	Sup-T1	++++	+	++++	++++	++	0
	Jurkat	++++	+++	++++	++++	++++	0
B-ALL	SUP-B15	+	0	++	+	0	0
myeloma	U266,	0	0	0	0	0	0
B-cell lymphoma	Ramos	0	0	++++	++++	0	0
	Toledo	0	0	++++	++++	+	++
	UF1[c]	0	0	+	0	0	0
	Mo2058	0	++	++	0	+	0
AML	NB-4 (APL)	+	0	++++	++++	0	0
	Kasumi-1	+++	0	++++	++++	++	0
Cells in normal bone marrow							
CD3 (+) T cells		0	0	0	0	0	0
mature B cells[a]		0	0	0	0	0	0
Immature B cells[b]		0	0	+	+	0	0
Granulocytes		0	0	0	0	0	0
Monocytes		0	0	+	+	0	0
Erythrocytes		0	0	++	++	0	0
Patient's samples							
T ALL 1		++	+++	+++	+++	+++	ND
T ALL 2		++	+	+++	++	+	0
T ALL 3		+	+	++++	+++	+	0
T ALL 4		+	+	++	+++	+	0
T ALL 5		+	+	++	+	+	0
T ALL 6		0	0	+	+	0	0
T ALL 7		0	0	++	++	0	0
T ALL 8		+	+	++	++	+	0
T ALL 9		+	0	+	+	0	0
TALL10		0	+	+	0	+	0
B ALL 1		0	0	++	++	0	0
B ALL 2		0	0	++	++	0	+
B ALL 3		++	0	++	++	0	+
B-ALL 4		0	0	+	+	0	0
AML 1		+	+	++	+	0	0

AML 2	+	0	++	+	0	0
AML 3	+	0	+	+	0	0
AML 4	0	0	++++	++++	0	0
AML 5	0	0	+	0	0	0
AML 6	+	0	0	0	0	0
AML 7	+	0	0	0	0	0
AML 8	+	0	+++	+++	0	0
1, Peripheral T-cell lymphoma	0	0	0	ND	ND	ND
2, follicular lymphoma	0	0	0	0	0	0
3, B-cell lymphoma	0	0	0	0	0	0
4, T-cell lymphoma,	0	0	0	0	0	0
5, B cell lymphoma	0	0	0	0	0	0
6, plasma cell neoplasm	0	0	+	+	0	0
7, follicular lymphoma	0	0	+	0	0	0

0 :< 10% + :10-35% ++ :35-60% +++ :60-85% ++++ :>85%

Note In the flow cytometry analysis, a threshold based on fluorescence intensity of FITC was chosen so that 99 % of cells incubated with the FITC-labeled unselected DNA library would have fluorescence intensity below it. When FITC-labeled aptamer was allowed to interact with the cells, the percentage of the cells with fluorescence above the set threshold was used to evaluate the binding capacity of the aptamer to the cells. 0 for <10 %; + for 10–35 %; ++ for 35–60 %; +++ for 60–85 %; ++++ for >85 % (Reprinted with the permission from Ref. [52], Copyright 2007 American Association for Clinical Chemistry)

target CCRF-CEM cells, a T-ALL cell line. In addition, aptamer binding patterns corresponded well with general categories pre-defined by antibodies.

Since one barrier to developing robust molecular profiling technologies is the use of expensive and difficult to standardize platforms, e.g. microarray technology [25, 53], it is important that this study featured the use of flow cytometry as the detection platform. By using this combination of cell-SELEX and flow cytometry, more labs and research facilities will begin to implement aptamer technology for molecular profiling. Similar to this demonstration of SELEX technology for molecular profiling, other studies have emerged that further support that aptamer-mediated molecular profiling and cancer cell specific recognition can be an essential reagent for personalized medicine [5–8].

In the journal Leukemia, Sefah et al. [7] reported the generation of aptamers that can distinguish between NB4 cells, acute promyelocytic leukemia (APL), and HL60 (AML) cells. This report is important for molecular profiling because there was no known probe that could distinguish between these 2 cell lines prior to this report. In fact, HL60 and NB4 cells are morphologically similar and can both be induced to differentiate toward monocytic and granulocytic pathways depending on the chemical induce. Gene expression profiling studies showed that NB4 and HL60

cell lines had the most closely related profiles of mRNA expression [54]. In this study, in addition to the differential recognition by specific aptamers, two other aptamers could respond to the pattern of differentiation in both cell lines (Figs. 9.3 and 9.4). The targets of these aptamers were down regulated when the cell lines were treated with all-trans retinoic acid (ATRA), which caused cells to differentiate into mature granulocytes. On the other hand targets were up regulated when treated with sodium butyrate, differentiation through the monocytic pathway. The ability to distinguish this off-on switch molecular event is important because these probes could be used to develop targeted therapy based on these markers and simultaneously monitor progress of course of the therapy.

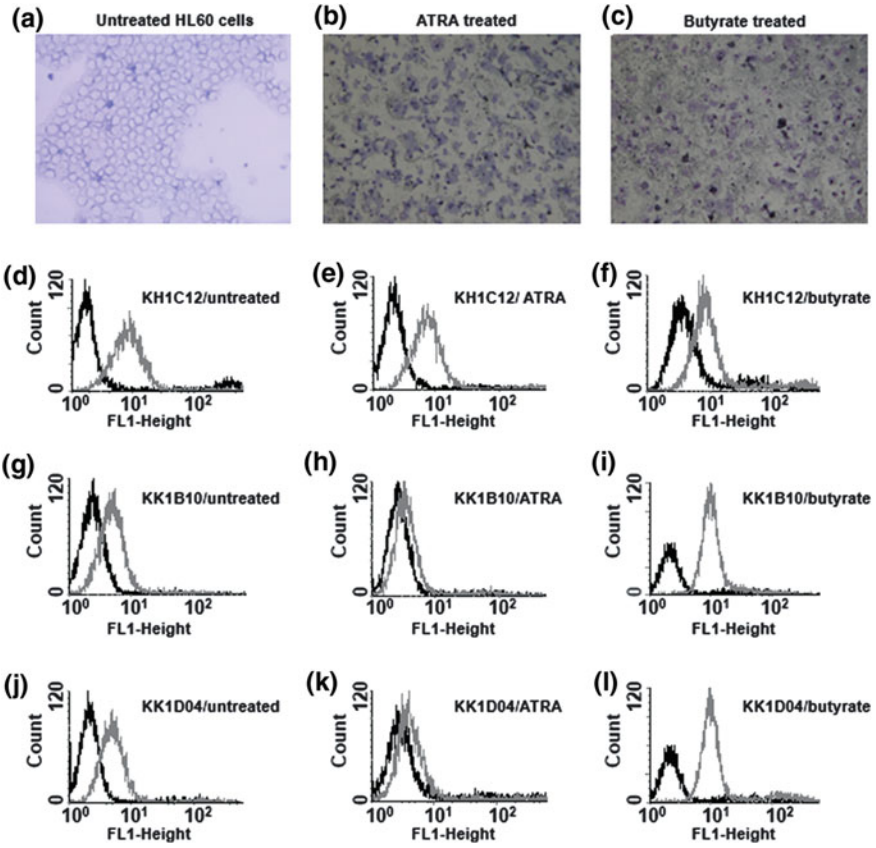

Fig. 9.3 Cytospin preparations followed by Accustain Wright staining of HL60 cells **a** untreated, **b** ATRA-induced differentiation, and **c** sodium butyrate-induced differentiation, showing the formation of formazan deposits (×10 magnification). The FACscan histograms (**d–l**) above show the binding profile of the selected aptamers to the untreated, ATRA-treated and sodium butyrate-treated cells. The *dark* histograms show fluorescence background using the unselected DNA library [7] (Reprinted with the permission from Ref. [7], Copyright 2009 Nature Publishing Group)

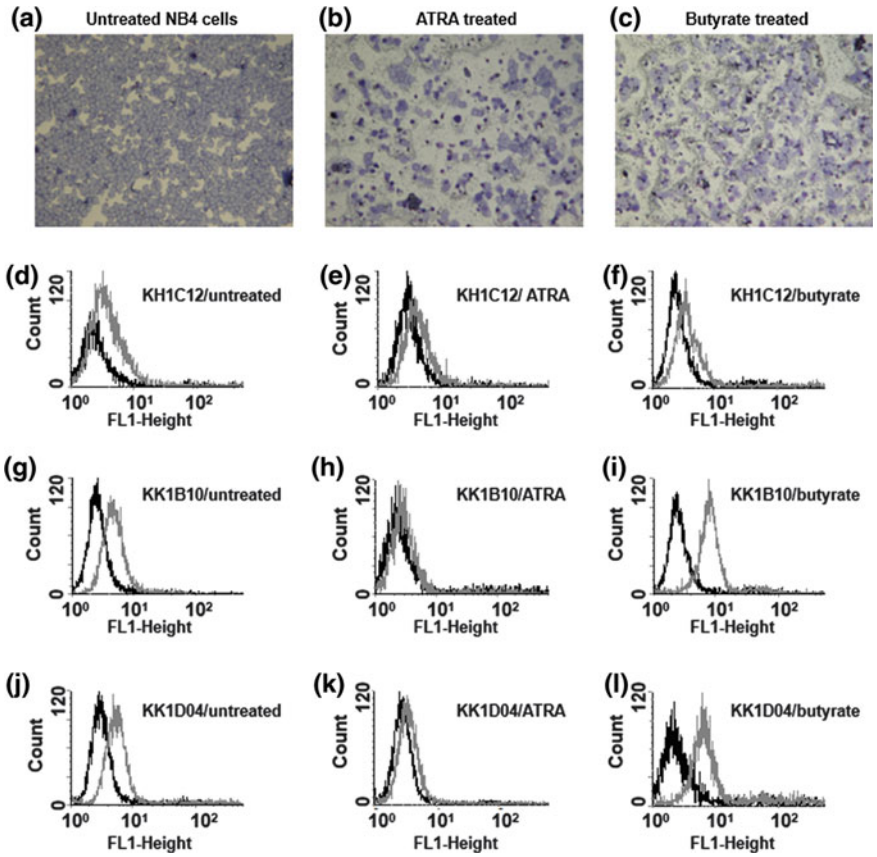

Fig. 9.4 Cytospin preparations followed by Accustain Wright staining of NB4 cells **a** untreated, **b** ATRA-induced differentiation, and **c** sodium butyrate-induced differentiation, showing the formation of formazan deposits (×10 magnification). The FACscan histograms (**d**–**l**) show the binding profile of the selected aptamers to the untreated, ATRA-treated and sodium butyrate-treated cells. The *dark* histograms show fluorescence background using the unselected DNA library (Reprinted with the permission from Ref. [7], Copyright 2009 Nature Publishing Group)

As the significance of these 2 cell lines has been well documented in leukemia research, most recently Yang et al. [55], has also developed aptamers that can differentiate between HL60 and NB4 cell lines. These aptamers could further differentiate between malignant and non-malignant cells (Fig. 9.3). The authors probed three groups of AML clinical samples, AML non-M3 CD34(+), AML non-M3 CD34(−), and 3) AML M3 with these aptamers and tested if the aptamers could differentially recognize any groups of AML cases. As expected, the aptamers showed low levels of reactivity on normal CD34(+) progenitors, but could recognize both CD34(+) and CD34(−) cells of AML non-M3 cases with the median values of fluorescence intensity higher than those of background binding. Also, they further

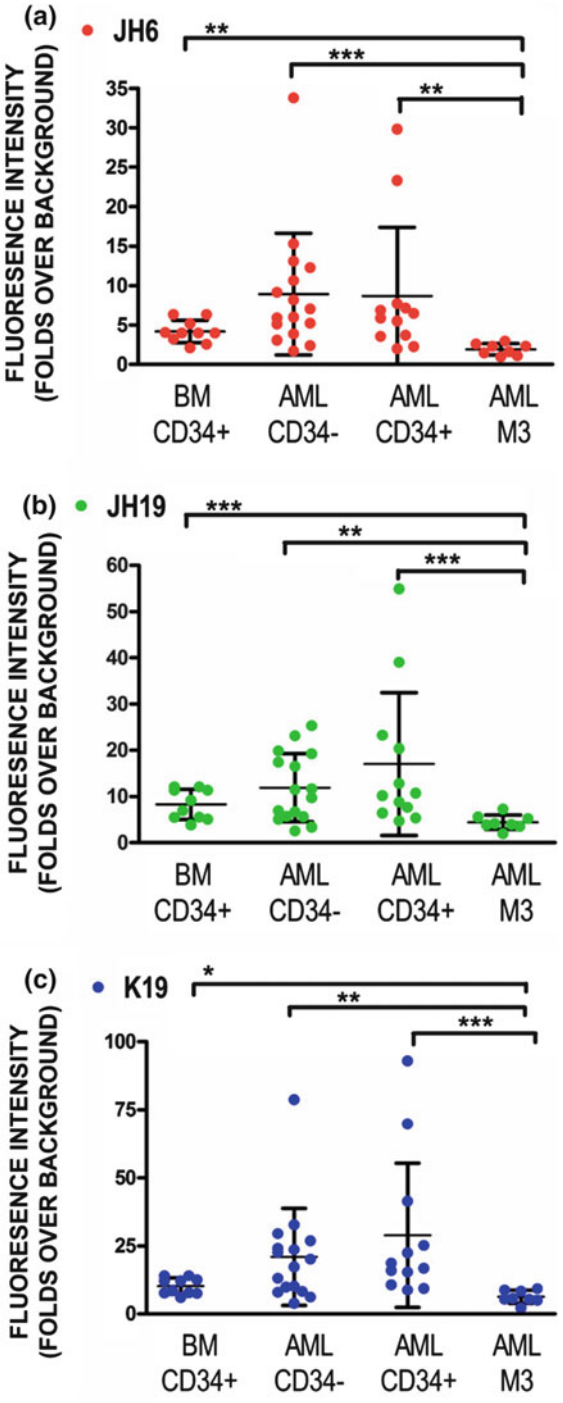

Fig. 9.5 Comparison of aptamer recognition of AML leukemic cells and non-malignant CD34(+) cells. The AML cases were separated into three groups: (1) CD34(+) AML non-M3; (2) CD34(−) AML non-M3; and (3) AML M3. The fluorescence levels of bound aptamers or single-stranded negative control DNA were determined by flow cytometry. The fluorescence intensity levels of bound aptamers (folds over background) were calculated (**a** JH6, **b** JH19, and **c** K19). Individual values for each aptamer bound on each case are shown as individual symbols, and mean ± standard deviation of individual groups are also shown. The P values are given as "*", "**", and "***" representing the P values of <0.05, <0.01, and <0.001, respectively (Reprinted from Ref. [55])

identified the binding molecule of one of the aptamers, called K19, to be Siglec-5, a specific but low expressed marker on NB4 cells. Based on these examples of aptamer technology providing panels of highly selective probes that are useful as molecular profiling reagents, we believe that the implementation of aptamers to manage these cancers is feasible. The unique nature of aptamers, i.e. ease of generation, sensitivity, specificity, ease of chemical modification, non-toxicity, make aptamer technology a solid platform for disease management (Fig. 9.5).

References

1. Tuerk C, Gold L (1990) Systematic evolution of ligands by exponential enrichment: RNA ligands to bacteriophage T4 DNA polymerase. Science 249:505–510
2. Ellington AD, Szostak JW (1990) In vitro selection of RNA molecules that bind specific ligands. Nature 346:818–822
3. Mallikaratchy P, Stahelin RV, Cao Z, Chob W, Tan W (2006) Selection of DNA ligands for protein kinase C-delta. Chem Commun 3229–3231
4. Shangguan D, Li Y, Tang ZW, Cao ZHC, Chen HW et al (2006) Aptamers evolved from live cells as effective molecular probes for cancer study. In: Proceedings of the national academy of sciences of the United States of America, vol 103, pp 11838–11843
5. Tang ZW, Shangguan D, Wang KM, Shi H, Sefah K et al (2007) Selection of aptamers for molecular recognition and characterization of cancer cells. Anal Chem 79:4900–4907
6. Chen HW, Medley CD, Sefah K, Shangguan D, Tang ZW et al (2008) Molecular recognition of small-cell lung cancer cells using aptamers. ChemMedChem 3:991–1001
7. Sefah K, Tang ZW, Shangguan DH, Chen H, Lopez-Colon D et al (2009) Molecular recognition of acute myeloid leukemia using aptamers. Leukemia 23:235–244
8. Sefah K, Meng L, Lopez-Colon D, Jimenez E, Liu C et al (2010) DNA aptamers as molecular probes for colorectal cancer study. PLoS One 5(12):e14269
9. Sefah K, Shangguan D, Xiong X, O'Donoghue MB, Tan W (2010) Development of DNA aptamers using cell-SELEX. Nat Protoc 5:1169–1185
10. Mattanovich D, Borth N (2006) Applications of cell sorting in biotechnology. Microb Cell Fact 5(1):12
11. Hong B, Zu Y (2013) Detecting circulating tumor cells: current challenges and new trends. Theranostics 3:377–394
12. Orfao A, RuizArguelles A (1996) General concepts about cell sorting techniques. Clin Biochem 29:5–9
13. Basu S, Campbell HM, Dittel BN, Ray A (2010) Purification of specific cell population by fluorescence activated cell sorting (FACS). J Visual Exp: JoVE
14. Pruszak J, Sonntag K-C, Aung MH, Sanchez-Pernaute R, Isacson O (2007) Markers and methods for cell sorting of human embryonic stem cell-derived neural cell populations. Stem Cells 25:2257–2268
15. Zehentner BK, Fritschle W, Stelzer T, Ghirardelli KM, Hunter K et al (2006) Minimal disease detection and confirmation in hematologic malignancies: combining cell sorting with clonality profiling. Clin Chem 52:430–437
16. Hou HW, Warkiani ME, Khoo BL, Li ZR, Soo RA et al (2013) Isolation and retrieval of circulating tumor cells using centrifugal forces. Scientific Reports 3
17. Phillips JA, Xu Y, Xia Z, Fan ZH, Tan W (2008) Enrichment of cancer cells using aptamers immobilized on a microfluidic channel. Anal Chem 81:1033–1039
18. Martin JA, Phillips JA, Parekh P, Sefah K, Tan W (2011) Capturing cancer cells using aptamer-immobilized square capillary channels. Mol BioSyst 7:1720–1727

19. Liu G, Mao X, Phillips JA, Xu H, Tan W et al (2009) Aptamer-nanoparticle strip biosensor for sensitive detection of cancer cells. Anal Chem 81:10013–10018
20. Liu Y, Bae SW, Wang K, Hong J-I, Zhu Z et al (2010) The effects of flow type on aptamer capture in differential mobility cytometry cell separations. Anal Chim Acta 673:95–100
21. Sheng W, Chen T, Katnath R, Xiong X, Tan W et al (2012) Aptamer-enabled efficient isolation of cancer cells from whole blood using a microfluidic device. Anal Chem 84:4199–4206
22. Sheng W, Chen T, Tan W, Fan ZH (2013) Multivalent DNA nanospheres for enhanced capture of cancer cells in microfluidic devices. ACS Nano 7:7067–7076
23. Zhao W, Cui CH, Bose S, Guo D, Shen C et al (2012) Bioinspired multivalent DNA network for capture and release of cells. In: Proceedings of the national academy of sciences of the United States of America, vol 109, pp 19626–19631
24. Xu Y, Phillips JA, Yan J, Li Q, Fan ZH et al (2009) Aptamer-based microfluidic device for enrichment, sorting, and detection of multiple cancer cells. Anal Chem 81:7436–7442
25. Cross D, Burmester JK (2004) The promise of molecular profiling for cancer identification and treatment. Clin Med Res 2:147–150
26. Weiss G (2013) Applied molecular profiling: evidence-based decision-making for anticancer therapy community oncology: frontline medical communications. pp. 115–121
27. Murphy CG, Fornier M (2010) HER2-positive breast cancer: beyond trastuzumab. Oncology 24:410–415
28. Paik S, Shak S, Tang G, Kim C, Baker J et al (2004) A multigene assay to predict recurrence of tamoxifen-treated, node-negative breast cancer. N Engl J Med 351:2817–2826
29. van't Veer LJ, Dai H, van de Vijver MJ, He YD, Hart AAM et al (2002) Gene expression profiling predicts clinical outcome of breast cancer. Nature 415:530–536
30. Wang YX, Klijn JGM, Zhang Y, Sieuwerts A, Look MP et al (2005) Gene-expression profiles to predict distant metastasis of lymph-node-negative primary breast cancer. Lancet 365:671–679
31. Chang HY, Nuyten DSA, Sneddon JB, Hastie T, Tibshirani R et al (2005) Robustness, scalability, and integration of a wound-response gene expression signature in predicting breast cancer survival. In: Proceedings of the national academy of sciences of the United States of America, vol 102, pp 3738–3743
32. Alizadeh A, Eisen M, Davis RE, Ma C, Sabet H et al (1999) The lymphochip: a specialized cDNA microarray for the genomic-scale analysis of gene expression in normal and malignant lymphocytes. Cold Spring Harb Symp Quant Biol 64:71–78
33. Alizadeh AA, Eisen MB, Davis RE, Ma C, Lossos IS et al (2000) Distinct types of diffuse large B-cell lymphoma identified by gene expression profiling. Nature 403:503–511
34. Valk PJM, Verhaak RGW, Beijen MA, Erpelinck CAJ, van Doorn-Khosrovani SBV et al (2004) Prognostically useful gene-expression profiles in acute myeloid leukemia. N Engl J Med 350:1617–1628
35. Bullinger L, Dohner K, Bair E, Frohling S, Schlenk RF et al (2004) Use of gene-expression profiling to identify prognostic subclasses in adult acute myeloid leukemia. N Engl J Med 350:1605–1616
36. Lapointe J, Li C, Higgins JP, van de Rijn M, Bair E et al (2004) Gene expression profiling identifies clinically relevant subtypes of prostate cancer. In: Proceedings of the national academy of sciences of the United States of America, vol 101, pp 811–816
37. Latil A, Bieche I, Chene L, Laurendeau I, Berthon P et al (2003) Gene expression profiling in clinically localized prostate cancer: a four-gene expression model predicts clinical behavior. Clin Cancer Res 9:5477–5485
38. Petty RD, Nicolson MC, Kerr KM, Collie-Duguid E, Murray GI (2004) Gene expression profiling in non-small cell lung cancer: from molecular mechanisms to clinical application. Clin Cancer Res 10:3237–3248
39. Borczuk AC, Shah L, Pearson GDN, Walter KL, Wang LQ et al (2004) Molecular signatures in biopsy specimens of lung cancer. Am J Respir Crit Care Med 170:167–174

40. Diatchenko L, Lau YFC, Campbell AP, Chenchik A, Moqadam F et al (1996) Suppression subtractive hybridization: a method for generating differentially regulated or tissue-specific cDNA probes and libraries. In: Proceedings of the national academy of sciences of the United States of America, vol 93, pp 6025–6030
41. Collisson EA, Campbell JD, Brooks AN, Berger AH, Lee W et al (2014) Comprehensive molecular profiling of lung adenocarcinoma. Nature 513:543–550
42. Pollack JR, Perou CM, Alizadeh AA, Eisen MB, Pergamenschikov A et al (1999) Genome-wide analysis of DNA copy-number changes using cDNA microarrays. Nat Genet 23:41–46
43. Yildirim MA, Goh K-I, Cusick ME, Barabasi A-L, Vidal M (2007) Drug—target network. Nat Biotech 25:1119–1126
44. Wu CC, Yates JR (2003) The application of mass spectrometry to membrane proteomics. Nat Biotech 21:262–267
45. Kong R-M, Zhang X-B, Chen Z, Tan W (2011) Aptamer-assembled nanomaterials for biosensing and biomedical applications. Small 7:2428–2436
46. Sefah K, Phillips JA, Xiong X, Meng L, Simaeys DV et al (2009) Nucleic acid aptamers for biosensors and bio-analytical applications. The Anal 134:1765–1775
47. Borbas KE, Ferreira CSM, Perkins A, Bruce JI, Missailidis S (2007) Design and synthesis of mono- and multimeric targeted radiopharmaceuticals based on novel cyclen ligands coupled to anti-MUC1 aptamers for the diagnostic imaging and targeted radiotherapy of cancer. Bioconjug Chem 18:1205–1212
48. Cerchia L, Ducongé F, Pestourie C, Boulay J, Aissouni Y et al (2005) Neutralizing aptamers from whole-cell SELEX inhibit the RET receptor tyrosine kinase. PLoS Biol 3:e123
49. Shangguan D, Cao ZH, Meng L, Mallikaratchy P, Sefah K et al (2008) Cell-specific aptamer probes for membrane protein elucidation in cancer cells. J Proteome Res 7:2133–2139
50. Mallikaratchy P, Tang ZW, Kwame S, Meng L, Shangguan DH et al (2007) Aptamer directly evolved from live cells recognizes membrane bound immunoglobin heavy mu chain in Burkitt's lymphoma cells. Mol Cell Proteomics 6:2230–2238
51. Van Simaeys D, Turek D, Champanhac C, Vaizer J, Sefah K et al (2014) Identification of cell membrane protein stress-induced phosphoprotein 1 as a potential ovarian cancer biomarker using aptamers selected by cell systematic evolution of ligands by exponential enrichment. Anal Chem 86:4521–4527
52. Shangguan DH, Cao ZHC, Li Y, Tan WH (2007) Aptamers evolved from cultured cancer cells reveal molecular differences of cancer cells in patient samples. Clin Chem 53:1153–1155
53. Ioannidis JPA (2007) Is molecular profiling ready for use in clinical decision making? Oncologist 12:301–311
54. Leupin N, Kuhn A, Hügli B, Grob TJ, Jaggi R et al (2006) Gene expression profiling reveals consistent differences between clinical samples of human leukaemias and their model cell lines. Br J Haematol 135:520–523
55. Yang M, Jiang G, Li W, Qiu K, Zhang M et al (2014) Developing aptamer probes for acute myelogenous leukemia detection and surface protein biomarker discovery. J Hematol Oncol 7 (5). doi:10.1186/1756-8722-7-5

Chapter 10
Using Cell-Specific Aptamer-Nanomaterial Conjugates for Cancer Cell Detection

Zhi Zhu

Abstract Early detection and treatment of cancer highly depends on developing highly sensitive and specific methods for targeting cancer cells. Aptamers, generated from cell-SELEX, have significant merits for cancer cell detection, such as high binding affinity and specificity, small size, easy and reproducible synthesis and modification, and minimal immunogenicity. In particular, the combination of aptamer and nanomaterials has resulted in an unprecedented improvement in the field of molecular recognition. With their unique physical and chemical properties, nanomaterials facilitate the sensing process and amplify the signal of recognition events. In this chapter, we discuss the recent advances of using the conjugations of cell-specific aptamers with various nanomaterials as novel molecular tools for enhanced cancer cell detection, including metallic, silica, and magnetic nanoparticles, nanocrystals, and DNA nanostructures.

Keywords Cell-specific aptamer · Nanomaterials · Bioconjugation · Molecular recognition · Cancer cell detection

10.1 Introduction

Cancer is the most leading cause of death today [1–3]. Detecting cancer cells is a very effective method to diagnosis of cancer, especially in their nascent stage, since the occurrence and development of cancer are closely related to the change of cells, such as cell-surface components, cell proliferation, and cell differentiation [4]. However, the level of cancer cells within the biological system at the early stages of cancer is particularly too low to be detected by the present available methods. Therefore, the development of novel approaches to detect cancer cells as sensitively

Z. Zhu (✉)
Department of Chemical Biology, College of Chemistry and Chemical Engineering, Xiamen University, Xiamen, China
e-mail: zhuzhi@xmu.edu.cn

W. Tan and X. Fang (eds.), *Aptamers Selected by Cell-SELEX for Theranostics*,
DOI 10.1007/978-3-662-46226-3_10

and selectively as possible is in crucial need. First, the selectivity is highly dependent on the development of highly specific molecular probes targeting cancer cell-surface molecules that differentiate the cancer cells from the normal counterparts [5–7]. Although antibodies have been widely applied for cancer cell targeting, their large molecular weight, high cost in preparation, batch-to-batch variation, narrow target range, instability, and immunogenicity cause serious limitations. Therefore, it is highly desired to develop new molecular probes with high affinity and specificity. From this perspective, a novel class of nucleic acid ligands, known as aptamers, has been isolated and identified as an alternative of antibodies [8, 9]. In particular, using cell-SELEX, whole living cells are regarded as targets for the selection of aptamers for specific cell recognition without any prior knowledge of targeting proteins on cell membrane [10–12]. Therefore, by carefully choosing the target cells and control cells, aptamer can be selected specifically against certain types of cancer cells, not normal cells or other types of cancer cells. The excellent biochemical properties of aptamers, such as small size, reproducible synthesis, easy modification, nontoxicity, and lack of immunogenicity, make aptamers as ideal molecular probes for cancer cell detection.

Second, the sensitivity is greatly determined by the format of signal readout. Over the past decade, rapid development in nanoscience and nanotechnology has resulted in the successful synthesis and characterization of various new nanomaterials, often with a size of 100 nm or smaller in at least one of their dimensions, including metallic [13, 14], silica [15], magnetic [16], and polymeric nanoparticles [17], nanocrystals (quantum dots) [18], nanorods [19], nanowires [20], carbon nanotubes (CNTs) [21], and DNA nanostructures [22, 23]. The unique optical, electronic, magnetic, mechanophysical, and chemical properties of these materials, induced by their extremely small size and large surface-to-volume ratio, make them highly suitable for a wide range of biological, electronic, optical, environmental, and medical applications [24, 25]. In particular, conjugating the signal properties of nanomaterials with recognition ability of aptamers offers increasingly exciting possibilities in sensitive and selective detection of cancer cells [26–32]. In this chapter, we will discuss recent advances in cancer cell detection using the conjugation of cell-specific aptamer with various nanomaterials, including metallic, silica, and magnetic nanoparticles, nanocrystals, and DNA nanostructures.

10.2 Aptamer-Metallic Nanoparticle Conjugate for Cancer Cell Detection

Metallic nanoparticles, such as gold nanoparticles (AuNPs), display attractive properties for their application in bioanalysis such as their size-related optical and electronic properties, chemical stability, biocompatibility, simple and controllable synthesis, and easy surface modification through gold–thiol chemistry [33, 34]. Meanwhile, the conjugation of AuNPs with aptamer can result in synergism effect

beyond simply AuNPs or aptamer [35]. First, the selectivity of aptamer enables the AuNP-based bioassay to be highly specific. Second, the large surface area of AuNPs can load high density of aptamers on the surface, leading to a higher binding strength with multivalent effect. Third, the high local salt concentration and steric effect can prevent the degradation of aptamer in biological environment. Therefore, Aptamer-AuNP conjugates provide a powerful platform for cancer cell detection [36].

10.2.1 AuNPs-Based Colorimetric Sensing

AuNPs possess strong distance-dependent optical properties by the variation of localized plasmon resonance [37]. When AuNPs come into close proximity, their absorption spectra shift and their scattering profiles change. This results in a change of color from red to blue. These properties, together with the aggregation or dissociation of AuNPs, formed the basis for colorimetric sensing of any target analyte. By using cancer cell aptamer-conjugated AuNPs (Apt-AuNPs), a direct colorimetric assay for sensitive cancer cell detection was first achieved by Tan and coworkers [38]. As schematically shown in Fig. 10.1a, the Apt-AuNPs are targeted to assemble on the surface of a specific type of cancer cell through the recognition of the aptamer to its target on the cell membrane surface. Once AuNPs have assembled on the cell surface, they behave as a larger gold cluster, having, as a consequence of

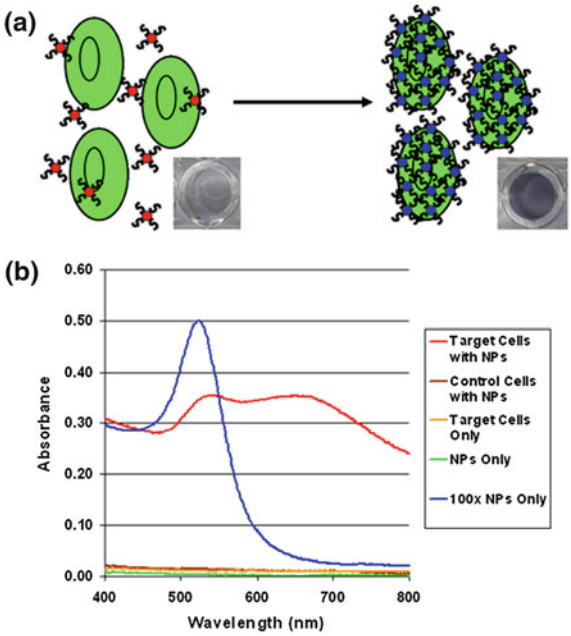

Fig. 10.1 **a** Schematic representation of the Apt-GNP-based colorimetric assay. **b** Plots depicting the absorption spectra obtained for various samples analyzed using Apt-GNPs. Reprinted with the permission from Ref. [38]. Copyright 2008 American Chemical Society

aggregation, sufficient proximity for surface plasmon resonance to overlap (Fig. 10.1b). This results in the alteration of light scattering and absorption properties as the signal transduction. In this way, the effective combination of the selectivity and affinity of aptamers with the spectroscopic advantages of AuNPs allows for the sensitive detection of cancer cells. After optimizing the particle size and concentration, 1.0×10^{10} AuNPs were incubated with increasing amounts of target cells and the same amounts of control cells for comparison. The results clearly showed that samples with the target cells present exhibited a distinct color change, while non-target samples did not elicit any change in color. Even a concentration of cells as low as 1,000 could be readily detected by the naked eye. For more complex samples containing variously colored species to confound the results, this method was still able to rely on spectroscopic detection without any further sample preparation steps. In addition, the assay was able to differentiate between different types of target and control cells based on the aptamer used in the assay, indicating the wide applicability of the assay for diseased cell detection.

Adapting a similar scheme, Liu et al. [39] transferred the reaction from solution to lateral flow device and developed an Apt-AuNP strip biosensor (ANSB) for the sensitive detection of circulating tumor cells (CTC), using Burkitt's lymphoma Ramos cells as proof of principle. The ANSB was prepared on a lateral flow device, consisting of four components: a sample application pad, an aptamer-nanoparticle conjugate pad, a nitrocellulose membrane, and an absorbent pad. A thiolated aptamer (thiol-TD05) was immobilized on the AuNPs, and a biotinylated aptamer (biotin-TE02) was immobilized on the strip's test zone. When a sample solution containing Ramos cells was applied on the ANSB sample pad, the cells migrated by capillary action, interacted with TD05-AuNPs to form Apt-AuNP-cell complexes which could then be captured in test zones by the reaction between Ramos cells and immobilized TE02 aptamers. The excessive Apt–AuNPs continued to migrate along the strip and pass the control zone, after which they were captured by hybridization events between the aptamer and immobilized DNA. The accumulation of AuNPs on the test and control zone was visualized as a characteristic red band. Under optimal conditions and 80 μL sample loading volume, 4,000 Ramos cells could be seen by the naked eye, and as low as 800 Ramos cells could be detected by a portable strip reader within 15 min. Moreover, the ANSB has been successfully applied in detecting Ramos cells in human blood, thus showing great promise for rapid, high-throughput, sensitive, and cost-effective point-of-care cancer diagnostics.

Similarly, Ray group reported a simple colorimetric and highly sensitive two-photon scattering (TPS) assay for highly selective and sensitive detection of breast cancer SK-BR-2 cell lines using an oval-shaped AuNP multifunctionalized with antibody and aptamer both targeting HER2 receptors on cell membrane [40]. In the presence of target cells, many nanoconjugates bound to HER2 receptors on the cancer cell surface, resulting in nanoparticle aggregates. Therefore, a distinct color change can be observed by naked eye and the TPS intensity increases of about 13-fold. The colorimetric assay can achieve sensitivity of 10^4 cells/mL, while as

low as 100 cells/mL could be detected by using the TPS technique. Instead of spherical AuNPs, oval-shaped AuNPs were introduced. During the aggregation, the particle aspect ratio increased and TPS intensity change became higher, leading to improved sensitivity.

10.2.2 Aptamer-Nanorods for Enhanced Detection

Although a group of aptamers can be selected against cancer cells by cell-SELEX, not all of them have high binding affinity. Meanwhile, some biomarkers on the cancer cell surface, especially those in the early stage of disease development, occur in very low density. This would result in poor signaling and hinder cell targeting. Under such conditions, multivalent binding is preferable to single binding events. Huang et al. [41] were able to improve the detection efficiency by using Au–Ag nanorods (NRs) as a nano-platform for multivalent binding by using multiple aptamers on the rod to increase both the signal and binding strengths of these aptamers in cancer cell recognition. The NRs were fabricated with 12 nm × 56 nm, and a monolayer of PEG was assembled onto the NR surfaces to minimize aggregation and protein nonspecific binding. Up to 80 fluorophore-labeled aptamers can be attached on a NR surface through simple thiol linkage, resulting in a much stronger fluorescence signal than that of an individual dye-labeled aptamer probe. When incubated with target and control cells, the aptamer-NRs maintained their selectivity and had a 26-fold higher binding affinity compared with that of single aptamer probes as a result of simultaneous multivalent interactions with the cell membrane receptors. As determined by flow cytometric measurements, an enhancement in fluorescence signal in excess of 300-fold was obtained for the NR-aptamer-labeled cells compared with those labeled by individual aptamer probes. Consequently, the target cells could be clearly visualized through the strong fluorescence under confocal microscopy. Overall, the molecular assembly of aptamers showed high fluorescence signal, minimal nonspecific binding, and enhanced binding affinity. Therefore, this conjugate has great potential for the elucidation of cells with low density of binding sites, or with relatively weak binding probes, and can greatly improve our ability to perform cellular imaging and targeting. This is an excellent example of integrating aptamers with nanomaterials to develop advanced molecular binders with greatly improved properties for cancer cell targeting.

10.2.3 Aptamer-Nanoclusters for Cancer Cell Targeting

The large AuNPs can have strong surface plasmon resonance effect. Once reducing the nanoparticle size to few atoms, the gold or silver nanoclusters exhibit strong, robust, and tunable fluorescence emission, which have been developed as a new

class of fluorophores for chemical sensing and biomedical imaging [42]. In particular, oligonucleotide-template silver nanoclusters (AgNCs) have attracted special attention, due to their outstanding spectral fluorescence property and biocompatibility [43–47]. Therefore, it is promising to prepare label-free one-step aptamer/nanomaterial-based strategy for cancer cell detection by design of chimeric oligonucleotides that contain one domain for luminescent nanomaterials formation and one domain for recognition of target cancer cells. Based on this principle, Wang and his coworkers reported a one-step engineering of intrinsically fluorescent Ag-NCs-aptamer assemblies that exhibited specific binding to target cancer cells with relatively high luminescence [48]. The sequence was optimized to contain aptamer sequence, C-rich sequence, and a linker in between. Based on the template synthesis of AgNCs, the aptamer sequence has been simply and inexpensively labeled with intrinsically fluorescent AgNCs and applied for cancer cell analysis by flow cytometry and confocal microscopy.

Although such a label-free strategy demonstrated effective recognition and imaging of cancer cells with high specificity, the Apt-AgNCs are "always-on" probes. Thus, extra washing and separation steps must be involved to reduce the background signal. Moreover, the fluorescence intensity of AgNCs was greatly diminished when the template contains extra aptamer portion. Meanwhile, as reported by Werner et al. [49], the fluorescence of DNA–AgNCs could be enhanced when AgNCs were in proximity to guanine-rich DNA sequences. Therefore, Wang and his coworkers further improved the system by developing a label-free and fluorescence turn-on aptamer strategy for cancer cell detection [50]. As shown in Fig. 10.2, in their design, two tailored probes were prepared, signaling probe (S-Probe) and recognition probe (R-Probe). The S-Probe contains a sequence for dark AgNCs template synthesis and a link sequence complementary to the arm

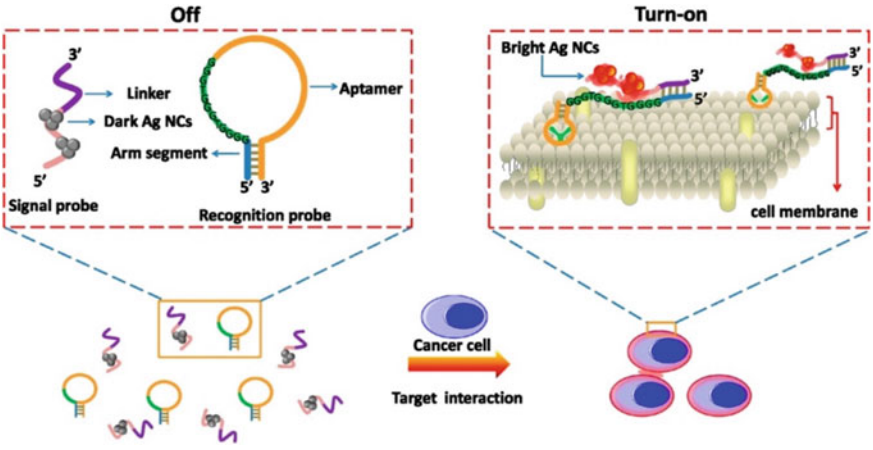

Fig. 10.2 Schematic representation of the label-free and turn-on aptamer strategy for cancer cell detection based on DNA-AgNC fluorescence upon recognition-induced hybridization. Reprinted with the permission from Ref. [50]. Copyright 2013 American Chemical Society

segment of R-Probe. The R-Probe is composed of an aptamer sequence for target recognition, a G-rich sequence for AgNC fluorescence enhancement, and an arm segment to form the hairpin structure with aptamer sequence. In the presence of target cancer cells, the aptamer-cell recognition induced the structure change of R-Probe that exposes the arm segment to hybridize with S-Probe and brings the AgNCs to be in proximity of G-rich sequence for fluorescence enhancement. Therefore, it provides a simple method to engineer a specific, conjugation-free, facile, one-step, turn-on fluorescence molecular probe for bio-recognition and analysis of cancer cells.

10.2.4 Au–Ag Bimetallic Nanoparticles with Special Properties

In recent year, Au–Ag bimetallic nanoparticles have been developed with some unique properties different from that of pure AuNPs or AgNCs. For example, Ag–Au nanostructures are attractive surface-enhanced Raman spectroscopy (SERS) substrates, because of the synergism of these metals, the tunability of the plasmon resonance, and superior SERS activity [51, 52]. SERS is a useful tool for cell detection and imaging given its low autofluorescence from biological samples and no photobleaching. Wu et al. [53] has reported using aptamer-conjugated Ag–Au nanostructures for the detection of breast cancer cells. The probes were synthesized by first performing the DNA-templated AgNC on aptamer and then photoreducing a layer of AuNPs on AgNC to form aptamer-Ag–Au nanostructure. The sensing was realized by specific tagging of MCF-7 cells with Rh6G-labeled aptamer-Ag–Au nanostructures, which displayed the characteristic peaks of Rh6G compared with nontarget cells in the SERS spectrum.

Not only gold ions can be photoreduced and deposited as AuNPs onto AgNC, the AuNPs could also serve as nucleation sites and automatically catalyze the chemical reduction of silver ion into silver metal in the presence of a reducing agent [54]. Based on this phenomenon, various novel detection schemes have been developed. Zhu et al. [55] designed hydrazine-AuNP-aptamer probe with silver enhancement for ultrasensitive and selective electrochemical detection of HER2 positive breast cancer cells (Fig. 10.3). Here, hydrazine acts as a reductant which has the capability of reducing silver ion to silver metal, and it is attached to AuNPs to make a bio-conjugate of hydrazine-AuNP-aptamer (Hyd-AuNP-Apt). Meanwhile, a sensor probe was prepared by covalently immobilizing the monoclonal anti-HER2 onto the nanocomposite. In the present of target cancer cells, the anti-HER2-immobilized probe, cancer cells, and Hyd-AuNP-Apt make a sandwich-type structure. Then, the silver ion is selectively reduced by hydrazine and specifically deposits onto AuNPs, which can be observed using a microscope and analyzed by square wave stripping voltammetry. Through such AuNP-promoted silver enhancement, as few as 26 cells/mL have been detected in human serum samples with high selectivity.

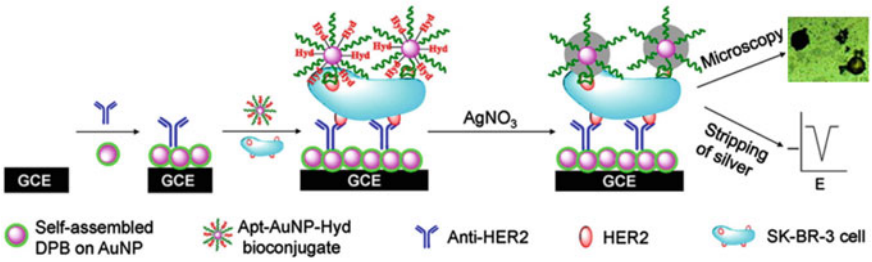

Fig. 10.3 Schematic representation of the immunosensor for detection of HER2 protein and HER2-overexpresing SK-BR-3 breast cancer cells based on Apt-AuNPs with silver enhancement. Reprinted with the permission from Ref. [55]. Copyright 2013 American Chemical Society

10.3 Aptamer-Quantum Dot Conjugate for Cancer Cell Detection

Fluorescent semiconductor nanocrystals, also known as Quantum dots (QDs), are single crystals a few nanometers in diameter whose size and shape can be precisely controlled by the duration, temperature, and ligand molecules used in the synthesis [56, 57]. Due to its significant advantages over traditional fluorophores, including size-dependent narrow photoluminescence with broad absorption, high quantum yield, low photobleaching, and resistance to chemical degradation, QDs have been increasingly utilized as biological imaging and labeling probes [58–63]. By modifying the QDs with cancer cell-specific aptamers, a wide variety of sensitive and specific sensing methods have been developed for targeted imaging and diagnostics of cancers. For instance, Xie and coworkers have developed QD-aptamer conjugates and used them to specifically recognize the mouse liver hepatoma cell line BNL 1ME A.7R.1 [64]. Li et al. [65] used GBI-10 aptamer-conjugated CdSe QDs for specifically targeting and imaging U251 human glioblastoma cells. In their work, polyamidoamine dendrimers were used to modify quantum dots and improve their solubility in water solution.

One of the significant features of QDs is their broad absorption with narrow and tunable photoluminescence spectra, which is highly suitable for multiplexing detection. Kim and coworkers conjugated the RGD peptide and AS1411 aptamer on the surfaces of QDs with different emission wavelengths (605 and 655 nm), enabling specific recognition of two putative cancer surface biomarkers, integrin $\alpha_v\beta_3$, and nucleolin, respectively [66]. They used these QDs for simultaneous fluorescence imaging of cellular distribution of nucleolin and integrin $\alpha_v\beta_3$ to study the difference of separate targets in the various cancer cell lines and normal healthy cells. Later, the same group further developed a multiplex cellular imaging system to simultaneously target three different molecular markers in a single cancer cell (Fig. 10.4). For the simultaneous evaluation of different genetic manifestations, three different QDs with distinct emission wavelengths of 605, 655, and 705 nm

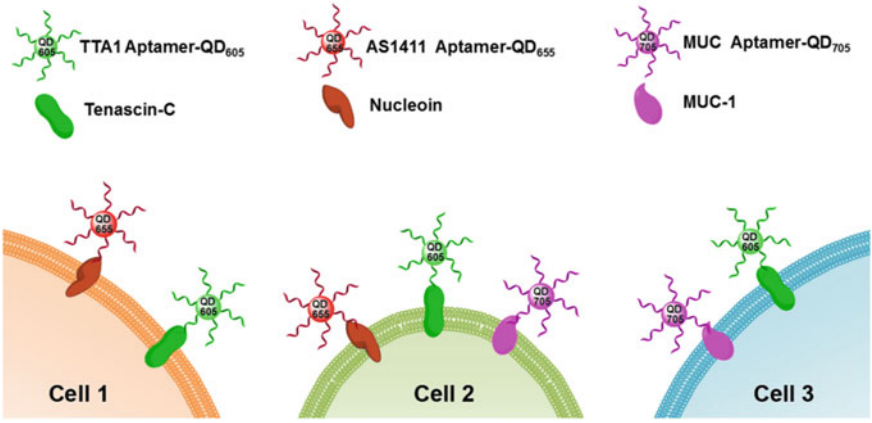

Fig. 10.4 Strategy for binding Apt-QDs to target molecules on cellular membrane. QDs were conjugated with three types of tumor-targeting aptamers. Tumor cells were treated with QD-TTA1 (605 nm, *green*), QD-AS1411 (655 nm, *red*), and QD-MUC (705 nm, *violet*). Binding of Apt-QDs to cells was different according to the target molecule expression on each cellular membrane

were used and labeled with aptamer AS1411, TTA1, and MUC, targeting nucleolin, tenascin-C, and mucin protein, respectively [67]. Simultaneous multiplex imaging demonstrated the colocalization and co-expression of different molecular markers in the cellular membrane of a single cancer cell. Therefore, QD-based multiplex imaging can enhance the accuracy of cancer cell detection by simultaneously evaluating the expression of different cancer markers in a single cancer cell.

In addition to its important role in the fluorescent field, QDs have also been widely used to establish electrochemical or electrochemiluminescence (ECL) sensing schemes. Ding et al. [68] reported the electrochemical detection of Ramos cells using aptamer-modified AuNPs with multiple CdS QDs anchored for target recognition and signal amplification, while the entire Au–CdS complex was immobilized on magnetic beads (MBs) for easy separation. Upon the recognition of target cancer cells by aptamers, the competitive disassociation of the Au-CdS complexes from the MBs changed the concentration of Cd^{2+} in the solution, which was reflected by the differential pulse voltammograms (DPVs). The DPV peak current was proportional to the cell concentration, reaching a calculated LOD of 67 cells per mL under optimal conditions in cell culture media. Later, the same group reported a reticular DNA-QD sheath constructed by self-assembly of DNA-modified CdTe QD probes and DNA nanowire frameworks functionalized with cell-binding aptamers for fluorescence microscopy imaging and the electrochemical detection of target cells with LOD of 10 cells per mL [69]. Moreover, they further reported a novel dendrimer nanocluster (NC)/CdSe-ZnS-QD as an electrochemiluminescence (ECL) probe with aptamer as recognition element for versatile assays of cancer cells. First, a large number of cDNA-modified CdSe-ZnS-quantum dots (QDs) were labeled on the NCs. Without target cells, the NCs were maintained on

electrode through DNA hybridization with aptamers conjugated on electrode, resulting in high ECL signal. In the present of target cells, the competitive reaction released the NCs away from electrode and decrease the ECL signal with LOD of 210 cells/mL. To further improve the sensitivity, they employed a DNA cycle-amplifying technique on MBs in the signal-on ECL assay to achieve LOD of 68 cells/mL. These electrochemical- and ECL-based methods are, in general, nondestructive and sensitive, but they are time-consuming, and the analytical volume is usually small.

10.4 Aptamer-Silica Nanoparticle Conjugate for Cancer Cell Detection

Various hybrid silica nanoparticles (SiNPs), such as dye-doped SiNPs, have been prepared and used in many areas of bioanalysis [70, 71]. The well-developed Stöber method [72] and water-in-oil reverse microemulsion method [73] enable simple, convenient, and controllable synthesis of dye-doped SiNPs. The dye-doped SiNPs possess several outstanding features, including small size, excellent photostability with the protection from silica matrix, and easy surface modification through silica surface conjugate chemistry [74]. Moreover, each SiNP can encapsulate hundreds to thousands of dye molecules, which can greatly amplify the signal and improve analytical sensitivity [75]. For example, compared with the traditional single-dye-labeled molecular probe, hundreds of dye molecules can be trapped in a single silica nanoparticle to produce a fluorescent signal approximately 10^4 times higher than that of single-dye-labeled probe [76]. Jiang et al. [77] have conjugated aptamers to near-infrared fluorescent SiNPs for sensitive leukemia cell detection by the fluorescence anisotropy technique and applied them in whole-blood detection.

Tan and coworkers have developed a two-NP assay with aptamers as the recognition element for specific targeting of CCRF-CEM acute leukemia cells in mixed cell and whole-blood samples [78]. The aptamer-modified magnetic nanoparticles (MNPs) were employed for the extraction of the target cancer cells, while the aptamer-conjugated $[Ru(bipy)_3]^{2+}$-doped SiNPs were simultaneously added for signal amplified detection and imaging of cancer cells. By using different aptamer-conjugated SiNPs, the Tan group has extended the use of the two-NP assay for multiple cancer cell recognition and imaging [79]. As shown in Fig. 10.5, three sets of MNPs were conjugated to aptamers targeting three different types of cancer cells, respectively (CEM cells, Ramos cells, non-Hodgkin's B cell lymphoma Toledo cells). After targeted cancer cell extraction and enrichment, dye-doped SiNPs conjugated with the same aptamer were added for imaging and detection by fluorescence imaging and microplate reader spectrometry. To improve the selectivity and sensitivity of such two-NP assay in a clinical setting, the Tan group systematically investigated several parameters, including nanoparticle size, conjugation

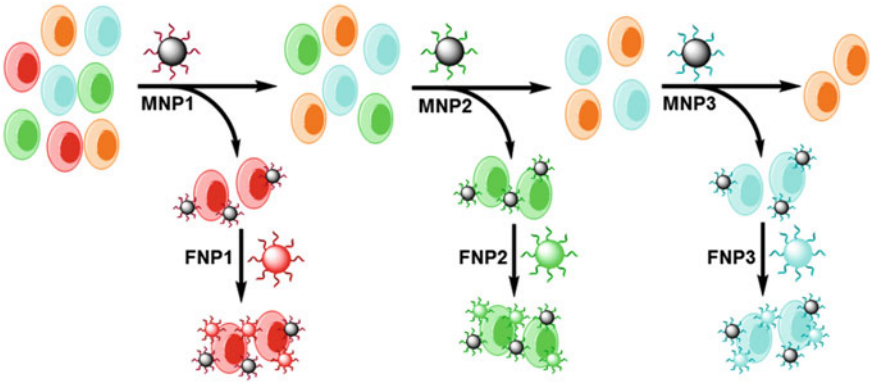

Fig. 10.5 Schematic representation of the multiple extraction procedure with the MNPs being added and extracted stepwise and the corresponding FNPs being added post magnetic extraction of cell samples

chemistry, use of multiple aptamer sequences on the nanoparticles, and use of multiple nanoparticles with different aptamer sequences [80].

Estévez et al. [75] reported the first example of using highly fluorescent SiNPs as a fluorescent label to efficiently increase the signal in flow cytometry for cancer cell detection. The fluorescein or Rubby dye-doped SiNPs were functionalized with polyethylene glycol (PEG) to reduce nonspecific interactions and with neutravidin to allow binding with biotinylated aptamers by neutravidin-biotin interaction. Compared with standard methods, these SiNPs showed one to two orders of magnitude increase in sensitivity. Later, Cai et al. [81] developed and compared three types of MUC-1 aptamer-conjugated Rubby-doped SiNPs for the detection of human breast carcinoma MCF-7 cells. The results showed that the prepared NPs-PEG-avidin-biotin-aptamer conjugate has the highest aptamer loading efficiency and best targeting performance compared with NPs–COOH–NH_2-aptamer and NPs-avidin-biotin-aptamer conjugates. Here, the PEG with flexible long chain as the bridge between the aptamer and NP can greatly enhance the freedom of aptamer. Therefore, the preparation method of SiNPs is highly important for its biological targeting performance.

To further extend the use of dye-doped silica nanoparticles, fluorescence resonance energy transfer (FRET) nanoparticles were developed by changing the doping ratio of three different dyes. Single-dye-, dual-dye-, and triple-dye-doped SiNPs were prepared according to this method [82]. These dyes possess appropriately overlapping excitation and emission spectra so that efficient energy transfer among them can occur. In this way, different FRET-mediated emission signatures can be obtained using a single wavelength to excite the SiNPs with varying ratio of three doping dyes. As shown in Fig. 10.6, by conjugating these FRET SiNPs with aptamers (T1, sgc8, and TD05) specific for different cancer cell lines (Toledo, CEM and Ramos, respectively), simultaneous and sensitive detection of multiple cancer cells has also been achieved [83].

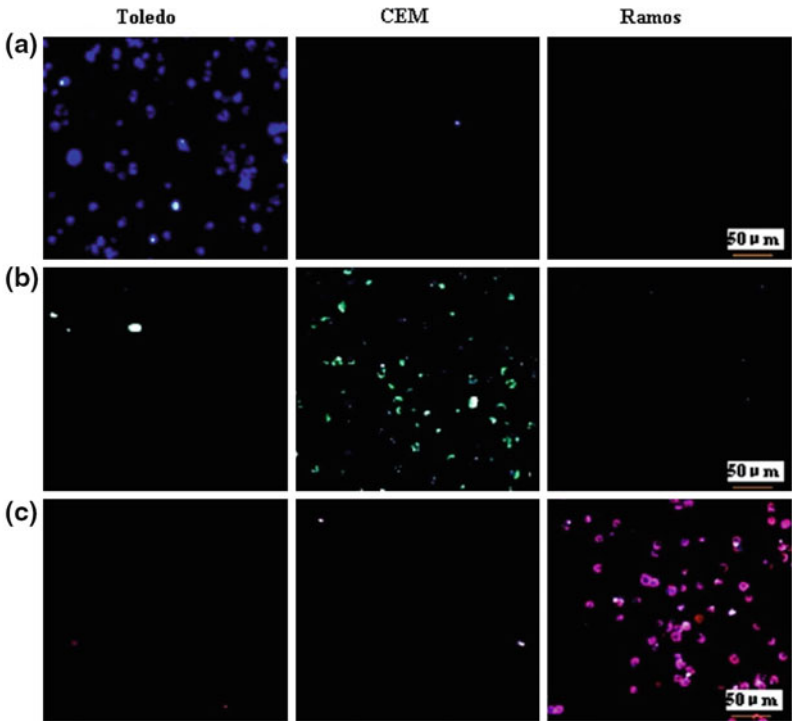

Fig. 10.6 Confocal microscopy images of individual SiNP-aptamer conjugates with the three different cells (Toledo, CEM, and Ramos): **a** NP (FAM)-T1, **b** NP (FAM-R6G)-sgc8, and **c** NP (FAM-R6GROX)-TDO5. Reprinted with the permission from Ref. [83]. Copyright 2009 American Chemical Society

10.5 Aptamer-Magnetic Nanoparticle Conjugate for Cancer Cell Detection

In recent years, researchers have developed various types of magnetic nanoparticles (MNPs) [84, 85]. The composition of these MNPs ranges from metals and alloys to metal oxides. The surface of MNPs can be modified through the creation of a few atomic layers of organic polymer, metallic or oxide surfaces for further functionalization with various bioactive molecules. One of the most outstanding aspects of MNPs is their high-throughput separation capabilities. As mentioned above, the aptamer-conjugated MNPs can be integrated with fluorescence SiNPs for cancer cell extraction and detection. Another significant feature of MNPs is their magnetism that can enhance the magnetic resonance (MR) signal of protons from surrounding water molecules [86]. Because most biological samples exhibit virtually no magnetic background, MNPs are highly suitable for ultrasensitive analysis of cells, especially in a complex biological environment. Briefly, the aggregation of

MNPs can induce the coupling of magnetic spin moments and generate strong local magnetic fields. Subsequently, local magnetic field inhomogeneities accelerate the spin dephasing of surrounding water protons, resulting in a decreased transverse or spin–spin relaxation times (T2). Thus, the target can be detected by a change in proton relaxation time (ΔT2) using nuclear magnetic resonance (NMR), magnetic resonance imaging (MRI), or relaxometry. Based on this principle, Bamrungsap et al. [87] could detect as few as 40 cells per mL in fetal bovine serum (FBS) containing buffer and 100 cells in a 250 μL whole-blood sample through the accumulation of cell-specific aptamer-modified MNPs on cell membranes. Moreover, with an array of aptamer-conjugated MNPs, pattern recognition of various cell types could be realized, and the expression level of different receptors on each cell type could be elucidated (Fig. 10.7). Compared with other techniques, the aptamer-conjugated MNPs provided robust and sensitive detection under different sample conditions, with minimal detection time and instrumentation.

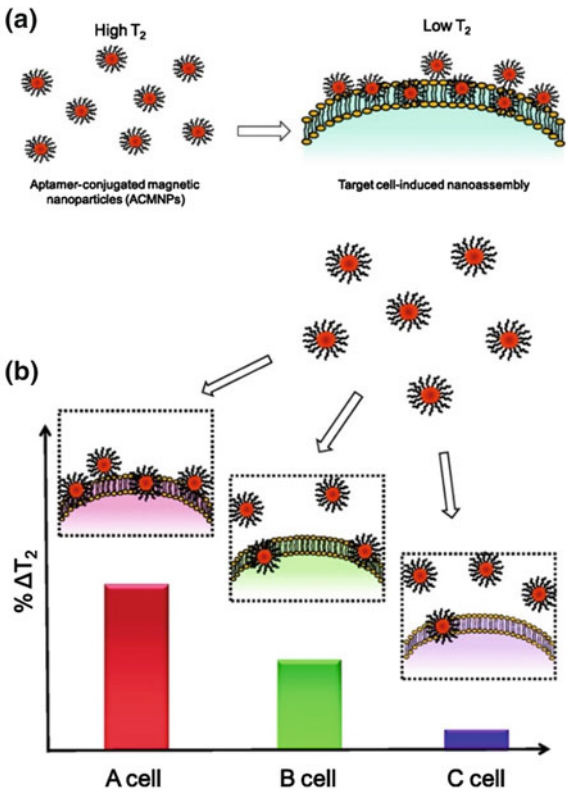

Fig. 10.7 Schematic illustration of using the magnetic nanosensor for cancer cell detection and pattern recognition. **a** The aptamer-conjugated MNPs have highly specific binding to their target cells. **b** Distinct recognition pattern generated for various cell lines with different receptor expression level using the magnetic nanosensors. Reprinted with the permission from Ref. [87]. Copyright 2012 American Chemical Society

Recently, a wide range of studies using multifunctional detection probes have provided more precise interpretation by overcoming the limitations of a single detection modality [16, 88]. For instance, Hwang et al. [89] synthesized cobalt–ferrite MNPs surrounding by fluorescent radamine with a silica shell matrix and labeled with AS1411 aptamer targeting nucleolin. After particle synthesis, the MNPs were further labeled with ^{67}Ga-citrate. Therefore, the MNPs were successfully used to target cancer cells by fluorescence imaging, radionuclide imaging, and MRI modalities in vivo and in vitro. This study illustrated that the aptamer-MNPs conjugate provides a versatile targeting tool that can enhance the diagnosis and therapy of cancer.

Zhao et al. [90] developed a novel dual-activatable fluorescence/MRI bimodal nanoprobe for cancer cell detection based on physisorption of Cy5-labeled aptamers on redoxable MnO_2 nanosheets. In the absence of target cells, aptamers were absorbed on MnO_2 nanosheets, and Cy5 fluorescence has been quenched by MnO_2 nanosheets. Neither fluorescence nor MRI signals of the nanoprobe were activated. In the presence of target cells (Fig. 10.8), the binding of aptamers to target cells induced the release of Cy5-labeled aptamers form MnO_2 nanosheets, causing partial fluorescence recovery to illuminate the target cells, and also facilitating the endocytosis of nanoprobes into target cells. After endocytosis, the reduction of MnO_2 nanosheets by intracellular GSH can generate large amounts of Mn^{2+} ions suitable for MRI. They have used sgc 8 aptamer-modified nanoprobe to realize fluorescence and MRI detection of CEM cells. Compared with "always-on" probe, the activatable probes would help to maximize the signal from the target cells and minimize the background signal, thus improving the detection sensitivity and specificity.

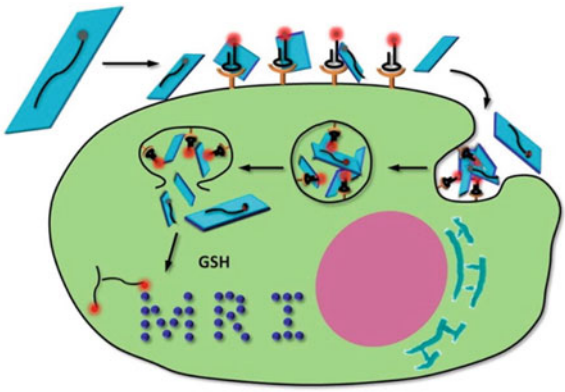

Fig. 10.8 Activation mechanism of the MnO_2 nanosheet-aptamer nanoprobe for fluorescence/MRI bimodal tumor cell detection. Reprinted with the permission from Ref. [90]. Copyright 2014 American Chemical Society

10.6 Aptamer-DNA Nanostructure Conjugate for Cancer Cell Detection

Owing to the unique feature of Watson–Crick base-pairing, DNA is an excellent structural building block for DNA nanotechnology [23, 91, 92]. The sequence programmability, automated controllable synthesis, high stability, and intrinsic functionalities make DNA nanostructures promising for applications in biomedicine and biotechnology [93, 94].

Inspired by the self-assembly of amphiphilic block copolymers, the copolymer that contains a hydrophilic DNA segment and a hydrophobic diacyllipid unit has been synthesized. Under certain conditions, the DNA amphiphiles could self-assemble into well-defined, homogeneous micelles with a desired size, and uniform size distribution [95]. In order to endow DNA micelles with more applicable properties and functions, Tan group have fabricated aptamer-functionalized micelles and demonstrated their enhanced binding ability [96]. Aptamer TD05, which selectively binds to IgG receptors on the surface of Ramos cells, was unable to bind with Ramos cells at physiological temperature (37 °C). However, the TD05-micelle conjugate displayed high affinity and selectivity for its target Ramos cells at 37 °C, as a result of a specific interaction-induced nonspecific insertion process which, in turn, led to the fusion between Apt-micelles and the cell membrane with extremely low off rate of aptamer (dissociation rate). Moreover, as shown in Fig. 10.9, the tumor cells were immobilized onto the surface of a flow channel device to mimic a tumor site in blood stream. By flushing the Apt-micelles through the channel in human whole-blood sample, the dynamic specificity of Apt-micelles in flow channel systems was demonstrated.

Inspired by the natural high packing efficiency of genomic dsDNA into a single nucleus micro-particles without relying on Watson–Crick base-pairing, Tan and his coworkers further fabricated hierarchical DNA nanoflowers (NFs) from the long DNA building blocks with tunable size from 200 nm to a few micrometers in diameter (Fig. 10.10) [97]. The long DNA building blocks were generated from a low amount of two DNA strands (one template and one primer) via rolling cycle replication (RCR), which is an isothermal enzymatic reaction involving the replication of many circular genomic DNAs. These assemblies were demonstrated to have high biostability that resist to nuclease degradation, denaturation by heating or urea treatment, or dissociation at extremely low concentration. By integrating fluorophores for signaling, cancer cell-targeting aptamers for recognition and drug loading sequences for delivery, the resultant multifunctional NFs have proven to be useful for bioimaging, selective cancer cell recognition, and targeted anticancer drug delivery. Furthermore, they have incorporated different fluorophores with different ratios into NFs via chemical modified deoxynucleotides to construct FRET-NFs for realizing single excitation multiplexed cellular imaging with multiple aptamers [98].

In another example, hybridization chain reaction (HCR) was employed for fabricating aptamer-tethered DNA nanodevices (aptNDs) [99]. In HCR, aptamers

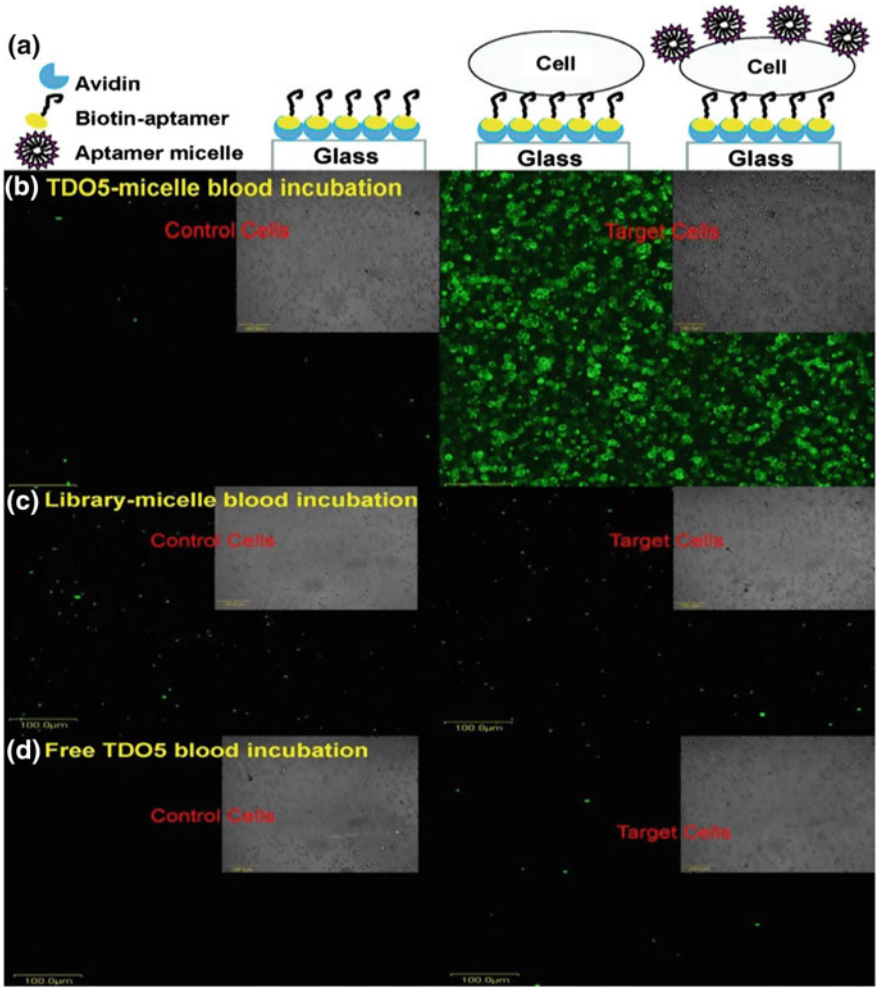

Fig. 10.9 Simplified flow channel response to cell-staining assay. Stepwise immobilization scheme of the flow channel (**a**). Representative images of the bright field and fluorescent images of control cells (CEM) and target cells (Ramos) captured on the flow channel surface incubated with FITC-TDO5-micelle (**b**), or FITC-library-micelle (**c**) or free FITC-TDO5 (**d**) spiked in human whole-blood sample under continuous flow at 300 nL/s at 37 °C for 5 min. All the scale bars are 100 μm. Reprinted from Ref. [96] by permission of PNAS

were engineered with initiator sequences that could activate cascading alternative hybridization of two partially complementary hairpin monomers to form a long linear nanostructure. To construct aptNDs for specific cancer cell recognition, aptamer sgc8, which can bind to target human protein tyrosine kinase 7 on CEM cells, was selected as a model. The aptNDs could efficiently anchor or in situ self-assemble on the target cell surfaces in cell mixtures, which enabled the loading of

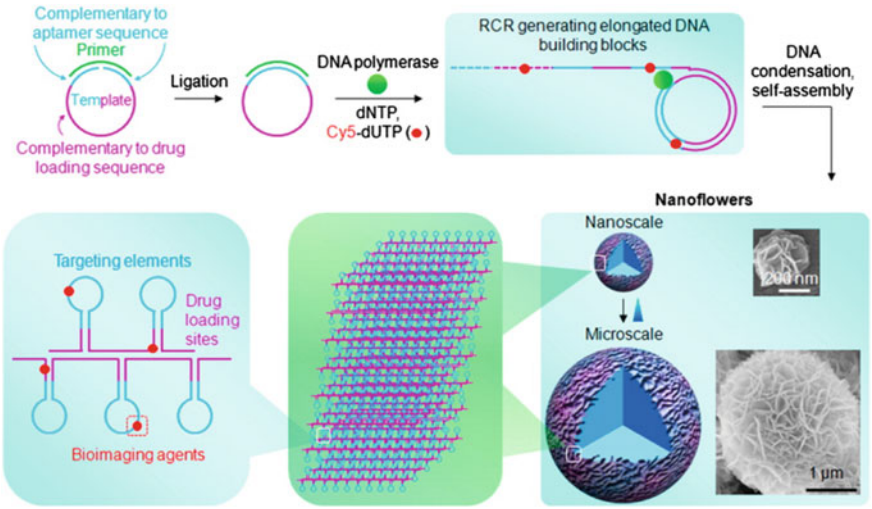

Fig. 10.10 Schematic illustration of noncanonical self-assembly of multifunctional DNA NFs. The linear DNA template was first ligated to form a circular template for RCR using Φ29 DNA polymerase and a primer. RCR generated a large amount of elongated non-nicked concatemer DNA with each unit complementary to the template. These DNAs then served as building blocks to self-assemble monodisperse, densely packed, and hierarchical DNA NFs. NF sizes are tunable with diameters ranging from ~200 nm to several micrometers, as shown by the representative SEM images. The multifunctional NFs can be generated by tailoring the template to carry multiple complements of functional nucleic acids, e.g., aptamers and drug loading sites, or incorporating via primers or modified deoxynucleotides, such as Cy5-dUTP, which can be applied for target cancer cell recognition, bioimaging, and targeted drug delivery. Reprinted with the permission from Ref. [97]. Copyright 2013 American Chemical Society

multiple fluorophores via either chemical conjugation or physical intercalation with enhanced fluorescence signals for effective cancer detection. The ability of self-assembling aptNDs in situ on target living cells could also be useful for cell surface localized bioanalysis and regulation of biological activity. However, DNA-based amplification methods usually require an extra 1–2 h of reaction time and washing steps, thereby hindering the real-time monitoring.

10.7 Conclusion and Outlook

Aptamers as chemical antibodies have become increasingly important molecular tools for cancer cell detection, because of their numerous merits, including high affinity, high specificity, small size, minimal immunogenicity, stable structures, and ease of synthesis. Moreover, aptamers can be readily modified with various functional groups for their conjugation with nanomaterials. Meanwhile, the excellent optical, electrochemical, magnetic, and mechanical properties of nanomaterials

make them good candidates for signal generation and transduction. Combining the unique properties of aptamers and nanomaterials, the aptamer-nanomaterial conjugates can serve as smart biosensing system for cancer diagnostics. While the specificity of aptamers can guarantee the targeted detection or binding of nanomaterials, the coupling of nanomaterials also enhance the binding ability of aptamers with high loading capacity, good stability, and significant signal amplification, leading to highly efficient cancer cell recognition.

While aptamer-nanomaterial conjugates have shown promise in their applications for cancer cell detection, most applications are still in the experimental stage with many challenges ahead. For example, compared with buffer solutions, the cellular environment is obviously much more complex. Proper attention is thus required to nonspecific adsorption of nontarget biomolecules in living cells onto nanomaterials, which might result in false signals. Therefore, the 3D nanostructures and surfaces of nanomaterials must be engineered for reducing nonspecific binding and maintaining aptamers' affinity, such as introducing spacers into the scaffold and changing the charge on the nanomaterial's surface. Meanwhile, the potential toxicity and long-term health effects of some nanomaterials to the human body are still not very clear [100–104]. To address this issue, surface charge, particle size, coating, the biocompatibility, and biodegradability of conjugates need to be carefully considered. From a natural perspective, DNA nanostructures without inorganic cores, such as DNA micelles and DNA nanoflowers, may be ideal platforms for cellular assays with low cytotoxicity even at high concentrations.

In the future, much attention should be paid to the transformation of these scientific achievements of aptamer-nanomaterial conjugates into clinical applications. It is necessary to strengthen the performance of the aptamers by developing novel aptamers directed toward clinically relevant targets. Meanwhile, the creation of novel nanomaterials suitable for clinical applications is also equally important. Many nanomaterials not only have signal transduction ability but also possess efficient therapeutic effect, which have been summarized in other chapters of this book. Therefore, multi-modularity of aptamer-nanomaterial conjugates for targeted cancer detection, image, and therapy is the trend for future clinical practicality of aptamer-nanomaterial conjugate systems. Meanwhile, circulating tumor cells (CTCs), which are the tumor cells identified in transit within the blood stream, are important for understanding the biology of metastasis and regarded as a biomarker for tumor genotype identification during treatment and disease progression [105–107]. However, CTCs are admixed with blood components and are thus rare, making their enrichment and detection a major technological challenge. The aptamer-nanomaterial conjugates with high sensitivity and high specificity have the great potential to solve this problem by enriching and detecting CTCs in blood for early cancer diagnosis.

References

1. Hanahan D, Weinberg RA (2011) Hallmarks of cancer: the next generation. Cell 144 (5):646–674
2. Siegel R, DeSantis C, Virgo K, Stein K, Mariotto A, Smith T, Cooper D, Gansler T, Lerro C, Fedewa S, Lin CC, Leach C, Cannady RS, Cho HS, Scoppa S, Hachey M, Kirch R, Jemal A, Ward E (2012) Cancer treatment and survivorship statistics. Ca-Cancer J Clin 62(4):220–241
3. Siegel R, Ma JM, Zou ZH, Jemal A (2014) Cancer statistics. Ca-Cancer J Clin 64(1):9–29
4. Balch WE, Morimoto RI, Dillin A, Kelly JW (2008) Adapting proteostasis for disease intervention. Science 319(5865):916–919
5. Sidransky D (2002) Emerging molecular markers of cancer. Nat Rev Cancer 2(3):210–219
6. Wulfkuhle JD, Liotta LA, Petricoin EF (2003) Proteomic applications for the early detection of cancer. Nat Rev Cancer 3(4):267–275
7. Finn OJ (2008) Molecular origins of cancer—cancer immunology. New Engl J Med 358 (25):2704–2715
8. Tuerk C, Gold L (1990) Systematic evolution of ligands by exponential enrichment: RNA ligands to bacteriophage T4 DNA polymerase. Science 249(4968):505–510
9. Ellington AD, Szostak JW (1990) In vitro selection of RNA molecules that bind specific ligands. Nature 346(6287):818–822
10. Shangguan D, Li Y, Tang ZW, Cao ZHC, Chen HW, Mallikaratchy P, Sefah K, Yang CYJ, Tan WH (2006) Aptamers evolved from live cells as effective molecular probes for cancer study. Proc Natl Acad Sci U S A 103(32):11838–11843
11. Fang XH, Tan WH (2010) Aptamers generated from cell-SELEX for molecular medicine: a chemical biology approach. Acc Chem Res 43(1):48–57
12. Tan WH, Donovan MJ, Jiang JH (2013) Aptamers from cell-based selection for bioanalytical applications. Chem Rev 113(4):2842–2862
13. Murphy CJ, San TK, Gole AM, Orendorff CJ, Gao JX, Gou L, Hunyadi SE, Li T (2005) Anisotropic metal nanoparticles: synthesis, assembly, and optical applications. J Phys Chem B 109(29):13857–13870
14. Murphy CJ, Gole AM, Stone JW, Sisco PN, Alkilany AM, Goldsmith EC, Baxter SC (2008) Gold nanoparticles in biology: beyond toxicity to cellular imaging. Acc Chem Res 41 (12):1721–1730
15. Burns A, Ow H, Wiesner U (2006) Fluorescent core-shell silica nanoparticles: towards "lab on a particle" architectures for nanobiotechnology. Chem Soc Rev 35(11):1028–1042
16. Gao JH, Gu HW, Xu B (2009) Multifunctional magnetic nanoparticles: design, synthesis, and biomedical applications. Acc Chem Res 42(8):1097–1107
17. Owens DE, Peppas NA (2006) Opsonization, biodistribution, and pharmacokinetics of polymeric nanoparticles. Int J Pharm 307(1):93–102
18. Zheng J, Nicovich PR, Dickson RM (2007) Highly fluorescent noble-metal quantum dots. Annu Rev Phys Chem 58:409–431
19. Huang XH, Neretina S, El-Sayed MA (2009) Gold nanorods: from synthesis and properties to biological and biomedical applications. Adv Mater 21(48):4880–4910
20. Lu W, Lieber CM (2006) Semiconductor nanowires. J Phys D Appl Phys 39(21):R387–R406
21. Tasis D, Tagmatarchis N, Bianco A, Prato M (2006) Chemistry of carbon nanotubes. Chem Rev 106(3):1105–1136
22. Feldkamp U, Niemeyer CM (2006) Rational design of DNA nanoarchitectures. Angew Chem Int Edit 45(12):1856–1876
23. Pinheiro AV, Han DR, Shih WM, Yan H (2011) Challenges and opportunities for structural DNA nanotechnology. Nat Nanotechnol 6(12):763–772
24. Rosi NL, Mirkin CA (2005) Nanostructures in biodiagnostics. Chem Rev 105(4):1547–1562
25. De M, Ghosh PS, Rotello VM (2008) Applications of nanoparticles in biology. Adv Mater 20 (22):4225–4241

26. Chen XL, Huang YF, Tan WH (2008) Using aptamer-nanoparticle conjugates for cancer cells detection. J Biomed Nanotechnol 4(4):400–409
27. Wang H, Yang RH, Yang L, Tan WH (2009) Nucleic acid conjugated nanomaterials for enhanced molecular recognition. ACS Nano 3(9):2451–2460
28. Chen T, Shukoor MI, Chen Y, Yuan QA, Zhu Z, Zhao ZL, Gulbakan B, Tan WH (2011) Aptamer-conjugated nanomaterials for bioanalysis and biotechnology applications. Nanoscale 3(2):546–556
29. Yang L, Zhang XB, Ye M, Jiang JH, Yang RH, Fu T, Chen Y, Wang KM, Liu C, Tan WH (2011) Aptamer-conjugated nanomaterials and their applications. Adv Drug Deliver Rev 63 (14–15):1361–1370
30. Kong RM, Chen Z, Ye M, Zhang XB, Tan WH (2011) Cell-SELEX-based aptamer-conjugated nanomaterials for enhanced targeting of cancer cells. Sci China Chem 54 (8):1218–1226
31. Liang H, Zhang XB, Lv YF, Gong L, Wang RW, Zhu XY, Yang RH, Tan WH (2014) Functional DNA-containing nanomaterials: cellular applications in biosensing, imaging, and targeted therapy. Acc Chem Res 47(6):1891–1901
32. Liu QL, Jin C, Wang YY, Fang XH, Zhang XB, Chen Z, Tan WH (2014) Aptamer-conjugated nanomaterials for specific cancer cell recognition and targeted cancer therapy. NPG Asia Mater 6:e95
33. Giljohann DA, Seferos DS, Daniel WL, Massich MD, Patel PC, Mirkin CA (2010) Gold nanoparticles for biology and medicine. Angew Chem Int Edit 49(19):3280–3294
34. Saha K, Agasti SS, Kim C, Li XN, Rotello VM (2012) Gold nanoparticles in chemical and biological sensing. Chem Rev 112(5):2739–2779
35. Zhang JN, Liu B, Liu HX, Zhang XB, Tan WH (2013) Aptamer-conjugated gold nanoparticles for bioanalysis. Nanomedicine 8(6):983–993
36. Dykman L, Khlebtsov N (2012) Gold nanoparticles in biomedical applications: recent advances and perspectives. Chem Soc Rev 41(6):2256–2282
37. Ghosh SK, Pal T (2007) Interparticle coupling effect on the surface plasmon resonance of gold nanoparticles: from theory to applications. Chem Rev 107(11):4797–4862
38. Medley CD, Smith JE, Tang Z, Wu Y, Bamrungsap S, Tan WH (2008) Gold nanoparticle-based colorimetric assay for the direct detection of cancerous cells. Anal Chem 80 (4):1067–1072
39. Liu GD, Mao X, Phillips JA, Xu H, Tan WH, Zeng LW (2009) Aptamer-nanoparticle Strip biosensor for sensitive detection of cancer cells. Anal Chem 81(24):10013–10018
40. Lu W, Arumugam SR, Senapati D, Singh AK, Arbneshi T, Khan SA, Yu H, Ray PC (2010) Multifunctional oval-shaped gold-nanoparticle-based selective detection of breast cancer cells using simple colorimetric and highly sensitive two-photon scattering assay. ACS Nano 4(3):1739–1749
41. Huang YF, Chang HT, Tan WH (2008) Cancer cell targeting using multiple aptamers conjugated on nanorods. Anal Chem 80(3):567–572
42. Yu JH, Choi SM, Richards CI, Antoku Y, Dickson RM (2008) Live cell surface labeling with fluorescent Ag nanocluster conjugates. Photochem Photobiol 84(6):1435–1439
43. Petty JT, Zheng J, Hud NV, Dickson RM (2004) DNA-templated Ag nanocluster formation. J Am Chem Soc 126(16):5207–5212
44. Richards CI, Choi S, Hsiang JC, Antoku Y, Vosch T, Bongiorno A, Tzeng YL, Dickson RM (2008) Oligonucleotide-stabilized Ag nanocluster fluorophores. J Am Chem Soc 130 (15):5038
45. Yu JH, Choi S, Dickson RM (2009) Shuttle-based fluorogenic silver-cluster biolabels. Angew Chem Int Edit 48(2):318–320
46. Yang SW, Vosch T (2011) Rapid detection of microRNA by a silver nanocluster DNA probe. Anal Chem 83(18):6935–6939
47. Sharma J, Rocha RC, Phipps ML, Yeh HC, Balatsky KA, Vu DM, Shreve AP, Werner JH, Martinez JS (2012) A DNA-templated fluorescent silver nanocluster with enhanced stability. Nanoscale 4(14):4107–4110

48. Yin JJ, He XX, Wang KM, Qing ZH, Wu X, Shi H, Yang XH (2012) One-step engineering of silver nanoclusters-aptamer assemblies as luminescent labels to target tumor cells. Nanoscale 4(1):110–112
49. Yeh HC, Sharma J, Han JJ, Martinez JS, Werner JH (2010) A DNA-silver nanocluster probe that fluoresces upon hybridization. Nano Lett 10(8):3106–3110
50. Yin JJ, He XX, Wang KM, Xu FZ, Shangguan JF, He DG, Shi H (2013) Label-free and turn-on aptamer strategy for cancer cells detection based on a DNA-silver nanocluster fluorescence upon recognition-induced hybridization. Anal Chem 85(24):12011–12019
51. Brus L (2008) Noble metal nanocrystals: plasmon electron transfer photochemistry and single-molecule Raman spectroscopy. Acc Chem Res 41(12):1742–1749
52. Sajanlal PR, Pradeep T (2010) Bimetallic flowers, beads, and buds: synthesis, characterization, and Raman imaging of unique mesostructures. Langmuir 26(1):456–465
53. Wu P, Gao Y, Zhang H, Cai C (2012) Aptamer-guided silver-gold bimetallic nanostructures with highly active surface-enhanced Raman scattering for specific detection and near-infrared photothermal therapy of human breast cancer cells. Anal Chem 84(18):7692–7699
54. Gupta S, Huda S, Kilpatrick PK, Velev OD (2007) Characterization and optimization of gold nanoparticle-based silver-enhanced immunoassays. Anal Chem 79(10):3810–3820
55. Zhu Y, Chandra P, Shim YB (2013) Ultrasensitive and selective electrochemical diagnosis of breast cancer based on a hydrazine-Au nanoparticle-aptamer bioconjugate. Anal Chem 85 (2):1058–1064
56. Alivisatos AP (1996) Semiconductor clusters, nanocrystals, and quantum dots. Science 271 (5251):933–937
57. Kim JY, Voznyy O, Zhitomirsky D, Sargent EH (2013) 25th anniversary article: colloidal quantum dot materials and devices: a quarter-century of advances. Adv Mater 25 (36):4986–5010
58. Michalet X, Pinaud FF, Bentolila LA, Tsay JM, Doose S, Li JJ, Sundaresan G, Wu AM, Gambhir SS, Weiss S (2005) Quantum dots for live cells, in vivo imaging, and diagnostics. Science 307(5709):538–544
59. Medintz IL, Uyeda HT, Goldman ER, Mattoussi H (2005) Quantum dot bioconjugates for imaging, labelling and sensing. Nat Mater 4(6):435–446
60. Resch-Genger U, Grabolle M, Cavaliere-Jaricot S, Nitschke R, Nann T (2008) Quantum dots versus organic dyes as fluorescent labels. Nat Methods 5(9):763–775
61. Pinaud F, Clarke S, Sittner A, Dahan M (2010) Probing cellular events, one quantum dot at a time. Nat Methods 7(4):275–285
62. Freeman R, Willner I (2012) Optical molecular sensing with semiconductor quantum dots (QDs). Chem Soc Rev 41(10):4067–4085
63. Wu P, Yan XP (2013) Doped quantum dots for chemo/biosensing and bioimaging. Chem Soc Rev 42(12):5489–5521
64. Zhang J, Jia X, Lv XJ, Deng YL, Xie HY (2010) Fluorescent quantum dot-labeled aptamer bioprobes specifically targeting mouse liver cancer cells. Talanta 81(1–2):505–509
65. Li ZM, Huang P, He R, Lin J, Yang S, Zhang XJ, Ren QS, Cui DX (2010) Aptamer-conjugated dendrimer-modified quantum dots for cancer cell targeting and imaging. Mater Lett 64(3):375–378
66. Ko MH, Kim S, Kang WJ, Lee JH, Kang H, Moon SH, Hwang DW, Ko HY, Lee DS (2009) In vitro derby imaging of cancer biomarkers using quantum dots. Small 5(10):1207–1212
67. Kang WJ, Chae JR, Cho YL, Lee JD, Kim S (2009) Multiplex imaging of single tumor cells using quantum-dot-conjugated aptamers. Small 5(22):2519–2522
68. Ding CF, Ge Y, Zhang SS (2010) Electrochemical and electrochemiluminescence determination of cancer cells based on aptamers and magnetic beads. Chem Eur J 16 (35):10707–10714
69. Zhong H, Zhang QL, Zhang SS (2011) High-intensity fluorescence imaging and sensitive electrochemical detection of cancer cells by using an extracellular supramolecular reticular dna-quantum dot sheath. Chem Eur J 17(30):8388–8394

70. Smith JE, Wang L, Tan WT (2006) Bioconjugated silica-coated nanoparticles for bioseparation and bioanalysis. Trac Trend Anal Chem 25(9):848–855
71. Wang L, Zhao WJ, Tan WH (2008) Bioconjugated silica nanoparticles: development and applications. Nano Res 1(2):99–115
72. Stöber W, Fink A (1968) Controlled growth of monodisperse silica spheres in the micron size range. J Colloid Interface Sci 26:62–66
73. Osseoasare K, Arriagada FJ (1990) Preparation of Sio_2 nanoparticles in a nonionic reverse micellar system. Colloid Surf 50:321–339
74. Yan JL, Estevez MC, Smith JE, Wang KM, He XX, Wang L, Tan WH (2007) Dye-doped nanoparticles for bioanalysis. Nano Today 2(3):44–50
75. Estévez MC, O'Donoghue MB, Chen XL, Tan WH (2009) Highly fluorescent dye-doped silica nanoparticles increase flow cytometry sensitivity for cancer cell monitoring. Nano Res 2(6):448–461
76. Zhao X, Hilliard LR, Mechery SJ, Wang Y, Bagwe RP, Jin S, Tan W (2004) A rapid bioassay for single bacterial cell quantitation using bioconjugated nanoparticles. Proc Natl Acad Sci U S A 101(42):15027–15032
77. Deng T, Li JS, Zhang LL, Jiang JH, Chen JN, Shen GL, Yu RQ (2010) A sensitive fluorescence anisotropy method for the direct detection of cancer cells in whole blood based on aptamer-conjugated near-infrared fluorescent nanoparticles. Biosens Bioelectron 25 (7):1587–1591
78. Herr JK, Smith JE, Medley CD, Shangguan DH, Tan WH (2006) Aptamer-conjugated nanoparticles for selective collection and detection of cancer cells. Anal Chem 78 (9):2918–2924
79. Smith JE, Medley CD, Tang ZW, Shangguan D, Lofton C, Tan WH (2007) Aptamer-conjugated nanoparticles for the collection and detection of multiple cancer cells. Anal Chem 79(8):3075–3082
80. Medley CD, Bamrungsap S, Tan WH, Smith JE (2011) Aptamer-conjugated nanoparticles for cancer cell detection. Anal Chem 83(3):727–734
81. Cai L, Chen ZZ, Chen MY, Tang HW, Pang DW (2013) MUC-1 aptamer-conjugated dye-doped silica nanoparticles for MCF-7 cells detection. Biomaterials 34(2):371–381
82. Wang L, Tan WH (2006) Multicolor FRET silica nanoparticles by single wavelength excitation. Nano Lett 6(1):84–88
83. Chen XL, Estevez MC, Zhu Z, Huang YF, Chen Y, Wang L, Tan WH (2009) Using aptamer-conjugated fluorescence resonance energy transfer nanoparticles for multiplexed cancer cell monitoring. Anal Chem 81(16):7009–7014
84. Lu AH, Salabas EL, Schuth F (2007) Magnetic nanoparticles: synthesis, protection, functionalization, and application. Angew Chem Int Edit 46(8):1222–1244
85. Laurent S, Forge D, Port M, Roch A, Robic C, Elst LV, Muller RN (2008) Magnetic iron oxide nanoparticles: synthesis, stabilization, vectorization, physicochemical characterizations, and biological applications. Chem Rev 108(6):2064–2110
86. Sun C, Lee JSH, Zhang MQ (2008) Magnetic nanoparticles in MR imaging and drug delivery. Adv Drug Deliver Rev 60(11):1252–1265
87. Bamrungsap S, Chen T, Shukoor MI, Chen Z, Sefah K, Chen Y, Tan WH (2012) Pattern recognition of cancer cells using aptamer-conjugated magnetic nanoparticles. ACS Nano 6 (5):3974–3981
88. Cheon J, Lee JH (2008) Synergistically integrated nanoparticles as multimodal probes for nanobiotechnology. Acc Chem Res 41(12):1630–1640
89. Hwang DW, Ko HY, Lee JH, Kang H, Ryu SH, Song IC, Lee DS, Kim S (2010) A nucleolin-targeted multimodal nanoparticle imaging probe for tracking cancer cells using an aptamer. J Nucl Med 51(1):98–105
90. Zhao Z, Fan H, Zhou G, Bai H, Liang H, Wang R, Zhang X, Tan W (2014) Activatable fluorescence/MRI bimodal platform for tumor cell imaging via MnO_2 nanosheet-aptamer nanoprobe. J Am Chem Soc 136(32):11220–11223
91. Bath J, Turberfield AJ (2007) DNA nanomachines. Nat Nanotechnol 2(5):275–284

92. Seeman NC (2010) Nanomaterials based on DNA. Annu Rev Biochem 79:65–87
93. Wilner OI, Willner I (2012) Functionalized DNA nanostructures. Chem Rev 112 (4):2528–2556
94. Sacca B, Niemeyer CM (2012) DNA origami: the art of folding DNA. Angew Chem Int Edit 51(1):58–66
95. Liu HP, Zhu Z, Kang HZ, Wu YR, Sefan K, Tan WH (2010) DNA-based micelles: synthesis, micellar properties and size-dependent cell permeability. Chem Eur J 16(12):3791–3797
96. Wu YR, Sefah K, Liu HP, Wang RW, Tan WH (2010) DNA aptamer-micelle as an efficient detection/delivery vehicle toward cancer cells. Proc Natl Acad Sci U S A 107(1):5–10
97. Zhu GZ, Hu R, Zhao ZL, Chen Z, Zhang XB, Tan WH (2013) Noncanonical self-assembly of multifunctional DNA nanoflowers for biomedical applications. J Am Chem Soc 135 (44):16438–16445
98. Hu R, Zhang XB, Zhao ZL, Zhu GZ, Chen T, Fu T, Tan WH (2014) DNA nanoflowers for multiplexed cellular imaging and traceable targeted drug delivery. Angew Chem Int Edit 53 (23):5821–5826
99. Zhu GZ, Zhang SF, Song EQ, Zheng J, Hu R, Fang XH, Tan WH (2013) Building fluorescent DNA nanodevices on target living cell surfaces. Angew Chem Int Edit 52 (21):5490–5496
100. Lewinski N, Colvin V, Drezek R (2008) Cytotoxicity of nanoparticles. Small 4(1):26–49
101. Aillon KL, Xie YM, El-Gendy N, Berkland CJ, Forrest ML (2009) Effects of nanomaterial physicochemical properties on in vivo toxicity. Adv Drug Deliver Rev 61(6):457–466
102. Sharifi S, Behzadi S, Laurent S, Forrest ML, Stroeve P, Mahmoudi M (2012) Toxicity of nanomaterials. Chem Soc Rev 41(6):2323–2343
103. Joris F, Manshian BB, Peynshaert K, De Smedt SC, Braeckmans K, Soenen SJ (2013) Assessing nanoparticle toxicity in cell-based assays: influence of cell culture parameters and optimized models for bridging the in vitro-in vivo gap. Chem Soc Rev 42(21):8339–8359
104. Peynshaert K, Manshian BB, Joris F, Braeckmans K, De Smedt SC, Demeester J, Soenen SJ (2014) Exploiting intrinsic nanoparticle toxicity: the pros and cons of nanoparticle-induced autophagy in biomedical research. Chem Rev 114(15):7581–7609
105. Pantel K, Alix-Panabieres C (2010) Circulating tumour cells in cancer patients: challenges and perspectives. Trends Mol Med 16(9):398–406
106. Chaffer CL, Weinberg RA (2011) A perspective on cancer cell metastasis. Science 331 (6024):1559–1564
107. Yu M, Stott S, Toner M, Maheswaran S, Haber DA (2011) Circulating tumor cells: approaches to isolation and characterization. J Cell Biol 192(3):373–382

Chapter 11
Cell-Specific Aptamers for Molecular Imaging

Jing Zheng, Chunmei Li and Ronghua Yang

Abstract Aptamers, single-stranded oligonucleotides, are an important class of molecular targeting ligands. Since their discovery, aptamers have been rapidly translated into bioanalytical practice. They have been approved as molecular imaging and therapeutics tools. Aptamers also possess several properties that make them uniquely suited to molecular imaging. This chapter aims to provide a summary of aptamers' advantages as targeting ligands and their applications in molecular imaging.

Keywords Aptamer · Molecular imaging · Optical imaging · Nanomaterials · MRI imaging

11.1 Introduction

Molecular imaging has been defined as the in vivo characterization and measurement of biological processes at the cellular and molecular level, or more broadly as a technique to directly or indirectly monitor and record the spatiotemporal distribution of molecular or cellular processes for biochemical, biological, diagnostic, or therapeutic application [1, 2]. To attain truly targeted imaging of specific molecules which exist in relatively low concentrations in living tissues, the imaging techniques must

J. Zheng (✉) · R. Yang (✉)
State Key Laboratory of Chemo/Biosensing and Chemometrics, College of Chemistry and Chemical Engineering, College of Biology, and Collaborative Innovation Center for Chemistry and Molecular Medicine, Hunan University, 410082 Changsha, China
e-mail: zhengjing2013@hnu.edu.cn

R. Yang
e-mail: yangrh@pku.edu.cn

C. Li
Key Laboratory of Luminescent and Real-Time Analytical Chemistry, Ministry of Education, College of Pharmaceutical Sciences, Southwest University, 400715 Chongqing, China

W. Tan and X. Fang (eds.), *Aptamers Selected by Cell-SELEX for Theranostics*,
DOI 10.1007/978-3-662-46226-3_11

be high sensitive. Imaging modalities in the clinic generally include optical imaging, magnetic resonance imaging (MRI), sound, and positron emission tomography (PET) or single-photon emission computed tomography (SPECT) [3].

Development of sensitive and specific molecular tools is one of the central challenges in cell, tissue, and animal imaging. Aptamers are single-stranded RNA or DNA oligonucleotides with unique intramolecular conformations that hold distinct binding properties to various targets, including small molecules, proteins, and even entire organisms [4–6]. As a small, polyanionic, and nonimmunogenic type of probe, aptamers may exhibit faster tissue penetration and uptake, shorter residence in blood and nontarget organs, and higher ratio of target accumulation, thus affording great potential for in vivo cancer imaging [7, 8]. Furthermore, aptamers have inherent advantages as imaging agents, such as the ability to withstand high heat and denaturants, rapid chemical synthesis, and nonimmunogenicity, thus affording great potential for in vivo tumor imaging [9, 10]. In this chapter, we will summarize cell-specific aptamers for molecular imaging including mice, tissue, and cell combing with various aforementioned imaging modes.

11.2 Optical Imaging

Optical methods offer several significant advantages over the routine imaging methods, including (a) noninvasiveness through the use of safe, nonionizing radiation, (b) display of contrast between soft tissues based on optical properties of the tissue, (c) a facility for continuous bedside monitoring, and (d) high spatial resolution (less than 0.5-μm lateral resolution in the visible range) [11]. Optical imaging, including fluorescence spectrum imaging and surface-enhanced Raman scattering (SERS) imaging, has sensitivity and can be "targeted" if the signal output element is conjugated to a targeting ligand. By virtue of being "switchable," optical imaging can result in very high target-to-background ratios. Switchable or activatable optical probes are unique in the field of molecular imaging since these agents can be turned on in specific environments but otherwise remain undetectable [12]. These advantages must be balanced against the lack of quantitation with optical imaging due to unpredictable light scattering and absorption, especially when the object of interest is deep within the tissue. Combing with aptamers, which is small, polyanionic types of probe, sensitive targeted-optical imaging could be realized.

First reported by Tyagi and Kramer in 1996, molecular beacons (MBs) are oligonucleotide hybridization probes that can report the presence of specific nucleic acids in homogeneous solutions [13]. This single-stranded DNA molecule consists of a stem-and-loop structure doubly labeled with a fluorophore and a quencher group on each end. In the absence of targets, MBs act like switches that are normally closed by the stem part, and in the "off" position, little fluorescence background is noted by the effect of quenching. However, upon binding with their targets, conformational changes open the hairpin, and fluorescence is turned "on" [14]. MBs are characterized by simple operation and high sensitivity and

specificity. As such, they have become a class of nucleic acid probes. A novel nucleic acid probe called molecular aptamer beacon (MAB) is developed by the excellent combination of the high binding affinity of aptamers and the sensitive signal transduction mechanism of MBs, thus, widely used in molecular imaging. MAB exhibit faster tissue penetration and uptake, shorter residence in blood and nontarget organs, and higher ratio of target accumulation, thus affording great potential for intracellular biomolecule such as mRNA, ATP imaging or even in vivo cancer imaging [15, 16]. Tan group designed a self-delivered MB for photoinitiated real-time imaging and detection of mRNA in living cells via direct hybridization of an extended internalizing aptamer and a MB. With this fluorescent aptamer as an internalizing carrier, the MB can be efficiently delivered into the cytoplasm of targeted cells, and its internalized amount as well as its intracellular distribution can be tracked before photoactivation [17]. As further important in vivo cancer imaging, Tan group firstly reported MAB probes with a fluorophore and a quencher attached at either terminus for tumor imaging in a mouse, as shown in Fig. 11.1 [18]. The results showed that the MAB can effectively recognize tumors with high sensitivity and specificity, thus establishing the efficacy of fluorescent MAB for diagnostic applications. In the absence of a target, the MAB was hairpin structured, resulting in quenched fluorescence. As expected, MAB could be activated by target cancer cells with fast restoration of fluorescence achieved in the tumor site compared to other areas. To further improve the serum stability and unabiding imaging window in vivo, Wang et al. develop a novel locked nucleic acid (LNA)/DNA chimeric aptamer probe through proper LNA incorporation and supplemented 3′-3′-thymidine (3′-3′-T) capping. TD05, a DNA aptamer against lymphoma Ramos cells, being used as the model and a series of modification strategies were designed and optimized [19]. The results show this strategy might be of great potentials to generate more aptamer probes that are stable and nuclease-resistant for tumor imaging in real biological systems.

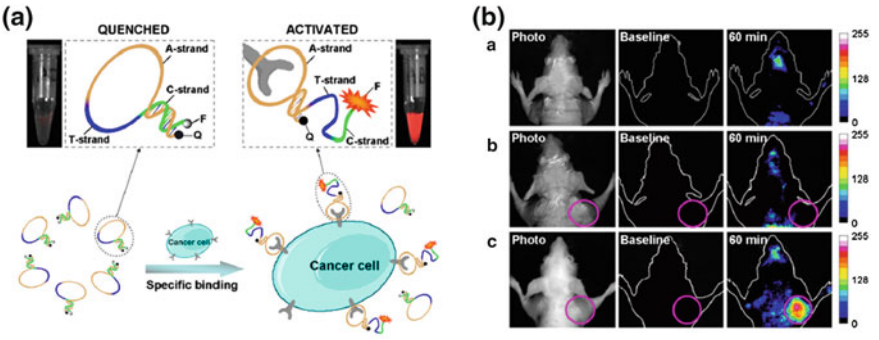

Fig. 11.1 **a** Schematic representation of the novel strategy for in vivo cancer imaging using activatable MAB based on cell membrane protein-triggered conformation alteration. **b** In vivo specific fluorescence imaging of the CCRF-CEM tumor with the activatable MAB. Reprinted from Ref. [18] by permission of PNAS

The past few years have also witnessed many advances in the synthesis and characterization of a variety of nanomaterials, such as metallic, carbon and silica, magnetic, semiconductor quantum dots [20, 21]. These nanomaterials normally have a large surface area coupled with unique size and shape, as well as composition-dependent physical and chemical properties, including surface plasmon resonance (SPR), fluorescence, magnetism, and/or loading ability [22]. Nanomaterial modification is the key to target specificity. By combining the inherent features of nanomaterials with the specific recognition ability of aptamers, a range of nanomaterial-aptamer conjugates have proven their utility in optical imaging.

11.2.1 Gold Nanomaterials

It is well known that gold nanomaterials have unusual optical and electronic properties, high stability and biological compatibility, controllable morphology and size dispersion, and easy surface functionalization [23–25]. From the standpoints of engineering and application, aptamer-conjugated gold nanomaterials provide a powerful platform to facilitate targeted recognition, detection, and imaging. Gold nanoparticles (AuNPs) used as a colorimetric reporter rely on their unique SPR property, which causes color changes that result from both scattering and electronic dipole–dipole coupling between neighboring particles [26]. Dispersed AuNPs having interparticle distances substantially greater than their average particle diameter appear red, whereas the color of the aggregates changes to purple as the interparticle distance drops below the average particle diameter. Based on this principle, there are two general types of target-induced colorimetric assays in homogeneous solution using oligonucleotide-modified AuNPs: assembly and disassembly. In assembly assays, the color of the AuNP solution changes from red (dispersed particles) to purple (aggregates). A classical work from the Mirkin group employed this assembly assay to detect DNA. Two designed pieces of DNA, which were each complementary to part of the target DNA, were immobilized onto the surfaces of the AuNPs. Target DNA acted as a cross-linker, leading to aggregation of the AuNPs. With the introduction of aptamers, many more kinds of analytes can be monitored using this platform, but on the basis of different mechanisms, to realize molecular imaging [27]. Wang et al. developed a dot-blot assay for the detection of thrombin based on aptamer–AuNP conjugates. They first immobilized protein on the membrane. A color change from colorless to red was produced when the aptamer–AuNPs bound to the active site of the protein. The aptasensor could be observed by the naked eye and had a detection limit of 14 pM with silver enhancement [28]. Medley et al. constructed a colorimetric assay for the direct imaging of cancer cells. Aptamer–AuNPs were targeted to assemble on the surface of a specific type of cancer cell through the recognition of the aptamer to its target on the cell membrane surface, as shown in the schematic in Fig. 11.2 [29]. In another application, Liu and Liu [30] utilized a pair of aptamers capable of specifically binding Ramos cells for a strip-based assay. A thiolated aptamer

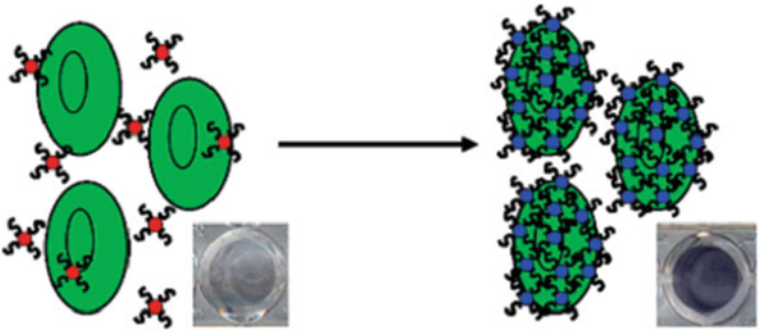

Fig. 11.2 Schematic representation of the ACGNP-based colorimetric assay. Reprinted with permission from Ref. [29]. Copyright (2008) American Chemical Society

(thiol-TD05) was immobilized on the AuNPs, and a biotinylated aptamer (biotin TE02) was immobilized on the strip's test zone. When a sample solution containing Ramos cells was applied to the sample pad, the solution migrated by capillary action past the conjugate pad and then rehydrated the aptamer–AuNP conjugates. Ramos cells interacted with aptamer–AuNPs and continued migrating along the strip until captured on the test zone by a second reaction between Ramos cells and the immobilized TE02 aptamers.

In addition to AuNPs, gold nanorods (NRs) have also been utilized as an effective tool for multiple aptamer immobilization to achieve molecular imaging. Through covalent linkages of fluorophore labeled aptamers on the nanorod surface, Huang et al. were able to increase the binding affinity of otherwise weak-binding aptamers by $\sim$26-fold compared to that of a single aptamer [31]. It was found that $\sim$80 aptamer molecules were bound on each NR. Because the cell surface is much larger than the aggregate of nanoparticles and, hence, contains more binding sites, the performance of molecular recognition could be improved by synergy, in which the combined effect of two or more like-acting components exceeds the sum of the individual effects. In this case, multiple aptamers on each NR contributed to the enhanced binding affinity.

Recent advances in fluorescent metal nanoclusters, especially gold and silver, have attracted a lot of interest in bioimaging and bionanotechnology [32, 33]. It was reported that nanoclusters had excellent photostability, subnanometersize, and low toxicity, which complement the properties of organic dyes and semiconductor quantum dots [34, 35]. Particularly, oligonucleotide-templated silver nanoclusters (AgNCs) have attracted special attention due to their facile synthesis, tunable fluorescence emission, and high photostability. Zhu et al. [36] present a strategy to synthesize aptamer AS1411-functionalized AgNCs with excellent fluorescence through a facile one-pot process, as shown in Fig. 11.3. Confocal laser scanning microscopy and Z-axis scanning confirmed that the AS1411-functionalized AgNCs could be internalized into MCF-7 human breast cancer cells and were able to specifically stain nuclei with red color. Due to the facile synthesis procedure and

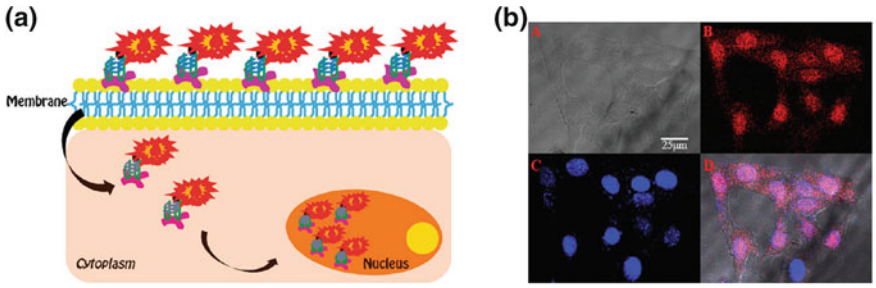

Fig. 11.3 **a** Schematic representation of one-pot synthesis of aptamer-functionalized silver nanoclusters for cell-type-specific imaging. **b** Intracellular distribution of internalized NC-AS1411-T5-stabilized AgNCs. Reprinted with permission from Ref. [36]. Copyright (2012) American Chemical Society

capability of specific target recognition, this fluorescent platform will potentially broaden the applications of AgNCs in biological imaging. In addition, Wang et al. reported a one-step method for the synthesis of DNA-aptamer-templated fluorescent AgNCs. The Sgc8c aptamer strands were immobilized onto AgNCs through cytosine-rich sequence, and the resulting Sgc8c-modified AgNCs showed specific targeting and fluorescent labeling capabilities to CCRF-CEM cancer cell over control cells [37].

SERS is an ultrasensitive vibrational spectroscopic technique to detect molecules on or near the surface of plasmonic nanostructures, greatly extending the role of standard Raman spectroscopy [38]. Since its discovery in the 1970s, SERS has been applied to many analyses, especially in biochemistry and life sciences [39, 40]. The classic application is the direct sensing of various analytes attached to a metallic SERS substrate, yielding both qualitative and quantitative information based on the analytes' SERS spectra. The SERS technique fulfills the requirements of live-cell imaging in the following aspects. First, the use of low laser powers can produce strong signals; therefore, SERS imaging avoids light-induced injury of the cells. Second, the excitation laser spot of the Raman microscope can be focused in a micrometer scale. Together with the nanosized SERS tags, the method can provide high-resolution images that reflect the microenvironment in cells. Third, data acquisition time are short when using the Raman system, enabling real-time and dynamic monitoring of biological processes. Ray's group used monoclonal anti-PSMA antibody- and A9 RNA aptamer-conjugated-shaped Au nanopopcorn as a heat nanogenerator and constructed a multifunctional system for targeted imaging, nanotherapy, and in situ monitoring of photothermal therapy response [41], as shown in Fig. 11.4. The localized heating that occurs during NIR irradiation can cause irreparable damage to the targeted LNCaP human prostate cancer cells. Interestingly, the data allowed linear plotting of percent cancer cell death an SERS intensity change, enabling one to imaging photothermal nanotherapy response during the therapy process. Encouraged by this work, this group also designed a new hybrid nanomaterial using popcorn-shaped, gold nanoparticle-attached, carbon

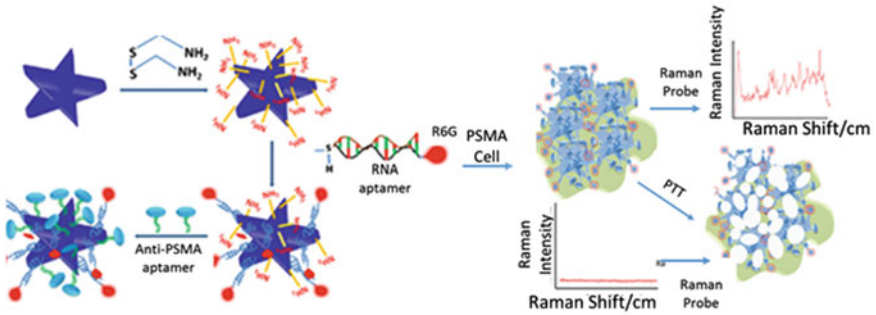

Fig. 11.4 Schematic representation of the synthesis of monoclonal anti-PSMA antibody- and A9 RNA aptamer-conjugated popcorn-shaped gold nanoparticles. Reprinted with permission from Ref. [41]. Copyright (2010) American Chemical Society

nanotubes (CNTs) for diagnosis and selective photothermal treatment [42]. For SERS imaging purposes, they directly incorporated Raman spectroscopic properties (D-band at 1,340 cm^{-1} and G-band at 1,590 cm^{-1}) in individual CNTs instead of using an organic Raman reporter. After labeling with S6 aptamer, the hybrid nanomaterial-based SERS assay is highly sensitive to imaging the targeted human breast cancer cells (SK-BR cell line).

11.2.2 Carbon Nanomaterials

Since the discovery of fullerene in 1985, CNTs in 1991, and graphene in 2004, various carbon nanomaterials (NMs) have been extensively studied [43–46]. The huge application potentials of these promising NMs in diverse areas, such as materials, electronic, environmental, and biomedical areas, have strongly stimulated the production and consumption of carbon NMs. Single-walled carbon nanotubes (SWNTs) and graphene oxide (GO) have powerful quenching capability for organic dyes. A variety of complexes, including DNA strands, can be adsorbed noncovalently onto the surface of SWNTs and GO by virtue of π–π stacking [45, 46]. Thus, traditional aptamer-based fluorescent systems can be prepared. In 2010, Li et al. reported the demonstration of cellular delivery and in situ molecular imaging in living cells by employing graphene oxide nanosheets (GO-nS) as DNA cargo and imaging platforms. Due to the particular interaction between GO and DNA molecules, an aptamer/GO-nS nanocomplex was designed and used as a real-time imaging platform in living cell systems, as shown in Fig. 11.5 [47]. An aptamer is an artificial oligonucleotide receptor derived from in vitro selection with high specificity, and affinity for ATP was chosen as model, and results demonstrate that uptake of aptamer-fluorescein/GO-nS nanocomplex and cellular target monitoring were realized successfully. Tan group designed an ATP aptamer molecular beacon

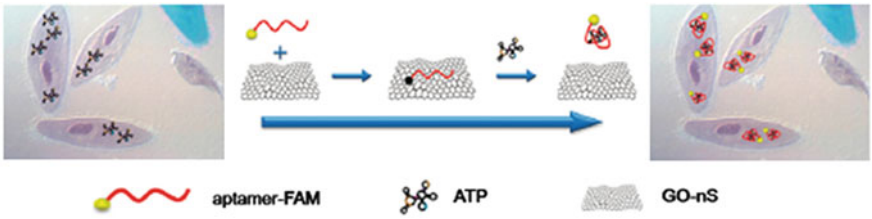

Fig. 11.5 Schematic illustration of in situ molecular probing in living cells by using aptamer/GO-nS nanocomplex. Reprinted with permission from Ref. [47]. Copyright (2010) American Chemical Society

(AAMB) which is adsorbed on GO to form a double quenching platform [48]. The AAMB/GO spontaneously enters cells, and then released and opened by intracellular ATP. The resulting fluorescence recovery can be used to perform ATP live-cell imaging with greatly improved background and signaling.

Two-photon excitation (TPE) with near-infrared (NIR) photons as the excitation source has the unique properties of lower tissue autofluorescence and self-absorption, reduced photodamage and photobleaching, higher spatial resolution, and deeper penetration depth (>500 μm). Recently, Yang group combined the carbon nanomaterials with the TPE technique to develop an aptamer-two-photon dye (TPdye)/GO TPE fluorescent nanosensing conjugate for molecular imaging in living cells and zebra fish [49]. This approach takes advantage of the exceptional quenching capability of GO for the proximate TP dyes and the higher affinity of single-stranded DNA on GO than the aptamer-target complex. Successful in vitro and in vivo imaging of ATP was demonstrated with this sensing strategy.

11.2.3 Functional DNA Self-assembled Nanomaterials

DNA is naturally water-soluble and biocompatible, and it is relatively simple to synthesize DNA with a commercial synthesizer. Recently, DNA has emerged as a favorable material for constructing DNA nanostructures with promising applications in molecular imaging. For functional DNAs, multivalent interaction can result in better affinity and selectivity in contrast to monovalent interaction in the design of high-performance ligands. Inspired by amphiphilic block copolymers, which can self-assemble into different morphologies, the copolymer that contains a hydrophilic DNA segment and a hydrophobic organic polymer unit can form a DNA micelle under certain conditions. Compared with other DNA-conjugated nanoparticles, DNA micelles have no inorganic cores, which would be cytotoxic at high concentrations, and the time required to synthesize DNA micelles can generally be abbreviated. In order to endow DNA micelles with more applicable properties and functions, we chose an aptamer to replace general DNA and conjugated it with a hydrophobic lipid tail. Recently, we reported an MAB-micelle system for

intracellular molecular imaging. This MAB was modified with a lipid tail to form the nanostructure of micelle flares. In the presence of ATP or mRNA, the conformation of the MAB containing the aptamer was altered, leading to the restoration of fluorescence [50, 51]. Thus, it can indicate the presence of the analyte and show exceptional promise for molecular imaging in bioanalysis, disease diagnosis, and drug delivery.

Instead of conventionally used short DNA, long DNA building blocks generated via hybridization chain reaction (HCR) and rolling circle replication (RCR) can also form nanoarchitectures for molecular imaging. Tan group successfully built fluorescent DNA nanodevices on target living cell surfaces by anchoring preformed model nanodevices and by in situ self-assembly of nanodevices through specific aptamer-target interaction [52]. These fluorescent DNA nanodevices consisted of aptamer-tethered nanodevices formed by cascading polymerization of monomeric building blocks. The features of multiple, repetitive, and alternating DNA building blocks in the resultant aptamer nanodevices provide an excellent platform for appropriate positioning of multi-chromophore arrays or multi-component nanofactories, implicating the feasibility of target living cell imaging and pinpoint biomolecular/pharmaceutical analysis or manipulation of biological activities. Latterly, we also present a facile approach to make aptamer-conjugated fluorescent resonance energy transfer (FRET) nanoflowers (NFs) through RCR for multiplexed cellular imaging [53]. The NFs can exhibit multi-fluorescence emissions by a single-wavelength excitation as a result of the DNA matrix covalently incorporated with three dye molecules able to perform FRET. Combined with the ability of traceable targeted drug delivery, these colorful DNA NFs provide a novel system for applications in multiplex fluorescent cellular imaging, effective screening of drugs, and therapeutic protocol development.

11.2.4 Silica Nanomaterials

Fluorescent silica nanomaterials represent an appealing class of nanosystems for optical biosensing and imaging. The most prominent among these materials are silica and organically modified silica, which have several attractive features such as optical transparency, low toxicity, simple and robust synthesis, as well as rich surface chemistry [54]. Functionalized silica nanoparticles (SiNPs) doped with fluorescent dyes appear to be an ideal and flexible platform for developing fluorescence imaging techniques used in living cells and the whole body. Since the silica matrix protects dyes from outside quenching and degrading factors, this enhances the photostability and biocompatibility of the SiNP-based probes. This makes them ideal for real-time and long-time tracking. One nanoparticle can encapsulate large numbers of dye molecules, which amplifies their optical signal and temporal–spatial resolution response. Along with the endocytosis, functionalized SiNPs can be efficiently internalized into cells for noninvasive localization, assessment, and monitoring. These unique characteristics of functionalized SiNPs

substantially support their applications in fluorescence imaging in vivo. Integrating fluorescent dye-doped SiNPs (FNPs) with targeting ligands such as aptamer using various surface modification techniques can greatly improve selective recognition. To fulfill specific recognition, our group immobilized the biotinylated aptamers onto the surfaces of neutravidin-coated FNPs [55]. The FNPs are then functionalized with polyethylene glycol (PEG) to prevent nonspecific interactions with neutravidin and to allow universal binding with biotinylated molecules. These aptamer-conjugated silica NPs have demonstrated low background signal, high signal enhancement, and efficient functionalization for molecular imaging. Multiplexed cancer cells can also be imaging by employing the combination of fluorescence resonance energy transfer (FRET) of FNPs and the conjugation of different aptamers [56]. In addition, Tan group combined fluorophore-doped silica and silica-coated magnetic nanoparticles modified with highly selective aptamers to image and extract CCRF-CEM targeted cells in a variety of mixtures [57]. They also systematically studied the effect of nanoparticle size, conjugation chemistry, and aptamer sequences on the selectivity and sensitivity of the dual-particle assays.

11.2.5 Upconversion Nanoparticles

Lanthanide-doped upconversion nanoparticles (UCNPs) are capable of emitting light in the visible range following photoexcitation with NIR light, typically at a wavelength of 980 nm. Among the various host materials for lanthanide ions (for example oxides, oxysulfides, phosphates, and fluorides), sodium yttrium fluoride ($NaYF_4$) turned out to be among the most efficient ones [58–60]. UCNPs have several outstanding features that make them highly attractive: their excitation is in the NIR spectral range and thus does not generate any interfering background luminescence (that is, in the visible), for example, by biomolecules. Obviously, resonance scattering and Raman bands cannot interfere either. NIR light also penetrates tissue much deeper than visible light but does not damage tissue, at least at the intensity levels that are applied for upconversion. Yuan et al. combined UCNPs with a DNA aptamer to image universal compound in fingerprints and provide a general and easily performed strategy for latent fingerprint imaging under NIR light excitation, as shown in Fig. 11.6 [61]. This approach also be applied to fingerprints on different surfaces and from different people, thus indicating the great practicality of this method. Recently, Tan group also combined the beneficial features of a DNA aptamer with the intercalation of photosensitizer TMPyP4 within the G-quadruplex DNA structure and NIR light-triggered upconversion nanomaterials to develop a smart cancer-specific imaging and photodynamic therapy system [62]. Utilizing sgc8 as a model for targeting, selective cancer cell labeling and tracking is realized which will possibly be useful for future imaging-guided therapy studies.

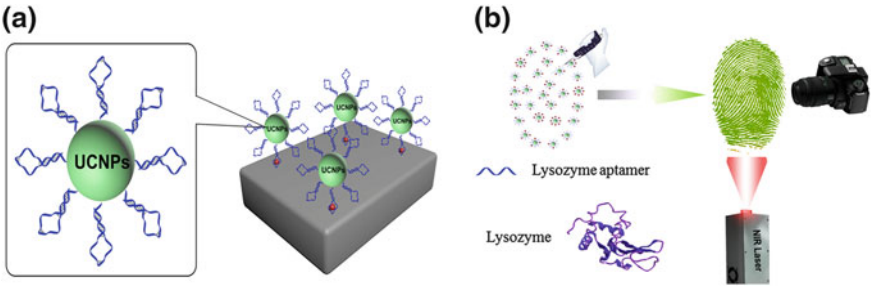

Fig. 11.6 **a** Strategy for latent fingerprint detection with UCNPs functionalized with a lysozyme-binding aptamer nanoconjugates. **b** Photograph of the marble with three latent fingerprints in the *black circles*

11.2.6 Quantum Dots

Semiconductor quantum dots (QDs), typically prepared as (core) shell nanocrystals, are a class of strained materials with novel optical and electronic properties. QD-based research has opened new opportunities for imaging living cells and in vivo animal models at unprecedented sensitivity and spatial resolution [63, 64]. With large extinction coefficients and high fluorescence quantum yields, inorganic semiconductor nanocrystals, or QDs, are a popular choice for fluorescence imaging applications. QDs have broad absorption spectra that enable excitation by a range of wavelengths, but narrow emission spectra, thus enabling simultaneous (multiplexed) imaging of multiple types of QDs, where different colors of QDs are used in a single assay with only one excitation source something unattainable with conventional fluorescent dyes.

An extracellular supramolecular reticular DNA-QD sheath was reported by Zhang and co-workers for high-intensity fluorescence imaging [65]. At physiological temperature, the DNA-QD sheath readily recognized and bound to Ramos cells in a cell-specific manner and was used to accurately image the Ramos cells within the range of 10–1,000 cells. Qin et al. reported a novel polymeric quantum dot/aptamer superstructure with a highly intense fluorescence was fabricated by a molecular engineering strategy and successfully applied to fluorescence imaging of cancer cells [66]. The polymeric superstructure, which is composed of both multiple cell-based aptamers and a high ratio of quantum dot (QD)-labeled DNA, exploits the target recognition capability of the aptamer, an enhanced cell internalization through multivalent effects, and cellular disruption by the polymeric conjugate. Importantly, the polymeric superstructure exhibits an increasingly enhanced fluorescence with recording time and is thus suitable for long-term fluorescent cellular imaging. The unique and excellent fluorescence property of the QD superstructure paves the way for developing polymeric QD superstructures that hold promise for applications such as in vivo imaging. In addition, Ma et al. [67] reported a new type of DNA-template heterobivalent QD nanoprobes with the

ability to target and image two spatially isolated cancer markers (nucleolin and mRNA) present on the cell surface and in the cell cytosol. By passing endolysosomal sequestration, this type of QD nanoprobes undergo micropinocytosis following the nucleolin targeting and then translocate to the cytosol for mRNA targeting. Fluorescence resonance energy transfer (FRET)-based confocal microscopy enables unambiguous signal deconvolution of mRNA-targeted QD nanoprobes inside cancer cells.

11.3 Magnetic Resonance Imaging

Except optical imaging, MRI is another powerful molecular imaging model for early clinical diagnosis of cancer and management of malignant tumors [68]. Especially, MRI is superior for deep tissue imaging as it provides tomographic images with high spatial and temporal resolution in a noninvasive manner [69, 70]. The MRI signal arises from the variation in relaxation rates of the abundant number of water protons (or lipids in some cases) in the tissues of interest, allowing for visualization and discrimination between tissue types [69].

However, most of the traditionally used imaging agents are small molecules, such as the gadolinium complexes used as longitudinal relaxation time (T1), MRI contrast agents, and anticancer chemical drugs. These small molecules are usually suffered from short blood circulation time and nonspecific bio-distribution, thus leading to many unwanted side effects [71]. Additionally, traditional techniques of MRI are hindered due to the lack of resolution at the cellular level, poor signal penetration through tissues, and low sensitivity to detect small size tumors [72]. And delivering sufficient contrast agents such as gadolinium into a cancer cell may cause serious toxicity [73]. With the rapid development of nanotechnology, nanoparticles with the diameter ranging from 5 to 100 nm can be variously functionalized on their surface, which are capable of multivalent conjugation to targeting, imaging, and therapeutic agents. These nanoparticles have been widely applied to molecular imaging to generate functional imaging nanoparticles. Therefore, to overcome the drawbacks of traditional MRI techniques, lots of nanoparticle contrast agents have been developed to produce sufficient contrast enhancement for accurate diagnosis [71, 74]. These contrast agents are able to alter T1 or transverse relaxation time (T2), hence producing significant contrast for improved visualization of a tumor-affected region [75]. Among them, superparamagnetic iron oxide nanoparticles (SPIOs) and paramagnetic metal chelates (e.g., gadolinium (Gd)-, europium (Eu)-, neodymium (Nd)-, and manganese (Mn)-containing materials) display the most efficient relaxation mechanism, thus becoming the most clinically successful and safe contrast agents [69, 76, 77]. Several SPIO and Gd-chelate-based contrast agents have been approved by the US Food and Drug Administration (FDA) for different clinical uses [69].

SPIOs create a decrease in signal intensity on T_2-weighted images (negative contrast, dark signal) by shortening the traverse relaxation time (T_2 and T_2*) of

surrounding water protons [78, 79]. To be effective MRI contrast agents, the blood circulation time of SPIOs is a very important parameter to be considered, which is greatly affected by the particle size and surface chemistry [80, 81]. SPIONs can be prematurely removed from circulation through two pathways, either via uptake by the reticuloendothelial system (RES) or through renal clearance mechanisms [80]. Particle size is regarded as the primary factor in determining which clearance pathway will be followed. Normally, particles with a hydrodynamic diameter larger than 200 nm are usually removed via the RES, whereas particles smaller than 5.5 nm (±10 %) can be cleared through renal filtration. Generally, particles in the range of 10–100 nm have comparatively minimized space available for adsorption of RES proteins, yet they can be large enough to evade renal clearance [80]. Therefore, to minimize the premature clearance from the bloodstream, particles with diameter in the range of 10–100 nm are optimized to have the longest circulation time when applying for molecular imaging.

In addition to the particle size, surface chemistry is also an important factor to prolong the circulation time of SPIOs. For example, if unprotected SPIONs are immersed in the blood stream, they may be recognized as invading agents and immediately be adsorbed on the surface of various kinds of plasma proteins [81]. Subsequently, they are rapidly endocytosed by the RES cells, causing their removal from blood stream and accumulation in organs with high phagocytic activity. Especially, SPIONs with negatively charged surfaces can facilitate the attachment of plasma proteins, thus leading to enhanced uptake and clearance via the RES [81]. On the other hand, SPIONs with positively charged surfaces can adhere to cells in nonspecific manners such as electrostatic interaction or hydrophobic interaction. Normally, hydrophilic and neutral surfaces interact the least with blood components; hence, they are preferred to minimize opsonization and clearance [82]. It has been reported that by coating with a dense packing of biocompatible polymers, the circulation time of SPIOs in the blood can also be prolonged [75]. Since SPIONs respond very strongly to a magnetic field, even at very low quantities, the resolution of the images can be greatly improved. Generally, this molecular imaging technique displays relatively low cytotoxicity, high magnetic signal strength, and longer-lasting contrast enhancement, hence possesses significant advantages over traditional contrast agents [80, 83, 84]. In addition, it is reported that the iron released from degrading SPIONs can be metabolized by the body, decreasing the potential for long-term cytotoxicity [80].

On the other hand, para-magnetic gadolinium chelates, such as the widely used Gd^{3+} or the recently introduced Mn^{2+}, usually have a large number of unpaired electrons [69]. They work by shortening the T_1 of surrounding water protons, causing an increase in signal intensity on T_1-weighted images (positive contrast, bright signal) [77, 85]. Compared to T_2-weighted images, T_1-weighted images show remarkable feature on signal-enhancing positive contrast ability, which can be clearly distinguished from other pathogenic or biological conditions. Additionally, since T_1 contrast agents are basically paramagnetic, they do not disrupt the magnetic homogeneity and other anatomic backgrounds [86, 87]. However, the limitation is that Gd-contrast materials may induce severe adverse effects, including

compromising renal function and subsequent deposition in different organs/tissues, and nephrogenic systemic fibrosis (NSF) caused by release of Gd^{3+} [81].

To achieve specifically targeting cancer cell imaging, various targeting agents such as folic acids [88], peptides [79], antibody [89], and, of particular interest, aptamers [90, 91] are commonly incorporated into the contrast agents. These new biomolecule-conjugated nanoparticles provide a chance to develop specific-targeted molecular imaging agents. Due to the remarkable features of long-term stability, rapid tissue penetration, and ease of synthesis and surface modification, aptamer-functionalized nanoparticles have been widely applied as molecular imaging agents for cell imaging and diagnosis [18, 78, 92–95]. Molecular imaging with cancer biomarkers has become an essential element of cancer diagnosis. Till now, various aptamers targeting cancer-specific biomarkers, such as nucleolin [96], platelet-derived growth factor (PDGF) [97], vascular endothelial growth factor receptor (VEGFR) [98], protein tyrosine kinase (PTK 7) [99, 100], and prostate-specific membrane antigen (PSMA) [101, 102], have been selected and applied for diagnostic studies of cancers.

11.3.1 Single Modality of MRI

By using these strategies, SPIONs have been functionalized with various kinds of aptamers to act as molecular imaging probes, which can specifically recognize different biomarkers located on malignant cells, thus distinguishing cancer cells from the healthy cells. Since the binding and concentration of molecular imaging agents enhances the contrast between cancer-affected and nonaffected cells, it greatly improved the accuracy of diagnosis [75].

Aptamer sgc8 was identified to well-recognized cancer cell CCRF-CEM (acute lymphoblastic leukemia T-cells) by specifically bind to the cell membrane receptor PTK 7 with high affinity and selectivity [99, 100]. To develop precise molecular imaging for targeted CCRF-CEM cells, Tan group has reported a smart multi-functional nanostructure (SMN) constructed from a porous hollow magnetite nanoparticle (PHMNP), a heterobifunctional PEG ligand, and a sgc8 aptamer. The hollow interior of the PHMNPs enables the high efficient loading of the anticancer drug doxorubicin (DOX), which can be released at lysosome pH. Moreover, T_2 relaxation measurements and T_2*-weighted MRI images demonstrated that this nanostructure showed great potential to be used as a T_2 contrast agent, which may enable real-time monitoring of the cancer treatment progress [78].

PSMA has been recognized as a biomarker for prostate cancer (PCa) [102]. A10 RNA aptamer, which can specifically bind the extracellular domain of the PSMA, was conjugated on the surface of thermally cross-linked SPION (TCL-SPION) by standard coupling chemistry of EDN/NHS reaction, as shown in Fig. 11.7. Then, a novel multifunctional TCL-SPION-Apt bioconjugate with diagnostic and therapeutic capabilities was synthesized and explored for the potential as an MRI

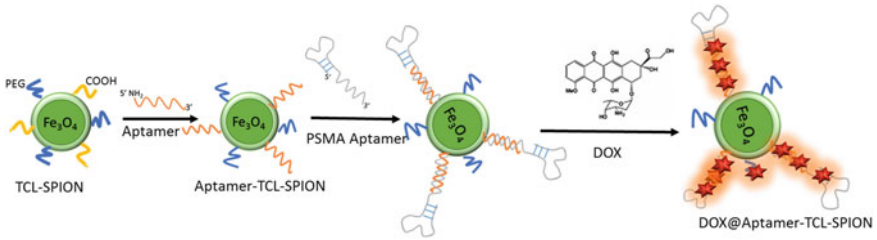

Fig. 11.7 Schematic representation of the preparation of Apt-hybr-TCL-SPIONs and Dox@Apt-hybr-TCL-SPIONs

contrast agent and as a therapeutic carrier for selectively targeting PSMA on PCa cells with high sensitivity [101, 102].

Integrin, a well-known important transmembrane molecule, participates in cell–cell and cell–matrix interactions. The αvβ3 subunit of integrin plays an important role in the regulation of diverse intracellular signaling pathways which modulate cell migration and invasion during angiogenesis [103, 104]. By modifying integrin αvβ3-targeting aptamer ($Apt_{\alpha v\beta 3}$) to magnetic nanoparticles, integrin-targeting magnetic nanoparticles ($Apt_{\alpha v\beta 3}$-MNPs) were developed to enable precise detection of integrin avb3 expression in cancer cells during angiogenesis using MRI. The nanoparticles with good cytocompatibility, efficient targeting ability, and high magnetic sensitivity through in vitro/in vivo studies were demonstrated to have the potential to be used for accurate tumor diagnosis and therapy [105].

Vascular endothelial growth factor receptor 2 (VEGFR2) was identified as one of the key angiogenic factors. Hence, precise molecular imaging of VEGFR2, which is overexpressed on angiogenic vessels, will benefit the treatment of glioblastoma. An ultrasensitive MR imaging contrast agent, MNC, was synthesized by the thermal decomposition method and enveloped using biocompatible carboxyl polysorbate 80. After surface modification with a VEGFR2-targetable aptamer, Apt-MNC exhibited good cytocompatibility, high magnetic resonance signal, and efficient VEGFR2-targeting ability. The orthotopic glioblastoma mouse model was used to investigate the potential of the aptamer-conjugated magnetic nanocrystal for targeted MR imaging of angiogenic vasculature from glioblastoma. It is proved to be a novel biomarker-detecting nanoprobe with high selectivity and sensitivity in vitro and in vivo [98].

11.3.2 Dual- or Multi-modality Molecular Imaging

The above examples exhibited the great potential of aptamer-conjugated SPIONs as excellent MRI contrast agents for highly selectively cancer cell-targeting detection ability. Even through, each imaging modality has its own advantages and intrinsic disadvantages in terms of sensitivity, spatial resolution, and complexity [3]. For

instance, this single modality of MRI with a depth insensitive technique can be used for deep tissue imaging, yet suffers from poor sensitivity and cannot be used in real time. To overcome the limitation of sensitivity of MRI, an unrecommended increase in the dose of the imaging agent can be used to enhance the imaging signal, while the application may be limited in humans due to the health risks resulting from the larger doses [106]. Even the imaging signal sensitivity can be improved by the development of imaging analysis software, it is still difficult to satisfy the accurate diagnoses of small size of tumors.

To achieve early accurate cancer cell imaging and provide additional information regarding the pathology of the tumor, other imaging moieties can be incorporated into the MRI contrast agents to integrate multimodality imaging systems [107]. Therefore, to acquire complementary information for accurate diagnosis, it is possible to rationally design a common imaging agent which can combine the imaging modalities with high sensitivity (PET, optical, etc.) and other modalities with high spatial resolution [computed tomography (CT), MRI, etc.] [81]. Hence, by synergistic combination of two or more imaging techniques, the multimodal imaging approach covers several advantages like high spatial resolution, high sensitivity, and high tissue penetration ability and tends to eliminate the limitations of individual imaging modalities, thus ensures enhanced visualization of biological materials and better reliability of collected data [3, 81, 107].

In terms of dual-modality imaging, MRI/optical imaging are the most well developed and have been significant increased to be applied in biomedical research and clinical practice [107]. Once fluorophores are attached to the MRI contrast agents to create dual-modal contrast agents, it can offer both the high spatial and temporal resolution and deep tissue penetration of MR imaging and rapid response and sensitivity of optical imaging.

Tan and co-workers have developed a gold-coated iron oxide (Fe_3O_4@Au) nanorose with five distinct functions, which integrates aptamer-based targeting, MRI, optical imaging, photothermal therapy, and chemotherapy into one single probe of about 70 nm in diameter [90]. As shown in Fig. 11.8, in this platform, the inner Fe_3O_4 core functions as an MRI agent, while coating by the gold shell, obvious NIR absorption at 805 nm was observed. Upon laser irradiation, a rapid rise in temperature can be achieved, resulting in a facilitated release of the anticancer drug doxorubicin carried by the nanoroses. The location of doxorubicin released is released can be monitored by its fluorescence. This paper demonstrated that the combination of dual-modality MRI and optical imaging has the potential to improve the specificity of cancer cell diagnosis and facilitate therapeutic drug monitoring. To perform each function effectively, the amounts of imaging agent, photothermal agent, or drug loaded into the system need to be adjusted to synergistically. This versatile theranostic system shows great advantages in multimodality and may be particularly useful for cancer therapy.

AS1411, a 26-mer guanine-rich oligonucleotide DNA aptamer, shows high binding affinity to the nucleolin in the plasma membrane, which is a cellular membrane protein highly expressed in continuously proliferating cells. AS1411 has been in phase II clinical trials for relapsed or refractory acute myeloid leukemia and

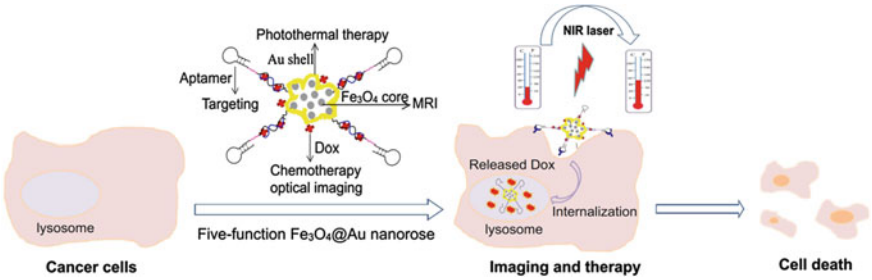

Fig. 11.8 Illustration of five-function Fe_3O_4@Au nanorose for cancer cell targeting, MRI, optical imaging, photothermal, and chemotherapy

for renal cell carcinoma [108]. It has been widely used as an example for molecular imaging. Qu et al. [108] have designed a multifunctional platform for simultaneous magnetofluorescent imaging and targeted cancer photodynamic therapy using photosensitizer-incorporated G-quadruplex DNA-functionalized magnetic nanoparticles. To prepare this platform, Fe_3O_4 and tris(2,2′-bipyridyl)-dichlororuthenium(II) hexahydrate ($Ru(bpy)_3^{2+}$) were first incorporated into the silica matrix. Then, anticancer aptamer AS1411 was conjugated on the surface of this nanoparticle for specifically recognize the nucleolin expressed in cancer cells. In this case, the multifunctional platform with excellent optical properties and cytocompatibility could be used as predominant contrast agents for targeting tumor cells with fluorescence and MRI simultaneously. This cell-type-specific aptamer was further used as caps to prepare a novel gadolinium-doped luminescent and mesoporous strontium hydroxyapatite nanorods (designated as Gd:SrHap nanorods) system [109]. In this system, aptamers were employed not only as a lid but also as a targeted molecular which can enable an effective way for therapeutically special cancer cells. This Gd-doped SrHap-aptamer system was demonstrated to be an ideal targeting contrast agent for fluorescence and MRI bioimaging simultaneously.

In addition, Yang and co-workers conjugated AS1411 on Mn_3O_4@SiO_2 core–shell nanoprobes and evaluate the quantitative biodistribution and toxicity of these core–shell nanoprobes (NPs) in human cervical carcinoma tumor-bearing mice. In this paper, aptamer-conjugated Mn_3O_4@SiO_2 core–shell nanoprobes have been successfully employed as a promising T1-MRI probe for targeting both in vitro fluorescence confocal imaging (cancer cells) and in vivo MRI (animal tumor model) [87]. Except Gd-and Mn-containing paramagnetic metal chelates, multifunctional lanthanide-doped porous nanoparticles are also prepared for the first time via a facile one-step solvothermal route by employing aptamers as the biotemplate. The nanoparticles feature excellent aqueous dispersibility and biospecific properties and could work as effective nanoprobes for targeted dual-modal cancer cell imaging and drug delivery with DNA aptamer as hydrophilic ligands [110].

This dual-modality imaging of MRI/optical imaging can be further incorporated with other imaging modalities such as CT imaging or radionuclide imaging to provide multimodal imaging probes. AS1411 aptamer-functionalized target-specific

Gd_2O_3:Eu nanoparticles (A-GdO:Eu nanoparticles) were synthesized with good biocompatibility. This multifunctional nanoparticles exhibited strong fluorescence in the visible range, excellent T1 contrast and strong CT signal, thus behaving as a trimodal molecular contrast agent for CT, MR, and fluorescence imaging [111]. Kim and co-workers develop a multi-modal imaging system which is capable of concurrent radionuclide imaging, MRI, and fluorescence imaging in vivo. This system is consisted of magnetic cobalt ferrite cores protected by a silica shell and coated by fluorescent rhodamine. The particles with carboxyl group and Fmoc-protected amine moiety on the surface were then coupled with amine-terminated AS1411 aptamer using EDC and further labeled with 67 Ga-citrate for radionuclide imaging [96].

Single biomarker imaging of cancer might cause low rate of cancer diagnosis, because it is not enough to acquire the complementary information about the various mechanisms and phases of neoplastic pathogenesis caused by multiple genetic changes [106]. A multitude of cancer biomarkers imaging by targeting different epitopes expressed in the cancer cells will help for accurate diagnosis. Kim et al. reported a Simultaneously Multiple Aptamers and RGD Targeting (SMART) cancer imaging probe which was conjugated to a multimodal nanoparticle with the capability of concurrent fluorescence, radionuclide, and MRI [106]. This multimodal SMART cancer probe can simultaneously target nucleolin, integrin αvβ3 and Tnc proteins in five different cancer cell lines, C6, NPA, DU145, HeLa, and A549, resulting in enhanced targeting efficacy and signals sensitivity. They claimed that this strategy has the potential for more selective identification of diseased cells than normal cells; thus, it can reduce the side effects and improve the patient's quality of life.

However, most of these aptamer probes for molecular imaging follow the "always on" strategy, in which the reporter-bearing aptamers are accumulated on the cancer site, resulting in an enhanced signal with reference to the surrounding environment [18, 112]. Since it is difficult to completely wash away the nonspecific binding aptamer probes, these "always on" probes with constant signals may cause a poor target-to-background signal ratio, thus critically limiting the image contrast [91]. Therefore, ideal aptamer probe for cancer imaging is that it always keeps quenched signal and can only be activated after specifically binding to the target cancer sites. Based on the target-triggered conformation alteration, this kind of activatable aptamer probe can greatly reduce the background signal and improve the sensitivity and specificity, thus enhancing the contrast imaging.

Inspired by this, Tan group developed a novel dual-activatable fluorescence/MRI bimodal platform via a MnO_2 nanosheet–aptamer nanoprobe [91]. As illustrated in Fig. 11.9, MnO_2 nanosheet behaves not only as an intracellular GSH-activated MRI contrast agent, but also as a quencher to quench the fluorescence of Cy_5 labeled on aptamers. Both the fluorescence signaling and MRI contrast of the nanoprobe are quenched in the absence of target cells. In the presence of target cells, aptamers specifically bind to the target cells and then can be released from the MnO_2 nanosheet, resulting in fluorescence recovery and illuminating the target cells. Endocytosed MnO_2 nanosheets can be reduced by intracellular GSH, thus causing the further recovery of fluorescence signal and generating large amounts of Mn^{2+}

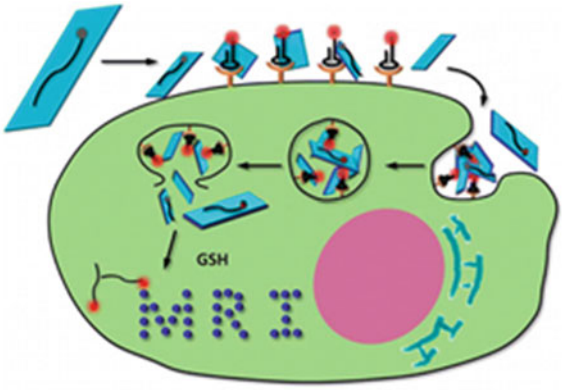

Fig. 11.9 Activation mechanism of the MnO_2 nanosheet–aptamer nanoprobe for fluorescence/MRI bimodal tumor cell imaging. Reprinted with permission from Refs. [91]. Copyright (2014) American Chemical Society

ions for MRI. This MnO_2 nanosheet–aptamer nanoprobe exhibited great potential to be used as a target-cell-activated fluorescence and intracellular GSH-activated MRI contrast agent with low background and high sensitivity.

11.4 Other Imaging Modalities

Aptamer-based molecular probes have also been used in CT imaging. Kim et al. conjugated the A10 aptamer, targeted against PSMA, to gold nanoparticles [113]. Gold nanoparticles, because of their high atomic number, can act as CT imaging contrast agents. The investigators showed that A10-targeted nanoparticles can bind to PSMA-expressing PCa cells with high sensitivity and specificity. More importantly, they showed that the A10-gold nanoparticle conjugate can be used as a molecular probe for the imaging of PSMA-expressing cancer cells by CT imaging.

Ultrasound is also one of the most commonly used clinical imaging modalities. Nakatsuka et al. engineered a novel aptamer-cross-linked microbubble as a molecular ultrasound imaging agent [114]. These microbubbles are designed to show ultrasound activation only at levels of thrombin associated with clot formation. To accomplish this, the microbubbles are coated with polymer–DNA strands and aptamers that can bind to thrombin. The aptamers also contain sequences that can bind to the DNA in a polymer–DNA complex, enabling cross-linking on the microbubble surface. However, the binding of thrombin to aptamer will displace the aptamers from the polymer–DNA complex. The investigators demonstrated that the semicrobubbles can act as a stimulus-responsive contrast agent and generate ultrasound signal in response to only the levels of thrombin. Such an aptamer-based ultrasound contrast agent can be useful for imaging thrombosis.

Nuclear imaging holds the highest potential for the clinical translation of aptamer-based molecular imaging probes. The very first report of an aptamer-based imaging probe was a radiolabeled (99mTc) aptamer targeted against human neutrophil elastase to identify sites of inflammation [115]. When compared with a radiolabeled IgG, the aptamer probe achieved a higher target-to-background ratio (fourfold) than that of IgG (threefold). This difference was attributed to the more rapid clearance of unbound aptamer probes than IgG probes. The study on radiolabeled TTA1 best demonstrated the potential of aptamers as nuclear imaging probes [115]. The investigators radiolabeled the aptamer TTA1 (38b, Kd is 5 nM) with ^{99m}Tc. TTA1 is targeted against the extracellular matrix protein tenascin-C, which is expressed during tissue remodeling processes including angiogenesis and tumor growth. Tenascin-C is also known to be overexpressed by a wide range of tumors, including lung, breast, and prostate. Radiolabeled TTA1 was evaluated in mouse xenograft models of brain and breast cancer. The investigators showed that TTA1 has a rapid clearance profile, with a blood half-life of 2 min. The aptamers penetrated tumors quickly, with 6 % of injected dose in tumor at 10 min. At 60 min after injection, there is still 3 % of the injected dose in tumor. The tumor-to-blood ratio was 50 within 3 h, highlighting its high potential for clinical translation.

11.5 Conclusions and Perspective

Because of these properties and combing with various nanomaterials, aptamers are studied in a wide range of applications in molecular imaging. There continues to be high interest in developing aptamer-based probes in preclinical research. These studies will improve the technology and identify the potential applications for aptamers in molecular imaging. The successful clinical translation of aptamer-based molecular imaging probes will also require the development of aptamers against biomarkers that have high clinical significance. In summary, aptamers are excellent molecular targeting ligands, and they hold great promise in improving molecular imaging.

References

1. Weissleder R, Mahmood U (2001) Molecular imaging. Radiology 219:316–333
2. Thakur M, Lentle BC (2005) Report of a summit on molecular imaging. Radiology 236:753–755
3. Lee DE, Koo H, Sun IC, Ryu JH, Kim K, Kwon IC (2012) Multifunctional nanoparticles for multimodal imaging and theragnosis. Chem Soc Rev 41:2656–2672
4. Ellington AD, Szostak JW (1990) In vitro selection of RNA molecules that bind specific ligands. Nature 346:818–822
5. Tuerk C, Gold L (1990) Systematic evolution of ligands by exponential enrichment: RNA ligands to bacteriophage T4 DNA polymerase. Science 249:505–510

6. Daniels DA, Chen H, Hicke BJ, Swiderek KM, Gold L (2003) A tenascin-C aptamer identified by tumor cell SELEX: systematic evolution of ligands by exponential enrichment. Proc Natl Acad Sci USA 100:15416–15421
7. Tavitian B, Terrazzino S, Kuhnast B, Marzabal S, Stettler O, Dolle F, Deverre JB, Jobert A, Hinnen F, Bendriem B, Crouzel C, Di Giamberardino L (1998) In vivo imaging of oligonucleotides with positron emission tomography. Nat Med 4:467–471
8. Schmidt KS, Borkowski S, Kurreck J, Stephens AW, Bald R, Hecht M, Friebe M, Dinkelborg L, Erdmann VA (2004) Application of locked nucleic acids to improve aptamer in vivo stability and targeting function. Nucleic Acids Res 32:5757–5765
9. Fang X, Tan W (2010) Aptamers generated from cell-SELEX for molecular medicine: a chemical biology approach. Acc Chem Res 43:48–57
10. Tan W, Donovan MJ, Jiang J (2013) Aptamers from cell-based selection for bioanalytical applications. Chem Rev 113:2842–2862
11. Amer M (2009) Wiley, Hoboken
12. Kobayashi H, Ogawa M, Alford R, Choyke PL, Urano Y (2009) New strategies for fluorescent probe design in medical diagnostic imaging. Chem Rev 110:2620–2640
13. Tyagi S, Kramer FR (1996) Molecular beacons: probes that fluoresce upon hybridization. Nat Biotech 14:303–308
14. Tan WH, Wang KM, Drake TJ (2004) Molecular beacons. Curr Opin Chem Biol 8:547–553
15. Stojanovic MN, de Prada P, Landry DW (2000) Fluorescent sensors based on aptamer self-assembly. J Am Chem Soc 122:11547–11548
16. Yang CJ, Jockusch S, Vicens M, Turro NJ, Tan WH (2005) Light-switching excimer probes for rapid protein monitoring in complex biological fluids. Proc Natl Acad Sci USA 102:17278–17283
17. Qiu L, Wu C, You M, Han D, Chen T, Zhu G, Jiang J, Yu R, Tan W (2013) A targeted, self-delivered, and photocontrolled molecular beacon for mRNA detection in living cells. J Am Chem Soc 135:12952–12955
18. Shi H, He XX, Wang KM, Wu X, Ye XS, Guo QP, Tan WH, Qing ZH, Yang XH, Zhou B (2011) Activatable aptamer probe for contrast-enhanced in vivo cancer imaging based on cell membrane protein-triggered conformation alteration. Proc Natl Acad Sci USA 108:3900–3905
19. Shi H, He X, Cui W, Wang K, Deng K, Li D, Xu F (2014) Locked nucleic acid/DNA chimeric aptamer probe for tumor diagnosis with improved serum stability and extended imaging window in vivo. Anal Chim Acta 812:138–144
20. Banerjee S, Wong SS (2002) Synthesis and characterization of carbon nanotube-nanocrystal heterostructures. Nano Lett 2:195–200
21. Lue JT (2001) A review of characterization and physical property studies of metallic nanoparticles. J Phys Chem Solids 62:1599–1612
22. Slowing II, Vivero-Escoto JL, Wu C-W, Lin VSY (2008) Mesoporous silica nanoparticles as controlled release drug delivery and gene transfection carriers. Adv Drug Deliv Rev 60:1278–1288
23. Daniel MC, Astruc D (2004) Gold nanoparticles: assembly, supramolecular chemistry, quantum-size-related properties, and applications toward biology, catalysis, and nanotechnology. Chem Rev 104:293–346
24. Rosi NL, Giljohann DA, Thaxton CS, Lytton-Jean AKR, Han MS, Mirkin CA (2006) Oligonucleotide-modified gold nanoparticles for intracellular gene regulation. Science 312:1027–1030
25. Sperling RA, Gil PR, Zhang F, Zanella M, Parak WJ (2008) Biological applications of gold nanoparticles. Chem Soc Rev 37:1896–1908
26. Storhoff JJ, Lazarides AA, Mucic RC, Mirkin CA, Letsinger RL, Schatz GC (2000) What controls the optical properties of DNA-linked gold nanoparticle assemblies? J Am Chem Soc 122:4640–4650

27. Elghanian R, Storhoff JJ, Mucic RC, Letsinger RL, Mirkin CA (1997) Selective colorimetric detection of polynucleotides based on the distance-dependent optical properties of gold nanoparticles. Science 277:1078–1081
28. Wang Y, Li D, Ren W, Liu Z, Dong S, Wang E (2008) Ultrasensitive colorimetric detection of protein by aptamer—Au nanoparticles conjugates based on a dot-blot assay. Chem Commun 2520–2522
29. Medley CD, Smith JE, Tang Z, Wu Y, Bamrungsap S, Tan W (2008) Gold nanoparticle-based colorimetric assay for the direct detection of cancerous cells. Anal Chem 80:1067–1072
30. Liu J, Lu Y (2006) Fast colorimetric sensing of adenosine and cocaine based on a general sensor design involving aptamers and nanoparticles. Angew Chem Int Ed 45:90–94
31. Huang Y-F, Chang H-T, Tan W (2008) Cancer cell targeting using multiple aptamers conjugated on nanorods. Anal Chem 80:567–572
32. Wang H-H, Lin C-AJ, Lee C-H, Lin Y-C, Tseng Y-M, Hsieh C-L, Chen C-H, Tsai C-H, Hsieh C-T, Shen J-L, Chan W-H, Chang WH, Yeh H-I (2011) Fluorescent gold nanoclusters as a biocompatible marker for in vitro and in vivo tracking of endothelial cells. ACS Nano 5:4337–4344
33. Wang Y, Chen J, Irudayaraj J (2011) Nuclear targeting dynamics of gold nanoclusters for enhanced therapy of HER2(+) breast cancer. ACS Nano 5:9718–9725
34. Vosch T, Antoku Y, Hsiang J-C, Richards CI, Gonzalez JI, Dickson RM (2007) Strongly emissive individual DNA-encapsulated Ag nanoclusters as single-molecule fluorophores. Proc Natl Acad Sci USA 104:12616–12621
35. de Souza N (2007) All that glitters but does not blink. Nat Meth 4:540
36. Li J, Zhong X, Cheng F, Zhang J-R, Jiang L-P, Zhu J-J (2012) One-pot synthesis of aptamer-functionalized silver nanoclusters for cell-type-specific imaging. Anal Chem 84:4140–4146
37. Yin J, He X, Wang K, Qing Z, Wu X, Shi H, Yang X (2012) One-step engineering of silver nanoclusters-aptamer assemblies as luminescent labels to target tumor cells. Nanoscale 4:110–112
38. Schluecker S (2009) SERS microscopy: nanoparticle probes and biomedical applications. ChemPhysChem 10:1344–1354
39. Jarvis RM, Goodacre R (2008) Characterisation and identification of bacteria using SERS. Chem Soc Rev 37:931–936
40. Qian XM, Nie SM (2008) Single-molecule and single-nanoparticle SERS: from fundamental mechanisms to biomedical applications. Chem Soc Rev 37:912–920
41. Lu W, Singh AK, Khan SA, Senapati D, Yu H, Ray PC (2010) Gold nano-popcorn-based targeted diagnosis, nanotherapy treatment, and in situ monitoring of photothermal therapy response of prostate cancer cells using surface-enhanced raman spectroscopy. J Am Chem Soc 132:18103–18114
42. Beqa L, Fan Z, Singh AK, Senapati D, Ray PC (2011) Gold nano-popcorn attached SWCNT hybrid nanomaterial for targeted diagnosis and photothermal therapy of human breast cancer cells. Acs Appl Mater Inter 3:3316–3324
43. Stankovich S, Dikin DA, Dommett GHB, Kohlhaas KM, Zimney EJ, Stach EA, Piner RD, Nguyen ST, Ruoff RS (2006) Graphene-based composite materials. Nature 442:282–286
44. Liu Y, Dong X, Chen P (2012) Biological and chemical sensors based on graphene materials. Chem Soc Rev 41:2283–2307
45. Wu Y, Phillips JA, Liu H, Yang R, Tan W (2008) Carbon nanotubes protect DNA strands during cellular delivery. ACS Nano 2:2023–2028
46. Lu C-H, Li J, Lin M-H, Wang Y-W, Yang H-H, Chen X, Chen G-N (2010) Amplified aptamer-based assay through catalytic recycling of the analyte. Angew Chem Int Ed 49:8454–8457
47. Wang Y, Li Z, Hu D, Lin C-T, Li J, Lin Y (2010) Aptamer/graphene oxide nanocomplex for in situ molecular probing in living cells. J Am Chem Soc 132:9274–9276

48. Tan XH, Chen T, Xiong XL, Mao Y, Zhu GZ, Yasun E, Li CM, Zhu Z, Tan WH (2012) Semiquantification of ATP in live cells using nonspecific desorption of DNA from graphene oxide as the internal reference. Anal Chem 84:8622–8627
49. Yi M, Yang S, Peng Z, Liu C, Li J, Zhong W, Yang R, Tan W (2014) Two-photon graphene oxide/aptamer nanosensing conjugate for in vitro or in vivo molecular probing. Anal Chem 86:3548–3554
50. Wu CC, Chen T, Han D, You MX, Peng L, Cansiz S, Zhu GZ, Li CM, Xiong XL, Jimenez E, Yang CJ, Tan WH (2013) Engineering of switchable aptamer micelle flares for molecular imaging in living cells. ACS Nano 7:5724–5731
51. Chen T, Wu CS, Jimenez E, Zhu Z, Dajac JG, You M, Han D, Zhang X, Tan W (2013) DNA micelle flares for intracellular mRNA imaging and gene therapy. Angew Chem Int Ed 52:2012–2016
52. Zhu G, Zhang S, Song E, Zheng J, Hu R, Fang X, Tan W (2013) Building fluorescent DNA nanodevices on target living cell surfaces. Angew Chem Int Ed 52:5490–5496
53. Hu R, Zhang X, Zhao Z, Zhu G, Chen T, Fu T, Tan W (2014) DNA nanoflowers for multiplexed cellular imaging and traceable targeted drug delivery. Angew Chem-Int Ed 53:5821–5826
54. Wang K, He X, Yang X, Shi H (2013) Functionalized silica nanoparticles: A platform for fluorescence imaging at the cell and small animal levels. Acc Chem Res 46:1367–1376
55. Estevez MC, O'Donoghue MB, Chen X, Tan W (2009) Highly fluorescent dye-doped silica nanoparticles increase flow cytometry sensitivity for cancer cell monitoring. Nano Res 2:448–461
56. Chen X, Estévez MC, Zhu Z, Huang Y-F, Chen Y, Wang L, Tan W (2009) Using aptamer-conjugated fluorescence resonance energy transfer nanoparticles for multiplexed cancer cell monitoring. Anal Chem 81:7009–7014
57. Medley CD, Bamrungsap S, Tan W, Smith JE (2011) Aptamer-conjugated nanoparticles for cancer cell detection. Anal Chem 83:727–734
58. Mader HS, Kele P, Saleh SM, Wolfbeis OS (2010) Upconverting luminescent nanoparticles for use in bioconjugation and bioimaging. Curr Opin Chem Biol 14:582–596
59. Cheng L, Wang C, Liu Z (2013) Upconversion nanoparticles and their composite nanostructures for biomedical imaging and cancer therapy. Nanoscale 5:23–37
60. Shen J, Zhao L, Han G (2013) Lanthanide-doped upconverting luminescent nanoparticle platforms for optical imaging-guided drug delivery and therapy. Adv Drug Deliv Rev 65:744–755
61. Wang J, Wei T, Li X, Zhang B, Wang J, Huang C, Yuan Q (2014) Near-infrared-light-mediated imaging of latent fingerprints based on molecular recognition. Angew Chem Int Ed 53:1616–1620
62. Yuan Q, Wu Y, Wang J, Lu D, Zhao Z, Liu T, Zhang X, Tan W (2013) Targeted bioimaging and photodynamic therapy nanoplatform using an aptamer-guided G-quadruplex DNA carrier and near-infrared light. Angew Chem Int Ed 52:13965–13969
63. Pinaud F, Clarke S, Sittner A, Dahan M (2010) Probing cellular events, one quantum dot at a time. Nat Meth 7:275–285
64. Stasiuk GJ, Tamang S, Imbert D, Poillot C, Giardiello M, Tisseyre C, Barbier EL, Fries PH, de Waard M, Reiss P, Mazzanti M (2011) Cell-permeable Ln(III) chelate-functionalized InP quantum dots as multimodal imaging agents. ACS Nano 5:8193–8201
65. Zhong H, Zhang Q, Zhang S (2011) High-intensity fluorescence imaging and sensitive electrochemical detection of cancer cells by using an extracellular supramolecular reticular DNA-quantum dot sheath. Chem-Eur J 17:8388–8394
66. Jie G, Zhao Y, Qin Y (2014) A fluorescent polymeric quantum dot/aptamer superstructure and its application for imaging of cancer cells. Chem-Asian J 9:1261–1264
67. Wei W, He X, Ma N (2014) DNA-templated assembly of a heterobivalent quantum dot nanoprobe for extra- and intracellular dual-targeting and imaging of live cancer cells. Angew Chem Int Ed 53:5573–5577

68. Louie AY, Huber MM, Ahrens ET, Rothbacher U, Moats R, Jacobs RE, Fraser SE, Meade TJ (2000) In vivo visualization of gene expression using magnetic resonance imaging. Nat Biotech 18:321–325
69. López-Cebral R, Martín-Pastor M, Seijo B, Sanchez A (2014) Progress in the characterization of bio-functionalized nanoparticles using NMR methods and their applications as MRI contrast agents. Prog Nucl Mag Res Sp 79:1–13
70. Weissleder R, Moore A, Mahmood U, Bhorade R, Benveniste H, Chiocca EA, Basilion JP (2000) In vivo magnetic resonance imaging of transgene expression. Nat Med 6:351–354
71. Kim J, Piao Y, Hyeon T (2009) Multifunctional nanostructured materials for multimodal imaging, and simultaneous imaging and therapy. Chem Soc Rev 38:372–390
72. Wu YL, Xu XZ, Tang Q, Li YX (2012) A new type of silica-coated $Gd_2(CO_3)_3$:Tb nanoparticle as a bifunctional agent for magnetic resonance imaging and fluorescent imaging. Nanotechnology 23:205103
73. Wadajkar AS, Menon JU, Nguyen KT (2012) Polymer-coated magnetic nanoparticles for cancer diagnosis and therapy. Rev Nanosci Nanotechnol 1:284–297
74. Peer D, Karp JM, Hong S, FaroKhzad OC, Margalit R, Langer R (2007) Nanocarriers as an emerging platform for cancer therapy. Nat Nanotech 2:751–760
75. Santhosh PB, Ulrih NP (2013) Multifunctional superparamagnetic iron oxide nanoparticles: promising tools in cancer theranostics. Cancer Lett 336:8–17
76. Veiseh O, Gunn JW, Zhang MQ (2010) Design and fabrication of magnetic nanoparticles for targeted drug delivery and imaging. Adv Drug Deliv Rev 62:284–304
77. Santra S, Jativa SD, Kaittanis C, Normand G, Grimm J, Perez JM (2012) Gadolinium-encapsulating iron oxide nanoprobe as activatable NMR/MRI contrast agent. ACS Nano 6:7281–7294
78. Chen T, Shukoor MI, Wang R, Zhao Z, Yuan Q, Bamrungsap S, Xiong X, Tan W (2011) Smart multifunctional nanostructure for targeted cancer chemotherapy and magnetic resonance imaging. ACS Nano 5:7866–7873
79. Park J-H, von Maltzahn G, Zhang L, Schwartz MP, Ruoslahti E, Bhatia SN, Sailor MJ (2008) Magnetic iron oxide nanoworms for tumor targeting and imaging. Adv Mater 20:1630–1635
80. Rosen JE, Chan L, Shieh D-B, Gu FX (2012) Iron oxide nanoparticles for targeted cancer imaging and diagnostics. Nanomedicine: nanotechnology. Biol Med 8:275–290
81. Colombo M, Carregal-Romero S, Casula MF, Gutierrez L, Morales MP, Bohm IB, Heverhagen JT, Prosperi D, Parak WJ (2012) Biological applications of magnetic nanoparticles. Chem Soc Rev 41:4306–4334
82. Brannon-Peppas L, Blanchette JO (2004) Nanoparticle and targeted systems for cancer therapy. Adv Drug Deliv Rev 56:1649–1659
83. Landmark KJ, DiMaggio S, Ward J, Kelly C, Vogt S, Hong S, Kotlyar A, Myc A, Thomas TP, Penner-Hahn JE, Baker JR, Holl MMB, Orr BG (2008) Synthesis, characterization, and in vitro testing of superparamagnetic iron oxide nanoparticles targeted using folic acid-conjugated dendrimers. ACS Nano 2:773–783
84. Corot C, Robert P, Idée J-M, Port M (2006) Recent advances in iron oxide nanocrystal technology for medical imaging. Adv Drug Deliv Rev 58:1471–1504
85. Song Y, Kohlmeir EK, Meade TJ (2008) Synthesis of multimeric MR contrast agents for cellular imaging. J Am Chem Soc 130:6662–6663
86. Qiao R, Yang C, Gao M (2009) Superparamagnetic iron oxide nanoparticles: from preparations to in vivo MRI applications. J Mater Chem 19:6274–6293
87. Hu H, Dai A, Sun J, Li X, Gao F, Wu L, Fang Y, Yang H, An L, Wu H, Yang S (2013) Aptamer-conjugated $Mn_3O_4@SiO_2$ core-shell nanoprobes for targeted magnetic resonance imaging. Nanoscale 5:10447–10454
88. Santra S, Kaittanis C, Santiesteban OJ, Perez JM (2011) Cell-specific, activatable, and theranostic prodrug for dual-targeted cancer imaging and therapy. J Am Chem Soc 133:16680–16688

89. Olariu CI, Yiu HHP, Bouffier L, Nedjadi T, Costello E, Williams SR, Halloran CM, Rosseinsky MJ (2011) Multifunctional Fe_3O_4 nanoparticles for targeted bi-modal imaging of pancreatic cancer. J Mater Chem 21:12650–12659
90. Li CM, Chen T, Ocsoy I, Zhu GZ, Yasun E, You MX, Wu CC, Zheng J, Song EQ, Huang CZ, Tan WH (2014) Gold-coated Fe_3O_4 nanoroses with five unique functions for cancer cell targeting, imaging, and therapy. Adv Funct Mater 24:1772–1780
91. Zhao Z, Fan H, Zhou G, Bai H, Liang H, Wang R, Zhang X, Tan W (2014) Activatable fluorescence/MRI bimodal platform for tumor cell imaging via MnO_2 nanosheet-aptamer nanoprobe. J Am Chem Soc 136:11220–11223
92. Kim JK, Choi K-J, Lee M, Jo M-H, Kim S (2012) Molecular imaging of a cancer-targeting theragnostics probe using a nucleolin aptamer-and microRNA-221 molecular beacon-conjugated nanoparticle. Biomaterials 33:207–217
93. Liang H, Zhang X-B, Lv Y, Gong L, Wang R, Zhu X, Yang R, Tan W (2014) Functional DNA-containing nanomaterials: cellular applications in biosensing, imaging, and targeted therapy. Acc Chem Res 47:1891–1901
94. Hu R, Zhang X-B, Kong R-M, Zhao X-H, Jiang J, Tan W (2011) Nucleic acid-functionalized nanomaterials for bioimaging applications. J Mater Chem 21:16323–16334
95. Song Y, Zhu Z, An Y, Zhang W, Zhang H, Liu D, Yu C, Duan W, Yang CJ (2013) Selection of DNA aptamers against epithelial cell adhesion molecule for cancer cell imaging and circulating tumor cell capture. Anal Chem 85:4141–4149
96. Hwang DW, Ko HY, Lee JH, Kang H, Ryu SH, Song IC, Lee DS, Kim S (2010) A nucleolin-targeted multimodal nanoparticle imaging probe for tracking cancer cells using an aptamer. J Nucl Med 51:98–105
97. Huang C-C, Huang Y-F, Cao Z, Tan W, Chang H-T (2005) Aptamer-modified gold nanoparticles for colorimetric determination of platelet-derived growth factors and their receptors. Anal Chem 77:5735–5741
98. Kim B, Yang J, Hwang M, Choi J, Kim HO, Jang E, Lee JH, Ryu SH, Suh JS, Huh YM, Haam S (2013) Aptamer-modified magnetic nanoprobe for molecular MR imaging of VEGFR2 on angiogenic vasculature. Nanoscale Res Lett 8:1–10
99. Shangguan D, Li Y, Tang Z, Cao ZC, Chen HW, Mallikaratchy P, Sefah K, Yang CJ, Tan W (2006) Aptamers evolved from live cells as effective molecular probes for cancer study. Proc Natl Acad Sci USA 103:11838–11843
100. Shangguan D, Cao Z, Meng L, Mallikaratchy P, Sefah K, Wang H, Li Y, Tan W (2008) Cell-specific aptamer probes for membrane protein elucidation in cancer cells. J Proteome Res 7:2133–2139
101. Wang AZ, Bagalkot V, Vasilliou CC, Gu F, Alexis F, Zhang L, Shaikh M, Yuet K, Cima MJ, Langer R, Kantoff PW, Bander NH, Jon SY, Farokhzad OC (2008) Superparamagnetic iron oxide nanoparticle-aptamer bioconjugates for combined prostate cancer imaging and therapy. ChemMedChem 3:1311–1315
102. Yu MK, Kim D, Lee IH, So JS, Jeong YY, Jon S (2011) Image-guided prostate cancer therapy using aptamer-functionalized thermally cross-linked superparamagnetic iron oxide nanoparticles. Small 7:2241–2249
103. Hood JD, Cheresh DA (2002) Role of integrins in cell invasion and migration. Nat Rev Cancer 2:91–100
104. Sancey L, Ardisson V, Riou L, Ahmadi M, Marti-Batlle D, Boturyn D, Dumy P, Fagret D, Ghezzi C, Vuillez J-P (2007) In vivo imaging of tumour angiogenesis in mice with the αvβ3 integrin-targeted tracer 99mTc-RAFT-RGD. Eur J Nucl Med Mol Imaging 34:2037–2047
105. Lim E-K, Kim B, Choi Y, Ro Y, Cho E-J, Lee JH, Ryu S-H, Suh J-S, Haam S, Huh Y-M (2014) Aptamer-conjugated magnetic nanoparticles enable efficient targeted detection of integrin αvβ3 via magnetic resonance imaging. J Biomed Mater Res A 102:49–59
106. Ko HY, Choi K-J, Lee CH, Kim S (2011) A multimodal nanoparticle-based cancer imaging probe simultaneously targeting nucleolin, integrin αvβ3 and tenascin-C proteins. Biomaterials 32:1130–1138

107. Jennings LE, Long NJ (2009) 'Two is better than one'-probes for dual-modality molecular imaging. Chem Commun 3511–3524
108. Yin M, Li Z, Liu Z, Ren J, Yang X, Qu X (2012) Photosensitizer-incorporated G-quadruplex DNA-functionalized magnetofluorescent nanoparticles for targeted magnetic resonance/fluorescence multimodal imaging and subsequent photodynamic therapy of cancer. Chem Commun 48:6556–6558
109. Li Z, Liu Z, Yin M, Yang X, Yuan Q, Ren J, Qu X (2012) Aptamer-capped multifunctional mesoporous strontium hydroxyapatite nanovehicle for cancer-cell-responsive drug delivery and imaging. Biomacromolecules 13:4257–4263
110. Zhou L, Li Z, Ju E, Liu Z, Ren J, Qu X (2013) Aptamer-directed synthesis of multifunctional lanthanide-doped porous nanoprobes for targeted imaging and drug delivery. Small 9:4262–4268
111. Kuo TR, Lai WY, Li CH, Wun YH, Chang HC, Chen JS, Yang P, Chen CC (2014) AS1411 aptamer-conjugated Gd_2O_3:Eu nanoparticles for target-specific computed tomography/magnetic resonance/fluorescence molecular imaging. Nano Res 7:658–669
112. Shi H, Ye X, He X, Wang K, Cui W, He D, Li D, Jia X (2014) Au@Ag/Au nanoparticles assembled with activatable aptamer probes as smart "nano-doctors" for image-guided cancer thermotherapy. Nanoscale 6:8754–8761
113. Nakatsuka MA, Mattrey RF, Esener SC, Cha JN, Goodwin AP (2012) Aptamer-crosslinked microbubbles: smart contrast agents for thrombin-activated ultrasound imaging. Adv Mater 24:6010–6016
114. Hong H, Goel S, Zhang Y, Cai W (2011) Molecular imaging with nucleic acid aptamers. Curr Med Chem 18:4195–4205
115. Winnard PT, Pathak AP, Dhara S, Cho SY, Raman V, Pomper MG (2008) Molecular imaging of metastatic potential. J Nucl Med 49:96S–112S

Chapter 12
Discovery of Biomarkers Using Aptamers Evolved in Cell-SELEX Method

Prabodhika Mallikaratchy, Hasan Zumrut and Naznin Ara

Abstract The knowledge of biomarkers relevant to diseases has a significant impact on the diagnosis, the prognosis, and the fundamental understanding of the disease. In the context of biomarker discovery in cell-SELEX, the definition of a biomarker referred to a molecular entity overly expressed in an immortalized cell line in which the origin of this cell is a diseased patient. This chapter focuses on an extensive discussion on how biomarkers can be discovered using aptamers evolved from cell-SELEX technology, with a particular emphasis on the systematic steps needs to follow to discover a biomarker. A comparison is made underlining current challenges of existing "omic"-based technologies of biomarker discovery. The utility of chemical versatility of aptamers in transforming aptamers evolved from cell-SELEX as a proteomic tool is discussed. Feasibility of post-proteomic target validation studies employing variety of biochemical techniques is highlighted with selected examples. The significant progress of aptamer-aided biomarker discovery is emphasized with six examples of aptamer-based biomarker discovery leading to the identification of novel marker or already established biomarker molecules. Chapter concludes with a discussion on current challenges that hinders the success of the field of aptamer-based biomarker discovery, and a discussion with potential solutions that could accelerate the progress of the field.

Keywords Aptamer-based biomarker discovery · Cell-SELEX · Proteomics · Flow cytometry · Chemical cross-linking · Protein tyrosine kinase 7 (PTK-7) · Immunoglobin heavy membrane (IGHM) · Stress-induced phosphoprotein 1 (STIP1) · Hemagglutinin (HA) · Sialic acid-binding Ig-like lectin (Siglec-5)

P. Mallikaratchy (✉) · H. Zumrut · N. Ara
Department of Chemistry, Lehman College-City University of New York,
New Science Hall-Office S-4404/Lab S-4401, 250 Bedford Park Blvd. West,
Bronx, NY 10468, USA
e-mail: prabodhika.mallikaratchy@lehman.cuny.edu

W. Tan and X. Fang (eds.), *Aptamers Selected by Cell-SELEX for Theranostics*,
DOI 10.1007/978-3-662-46226-3_12

12.1 What Is a Biomarker?

According to the National Institute of Health, USA, a biomarker is defined as a "characteristic that is objectively measured and elevated as an indicator of normal biological processes, pathogenic processes or pharmacologic response to a therapeutic intervention" [1]. Under this broad definition, for a particular disease such as cancer, the definition of a biomarker is "a biological molecule found in blood, other body fluids, or tissues that is a sign of a normal or an abnormal process, or of a condition or a disease such as cancer" [2]. Based on the aforementioned definition, a biomarker molecule usually assists in differentiating what is a "normal" cell or condition from an "abnormal" cell or condition. Thus, a biomarker could be used in diagnostic or prognostic evaluations in a clinical setting or could be used to discover underlying biochemical mechanisms of the origin and progression of a disease using an immortalized cell line related to cancer. Currently, the established molecular markers include serum proteins, nucleic acids, antibodies, peptides, and small molecules such as sugars, steroids, or any other molecule present in cells, tissues, or biological fluids [3].

12.2 Relevance of Biomarker Discovery

The relevance of biomarker discovery directly aims at early detection in a clinical setting. Early detection is identifying a disease at an early point by detecting molecules specific for a disease or abnormal pathological changes of a cell due to a disease, so that a cure is probable. In cancer, in particular, the prognosis is directly related to the stage of the cancer, which is how far the cancer had spread at the point of diagnosis; thus, early detection plays a crucial role in survival rate [4, 5]. For example, though contradictory, prostate-specific membrane antigen levels are commonly used as a marker for prostate cancer [6] and routine mammograms are advisable for women of 40 years or older to detect early signs of malignancy with no other observable significant signs of the disease [7]. However, these types of methods have shown only a limited success due to the lack of sensitivity needed to reliably detect the disease at an early stage. Therefore, implementation of methods that could successfully detect biomarker proteins relevant to a disease or stages of a disease is in great demand. For this reason, investigations and investments related to discovery of biomarkers have been significantly high both in academic and industrial communities. In a clinical setting, clinicians make an extensive use of existing validated biomarkers to screen patients, diagnose the severity of the disease, and assess patient's response to a treatment and possibility of a recurrence, or to derive prognostic predictions [4–6]. To name a few, plasma troponin is being used to assess patient with chest pain for possible cardiovascular conditions [8], lipoprotein levels are important in prognosis of metabolic and cardiovascular

disease [9], and levels of carcinoembryonic antigen are being assessed to monitor patients with gastrointestinal cancer [2, 4]. In addition, the knowledge of biomarkers can be used to determine the risk of an individual in developing a particular disease and might be helpful in risk reduction steps prior to occurrence of the disease. For example, genetic screening of BRCA1 gene for women with strong family history of ovarian and breast cancer is being used to predict the risk of developing breast cancer, and this approach is clinically validated and often used as a preliminary step in preventative medicine [10, 11]. The traits of biomarker discovery are therefore very important both in a clinical setting to introduce effective treatments and in an academic setting to expand the fundamental understanding of diseases in a molecular level. Such basic understanding will also make grounds for developing new and effective therapeutic molecules.

In the context of biomarker discovery in cell-SELEX, the definition of a biomarker referred to a molecular entity overly expressed in an immortalized cell line in which the origin of this cell is a diseased patient, i.e., a cancer patient [12]. In addition to cancer cell lines, cell-SELEX has been utilized in identifying molecular markers over-expressed on a cell as a result of transfection of a gene or over-expression of a molecule as a result of an infection with a pathogen [13]. The biomarker discovery using cell-SELEX consists of following systematic steps:

1. Identification of a target cell pertaining to a disease model
2. Cell-SELEX followed by identification of aptameric sequences.
3. Post-cell-SELEX screening assays to identify unique binding patterns of each aptamer sequence
4. Identification of unique aptamers sequences followed by aptamer-aided protein capture and proteomic identification.
5. Post-proteomic target validation using biochemical techniques and assays.

The hypothesis of biomarker discovery by cell-SELEX is that the biomarker proteins that are overly expressed in an immortalized cell line or in a cell upon treatment of a gene, or a virus particle. Cell-SELEX against these types of cells will lead to the discovery of new aptamer sequences that could specifically recognize the overly expressed molecules on the target cell line. Then, the identification of the target molecule of the aptamer will lead to finding new molecular signatures of the target cell relevant to a respective disease. This new acquired information will likely correlate with expression patterns of the same proteins in a patient primary cell samples obtained in a clinical setting with the same type of disease. This hypothesis could be justified since any disease originates from the differential expression patterns of molecules leading to alteration of biological process of cells. The altered biological processes of cells will then lead to diseases including malignancies. In addition to discovering biomarkers, if the protein target is an already established biomarker, a new targeting molecule based on aptamers will be introduced.

12.3 Existing Methods of Biomarker Discovery

The methods of biomarker discovery can vary based on the classification of the biomarker. For example, gene expression analyses are being used to detect differential expression of genes in a diseased cell and in a healthy cell [14, 15]. Based on the expression of patterns of a single gene or a cluster of genes, conclusions are being derived. Also, further investigations are conducted to identify potential abnormal expression patterns of one or clusters of genes and its relation to the disease state or origin of the disease. Most common methods of gene expression analysis include whole-genome expression array [15], serial analysis of gene expression [16], expressed sequence tag analysis [17], and gene expression profiling based on alternative RNA splicing [18]]. Also, individual sequences are being analyzed using real-time RT-PCR [19] and competitive quantitative RT-PCR [20]. In addition, epigenetic technologies are used to determine DNA methylation sites, when and how genes are switched "on" and "off" leading to differential expression of genes, that eventually act as triggering points to alter biochemical mechanisms [21]. While genetic testing has shown much promise in distinguishing expression patterns of genes in relation to diseases, biochemical alterations at the posttranslational levels, changes of folding of the proteins, and other biochemical modifications such as phosphorylation, acetylation, and glycosylation, capable of altering the function of the protein leading to disease development cannot be predicted. Also, gene expression analysis might not reflect the alteration of expression levels of proteins. Therefore, the analysis of proteome is better suited due to the fact that over-expression of a protein accounts for the over-expression of genes as well as changes in the posttranslational modifications of proteins, leading to the transformation of a healthy cell into a diseased cell. Here, the detailed focus of the discussion of existing methods will be aimed at identification of cell membrane proteins expressed on a disease cell compared to a "healthy" cell and what are the existing methods available to recognize such patterns. In this regard, two-dimensional gel electrophoresis followed by mass spectroscopy is a technique widely used to discover biomarkers [22]. Utilization of the two-separation strategy for a mixture of proteins through a first dimension separation based on the charge of the protein, and a second dimension based on the molecular mass of the protein, offers high resolution separation of a complex mixture of proteins. This method has been used to successfully identify expression patterns of protein of normal and tumor tissues obtained from liver, bladder, lung, esophageal, prostate, and breast [23]. At its highest resolution, 2-D gel electrophoresis can distinguish distinct as many as 10,000 spots of proteins and peptides [24]. However, due to technical limitations of protein sequencing, even with a highest achievable sensitivity, number of detectable spots is limited [25]. Another disadvantage is that this method requires a large amount of proteins to be analyzed and the technique is unable to identify low-abundance proteins [23].

Direct identification of proteins using tissue samples of a "normal" and an "abnormal" tissues using mass spectrometric (MS) methods to verify expression levels, location in the cell, and information on protein–protein interactions is

well known, and this method is well accepted in identifying biomarkers. Typically, in MS methods, what is observed is a spectrum of mass-to-charge ratio of ions as a function of abundance of each ion of the analyte. Subsequent interpretation of the data is done using bioinformatics approaches using large database of sequences of proteins and peptides. Due to the high-throughput capabilities, resolution, and precision, matrix-assisted desorption–ionization–time-of-flight–MS (MALDI-TOF-MS) and closely related surface-enhanced laser desorption–ionization–time-of-flight (SELDI-TOF) are two well-known approaches used in biomarker discovery [26–28]. For example, it has been reported that direct analysis of tissue samples using MALDI-TOF-MS can detect hundreds of proteins with molecular weights ranging from 2000–70,000 Da in one analysis [27, 29]. Profiling data obtained from analyzing tissues from mouse brain to human glioma had been analyzed using MALDI-TOF-MS that could successfully correlate to disease state, drug resistance patterns, and prognosis [27]. SELDI-TOF-MS also shows a substantial potential in biomarker discovery due to its versatility [28]. One of the key uses of this technique is its use in detecting proteins in biological fluids. For example, levels of serum prostate-specific membrane antigen in prostrate cancer patients and biomarker identification for breast cancer using nipple aspirate fluids had been done using SELDI-TOF-MS method [30]. SELDI-TOF-MS is effective in detecting low molecular weight proteins, usually proteins with molecular weight < 20,000 Da [28]. While both MALDI-TOF-MS and SELDI-TOF-MS are effective in identifying biomarkers, these methods are well suited for the detection of most abundant serum proteins and peptides [23]. Apart from proteomic and genomic approaches, one of the emerging fields of biomarker discovery is the field of metabolomics, i.e., it is the rapid in vivo screening of pathophysiological processes in response to drug interactions [31].

12.4 Cell-SELEX Method in the Context of Biomarker Discovery

The method of aptamer selection, i.e., SELEX ("Systematic Evolution of Ligands by EXponential enrichment") involves a repeated incubation with a specific target, separation, and amplification of DNA or RNA libraries to evolve aptameric sequences toward a specific target [32]. Therefore, the initial aptamer candidate libraries contain a large number of DNA/RNA sequences folded into unique three-dimensional structures. Some of these unique structures are able to specifically recognize epitopes of proteins or "trap" small molecules with high affinity or high specificity [33]. While binding affinity is an important parameter of a ligand, one of the most important features of an aptamer is the high target specificity. The short aptameric sequences are folded into 3-D fold and binding with an epitope in non-covalent fashion with affinities ranging from micro- to picomoles [34]. Due to the high specificity of aptamers, one of the proven hypotheses is that the aptamers can

be used to detect biomolecules with high precision. Therefore, aptamers in the context of biomarker discovery are most ideal candidates. While SELEX method is successful in developing aptameric sequences toward a purified protein, peptides, and small molecules, due to the unique specificity of aptamer–epitope interaction, most of the interaction could only be mimicked in conditions that used for aptamer selection, i.e., aptamer selected using purified protein may not recognize the same protein at its endogenous levels or conditions in a cell. The method cell-SELEX is designed to target a whole cell and uses a subtractive strategy to enrich sequences specific for the target cell [35]. Therefore, the aptamers developed could be used as molecular probes to discover its targeting entity.

To discover biomarkers using cell-SELEX, a prior knowledge of the diseases is important, but prior knowledge of biomarkers is not required. However, upon selection of the target cell line, the choice of the negative cell line will predefine the nature of the molecular differences between the cell lines; thus, the aptamers will be evolved accordingly. For example, (1) Shanguan et al. selected aptamers using CCRF-CEM, a human ALL, T-cell line as the target cell [35], and human Burkitt's cell line Ramos cells as the negative cells to emphasize unique expression levels of molecular entities on CCRF-CEM cells and discovered a new biomarker expressed in CCRF-CEM cells. (2) Tang et al. discovered aptamers specific toward a human lung carcinoma cells infected with vaccinia virus and used uninfected human lung carcinoma cells as a way to emphasize differential expression patterns of vaccinia virus-infected cells with respect to uninfected cells [13] (3) Sefah et al. discovered aptamers toward cell line HL60, an acute myeloid leukemia cells using closely related acute promyelocytic leukemia as the negative cell line [36] Aforementioned selections were designed such that desired molecular differences are emphasized to evolve aptamer molecules that uniquely identify a molecular patterns on the target cell of interest. In order to discover biomarkers uniquely expressed in a given cell, these types of predefined conditions are important to minimize the preexisting complexities of the cellular membrane itself leading to false-positive aptamers. However, cell-SELEX has been used to discover aptamers without using a subtractive strategy; for example, Tang et al. selected aptamers toward human Burkitt's lymphoma cells without using a subtractive strategy and discovered aptamers identified to be interacting with proteins already established as biomarkers for non-Hodgkin's lymphoma [37]. Therefore, based on the need, the cell-SELEX technology could be employed to discover aptamers toward predefined biomarkers or to discover new biomarkers.

Once the target cells are identified, and a negative cell line is defined, a library of DNA/RNA molecules consisting of approximately a 10^{16} number of uniquely folded DNA sequences is incubated with target cells, and following the incubation, washing, and elution, the eluted pool of DNA molecules is incubated with negative cell line to perform a subtractive cell-SELEX. Subtractive step is the most important step in cell-SELEX in the context of biomarker discovery. The hypothesis of introducing a subtractive step is to remove nonspecific DNA/RNA interacting with

cell membrane or to remove aptamers binding to cellular receptor commonly present in a cell not necessarily relevant to specific diseases. While finding a new biomarker is significant, cell-SELEX is also capable of generating aptamers toward receptor molecules expressed in abnormally high levels on a cell due to an underlying biological phenomenon. Therefore, if introducing a negative step will assist in removing aptamer sequences binding to epitopes, then those are not considered biomarkers in terms of either its expression levels or distinctive expression. Thus, aptamer sequences specific for targets uniquely expressed on the target cell line are enriched. Since an aptamer sequence is specific toward one target epitope, a library of molecules consisting of potential aptamer candidates should identify epitopes on a given cell unique to that cell. In this regard, cell-SELEX strategy exploits this key feature of aptamer specificity to identify aptamers toward a single cell type. The simplicity of cell-SELEX method in generating aptamers is also an advantage. On the other hand, closely related phage display techniques [38] require meticulous biological manipulation strategies to discover biomarkers. Even with meticulous biological manipulations, it is challenging to use whole cells as target to discover new antibody fragments specific for biomarkers.

12.5 Aptamers in Biomarker Discovery

Aptamers selected using cell-SELEX is better suited for biomarker discovery than methods based on peptide aptamers or antibodies. The most important parameters of aptamers are specificity and stability as well as simplicity of selection strategies. Due to the simplicity of selection and ease of handling the aptamer, significant number of aptamers is introduced toward number of cancer cell lines.

Aptamers are directly compared with antibodies; antibodies are inherently multivalent and show higher affinity than aptamers. Antibody-based biomarker identification is mainly focused on identifying overly expressed proteins and employs sandwich type of assays. In particular, enzyme-linked immuno sorbant assays (ELISA) had shown high sensitivity and specificity [39]. However, non-specific protein–protein interactions, batch-to-batch variations of antibodies, high cost of production, and low stability of an antibody are the challenges when antibodies are used as molecular probes [40]. Furthermore, ELISA techniques cannot be multiplexed due to nonspecific interactions [41]. Generation of monoclonal antibodies toward a single cell line to distinguish molecular-level differences is not possible due to the nature of monoclonal antibody production technology.

Ease of synthesis and structural homogeneity due to chemical nature of the aptamer allows them to be modified without compromising its specificity and affinity. Also, in biomarker discovery, variety of structural manipulations have been introduced into an aptamer that allow the efficient capturing process.

12.6 Protocols/Methods

The typical method of target protein isolation using aptamers generated by cell-SELEX is depicted in Fig. 12.1.

12.6.1 Isolation of Aptamer–Protein Complex

12.6.1.1 Chemical Modification of Aptamers

Since the interaction of aptamer with its protein target is non-covalent, the fold of the protein and the fold of the aptamer are important in stabilizing the quaternary structure of aptamer–protein complex.

Due to the synthetic nature of aptamers, a precise chemical modification by incorporating different functionalities to improve their performance as molecular probes is feasible. Following is a list of chemical modifications in aptamers that has been shown to improve and aid in isolation of aptamer–protein complex.

Modification of aptamers with biotin: Aptamers used in biomarker discovery are modified with a biotin tag, which allows the isolation and enrichment of the aptamer–protein complex. Typically, aptamer–protein complex is enriched by incorporating a biotin tag at one of the ends of the aptamer. The biotin modification of the aptamer is most common due to the availability of streptavidin beads with or without magnetic properties to separate and enrich the protein–aptamer target prior to get electrophoresis. Since the cell lysate is a complex mixture with high concentration of DNA/RNA binding proteins, enrichment of the aptamer–protein complex is important to avoid false-positive analysis. Also, the proteins are being captured in its endogenous levels typically low in abundance, adding a significant challenge in capturing aptamer–protein complex.

Photocrosslinkable agents: Chemical cross-linking of the aptamer with its target will enable precisely isolating the complex without disrupting the quaternary structure. Also, chemical cross-link will avoid loss of target protein due to disruptions introduced during cell lysis keeping aptamer–protein complex intact. Moreover, chemical cross-linking modification of the aptamer with photocrosslinkable phosphoramidites is done without comprising the specificity to covalently attach the aptamer with its target [42] One way of modifying the structure of the aptamers is the incorporation of 5-iododeoxyuridine (5-dUI), which allows the covalent cross-linking of the aptamer–protein complex leading to enhance the stability of the aptamer–protein complex [42]. Aptamer–protein complex can also be covalently cross-linked using the cross-linking agent called formaldehyde. Formaldehyde had been used in variety of biological assays to cross-link proteins and protein–DNA/RNA complexes [43]. The use of formaldehyde to cross-link aptamer–protein complex further simplifies the aptamer-based biomarker discovery, and post-SELEX structural modification of the aptamer could be substantially

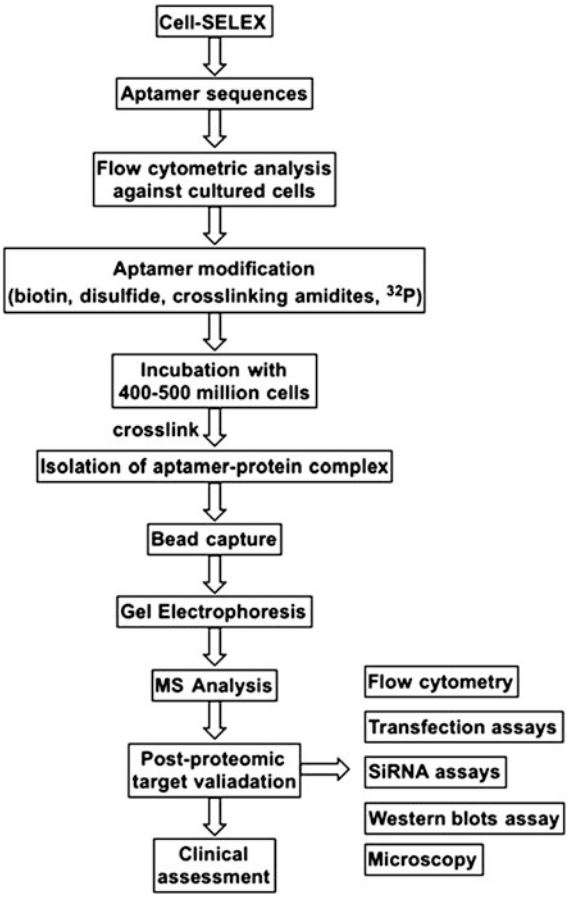

Fig. 12.1 Schematic of the discovery and the validation of biomarkers with aptamers evolved from cell-SELEX method. Upon generating aptamers by cell-SELEX, individual aptamer sequences are evaluated for unique binding patterns. Aptamers with unique binding patterns against cultured cells or clinical samples are then modified with chemical entities that facilitate the biomarker discovery. Typically, 400–500 million cells are used for incubation of the aptamer, and after optional chemical cross-linking step, cells are lysed using a lysis buffer. Aptamer bound membrane is solubilized in an appropriate detergent solution, and aptamer–protein complex is isolated using magnetic beads containing streptavidin. Isolated complex is released from the beads and subjected to protein gel electrophoresis followed by visualization of proteins using commercially available protein staining reagent. Bands corresponding to protein specific for aptamer sequence are excised and subjected to appropriate proteomic analysis. The post-proteomic validation with number of methods is used to confirm the target, and upon clinical sample evaluation, a new biomarker is established

avoided [43] Covalent cross-linking of the aptamer–protein complex also aid in sustaining harsh washing conditions in extraction, an important step in purification and enrichment of targeted proteins from a cell lysate sample.

Disulfide linkers: The cleavable linker such as disulfide linkers can also be introduced to improve the separation of the complex [42]. Efficient removal of aptamer–protein complex after washing could be done either by dramatically changing the pH and heat or appending a readily cleavable disulfide bond between the aptamer and biotin tag.

Radioactive tracers: Finally, aptamers can be modified with radioactive tracers either ^{32}P or ^{3}H for the sensitive detection [42].

These modifications have successfully been used to increase the separation efficiency or detection. Unlike antibodies, which the modification site is preselected based on the functional side chains of amino acids often leads to disruption of the stability, one of the advantages of DNA aptamers is that easy modification can be done to increase the desired features without altering the probe binding ability nor significantly disrupting the stability.

12.6.1.2 Separation of Aptamer–Protein Complex

Typically, the separation of the aptamer–protein complex following the extraction from the rest of the cell lysate is done by protein gel electrophoresis followed by staining of the protein using commercially available protein stain such as coomassie blue. Also, the aptamer–protein complex could be traced during the isolation or separation by incorporating radioactive beta particle emitter ^{32}P at the 5′ end of the aptamer, and aptamer–protein complex could be visualized by gel imaging software prior to excising the band. Following the gel electrophoresis using a 10 % tris-bis-PAGE precast gel, aptamer–protein complex is digested in situ and the resulting peptides are analyzed using mass spectrometry.

12.6.1.3 Criteria for Selection of Target Protein

Upon generation of a list of potential protein hits based on the peptides identified during MS analysis, usually, probable targets are narrowed down based on the nature of the protein target itself. The criteria of selection of the protein are as follows:

1. It is common to observe a significant number of DNA/RNA binding proteins as potential hits due to nonspecific interaction between aptamer and DNA/RNA binding proteins. Therefore, most DNA/RNA binding plasma proteins are eliminated.
2. Elimination of common housekeeping proteins: Transport proteins are commonly present in a cell membrane and can lead to false-positive targets.
3. In the observed size of the protein–aptamer band excised in gel electrophoresis, the protein candidates with significantly higher or lower molecule weights are eliminated.

Typically, these criteria narrow the list of protein candidates, that is, 3–4 candidates for post-proteomic validation assessments.

12.6.1.4 Post-proteomic Validation of Target

Upon determination of the probable target, post-proteomic validation of the target protein is done by a number of methods.

Antibody and aptamer screening with target cells: The first step in target validation is done by comparing the binding patterns of the aptamer and its respective antibody against cells expressing target of interest. For example, Shanguuan et al. evaluated the binding patterns of anti-PTK7 antibody and aptamer Sgc8 in both cultured cells and clinical samples to investigate the similarity of binding patterns [44] (Fig. 12.2).

Similarly, Mallikaratchy et al. evaluated the anti-IGHM antibody binding and aptamer TD05 binding with number of cell lines known to express or not known to express target protein IGHM [42], and Dimitri Van Simaeys et al. used anti-STIP1 antibody and cell lines known to express the target protein [43]. Ara et al. used anti-troponin antibody against target cells, and Yang et al. used anti-Siglec5 antibody against target cell lines [45].

Competition assays with the antibody and aptamer: Following the initial validation, in order to further validate the target, competition assays between the aptamer and antibody are investigated. If the antibody displaces the aptamer upon binding to its epitope, then the target is most likely the protein target of antibody [42, 45].

Validation using biochemical techniques: If the competition is not observed, it is most likely that the aptamer and the antibody binding to two different sites of the protein. Therefore, further validation studies biochemical techniques such as transfection of the protein in a cell line not known to express the target protein [44], Western blot analysis [46], knockdown of the target protein using siRNA followed by binding analysis using flow cytometry [43], proximity assays such as Alpha-Screen assay to investigate how close the aptamer and antibody interacting with target entity [47] is performed. These types of biochemical techniques and assays further validate the target in the post-proteomic validation step.

12.7 Examples of Biomarker Discovery

Examples of biomarker discovery were selected based on the post-proteomic validation steps employed in validation of the protein target.

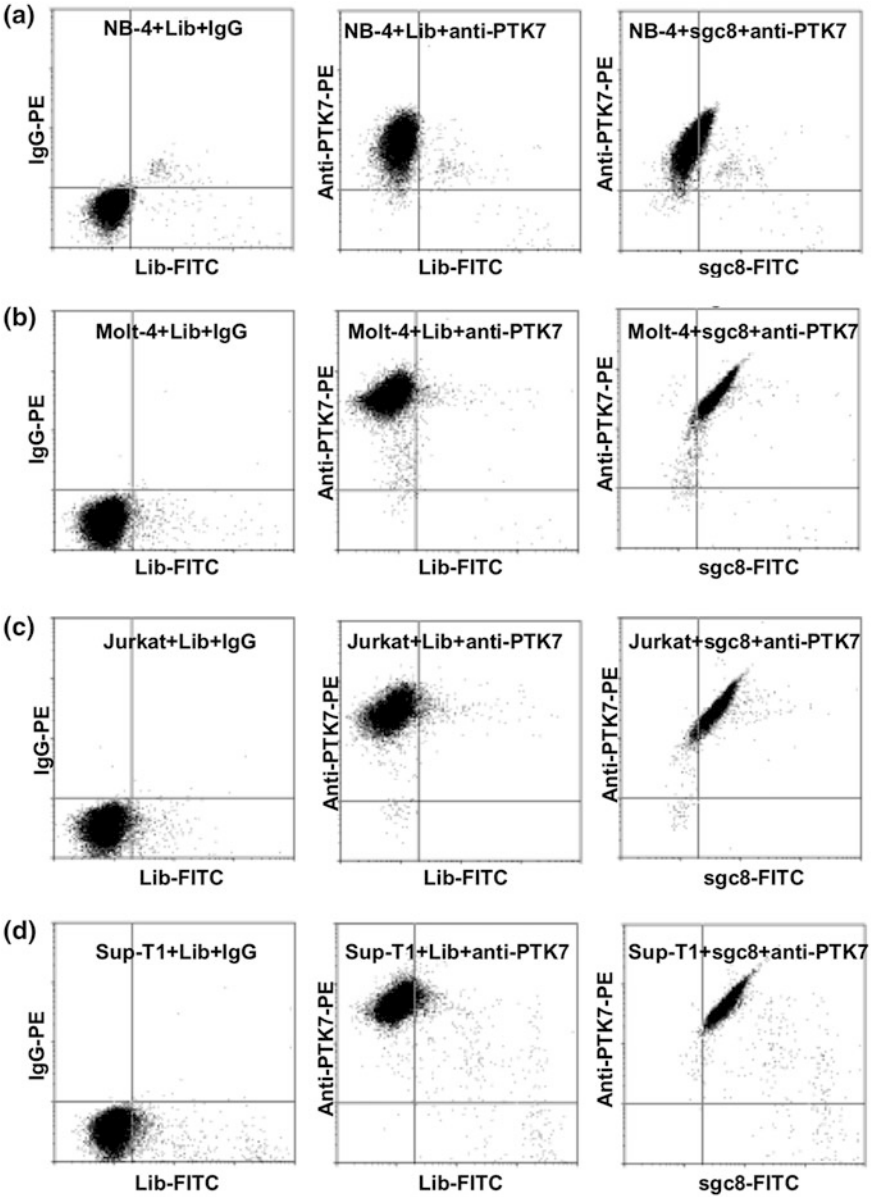

Fig. 12.2 Post-proteomic validation of biomarker target of aptamer Sgc8 was done by flow cytometry. A flow cytometric assay conducted with biomarker candidate anti-PTK7 antibody labeled with PE and Sgc8 labeled with FITC against cultured leukemia cells. **a** Acute promyelocytic leukemia, NB-4; **b** human acute lymphoblastic leukemia (T-cell line), Molt-4; **c** human acute T cell leukemia, Jurkat; **d** human lymphoblastic leukemia (T-cell line), Sup-T1. FITC-labeled random DNA library (Lib) and IgG-PE were used as negative control. Reprinted with the permission from Ref. [44] Copyright 2008 American Chemical Society

12.7.1 Discovery of Expression of PTK7 on T-Cell Acute Lymphoblastic Leukemia (T-ALL) Cell Line, and CCRF-CEM

The discovery of expression of PTK7 on CCRF cells is one of the first examples of aptamers generated using cell-SELEX that could be utilized in discovering biomarkers expressed on cells used as targets in cell-SELEX. The initial hypothesis of cell-SELEX was to discover the molecular differences between two cell types [48]. In doing so, the cell-based SELEX was conducted with T-cell acute lymphoblastic leukemia (T-ALL) cell line, i.e., CCRF-CEM utilizing as a target cell line and as a negative cell line a non-Hodgkin's lymphoma cell line, i.e., Ramos cells as a negative cell line [35]. Following the post-SELEX validation and the screening studies with selected aptamer candidates against cultured cells and clinical samples, one particular sequence, Sgc8, showed high affinity and specificity toward a surface target molecule on T-ALL, acute myeloid leukemia (AML), and B-cell acute lymphoblastic leukemia (B-ALL) suggesting that Sgc8 might be recognizing a specific protein unique to T-ALL, AML, and B-ALL [49]. It was also found that Sgc8 did not bind to normal bone marrow or lymphoma, further confirming that Sgc8 is specific to leukemia.

Since there is no prior knowledge on the nature of the binding entity of Sgc8, initial validation of target of Sgc8 was done by a simple trypsin digestion assays. It was hypothesized that the partial digestion of cell membrane with trypsin to cleave extracellular proteins would shed light on nature of the binding entity on the membrane of CCRF-CEM. Loss of binding ability upon treatment of trypsin and proteinase K revealed that SgC8 does indeed interact with a protease cleavable binding entity suggesting that aptamer Sgc8 might be binding to a protein. A truncated version of Sgc8 was designed and synthesized incorporating a biotin molecule as a capturing moiety to capture Sgc8-target protein.

Proteomic discovery of the target Sgc8 was done by first incubation, lysis, and resolubilization with PBS containing 5 mM $MgCl_2$ and 1 % Triton X-100 buffer to solubilize the membrane proteins using a modified version of Sgc8: Biotin-Sgc8c (Biotin-S-S-S-S-ATCTAACTGCTGCGCCGCCGGGAAAATACTGTACGGTT-AGA, where S denotes an 18-atom ethylene glycol spacer). The biotin–Sgc8c–protein complex was separated from the bulk mixture of cell lysate using streptavidin-coated magnetic beads. The magnetically enriched Biotin-Sgc8c-protein complex was washed to remove nonspecific binders followed by denatured utilizing heat and subjected to SDS-PAGE. Extra protein bands appeared in the coomassie stained gel compared to controls were excised from the gel and analyzed by standard proteomic analysis using LC-MS/MS QSTAR. The MS results revealed that the target of the aptamer could be one of the proteins among 25 hits, which included keratins, ribonucleoproteins, DNA binding proteins, and cell membrane proteins. Justifiably, according to the criteria of protein selection outlined in the method section, the post-proteomic validation was focused on the protein hits that are expressed on the cell membrane. This is due to the experimental observations of

initial validation studies utilizing trypsin/proteinase K suggested that the protein target of Sgc8 might be an extracellular membrane protein. Based on the score obtained in MASCOT database, on the correlation between molecular weight of the band excised from the gel for analysis and due to the fact that PTK-7-5 (an isoform of protein tyrosine kinase 7) is a membrane protein, post-proteomic validation experiments were aimed at confirming PTKC-7-5 as the target of Sgc8 aptamer.

Competition experiments with anti-PTK7 antibody and unlabeled Sgc8 showed no substantial reduction of binding when Sgc8 bound CEM-CCRF cells. However, binding of fluorescently tagged Sgc8 and anti-PTKC7-5 showed a linear relationship when the binding was analyzed using flow cytometry and loss of linearity when control antibodies or control sequences were used. This observation suggested that both Sgc8 and anti-PTK7-5 antibody might be binding to the same protein but two different epitopes. Furthermore, microscopic studies using fluorescently tagged Sgc8 and anti-PTK7-5 antibody showed clear colocalization of the aptamer and the antibody and loss of co-localization when either a control antibody or random aptamer sequences were used. Next, further validation experiments using negative cells used in the initial screening of the aptamer were conducted by transfecting PTK7-5 gene into Ramos cells, followed by flow cytometric analysis of binding of anti-PTK7-5 antibody and Sgc8 aptamer. The binding analysis suggested that both anti-PTK7-5 and Sgc8 aptamer indeed binding to Ramos cells that were transfected and expressed with PTK7-5 (Fig. 12.3).

Further validation of the target was conducted by investigation of internalization of PTK7-5 upon binding with anti-PTK7-5 and Sgc8 and further confirmed that both the antibody and the aptamer show identical colocalization in the endosome confirming that the target of aptamer Sgc8 was indeed PTK-7-5 [50].

The discovery of over-expression PTK7-5 on CCRF-CEM cells and observed over-expression of clinical samples have demonstrated that the upregulated membrane proteins could be identified using aptamers generated by cell-SELEX. PTK-7-5 has been identified as an overly expressed protein in number of tumors but not an established marker for T-ALL or AML [44]. The exact function of PTK7-5 is not clear; however, it has been shown that PTK7-5 plays an important role in metastatic melanoma and other cancers [51]. Finding of PTK7-5 exemplifies that the approach of cell-SELEX followed by biomarker discovery is feasible and can discover new marker molecules expressed in cultured cells.

12.7.2 Discovery of Expression of Membrane IgM in Burkitt's Lymphoma Cells

Modified version of cell-SELEX without employing negative selection has also been used to generate aptamers against immortalized cell lines [37]. In particular, the cell-SELEX carried out against Ramos cells, a Burkitt's lymphoma cell line, eliminating the negative selection, resulted multiple sequences against Ramos cells.

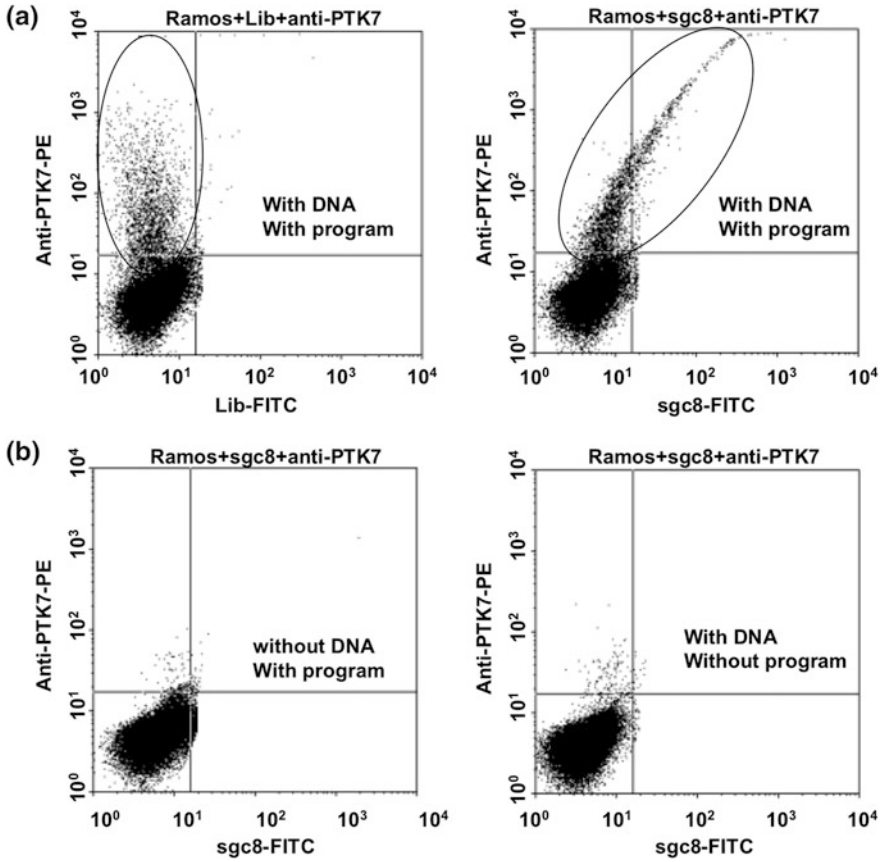

Fig. 12.3 Post-proteomic validation assays against PTK7-negative Ramos cells nucleofected with cDNA of PTK7. **a** Ramos cells nucleofected with plasma containing cDNA of PTK7: *left*, stained with anti-PTK7-PE; *right*, stained with anti-PTK7-PE and Sgc8-FITC. The elliptical area represents the cells that expressed PTK7. **b** Negative control cells stained with anti-PTK7-PE and Sgc8-FITC: *left*, Ramos cells without plasmid with nucleofection program; *right*, Ramos cells with plasmid without nucleofection program. Reprinted with the permission from Ref. [44], Copyright 2008 American Chemical Society

Among the sequences identified, one particular sequence, TD05, showed unique specificity against the target Ramos cells. Partial digestion of cell membrane using proteinase K followed by cell binding assays confirmed that the TD05 binds to a moiety on a membrane receptor [37]. Modified version of TD05 incorporating 5-iododeoxyuridine and biotin and disulfide linkages and ^{32}P, i.e., 5′-ACCGGG AGGAUAGTUCGGTGGCTGTTCAGGGUCTCCUCCCGGTG-S-S-T-PEG-biotin was employed in aptamer-aided receptor isolation experiments. The detailed description of probe modifications can be found under methods. Following incubation with target Ramos cells, and the lysis, streptavidin-coated magnetic bead was

used to isolate the aptamer–receptor complex. Finally, the isolated aptamer–receptor complex was cleaved from the beads and separated from the nonspecific protein using gel electrophoresis. Here, Mallikaratchy et al. reported the utilization of ability of ^{32}P labeling of the DNA aptamer, which allowed the sensitive detection of the complex based on the radioactive emission of the beta particles. Excised gel was analyzed using mass spectrometry. Based on the molecular weight of the excised band, and the fact the aptamer should be binding to a membrane target, four candidates were identified as a potential target of TD05 from the list of proteins generated based on the analyzed peptide sequences from the MASCOT database.

Out of these candidates, authors focused on post-proteomic validation of IGHM as the most probable target of TD05. This is due to the fact that IGHM protein is known to be expressed specifically on B cells [52]. Target validation of IGHM was done by first comparing the binding of corresponding antibody with number of cells lines that are known to express and do not express IGHM.

In doing so, studies were carried out investigating the correlation of binding patterns of anti-IGHM antibody and TD05 aptamers by utilizing a B-cell line known to express IGHM, a B-cell line that does not express IGHM, and a number of T-ALL cell lines. Binding analysis of these cell lines revealed that both the aptamer and the corresponding antibody exhibit similar binding patterns. In particular, the lack of binding of both aptamer and the antibody with Toledo cells, a cell line that closely resembles with Burkitt's lymphoma cells, but does not express cytoplasmic or membrane immunoglobulins due to absence of chromosomal translocations of Burkitt's lymphoma, strongly suggested that IGHM is the protein target of TD05 (Fig. 12.4).

Second validation study was focused on demonstrating that the anti-IGHM aptamer competes with TD05 aptamer. The competition assay was performed based on the hypothesis that if both TD05 and anti-IGHM bind to a similar epitope, the antibody against IGHM might be able to replace the aptamer. Thus, the competition experiment between anti-IGHM antibody and aptamer TD05 revealed that anti-IGHM antibody can replace TD05, suggesting that both probes bind to same target entity with different affinities further confirming the target of TD05 is IGHM (Fig. 12.5).

One unique observation reported was the investigation of aptamer and antibody binding in response to the protease treatment by trypsin. The IGHM is resistant to partial trypsin digestion. An investigation of binding of IGHM and TD05 upon trypsin treatment revealed that both the anti-IGHM antibody and aptamer showed similar binding upon partial digestion of trypsin. These series of post-proteomic validation analysis led the authors to conclude that target of TD05 is IGHM protein.

The most important finding reported is that an aptamer generated using cell-SELEX against Ramos cells, with no prior knowledge of expression levels of IGHM on Ramos cells, led to discover an aptamer that binds to endogenous levels IGHM on Burkitt's lymphoma cells. Since IGHM is one of the major components of B-cell receptor complex expressed in mature Burkitt's lymphoma cells, the discovery of IGHM using TD05 on Ramos cells validates the initial hypothesis of cell-SELEX-aided biomarker discovery [42]. It has also been known that lymphoma development is closely related to IGHM expression on premature B lymphocytes [52].

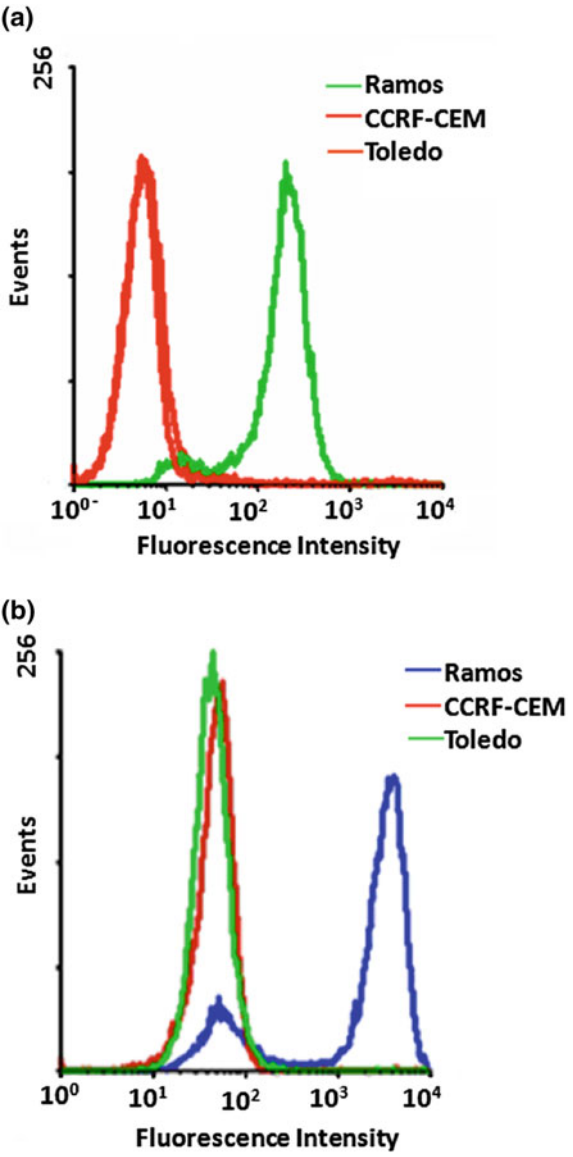

Fig. 12.4 Post-proteomic validation studies to confirm the biomarker: Flow cytometric analysis with anti-IGHM labeled with Alexa Fluor 488 binding with IGHM-negative Toledo cells and CEM cells and IGHM-positive Ramos cells, similarly, binding of FITC-labeled TD05 against Toledo, CEM and Ramos cells was conducted. This research was originally published in Molecular and Cellular Proteomics [42] © the American Society for Biochemistry and Molecular Biology

Furthermore, IGHM is a receptor that has a role in development of Burkitt's lymphoma, and this protein is a marker for Burkitt's lymphomas [52]. Accordingly, these findings demonstrate the applicability of the approach of cell-SELEX followed by the identification of cell membrane receptors that have altered expression levels in tumor cells as one of the best methods to discover biomarkers. In this example, the elimination of the counter selection shows that even with no negative selection, it is feasible to identify upregulated protein candidate in a cell line.

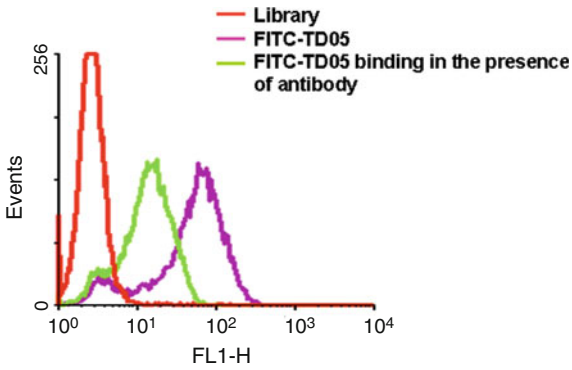

Fig. 12.5 Post-proteomic validation analysis by competition between TD05 and anti-IGHM antibody. After incubation with the antibody, the binding of FITC-labeled TD05 shifts back, compared to FITC-TD05 binding in absence of Alexa Fluor 448 anti-IGHM antibody. This research was originally published in molecular and cellular proteomics [42] © the American Society for Biochemistry and Molecular Biology

12.7.3 Aptamers Recognize Glycosylated Hemagglutinin Expressed on the Surface of Vaccinia Virus-infected Cells

Third example of utilizing cell-SELEX technology for biomarker discovery is aimed at identifying biomarker proteins upon infection of virus on an immortalized cell line published by Parekh et al. [47]. Cell-SELEX against vaccinia virus-infected HeLa cells generated aptamer probes targeting specifically against vaccinia virus (VV)-infected cells. Vaccinia virus has been chosen for this study because it is an established model to study variola virus, which causes smallpox [53]. The method known as "infected cell-SELEX" takes the advantage of the modification of cell surface due to a virus infection to generate aptamer-based molecular probes against infected cells and to discover proteins expressed on the cell surface upon infection using the aptamer molecules as capturing agent.

During selection, in order to minimize the loss of DNA due to porosity resulted in the infected cells in later stages of infection, the infection time was optimized using VV strain expressing GFP in HeLa cells and concluded that the 15 hour post-infection as the optimized infection time to be utilized in the "infected cell-SELEX." Infected cell-SELEX was performed against HeLa cells treated with VV and uninfected HeLa cells. The counter selection with uninfected HeLa cells was introduced after the first five rounds of selection. Progress of the selection was monitored using flow cytometric assays, an enrichment of aptamer candidates obtained at round 12; however, the selection was continued up to the 20th round. Aptamer pools from 12th, 14th, and 20th rounds are cloned and sequenced.

To test the specificity of the obtained aptamers against a virus-infected cells, authors used 3 additional cell lines (CV1, PK15, and RK13) infected with VV and

showed that all the aptamers binding to cells infected VV but not with uninfected cells. This observation suggested that tested aptamers were binding to target molecule expressed due to virus infection and the expression of this protein is cell independent.

Following the initial observation, a competition assay was performed among discovered aptamer sequences in order to determine if the aptamers from different families binding to the same or different target protein. Competition assays confirmed that all four aptamers bind to same protein target and competing among each other. The screening assays using aptamer PP3 (ATCCAGAGTGACGCAGCA CGAGCCAGAC ATCTCACACCTGTTGCATATACATTTTGCATGGACACG GTGGCTTAGT), in particular, against HeLa cells infected with additional orthopox viruses, namely cowpox, vaccinia IHD-j, vaccinia IHD-W and rabbitpox virus, non-orthopox virus, and myxoma virus as a control revealed that aptamer PP3 binds to cells infected with all viruses except rabbitpox virus suggesting that the aptamer PP3 might be interacting with a protein entity unique to specific strain of virus infection (Fig. 12.6). Analysis of the binding patterns of aptamer PP3 and the existing literature of families of virus used in the investigation suggested that aptamer PP3 did not bind to any of the target cells infected with a virus that lacks the expression of hemagglutinin (HA) protein upon infection, even if they are from orthopox family, indicating that HA might be the target. A proximity-based assay known as "AlphaScreen" (amplified luminescent proximity homogenous assay) was used to investigate the biomolecular interactions of aptamer PP3 and HA which are binding to a molecule in close proximity, confirming HA as the target of PP3 (Fig. 12.7).

The target epitope of the generated aptamers is identified as a glycosylated hemagglutinin, which is expressed on virus-infected cells but not on uninfected cells. This study shows that cell surface alterations during viral infection can be distinguished with aptamers evolved utilizing cell-SELEX, and novel biomarkers could be discovered using identified aptamers. Since HA is known to be heavily glycosylated, and glycosylation is important for its activity [54], further investigations were carried out to determine whether the glycosylation pattern is important for aptamer binding. The infected cells are incubated with aptamer PP3 in the presence of glycosylation inhibitors subsequently evaluating the binding of aptamers using flow cytometry. Authors observed a decreased fluorescence signal upon treatment of glycosylation inhibitors, demonstrating that the glycosylation of HA is important in aptamer recognition of HA on infected cells.

Finding of expression of HA using an aptamer discovered using infected cell-SELEX technology demonstrates that the aptamers could be utilized to identify the differential expression of target cell surface proteins due to a viral infection. Once the target is identified, it can be used as a biomarker for that type of infection. The findings also showed that different virus strains could show the same result provided that they express same viral protein.

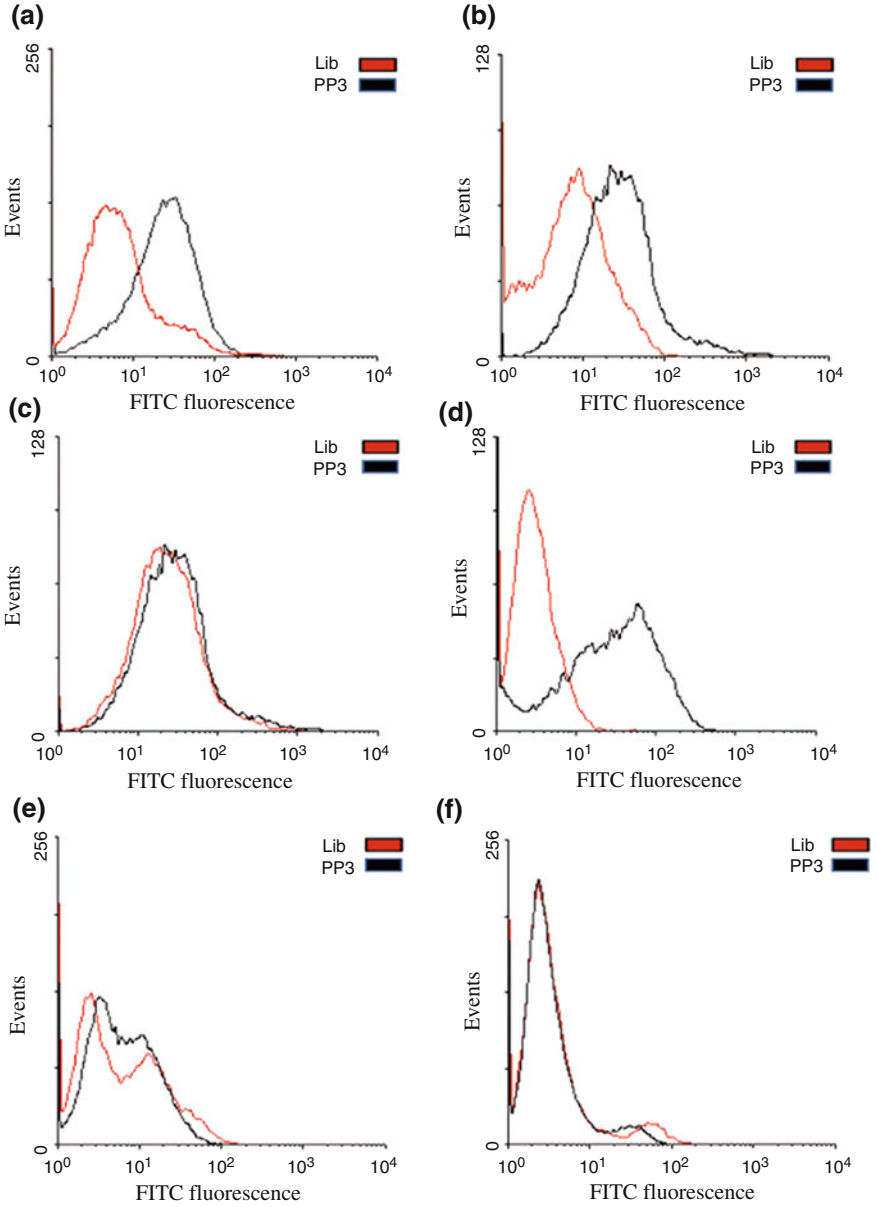

Fig. 12.6 Aptamer PP3 binds HeLa cells infected with different viruses. HeLa cells infected with hemagglutinin (HA)-expressing strains such as **a** VV WR, **b** VV IHDJ, **d** cowpox virus. Non-HA expressing strains **c** VV IHDW; **e** rabbitpox virus; and **f** myxoma, a leporipoxvirus. Reprinted with the permission from Ref. [47] Copyright 2010 American Chemical Society

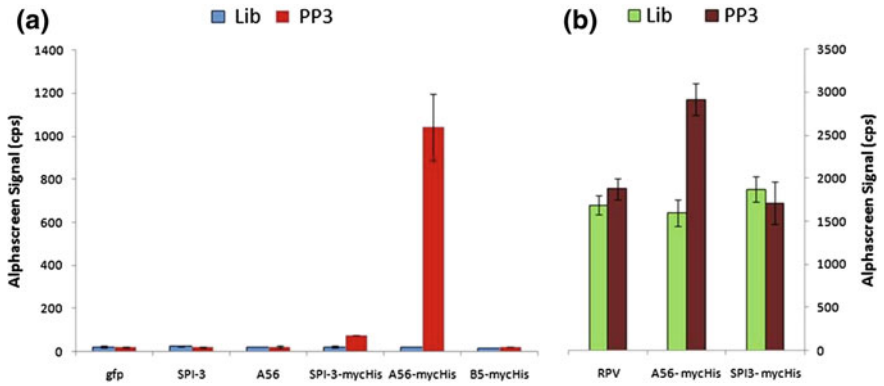

Fig. 12.7 Post-proteomic validation assays using a proximity base assay AlphaScreen™ confirming Hemagglutinin (HA) as the target of PP3. **a** CV 1 cell lysates infected with VV T7 and over-expressing myc-His-tagged proteins GFP (control), SPI-3, HA, and B5 were probed using biotinylated aptamer PP3 and a control DNA library. The control DNA library did not show a signal for any sample. **b** AlphaScreen™ with cell lysates from BSR T7 cells, which express T7 RNA polymerase infected with RPV at moi = 5.0, transfected with plasmids to overexpress myc-His-tagged VV HA and SPI-3. RPV-infected only cells and SPI-3 samples show a nonspecific background signal with aptamer PP3 and DNA library. Reprinted with the permission from Ref. [47] Copyright 2010 American Chemical Society

12.7.4 Identification of Cell Membrane Protein Stress-Induced Phosphoprotein 1 (STIP1) as a Potential Ovarian Cancer Biomarker Using Aptamers Selected by Cell-SELEX

Fourth example of the discovery of biomarker using aptamers generated by cell-SELEX reported by van Simaeys et al. [43] using an aptamer TOV6 selected against ovarian cancer cell line TOV-21G [55]. Initial screening assays of aptamer TOV6 (5′-ATCCAGAGTGACGCAGCACGGCACTCACTCTTTGTTAAGTGGT CTGCTTC TTAACCTTCATCGACACGGTGG CTTA-3′) revealed that it is binding to TOV-21G which is an ovarian adenocarcinoma cell line but not with cervical cancer cell line HeLa or ovarian serous adenocarcinoma CAOV3 [55].

In order to identify the protein target of aptamer TOV6, the authors used a novel cross-linking strategy by using formaldehyde to induce cross-linking between DNA aptamer and the target protein. Upon cross-linking of aptamer to its target, the extraction of the membrane protein–aptamer complex from the cell lysate was done using streptavidin-coated magnetic beads and the identification of target was done by mass spectrometry (MS). Based on the MS analysis, post-proteomic target validation aimed at STIP1 as the target, which is a part of the cell peripheral complex with heat-shock protein 90 [56]. HSP 90 activates metalloproteases, and an HSP 90 complex is an important marker suggesting that discovery of STIP1

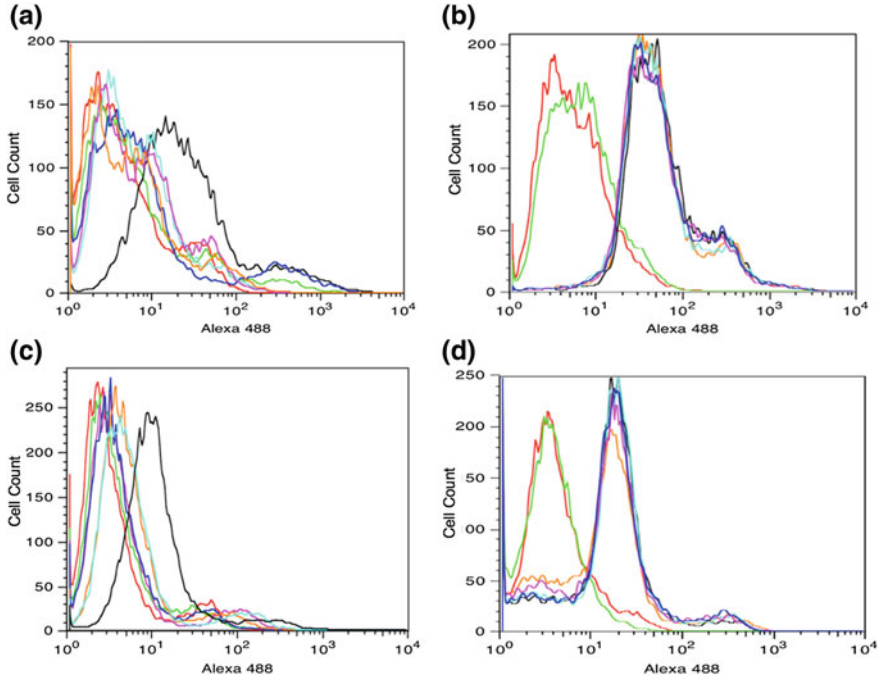

Fig. 12.8 **a** Post-proteomic validation of STIP1 as the target of aptamer TOV6 on TOV-21G cells by silencing of STIP1 in TOV-21G cells followed by flow cytometric analysis. The cells were tested for TOV6 binding after 72 h of siRNA treatment. **b** Absence of PTK7 silencing with STIP1 siRNA treatment in TOV-21G cells. The cells were tested for Sgc8 binding after 72 h of siRNA treatment. **c** Silencing of STIP1 in A172 cells. The cells were tested for TOV6 binding after 72 h of siRNA treatment. **d** Absence of PTK7 silencing with STIP1 siRNA treatment in A172 cells. The cells were tested for Sgc8 binding after 72 h of siRNA treatment. *Red* A172 cells incubated with Streptavidin-Alexa 488 only; *Green* Library-incubated cells; *Black* Scrambled siRNA-treated cells; *Dark blue* STIP1 siRNA 5; *Orange* STIP1 siRNA 6; *Light blue* STIP1 siRNA 10; *Magenta* STIP1 siRNA 11. Reproduced from Ref. [43]

further confirms the feasibility of detecting biomarkers using aptamers evolved from cell-SELEX.

In order to confirm the target STIPI, a number of post-proteomic validation experiments were conducted: First, a siRNA silencing of STIP1 in TOV-21G cells and screening of the aptamer and STIP1 antibody against TOV-21G cell lines were conducted. Silencing of STIP1 using siRNA revealed that STIP1 indeed is the target of TOV6 aptamer (Fig. 12.8). In parallel, a positive control analysis was conducted by evaluating the binding of ant-STIP1 antibody on TOV-21G cells used in silencing experiments. Anti-STIP1 did not recognized cells due to lack of STIP1 expression as a result of silencing experiments suggesting that both TOV6 antibody and anti-STIP1 antibody show similar binding patterns (Fig. 12.9).

Further validation studies were performed using an aptamer blot on rhSTIP1 and showed that aptamer clearly recognized the recombinant protein but not control

BSA. Finally, post-proteomic validation screening with different ovarian cancer cell lines against TOV6 showed that the aptamer was able to bind all the cell lines that express STIP1, including serous-type ovarian adenocarcinoma cell lines (SKOV3 and OVCAR3).

STIP1 (stress-induced phosphoprotein 1) that is also named as Hop (Hsp70/Hsp90 organizing protein) mediates the association of Hsp70 and Hsp90 heat-shock proteins and forms a molecular chaperone complex [56]. STIP1 is shown to have a role in cell invasion in pancreatic cancer since inhibition of STIP1 decreased invasion by downregulating matrix metalloproteinases-2 (MMP-2), an enzyme that is important for metastasis [56]. The invasiveness of TOV-21G cells has been tested in this report by using STIP1 silencing, and results showed that STIP1 silencing decreased the invasion ability [43]. To investigate the ability of aptamer TOV on cell invasiveness by blocking Hsp90-STIP1 interaction, a cell invasion assay was conducted and showed a reduction in invasion ability similar to that observed upon STIP1 silencing, suggesting that binding of the aptamer inhibits biological function of STIP1.

In an independent study, STIP1 is identified as a potential serum biomarker for ovarian cancer, by serum proteomics analysis [57]. The discovery of STIP1 using aptamer TOV6 generated utilizing cell-SELEX shows that cell-SELEX method is a feasible technique for biomarker discovery. This report also introduces novel crosslinking agent to crosslink aptamer-protein complexes utilizing formaldehyde as a crosslinking agent. Use of formaldehyde as a crosslinking agent further simplifies the aptamer aided biomarker discovery. Since the targets of the aptamers generated by cell-SELEX are normally membrane proteins, the aptamer TOV6 has inhibitory effects on cell invasiveness upon binding to its target and might be a potential drug candidate against ovarian cancer.

12.7.5 Identification and Expression of Troponin T, a New Marker on the Surface of the Cultured Tumor Endothelial Cells

Fifth example shows that aptamer-mediated identification of troponin T marker on the cultured tumor endothelial cells using aptamer AraHH001 (5-CGTAGAATTCATGAGGACGTTACGTACCGACTTCGTATGCCAACAGCCCTTTATCCACCTCAGCTAAGCTTACCAGTGCGAT) discovered using cell-SELEX [46]. The cell-SELEX approach was employed against primary cultured tumor endothelial cells (mTECs). Due to the fact that a single tumor endothelial cell can support many tumor cells, tumor endothelial cells from all tumor types are very similar, and also, tumor blood vessels have been shown to differ from their normal counterparts due to leakiness, uneven thickness, and the target cell line mTEC was chosen to discover novel molecules using aptamers discovered using cell-SELEX against mTEC [58]. A 12-round cell-SELEX selection was performed against mTECs to obtain

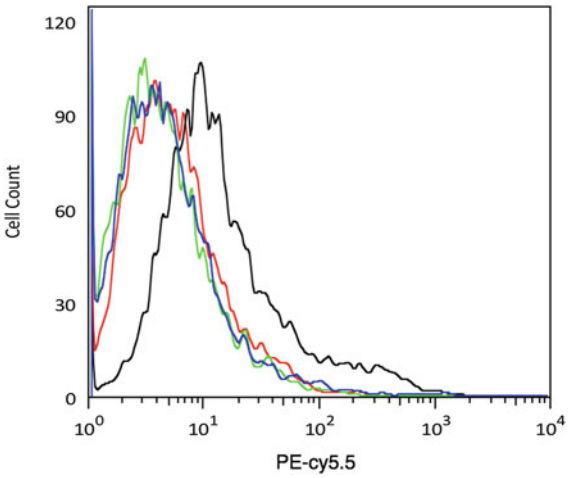

Fig. 12.9 Effect of STIP1 silencing on STIP1 antibody binding. *Red* TOV-21G cells incubated with Streptavidin PE-Cy5.5 only; *Green* Biotinylated IgG Streptavidin PE-Cy5.5; *Black* Biotinylated M33 antibody on scrambled siRNA-treated cells; *Blue* Biotinylated M33 antibody on STIP1 siRNA 5. Reproduced from Ref. [43]

high-affinity aptamer AraHH01. The aptamer AraHH01 has shown to bind selectively to mTECs, it also showed the similar binding affinity against cultured human tumor endothelial cells [58] (Fig. 12.10). In addition, this aptamer has shown to be internalized into the tumor endothelial cells and aptamer–PEG–liposomes nanoparticles enhanced the uptake into mTECs in vitro as well as in vivo [59].

Due to observed binding with human tumor endothelial cells and uptake, the molecular target of the aptamer AraHH01 investigated in a subsequent study [46].

To isolate the molecular target of AraHH01, typical aptamer–protein techniques were followed. The desired protein band following gel electrophoresis was excised and analyzed by the peptide mass fingerprinting (PMF). The PMF analysis showed that the target of aptamer AraHH001 as slow skeletal muscle troponin T (TNNT1) exhibited similarity to cardiac troponin T. There are no reports of TNNT1 surface expression on primary cultured tumor endothelial cells to date. The post-proteomic validation experiments for validating the target was first done by a flow cytometry binding assay and confirmed that the surface expression of troponin T using FITC-conjugated anti-troponin T cardiac antibody on mTECs and skin-ECs. Troponin T was expressed on mTECs, but not on skin-ECs (control normal endothelial cells) (Fig. 12.11). In addition, binding of FITC-tagged anti-troponin T monoclonal antibody using cells partial digested by the protease enzyme trypsin was evaluated by flow cytometry. Flow cytometric analysis showed that anti-troponin T antibody looses its binding ability when the cells are treated with trypsin compared to untreated cells suggesting that the mTECs express troponin T protein. Second validation study was aimed at a quantitative RT-PCR to measure troponin T mRNA

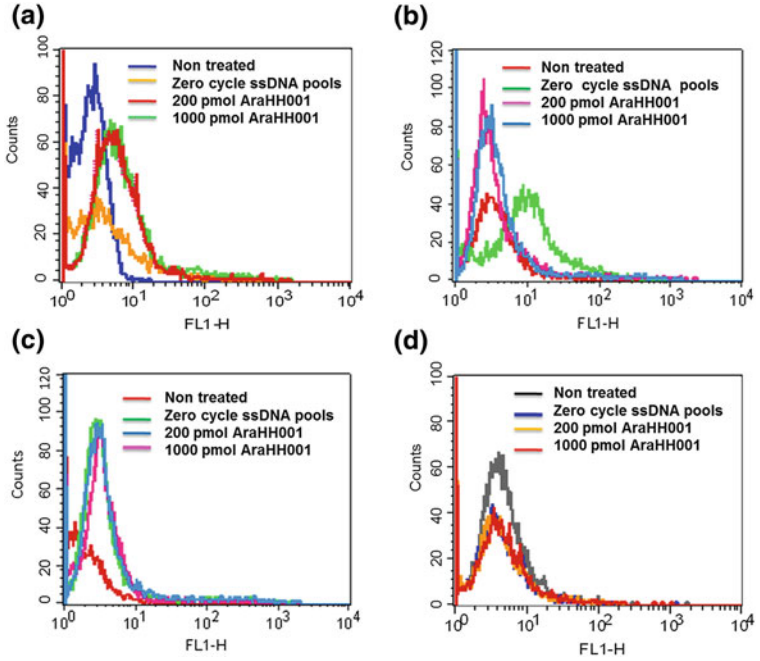

Fig. 12.10 Aptamer araHH01 binding with a series of cells and cell lines by a flow cytometric assay. **a** Normal skin-ECs, **b** OS-RC-2, **c** RFP-SM, **d** HUVEC, **e** HMVEC, **f** m OS-RC-EC, and **g** hTEC. In all cases, the results show non-treated, treated with 200 pmol FITC-labeled zero cycle ssDNA pools, treated with 200 pmol and 1,000 pmol FITC-labeled DNA aptamer AraHH001. Reproduced from Ref. [58]

level on mTECs and skin-ECs normalized to GADPH. The total relative troponin T mRNA levels on mTECs were found higher than normal endothelial cells, skin-ECs. These high expression levels of mRNA encoding troponin T in mTECs suggested that the molecular target of AraHH001 might be troponin T (Fig. 12.11). Third validation was done with electrophoretic mobility shift (EMSA) analysis, using a fixed concentration of Cy5-tagged aptamer AraHH001 with series concentration of recombinant troponin T and analyzed binding using EMSA. A substantial shift of aptamer–protein binding was detected under Luminescent image analyzer, indicating that aptamer AraHH001 binds to purified troponin T. The binding results for a gel shift assay of the aptamer with cardiac troponin T also provided strong evidence that troponin T is the molecular target of ARAHH001 (Fig. 12.11).

Finally, Western blot (WB) experiment was done, using mTECs cellular lysates containing protein sample was separated by SDS-PAGE and transferring to nitrocellulose membrane. The membrane was stained with primary anti-troponin T monoclonal antibody. A recombinant cardiac troponin T was used as a positive control. Western blot experiment also recognized troponin T near 60 kDa as a dimer, which was identical in size of the protein band observed in gel

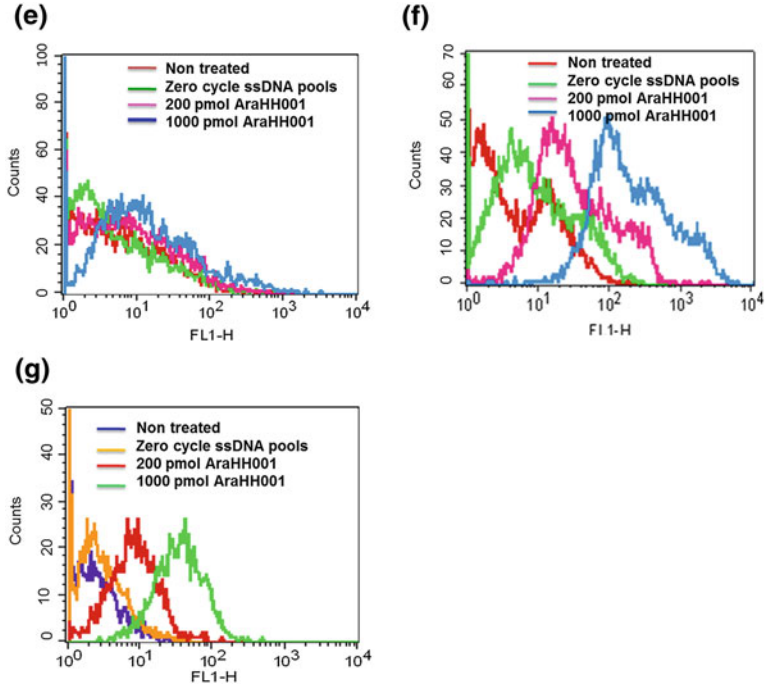

Fig. 12.10 (continued)

electrophoresis during biomarker discovery confirming that troponin T is the protein target of AraHH001 (Fig. 12.12).

Further validation studies were performed with immune-staining experiments using clinical patient samples obtained from excised renal cell carcinoma tissues of 3 patients at the Hokkaido University Hospital, Japan. Human sections were double-stained with Alexa Fluor 647-anti-human CD31 antibody and FITC-conjugated mouse anti-cardiac troponin T antibody to assess troponin T colocalization in hTECs. Expression of troponin T in hTEC was observed based on confocal laser scanning microscopic imaging analysis suggesting that troponin T might be novel biomarker for tumor endothelial cells.

Biologically, troponin is a complex of 3 units of troponin I, C, and T along with tropomyosin and is located on actin filaments, which are essential for the calcium-mediated regulation of skeletal and cardiac muscle contraction [60]. Generally, troponin T is well recognized as a cardiac marker for cardiac injury [8]. The discovery of troponin T expressed on mTECs and the molecular target of aptamer AraHH001 clearly demonstrate the ability of cell-SELX-generated aptamers to discover novel biomarkers that was not known expressed before. Although the exact reason and the mechanistic role of troponin T on mTECs is unknown, novelty demonstrated in this study is that the discovery of a biomarker was not known to express in tumor endothelial cells.

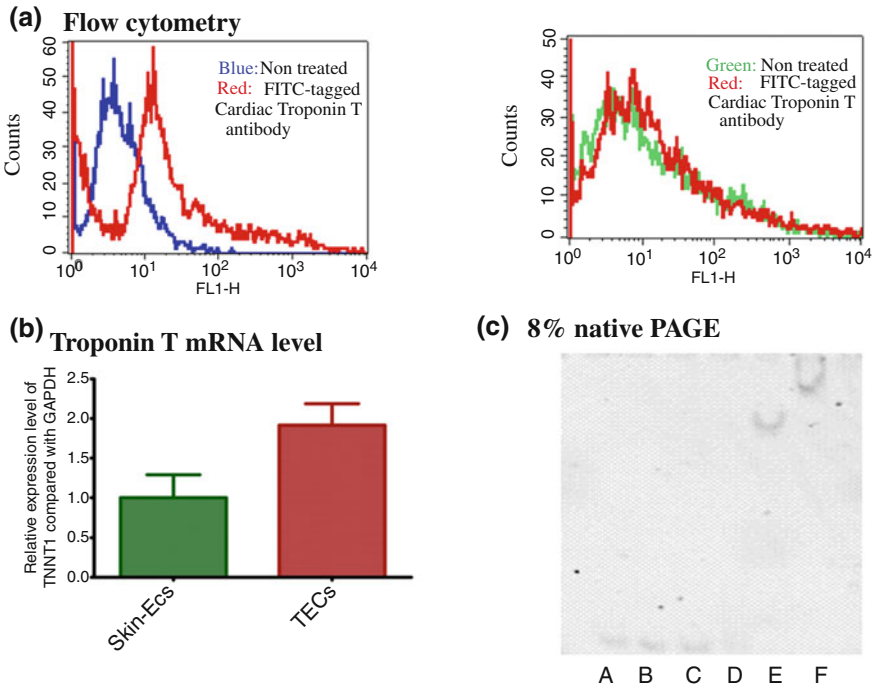

Fig. 12.11 Post-proteomic validation assays to confirm aptamer AraHH001 target protein troponin T. **a** Troponin T expressed on mTECs. flow cytometric assay of a FITC-conjugated cardiac troponin T (cTnT) antibody with mTECs and skin-ECs. The *blue* and *red curves* represent non-treated and treated mTECs with a FITC-conjugated cTnT antibody. The *green* and *red curves* represent non-treated and treated skin-ECs with the FITC-conjugated cTnT antibody. **b** Relative expression of troponin T mRNA level in mTECs and skin-ECs. RT-PCR analyses of the relative expression of troponin T in mTECs as well as in skin-ECs, compared with standard GAPDH. **c** Electrophoretic mobility shift assay (EMSA) of an AraHH001 aptamer with its target protein troponin T. EMSA result represents the binding of 10 nmol/L AraHH001 with 0, 5.33, 16, 80, 400, and 2,000 nmol/L cTnT. Reproduced from Ref. [46]

12.7.6 Developing Aptamer Probes for Acute Myelogenous Leukemia Detection and Surface Protein Biomarker Discovery

Yang et al. recently discovered a panel aptamers against NB4 cell, acute myelogenous (AML) cell line {45}. A significant improvement of this work is that the authors designed a pipeline approach for biomarker discovery including cell-based SELEX technique to select high-affinity aptamer pools against live leukemia cells and to test selected aptamers by phenotyping normal human bone marrow cells or clinical specimens followed by to identify target proteins on the leukemia cell

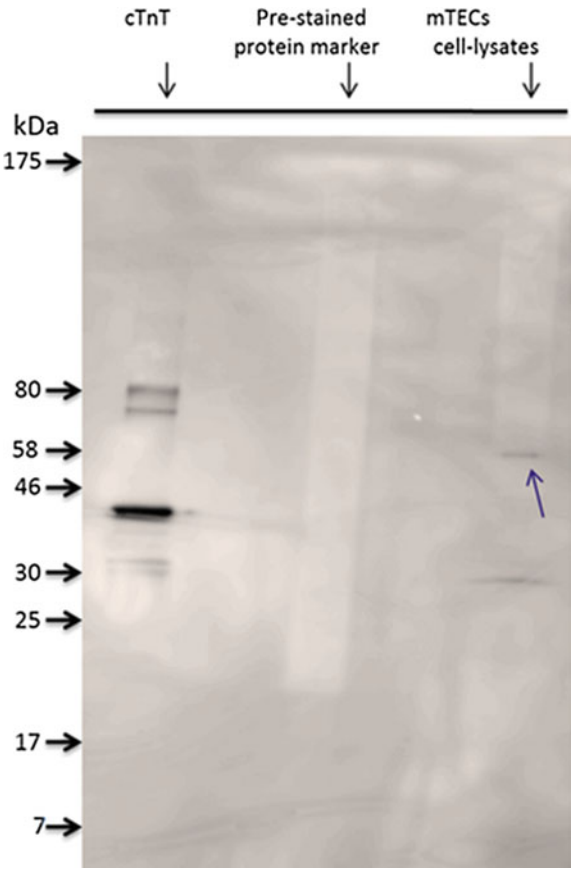

Fig. 12.12 Post-proteomic validation of target using Western blot analysis from mTECs cellular extracts contains membrane proteins. In WB analysis, cardiac TnT in first lane recognized by anti-cardiac troponin T (cTnT) antibody. In the second and third lane, non-recognized prestained protein marker and recognized troponin T from mTECs cellular lysates by anti-cTnT antibody. Reproduced from Ref. [46]

surfaces using aptamer-based proteomic approach. Aptamer selection was performed against NB-4 cells using cell-SLEX method, and after 8–20 rounds of selection, high-affinity aptamers were identified. Authors focused on three aptamers, namely JH6, JH19, and K19 and evaluated their ability to recognize different types of leukocytes from human bone marrow specimens. All three aptamers showed binding with mature and immature granulocytes and monocytes but not with lymphocytes suggesting that three aptamers recognize myeloid-specific surface markers. Out of the three aptamer K19 (showed higher binding with granulocytes, monocytes, and cultured NB4 cells and due to the unique binding pattern of K19), the identification of the molecular target was done. First, a biotin-labeled aptamer K19 designed and synthesized and was incubated with cultured NB4 cells. Aptamer–protein complex was captured using streptavidin-coated magnetic beads, separated by SDS-PAGE, and finally stained with commercially available protein staining agent silver stain. The band corresponding to aptamer–protein complex was excised for trypsin digestion, subsequently analyzed by mass spectrometry. The target of K19 was identified as Siglec-5, sialic acid-binding Ig-like lectin

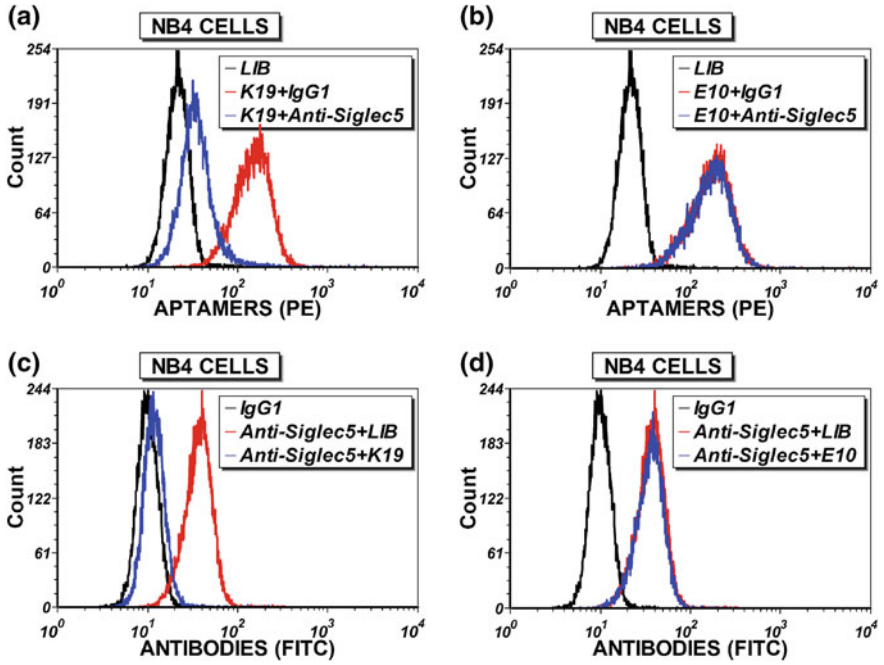

Fig. 12.13 Post-proteomic validation assays to confirm the target protein of aptamer K19 by competition assays of aptamer K19 and anti-Siglec-5 antibody. For blocking aptamer binding with antibodies, NB4 cells were preincubated with anti-Siglec-5 or isotype control antibodies before binding to biotin-labeled aptamers K19 (**a**) or E10 (**b**). The fluorescence intensities of bound aptamers were determined by flow cytometry. Similar approaches were employed with aptamers K19 (**c**) or E10 (**d**) used to block binding of the FITC-anti-Siglec-5 antibody on NB4 cells. The FITC-isotype control (IgG1) was used as a negative control for specific antibody binding. Reproduced from Ref. [45]

protein. Post-proteomic validation was done to confirm the target protein of aptamer K19. In doing so, a competition assay with fluorescein-conjugated anti-human anti-Siglec 5 antibody was performed against aptamer K19 using NB4 and observed that the aptamer K19 and Siglec 5 antibody can compete against each other on the cultured NB4 cells. Thus, authors confirmed that the aptamer k19 recognizes the target protein Siglec-5 and that the binding sites of aptamer K19 and antibody on Siglec-5 might be in close proximity (Fig. 12.13).

The expression of Siglec-5 on granulocytes was reported [61]. However, their expression during granulocytic or monocytic maturation was not well characterized [61]. In order to further investigate the target protein, in particular to determine the binding site of Siglec-5 varies with respect to maturation levels of granulocytes, a series of analysis was done against three subsets of granulocytes, i.e., early, intermediate, and mature. An increase in binding of K19 was observed with increasing maturity of granulocytes suggesting that Siglec-5 upregulated in mature

granulocytes. This report successfully exemplifies the use of cell-SELEX against cultured cells followed by proteomic identification which could successfully be used in molecular recognition in primary cells.

12.8 Challenges and Future Work

There are two important parameters of aptamer binding to it targets is that it is specific three-dimensional fold of the aptamer and three-dimensional fold of the protein and its posttranslational modifications. Therefore, when using whole cells as the target, measures are needed to be taken to avoid introducing differential protein expression patterns due to bias of the cell culture techniques employed. Because such bias with cell culture technique can lead to changes of protein folding, changes of posttranslational modifications and changes in expression levels of certain proteins. Since aptamer recognition is very specific, and aptamers are able to recognize the subtle differences of molecular expression patterns, the maintenance of cell lines with meticulous care is necessary to discover novel marker molecules with clinical relevance. For example, a presence of dead cells in the sample has been an issue with cell-SELEX and new method based on cell-SELEX called FACS-cell-SELEX was introduced to avoid interference from dead cells in culture [62]. Another challenge of aptamer-based biomarker discovery is low signal of the fluorescence tag of the aptamer itself. Due to high heterogeneity of clinical samples, the clinical samples might not express the same protein in question in the levels compared to that of cultured samples. Failure to identify low levels of proteins can lead to false-negative validation results of the biomarker. Methods were introduced and enhanced the signal of an aptamer by incorporating dye-coated silica particles [63]. However, use of particles especially with complex clinical sample can further complicate the process. Therefore, measures needed are taken to design better fluorophores or nanoparticles with enhanced signaling capability to be used against clinical samples. Also, overgrown cells in culture tend to express protein may not necessarily over-expressed in a clinical samples leading to false-positive aptamers. Also, improper techniques of cell culture from the type of plasticware used to how the media is prepared and composition of the cell media, and quality of the incubator could introduce posttranslational modification that might not be present in the same type of disease obtained from primary clinical samples. Maintenance of the three-dimensional structure of the aptamer is important by carefully balancing salt composition. However, during the selection, cells in culture with same salt composition may implicate the folding of proteins. Therefore, these compositions needed to be maintained in exact amounts when clinical samples are screened during biomarker validation step.

One way of avoiding the bias introduced during cell culture procedure is to use clinical samples of the same type of disease during cell-SELEX process. However, it is commonly known that the accessibility to clinical samples from academic laboratories is nearly impossible and requires an extensive amount of regulatory

procedures. Limited access to clinical samples for both during the validation phase and selection phase has a significant impact on aptamer-based biomarker discovery. Discovery of biomarkers using aptamers evolved using cell-SELEX method has shown significant success. So far, number of reports already shown that it is possible to discover biomarkers using this method. However, in order to expand the biomarker discovery using cell-SELEX, a systematic approach of cell-SELEX first with cultured cells and clinical specimens would be more ideal to avoid bias introduced during cell culture in protein expression levels. The success of aptamer-based biomarker discovery will be most likely determined by investigations led by cross-disciplinary collaborative teams consisting of clinicians and aptamer researchers with basic science research capabilities. These types of cross-disciplinary teams will be able to merge technical expertise to propose systematic approaches to address current issues of biomarker discovery.

References

1. Strimbu K, Tavel JA (2010) What are biomarkers? Current opinion in HIV and AIDS 5 (6):463–466. doi:10.1097/COH.0b013e32833ed177
2. Henry NL, Hayes DF (2012) Cancer biomarkers. Molecular oncology 6(2):140–146. doi:10.1016/j.molonc.2012.01.010
3. Frangogiannis NG (2012) Biomarkers: hopes and challenges in the path from discovery to clinical practice. Translational research : the journal of laboratory and clinical medicine 159 (4):197–204. doi:10.1016/j.trsl.2012.01.023
4. Ludwig JA, Weinstein JN (2005) Biomarkers in cancer staging, prognosis and treatment selection. Nat Rev Cancer 5(11):845–856. doi:10.1038/nrc1739
5. Etzioni R, Urban N, Ramsey S, McIntosh M, Schwartz S, Reid B, Radich J, Anderson G, Hartwell L (2003) The case for early detection. Nat Rev Cancer 3(4):243–252. doi:10.1038/nrc1041
6. Lin K, Lipsitz R, Miller T, Janakiraman S, Force USPST (2008) Benefits and harms of prostate-specific antigen screening for prostate cancer: an evidence update for the U.S. Preventive Services Task Force. Ann Intern Med 149(3):192–199
7. Health Quality O (2007) Screening mammography for women aged 40 to 49 years at average risk for breast cancer: an evidence-based analysis. Ontario health technology assessment series 7(1):1–32
8. Babuin L, Jaffe AS (2005) Troponin: the biomarker of choice for the detection of cardiac injury. CMAJ : Canadian Medical Association journal = journal de l'Association medicale canadienne 173 (10):1191-1202. doi:10.1503/cmaj/051291
9. Vasan RS (2006) Biomarkers of cardiovascular disease: molecular basis and practical considerations. Circulation 113(19):2335–2362. doi:10.1161/CIRCULATIONAHA.104.482570
10. Hall JM, Lee MK, Newman B, Morrow JE, Anderson LA, Huey B, King MC (1990) Linkage of early-onset familial breast cancer to chromosome 17q21. Science 250(4988):1684–1689
11. Easton DF, Ford D, Bishop DT (1995) Breast and ovarian cancer incidence in BRCA1-mutation carriers. Breast Cancer Linkage Consortium. Am J Hum Genet 56(1):265–271
12. Fang X, Tan W (2010) Aptamers generated from cell-SELEX for molecular medicine: a chemical biology approach. Acc Chem Res 43(1):48–57. doi:10.1021/ar900101s

13. Tang Z, Parekh P, Turner P, Moyer RW, Tan W (2009) Generating aptamers for recognition of virus-infected cells. Clin Chem 55(4):813–822. doi:10.1373/clinchem.2008.113514
14. Ilyin SE, Belkowski SM, Plata-Salaman CR (2004) Biomarker discovery and validation: technologies and integrative approaches. Trends Biotechnol 22(8):411–416. doi:10.1016/j.tibtech.2004.06.005
15. Welsh JB, Zarrinkar PP, Sapinoso LM, Kern SG, Behling CA, Monk BJ, Lockhart DJ, Burger RA, Hampton GM (2001) Analysis of gene expression profiles in normal and neoplastic ovarian tissue samples identifies candidate molecular markers of epithelial ovarian cancer. Proceedings of the National Academy of Sciences of the United States of America 98 (3):1176-1181. doi:10.1073/pnas.98.3.1176
16. Velculescu VE, Zhang L, Vogelstein B, Kinzler KW (1995) Serial analysis of gene expression. Science 270(5235):484–487
17. Ewing B, Green P (2000) Analysis of expressed sequence tags indicates 35,000 human genes. Nat Genet 25(2):232–234. doi:10.1038/76115
18. Brinkman BM (2004) Splice variants as cancer biomarkers. Clin Biochem 37(7):584–594. doi:10.1016/j.clinbiochem.2004.05.015
19. Scott A, Ambannavar R, Jeong J, Liu ML, Cronin MT (2011) RT-PCR-based gene expression profiling for cancer biomarker discovery from fixed, paraffin-embedded tissues. Methods Mol Biol 724:239–257. doi:10.1007/978-1-61779-055-3_15
20. Evans CW, Wilson DA, Mills GN (2001) Quantitative competitive (qc) RT-PCR as a tool in biomarker analysis. Biomarkers : biochemical indicators of exposure, response, and susceptibility to chemicals 6(1):7–14. doi:10.1080/135475001452733
21. Stenvinkel P, Karimi M, Johansson S, Axelsson J, Suliman M, Lindholm B, Heimburger O, Barany P, Alvestrand A, Nordfors L, Qureshi AR, Ekstrom TJ, Schalling M (2007) Impact of inflammation on epigenetic DNA methylation - a novel risk factor for cardiovascular disease? J Intern Med 261(5):488–499. doi:10.1111/j.1365-2796.2007.01777.x
22. Gorg A, Obermaier C, Boguth G, Harder A, Scheibe B, Wildgruber R, Weiss W (2000) The current state of two-dimensional electrophoresis with immobilized pH gradients. Electrophoresis 21(6):1037–1053. doi:10.1002/(SICI)1522-2683(20000401)21:6<1037:AID-ELPS1037>3.0.CO;2-V
23. Wulfkuhle JD, Liotta LA, Petricoin EF (2003) Proteomic applications for the early detection of cancer. Nat Rev Cancer 3(4):267–275. doi:10.1038/nrc1043
24. Tannu NS, Hemby SE (2006) Two-dimensional fluorescence difference gel electrophoresis for comparative proteomics profiling. Nat Protoc 1(4):1732–1742. doi:10.1038/nprot.2006.256
25. Jain KK (2010) The handbook of biomarkers. Springer, New York
26. Rifai N, Gillette MA, Carr SA (2006) Protein biomarker discovery and validation: the long and uncertain path to clinical utility. Nat Biotechnol 24(8):971–983. doi:10.1038/nbt1235
27. Reyzer ML, Caprioli RM (2005) MALDI mass spectrometry for direct tissue analysis: a new tool for biomarker discovery. J Proteome Res 4(4):1138–1142. doi:10.1021/pr050095+
28. Issaq HJ, Veenstra TD, Conrads TP, Felschow D (2002) The SELDI-TOF MS approach to proteomics: protein profiling and biomarker identification. Biochemical and biophysical research communications 292(3):587–592. doi:10.1006/bbrc.2002.6678
29. Chaurand P, Sanders ME, Jensen RA, Caprioli RM (2004) Proteomics in diagnostic pathology: profiling and imaging proteins directly in tissue sections. Am J Pathol 165 (4):1057–1068. doi:10.1016/S0002-9440(10)63367-6
30. Paweletz CP, Trock B, Pennanen M, Tsangaris T, Magnant C, Liotta LA, Petricoin EF 3rd (2001) Proteomic patterns of nipple aspirate fluids obtained by SELDI-TOF: potential for new biomarkers to aid in the diagnosis of breast cancer. Dis Markers 17(4):301–307
31. Robosky LC, Robertson DG, Baker JD, Rane S, Reily MD (2002) In vivo toxicity screening programs using metabonomics. Comb Chem High Throughput Screening 5(8):651–662

32. Tuerk C, Gold L (1990) Systematic evolution of ligands by exponential enrichment: RNA ligands to bacteriophage T4 DNA polymerase. Science 249(4968):505–510
33. Ellington AD, Szostak JW (1990) In vitro selection of RNA molecules that bind specific ligands. Nature 346(6287):818–822. doi:10.1038/346818a0
34. Jayasena SD (1999) Aptamers: an emerging class of molecules that rival antibodies in diagnostics. Clin Chem 45(9):1628–1650
35. Shangguan D, Li Y, Tang Z, Cao ZC, Chen HW, Mallikaratchy P, Sefah K, Yang CJ, Tan W (2006) Aptamers evolved from live cells as effective molecular probes for cancer study. Proceedings of the National Academy of Sciences of the United States of America 103 (32):11838-11843. doi:10.1073/pnas.0602615103
36. Sefah K, Tang ZW, Shangguan DH, Chen H, Lopez-Colon D, Li Y, Parekh P, Martin J, Meng L, Phillips JA, Kim YM, Tan WH (2009) Molecular recognition of acute myeloid leukemia using aptamers. Leukemia 23(2):235–244. doi:10.1038/leu.2008.335
37. Tang Z, Shangguan D, Wang K, Shi H, Sefah K, Mallikratchy P, Chen HW, Li Y, Tan W (2007) Selection of aptamers for molecular recognition and characterization of cancer cells. Anal Chem 79(13):4900–4907. doi:10.1021/ac070189y
38. Ballew JT, Murray JA, Collin P, Maki M, Kagnoff MF, Kaukinen K, Daugherty PS (2013) Antibody biomarker discovery through in vitro directed evolution of consensus recognition epitopes. Proceedings of the National Academy of Sciences of the United States of America 110 (48):19330-19335. doi:10.1073/pnas.1314792110
39. Chang YM, Donovan MJ, Tan W (2013) Using aptamers for cancer biomarker discovery. Journal of nucleic acids 2013:817350. doi:10.1155/2013/817350
40. Bunka DH, Stockley PG (2006) Aptamers come of age - at last. Nat Rev Microbiol 4596. doi:10.1038/nrmicro1458
41. Gold L, Ayers D, Bertino J, Bock C, Bock A, Brody EN, Carter J, Dalby AB, Eaton BE, Fitzwater T, Flather D, Forbes A, Foreman T, Fowler C, Gawande B, Goss M, Gunn M, Gupta S, Halladay D, Heil J, Heilig J, Hicke B, Husar G, Janjic N, Jarvis T, Jennings S, Katilius E, Keeney TR, Kim N, Koch TH, Kraemer S, Kroiss L, Le N, Levine D, Lindsey W, Lollo B, Mayfield W, Mehan M, Mehler R, Nelson SK, Nelson M, Nieuwlandt D, Nikrad M, Ochsner U, Ostroff RM, Otis M, Parker T, Pietrasiewicz S, Resnicow DI, Rohloff J, Sanders G, Sattin S, Schneider D, Singer B, Stanton M, Sterkel A, Stewart A, Stratford S, Vaught JD, Vrkljan M, Walker JJ, Watrobka M, Waugh S, Weiss A, Wilcox SK, Wolfson A, Wolk SK, Zhang C, Zichi D (2010) Aptamer-based multiplexed proteomic technology for biomarker discovery. PLoS ONE 5(12):e15004. doi:10.1371/journal.pone.0015004
42. Mallikaratchy P, Tang Z, Kwame S, Meng L, Shangguan D, Tan W (2007) Aptamer directly evolved from live cells recognizes membrane bound immunoglobin heavy mu chain in Burkitt's lymphoma cells. Molecular & cellular proteomics : MCP 6(12):2230–2238. doi:10.1074/mcp.M700026-MCP200
43. Van Simaeys D, Turek D, Champanhac C, Vaizer J, Sefah K, Zhen J, Sutphen R, Tan W (2014) Identification of cell membrane protein stress-induced phosphoprotein 1 as a potential ovarian cancer biomarker using aptamers selected by cell systematic evolution of ligands by exponential enrichment. Anal Chem 86(9):4521–4527. doi:10.1021/ac500466x
44. Shangguan D, Cao Z, Meng L, Mallikaratchy P, Sefah K, Wang H, Li Y, Tan W (2008) Cell-specific aptamer probes for membrane protein elucidation in cancer cells. J Proteome Res 7 (5):2133–2139. doi:10.1021/pr700894d
45. Yang M, Jiang G, Li W, Qiu K, Zhang M, Carter CM, Al-Quran SZ, Li Y (2014) Developing aptamer probes for acute myelogenous leukemia detection and surface protein biomarker discovery. Journal of hematology & oncology 7(1):5. doi:10.1186/1756-8722-7-5

46. Ara MN, Hyodo M, Ohga N, Akiyama K, Hida K, Hida Y, Shinohara N, Harashima H (2014) Identification and expression of troponin T, a new marker on the surface of cultured tumor endothelial cells by aptamer ligand. Cancer medicine 3(4):825–834. doi:10.1002/cam4.260
47. Parekh P, Tang Z, Turner PC, Moyer RW, Tan W (2010) Aptamers recognizing glycosylated hemagglutinin expressed on the surface of vaccinia virus-infected cells. Anal Chem 82 (20):8642–8649. doi:10.1021/ac101801j
48. Tan W, Donovan MJ, Jiang J (2013) Aptamers from cell-based selection for bioanalytical applications. Chem Rev 113(4):2842–2862. doi:10.1021/cr300468w
49. Shangguan D, Cao ZC, Li Y, Tan W (2007) Aptamers evolved from cultured cancer cells reveal molecular differences of cancer cells in patient samples. Clin Chem 53(6):1153–1155. doi:10.1373/clinchem.2006.083246
50. Xiao Z, Shangguan D, Cao Z, Fang X, Tan W (2008) Cell-specific internalization study of an aptamer from whole cell selection. Chemistry 14(6):1769–1775. doi:10.1002/chem.200701330
51. Easty DJ, Mitchell PJ, Patel K, Florenes VA, Spritz RA, Bennett DC (1997) Loss of expression of receptor tyrosine kinase family genes PTK7 and SEK in metastatic melanoma. International journal of cancer Journal international du cancer 71(6):1061–1065
52. Cambier JC, Campbell KS (1992) Membrane immunoglobulin and its accomplices: new lessons from an old receptor. FASEB journal : official publication of the Federation of American Societies for Experimental Biology 6(13):3207–3217
53. Adams MM, Rice AD, Moyer RW (2007) Rabbitpox virus and vaccinia virus infection of rabbits as a model for human smallpox. J Virol 81(20):11084–11095. doi:10.1128/JVI.00423-07
54. Shida H, Dales S (1981) Biogenesis of vaccinia: carbohydrate of the hemagglutinin molecules. Virology 111(1):56–72
55. Van Simaeys D, Lopez-Colon D, Sefah K, Sutphen R, Jimenez E, Tan W (2010) Study of the molecular recognition of aptamers selected through ovarian cancer cell-SELEX. PLoS ONE 5 (11):e13770. doi:10.1371/journal.pone.0013770
56. Walsh N, Larkin A, Swan N, Conlon K, Dowling P, McDermott R, Clynes M (2011) RNAi knockdown of Hop (Hsp70/Hsp90 organising protein) decreases invasion via MMP-2 down regulation. Cancer Lett 306(2):180–189. doi:10.1016/j.canlet.2011.03.004
57. Wang TH, Chao A, Tsai CL, Chang CL, Chen SH, Lee YS, Chen JK, Lin YJ, Chang PY, Wang CJ, Chao AS, Chang SD, Chang TC, Lai CH, Wang HS (2010) Stress-induced phosphoprotein 1 as a secreted biomarker for human ovarian cancer promotes cancer cell proliferation. Molecular & cellular proteomics : MCP 9(9):1873–1884. doi:10.1074/mcp.M110.000802
58. Ara MN, Hyodo M, Ohga N, Hida K, Harashima H (2012) Development of a novel DNA aptamer ligand targeting to primary cultured tumor endothelial cells by a cell-based SELEX method. PLoS ONE 7(12):e50174. doi:10.1371/journal.pone.0050174
59. Ara MN, Matsuda T, Hyodo M, Sakurai Y, Hatakeyama H, Ohga N, Hida K, Harashima H (2014) An aptamer ligand based liposomal nanocarrier system that targets tumor endothelial cells. Biomaterials 35(25):7110–7120. doi:10.1016/j.biomaterials.2014.04.087
60. Risnik VV, Verin AD, Gusev NB (1985) Comparison of the structure of two cardiac troponin T isoforms. Biochem J 225(2):549–552
61. Virgo P, Denning-Kendall PA, Erickson-Miller CL, Singha S, Evely R, Hows JM, Freeman SD (2003) Identification of the CD33-related Siglec receptor, Siglec-5 (CD170), as a useful marker in both normal myelopoiesis and acute myeloid leukaemias. Br J Haematol 123 (3):420–430

62. Mayer G, Ahmed MS, Dolf A, Endl E, Knolle PA, Famulok M (2010) Fluorescence-activated cell sorting for aptamer SELEX with cell mixtures. Nat Protoc 5(12):1993–2004. doi:10.1038/nprot.2010.163
63. Yang L, Zhang X, Ye M, Jiang J, Yang R, Fu T, Chen Y, Wang K, Liu C, Tan W (2011) Aptamer-conjugated nanomaterials and their applications. Adv Drug Deliv Rev 63(14–15):1361–1370. doi:10.1016/j.addr.2011.10.002

Chapter 13
Cell-Specific Aptamers for Targeted Therapy

Yue He, Andrea del Valle and Yu-Fen Huang

Abstract Aptamers provide several advantages such as efficient and widely applicable selection technology, reproducible chemical synthesis and modification, generally impressive target binding selectivity and affinity, as well as relatively rapid tissue penetration and low immunogenicity, making them as emerging probes that rivals antibodies in biomedical applications. Recent studies showed that the development of aptamer–drug conjugates and aptamer-conjugated nanoparticles (e.g., gold and magnetic nanoparticles) offers new theranostic opportunities for cancer treatment with better efficacy and lower side effects than traditional chemotherapeutic methods. In this chapter, we discuss the current progress in aptamer-mediated targeted delivery for chemotherapy, phototherapy (e.g., photodynamic therapy and photothermal therapy), and combinational therapy. Conjugation strategies operative through a variety of chemical reactions or physical interactions are also highlighted.

Keywords Aptamer · Aptamer–drug conjugates · Gold nanoparticles · Magnetic nanoparticles · Targeted cancer therapy

13.1 Introduction

Cancer is a complex disease involving numerous tempo-spatial changes in cell physiology. Six biological capabilities, which can be described as sustaining proliferative signaling, evading growth suppressors, resisting cell death, enabling replicative immortality, inducing angiogenesis, and activating invasion and metastasis, are considered essential progressions during the development of malignant tumors [1, 2]. Although the origin of cancer is far from settled, unspecific

Y. He · A. del Valle · Y.-F. Huang (✉)
Department of Biomedical Engineering and Environmental Sciences,
National Tsing Hua University, Hsinchu, Taiwan, ROC
e-mail: yufen@mx.nthu.edu.tw

W. Tan and X. Fang (eds.), *Aptamers Selected by Cell-SELEX for Theranostics*,
DOI 10.1007/978-3-662-46226-3_13

factors, including radiation, chemicals, viruses, inflammation, and carcinogens, can initiate the disease [3]. The processes underlying the transformation of normal cells to cancerous cells have been the focus of intense research efforts [4–6]. Unfortunately, despite decades of basic and clinical studies and a multitude of trials of promising therapeutic strategies, cancer remains a major cause of morbidity and mortality, as well as the top public health problem worldwide [7]. As of 2014, cancer has been reported to be the second major cause of mortality in the USA with 1,665,540 new cases and 585,720 deaths [8]. A skyrocketing level of investment has been devoted to the battle against cancer, which has become one of the top priorities for biotechnological research and pharmaceutical innovation worldwide.

Cancer treatments commonly employed by clinicians include surgery, radiotherapy, and chemotherapy. The choice of therapy depends upon the type of cancer, its location, and its state of advancement [9]. Optimal tumor control sometimes requires a combination of different modalities. For patients with systemic cancers, such as leukemia or lymphoma, or advanced cancers with a high risk of spreading, chemotherapy is considered the most effective anticancer treatment [10]. The drugs adopted in chemotherapeutics are toxic compounds designed to target and disrupt actively dividing cancerous cells. Many of these drugs interfere with the synthesis of precursor molecules needed for DNA replication. These agents include antifolates (e.g., methotrexate), pyrimidines such as 5-fluorouracil, and purines such as 6-mercaptopurine and 6-thioguanine, which can damage cells during the S phase of the cell cycle. Other drugs, such as nitrogen mustards and platinum compounds belonging to a class of alkylating agents, can cause extensive DNA damage and therefore prevent the cancerous cells from reproducing. Several other categories of medications including anti-tumor antibiotics (e.g., anthracyclines) and mitotic inhibitors, such as taxanes and topoisomerase inhibitors, are currently available for cancer treatment via various mechanisms of action [11].

Although the aim of traditional chemotherapy regimens is to target rapidly dividing cancerous cells, cytotoxic medicines also affect certain normal cells (e.g., hair, gastrointestinal epithelium, and bone marrow), which ultimately leads to adverse side effects including alopecia, gastrointestinal symptoms, and myelosuppression. Targeted therapy has therefore become the focus for the development of modern medications [12]. Among the new anticancer drugs approved by the US Food and Drug Administration (FDA) since 2000, fifteen have been targeted therapies, while only five have been traditional chemotherapeutic agents [13]. Targeted therapy nowadays includes two major classifications comprised of monoclonal antibodies and small-molecule inhibitors [14]. In spite of their distinct mechanisms of action and toxicities targeted, the distinctive function of these therapeutic agents is to block the proliferation of cancer cells by interfering with specific molecules (molecular targets) that are involved in tumor development and growth. Targeted therapy is currently a component of treatment modality for various types of cancer, including breast, colorectal, lung, and pancreatic cancers, as well as lymphoma, leukemia, and multiple myeloma [13]. The concept of tailored cancer treatment has been further expanded to individual patients, which has paved the way to a new era of personalized medicine [15].

A particularly successful event in the targeted therapy revolution has been the discovery and development of monoclonal antibodies directed against molecules that are either unique to, over expressed in, or mutated in cancer cells. A broad array of targets, such as epidermal growth factor receptor (EGFR), vascular endothelial growth factor (VEGF), and human epidermal growth factor receptor 2 (HER2/neu), have garnered attention as potential molecular signatures associated with malignant tumor progression. Bevacizumab (Avastin) and trastuzumab (Herceptin) are representative candidates approved by the FDA for antibody-based therapeutics applicable to solid tumors [16]. Monoclonal antibodies can be used either alone or conjugated with radioactive isotopes or other toxic agents for targeted delivery. Once the antibody binds to a specific tumor antigen expressed on a carcinoma, toxins are delivered to the tumor site without damaging nearby healthy tissue. Numerous preclinical efficacy studies have demonstrated that antibody–drug conjugates (ADCs) present a beneficial combination of selectivity and potency to reduce the risk of systemic toxicity. Recent advances in conjugation technology have also greatly improved the therapeutic effectiveness of ADCs for carcinoma patients. So far, the FDA has approved four ADCs for market, and more ADCs are currently being evaluated in clinical trials [17–19].

In addition to antibodies, aptamers comprise another class of molecular probes for selective disease tissue recognition in targeted therapy. Aptamers are single-stranded oligonucleotides that fold into unique three-dimensional structures [20]. Through structural recognition, these probe elements demonstrate a particularly high binding affinity for their targets, which include small organic molecules, proteins, and live cancer cells [21–23]. Aptamers applicable to a specific target can be identified using the systematic evolution of ligands by exponential enrichment (SELEX) process. In this process, aptamers are selected from a random library of DNA or RNA and, via multiple selection cycles, are enriched by repetitive binding to their target molecules. Presently, several kinds of aptamers have been developed for cancer-related proteins, such as VEGF, platelet-derived growth factor (PDGF), human epidermal growth factor receptor 3 (HER3), nuclear factor kB (NF-kB), and prostate-specific membrane antigen (PMSA) [24]. Aptamer selection appropriate for complex targets, in particular, for entire cells, has also been successfully demonstrated using a cell-based SELEX technology [25]. Recent reports indicate that panels of new aptamer probes have been generated for various types of cancer cells, such as lymphocytic leukemia, myeloid leukemia, liver cancer, and colon cancer, as well as small cell and non-small cell lung cancer. These aptamers exhibit high specificity and binding affinity (K_d values in the nanomolar to picomolar ranges) for the targeted cells, thus increasingly arising as an alternative to conventional antibody treatment [26].

As an emerging probe that rivals antibodies in both therapeutics and diagnostics, synthetic aptamers possess a number of beneficial properties over those of natural antibodies. Aptamers are easy to synthesize and manipulate with high reproducibility at low cost. Their inherent stability makes them suitable for long-term storage and allows for reversible denaturation. Additional advantages, such as biocompatibility, lack of toxicity and unwanted immunogenicity, and rapid tissue

penetration, also make aptamers ideal candidates for applications in molecular medicine [23]. Similar to antibodies, certain aptamers themselves have been exploited as macromolecular drugs [24, 27]. For instance, pegaptanib (Macugen, Pfizer) was the first therapeutic aptamer approved by the FDA in 2004 for anti-VEGF treatment of neovascular age-related macular degeneration. Another example is AS1411, a well-known aptamer that recognizes nucleolin, a BCL-2 mRNA-binding protein involved in cell proliferation. Once bound, the AS1411 aptamer can be internalized by the target cell, and then interferes with intracellular pathways. AS1411 is currently in phase II clinical trials for the potential treatment of a broad range of cancers including acute myelogenous leukemia (AML) [28].

In addition to the therapeutic modulation of protein activities implicated in pathological conditions, aptamers that can differentiate ex vivo and in vivo tumor cells from healthy cells also enable selective delivery of therapeutic cargos (e.g., siRNA, chemotherapeutics, or toxins) in targeted cancer therapy. Considerable effort has also been applied for developing a variety of aptamer-mediated delivery vesicles [29–32]. With the increasing enthusiasm for nanotechnology, nanoparticle-based drug delivery systems have received extensive attention among researchers over the past decades [33–36]. Nanoparticles, owing to their small size, particularly from 10 to 200 nm, can extravasate across the leaky endothelium barrier and become concentrated preferentially in tumors and inflamed tissues by virtue of the enhanced permeability and retention (EPR) effect of the vasculature [37–39]. The drug of interest is typically entrapped, encapsulated, adsorbed, or attached in or onto the nanocarrier to reduce drug leakage, to protect the drug against enzymatic degradation, and, ultimately, to improve their bioavailability for systemic delivery. Moreover, the physicochemical characteristics, including the drug release profile and pharmacokinetic and pharmacodynamic behaviors of the delivery vesicles, can also be tailor-made with respect to their materials and surface chemistry. To date, various inorganic nanoparticles, such as gold nanoparticles [40], iron oxide nanoparticles [41], carbon nanotubes [42], and mesoporous silica nanoparticles [43], as well as organic nanoparticles, including liposomes [44], micelles [45], and polymers [46], have been developed as effective delivery platforms. Although the approach based on EPR effects, called passive targeting, can enhance drug accumulation in a tumor area, the approach does suffer from certain limitations such as the limited control of the process owing to the random diffusion of drugs inside tumor tissue. In addition, this strategy is further restricted because certain tumors do not exhibit EPR effects, and the permeability of vessels may not be equivalent throughout a single tumor [47, 48]. To overcome these limitations, active and tumor-specific targeting of nanomaterials has begun to develop into a potentially powerful technology in cancer treatment. In combination with cell-specific aptamers, nanovesicles could be directionally transported to tumor sites, leading to an increased accumulation of therapeutic agents to specific cells or tissues while minimizing harmful toxicity to non-targeted cells. In addition, the ability of some aptamers to be internalized into cells also allows for an efficient intracellular delivery of nanocarriers as well as for selective drug accumulation at target sites.

In this chapter, we summarize recent advances in the use of cell-specific aptamers as recognition moieties for targeted cancer therapy. Promising strategies for targeted delivery using aptamer-based conjugates can be divided into two major categories: (1) aptamer-tethered therapeutic agents and (2) aptamer-functionalized nanoparticles including gold nanoparticles and magnetic nanoparticles. Current progress in aptamer-mediated targeted delivery for chemotherapy, phototherapy, and combined therapy is highlighted. Conjugation strategies operative through a variety of chemical reactions or physical interactions will also be discussed. Importantly, aptamer-based conjugates have demonstrated high efficacy and low side effects for cancer treatment in targeted therapy, making them promising candidates for advanced applications in future cancer therapy.

13.2 Aptamer-Conjugated Chemotherapeutic Drugs for Specific Cancer Cell Therapy

13.2.1 Aptamer–Drug Conjugates in Targeted Chemotherapy

The lack of specificity of traditional chemotherapeutic agents for tumor cells often results in adverse and even life-threatening effects for patients [49]. To overcome this drawback, new therapeutic approaches based on aptamer-mediated specific drug delivery have been explored [50]. Aptamers have been designed as targeting moieties and, when linked with anticancer drugs, have enabled the selective delivery of therapeutic compounds to diseased sites. The chemical stability and ease of manipulation of oligonucleotides also provides tremendous opportunities for scientists to design various aptamer linkage strategies [30]. Some of the representative aptamer–drug conjugates in which aptamer is directly conjugated to drug molecules via either a chemical cross-linker or physical intercalation will be described in the section below. These studies have revealed the numerous advantages offered by aptamer technology, which is poised to play an important role in the targeted delivery of therapeutics.

13.2.1.1 Covalent Conjugation of Aptamers to Chemotherapeutic Agents via Chemical Linkages

Site-specific modifications of aptamers with different functional groups, such as thiol, amino, or azide, can be readily synthesized using a solid-phase method. These modifications enable further derivatization of aptamers to various drug compounds through stable chemical bonds. Huang et al. [29] succeeded for the first time in the covalent attachment of the DNA aptamer sgc8c to the anti-tumor drug doxorubicin (Dox) through a hydrazone linkage (Fig. 13.1). The aptamer sgc8c, which was selected for human T-cell acute lymphoblastic leukemia (T-ALL), CCRF-CEM cell lines, binds to its target, protein tyrosine kinase 7 (PTK7), with a high binding

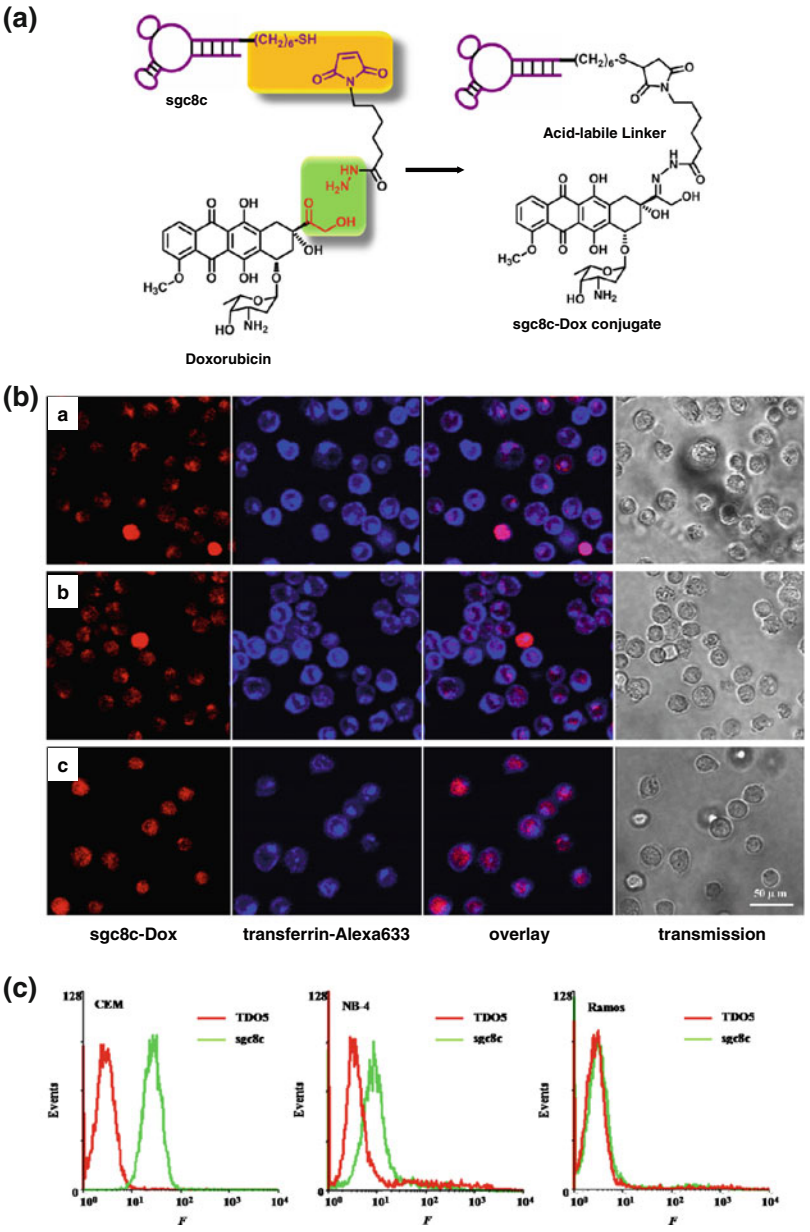

Fig. 13.1 Sgc8c–Dox conjugates for targeted drug delivery. **a** Schematic diagrams depicting the covalent conjugation between aptamers sgc8c and chemotherapeutic agents Dox via acid-labile linkages. **b** Distribution of sgc8c–Dox conjugates inside CCRF-CEM cells after incubation with cells for (*a*) 30 min, (*b*) 1 h, and (*c*) 2 h, respectively. From *left* to *right*, the fluorescence confocal images were monitored for sgc8c–Dox, transferrin–alexa633, overlay of these two channels, and bright field channel, respectively. **c** Flow cytometry assay for the binding of biotin-labeled TDO5 and sgc8c with three different cell lines: CCRF-CEM, NB-4, and Ramos cells. Cells (10^5/mL) were incubated with biotin-labeled TDO5 and sgc8c at 37 °C for 20 min in 100 μL culture medium without FBS. After washing twice, cells were mixed with streptavidin-(R-phycoerythrin) (20 min on ice), and the fluorescence was determined by flow cytometry. Reproduced from Ref. [29] by permission of John Wiley & Sons Ltd

affinity (K_d approximately 1 nM) and high specificity. PTK7, a transmembrane receptor that is highly expressed on CCRF-CEM cells, has been recently recognized as a new potential biomarker for leukemia [51]. After specific binding to PTK7, the sgc8c–Dox conjugate undergoes efficient uptake by the target cell and accumulates inside the endosomal compartment. The acidic environment (pH 4.5–5.5) of endosomes leads to a specific cleavage of the acid-labile hydrazone linker, allowing the rapid transport and function of Dox molecules in the nucleus. Analysis of cell viability demonstrated that the sgc8c–Dox conjugate possesses a potency similar to the unconjugated parent Dox, but with minimal toxicity toward non-targeted cells. Therefore, the molecular assembly of Dox to the aptamer probe through a simple conjugation strategy is highly promising for target-specific intracellular drug delivery. When compared to the less effective reported Dox immunoconjugates [12], the beneficial properties of the developed sgc8c–Dox conjugate also make targeted chemotherapy more feasible with drugs having various potencies.

To achieve high-capacity targeted drug delivery, a novel dimeric aptamer complex (DAC) has recently been developed by Boyaciogul et al. [52]. In the DAC, two individual aptamers, termed SZTI01, are linked together through the complementary overhang added to the 3′-end of each DNA strand (Fig. 13.2a). The duplex bridging is designed to be sufficiently stable under physiological conditions to achieve a prolonged half-life (approximately 8 h) for optimal in vivo activity. The SZTI01 used herein is a new DNA aptamer identified after SELEX processing directed at the PSMA. PSMA expression is elevated in prostate epithelial cells; thus, the antigen can be considered as a potential prognostic marker for lethal prostate cancers [53]. Because PSMA is expressed as a dimer on the apical plasma membrane of tumor cells [54], a DAC with the dimeric aptamer construct suggests an improved activity toward PSMA targeting relative to monovalent ligands [55]. To promote multiple drug loading, CpG sequences that reveal a preferential binding for Dox were also appended to the duplex-forming counterpart. The covalent attachment of Dox to DAC using formaldehyde results in a complex, denoted as DAC-D, which presents a high payload capacity with a stoichiometry of four equivalents of Dox per complex. DAC-D has been used to selectively deliver Dox to PSMA-positive C4-2 cells with minimal uptake into PSMA-null cells. After cellular internalization, Dox is readily released from the DAC-D and translocated to the nucleus upon acid-mediated dissociation in endosomes. As a result, the complex exhibited cytotoxicity to a similar extent as free drug molecules of an equivalent amount. Overall, the specificity and stability features of DAC-D are highly useful for improved delivery of Dox selectively to malignant tissue in vivo.

A more efficient strategy to enhance the drug-loading capacities of aptamer–drug conjugates has been proposed by our group (Fig. 13.2b) [56]. A phosphoramdite monomer, called a therapeutic module (D), was first designed and synthesized to contain an anticancer drug moiety (fluorouracil, 5-FU) and a photocleavable linker (a nitrobenzene derivative). The aptamer–drug conjugate, ApDC, was then integrated from module D as well as the other phosphoramidite building blocks A, T, C, and G in a stepwise manner using an automated DNA synthesizer. Multiple drug moieties could also be successfully incorporated into one aptamer at predesigned

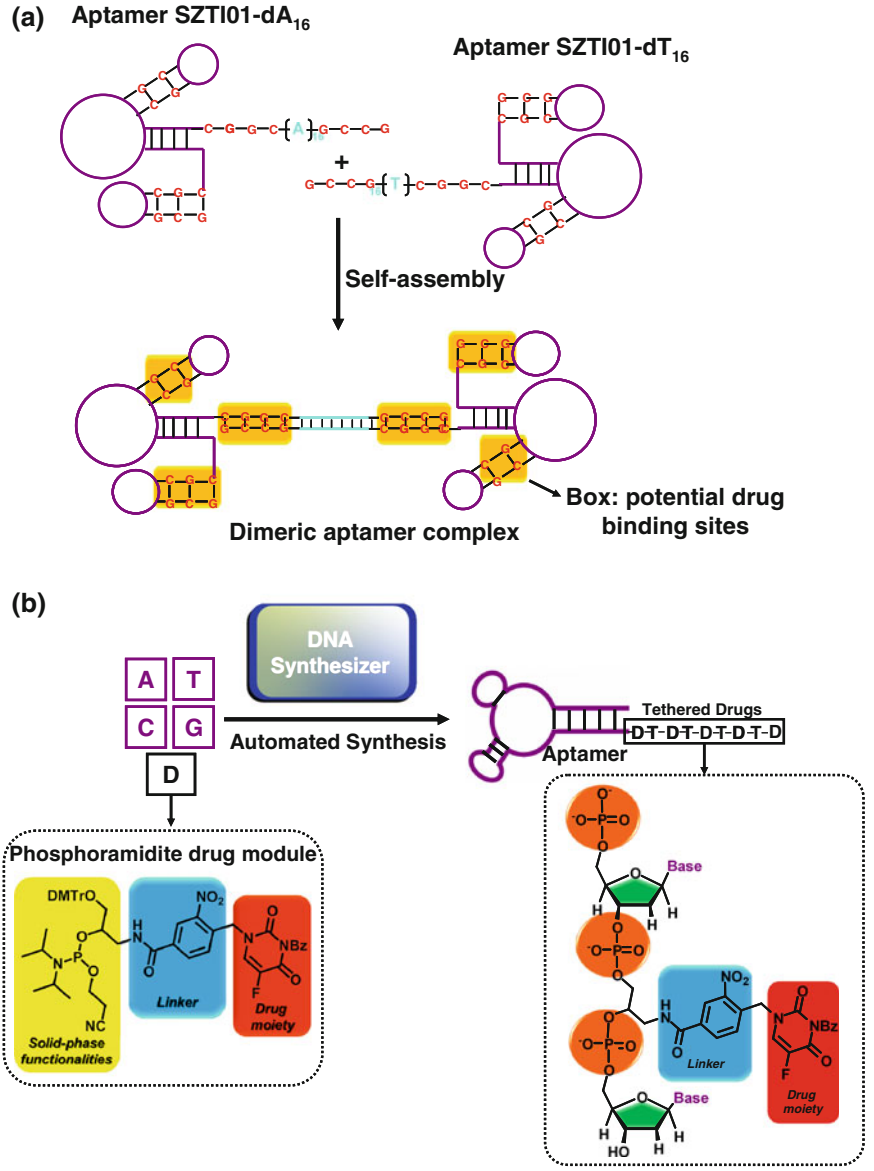

Fig. 13.2 Schematic diagrams of covalent conjugation between aptamers and chemotherapeutic agents via **a** intercalation at multiple GC sites, followed by formaldehyde fixation, and **b** phosphoramidite solid-phase synthesis

positions during the process of solid-phase synthesis. For the present work, aptamer sgc8 was chosen as a model for the automated and modular synthesis of ApDCs tethered with a high drug molecule capacity. Analysis of flow cytometry and

confocal microscopy images displayed a specific binding and internalization of the resultant ApDCs by targeted HCT116 colon cancer cells. The photocleavable linkage also allows a spatiotemporal controllability of intracellular drug release by light irradiation. Compared with traditional ADCs, this new generation of ApDCs provides unique advantages, including economy, procedural simplicity, as well as site-specific and multiple drug-loading capabilities. The highly controllable synthesis method is capable of generating a broad panel of molecular ApDCs and is particular beneficial for targeted drug delivery.

13.2.1.2 Non-covalent Conjugation of Aptamers to Chemotherapeutic Agents Through Intercalation

In addition to the direct association of drug copies to an aptamer through stable chemical bonding, physical conjugation of aptamers and chemotherapeutic agents represents another attractive synthesis strategy developed for targeted therapy. Some anticancer reagents, such as Dox and its closely related analog daunorubicin, are well-known to intercalate within the double helix of DNA owing to the presence of flat aromatic rings in these molecules. Professor Farokhzad and his colleagues were the first group to claim that tertiary conformations comprised of short double-stranded regions of aptamers can form a physical complex with drug molecules requiring no covalent modifications (Fig. 13.3a) [57]. In their study, an RNA aptamer–Dox physical conjugate was contrived as a novel targeted drug delivery platform. The RNA aptamer, A10, which had been selected to inhibit PSMA enzymatic activity, is a potential candidate for the targeting of prostate cancer cells [58]. To circumvent the vulnerability of RNA to nuclease degradation, 2′-fluoropyrimidine-modified RNA aptamers were used to improve the treatment outcomes. The fluorescence quenching study demonstrated that approximately 1.2 Dox were physically intercalated into the A10 aptamer with a dissociation constant value of 600 nM. The resultant aptamer–Dox physical conjugate retains its binding activity to the target antigen, leading to a selective cytotoxicity against PSMA-positive cells. In a similar manner, another aptamer–Dox complex was explored by Liu et al. [59] for delivering Dox to breast cancer cells. A new aptamer, HB5, was developed to target human EGFR 2 (HER2), which is overexpressed by multiple malignancies including breast cancers [60, 61]. A complex of this newly developed aptamer and Dox could specifically target HER2-positive breast cancer cells, minimizing the non-specific drug uptake by negative control cells. This result suggests a measure for the application potentials of aptamers that target HER2 in targeted chemotherapy.

To achieve a high drug-loading capacity for in vivo cancer treatment, a dimeric aptamer conjugate that concurrently carries multiple copies of anticancer drugs in a single platform has been described. The oligonucleotide TLS11a used in this study is the first aptamer to be identified as specific for human liver cancer cells [62]. A long GC tail was appended to the 5′-end of TLS11a to form a dimer structure through base-pairing. The resultant carrier of the TLS11a–GC dimer was shown to intercalate up to 56 Dox molecules (Fig. 13.3b), in sharp contrast to the original TLS11a

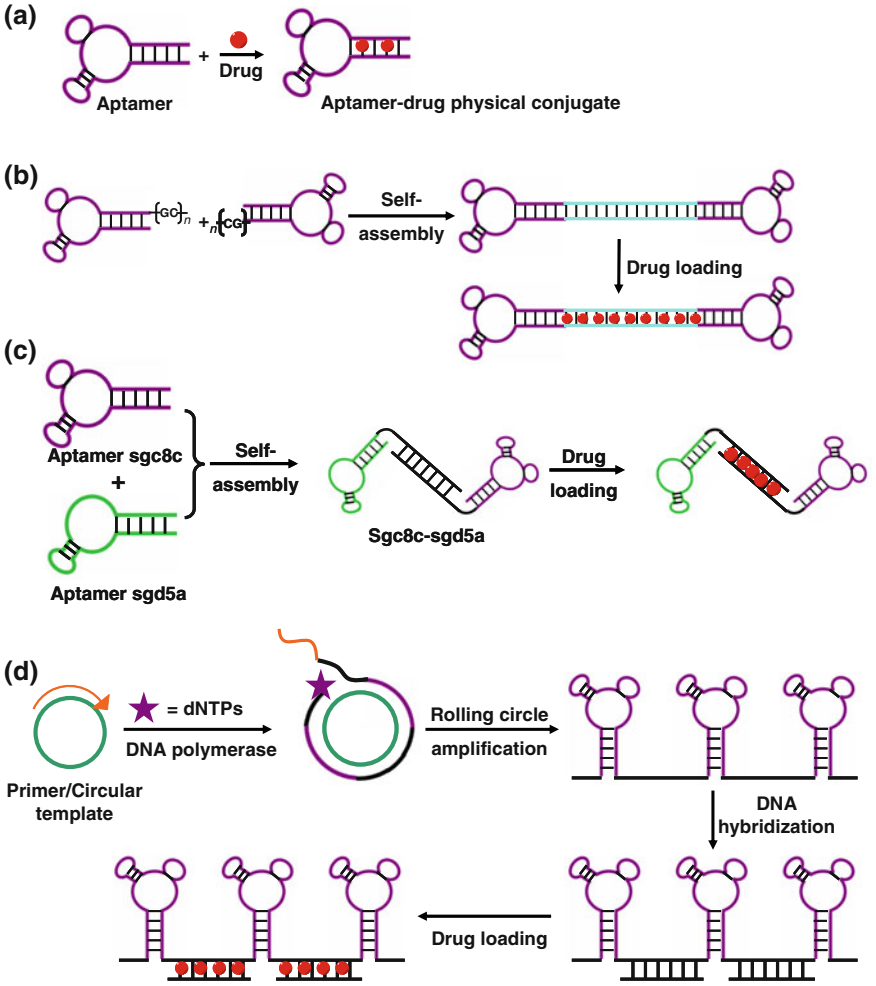

Fig. 13.3 Schematic diagrams of non-covalent conjugation between aptamers and chemotherapeutic agents through intercalation. **a** A physical conjugate formation between an aptamer and a model drug. **b**, **c** High-drug-loading systems based on self-assembly of (**b**) GC tail-modified aptamers, as well as (**c**) engineered aptamers sgc8c and sgd5a. **d** A polyvalent aptamer drug-loading system constructed by the rolling circle amplification and DNA hybridization reaction

that was able to bind only two Dox molecules. The in vitro study demonstrated the selective toxicity of the drug-loaded aptamer conjugates, indicating that the dimeric structure retained its specific binding affinity to the target cells. The simultaneous release of multiple drug copies to the site of action upon internalization also suggests a significant in vitro and in vivo inhibition of tumor cell proliferation.

Owing to the fact that a single type of aptamer cannot recognize all clinical samples from different patients, even for patients having the same type of cancer, a

bispecific aptamer-based drug carrier was therefore investigated to facilitate aptamer applications for heterogeneous cancer subtypes [63]. Similar to the strategy described previously, this carrier, sgc8c–sgd5a (SD), was designed to be self-assembled from two individually modified aptamers through a double-stranded linker with preferential Dox loading sites (Fig. 13.3c) [64]. After the physical intercalation of multiple copies of Dox, the SD-mediated drug carrier was able to recognize two distinct target cells, leading to a respective cytotoxicity in a mixed cell environment. Whereas the recognition ability of monovalent aptamers is necessarily limited, the development of mutispecific, aptamer-based drug carriers allows drug cytotoxic effects to be directed to multiple types of target cells. Development of aptamers capable of recognizing a broader range of target cells is expected to overcome many diagnostic and therapeutic complications for future clinical applications.

Despite the promising outlook, the majority of these approaches still suffer from restrictions regarding the limited drug-carrying capacity and the attendant disadvantages of high cost. From this perspective, an innovative design called aptamer-tethered DNA nanotrains (aptNTrs) was introduced by Zhu et al. [65] to address these issues. In this study, the structure of the sgc8 aptamer, which targets PTK7, was modified by adding a DNA trigger probe on the 5′-end. A relatively long chain of dsDNA was then self-assembled from two partially complementary short hairpin monomers upon initiation by an aptamer-tethered probe through a hybridization chain reaction (Fig. 13.4). Consequently, the modified aptamer acted as a locomotive for targeting, while the reaming dsDNA nanoconstructs containing numerous Dox intercalation sites acted as boxcars to deliver the drug. The resultant sgc8c–NTrs displayed high cargo-loading capacity with a Dox/sgc8–NTr molar ratio of 50:1. The use of short DNA monomers in aptNTrs also contributed to a high DNA synthesis yield compared to that with the use of long monomers. Significantly, this delivery platform allowed for efficient targeting in cancer therapy and demonstrated a potent anti-tumor efficacy with minimized side effects in a mouse xenograft tumor model. With basic substitution of aptamers and drugs, this applied DNA technology will have broad implications for targeted drug delivery.

The generation of long single-stranded DNA scaffolds with repetitive aptamer units has also been realized by the rolling circle amplification (RCA) reaction (Fig. 13.3d) [66]. The duplex drug-loading domains in this multivalent drug delivery system were then constructed by hybridizing the spacer regions between aptamers and complementary strands. It has been determined that the Dox payload capacity of this polyvalent aptamer increased approximately tenfold, as compared to the monovalent sgc8 aptamer. Moreover, the greater binding affinity (40-fold) also makes poly-aptamer–drug conjugates more effective than their monovalent counterparts in targeting and killing leukemia cells. In accord with previous studies [67], the polyvalent interactions involving the simultaneous binding of multiple aptamers to the multiple receptors of a target results in a stronger binding property, which provides higher target selectivity as well as a more rapid internalization by their target cells. Undoubtedly, engineered multivalency has become a powerful emerging approach to improve targeting efficacy and selectivity in drug delivery.

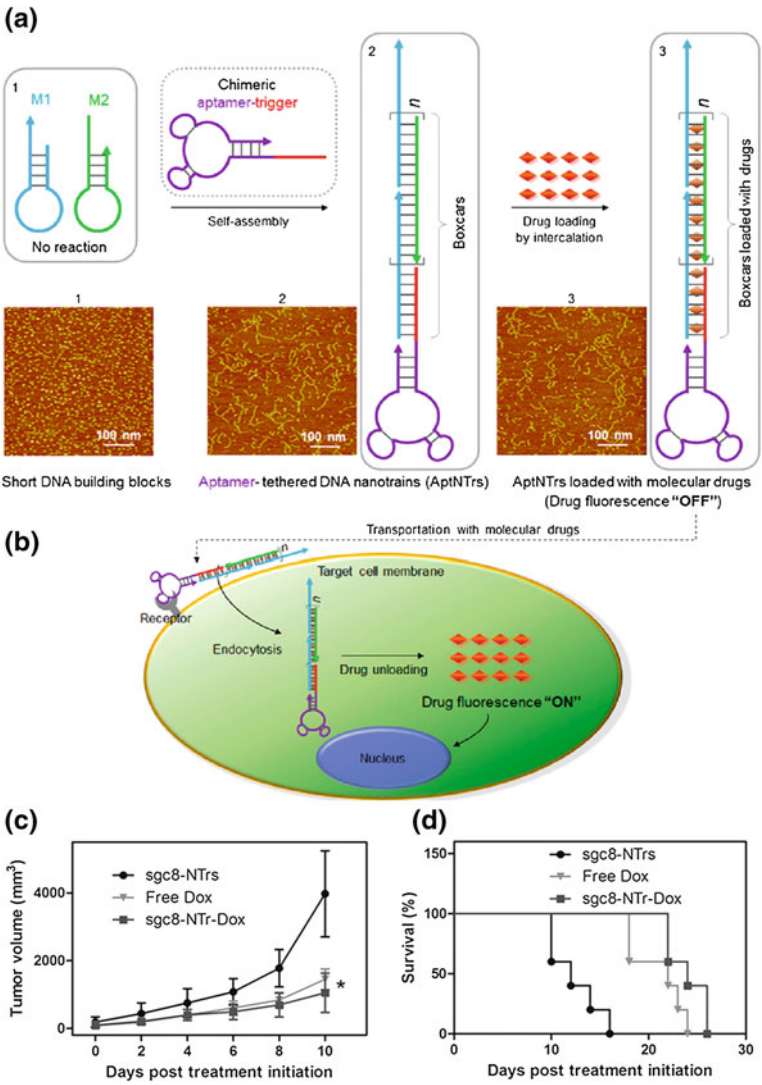

Fig. 13.4 Aptamer-tethered DNA nanotrains (aptNTrs) for transport of molecular drugs in theranostic applications. **a** Schematic diagram depicting the self-assembly of aptNTrs from two partially complementary short hairpin monomers upon initiation by an aptamer-tethered probe through a hybridization chain reaction. AFM images (*1–3*) showed the morphologies of the corresponding nanostructures. **b** The drugs were specifically transported to target cancer cells via aptNTrs, unloaded, and induced cytotoxicity to target cells. **c** Potent anti-tumor efficacy and reduced side effects of drugs transported via aptNTrs. Tumor volumes of subcutaneous CEM xenograft mouse tumors were measured after drug administration up to date 10 ($n = 5$). *Asterisk* on day 10 represents significant differences between tumor volumes of free Dox- and sgc8–NTr–Dox-treated mice ($^*P < 0.05$, $n = 5$; Student's t test). **d** Survival percentage of mice after treatment initiation. Reprinted from Ref. [65] by permission of PNAS

13.2.2 Aptamer–Drug Conjugates in Targeted Photodynamic Therapy

Photodynamic therapy (PDT) is a promising modality that destroys target cells in the presence of oxygen when light irradiates a photosensitizer (PS), generating highly reactive oxygen species (ROS). ROS, including singlet oxygen ($^1O_2$), then attacks cellular targets, causing destruction through direct cellular damage, vascular shutdown, and activation of an immune response against target cells [68, 69]. Current clinical applications of PDT include treatment of superficial cancers in the skin, head, neck, esophagus, bladder, bronchus, etc. [70]. PDT has several advantages over conventional therapies because of its noninvasive nature, high spatial–temporal resolution with regional light irradiation, and minimal associated side effects [71]. However, the lack of targeting specificity of most PS reagents results in an indiscriminate release of ROS, thereby causing damage to surrounding normal tissue. Additionally, because $^1O_2$ has a limited lifetime and diffusion distance [72], controllable $^1O_2$ generation with high selectivity and localization would lead to more efficient and reliable PDT. New approaches to achieve site-specific drug delivery for PDT are therefore highly desirable [73–75]. In the following section, we provide an overview of recent achievements in aptamer-mediated PS delivery, which has been applied for targeted PDT in cancer treatment.

13.2.2.1 Aptamer–Photosensitizer Conjugates for Targeted Photodynamic Cancer Therapy

One of the common methods to improve the specific accumulation of PS at a diseased site has been accomplished with aptamers via direct covalent coupling. For example, a PS agent, chlorin e6 (Ce6), has been chemically linked to a highly selective aptamer, TDO5, which very specifically targets Burkitt's lymphoma Ramos cells [76]. The introduction of TDO5-Ce6, followed by light irradiation, can effectively destroy the targeted Ramos cells. Toxicity observed in control CCRF-CEM cells and other myeloid leukemia cell lines was over 50 % less than that of targeted cells. It is also worth noting that in conjugation with an oligonucleotide, aptamer greatly increases the aqueous solubility of Ce6, resulting in an enhanced bioavailability of this PS for increased cellular toxicity [77]. In another example, Ce6 was chemically bound to a human interleukin-6 receptor (IL-6R)-binding RNA aptamer, AIR-3A, through an EDC coupling reaction. The resultant conjugate, AIR-3A-Ce6, was capable of rapid and specific internalization by IL-6R presenting cells. Followed by light irradiation, the targeted cells were selectively killed, while free Ce6 demonstrated no toxic effect [78]. Together, the selective cytotoxicity of these aptamer–PS conjugates demonstrates that the use of aptamers for targeted PS delivery is a promising therapeutic strategy to overcome the aforementioned issues with PDT.

G-quadruplex, composed of four guanines (also known as a G-quartet) by Hoogsteen hydrogen binding, is a specialized G-rich DNA structure. This structure

can be stabilized by monovalent cations such as potassium or sodium [79]. Several important G-rich genomic regions, including telomeres and promoters, were found to potentially form G-quadruplex structures and play many important regulatory roles at an intracellular level [80, 81]. Owing to its aromatic and cationic properties, the porphyrin-derived compound, $TMPyP_4$ (5, 10, 15, 20-tetrakis (1-methylpyridinium-4-yl) porphyrin), is a G-quadruplex ligand. $TMPyP_4$ can bind to and stabilize the G-quadruplex in human telomere sequences, resulting in inhibition of telomerase activity. In addition, porphyrins in general have been used in PDT for their ability to produce ROS. These species have been widely explored as possible anticancer agents owing to their intrinsic capability to cause cellular senescence [82, 83]. However, $TMPyP_4$ is poorly selective, and toxic to some normal cell lines, particularly in normal fibroblast and epithelial cells upon light exposure [84]. An innovative delivery platform for $TMPyP_4$ has been developed by Shieh et al. [85] for photodynamic cancer treatment. In this work, an aptamer, AS1411, which tends to form an intramolecular G-quadruplex, was able to carry six molecules of $TMPyP_4$ by means of intercalation and electrostatic attraction (Fig. 13.5a). The resultant aptamer–$TMPyP_4$ physical complex was resistant to degradation and digestion by the enzyme DNase I. It was further identified to recognize the overexpressed nucleolin in breast cancer cells, thus delivering a greater quantity of PS into target MCF7 cancer cells than into normal M10 epithelial cells. Consequently, the use of light irradiation to activate TMPyP4 results in selective photodamage to diseased cancer cells.

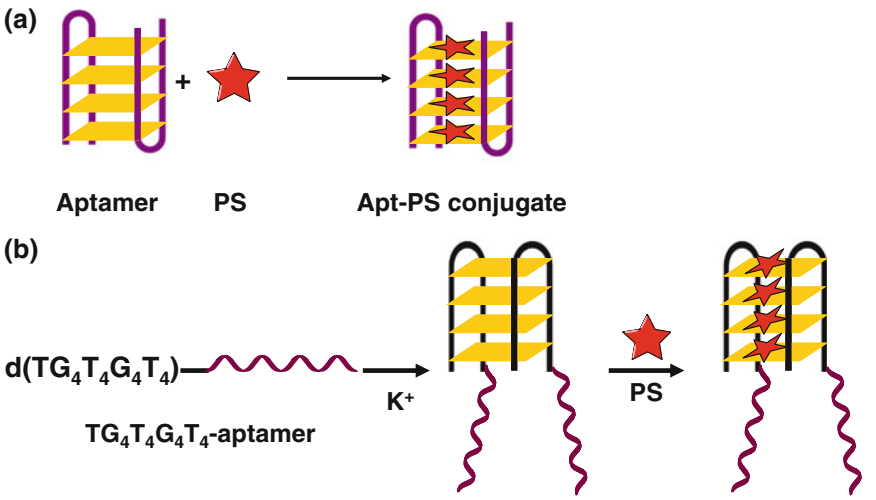

Fig. 13.5 Schematic diagrams of non-covalent conjugation of aptamers with photosensitizer (PS). **a** A G-quadruplex Apt–PS physical complexion via intercalation and electrostatic attraction. **b** A bifunctional DNA drug carrier constructed by utilizing the G-quadruplex as the drug carrier and the aptamer as the targeting molecule

Notably, not all aptamers need to be guanosine rich for a preferential G-quadruplex conformation. With careful design on the basis of DNA self-assembly, a novel delivery platform, which combines the target recognition function of a DNA aptamer and the drug-loading ability of a G-quadruplex, was constructed in a predictable and programmable manner (Fig. 13.5b) [86]. Briefly, the aptamer sgc8c was tethered with a guanine-rich segment capable of forming intermolecular G-quadruplexes after annealing. The modified aptamer formed a dimer structure, which has been denoted as G-quadruplex–sgc8. The resultant carrier module generated high toxicity for target cells and low cellular damage to control cells upon irradiation. In addition, G-quadruplex–sgc8 achieved higher cellular accumulation and cytotoxicity to target CEM cells than the $TMPyP_4$ itself. The assembly strategy described here in may serve as a universal method for joining two functional groups of DNA into a well-defined geometry, which would greatly enable a future of aptamer-based therapeutics.

13.2.2.2 Aptamer–Photosensitizer Conjugates for Activatable Photodynamic Cancer Therapy

In addition to controlling the spatial localization of PS reagents as well as the position for optimal light delivery, a new direction for improving PDT selectivity is to exert additional control of the conditions under which the PS will produce ROS [87]. At this level of control, the probe remains in a non-toxic state and can only be activated when it interacts with its corresponding trigger, e.g., tumor-associated biomarkers at specific sites. For example, an artificial molecular switch has been developed to achieve molecular mediation of $^1O_2$ generation upon the binding of an aptamer with its target [88]. In this work, a PS and a quencher moiety are linked in close proximity through a DNA switch that comprises an aptamer, a partial complementary DNA, and a polyethylene glycol (PEG) linker uniting these two components (Fig. 13.6a). The resultant photosensitizer aptamer switch remains photodynamically inactive until target binding, leading to a conformation restoration that activates its PS function. Thus, incorporating molecular activation allows the PS to more readily distinguish diseased cells from healthy cells, resulting in a significant improvement in PDT selectivity.

The manipulation of $^1O_2$ production for targeted PDT could further be conducted in a programmable catalytic manner to achieve amplified therapeutic efficacy. Oligonucleotides, which have been considered as promising building blocks for self-assembly, can generate a well-regulated amplification circuit via simple nucleic acid hybridization such as hybridization chain reaction [89], entropy-triggered hybridization catalysis [90], and DNA hairpin fuel catalysis [91]. By introducing the aforementioned concept, an aptamer-based circuit was developed for activatable PDT in targeted therapy [92]. As displayed in Fig. 13.6b, the aptamers can selectively recognize target cancer cells and bind to the specific receptors on cell membranes. Then, the overhanging catalyst sequence on the aptamer can trigger a toehold-mediated catalytic strand displacement to continually activate the PS. The specific binding-induced activation allows the DNA circuit to distinguish

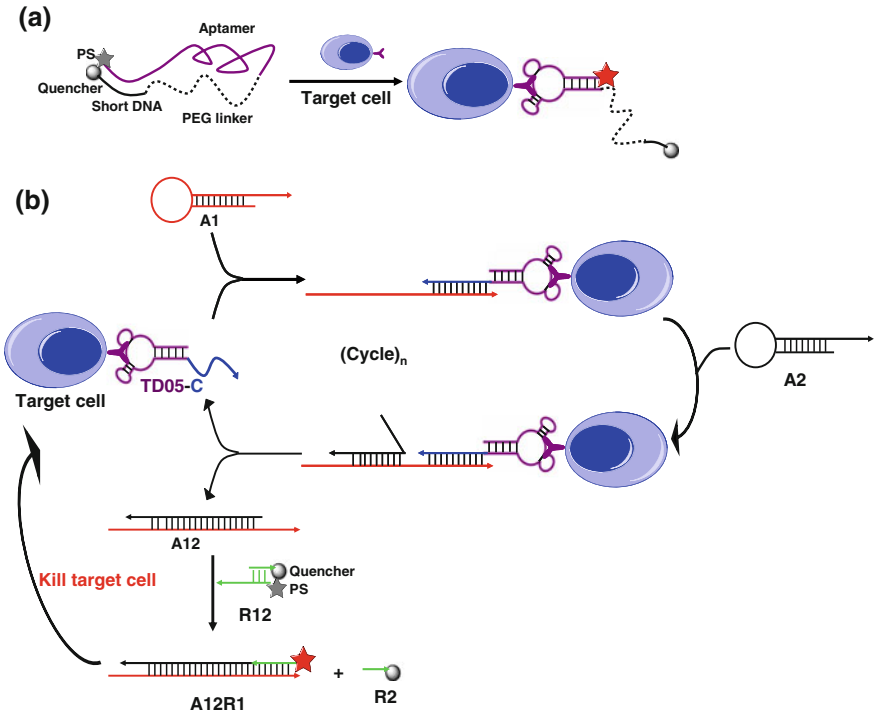

Fig. 13.6 Schematic diagrams of **a** photosensitizer aptamer switch probe, and **b** cell-mediated DNA aptamer amplification circuit for activatable photodynamic cancer therapy

between diseased and healthy cells, thus reducing damage to nearby healthy cells. Moreover, the catalytic amplification reaction occurs close to the target cancer cells, resulting in a high local concentration of $^1O_2$ for selective destruction. By combining the recognition and amplification abilities of these oligonucleotides, a more specific, controllable, and efficient PDT method was successfully demonstrated.

13.3 Aptamer-Conjugated Nanomaterials for Cancer Therapy

13.3.1 Aptamer-Conjugated Gold Nanoparticles for Targeted Cancer Therapy

As the most common and stable metallic nanomaterials, gold nanoparticles (AuNPs) have received substantial attention over the past decades owing to their unique features and properties [93]. AuNPs possess a large surface area and afford a

high capacity for surface manipulation through simple, stable Au:S bonds. These thiolated ligands can be used to introduce diverse molecules, such as targeting ligands, polymer linkers, or drug molecules, enabling AuNPs to incorporate multiple functionalities [94]. Although AuNPs are relatively inert and chemically unreactive, surface modification is required to assure high biocompatibility for future biomedical applications. The most widely applied coating polymer is PEG, which is neutral in charge and highly hydrophilic. These characteristics prevent non-specific protein adsorption on the nanoparticle surface, as well as the uptake of nanoparticles by the reticuloendothelial system, and finally, providing a lengthened blood circulation time [95, 96]. Recent in vitro studies suggest that AuNPs are non-toxic to human cells, which makes AuNPs an excellent candidate as a drug delivery carrier [97, 98].

AuNPs of different size and shape (e.g., nanospheres, nanorods, nanoshells, and nanocages) can be precisely controlled through a variety of synthetic methods [99–102]. The resultant nanostructures exhibit unusual and tunable optical properties owing to localized surface plasmon resonance (SPR) [103]. Light is most strongly absorbed and/or scattered at the resonant frequency of the individual AuNP, with their absorption cross sections being orders of magnitude greater than those of typical absorbing organic molecules. In addition, photon energies that have been absorbed by AuNPs can be efficiently converted into heat on a picosecond time scale via a series of non-radiative processes. Collectively, AuNPs are considered a highly potent therapeutic agent in photothermal therapy (PTT) [104]. PTT is a relatively noninvasive and benign alternative for cancer treatment. This treatment modality exposes biological tissues to higher-than-normal temperatures to promote the destruction of abnormal cells [105]. For sufficient heating, continuous laser light in the near-infrared region (NIR) is generally used to achieve deep-tissue penetration with high spatial precision. Among all types of AuNPs, gold nanorods (AuNRs) are more feasible for future clinical PTT for the following reasons. AuNRs can be readily synthesized with various aspect ratios, which enable selective absorption in the NIR region. They also support a higher absorption cross section at NIR frequencies per unit volume than nanoshells and nanocages. A number of recent studies have demonstrated the feasibility of AuNRs for successful tumor remission in mice via PTT treatment [106, 107].

13.3.1.1 Aptamer-Conjugated Gold Nanoparticles for Targeted Photothermal Therapy

To achieve effective hyperthermia specific to target cancer cells, Huang et al. [108] demonstrated the conjugation of aptamer sgc8c to Au–Ag NRs for selective PTT in vitro. Au–Ag NRs have been utilized as a nanoscaffold for covalent linkage of multiple aptamer copies, leading a simultaneous multivalent ligand–receptor interaction. The binding affinity of the resultant sgc8c–NR conjugates for targeted CCRF-CEM cells was found to be approximately 26-fold greater than that of a single sgc8c probe [109]. In addition, the high absorption efficiency and superior

photothermal transfer capability of Au–Ag NRs further make this novel platform highly promising for selective cell recognition and targeted PTT. Consequently, under a specific laser intensity and duration of laser exposure, about (50 ± 1) % of targeted CCRF-CEM cells were severely damaged, while more than (87 ± 1) % of the control cells remained intact in a suspension cell mixture. AuNRs modified with two different aptamers were also used to destroy different cancer cells simultaneously [110]. Aptamers targeting DU145 prostate cancer cells (aptamer CSC1) and their subpopulation of cancer stem cells (aptamer CSC13) were linked to the surface of AuNRs, and the resulting conjugates were successfully used to target and kill both cancer cells and cancer stem cells using NIR laser irradiation.

13.3.1.2 Aptamer-Conjugated Gold Nanoparticles for Combinational Therapy: Photothermal and Chemotherapy

In addition to the role as hyperthermia agents in PTT, AuNPs have emerged as attractive candidates for further exploration in combinational therapy: PTT and chemotherapy [111]. The large surface area permits AuNPs to accommodate a high capacity of payload attachment, which makes them ideal candidates for drug delivery [112]. It has also been reported that, with mild hyperthermia (39–45 °C), cancer cells become sensitized to cytotoxic agents as a result of increasing membrane permeability and decreasing hydrostatic pressure [113]. Under these circumstances, smaller drug doses may be sufficient for the desired therapeutic outcome. The synergistic effect of toxicity and hyperthermia presents an advantage of combinational therapy, providing for more efficient destruction of cancer cells. Therefore, it may be the most effective way to improve treatment efficacy and conquer resistance in oncotherapy.

Hollow gold nanospheres (HAuNS) are a novel class of AuNPs composed of an Au shell with a hollow interior. It has been reported that for HAuNS and AuNPs of similar size, similar surface charge, and an equivalent Au concentration, the drug-loading capacity of HAuNS is 3.5-fold greater than that of AuNPs [114]. By utilizing the superior drug-loading capacity of HAuNS and the high specificity of an RNA aptamer for targeting CD30, a novel delivery vehicle has been explored for targeted chemotherapy in lymphoma cells (Fig. 13.7a) [115]. Through the aptamer-mediated guidance, the resultant Apt–HAuNS–Dox demonstrated the selective destruction of lymphoma tumor cells with minimal effect on the growth of the off-target cells in the cell mixtures.

The coating of AuNRs with mesoporous silica (AuMPs) has attracted increasing attention as a potential drug delivery system owing to the large pore volume and high surface area for effective drug loading [116]. To enable successful in vivo delivery, guest molecules are entrapped inside the mesoporous cavities; the molecules are released as required in the affected tissues during circulation. To facilitate this goal, nucleic acids have been used as molecular gates on the pore outlets to close and open the pore system in smart response to external stimulus. Specifically, aptamer AS1411 grafted onto the surface of an AuMP can form a dimeric structure

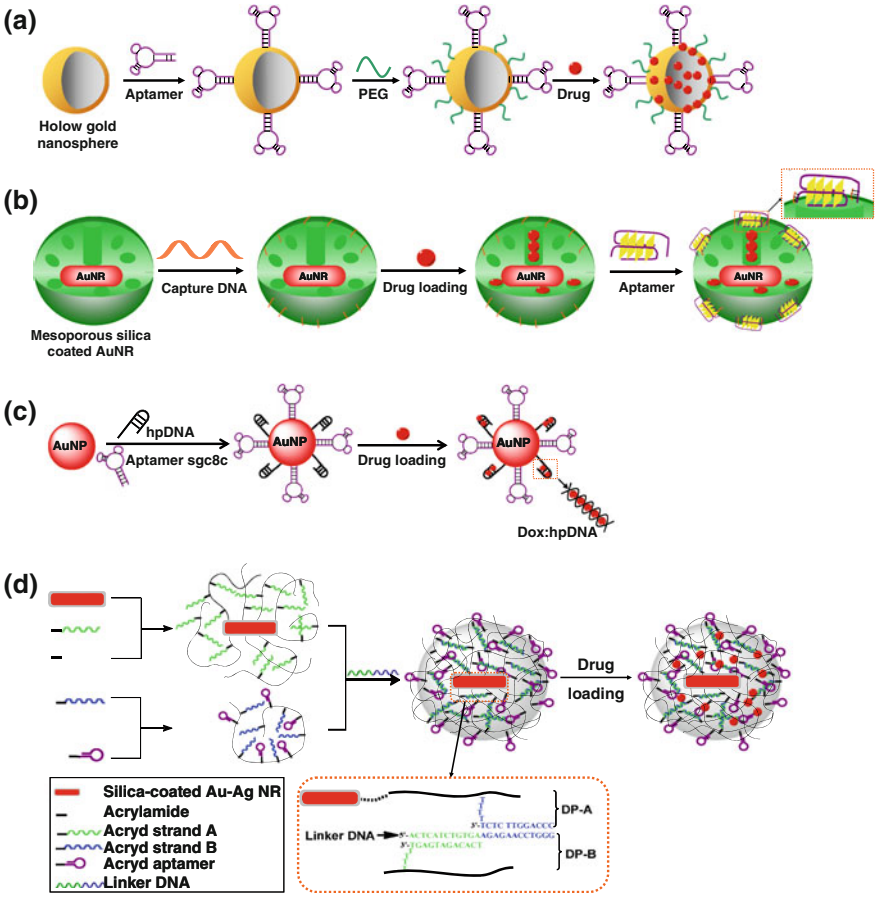

Fig. 13.7 Schematic diagrams of nanoplatforms based on aptamer-conjugated gold nanoparticles for targeted drug delivery. **a** Apt–HAuNS–Dox nanoscale drug carrier. **b** AuNR-based mesoporous silica nanocarrier. **c** Dox:Apt/hp–AuNP nanocomplexes. **d** Aptamer-functionalized core–shell nanogels

of G-quadruplex, which is sufficiently large to cap the pores (Fig. 13.7b) [117]. Upon irradiation by NIR light, the photothermal effect of AuNRs encapsulated within the mesoporous silica framework leads to a rapid rise in the local temperature. This results in the dehybridization of the linkage DNA duplex that anchors the capping molecules, herein G-quadruplex DNA, allowing the specific release of the loaded cargo. More importantly, the use of a DNA aptamer, as both the capping and targeting agent, makes this AuNR-based porous nanocarrier widely useful for targeted delivery of drugs with remote control capability by laser-induced thermal stimulus [118].

In addition, by taking advantage of the non-covalent interactions between oligonucleotides and various therapeutics, AuNPs assembled with multiple copies of

DNA containing consecutive C-G base pairs have been developed to accommodate a high level of drug loading (Fig. 13.7c). Under optimal conditions, about 25 sgc8c aptamers and 305 Dox molecules were successfully loaded, and the resultant nanoconjugates provided an ideal platform to simultaneously deliver heat and anticancer drugs in a laser activation process [119]. Moreover, Kang et al. [120] have proceeded to coat DNA cross-linked polymeric shells onto the surface of Au–Ag NRs and developed a thermosensitive nanogel (Fig. 13.7d). When illuminated with plasmon-resonant light, the thermal energy generated from Au–Ag NRs heats the surrounding gel, facilitating a rapid release of the encapsulated drug with spatiotemporal controllability. Moreover, in vivo studies confirmed that the aptamer-functionalized nanogels developed herein are suitable carriers for targeted and noninvasive remote drug delivery. A superior therapeutic efficacy could be observed upon NIR light irradiation. Because the NIR region lies between the "biological window" (700–1,300 nm), defined as the wavelength where absorption, scattering, and autofluorescence by tissues, blood, and water are minimized, it is extremely useful for future in vivo applications [35].

13.3.1.3 Aptamer-Conjugated Gold Nanoparticles for Combinational Therapy: Photothermal and Photodynamic Therapies

The efficient photothermal response of gold nanomaterials has also promoted recent investigation on combinational PTT/PDT dual therapy [121, 122]. Based on the strong surface plasmon absorption in the NIR region, AuNRs can be utilized as ultra-efficient energy quenchers to control the selective action of PS reagents by manipulating the distance between the donor and acceptor [123–125]. For example, aptamer switch probes (ASP), which comprise three components—aptamer, poly-T, and 8bt-cDNA—have been designed and assembled onto AuNRs to bring the PS molecule, Ce6, into close proximity with the gold surface. No phototoxicity was observed as a consequence of an effective energy transfer quenching from the excited Ce6 to the AuNR. However, in the presence of target cancer cells, the ASP changes conformation to drive the Ce6 away from the gold surface, thereby producing $^1O_2$ for PDT upon light irradiation (Fig. 13.8a) [126]. In another study, aptamers were conjugated to AuNRs through simple thiol–Au linkages and then hybridized with a Ce6-labeled oligonucleotide to form a DNA double helix (Fig. 13.8b). During NIR irradiation, AuNRs were able to convert the absorbed photoenergy into heat to accelerate the release of Ce6 from their surface. The quenching of the PDT effect was therefore recovered in a selective manner by regional irradiation to minimize phototoxic tissue damage of non-targeted cells. The therapeutic outcomes of the aforementioned AuNR–PS nanoconjugates were furthermore greatly enhanced by the additional PTT effect using AuNRs. Overall, the strategy of utilizing a highly selective aptamer combined with the synergistic effect of PTT and PDT promises to be a more efficient therapeutic regimen against cancer cells than non-specific methods using either PTT or PDT alone [127].

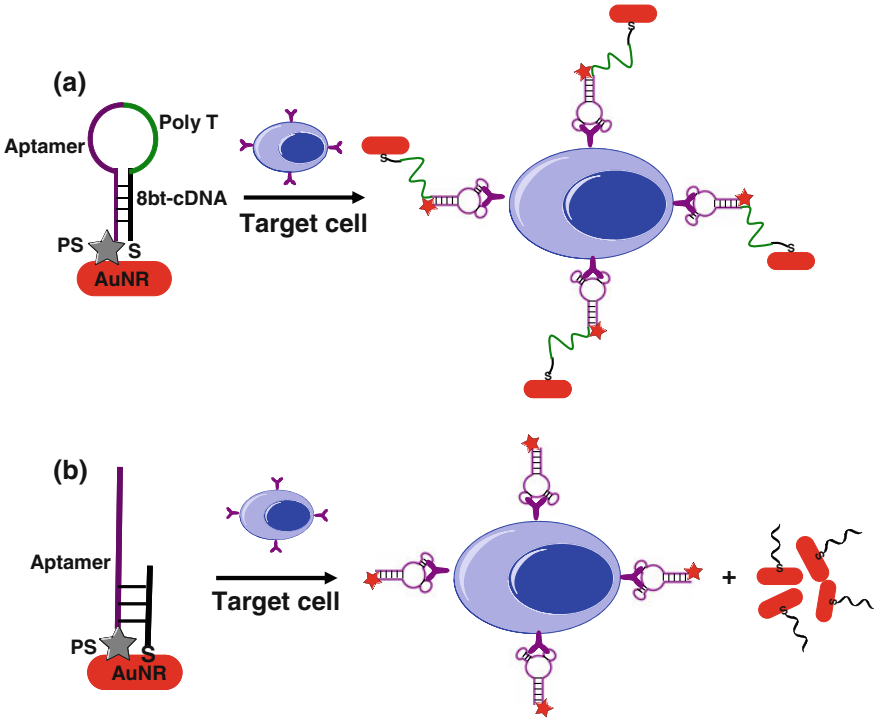

Fig. 13.8 Schematic diagrams of gold nanorods assembled with multiple copies of **a** ASP–PS, and **b** PS-tethered DNA double helix for combinational therapy: PTT and PDT

13.3.1.4 Aptamer-Conjugated Gold Nanoparticles for Theranostics

Cancers by their nature are immensely heterogeneous, and all existing clinical treatments face limited effectivity for restricted stages of the disease. In consequence, a close marriage of diagnosis and therapeutics may provide a therapeutic paradigm that is more specific to individuals and, therefore, pave the way toward the goal of personalized medicine [128, 129]. AuNPs with multiple functionalities have emerged as one of the most actively investigated nanoparticle-based theranostic agents. With further integration of aptamers, the resulting nanoplatforms become targeted specific, offering a great opportunity for simultaneous diagnosis, drug delivery, and monitoring of therapeutic response.

X-ray computed tomography (CT) is a commonly used diagnostic tool for medical imaging [130]. The ability of CT to visualize different tissues is based on the variable attenuation of the X-ray beam as it passes through tissue. It has been reported that PEG-modified AuNPs are an appealing CT contrast agent for in vivo angiography and hepatoma detection [131–133]. The in vivo measurement of the X-ray absorption coefficient also reveals that the attenuation of PEG–AuNPs is 5.7

times higher than that of the conventional iodine-based CT contrast agent [131]. Recently, a multifunctional drug-loaded aptamer-conjugated AuNP agent has been presented by Kim et al. [134] for combinational CT imaging and chemotherapy of prostate cancer cells. In this study, an extended A10 aptamer, the extension of which was complementary to an oligonucleotide sequence attached to the surface of AuNPs, was devised to achieve a high level of drug loading. Through the specific aptamer guidance, the resulting aptamer–AuNP nanoconjugates displayed more than fourfold greater CT intensity for PSAM-positive prostate cancer cells than that for non-targeted cell lines. Moreover, the drug-loaded nanoplatforms also exhibited targeted cell-specific cytotoxicity, suggesting a new perspective for tumor treatment by targeted theranostic agents employing aptamer-based multifunctional AuNPs.

Magnetic resonance imaging (MRI) is another powerful diagnosis tool for obtaining functional and anatomic information with high temporal and spatial resolution [135]. MRI records magnetization changes, which in turn affect the relaxation rates of nuclear spins, particularly the hydrogen protons, under different environments in the human body [136]. Superparamagnetic iron oxides that are capable of shortening the T_2 transverse relaxation time are predominantly used as negative contrast agents for MRI in clinical practice [137]. To fulfill the multimodality needed for accurate diagnosis and targeted therapy, a core–shell nanostructure that consists of a magnetic nanorose core coated with gold shells was developed by Li et al. After aptamer grafting, the resulting nanocomposties, Fe_3O_4@Au, offer tremendous potential for integrating distinct functions, including aptamer-based targeting, optical imaging, and MRI capability as well as PTT and chemotherapy, into a single platform. For in vitro tests, it enables efficient target cell binding and selective drug delivery as well as a desirable synergistic anticancer effect with minimum non-specific toxicity and side effects. The combination of dual-modality MRI and optical imaging further suggests an enhanced specificity toward tumor diagnosis; this is followed by the tailored guidance of therapeutic treatment. It is expected that this novel theranostic system will have wide biomedical applications, and it may be particularly promising for future cancer therapy [138].

13.3.2 Aptamer-Conjugated Magnetic Nanoparticles for Targeted Cancer Therapy

Iron oxide-based magnetic nanomaterials such as magnetite (Fe_3O_4) and maghemite (γ-Fe_2O_3) have attracted broad attention in the biomedical field owing to their unique magnetic properties, inherent biocompatibility, and low cost [139–141]. For example, superparamagnetic iron oxide nanoparticles (SPIONs), including bowel contrast agents (such as Lumiren® and Gastromark®) and liver/spleen imaging agents (such as Endorem® and Feridex IV®), are MRI contrast agents currently used in clinical diagnostics [142]. The success of SPIONs in MR imaging has paved the way for the development of iron oxide NPs as novel nanomedicines to combat cancer [143].

Most FDA-approved SPION contrast agents are synthesized by an aqueous coprecipitation method in the presence of stabilizing agents (e.g., dextran) [144]. Unfortunately, the typical synthetic route presents several disadvantages, particularly the broad particle size distribution and low degree of crystallinity. Accordingly, non-hydrolytic approaches have been intensively pursued toward high-quality iron oxide nanocrystals. The thermal decomposition method was firstly introduced by Alivisatos et al. [145] and was latterly developed by Sun and Zeng [146] to fabricate SPIONs with high monodispersity and magnetic susceptibility [147]. Owing to the existence of surfactant molecules (e.g., oleic acid and oleylamine), the pyrolysis of iron precursors followed by particle growth is carried out in a controlled fashion. SPIONs of uniform size and high crystallinity were then obtained in boiling solvents under high temperature. This procedure was found to be effective, productive, and facile to scaling up, thus offering substantial opportunities for high-performance MRI [144]. Nevertheless, products produced by the thermal decomposition method are not water soluble, and thus, a suitable surface coating is necessary to assure the desirable solubility of SPIONs in an aqueous environment [148]. General strategies, including ligand exchange (e.g., the use of high-affinity, hydrophilic ligands to replace the original hydrophobic coating) and ligand addition (e.g., the use of amphiphilic materials, which are added to the particle surface by forming a bilayer structure with the existing alkyl coating), have been extensively explored to confer high water dispersibility, colloidal stability, biocompatibility, and conjugation capability to SPIONs [149]. In the following section, we will summarize recent advances in the development of aptamer-conjugated magnetic NPs for a variety of biomedical applications including drug delivery, targeted therapy, and MRI.

13.3.2.1 Aptamer-Conjugated Magnetic Nanoparticles for Targeted Drug Delivery

Aptamer–magnetic NP conjugates have been formulated to meet the specific requirements of codelivery anticancer drugs and imaging probes for cancer-specific targeting. Anti-PSMA A10 aptamers have been assembled onto the surface of SPIONs with the aim of combined prostate cancer imaging and chemotherapy in vitro. Because the GC segments of the aptamer can intercalate with Dox molecules, the resulting aptamer-conjugated SPIONs (Apt–SPIONs) can act as both an MRI contrast agent and drug carrier. The conducted cytotoxicity assay indicated that the aptamer-mediated drug delivery resulted in selective targeting to PSMA-expressing cells without significant loss in the drug potency. Meanwhile, the observation of dramatic decreases in T_1 and T_2 relaxation times indicated that the Apt–SPIONs have the potential for highly sensitive cancer cell detection [150]. In a similar manner, another Apt–SPION conjugate was explored by Jalalian et al. for delivering the anthracycline drug epirubicin (an intercalating agent, preferentially binding to GC sequences) to target cells. A new aptamer, 5TR1, was selected to recognize mucin-1 (MUC-1), a cell surface-associated glycoprotein that is highly expressed in various epithelial cancer cells, including colon carcinoma cells. After

drug loading, the developed epirubicin–Apt–SPIONs were capable of targeting MUC-1-positive colon C-26 cells, thus minimizing the non-specific drug uptake by negative control cells. Most importantly, for in vivo delivery, these conjugates could be used for specific tumor MRI and tumor growth inhibition [151]. To increase the drug-loading capacity of the anti-PSMA Apt–SPIONs reported previously, a $(CGA)_7$ tail complementary to the $(TCG)_7$ sequence grafted onto the surface of SPIONs was appended to the 3′-end of the A10 aptamer. After hybridization, the resulting CG-rich duplex in Apt–*hybr*–TCL–SPIONs enabled loading of multiple Dox molecules onto the nanoconjugates (Fig. 13.9). In vitro and in vivo studies demonstrated that the developed Dox@Apt–*hybr*–SPION showed selective drug delivery efficacy for PSMA-positive prostate cancer cells. With the aid of the diagnostic capability of MRI, this nanoplatform has a potential for future use as novel prostate cancer-specific nanotheranostics [152].

Although promising, the majority of these approaches still suffer from limited drug-carrying capacity. From this perspective, Zheng et al. [153] developed a SPION-based spherical nucleic acid (SPION-SNA) to accommodate higher drug-loading levels, thereby reducing the dosage to avoid non-specific toxicity (Fig. 13.10a). In this study, a SPION-tethered initiator, two partially complementary hairpin monomers, and an aptamer probe were self-assembled to construct a novel multifunctional SNA platform. Because each copy of the initiator on the SPION can trigger the propagation of hybridization chain reaction events between the two hairpin monomers to form a nicked double-helix, multiple copies of the aptamer can therefore be embedded in the long DNA biopolymer on the surface of the SPION. The aptamer on the resulting SPION-SNA can act as a targeting element, while the double-helix polymer containing numerous Dox intercalation sites acts as a drug-loading module. In addition, simultaneous fluorescence imaging could also be realized by appropriate positioning of multiple chromophores in the self-assembled biopolymer. This nanoplatform providing multimodal functionality including targeting, drug delivery, and imaging is expected to be a promising approach for cancer diagnosis and therapy.

Moreover, porous hollow magnetite nanoparticles (PHMNPs) have also been devised as smart multimodality vesicles for targeted theranostics. PHMNPs have been reported as an ideal nanoplatform for drug storage and targeted delivery. The porous nature of PHMNPs facilitates drug diffusion into the cavity of the hollow structure; hence, this increases the drug loading of the entire system. In addition, the porous shell is stable under neutral or basic physiological conditions, but exposure of the pores to an acidic environment leads to acidic etching, wider pore opening, and faster drug release [154]. To improve the biocompatibility of a PHMNP, the hydrophobic surface has been modified with a heterobifunctional PEG ligand. The resultant PEGylated PHMNPs (PPHMNPs) with active carboxyl functional groups were easily dispersed in an aqueous solution for further conjugation. By conjugating PPHMNPs with aptamer sgc8, this smart multifunctional nanostructure (SMN) was used for CEM cell-targeted therapy (Fig. 13.10b). Aptamers modified on the outer layer of the SMN resulted in a multivalent effect, leading to enhanced

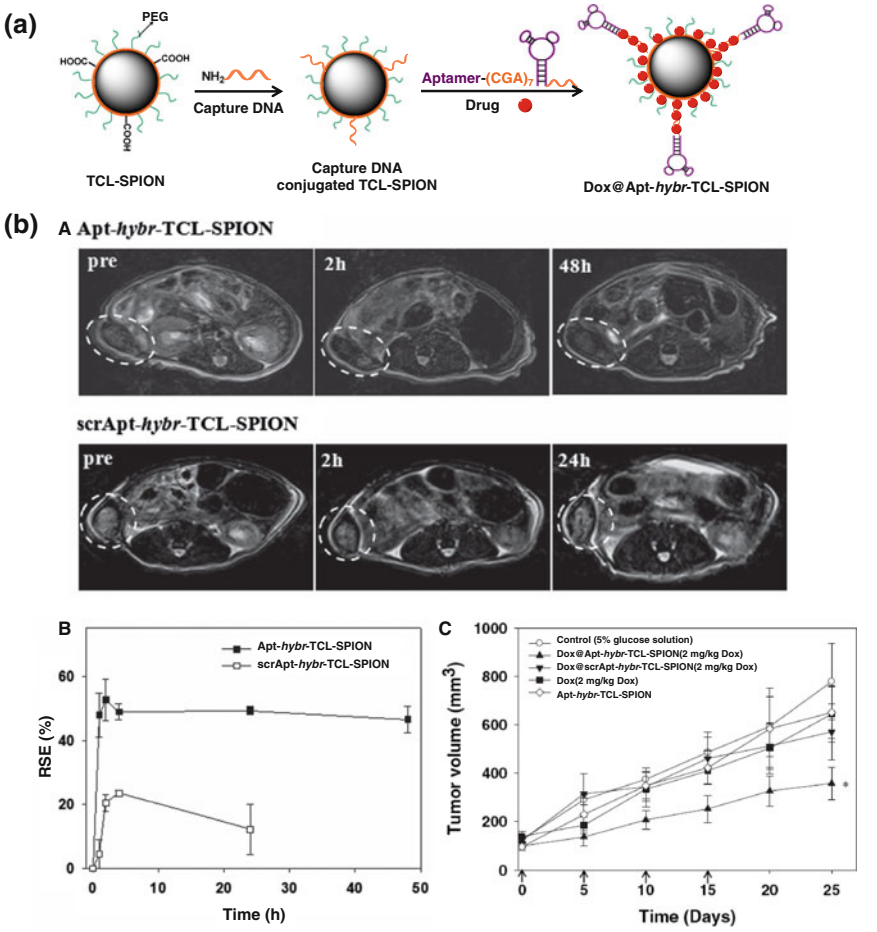

Fig. 13.9 Image-guided prostate cancer therapy using aptamer-functionalized thermally cross-linked SPIONs (Apt–*hybr*–TCL–SPIONs). **a** Schematic diagrams depicting the preparation of Dox-loaded Apt–*hybr*–TCL–SPIONs. **b** T_2-weighted fast-spin echo images (*a*) at the level of the LNCaP mouse tumor taken at 0, 2, 24, and 48 h after injection of Apt–*hybr*–TCL–SPIONs or scrApt–*hybr*–TCL–SPIONs. The *dashed circle* indicates the xenorafted tumor region. (*b*) Relative signal enhancement (RSE, %) at the tumor areas of Apt–*hybr*–TCL–SPION or scrApt–*hybr*–TCL–SPION-treated mice was recorded from T_2-weighted images as a function of time. (*c*) Antitumor activity of Dox@Apt–hybr–TCL–SPIONs in the LNCaP xenograft animal model. Inhibition of tumor growth in each treatment group ($^*P < 0.05$, $n = 6$). Reproduced from Ref. [152] by permission of John Wiley & Sons Ltd

specific binding and internalization of SMNs to target cancer cells. For the acid-labile pores, the lysosome localization of SMNs facilitates the release of Dox from the SMNs, enabling efficient killing of target cancer cells. In addition, T_2 relaxation measurements and T_2*-weighted magnetic resonance images revealed that this nanostructure can be used as a T_2 contrast agent [155].

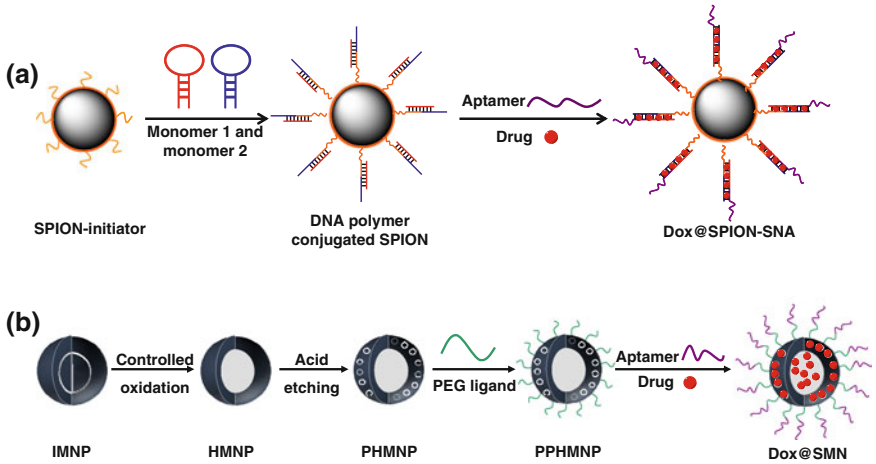

Fig. 13.10 Schematic diagrams of aptamer–magnetic nanoparticle nanoplatforms: **a** SPION-SNAs and **b** SMNs for targeted drug delivery

13.3.2.2 Aptamer–Magnetic Nanoparticle Conjugates for Targeted Magnetic Hyperthermia Therapy

In addition to their suitability as theranostic agents, magnetic NPs have also attracted a great deal of attention in magnetic hyperthermia therapy owing to their associated hyperthermic effects [156]. When subjected to alternating AC magnetic fields, magnetic NPs cause heating of the local area due to losses during magnetization reversal, making magnetic hyperthermia a promising therapeutic method. Generally, magnetic hyperthermia is a two-step procedure: MNPs are first injected into the tumor site, and the patient is then immersed in an alternating magnetic field with frequency f and amplitude $\mu_0 H_{\max}$ appropriately chosen [157]. Because of the excitation of the MNPs, the temperature of the tumor tissue rises. The rise in temperature induces the cancer cells to undergo apoptosis or necrosis and makes the tumor more vulnerable to radio or chemotherapy [158]. To demonstrate specific tumor destruction, Pala et al. applied HER2 aptamer-conjugated SPIONs to hyperthermic therapy targeted for human adenocarcinoma SK-BR3 cancer cells. These Apt–SIPONs were found to be particularly effective in the hyperthermic killing of SK-BR3 at a dosage that was approximately 100-fold lower than that of non-aptamer-tagged SPIONs; however, the treatment was observed to be harmless for the off-targeted U-87 MG cells. The potential for using lower doses of SIPONs is highly desirable in light of the side effects associated with treatment [159].

Other than hyperthermia, SPIONs have also been found to be capable of destroying targeted cancer cells through a magnetocytolytic approach under a DC magnetic field. Nair et al. for the first time employed aptamer-conjugated SPIONs controlled by an externally applied three-dimensional rotational magnetic field to perform nanosurgery for the selective removal of target cells. The cancer cells thus

excised by nanosurgery were confirmed dead, which in turn nullifies the possibility of their proliferation. These results demonstrate that nanosurgery can be a useful tool in the medical field for selective surgery and cell manipulation studies. Additionally, this system could be upgraded for the selective removal of complex cancers from diverse tissues by incorporating various target-specific ligands on SPIONs [160].

13.3.2.3 Aptamer–Magnetic Nanoparticle Conjugates for Targeted Combinational Therapy

While magnetic hyperthermia alone is often not a sufficient cancer treatment, it, however, greatly enhances the treatment of other conventional modalities such as chemotherapy, making SPIONs an attractive candidate for combinational therapy. Aravind et al. [161] developed a multifunctional nanoplatform based on SPIONs for MCF-7 cancer cell theranostics. In this work, poly(D, L-lactide-co-glycolide) (PLGA), an FDA-approved polymer, was chosen as the nanocarrier. PLGA exhibits attractive properties, such as diffusion and erosion-controlled drug release, pH sensitivity as well as temperature-dependent degradation capability, making it a popular choice for drug delivery applications [162, 163]. Paclitaxel (PTX), a broad spectrum anticancer drug, was chosen for encapsulation by the polymer as the drug content [164]. A fluorescent dye, Nile red (NR), was also used to label the PLGA. Further incorporation of SPIONs into PLGA provides benefits in medical applications for hyperthermia therapy, magnetic manipulation, and MRI. Moreover, combination of NR and SPIONs along with chemotherapeutic PTX in the PLGA simultaneously provide for bimodal imaging (via fluorescence and magnetic resonance) and therapeutic features. The specific binding and uptake of the resulting nanocomposites (Apt–SPIONs–NR–PLGANPs) to the target cancer cells through aptamer guidance was observed using confocal microscopy. In addition, combined chemotherapy and hyperthermia therapy exhibited an increased therapeutic effect for the target cancer cells.

Subsequently, the same group developed another multifunctional nanoplatform for pancreatic cancer therapy. In contrast to the previous study, dual drugs, curcumin (Cur) and gemcitabine (Gem), were simultaneously loaded in the formulation for cancer cell chemotherapy. Cur, the natural wonder rhizome, possesses extraordinary properties such as anti-inflammatory, antioxidant, anticancer, and anti-angiogenic effects. In addition, the inherent fluorescence from Cur was used for in vitro cellular imaging [165]. Gem, which is a nucleoside analog, has been broadly used as a standard chemotherapeutic agent for advanced pancreatic cancer [166]. By monitoring the fluorescence of Cur, the successful targeting of Apt–SPIONs–Cur–Gem–PLGANPs to pancreatic cancer cells was observed. Moreover, the ability of SPIONs for hyperthermia therapy and magnetic manipulation of pancreatic cell lines was also monitored. Owing to the synergistic action of Cur, Gem, and magnetic ablation, the induced cell death was extremely significant. Overall, the use of Apt–SPIONs–Cur–Gem–PLGANPs for the targeting of pancreatic cancer cells offers a versatile tool,

providing a platform for both diagnosis and therapy. Multifunctional theragnostic biotechnology and nanotechnology provide the best example of leading research and development for novel cancer annihilation in the near future [167].

13.4 Conclusions

Conventional anticancer therapy is currently facing a diverse range of increasing challenges that detract from the therapeutic success of cancer treatment. On the other hand, these challenges have provided an impetus for developing new therapeutic methods and technology that improve therapeutic efficiency and reduce nondesired side effects. As an example of this development, in recent research, targeted therapy has become the main goal for anticancer drug delivery. Nowadays, with Cell-SELEX technology development, recent studies have demonstrated a variety of applications where aptamers act as target ligands for specific cancer cell therapy. In the present work, we discussed diverse studies where aptamer-based conjugates have provided several novel pathways that serve as platforms for a successful targeted therapy. Overall, aptamer-based conjugates present an approach for the novel development of anticancer therapy that includes four major benefits: (1) The specificity of aptamers provides for targeted binding to cancer cells. (2) The simplicity of aptamer synthesis and modification facilitates their translation into clinical practice. (3) The diverse coupling of aptamers with nanomaterial-based compatible platforms enhances drug-loading capacity. (4) The theranostic capability of aptamer-based nanoconjugates provides controllable optical, electrochemical, magnetic, and mechanical properties for cancer therapy.

While new cancer treatment modalities based on aptamer-mediated targeted delivery are emerging, clinical applications of aptamer-based conjugate/nanoconjugate therapy are still relatively new. Most of the experimental studies have only been conducted in vitro, and parameters such as preparation methods, loading efficiency, biostability, bioavailability, biocompatibility, pharmacokinetics, controlled release, and biodistribution remain to be evaluated for further clinical practices. Specifically, researchers must improve target efficacy, minimize systemic toxicity, and also study nanoparticle behavior in biological microenvironments. For example, to improve target efficiency, it is necessary to optimize the surface modification of conjugates. In this case, the polyvalent-mediated enhancement affinity is achieved by the use of multiple aptamers on the surface, which will increase the binding strengths of aptamers with cancer cells. In addition, to minimize systemic toxicity, key factors must be considered such as surface charge, particle size, coating, biocompatibility, and biodegradability. Finally, to modulate aptamer density, the encapsulation of nanoparticles with PEG coatings prolongs the nanoconjugate half-life in the blood stream. Research on animal models is also required to evaluate the safety and efficacy of aptamer-based therapy, which will posteriorly provide the fundamental parameters for human clinical practice.

Taken together, although several challenges remain to be addressed, oligonucleotide aptamers have become an attractive and promising tool for targeted cancer therapy. As more clinical data are accumulated, we will witness a continued and rapid development of aptamer-based conjugates/nanoconjugates for future cancer therapy in clinical practice.

Acknowledgments We thank the National Tsing Hua University (101N7046E1), the Ministry of Science and Technology (NSC 102-2113-M-007-005-MY3, NSC 102-2627-M-007-004), and the postdoctoral fund of Ministry of Science and Technology (MOST 103-2811-M-007-039) of Taiwan, ROC. Dr. He also thanks the National Natural Science Foundation of China (21405125) and the Fundamental Research Funds for the Central Universities (no. SWU113099) of China.

References

1. Hanahan D, Weinberg RA (2000) The hallmarks of cancer. Cell 100:57–70
2. Hanahan D, Weinberg RA (2011) Hallmarks of cancer: the next generation. Cell 144:646–674
3. Seyfried TN, Shelton LM (2010) Cancer as a metabolic disease. Nutr Metab 7:7
4. Wang ZW, Li YW, Ahmad A, Azmi AS, Kong DJ, Banerjee S, Sarkar FH (2010) Targeting miRNAs involved in cancer stem cell and EMT regulation: an emerging concept in overcoming drug resistance. Drug Resist Update 13:109–118
5. Xu L (2013) Cancer stem cell in the progression and therapy of pancreatic cancer. Front Biosci-Landmrk 18:795–802
6. Haq R, Fisher DE (2011) Biology and clinical relevance of the micropthalmia family of transcription factors in human cancer. J Clin Oncol 29:3474–3482
7. Kanavos P (2006) The rising burden of cancer in the developing world. Ann Oncol 17:15–23
8. Siegel R, Ma JM, Zou ZH, Jemal A (2014) Cancer statistics, 2014. Ca-Cancer J Clin 64:9–29
9. DeSantis CE, Lin CC, Mariotto AB, Siegel RL, Stein KD, Kramer JL, Alteri R, Robbins AS, Jemal A (2014) Cancer treatment and survivorship statistics, 2014. Ca-Cancer J Clin 64: 252–271
10. Chabner BA, Roberts TG (2005) Timeline—chemotherapy and the war on cancer. Nat Rev Cancer 5:65–72
11. DeVita VT, Chu E (2008) A history of cancer chemotherapy. Cancer Res 68:8643–8653
12. Chari RVJ (2008) Targeted cancer therapy: conferring specificity to cytotoxic drugs. Acc Chem Res 41:98–107
13. Gerber DE (2008) Targeted therapies: a new generation of cancer treatments. Am Fam Phys 77:311–319
14. Imai K, Takaoka A (2006) Comparing antibody and small-molecule therapies for cancer. Nat Rev Cancer 6:714–727
15. Andre N, Carre M, Pasquier E (2014) Metronomics: towards personalized chemotherapy? Nat Rev Clin Oncol 11:413–431
16. Yan L, Hsu K, Beckman RA (2008) Antibody-based therapy for solid tumors. Cancer J 14:178–183
17. Schrama D, Reisfeld RA, Becker JC (2006) Antibody targeted drugs as cancer therapeutics. Nat Rev Drug Discov 5:147–159
18. Alley SC, Okeley NM, Senter PD (2010) Antibody-drug conjugates: targeted drug delivery for cancer. Curr Opin Chem Biol 14:529–537
19. Sievers EL, Senter PD (2013) Antibody-drug conjugates in cancer therapy. Annu Rev Med 64:15–29

20. Ellington AD, Szostak JW (1990) In vitro selection of RNA molecules that bind specific ligands. Nature 346:818–822
21. Shangguan D, Li Y, Tang ZW, Cao ZHC, Chen HW, Mallikaratchy P, Sefah K, Yang CYJ, Tan WH (2006) Aptamers evolved from live cells as effective molecular probes for cancer study. P Natl Acad Sci USA 103:11838–11843
22. Sefah K, Shangguan D, Xiong XL, O'Donoghue MB, Tan WH (2010) Development of DNA aptamers using Cell-SELEX. Nat Protoc 5:1169–1185
23. Mayer G (2009) The chemical biology of aptamers. Angew Chem Int Edit 48:2672–2689
24. Ireson CR, Kelland LR (2006) Discovery and development of anticancer aptamers. Mol Cancer Ther 5:2957–2962
25. Guo KT, Paul A, Schichor C, Ziemer G, Wendel HP (2008) Cell-SELEX: novel perspectives of aptamer-based therapeutics. Int J Mol Sci 9:668–678
26. Fang XH, Tan WH (2010) Aptamers generated from Cell-SELEX for molecular medicine: a chemical biology approach. Acc Chem Res 43:48–57
27. Sundaram P, Kurniawan H, Byrne ME, Wower J (2013) Therapeutic RNA aptamers in clinical trials. Eur J Pharm Sci 48:259–271
28. Bates PJ, Laber DA, Miller DM, Thomas SD, Trent JO (2009) Discovery and development of the G-rich oligonucleotide AS1411 as a novel treatment for cancer. Exp Mol Pathol 86:151–164
29. Huang YF, Shangguan DH, Liu HP, Phillips JA, Zhang XL, Chen Y, Tan WH (2009) Molecular assembly of an aptamer-drug conjugate for targeted drug delivery to tumor cells. ChemBioChem 10:862–868
30. Tan WH, Wang H, Chen Y, Zhang XB, Zhu HZ, Yang CY, Yang RH, Liu C (2011) Molecular aptamers for drug delivery. Trends Biotechnol 29:634–640
31. Huang YF, Kim Y, Meng L, Tan WH (2009) Assembly of aptamer conjugates as molecular tools in therapeutics. Chim Oggi 27:52–54
32. Wu Z, Tang LJ, Zhang XB, Jiang JH, Tan WH (2011) Aptamer-modified nanodrug delivery systems. Acs NANO 5:7696–7699
33. Liu QL, Jin C, Wang YY, Fang XH, Zhang XB, Chen Z, Tan WH (2014) Aptamer-conjugated nanomaterials for specific cancer cell recognition and targeted cancer therapy. Npg Asia Mater 6:e95
34. Chen T, Shukoor MI, Chen Y, Yuan QA, Zhu Z, Zhao ZL, Gulbakan B, Tan WH (2011) Aptamer-conjugated nanomaterials for bioanalysis and biotechnology applications. Nanoscale 3:546–556
35. Yang L, Zhang XB, Ye M, Jiang JH, Yang RH, Fu T, Chen Y, Wang KM, Liu C, Tan WH (2011) Aptamer-conjugated nanomaterials and their applications. Adv Drug Deliver Rev 63:1361–1370
36. Kong RM, Zhang XB, Chen Z, Tan WH (2011) Aptamer-assembled nanomaterials for biosensing and biomedical applications. Small 7:2428–2436
37. Aslan B, Ozpolat B, Sood AK, Lopez-Berestein G (2013) Nanotechnology in cancer therapy. J Drug Target 21:904–913
38. Peer D, Karp JM, Hong S, FaroKHzad OC, Margalit R, Langer R (2007) Nanocarriers as an emerging platform for cancer therapy. Nat Nanotechnol 2:751–760
39. Maeda H, Nakamura H, Fang J (2013) The EPR effect for macromolecular drug delivery to solid tumors: improvement of tumor uptake, lowering of systemic toxicity, and distinct tumor imaging in vivo. Adv Drug Deliv Rev 65:71–79
40. Kumar A, Zhang X, Liang XJ (2013) Gold nanoparticles: emerging paradigm for targeted drug delivery system. Biotechnol Adv 31:593–606
41. Peng XH, Qian XM, Mao H, Wang AY, Chen Z, Nie SM, Shin DM (2008) Targeted magnetic iron oxide nanoparticles for tumor imaging and therapy. Int J Nanomed 3:311–321
42. Ji SR, Liu C, Zhang B, Yang F, Xu J, Long JA, Jin C, Fu DL, Ni QX, Yu XJ (2010) Carbon nanotubes in cancer diagnosis and therapy. Bba-Rev Cancer 1806:29–35

43. Lee JE, Lee N, Kim T, Kim J, Hyeon T (2011) Multifunctional mesoporous silica nanocomposite nanoparticles for theranostic applications. Acc Chem Res 44:893–902
44. Andresen TL, Jensen SS, Jorgensen K (2005) Advanced strategies in liposomal cancer therapy: problems and prospects of active and tumor specific drug release. Prog Lipid Res 44:68–97
45. Blanco E, Kessinger CW, Sumer BD, Gao J (2009) Multifunctional micellar nanomedicine for cancer therapy. Exp Biol Med 234:123–131
46. Maeda H, Bharate GY, Daruwalla J (2009) Polymeric drugs for efficient tumor-targeted drug delivery based on EPR-effect. Eur J Pharm Biopharm 71:409–419
47. Jain RK (1994) Barriers to drug-delivery in solid tumors. Sci Am 271:58–65
48. Bamrungsap S, Zhao ZL, Chen T, Wang L, Li CM, Fu T, Tan WH (2012) Nanotechnology in therapeutics: a focus on nanoparticles as a drug delivery system. Nanomedicine-Uk 7:1253–1271
49. Berdel WE, Fink U (1984) Cancer-chemotherapy—situation problems, perspectives. Munchen Med Wochen 126:1166–1171
50. Zhou JH, Rossi JJ (2011) Cell-specific aptamer-mediated targeted drug delivery. Oligonucleotides 21:1–10
51. Shangguan D, Cao ZH, Meng L, Mallikaratchy P, Sefah K, Wang H, Li Y, Tan WH (2008) Cell-specific aptamer probes for membrane protein elucidation in cancer cells. J Proteome Res 7:2133–2139
52. Boyacioglu O, Stuart CH, Kulik G, Gmeiner WH (2013) Dimeric DNA aptamer complexes for high-capacity-targeted drug delivery using pH-sensitive covalent linkages. Mol Ther-Nucl Acids 2:e107
53. Perner S, Hofer MD, Kim R, Shah RB, Li HJ, Moller P, Hautmann RE, Gschwend JE, Kuefer R, Rubin MA (2007) Prostate-specific membrane antigen expression as a predictor of prostate cancer progression. Hum Pathol 38:696–701
54. Schulke N, Varlamova OA, Donovan GP, Ma DS, Gardner JP, Morrissey DM, Arrigale RR, Zhan CC, Chodera AJ, Surowitz KG, Maddon PJ, Heston WDW, Olson WC (2003) The homodimer of prostate-specific membrane antigen is a functional target for cancer therapy. P Natl Acad Sci USA 100:12590–12595
55. Aggarwal S, Singh P, Topaloglu O, Isaacs JT, Denmeade SR (2006) A dimeric peptide that binds selectively to prostate-specific membrane antigen and inhibits its enzymatic activity. Cancer Res 66:9171–9177
56. Wang RW, Zhu GZ, Mei L, Xie Y, Ma HB, Ye M, Qing FL, Tan WH (2014) Automated modular synthesis of aptamer-drug conjugates for targeted drug delivery. J Am Chem Soc 136:2731–2734
57. Bagalkot V, Farokhzad OC, Langer R, Jon S (2006) An aptamer-doxorubicin physical conjugate as a novel targeted drug-delivery platform. Angew Chem Int Edit 45:8149–8152
58. Lupold SE, Hicke BJ, Lin Y, Coffey DS (2002) Identification and characterization of nuclease-stabilized RNA molecules that bind human prostate cancer cells via the prostate-specific membrane antigen. Cancer Res 62:4029–4033
59. Liu Z, Duan JH, Song YM, Ma J, Wang FD, Lu X, Yang XD (2012) Novel HER2 aptamer selectively delivers cytotoxic drug to HER2-positive breast cancer cells in vitro. J Transl Med 10:148
60. Ross JS, Slodkowska EA, Symmans WF, Pusztai L, Ravdin PM, Hortobagyi GN (2009) The HER-2 receptor and breast cancer: ten years of targeted Anti-HER-2 therapy and personalized medicine. Oncologist 14:320–368
61. Goldhirsch A, Ingle JN, Gelber RD, Coates AS, Thurlimann B, Senn HJ (2009) Thresholds for therapies: highlights of the St Gallen International Expert Consensus on the primary therapy of early breast cancer 2009. Ann Oncol 20:1319–1329
62. Shangguan DH, Meng L, Cao ZHC, Xiao ZY, Fang XH, Li Y, Cardona D, Witek RP, Liu C, Tan WH (2008) Identification of liver cancer-specific aptamers using whole live cells. Anal Chem 80:721–728

63. Shangguan DH, Cao ZHC, Li Y, Tan WH (2007) Aptamers evolved from cultured cancer cells reveal molecular differences of cancer cells in patient samples. Clin Chem 53:1153–1155
64. Zhu GZ, Meng L, Ye M, Yang L, Sefah K, O'Donoghue MB, Chen Y, Xiong XL, Huang J, Song EQ, Tan WH (2012) Self-assembled aptamer-based drug carriers for bispecific cytotoxicity to cancer cells. Chem-Asian J 7:1630–1636
65. Zhu GZ, Zheng J, Song EQ, Donovan M, Zhang KJ, Liu C, Tan WH (2013) Self-assembled, aptamer-tethered DNA nanotrains for targeted transport of molecular drugs in cancer theranostics. P Natl Acad Sci USA 110:7998–8003
66. Zhang ZQ, Ali MM, Eckert MA, Kang DK, Chen YY, Sender LS, Fruman DA, Zhao WA (2013) A polyvalent aptamer system for targeted drug delivery. Biomaterials 34:9728–9735
67. Kim Y, Cao Z, Tan W (2008) Molecular assembly for high-performance bivalent nucleic acid inhibitor. P Natl Acad Sci USA 105:5664–5669
68. Dougherty TJ, Gomer CJ, Henderson BW, Jori G, Kessel D, Korbelik M, Moan J, Peng Q (1998) Photodynamic therapy. J Natl Cancer I 90:889–905
69. Nseyo UO, DeHaven J, Dougherty TJ, Potter WR, Merrill DL, Lundahl SL, Lamm DL (1998) Photodynamic therapy (PDT) in the treatment of patients with resistant superficial bladder cancer: a long term experience. J Clin Laser Med Sur 16:61–68
70. Huang Z (2005) A review of progress in clinical photodynamic therapy. Technol Cancer Res T 4:283–293
71. Wilson BC, Patterson MS (2008) The physics, biophysics and technology of photodynamic therapy. Phys Med Biol 53:R61–R109
72. Moan J (1990) On the diffusion length of singlet oxygen in cells and tissues. J Photoch Photobio B 6:343–347
73. Bugaj AM (2011) Targeted photodynamic therapy—a promising strategy of tumor treatment. Photoch Photobio Sci 10:1097–1109
74. Lovell JF, Liu TWB, Chen J, Zheng G (2010) Activatable photosensitizers for imaging and therapy. Chem Rev 110:2839–2857
75. Verma S, Watt GM, Mal Z, Hasan T (2007) Strategies for enhanced photodynamic therapy effects. Photochem Photobiol 83:996–1005
76. Tang ZW, Shangguan D, Wang KM, Shi H, Sefah K, Mallikratchy P, Chen HW, Li Y, Tan WH (2007) Selection of aptamers for molecular recognition and characterization of cancer cells. Anal Chem 79:4900–4907
77. Mallikaratchy P, Tang ZW, Tan WH (2008) Cell specific aptamer-photosensitizer conjugates as a molecular tool in photodynamic therapy. ChemMedChem 3:425–428
78. Kruspe S, Meyer C, Hahn U (2014) Chlorin e6 conjugated interleukin-6 receptor aptamers selectively kill target cells upon irradiation. Mol Ther-Nucl Acids 3:e143
79. Sen D, Gilbert W (1988) Formation of parallel 4-stranded complexes by guanine-rich motifs in DNA and its implications for meiosis. Nature 334:364–366
80. Ambrus A, Chen D, Dai JX, Bialis T, Jones RA, Yang DZ (2006) Human telomeric sequence forms a hybrid-type intramolecular G-quadruplex structure with mixed parallel/antiparallel strands in potassium solution. Nucleic Acids Res 34:2723–2735
81. Evans T, Schon E, Goramaslak G, Patterson J, Efstratiadis A (1984) S1-hypersensitive sites in eukaryotic promoter regions. Nucleic Acids Res 12:8043–8058
82. Granotier C, Pennarun G, Riou L, Hoffschir F, Gauthier LR, De Cian A, Gomez D, Mandine E, Riou JF, Mergny JL, Mailliet P, Dutrillaux B, Boussin FD (2005) Preferential binding of a G-quadruplex ligand to human chromosome ends. Nucleic Acids Res 33:4182–4190
83. Zahler AM, Williamson JR, Cech TR, Prescott DM (1991) Inhibition of telomerase by G-quartet DNA structures. Nature 350:718–720
84. Rha SY, Izbicka E, Lawrence R, Davidson K, Sun DK, Moyer MP, Roodman GD, Hurley L, Von Hoff D (2000) Effect of telomere and telomerase interactive agents on human tumor and normal cell lines. Clin Cancer Res 6:987–993

85. Shieh YA, Yang SJ, Wei MF, Shieh MJ (2010) Aptamer-based tumor-targeted drug delivery for photodynamic therapy. ACS Nano 4:1433–1442
86. Wang KL, You MX, Chen Y, Han D, Zhu Z, Huang J, Williams K, Yang CJ, Tan WH (2011) Self-assembly of a bifunctional DNA carrier for drug delivery. Angew Chem Int Edit 50:6098–6101
87. Zheng G, Chen J, Stefflova K, Jarvi M, Li H, Wilson BC (2007) Photodynamic molecular beacon as an activatable photosensitizer based on protease-controlled singlet oxygen quenching and activation. P Natl Acad Sci USA 104:8989–8994
88. Tang ZW, Zhu Z, Mallikaratchy P, Yang RH, Sefah K, Tan WH (2010) Aptamer-target binding triggered molecular mediation of singlet oxygen generation. Chem-Asian J 5:783–786
89. Dirks RM, Pierce NA (2004) Triggered amplification by hybridization chain reaction. P Natl Acad Sci USA 101:15275–15278
90. Zhang DY, Turberfield AJ, Yurke B, Winfree E (2007) Engineering entropy-driven reactions and networks catalyzed by DNA. Science 318:1121–1125
91. Yin P, Choi HMT, Calvert CR, Pierce NA (2008) Programming biomolecular self-assembly pathways. Nature 451:318–322
92. Han D, Zhu GZ, Wu CC, Zhu Z, Chen T, Zhang XB, Tan WH (2013) Engineering a cell-surface aptamer circuit for targeted and amplified photodynamic cancer therapy. ACS Nano 7:2312–2319
93. Daniel MC, Astruc D (2004) Gold nanoparticles: assembly, supramolecular chemistry, quantum-size-related properties, and applications toward biology, catalysis, and nanotechnology. Chem Rev 104:293–346
94. Hakkinen H (2012) The gold-sulfur interface at the nanoscale. Nat Chem 4:443–455
95. Niidome T, Yamagata M, Okamoto Y, Akiyama Y, Takahashi H, Kawano T, Katayama Y, Niidome Y (2006) PEG-modified gold nanorods with a stealth character for in vivo applications. J Control Release 114:343–347
96. Boca SC, Astilean S (2010) Detoxification of gold nanorods by conjugation with thiolated poly(ethylene glycol) and their assessment as SERS-active carriers of Raman tags. Nanotechnology 21:235601
97. Alkilany AM, Murphy CJ (2010) Toxicity and cellular uptake of gold nanoparticles: what we have learned so far? J Nanopart Res 12:2313–2333
98. Gerber A, Bundschuh M, Klingelhofer D, Groneberg DA (2013) Gold nanoparticles: recent aspects for human toxicology. J Occup Med Toxicol 8:32
99. Nikoobakht B, El-Sayed MA (2003) Preparation and growth mechanism of gold nanorods (NRs) using seed-mediated growth method. Chem Mater 15:1957–1962
100. Schwartzberg AM, Olson TY, Talley CE, Zhang JZ (2006) Synthesis, characterization, and tunable optical properties of hollow gold nanospheres. J Phys Chem B 110:19935–19944
101. Skrabalak SE, Chen JY, Sun YG, Lu XM, Au L, Cobley CM, Xia YN (2008) Gold nanocages: synthesis, properties, and applications. Acc Chem Res 41:1587–1595
102. Huang XH, Neretina S, El-Sayed MA (2009) Gold nanorods: from synthesis and properties to biological and biomedical applications. Adv Mater 21:4880–4910
103. Hu M, Chen JY, Li ZY, Au L, Hartland GV, Li XD, Marquez M, Xia YN (2006) Gold nanostructures: engineering their plasmonic properties for biomedical applications. Chem Soc Rev 35:1084–1094
104. Schoen PAE, Walther JH, Poulikakos D, Koumoutsakos P (2007) Phonon assisted thermophoretic motion of gold nanoparticles inside carbon nanotubes. Appl Phys Lett 90:253116
105. Fisher JW, Sarkar S, Buchanan CF, Szot CS, Whitney J, Hatcher HC, Torti SV, Rylander CG, Rylander MN (2010) Photothermal response of human and murine cancer cells to multiwalled carbon nanotubes after laser irradiation. Cancer Res 70:9855–9864
106. Dickerson EB, Dreaden EC, Huang XH, El-Sayed IH, Chu HH, Pushpanketh S, McDonald JF, El-Sayed MA (2008) Gold nanorod assisted near-infrared plasmonic photothermal therapy (PPTT) of squamous cell carcinoma in mice. Cancer Lett 269:57–66

107. Choi WI, Kim JY, Kang C, Byeon CC, Kim YH, Tee G (2011) Tumor regression in vivo by photothermal therapy based on gold-nanorod-loaded, functional nanocarriers. ACS Nano 5:1995–2003
108. Huang YF, Sefah K, Bamrungsap S, Chang HT, Tan W (2008) Selective photothermal therapy for mixed cancer cells using aptamer-conjugated nanorods. Langmuir 24:11860–11865
109. Huang YF, Chang HT, Tan WH (2008) Cancer cell targeting using multiple aptamers conjugated on nanorods. Anal Chem 80:567–572
110. Wang J, Sefah K, Altman MB, Chen T, You MX, Zhao ZL, Huang CZ, Tan WH (2013) Aptamer-conjugated nanorods for targeted photothermal therapy of prostate cancer stem cells. Chem-Asian J 8:2417–2422
111. Yang HW, Lu YJ, Lin KJ, Hsu SC, Huang CY, She SH, Liu HL, Lin CW, Xiao MC, Wey SP, Chen PY, Yen TC, Wei KC, Ma CCM (2013) EGRF conjugated PEGylated nanographene oxide for targeted chemotherapy and photothermal therapy. Biomaterials 34:7204–7214
112. Pissuwan D, Niidome T, Cortie MB (2011) The forthcoming applications of gold nanoparticles in drug and gene delivery systems. J Control Release 149:65–71
113. Hegyi G, Szigeti GP, Szasz A (2013) Hyperthermia versus oncothermia: cellular effects in complementary cancer therapy. Evid-Based Compl Alt 2013:672873
114. You J, Zhang GD, Li C (2010) Exceptionally high payload of doxorubicin in hollow gold nanospheres for near-infrared light-triggered drug release. ACS Nano 4:1033–1041
115. Zhao NX, You J, Zeng ZH, Li C, Zu YL (2013) An ultra pH-sensitive and aptamer-equipped nanoscale drug-delivery system for selective killing of tumor cells. Small 9:3477–3484
116. Slowing II, Vivero-Escoto JL, Wu CW, Lin VSY (2008) Mesoporous silica nanoparticles as controlled release drug delivery and gene transfection carriers. Adv Drug Deliv Rev 60:1278–1288
117. Marsh TC, Vesenka J, Henderson E (1995) A new DNA nanostructure, the G-wire, imaged by scanning probe microscopy. Nucleic Acids Res 23:696–700
118. Yang XJ, Liu X, Liu Z, Pu F, Ren JS, Qu XG (2012) Near-infrared light-triggered, targeted drug delivery to cancer cells by aptamer gated nanovehicles. Adv Mater 24:2890–2895
119. Luo YL, Shiao YS, Huang YF (2011) Release of photoactivatable drugs from plasmonic nanoparticles for targeted cancer therapy. ACS Nano 5:7796–7804
120. Kang HZ, Trondoli AC, Zhu GZ, Chen Y, Chang YJ, Liu HP, Huang YF, Zhang XL, Tan WH (2011) Near-infrared light-responsive core-shell nanogels for targeted drug delivery. ACS Nano 5:5094–5099
121. Jang B, Park JY, Tung CH, Kim IH, Choi Y (2011) Gold nanorod-photosensitizer complex for near-infrared fluorescence imaging and photodynamic/photothermal therapy in vivo. ACS Nano 5:1086–1094
122. Kuo WS, Chang CN, Chang YT, Yang MH, Chien YH, Chen SJ, Yeh CS (2010) Gold nanorods in photodynamic therapy, as hyperthermia agents, and in near-infrared optical imaging. Angew Chem Int Edit 49:2711–2715
123. Dulkeith E, Ringler M, Klar TA, Feldmann J, Javier AM, Parak WJ (2005) Gold nanoparticles quench fluorescence by phase induced radiative rate suppression. Nano Lett 5:585–589
124. Jain PK, Lee KS, El-Sayed IH, El-Sayed MA (2006) Calculated absorption and scattering properties of gold nanoparticles of different size, shape, and composition: Applications in biological imaging and biomedicine. J Phys Chem B 110:7238–7248
125. Griffin J, Singh AK, Senapati D, Rhodes P, Mitchell K, Robinson B, Yu E, Ray PC (2009) Size- and distance-dependent nanoparticle surface-energy transfer (NSET) method for selective sensing of Hepatitis C Virus RNA. Chem-Eur J 15:342–351
126. Wang J, Zhu GZ, You MX, Song EQ, Shukoor MI, Zhang KJ, Altman MB, Chen Y, Zhu Z, Huang CZ, Tan WH (2012) Assembly of aptamer switch probes and photosensitizer on gold nanorods for targeted photothermal and photodynamic cancer therapy. ACS Nano 6:5070–5077

127. Poon L, Zandberg W, Hsiao D, Erno Z, Sen D, Gates BD, Branda NR (2010) Photothermal release of single-stranded DNA from the surface of gold nanoparticles through controlled denaturating and Au–S bond breaking. ACS Nano 4:6395–6403
128. Lee DE, Koo H, Sun IC, Ryu JH, Kim K, Kwon IC (2012) Multifunctional nanoparticles for multimodal imaging and theragnosis. Chem Soc Rev 41:2656–2672
129. Yin ML, Li ZH, Liu Z, Ren JS, Yang XJ, Qu XG (2012) Photosensitizer-incorporated G-quadruplex DNA-functionalized magnetofluorescent nanoparticles for targeted magnetic resonance/fluorescence multimodal imaging and subsequent photodynamic therapy of cancer. Chem Commun 48:6556–6558
130. Natterer F, Ritman EL (2002) Past and future directions in X-ray computed tomography (CT). Int J Imag Syst Tech 12:175–187
131. Kim D, Park S, Lee JH, Jeong YY, Jon S (2007) Antibiofouling polymer-coated gold nanoparticles as a contrast agent for in vivo x-ray computed tomography imaging. J Am Chem Soc 129:7661–7665
132. Kattumuri V, Katti K, Bhaskaran S, Boote EJ, Casteel SW, Fent GM, Robertson DJ, Chandrasekhar M, Kannan R, Katti KV (2007) Gum Arabic as a phytochemical construct for the stabilization of gold nanoparticles: in vivo pharmacokinetics and X-ray-contrast-imaging studies. Small 3:333–341
133. Alric C, Taleb J, Le Duc G, Mandon C, Billotey C, Le Meur-Herland A, Brochard T, Vocanson F, Janier M, Perriat P, Roux S, Tillement O (2008) Gadolinium chelate coated gold nanoparticles as contrast agents for both X-ray computed tomography and magnetic resonance imaging. J Am Chem Soc 130:5908–5915
134. Kim D, Jeong YY, Jon S (2010) A drug-loaded aptamer-gold nanoparticle bioconjugate for combined CT imaging and therapy of prostate cancer. ACS Nano 4:3689–3696
135. Fox MD, Raichle ME (2007) Spontaneous fluctuations in brain activity observed with functional magnetic resonance imaging. Nat Rev Neurosci 8:700–711
136. Munowitz M, Pines A (1987) Principles and applications of multiple-quantum NMR. Adv Chem Phys 66:1–152
137. Pan DPJ, Schmieder AH, Wickline SA, Lanza GM (2011) Manganese-based MRI contrast agents: past, present, and future. Tetrahedron 67:8431–8444
138. Li CM, Chen T, Ocsoy I, Zhu GZ, Yasun E, You MX, Wu CC, Zheng J, Song EQ, Huang CZ, Tan WH (2014) Gold-coated Fe_3O_4 nanoroses with five unique functions for cancer cell targeting, imaging, and therapy. Adv Funct Mater 24:1772–1780
139. Colombo M, Carregal-Romero S, Casula MF, Gutierrez L, Morales MP, Bohm IB, Heverhagen JT, Prosperi D, Parak WJ (2012) Biological applications of magnetic nanoparticles. Chem Soc Rev 41:4306–4334
140. Mahmoudi M, Hofmann H, Rothen-Rutishauser B, Petri-Fink A (2012) Assessing the in vitro and in vivo toxicity of superparamagnetic iron oxide nanoparticles. Chem Rev 112:2323–2338
141. Shubayev VI, Pisanic TR, Jin SH (2009) Magnetic nanoparticles for theragnostics. Adv Drug Deliv Rev 61:467–477
142. Sun C, Lee JSH, Zhang MQ (2008) Magnetic nanoparticles in MR imaging and drug delivery. Adv Drug Deliv Rev 60:1252–1265
143. Jun YW, Seo JW, Cheon A (2008) Nanoscaling laws of magnetic nanoparticles and their applicabilities in biomedical sciences. Acc Chem Res 41:179–189
144. Laurent S, Forge D, Port M, Roch A, Robic C, Elst LV, Muller RN (2008) Magnetic iron oxide nanoparticles: synthesis, stabilization, vectorization, physicochemical characterizations, and biological applications. Chem Rev 108:2064–2110
145. Rockenberger J, Scher EC, Alivisatos AP (1999) A new nonhydrolytic single-precursor approach to surfactant-capped nanocrystals of transition metal oxides. J Am Chem Soc 121:11595–11596

146. Sun SH, Zeng H (2002) Size-controlled synthesis of magnetite nanoparticles. J Am Chem Soc 124:8204–8205
147. Zhao FY, Zhang BL, Feng LY (2012) Preparation and magnetic properties of magnetite nanoparticles. Mater Lett 68:112–114
148. Wu W, He QG, Jiang CZ (2008) Magnetic iron oxide nanoparticles: synthesis and surface functionalization strategies. Nanoscale Res Lett 3:397–415
149. Gupta AK, Gupta M (2005) Synthesis and surface engineering of iron oxide nanoparticles for biomedical applications. Biomaterials 26:3995–4021
150. Wang AZ, Bagalkot V, Vasilliou CC, Gu F, Alexis F, Zhang L, Shaikh M, Yuet K, Cima MJ, Langer R, Kantoff PW, Bander NH, Jon SY, Farokhzad OC (2008) Superparamagnetic iron oxide nanoparticle-aptamer bioconjugates for combined prostate cancer imaging and therapy. ChemMedChem 3:1311–1315
151. Jalalian SH, Taghdisi SM, Hamedani NS, Kalat SAM, Lavaee P, ZandKarimi M, Ghows N, Jaafari MR, Naghibi S, Danesh NM, Ramezani M, Abnous K (2013) Epirubicin loaded super paramagnetic iron oxide nanoparticle-aptamer bioconjugate for combined colon cancer therapy and imaging in vivo. Eur J Pharm Sci 50:191–197
152. Yu MK, Kim D, Lee IH, So JS, Jeong YY, Jon S (2011) Image-guided prostate cancer therapy using aptamer-functionalized thermally cross-linked superparamagnetic iron oxide nanoparticles. Small 7:2241–2249
153. Zheng J, Zhu GZ, Li YH, Li CM, You MX, Chen T, Song EQ, Yang RH, Tan WH (2013) A spherical nucleic acid platform based on self-assembled DNA biopolymer for high-performance cancer therapy. ACS Nano 7:6545–6554
154. Cheng K, Peng S, Xu CJ, Sun SH (2009) Porous hollow Fe_3O_4 nanoparticles for targeted delivery and controlled release of cisplatin. J Am Chem Soc 131:10637–10644
155. Chen T, Shukoor MI, Wang RW, Zhao ZL, Yuan Q, Bamrungsap S, Xiong XL, Tan WH (2011) Smart multifunctional nanostructure for targeted cancer chemotherapy and magnetic resonance imaging. ACS Nano 5:7866–7873
156. Kumar CSSR, Mohammad F (2011) Magnetic nanomaterials for hyperthermia-based therapy and controlled drug delivery. Adv Drug Deliv Rev 63:789–808
157. Mehdaoui B, Meffre A, Carrey J, Lachaize S, Lacroix LM, Gougeon M, Chaudret B, Respaud M (2011) Optimal size of nanoparticles for magnetic hyperthermia: a combined theoretical and experimental study. Adv Funct Mater 21:4573–4581
158. Johannsen M, Gneueckow U, Thiesen B, Taymoorian K, Cho CH, Waldofner N, Scholz R, Jordan A, Loening SA, Wust P (2007) Thermotherapy of prostate cancer using magnetic nanoparticles: feasibility, imaging, and three-dimensional temperature distribution. Eur Urol 52:1653–1662
159. Pala K, Serwotka A, Jelen F, Jakimowicz P, Otlewski J (2014) Tumor-specific hyperthermia with aptamer-tagged superparamagnetic nanoparticles. Int J Nanomed 9:67–76
160. Nair BG, Nagaoka Y, Morimoto H, Yoshida Y, Maekawa T, Kumar DS (2010) Aptamer conjugated magnetic nanoparticles as nanosurgeons. Nanotechnology 21:455102
161. Aravind A, Nair R, Raveendran S, Veeranarayanan S, Nagaoka Y, Fukuda T, Hasumura T, Morimoto H, Yoshida Y, Maekawa T, Kumar DS (2013) Aptamer conjugated paclitaxel and magnetic fluid loaded fluorescently tagged PLGA nanoparticles for targeted cancer therapy. J Magn Magn Mater 344:116–123
162. Dunne M, Corrigan OI, Ramtoola Z (2000) Influence of particle size and dissolution conditions on the degradation properties of polylactide-co-glycolide particles. Biomaterials 21:1659–1668
163. Grayson ACR, Cima MJ, Langer R (2005) Size and temperature effects on poly(lactic-co-glycolic acid) degradation and microreservoir device performance. Biomaterials 26:2137–2145
164. Koziara JM, Lockman PR, Allen DD, Mumper RJ (2004) Paclitaxel nanoparticles for the potential treatment of brain tumors. J Control Release 99:259–269

165. Goel A, Kunnumakkara AB, Aggarwal BB (2008) Curcumin as "Curecumin": from kitchen to clinic. Biochem Pharmacol 75:787–809
166. Burris HA, Moore MJ, Andersen J, Green MR, Rothenberg ML, Madiano MR, Cripps MC, Portenoy RK, Storniolo AM, Tarassoff P, Nelson R, Dorr FA, Stephens CD, VanHoff DD (1997) Improvements in survival and clinical benefit with gemcitabine as first-line therapy for patients with advanced pancreas cancer: a randomized trial. J Clin Oncol 15:2403–2413
167. Sivakumar B, Aswathy RG, Nagaoka Y, Iwai S, Venugopal K, Kato K, Yoshida Y, Maekawa T, Kumar DNS (2013) Aptamer conjugated theragnostic multifunctional magnetic nanoparticles as a nanoplatform for pancreatic cancer therapy. RSC Adv 3:20579–20598

Chapter 14
The Clinical Application of Aptamers: Future Challenges and Prospects

Yanling Song, Huimin Zhang, Zhi Zhu and Chaoyong Yang

Abstract This final chapter attempts to search for reasons to explain why so little progress has been made in the practical clinical application of aptamers and propose potential solutions to the problem. The advantages and limitations of aptamers in clinical settings are first carefully evaluated. It is suggested that in order to increase the clinical application of aptamers, new selection methods are needed to further improve the success rate of aptamer selection and to efficiently generate stable aptamers for in vivo application with low cost. Several new and promising aptamer selection methods are then reviewed. Strategies for improving selection success rate are highlighted. Finally, efforts leading to the selection of stable aptamers and, hence, increasing the potential for the practical use of aptamer-based technology in clinical settings, are discussed.

Keywords Aptamer · Base modification · Spiegelmer · Microfluidics · SELEX

14.1 Introduction

Based on their unique functions and features, as discussed throughout the chapters of this book, aptamers have been developed over the past 25 years for applications in chemical sensing, clinical diagnosis, targeted drug delivery, and therapy [1–6]. Moreover, the utility of aptamers has been amplified by their compatibility with such detection schemes as electrochemistry [7], fluorescence [8, 9], colorimetrics [6, 10–12], chemiluminescence [13], field effect transistors [14], and surface plasmon resonance (SPR) [15, 16]. However, while aptamer development has flourished in the laboratory, the commercialization of aptamers, especially for biomedical applications, has lagged far behind. Since the invention of aptamer

Y. Song · H. Zhang · Z. Zhu · C. Yang (✉)
Department of Chemical Biology, College of Chemistry and Chemical Engineering, Xiamen University, Xiamen, People's Republic of China
e-mail: cyyang@xmu.edu.cn

W. Tan and X. Fang (eds.), *Aptamers Selected by Cell-SELEX for Theranostics*,
DOI 10.1007/978-3-662-46226-3_14

selection technique by the Gold and Szostak labs in 1990 [17, 18], it took more than a decade to develop the first FDA-approved therapeutic aptamer, Macugen, a drug for age-related macular degeneration [19]. Macugen was developed using an aptamer against its target molecule vascular endothelial growth factor hormone (VEGF). Although several therapeutic aptamers are currently being developed for nucleolin, thrombin, platelet-derived growth factor (PDGF), and human neutrophil elastase (hNE), none has been approved by FDA. In this final chapter, then, we search for reasons to explain why so little progress has been made in the practical application of aptamers for therapeutic and clinical diagnostics. To accomplish this, we take a hard look at the advantages and limitations of aptamers in clinical settings, in particular, comparing them against commonly used affinity probes-antibodies. We also review several methods that have been developed to improve the selection and stability of aptamers, as we look ahead to their increased use in clinical applications.

14.2 Comparison of Aptamers Against Antibodies

One of the attractive features of aptamers is that they can be selected against targets not otherwise possible for antibodies. Using the in vitro method known as SELEX (systematic evolution of ligands by exponential enrichment), as discussed throughout this work, toxins, as well as molecules that do not elicit good immune responses, can be used to detect a wide variety of targets, ranging from small molecules to supramolecular complexes, even tissue. More importantly, aptamers that bind their cognate target in nonphysiological buffer and temperature are easy to identify, making it possible to change their properties on demand and thus obtain aptamers desirable for in vitro diagnostics. On the other hand, many challenges confront the identification and production of antibodies. Since the identification process starts within an animal, molecules that are poorly tolerated, or less immunogenic, immediately complicate antibody generation. The production of monoclonal antibodies is often labor-intensive as screening a large number of colonies is a requirement. Since antibodies are produced in vivo, it follows that the identification of antibodies is restricted by in vivo parameters, making it impossible to change the properties of antibodies on demand.

Another attractive feature of aptamers is that they are easy to manufacture. Aptamers can be chemically synthesized, and their sequence information can be shared digitally as a blueprint for their manufacture. This eliminates any batch-to-batch variations and reduces the cost and the time needed for production. In contrast the performance of the same antibody tends to vary from batch to batch, requiring immunoassays to be checked with each new batch.

Unlike temperature-sensitive antibodies with limited shelf-life and susceptibility to irreversible denaturation, aptamers can easily reform within minutes and are stable enough for long-term storage and transportation at ambient temperature. Because of these features, aptamer-based ELISA offers the advantage of reusability

and regenerability. Unlike antibodies, which suffer from permanent degradation, an aptamer-immobilized ELISA system can be easily reused for different protocols after the target has been unbound. In one experiment, for example, temperature change was used to regenerate aptamers more than 40 times, and 90 % of these aptamers were able to refold into their original configuration [20].

More importantly, aptamers can be easily labeled and modified with a variety of reporter molecules, linkers, and other functional groups at precise locations during or after chemical synthesis, whereas antibodies are subject to denaturation of the protein or loss of function.

Finally, aptamers are smaller in size when compared to antibodies. As such, aptamers can penetrate tumor tissue much more efficiently than conventional immunotherapy options, and these nucleic acids also lack immunogenicity, leading to far fewer side effects. For example, CD133-specific aptamers were demonstrated to outperform CD133 antibodies in penetrating tumor spheres. CD133 RNA aptamers could penetrate a tumor sphere and maintain cellular residence for a minimum of 24 h. In contrast, antibodies could not penetrate the tumor sphere core, even at a concentration 300-fold higher than that of aptamers [21].

On the other hand, compared to antibodies, aptamers do have some limitations. Theoretically, aptamers can be selected for any kind of target, but as a practical matter, comparatively few aptamers sequences are currently available. It is astonishing that only a limited number of aptamer–target pairs have been intensively used, mainly for proof-of-principle of novel aptamer assays [22]. For example, by far the most frequently used aptamer in the literature is the antithrombin aptamer, which has been reported in over 1,000 publications, followed by aptamers targeting adenosine, cocaine, and platelet-derived growth factor, all of which account for over one-third of the total publications on aptamers (Fig. 14.1). This lack of variation severely impedes the development and application of aptamers.

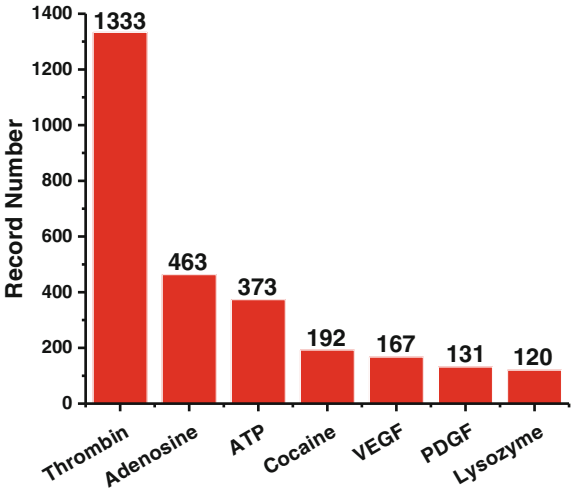

Fig. 14.1 Based on the web of science database, a total of 7,684 publications were found between 1990 and 2014 by using the keyword "aptamer*" (* is a wildcard character)

The low success rate of aptamer selection is believed to account for limited availability of aptamers. Two reasons have been proposed to explain to the low success of aptamer selection. First, the conventional selection technique, known as SELEX [17, 18], is time-consuming, labor-intensive, inefficient, and expensive. Second, limited chemical diversity is intrinsic to natural DNA, which has led to difficulty in selecting aptamers against some targets, especially proteins [23]. Compared to antibodies that have building blocks consisting of 20 amino acids, aptamers only consist of A, T(U), C, and G, resulting in limited chemical and structural diversity. In additional, unlike antibodies that have local positive or negative surfaces, aptamer sequences are ubiquitously negative-charge under physiological conditions.

Another limitation of aptamers for their biomedical applications is that they tend to be very sensitive to nucleases. Therefore, extra effort is required in order to modify these aptamer sequences to make them nuclease-resistant, a process which, in turn, involves expensive and lengthy steps.

To overcome these limitations, new selection methods are needed to further improve the success rate of aptamer selection and to efficiently generate stable aptamers for in vivo application with low cost. In the following sections, several new and promising aptamer selection methods will be reviewed. Strategies for improving selection success rate will be highlighted. Finally, efforts leading to the selection of stable aptamers and, hence, increasing the potential for the practical use of aptamer-based technology in clinical settings, will be discussed.

14.3 New Methods to Improve the Efficiency of Aptamer Selection

SELEX involves enrichment from a large initial library after many iterative rounds of selection and the screening of tens to hundreds of aptamer candidates from the enriched library [24]. This lengthy and inefficient process calls for the development of innovative methods for rapid, efficient, and high-throughput generation of aptamers. Over the past decade, several new SELEX enrichment and screening methods have been developed to facilitate aptamer discovery.

For example, taking advantage of the excellent separation efficiency of capillary electrophoresis (CE), Mendonsa and Bowser developed CE-SELEX (Fig. 14.2), which significantly reduces the number of selection rounds to as low as four. So far, CE-SELEX has been successfully used to isolate aptamers for large targets including human immunoglobulin E [25, 26], HIV reverse transcriptase [27], protein kinase K [28], protein farnesyltransferase [29], protein MutS [30, 31], and small targets such as neuropeptide Y [32] and N-methyl mesoporphyrin [33].

Another exciting progress made in this field is the introduction of microfluidics technology to aptamer selection. Due to the advantages of reduced reagent consumption, high throughput, and automation potential, microfluidic technology has revolutionized the field of aptamer selection in terms of increased speed, reduced costs, improved resolving power, high throughput, and automation [34–37]. One of

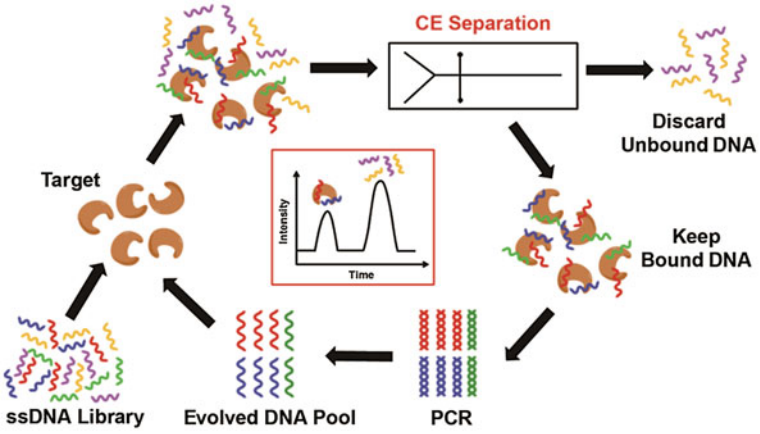

Fig. 14.2 Schematic illustration of CE-SELEX. A library of ssDNA is incubated with the target molecules. Capillary electrophoresis is used to separate bound from unbound sequences. Binding sequences are amplified by PCR and evolved as an enriched ssDNA pool suitable for further rounds of selection

the successful examples of the integrating microfluidics with aptamer selection was illustrated by Soh group, where they integrated the high separation efficiency of microfluidics with target-bound magnetic beads to develop a magnetic beads-based microfluidic SELEX, or M-SELEX, for highly efficient isolation of aptamers [38]. Using this M-SELEX method, an enriched aptamer pool was obtained that tightly bound to the light chain of recombinant botulinum neurotoxin type A after a single round of selection with a K_d value of 33 nM.

In addition to the enrichment process, screening active aptamers from a large enriched library is also an important step for aptamer selection. In a normal screening process, the enriched DNA library has to be cloned into plasmids, followed by transfection into bacteria. Bacteria are then grown, and colonies are picked and sequenced in large quantities to obtain aptamer candidates. After bioinformatics analysis, possible candidates are then chemically synthesized, and their binding affinities are measured individually. To reduce and simplify this time-consuming, labor-intensive process, agarose droplet SELEX (Fig. 14.3) and surface display SELEX were developed for efficiently screening aptamers from a complex ssDNA library by employing single-molecule emulsion PCR (ePCR) in agarose droplets [39] or on the surface of microbeads [40]. Compared to the conventional cloning–sequencing–synthesis–screening work flow, these methods take advantage of the compartmentalization of droplets and allow rapid screening of individual DNA sequences from an enriched library prior to knowing their exact sequence information, thereby accelerating and simplifying the entire process at reduced cost.

Another game-changing technology for aptamer selection is next-generation sequencing (NGS). NGS possesses unprecedented sequencing speed, thereby enabling impressive scientific achievements and novel biological applications

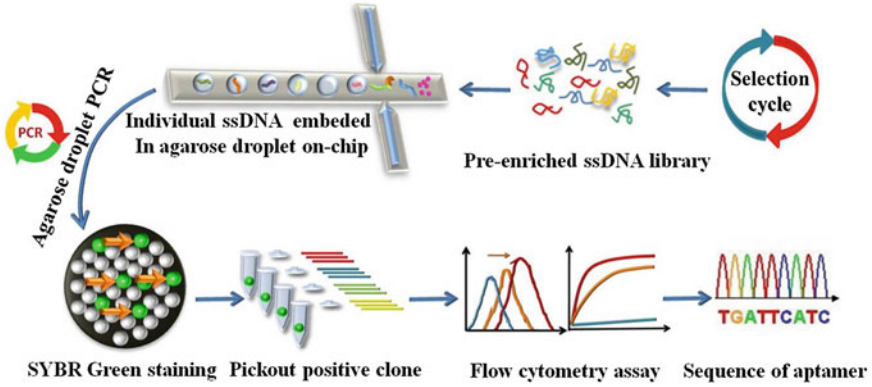

Fig. 14.3 Schematic illustration of direct evaluation of enriched sequences by agarose droplet microfluidics. Single DNA sequences of an enriched library obtained by traditional SELEX are encapsulated individually into agarose droplets for high-throughput single-copy DNA amplification. The resulting agarose droplets are cooled to become agarose beads and stained with SYBR Green to enable selection of highly fluorescent beads containing DNA colonies. The binding affinity of DNA in each fluorescent bead against the target molecule is screened. DNA sequences with low K_d values and good selectivity can be directly used as aptamers, or they can be sequenced and synthesized for further study. Adapted from Ref. [39]. Copyright 2012 American Chemical Society

[41, 42]. Accordingly, this high-throughput NGS has also been introduced into aptamer selection [43–48]. In traditional aptamer selection, Sanger sequencing can only identify some hundred clones, requiring the successive shrinking of the enriched library to a small number of sequences through many rounds of selection. In contrast, NGS, together with bioinformatics, allows the successful isolation of high-quality target binders after very few selection rounds. Moreover, NGS also offers the opportunity to open the black box of SELEX and observe a large part of the population dynamics during the selection process. For example, Schütze et al. [44] performed SELEX on the model target streptavidin immobilized on magnetic beads and compared the results obtained between conventional cloning with Sanger sequencing and NGS. In order to follow the selection process, pools from all selection rounds were barcoded and sequenced in parallel. Ten rounds of selection were performed. It was found that high-affinity aptamers could be readily identified simply by copy number enrichment in the first selection rounds. Interestingly, the most abundant clones analyzed in the final selection round did not directly coincide with the strongest binding behavior, which indicates a strong selection bias in favor of PCR performance over binding properties. It was also observed mutant clones introduced by Taq polymerase arise during the selection. Based on these results, they suggested that performing three rounds of selection, followed by sequencing the pools by NGS, could avoid the high number of iterative selection rounds typical of traditional SELEX, while, at the same time, reducing time, PCR bias, and artifacts. Moreover, one round of positive selection, followed by NGS and bioinformatics analysis, has proven successful in selecting high-affinity aptamers against thrombin [45].

14.4 Aptamers with Modified and Unnatural Bases for Better Binding Affinity

Because of their limited number of building blocks and ubiquitous negative-charge, DNA or RNA molecules have limited chemical, structural, and molecular interaction diversity as compared to antibodies. This intrinsic limitation of natural nucleic acids may, in turn, lead to low success rate for generating aptamers against some proteins. By doping modified bases with hydrophobic moieties, positive charges, or non-Watson–Crick hydrogen bonds into aptamer sequences, the chemical, structural, and interaction diversity of the aptamers could be significantly expanded, leading to greatly improved binding properties.

Eaton and coworkers have pioneered the field by synthesizing nucleotides modified with diverse functional groups for use in SELEX [49, 50]. By using pyridine-modified RNA molecules, RNA aptamers capable of catalyzing a Diels–Alder [4 + 2]cycloaddition by a factor of up to 800, relative to the uncatalyzed reaction, were reported [51]. Recently, based on this technology, Gold and coworkers proposed modifying bases with a functional group that mimics amino acid side chains to yield protein-like properties (Fig. 14.4). Such modification was found to significantly increase the success rate of SELEX. The group has selected high-quality aptamers against over 1,000 human proteins that were initially unsuccessful in SELEX with unmodified SELEX [52].

In addition to using modified natural nucleotides, unnatural nucleotides have been successfully used in aptamer selection. Unlike modified natural nucleotides, which still pair with their natural complementary nucleotides, unnatural nucleotides pair with each other, but not with any of the four natural nucleotides. Use of unnatural nucleotides provides additional structural and chemical diversity beyond that available with modified natural nucleic acids, which could increase the functionality of aptamers and improve the success rate of aptamer selection. Hirao and coworkers generated aptamers containing adenine, guanine, thymine, cytosine, and the highly hydrophobic unnatural base 7-(2-thienyl)imidazo[4,5-b]pyridine (Ds) [53]. Based on the hydrophilic property of nucleic acids, conventional aptamers bind less effectively to the hydrophobic parts of target protein. However, the

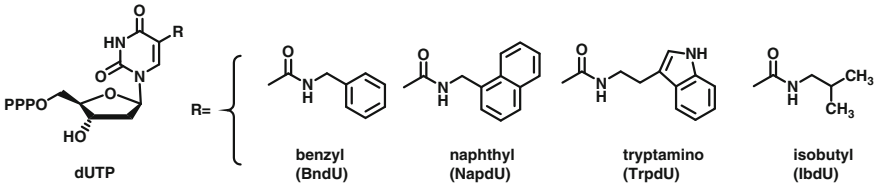

Fig. 14.4 Nucleotides modified with a functional group that mimics amino acid side chains. Nucleotide triphosphate analogs modified at the 5-position (R) of uridine (dUTP):5-benzylaminocarbonyl-dU (BndU); 5-naphthylmethylaminocarbonyl-dU (NapdU); 5-tryptaminocarbonyl-dU (TrpdU); and 5-isobutylaminocarbonyl-dU (iBudU)

introduction of a hydrophobic cavity provided by unnatural Ds bases extends additional hydrophobic binding forces to aptamer candidates. Aptamers identified against two protein targets were used in their experiment, including vascular endothelial cell growth factor-165 (VEGF-165) and interferon-γ(IFN-γ), and they displayed affinity in the pM range, which is >100-fold stronger over that of aptamers containing only natural bases.

Instead of using natural bases with hydrophobic functionality, Tan and coworkers incorporated artificially expanded genetic information systems, or AEGISs, to expand the structure and chemical diversity of the DNA library for aptamer selection [54]. AEGISs are unnatural forms of DNA with different arrangements of hydrogen bond donor and acceptor groups on the nucleobases not found in natural nucleobases. Introduction of AEGISs can significantly increase information density and provide more functional groups for molecular interaction. Using a DNA library built from 6 nucleobases, A, T, C, G, and the AEGIS non-standard P and Z nucleotides, aptamers against a line of breast cancer cells were successfully identified. These results demonstrate the potential of genetic alphabet expansion to increase the chemical and structural diversity of nucleic acid library for aptamer selections.

14.5 Selection of Stable Aptamers

One of the major barriers against the in vivo application of aptamers built from natural nucleic acids is their quick degradation by nucleases under physiological conditions. Depending on the sequence and secondary structure, RNA is degraded by nucleases in seconds and DNA in minutes in biological media, such as serum [55]. As such, natural nucleic acids are not suitable building blocks for therapeutics or imaging reagents where prolonged activity is required. However, the rate of nuclease digestion can be inhibited with backbone modification of the nucleic acids, e.g., substitution at the 2′ position of pyrimidines, which are the primary targets for serum nucleases [56]. Another highly stabilizing modification commonly used for antisense oligonucleotides is the substitution of the internucleotide phosphodiester linkage with a phosphorothioate linkage. Unfortunately, post-SELEX modification risks weakening aptamer-target binding by altering aptamer structure, disrupting specific interactions with the target, or a combination of both.

In addition, the isolation of nuclease-resistant aptamers could be achieved by using a library of oligonucleotides with the chemical substitutions already present (Mod-SELEX) [55]. Mod-SELEX uses a polymerase to incorporate modified nucleotides into the oligonucleotide library. Wild-type polymerases are evolved in nature to work efficiently with wild-type nucleotides. However, these polymerases are generally specific for their substrates to ensure high-fidelity amplification; therefore, the incorporation of nucleotides containing modifications in such wild-type polymerases is often a challenge. As a consequence, considerable effort has been expended to discover variants of wild-type polymerases that are able to accept

modified nucleotides. Among these, Y639F T7 RNA polymerase was found to polymerize 2′-deoxy nucleotides (A, C, and U), 2′-fluoro-pyrimidines, and 2′-amino-pyrimidine nucleotides [57]. Compared to other modifications, 2′-O-methyl modification is more attractive for a number of reasons. First of all, 2-O-methyl nucleotides are much cheaper to synthesize. Second, they are naturally occurring nucleotides that are commonly found in ribosomes and thus safe to use for therapeutic applications. Based on Y639F, the double mutant Y639F/H784A T7 RNA polymerase was found to polymerize pyrimidines with more bulky groups, including 2′-azido and 2′-O-methyl [58]. More recently, a T7 RNA polymerase variant, R425C, was discovered, which permits the enzymatic synthesis of fully 2-O-methyl-modified RNA [59].

Early examples of Mod-SELEX used wild-type polymerase to synthesize 2′-fluoropyrimidine and 2′-hydroxyl-purine oligonucleotide for the selection of nuclease-resistant aptamers, which were further developed later as Macugen (pegaptanib sodium) [19], the first aptamer to be clinically approved for human therapeutic use in the USA, and other drugs currently in clinical development. With the availability of polymerase capable of incorporating different modified bases, it is expected that more nuclease-resistant aptamers will be reported.

Another approach for generating stable aptamers involves the use of nucleic acids consisting of L-nucleotides for aptamer synthesis. The resulting L-aptamers, called Spiegelmers, have shown good resistance to nuclease degradation, and, as a result, they have been selected to target a variety of small molecules, including gonadotropin-releasing hormone [60], ghrelin [61], and more recently, proteins such as cardiac troponin I [62].

14.6 Summary and Outlook

The advantages of aptamers, as discussed above, fully position these DNA/RNA oligonucleotides as promising affinity ligands for therapeutic and diagnostic applications. Although significant progress has been made in fundamental research in the areas of chemical sensing, clinical diagnosis, and targeted drug delivery and therapy, the practical and commercial use of aptamers, especially for clinical applications, has lagged far behind. It is true that aptamers suffer such limitations as low efficiency and low rate of successful selection, as well as susceptibility to nuclease digestion. However, novel selection methods have been developed to address these obstacles. For example, next-generation sequencing allows observation of the population dynamics during the selection process and allows the successful isolation of high-quality target binders after very few rounds of selection. To improve the success rate of aptamer selection, a variety of chemical functional groups have been introduced to expand the structural and chemical diversity of the nucleic acid library. Furthermore, progress in enzymology has allowed the enzymatic introduction of different moieties to the 2′ position of the sugar ring to prepare a nuclease-resistant library for stable aptamer selection. Other novel strategies, like

Spiegelmers, consisting of the enantiomers of natural oligonucleotides, further improve the selection of robust aptamers for small molecule and, more recently, protein targets.

Unlike the identification of small-molecule ligands, where computational approaches have been the indispensable main force in the drug screening pipeline for lead compound identification, computational screening remains a fundamentally uncharted area for aptamer selection. Nonetheless, some progress in this direction has been demonstrated by Tseng and coworkers, who used an in silico, entropic fragment-based approach (EFBA) to design aptamer templates that selectively bind to the phospholipid membrane component phosphatidylserine [63].

Another under-explored area is the structural study of aptamers. Accurate elucidation of aptamer structure allows one to study structure–function relationship, which would further help optimization of aptamer sequence. More importantly, based on the structure of aptamer obtained, a variety of sensing schemes, such as fluorescence resonance energy transfer, pyrene-based monomer–excimer switching, and target responsive aptamer-crosslinked hydrogel, could be adopted for robust yet sensitive detection of related targets. In addition, the availability of aptamer structure could guide one to further stabilize the structure of aptamer. Unlike the globular structure of antibodies, aptamer structures are floppy, which leads to their affinity sensitive to environmental changes. Stem structures or covalent crosslinks by photo-affinity moieties could be possibly introduced to fix the structure of non-active sites to enhance the overall structural stability of aptamers thus their binding properties.

With the broad availability of novel selection methods, modification strategies, the introduction of powerful computational approaches, as well as the increased effort in aptamer structure elucidation and stabilization, it is anticipated that more and more aptamers will emerge for practical therapeutic and diagnostic applications.

References

1. Fang X, Tan W (2010) Aptamers generated from cell-SELEX for molecular medicine: a chemical biology approach. Acc Chem Res 43(1):48–57. doi:10.1021/ar900101s
2. Keefe AD, Pai S, Ellington A (2010) Aptamers as therapeutics. Nat Rev Drug Discovery 9 (7):537–550. doi:10.1038/nrd3141
3. Iliuk AB, Hu L, Tao WA (2011) Aptamer in bioanalytical applications. Anal Chem 83 (12):4440–4452. doi:10.1021/ac201057w
4. Tan W, Wang H, Chen Y, Zhang X, Zhu H, Yang C, Yang R, Liu C (2011) Molecular aptamers for drug delivery. Trends Biotechnol 29(12):634–640. doi:10.1016/j.tibtech.2011.06.009
5. Tan W, Donovan MJ, Jiang J (2013) Aptamers from cell-based selection for bioanalytical applications. Chem Rev 113(4):2842–2862. doi:10.1021/cr300468w
6. Yan L, Zhu Z, Zou Y, Huang Y, Liu D, Jia S, Xu D, Wu M, Zhou Y, Zhou S, Yang CJ (2013) Target-responsive "sweet" hydrogel with glucometer readout for portable and quantitative detection of non-glucose targets. J Am Chem Soc 135(10):3748–3751. doi:10.1021/ja3114714

7. Willner I, Zayats M (2007) Electronic aptamer-based sensors. Angew Chem 46(34):6408–6418. doi:10.1002/anie.200604524
8. Yang CJ, Jockusch S, Vicens M, Turro NJ, Tan W (2005) Light-switching excimer probes for rapid protein monitoring in complex biological fluids. Proc Nat Acad Sci USA 102 (48):17278–17283. doi:10.1073/pnas.0508821102
9. Rupcich N, Nutiu R, Li Y, Brennan JD (2006) Solid-phase enzyme activity assay utilizing an entrapped fluorescence-signaling DNA aptamer. Angew Chem 45(20):3295–3299. doi: 10.1002/anie.200504576
10. Liu J, Lu Y (2005) Fast colorimetric sensing of adenosine and cocaine based on a general sensor design involving aptamers and nanoparticles. Angew Chem 45(1):90–94. doi:10.1002/anie.200502589
11. Liu J, Lu Y (2006) Preparation of aptamer-linked gold nanoparticle purple aggregates for colorimetric sensing of analytes. Nat Protoc 1(1):246–252. doi:10.1038/nprot.2006.38
12. Zhu Z, Wu C, Liu H, Zou Y, Zhang X, Kang H, Yang CJ, Tan W (2010) An aptamer cross-linked hydrogel as a colorimetric platform for visual detection. Angew Chem 49(6):1052–1056. doi:10.1002/anie.200905570
13. Freeman R, Liu X, Willner I (2011) Chemiluminescent and chemiluminescence resonance energy transfer (CRET) detection of DNA, metal ions, and aptamer-substrate complexes using hemin/G-quadruplexes and CdSe/ZnS quantum dots. J Am Chem Soc 133(30):11597–11604. doi:10.1021/ja202639m
14. Ohno Y, Maehashi K, Matsumoto K (2010) Label-free biosensors based on aptamer-modified graphene field-effect transistors. J Am Chem Soc 132(51):18012–18013. doi:10.1021/ja108127r
15. Lee SJ, Youn BS, Park JW, Niazi JH, Kim YS, Gu MB (2008) ssDNA aptamer-based surface plasmon resonance biosensor for the detection of retinol binding protein 4 for the early diagnosis of type 2 diabetes. Anal Chem 80(8):2867–2873. doi:10.1021/ac800050a
16. Zhou WJ, Halpern AR, Seefeld TH, Corn RM (2012) Near infrared surface plasmon resonance phase imaging and nanoparticle-enhanced surface plasmon resonance phase imaging for ultrasensitive protein and DNA biosensing with oligonucleotide and aptamer microarrays. Anal Chem 84(1):440–445. doi:10.1021/ac202863k
17. Tuerk C, Gold L (1990) Systematic evolution of ligands by exponential enrichment: RNA ligands to bacteriophage T4 DNA polymerase. Science 249(4968):505–510
18. Ellington AD, Szostak JW (1990) In vitro selection of RNA molecules that bind specific ligands. Nature 346(6287):818–822
19. Ruckman J, Green LS, Beeson J, Waugh S, Gillette WL, Henninger DD, Claesson-Welsh L, Janjic N (1998) 2′-Fluoropyrimidine RNA-based aptamers to the 165-amino acid form of vascular endothelial growth factor (VEGF165). Inhibition of receptor binding and VEGF-induced vascular permeability through interactions requiring the exon 7-encoded domain. J Biol Chem 273(32):20556–20567
20. Wu ZS, Guo MM, Zhang SB, Chen CR, Jiang JH, Shen GL, Yu RQ (2007) Reusable electrochemical sensing platform for highly sensitive detection of small molecules based on structure-switching signaling aptamers. Anal Chem 79(7):2933–2939. doi:10.1021/ac0622936
21. Shigdar S, Qiao L, Zhou S-F, Xiang D, Wang T, Li Y, Lim LY, Kong L, Li L, Duan W (2013) RNA aptamers targeting cancer stem cell marker CD133. Cancer Lett 330(1):84–95
22. Famulok M, Mayer G (2011) Aptamer modules as sensors and detectors. Acc Chem Res 44 (12):1349–1358. doi:10.1021/ar2000293
23. Davies DR, Gelinas AD, Zhang C, Rohloff JC, Carter JD, O'Connell D, Waugh SM, Wolk SK, Mayfield WS, Burgin AB, Edwards TE, Stewart LJ, Gold L, Janjic N, Jarvis TC (2012) Unique motifs and hydrophobic interactions shape the binding of modified DNA ligands to protein targets. Proc Nat Acad Sci USA 109(49):19971–19976. doi:10.1073/pnas.1213933109
24. Sefah K, Shangguan D, Xiong X, O'Donoghue MB, Tan W (2010) Development of DNA aptamers using cell-SELEX. Nat Protocols 5(6):1169–1185

25. Mendonsa SD, Bowser MT (2004) In vitro evolution of functional DNA using capillary electrophoresis. J Am Chem Soc 126(1):20–21. doi:10.1021/ja037832s
26. Mendonsa SD, Bowser MT (2004) In vitro selection of high-affinity DNA ligands for human IgE using capillary electrophoresis. Anal Chem 76(18):5387–5392. doi:10.1021/ac049857v
27. Mosing RK, Mendonsa SD, Bowser MT (2005) Capillary electrophoresis-SELEX selection of aptamers with affinity for HIV-1 reverse transcriptase. Anal Chem 77(19):6107–6112. doi:10.1021/ac050836q
28. Tok J, Lai J, Leung T, Li SF (2010) Selection of aptamers for signal transduction proteins by capillary electrophoresis. Electrophoresis 31(12):2055–2062. doi:10.1002/elps.200900543
29. Berezovski M, Drabovich A, Krylova SM, Musheev M, Okhonin V, Petrov A, Krylov SN (2005) Nonequilibrium capillary electrophoresis of equilibrium mixtures: a universal tool for development of aptamers. J Am Chem Soc 127(9):3165–3171. doi:10.1021/ja042394q
30. Drabovich A, Berezovski M, Krylov SN (2005) Selection of smart aptamers by equilibrium capillary electrophoresis of equilibrium mixtures (ECEEM). J Am Chem Soc 127(32):11224–11225. doi:10.1021/ja0530016
31. Drabovich AP, Berezovski M, Okhonin V, Krylov SN (2006) Selection of smart aptamers by methods of kinetic capillary electrophoresis. Anal Chem 78(9):3171–3178. doi:10.1021/ac060144h
32. Mendonsa SD, Bowser MT (2005) In vitro selection of aptamers with affinity for neuropeptide Y using capillary electrophoresis. J Am Chem Soc 127(26):9382–9383. doi:10.1021/ja052406n
33. Yang J, Bowser MT (2013) Capillary electrophoresis-SELEX selection of catalytic DNA aptamers for a small-molecule porphyrin target. Anal Chem 85(3):1525–1530. doi:10.1021/ac302721j
34. Mosing RK, Bowser MT (2007) Microfluidic selection and applications of aptamers. J Sep Sci 30(10):1420–1426. doi:10.1002/jssc.200600483
35. Xu Y, Yang X, Wang E (2010) Review: aptamers in microfluidic chips. Anal Chim Acta 683(1):12–20. doi:10.1016/j.aca.2010.10.007
36. Weng CH, Huang CJ, Lee GB (2012) Screening of aptamers on microfluidic systems for clinical applications. Sensors 12(7):9514–9529. doi:10.3390/s120709514
37. Lin H, Zhang W, Jia S, Guan Z, Yang CJ, Zhu Z (2014) Microfluidic approaches to rapid and efficient aptamer selection. Biomicrofluidics 8(4):041501. doi:10.1063/1.4890542
38. Lou X, Qian J, Xiao Y, Viel L, Gerdon AE, Lagally ET, Atzberger P, Tarasow TM, Heeger AJ, Soh HT (2009) Micromagnetic selection of aptamers in microfluidic channels. Proc Nat Acad Sci USA 106(9):2989–2994. doi:10.1073/pnas.0813135106
39. Zhang WY, Zhang WH, Liu ZY, Li C, Zhu Z, Yang CJ (2011) A highly parallel single molecule amplification approach based on agarose droplet PCR for efficient and cost-effective aptamer selection. analytical chemistry, Washington, DC, United States 83 (in press)
40. Zhu Z, Song Y, Li C, Zou Y, Zhu L, An Y, Yang CJ (2014) Monoclonal surface display SELEX for simple, rapid, efficient, and cost-effective aptamer enrichment and identification. Anal Chem 86:5881–5888. doi:10.1021/ac501423g
41. Metzker ML (2010) Applications of next-generation sequencing sequencing technologies—the next generation. Nat Rev Genet 11(1):31–46. doi:10.1038/Nrg2626
42. Shendure J, Ji HL (2008) Next-generation DNA sequencing. Nat Biotechnol 26(10):1135–1145. doi:10.1038/Nbt1486
43. Zimmermann B, Gesell T, Chen D, Lorenz C, Schroeder R (2010) Monitoring genomic sequences during SELEX using high-throughput sequencing: neutral SELEX. Plos ONE 5(2):e9169. doi:10.1371/Journal.Pone.0009169 Artn
44. Schütze T, Wilhelm B, Greiner N, Braun H, Peter F, Morl M, Erdmann VA, Lehrach H, Konthur Z, Menger M, Arndt PF, Glokler J (2011) Probing the SELEX process with next-generation sequencing. Plos ONE 6(12):e29604. doi:10.1371/journal.pone.0029604 ARTN

45. Hoon S, Zhou B, Janda KD, Brenner S, Scolnick J (2011) Aptamer selection by high-throughput sequencing and informatic analysis. Biotechniques 51(6):413–416. doi:10.2144/000113786
46. Cho M, Xiao Y, Nie J, Stewart R, Csordas AT, Oh SS, Thomson JA, Soh HT (2010) Quantitative selection of DNA aptamers through microfluidic selection and high-throughput sequencing. P Natl Acad Sci USA 107(35):15373–15378. doi:10.1073/pnas.1009331107
47. Cho M, Oh SS, Nie J, Stewart R, Eisenstein M, Chambers J, Marth JD, Walker F, Thomson JA, Soh HT (2013) Quantitative selection and parallel characterization of aptamers. Proc Nat Acad Sci USA 110(46):18460–18465. doi:10.1073/pnas.1315866110
48. Wilson R, Bourne C, Chaudhuri RR, Gregory R, Kenny J, Cossins A (2014) Single-step selection of bivalent aptamers validated by comparison with SELEX using high-throughput sequencing. Plos ONE 9(6):e100572. doi:10.1371/journal.pone.0100572 ARTN
49. Dewey TM, Mundit A, Crouch GJ, Zyzniewski MC, Eaton BE (1995) New uridine derivatives for systematic evolution of RNA ligands by exponential enrichment. J Am Chem Soc 117 (32):8474–8475. doi:10.1021/Ja00137a027
50. Eaton BE (1997) The joys of in vitro selection: chemically dressing oligonucleotides to satiate protein targets. Curr Opin Chem Biol 1(1):10–16
51. Tarasow TM, Tarasow SL, Eaton BE (1997) RNA-catalysed carbon-carbon bond formation. Nature 389(6646):54–57. doi:10.1038/37950
52. Gold L, Ayers D, Bertino J, Bock C, Bock A, Brody EN, Carter J, Dalby AB, Eaton BE, Fitzwater T, Flather D, Forbes A, Foreman T, Fowler C, Gawande B, Goss M, Gunn M, Gupta S, Halladay D, Heil J, Heilig J, Hicke B, Husar G, Janjic N, Jarvis T, Jennings S, Katilius E, Keeney TR, Kim N, Koch TH, Kraemer S, Kroiss L, Le N, Levine D, Lindsey W, Lollo B, Mayfield W, Mehan M, Mehler R, Nelson SK, Nelson M, Nieuwlandt D, Nikrad M, Ochsner U, Ostroff RM, Otis M, Parker T, Pietrasiewicz S, Resnicow DI, Rohloff J, Sanders G, Sattin S, Schneider D, Singer B, Stanton M, Sterkel A, Stewart A, Stratford S, Vaught JD, Vrkljan M, Walker JJ, Watrobka M, Waugh S, Weiss A, Wilcox SK, Wolfson A, Wolk SK, Zhang C, Zichi D (2010) Aptamer-based multiplexed proteomic technology for biomarker discovery. PLoS ONE 5(12):e15004. doi:10.1371/journal.pone.0015004
53. Kimoto M, Yamashige R, Matsunaga K, Yokoyama S, Hirao I (2013) Generation of high-affinity DNA aptamers using an expanded genetic alphabet. Nat Biotechnol 31(5):453–457. doi:10.1038/nbt.2556
54. Sefah K, Yang Z, Bradley KM, Hoshika S, Jimenez E, Zhang L, Zhu G, Shanker S, Yu F, Turek D, Tan W, Benner SA (2014) In vitro selection with artificial expanded genetic information systems. Proc Nat Acad Sci USA 111(4):1449–1454. doi:10.1073/pnas.1311778111
55. Keefe AD, Cload ST (2008) SELEX with modified nucleotides. Curr Opin Chem Biol 12 (4):448–456. doi:10.1016/j.cbpa.2008.06.028
56. Uhlmann E, Peyman A, Ryte A, Schmidt A, Buddecke E (2000) Use of minimally modified antisense oligonucleotides for specific inhibition of gene expression. Methods Enzymol 313:268–284
57. Sousa R, Padilla R (1995) A mutant T7 RNA polymerase as a DNA polymerase. EMBO J 14 (18):4609–4621
58. Padilla R, Sousa R (2002) A Y639F/H784A T7 RNA polymerase double mutant displays superior properties for synthesizing RNAs with non-canonical NTPs. Nucleic Acids Res 30 (24):e138
59. Ibach J, Dietrich L, Koopmans KR, Nobel N, Skoupi M, Brakmann S (2013) Identification of a T7 RNA polymerase variant that permits the enzymatic synthesis of fully 2′-O-methyl-modified RNA. J Biotechnol 167(3):287–295. doi:10.1016/j.jbiotec.2013.07.005
60. Leva S, Lichte A, Burmeister J, Muhn P, Jahnke B, Fesser D, Erfurth J, Burgstaller P, Klussmann S (2002) GnRH binding RNA and DNA Spiegelmers: a novel approach toward GnRH antagonism. Chem Biol 9(3):351–359

61. Hornby PJ (2006) Designing Spiegelmers to antagonise ghrelin. Gut 55(6):754–755. doi: 10.1136/gut.2005.076067
62. Szeitner Z, Lautner G, Nagy SK, Gyurcsanyi RE, Meszaros T (2014) A rational approach for generating cardiac troponin I selective Spiegelmers. Chem Commun 50(51):6801–6804. doi:10.1039/c4cc00447g
63. Ashrafuzzaman M, Tseng CY, Kapty J, Mercer JR, Tuszynski JA (2013) A computationally designed DNA aptamer template with specific binding to phosphatidylserine. Nucleic Acid Therapeutics 23(6):418–426. doi:10.1089/nat.2013.0415